

Volume II
Chapters 3-9

PPG-909
UCLA-ENG-85-39

Technical Issues and Requirements of Experiments and Facilities for Fusion Nuclear Technology

FINESSE Phase I Report

December 1985



Fusion Engineering
University of California, Los Angeles
Los Angeles, California

DISCLAIMER

This report was prepared as an account of work sponsored by an agency of the United States Government. Neither the United States Government nor any agency thereof, nor any of their employees, makes any warranty, express or implied, or assumes any legal liability or responsibility for the accuracy, completeness, or usefulness of any information, apparatus, product, or process disclosed, or represents that its use would not infringe privately owned rights. Reference herein to any specific commercial product, process, or service by trade name, trademark, manufacturer, or otherwise, does not necessarily constitute or imply its endorsement, recommendation, or favoring by the United States Government or any agency thereof. The views and opinions of authors expressed herein do not necessarily state or reflect those of the United States Government or any agency thereof.

Technical Issues and Requirements of Experiments and Facilities
for Fusion Nuclear Technology

FINESSE Phase I Report

December 1985

Work supported by U.S. Department of Energy Contract No. DE-AS03-84ER52105.

FINESSE Phase I Report

Technical Issues and Requirements of Experiments and
Facilities for Fusion Nuclear Technology

Volume II

Contributors

M. Abdou	(UCLA)	R. Krakowski	(LANL)
J. Bartlit	(LANL)	G. Listvinsky	(TRW)
C. Bathke	(LANL)	H. Madarame	(UCLA/U. Tokyo)
G. Bell	(UCLA)	R. McGrath	(SNLA)
D. Berwald	(TRW)	G. Morgan	(MDAC)
L. Bogart	(EASI)	M. Nakagawa	(UCLA/JAERI)
T. Carpenter	(Grumman)	B. Picologlou	(ANL)
Y. Cha	(ANL)	R. Puigh	(HEDL)
J. Doggett	(LLNL)	R. Raffray	(UCLA)
J. Garner	(TRW)	J. Reimann	(UCLA/KfK)
P. Gierszewski	(UCLA/CFFTP)	D. K. Sze	(ANL)
D. Greenslade	(HEDL)	M. Tillack	(UCLA)
J. Grover	(HEDL)	C. Walthers	(LANL)
R. Jalbert	(LANL)	M. Youssef	(UCLA)
C. Johnson	(ANL)		

December 1985

FINESSE Phase I Report

Technical Issues and Requirements of Experiments and Facilities for Fusion Nuclear Technology

Volume II

Task Leaders

M. Abdou, UCLA	Principal Investigator
J. Bartlit, LANL	Tritium and Vacuum Systems
D. Berwald, TRW	Test Plan Considerations
P. Gierszewski, UCLA/CFFTP	Solid Breeder Blankets, Plasma Interac- tive Components, Fusion Test Facilities
J. Grover, HEDL	Non-Fusion Irradiation Facilities
R. McGrath, SNLA	Plasma Interactive Components
M. Nakagawa, UCLA/JAERI	Radiation Shielding
R. Puigh, HEDL	Solid Breeder Blankets
J. Reimann, UCLA/KfK	Tritium and Vacuum Systems
D. K. Sze, ANL	Liquid Metal Blankets
M. Tillack, UCLA	Liquid Metal Blankets

Acknowledgements

The authors wish to thank the following people for their technical advice and for their assistance in editing this report:

C. Baker	(ANL)	F. Mann	(HEDL)
L. Bromberg	(MIT)	R. Mattas	(ANL)
J. Brooks	(ANL)	J. Peerenboom	(ANL)
D. Dolan	(HEDL)	M. Peng	(ORNL)
J. Downing	(LANL)	M. Sawan	(U. Wisconsin)
A. Hadid	(UCLA)	R. Watson	(SNLA)
G. Hollenberg	(HEDL)	R. Whitfield	(ANL)
D. Jassby	(PPPL)	K. Wilson	(SNLL)
D. Johnson	(HEDL)		

We also gratefully acknowledge L. Lane, S. Ehrlich, and especially M. Pagnusat for their assistance in assembling the report.

FINESSE Phase I Report

Technical Issues and Requirements of Experiments and Facilities
for Fusion Nuclear Technology

TABLE OF CONTENTS

Volume I

Executive Summary

1. Introduction and Technical Summary
2. Blanket Test Plan

Volume II

	<u>Page</u>
3. Liquid Metal Blankets	
3.1 Introduction.....	3-1
3.1.1 Overview of Chapter 3.....	3-1
3.1.2 Summary of Critical Liquid Metal Blanket Issues.....	3-4
References for Section 3.1.....	3-9
3.2 Survey of Existing Data and Facilities.....	3-10
3.2.1 Survey of Existing Data.....	3-10
3.2.1.1 Materials Properties Data.....	3-10
3.2.1.2 Data on Liquid Metal Corrosion.....	3-11
3.2.1.3 Data on MHD Effects in Liquid Metals.....	3-14
3.2.2 Test Facilities.....	3-14
3.2.2.1 Corrosion Loops.....	3-14
3.2.2.2 LMMHD Loops.....	3-22
References for Section 3.2.....	3-26
3.3 Basic Measurements.....	3-28
3.4 Separate and Multiple Effects Experiments.....	3-29
3.4.1 MHD Flow Phenomena.....	3-32
3.4.1.1 Introduction.....	3-32
3.4.1.2 Scaling of MHD Flow Phenomena.....	3-34
3.4.1.3 Analysis of Minimum Test Requirements.....	3-36
3.4.1.4 Modeling Needs.....	3-46
3.4.1.5 Facility Requirements.....	3-47
References for Section 3.4.1.....	3-50
3.4.2 Heat Transfer.....	3-51

TABLE OF CONTENTS (cont.)

3.4.2.1	Testing Needs.....	3-51
3.4.2.2	Modeling Needs.....	3-52
3.4.2.3	Analysis and Scaling.....	3-52
3.4.2.4	Test Scenarios.....	3-58
3.4.2.5	Facility Descriptions.....	3-59
References for Section 3.4.2.....		3-61
3.4.3	Materials Interactions and Mass Transfer.....	3-62
3.4.3.1	Testing Needs.....	3-62
3.4.3.2	Modeling Needs.....	3-69
3.4.3.3	Analysis and Scaling.....	3-71
3.4.3.4	Test Scenarios and Test Strategies.....	3-72
3.4.3.5	Facility Descriptions.....	3-75
References for Section 3.4.3.....		3-81
3.4.4	Tritium Recovery.....	3-82
3.4.4.1	Testing Needs.....	3-82
3.4.4.2	Modeling Needs.....	3-82
3.4.4.3	Analysis and Scaling.....	3-85
3.4.4.4	Test Scenarios.....	3-86
3.4.4.5	Facility Descriptions.....	3-87
References for Section 3.4.4.....		3-92
3.4.5	MHD Insulators.....	3-93
3.4.5.1	Introduction.....	3-94
3.4.5.2	Testing Needs for MHD Insulators.....	3-95
3.4.5.3	Test Scenarios.....	3-95
3.4.6	Electromagnetics.....	3-97
3.4.6.1	Testing Needs.....	3-97
3.4.6.2	Modeling Needs.....	3-99
3.4.6.3	Analysis and Scaling.....	3-100
3.4.6.4	Electromagnetic Test Facilities.....	3-107
References for 3.4.6.....		3-109
3.4.7	Tritium Breeding.....	3-110
3.5	Partially Integrated Experiments.....	3-110
3.5.1	Non-Neutron TMIF.....	3-111
3.5.1.1	Purpose of TMIF and Its Role in the Test Plan...	3-111

TABLE OF CONTENTS (cont.)

3.5.1.2	Test Scenarios.....	3-112
3.5.1.3	Facility Description.....	3-114
3.5.2	Characteristics of a Single PITF	
Non-Neutron Test Facility.....		3-114
3.6	Integrated Experiments.....	3-115
3.6.1	Purpose of Integrated Experiments.....	3-115
3.6.2	Data Requirements.....	3-116
3.7	Liquid Metal Blanket Facilities Costing.....	3-117
3.7.1	Methodology for FINESSE Costing.....	3-117
3.7.2	Groundrules for Estimates.....	3-121
3.7.3	Cost Data for the Liquid Metal Blanket Test Program.....	3-123
3.8	Summary of Testing and Modeling Needs.....	3-128
3.8.1	Thermal/Mechanical and Materials Compatibility Test Sequence.....	3-128
3.8.2	Tritium Recovery and Control Test Sequence.....	3-136
3.8.3	Tritium Breeding Test Sequence.....	3-137
3.8.4	Summary of Model Development Needs.....	3-137
3.A	Appendix: Materials Properties for Li and LiPb.....	3-139
4.	Solid Breeder Blankets	
4.1	Introduction and Critical Issues.....	4-1
4.2	Survey of Existing Experiments.....	4-5
4.2.1	Materials Development and Characterization.....	4-5
4.2.2	Tritium Inventory Recovery.....	4-11
4.2.3	Breeder/Multiplier/Structure Mechanical Interaction.....	4-13
4.2.4	Structure Mechanical Behavior.....	4-13
4.2.5	Corrosion and Mass Transfer.....	4-13
4.2.6	Tritium Permeation and Processing.....	4-14
4.2.7	Neutronics	4-14
4.3	Material Development and Characterization.....	4-17
4.3.1	Structure.....	4-17
4.3.2	Solid Breeder.....	4-23
4.3.3	Multiplier.....	4-29
4.4	Separate and Multiple Effect Experiments.....	4-38
4.4.1	Tritium Inventory and Recovery.....	4-38

TABLE OF CONTENTS (cont.)

4.4.1.1	Testing and Modelling Needs.....	4-38
4.4.1.2	Experiments and Facilities.....	4-48
4.4.1.3	Test Plan Considerations.....	4-64
4.4.2	Breeder/Multiplier/Structure Mechanical Interaction.....	4-68
4.4.2.1	Testing and Modelling Needs.....	4-68
4.4.2.2	Experiments and Facilities.....	4-71
4.4.2.3	Test Plan Considerations.....	4-77
4.4.3	Structure Mechanical Behavior.....	4-78
4.4.4	Corrosion and Mass Transfer.....	4-80
4.4.4.1	Testing and Modelling Needs.....	4-80
4.4.4.2	Experiments and Facilities.....	4-85
4.4.4.3	Test Plan Considerations.....	4-87
4.4.5	Tritium Permeation and Processing.....	4-90
4.4.6	Neutronics and Tritium Breeding.....	4-91
4.4.6.1	Uncertainty in Tritium Self-Sufficiency.....	4-91
4.4.6.2	Review of Present Status.....	4-92
4.4.6.3	Point Neutron Source Tests.....	4-94
4.4.6.4	Fission Reactor Tests.....	4-100
4.4.6.5	Fusion Test Facilities.....	4-101
4.5	Partially Integrated and Integrated Experiments.....	4-109
4.5.1	Non-Neutron Thermomechanical Integrity Tests.....	4-109
4.5.2	Nuclear Submodule.....	4-124
4.5.3	Fusion Experiments.....	4-140
4.5.4	Test Plan Considerations.....	4-141
4.6	Experiment Cost and Time Characteristics.....	4-143
4.7	Summary.....	4-154
5.	Tritium Processing and Vacuum Systems	
5.1	Introduction.....	5-1
5.2	Tritium Monitoring and Accountability.....	5-6
5.2.1	Monitor Sensitivity.....	5-6
5.2.2	Accountability.....	5-7
5.3	Tritium Permeation and Inventory.....	5-10
5.3.1	Issues.....	5-10
5.3.2	Phenomena and Key Parameters.....	5-10

TABLE OF CONTENTS (cont.)

5.3.3	Experiments and Facilities.....	5-12
5.4	Fuel Cleanup System.....	5-15
5.4.1	Plasma Impurity Content.....	5-15
5.4.2	Component Reliability and Inventory.....	5-18
5.5	Breeder Tritium Extraction.....	5-20
5.5.1	Issues and Key Parameters.....	5-20
5.5.2	Breeder Tritium Extraction Methods.....	5-24
5.5.3	Experiments and Facilities.....	5-33
5.6	Detritiation Systems.....	5-41
5.6.1	Air Detritiation.....	5-41
5.6.2	Water Coolant Detritiation.....	5-43
5.6.3	Helium and Liquid Metal Detritiation.....	5-45
5.7	Vacuum Pumps and Valves.....	5-46
5.7.1	Compound Cryopumps.....	5-46
5.7.2	Vacuum Valves.....	5-48
5.8	Integrated System Behavior.....	5-53
5.8.1	Operation and Control.....	5-53
5.8.2	DT Losses from System.....	5-55
	References.....	5-60

6. Plasma Interactive Components

6.1	Introduction.....	6-1
6.2	Issues for Plasma Interactive Components.....	6-2
6.2.1	Particle Exhaust, Erosion and Recycling.....	6-4
6.2.2	Permeation and Retention of Hydrogen Isotopes and Helium...6-7	
6.2.3	High Heat Flux Removal.....	6-9
6.2.4	Disruptions.....	6-12
6.2.5	Radiation Effects.....	6-13
6.2.6	System Integration.....	6-13
6.3	Parameter Ranges for Testing.....	6-14
6.4	Survey of Existing Facilities.....	6-17
6.4.1	Erosion/Redeposition and Conditioning.....	6-17
6.4.2	Tritium Permeation and Retention.....	6-19
6.4.3	High Heat Flux Removal.....	6-20

TABLE OF CONTENTS (cont.)

6.4.4	Disruptions.....	6-22
6.4.5	Radiation Effects.....	6-23
6.5	Testing Needs.....	6-23
	References.....	6-27
7. Radiation Shielding		
7.1	Introduction and Issues.....	7-1
7.2	Status of Experiments, Data and Methods.....	7-6
7.2.1	Required Accuracies and Status of Experiments.....	7-7
7.2.2	Status of Data Base and Methods.....	7-12
7.3	Experiments and Facilities.....	7-17
7.3.1	Experiments.....	7-19
7.3.2	Point Neutron Source Facility.....	7-26
7.3.3	Fission Neutron Source.....	7-30
7.4	Shielding Experiments in Fusion Test Facility.....	7-35
7.4.1	Operating Condition Requirements.....	7-35
7.4.2	Test Matrix Requirements.....	7-36
	References.....	7-52
8. Nonfusion Irradiation Facilities		
8.1	Introduction.....	8-1
8.2	Fission Reactors.....	8-1
8.2.1	Environmental Relevance.....	8-1
8.2.2	Facility Availability.....	8-8
8.2.3	Cost of Utilization.....	8-8
8.3	Accelerator-Based Neutron Sources.....	8-11
8.3.1	RTNS-II Facility.....	8-13
8.3.1.1	Description.....	8-13
8.3.1.2	Environmental Relevance.....	8-14
8.3.1.3	Availability.....	8-14
8.3.2	UC Davis Cyclotron Facility.....	8-16
8.3.2.1	Description.....	8-16
8.3.2.2	Environmental Relevance.....	8-16

TABLE OF CONTENTS (cont.)

8.3.2.3	Availability.....	8-17
8.3.3	The A-6 Radiation Effects Facility at LAMPF.....	8-17
8.3.3.1	Description.....	8-17
8.3.3.2	Environmental Relevance.....	8-19
8.3.3.3	Availability.....	8-22
8.3.4	The Fusion Materials Test (FMIT) Facility.....	8-22
8.3.4.1	Description.....	8-22
8.3.4.2	Environmental Relevance.....	8-22
8.3.4.3	Availability.....	8-29
8.3.5	Multiple Beam Facility.....	8-29
8.4	Conclusion.....	8-29
	References.....	8-32

9. Fusion Test Facilities

9.1	Introduction.....	9-1
9.2	Test Requirements.....	9-3
9.2.1	Introduction and Engineering Scaling	9-3
9.2.2	Blankets.....	9-4
9.2.3	Non-blanket Components.....	9-21
9.2.4	Summary.....	9-22
9.3	LITE Tokamak (TRW/MIT/U.Texas)	9-25
9.3.1	Concept Description.....	9-26
9.3.2	Representative Design.....	9-31
9.3.3	Development Needs.....	9-35
9.4	Demountable Toroidal Fusion Core (EASI).....	9-37
9.4.1	Concept Description.....	9-37
9.4.2	Representative Designs.....	9-39
9.4.3	Development Needs.....	9-43
9.5	Tokamak Test Facility (PPPL).....	9-44
9.5.1	Concept Description.....	9-44
9.5.2	Representative Design.....	9-44
9.5.3	Development Needs.....	9-45
9.6	Spherical Torus (FEDC).....	9-47
9.6.1	Concept Description.....	9-47
9.6.2	Representative Designs.....	9-52

TABLE OF CONTENTS (cont.)

9.6.3	Development Needs.....	9-52
9.7	Mirrors (LLNL).....	9-55
9.7.1	Concept Description.....	9-55
9.7.2	Representative Designs.....	9-59
9.7.3	Development Needs.....	9-61
9.8	Reverse Field Pinch (LANL/Philips Petroleum).....	9-62
9.8.1	Concept Description.....	9-62
9.8.2	Representative Design.....	9-68
9.8.3	Development Needs.....	9-74
9.9	Comparison of Fusion Test Facilities	9-77
9.9.1	Introduction.....	9-77
9.9.2	Performance.....	9-78
9.9.3	Cost.....	9-80
9.9.4	Risk.....	9-84
9.9.5	Summary.....	9-85
9.10	Conclusions.....	9-91
	References.....	9-93
Appendix A.	Blanket Development Planning Considerations.....	A-1
A.1	Introduction.....	A-1
A.2	Decision Framework.....	A-2
A.3	Objectives, Sub-objectives and Attributes.....	A-5
A.4	Issues and Facilities for First Wall/Blanket Development.....	A-7
A.4.1	First Wall/Blanket Development Issues.....	A-8
A.5	Useful Nuclear Technology Facilities.....	A-10
A.6	Consistency with Magnetic Fusion Program Plan (MFPP).....	A-12
A.6.1	General Time Phasing of Development.....	A-12
A.6.2	Periodic Re-evaluation.....	A-13
A.6.3	Frugality and Near Term Planning.....	A-13
A.6.4	Long Term Planning.....	A-14
A.6.5	Summary.....	A-14

CHAPTER 3

LIQUID METAL BLANKETS

TABLE OF CONTENTS

3. LIQUID METAL BLANKETS

	<u>Page</u>
3.1 Introduction.....	3-1
3.1.1 Overview of Chapter 3.....	3-1
3.1.2 Summary of Critical Liquid Metal Blanket Issues.....	3-4
References for Section 3.1.....	3-9
3.2 Survey of Existing Data and Facilities.....	3-10
3.2.1 Survey of Existing Data.....	3-10
3.2.1.1 Materials Properties Data.....	3-10
3.2.1.2 Data on Liquid Metal Corrosion.....	3-11
3.2.1.3 Data on MHD Effects in Liquid Metals.....	3-14
3.2.2 Test Facilities.....	3-14
3.2.2.1 Corrosion Loops.....	3-14
3.2.2.2 LMMHD Loops.....	3-22
References for Section 3.2.....	3-26
3.3 Basic Measurements.....	3-28
3.4 Separate and Multiple Effects Experiments.....	3-29
3.4.1 MHD Flow Phenomena.....	3-32
3.4.1.1 Introduction.....	3-32
3.4.1.2 Scaling of MHD Flow Phenomena.....	3-34
3.4.1.3 Analysis of Minimum Test Requirements.....	3-36
3.4.1.4 Modeling Needs.....	3-46
3.4.1.5 Facility Requirements.....	3-47
References for Section 3.4.1.....	3-50
3.4.2 Heat Transfer.....	3-51
3.4.2.1 Testing Needs.....	3-51
3.4.2.2 Modeling Needs.....	3-52
3.4.2.3 Analysis and Scaling.....	3-52

TABLE OF CONTENTS (cont.)

3.4.2.4	Test Scenarios.....	3-58
3.4.2.5	Facility Descriptions.....	3-59
	References for Sectin 3.4.2.....	3-61
3.4.3	Materials Interactions and Mass Transfer.....	3-62
3.4.3.1	Testing Needs.....	3-62
3.4.3.2	Modeling Needs.....	3-69
3.4.3.3	Analysis and Scaling.....	3-71
3.4.3.4	Test Scenarios and Test Strategies.....	3-72
3.4.3.5	Facility Descriptions.....	3-75
	References for Section 3.4.3.....	3-81
3.4.4	Tritium Recovery.....	3-82
3.4.4.1	Testing Needs.....	3-82
3.4.4.2	Modeling Needs.....	3-82
3.4.4.3	Analysis and Scaling.....	3-85
3.4.4.4	Test Scenarios.....	3-86
3.4.4.5	Facility Descriptions.....	3-87
	References for Section 3.4.4.....	3-92
3.4.5	MHD Insulators.....	3-93
3.4.5.1	Introduction.....	3-94
3.4.5.2	Testing Needs for MHD Insulators.....	3-95
3.4.5.3	Test Scenarios.....	3-95
3.4.6	Electromagnetics.....	3-97
3.4.6.1	Testing Needs.....	3-97
3.4.6.2	Modeling Needs.....	3-99
3.4.6.3	Analysis and Scaling.....	3-100
3.4.6.4	Electromagnetics Test Facilities.....	3-107
	References for Section 3.4.6.....	3-109
3.4.7	Tritium Breeding.....	3-110
3.5	Partially Integrated Experiments.....	3-110
3.5.1	Non-Neutron TMIF.....	3-111
3.5.1.1	Purpose of TMTF and Its Role in the Test Plan.....	3-111
3.5.1.2	Test Scenarios.....	3-112
3.5.1.3	Facility Description.....	3-114

TABLE OF CONTENTS (cont.)

3.5.2	Characteristics of a Single PITF Non-Neutron Test Facility.....	3-114
3.6	Integrated Experiments.....	3-115
3.6.1	Purpose of Integrated Experiments.....	3-115
3.6.2	Data Requirements.....	3-116
3.7	Liquid Metal Blanket Facilities Costing.....	3-117
3.7.1	Methodology for FINESSE Costing.....	3-117
3.7.2	Groundrules for Estimates.....	3-121
3.7.3	Cost Data for the Liquid Metal Blanket Test Program.....	3-123
3.8	Summary of Testing and Model Development Needs.....	3-128
3.8.1	Thermal/Mechanical and Materials Compatibility Test Sequence.....	3-128
3.8.2	Tritium Recovery and Control Test Sequence.....	3-136
3.8.3	Tritium Breeding Test Sequence.....	3-137
3.8.4	Summary of Model Development Needs.....	3-137
3.A	Appendix: Materials Properties for Li and LiPb.....	3-139

LIST OF TABLES

<u>Figure</u>	<u>Page</u>
3.1-1	Major Device Parameters and Blanket Characteristics Considered....3-2
3.1-2	Levels of Integration and Types of Information Obtained from Experiments.....3-3
3.1-3	Characterization of Issues.....3-5
3.1-4	Generic Liquid Metal Blanket Issues.....3-5
3.2-1	Material Properties Available for LiPb.....3-10
3.2-2	Material Properties Unavailable for LiPb.....3-11
3.2-3	Summary of System and Material Conditions for Corrosion Data in Liquid Lithium.....3-12
3.2-4	Summary of System and Material Conditions for Corrosion Data in Liquid Lead - 17 at.% Lithium.....3-13
3.4-1	Separate and Multiple Effects Testing Issues.....3-30
3.4-2	Requirements for Non-nuclear Heat Transfer Tests of a Liquid Metal First Wall/Blanket.....3-57
3.4-3	Comparison of Parameters between Proposed Experiments and Actual Fusion Environment.....3-59
3.4-4	Comparison of Dimensionless Parameters between Proposed Experiments and Actual Fusion First Wall/Blanket.....3-60
3.4-5	Sequence and Schedule of Heat Transfer Experiments.....3-61
3.4-6	Major Characteristics of the MHD Heat Transfer Facility.....3-62
3.4-7	Materials Interactions Issues.....3-63
3.4-8	Materials Interactions Testing Needs.....3-66
3.4-9	Reactor Relevant Conditions Required for Testing of Heat, Mass, and Momentum Transport Issues.....3-72

LIST OF TABLES (cont.)

3.4-10	Types of Corrosion Facilities and Their Distinguishing Environmental Conditions.....	3-76
3.4-11	Shared Facilities Requirements for Most Corrosion Tests.....	3-77
3.4-12	Parameter Ranges for Tritium Recovery Systems.....	3-82
3.4-13	Some Operational Considerations for the Molten-Salt Extraction Process.....	3-88
3.4-14	Summary of Analytical Methods for Impurity Measurement.....	3-90
3.4-15	LiPb Tritium Recovery System Parameters.....	3-91
3.4-16	Issues for MHD Insulators.....	3-94
3.4-17	Evaluation of Ceramic Electrical Insulators for Liquid Metal Blankets.....	3-96
3.4-18	Electromagnetics Issues.....	3-98
3.4-19	Data for Evaluation of Time Constants.....	3-106
3.4-20	Scaling Relations for Electromagnetic Effects.....	3-107
3.4-21	Test Requirements for Electromagnetics Issues.....	3-108
3.4-22	FELIX Device Parameters.....	3-109
3.5-1	Comparison of Testing Goals.....	3-111
3.5-2	TMIF Proposed Testing Sequence.....	3-113
3.5-3	Parameter Range for TMIF.....	3-113
3.7-1	Key Liquid Metal Blanket Facilities Which Were Costed.....	3-117
3.7-2	Direct and Indirect Costs Associated with Experiments.....	3-119
3.7-3	Groundrules and Assumptions for Facilities Costing.....	3-122
3.7-4	Liquid Metal Blanket Facilities Costs.....	3-125
3.7-5	Capital Costs.....	3-126
3.7-6	Materials and Systems Costs.....	3-127
3.8-1	Principal Facility Characteristics for the Three Test Sequences.....	3-130

LIST OF TABLES (cont.)

3.8-2	Summary of Model Development Needs.....	3-138
3.A.1	General Properties of Lithium.....	3-139
3.A.2	Enthalpies (ΔH^0) and Free Energies (ΔG^0) for Various Lithium reactions at 25°C.....	3-140

LIST OF FIGURES

<u>Figure</u>	<u>Page</u>
3.1-1 Thermomechanical design window.....	3-7
3.1-2 Design window uncertainties.....	3-8
3.2-1 Hartmann number and interaction parameter ranges for proposed experiments.....	3-15
3.2-2 ANL Facility for fatigue testing in lithium.....	3-17
3.2-3 ANL LiPb loop.....	3-18
3.2-4 ORNL natural convection loop.....	3-19
3.2-5 Isometric diagram of BLIP loop.....	3-21
3.2-6 Experimental lithium system.....	3-23
3.2-7 Lithium loop at the University of Wisconsin.....	3-24
3.2-8 Schematic of facility for LMMHD experiments.....	3-25
3.4-1 Prototype ducting, showing regions for analyzing flow when Ha, N, and Re are large.....	3-37
3.4-2 Velocity profiles in parallel layer.....	3-39
3.4-3 Eddy current induced by nonuniform potential distribution in axial direction.....	3-40
3.4-4 Required parameter range for MHD pressure drop and fluid flow....	3-43
3.4-5 Required conditions for MHD flow tests with lithium.....	3-44
3.4-6 Required conditions for MHD flow tests with NaK.....	3-45
3.4-7 Required conditions for MHD flow tests with mercury.....	3-46
3.4-8 The effect of impurities on the DBTT of unalloyed vanadium.....	3-64
3.4-9 Flow diagram of the continuous tritium recovery process loop....	3-88
3.4-10 Conceptual design of the mixer/separator.....	3-89
3.4-11 Plasma-blanket equivalent circuit.....	3-100
3.4-12 Geometry for calculation of blanket time constants.....	3-101
3.4-13 Flat current distribution.....	3-104
3.4-14 Linear current distribution.....	3-104

LIST OF FIGURES (cont.)

3.4-15	Surface current distribution.....	3-104
3.4-16	Coupling of blanket flux to the plasma (shaded region indicates all of the flux passes through the core of the torus).....	3-105
3.7-1	The relationship of the costing task to the FINESSE process.....	3-118
3.8-1	Types of experiments and facilities for liquid metal blankets...	3-129
3.A-1	Heat capacity of lithium as a function of temperature.....	3-141
3.A-2	Enthalpy of lithium as a function of temperature.....	3-141
3.A-3	Thermal conductivity of lithium as a function of temperature....	3-141
3.A-4	Electrical resistivity of lithium as a function of temperature..	3-141
3.A-5	Surface tension of lithium as a function of temperature.....	3-142
3.A-6	Viscosity of lithium as a function of temperature.....	3-142
3.A-7	Vapor pressure of lithium as a function of temperature.....	3-142
3.A-8	Density of lithium as a function of temperature.....	3-142
3.A-9	Phase diagram of LiPb.....	3-143
3.A-10	Sievert's constants for solutions of hydrogen isotopes in liquid LiPb alloys.....	3-144
3.A-11	Activity coefficients for lithium and lead.....	3-146
3.A-12	Density and thermal expansion coefficient of LiPb at liquidus temperature.....	3-146
3.A-13	Electrical conductivity of LiPb.....	3-147
3.A-14	Electrical resistivity of LiPb at 800°C.....	3-147
3.A-15	Specific heat at constant pressure C_p of ^{17}Li - ^{83}Pb	3-148
3.A-16	Arrhenius plot of dissolution rate data for austenitic and ferritic steels exposed to flowing lithium.....	3-150
3.A-17	Arrhenius plot of dissolution rate data for austenitic and ferritic steels exposed to flowing Pb - ^{17}Li	3-151
3.A-18	The solubility of hydrogen in selected metals and alloys as a function of temperature.....	3-152

3. LIQUID METAL BLANKETS

3.1 Introduction

In order to assess the feasibility and attractiveness of fusion nuclear components, it is necessary first to characterize the environment in which they will operate and to provide at least general design features: for example, possible geometries, materials, etc. In the past several years, fusion reactors have become sufficiently well characterized to allow for detailed, self-consistent designs of nuclear components, including the blanket.

However, current designs of liquid metal blankets possess a large number of uncertainties, covering a wide range of technical disciplines. In many cases, the level of uncertainty is so great and the amount of data so small that a judgement on blanket feasibility cannot be confidently made at the present time. A large and comprehensive program of research and testing will be required in order to reasonably meet the goal of providing information to judge the feasibility and attractiveness of fusion reactor blankets. Using the reactor and blanket designs which are known today, the most critical uncertainties in blanket operation have been identified and possible scenarios for resolving these uncertainties have been examined.

The results and conclusions have been made as generic as possible. Nevertheless, in many cases it is necessary to adopt a specific design or set of designs for quantitative analysis. Throughout this study there are implicit and explicit assumptions regarding the blanket and its operating environment. This is true in the definition of the issues, in the evaluation of dimensionless ratios and properties, and in the choice of experiments. When specific parameters or design features are critical, the BCSS self-cooled lithium design with vanadium alloy structure^[1] and the MARS self-cooled LiPb design with ferritic steel structure^[2] are used. Reference values of the major device parameters are given in Table 3.1-1. Assumptions about the blanket operating environment can have as strong an impact on testing as the designs themselves.

3.1.1 Overview of Chapter 3

The major blanket issues are first surveyed in Section 3.1. The survey

Table 3.1-1. Major Device Parameters and Blanket Characteristics Considered

neutron wall load	5 MW/m ²
surface heat flux	0-1 MW/m ²
peak magnetic field in blanket	up to 7 T
flow path length	up to 9 m
blanket fluence lifetime	10-15 MW-yr/m ²
burn cycle	long burn and steady state
channel geometry	self-cooled geometries

is brief, since a more thorough study has already been completed^[3]. In addition, further details exist in the separate subsections of this chapter. In Section 3.2, existing data and experimental facilities are summarized in order to provide a frame of reference for the proposed new experiments. New testing needs are then considered and the key experiments are described in Sections 3.3-3.6.

The experiments are classified according to their level of integration. An increased level of integration corresponds roughly to increasing design detail and an increasing number of environmental conditions. The type of information obtained from an experiment depends strongly on the level of integration. Less integrated tests explore individual phenomena and verify detailed theoretical models. More highly integrated tests provide verification of global systems models and serve to partially validate component operation.

In FINESSE, five classes of tests have been defined, as shown in Table 3.1-2. Section 3.3 describes basic measurements, 3.4 describes single and multiple effects tests, 3.5 describes partially integrated tests, and 3.6 describes integrated tests. The experiments are described in enough detail to determine the major cost items and the nature of the information which will be obtained.

For blanket research and development, more emphasis has been placed on the required **testing** rather than required **theory**. It is acknowledged that a substantial theoretical and modeling effort will also be required to adequate-

ly resolve the issues. In general, experiments and theory go hand-in-hand: experiments are designed to validate theory, as well as to provide empirical information and for proof testing. Experiments act as more visible elements in the development program and amount to larger single expenditures. It is intended that more detailed analysis of theory needs will be performed in the future.

In order to minimize the cost of performing experiments, it is important to determine the essential parameters which affect the phenomena being explored and their relevant ranges. In some cases this requires detailed analysis to obtain appropriate scaling relations. We have attempted to provide a sound basis for the choices of sizes and parameter ranges for the proposed experiments. In some cases, the existing data are so scarce that scaling of design parameters is difficult.

Table 3.1-2. Levels of Integration and Types of Information
Obtained from Experiments

Basic Measurements	properties; no geometric effects
Separate Effects	phenomena exploration under individual environmental conditions; simple geometries
Mutiple Effects	phenomena exploration, multiple environments, more relevant geometries; semi-empirical
Partially Integrated	component/sub-system verification and empirical correlations with most environmental conditions
Integrated	component/sub-system verification under all environmental conditions; evaluation of reliability and failure modes

Having defined the testing needs and the minimum requirements for adequate testing, it is possible to define facilities and test scenarios. The facilities are defined by identifying the major elements, so that the general characteristics of the facilities can be understood and order of magnitude cost estimates can be made.

Section 3.7 contains rough cost estimates for the key experiments identified. Both capital costs and operating costs are treated, including staff requirements to operate the experiments and to analyze data. Finally, in Section 3.8, the experiments are considered together as constituting a complete test plan. Characteristics of test plans are discussed and several alternatives are given. These alternatives attempt to indicate the effect of cost constraints, number of design options, time constraints, and other aspects of the test plan. A method for evaluating test plans is presented such that the cost and benefit of different possible nuclear technology development pathways can be compared.

3.1.2 Summary of Critical Liquid Metal Blanket Issues

A testing issue is defined as an uncertainty which has a significant impact on blanket behavior. The significance of an issue is related to the level of uncertainty and the potential impact. Issues which have such a large impact on blanket design that their resolution could rule out the blanket on strictly technical grounds are called feasibility issues. The resolution of other, less serious issues may demonstrate that a particular blanket is economically or environmentally undesirable. These are known as attractiveness issues.

Table 3.1-3 summarizes the different types of issues. Generally, a feasibility issue is more important than an attractiveness issue, but in many cases the difference between feasibility and performance is only a matter of degree, such that a judgement on the nature of the issue is subjective. The testing issues have been described in great detail in previous work^[2] and are also summarized in Chapter 2. Table 3.1.4 reviews the broad categories of most critical issues, each of which contains many aspects, or sub-issues. These broad issues are described here to give a general understanding of the nature of the issues and their uncertainties. More detail can be found in the individual sections describing the experiments.

Table 3.1-3. Characterization of Issues

Feasibility Issues

- May Close the Design Window
- May Result in Unacceptable Safety Risk
- May Result in Unacceptable Reliability,
Availability, or Lifetime

Attractiveness Issues

- May Reduce System Performance
 - May Reduce Component Lifetime
 - May Increase System Cost
 - May Have Less Desirable Safety or
Environmental Implications
-

Table 3.1-4. Generic Liquid Metal Blanket Issues

1. MHD Effects
 - A. Pressure Drop and Pressure Stresses
 - B. Fluid Flow and Heat Transfer
 2. Materials Interactions (Corrosion)
 - A. Mass Transport
 - B. Structural Properties Degradation
 3. Tritium Control
 - A. Tritium Extraction from the Breeder
 - B. Tritium Transport in the Primary Cooling System
 4. Irradiation Effects on Material Properties
 5. Structural Response in the Fusion Environment
 6. Failure Modes
 7. DT Fuel Self-Sufficiency
-

In general, the magnetic field plays an important role in many aspects of liquid metal blanket operation. Because of its dominant influence on the velocity profiles, both heat transfer and mass transfer are strongly affected. Hence, thermal stresses, pressure stresses, and failure modes are all highly dependent on magnetohydrodynamic (MHD) effects. MHD provides a great deal of added uncertainties to problems which are either simple to describe or well studied in the absence of a magnetic field. The critical MHD uncertainties relate to pressure drop, fluid flow, and heat transfer in complex geometries.

Materials compatibility is a special problem for liquid metal blankets, both because of a general lack of data and because the design window can be strongly affected. Both lithium and LiPb are much more corrosive than sodium, which is relatively well-studied. Relatively low temperature limits due to dissolution of steel force us to explore advanced high temperature alloys, such as vanadium alloy, as well as innovative techniques for impurity control.

Tritium inventory control in liquid metal systems is generally easier to handle as compared to solid breeder blankets. The principal problem areas relate to efficient extraction from the breeder and adequate control over permeation. At present, the issue of tritium control in lithium blankets is not considered a feasibility issue. For $\text{Li}_{17}\text{Pb}_{83}$, the very low solubility leads to very high required extraction efficiency in order to maintain loss rates through the heat exchanger within acceptable limits. Effectiveness of tritium permeation barriers and double-walled piping are both important issues.

The mechanical response of liquid metal blankets is very complicated, owing to the complex loading conditions (MHD pressure stresses, thermal stresses, etc.) and to the effects of irradiation on the basic materials behavior. Irradiation swelling and creep, changes in ductility and other basic properties, helium embrittlement, and other irradiation effects are all important to a greater or lesser degree in the primary candidate structural alloys, which includes austenitic and ferritic steels, and refractory alloys. Modes of failure have been examined, but determination of unknown failure modes, failure rates and probabilities will require integrated testing.

The final issue listed in Table 3.1-4 is tritium breeding. The margin for tritium self-sufficiency is fairly high in self-cooled liquid metal blankets. This margin could be reduced in helium cooled designs and may

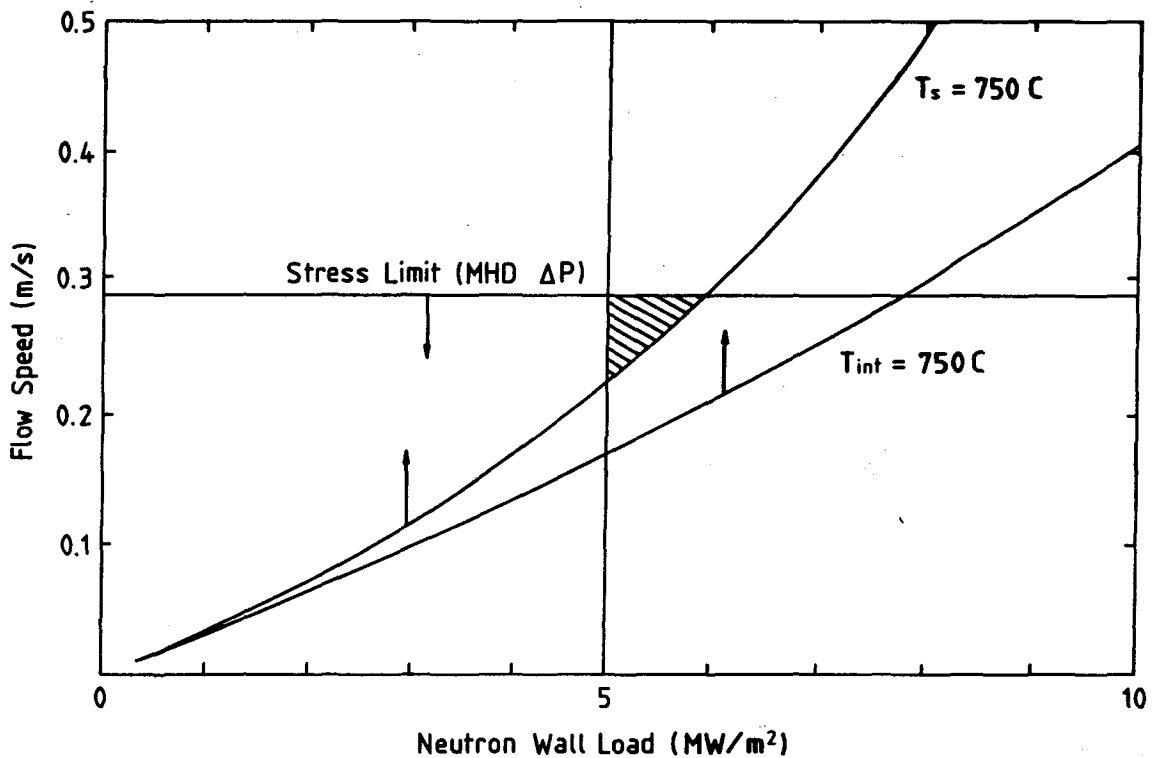


Figure 3.1-1. Thermomechanical design window

become critical if partial coverage is mandated by blanket cooling constraints.

The importance of feasibility issues is well characterized by the design window concept. An example of a design window is illustrated in Figure 3.1-1, which demonstrates the importance of heat transfer, fluid flow, corrosion, and pressure stresses in determining the feasibility of a self-cooled blanket with poloidal manifolds and toroidal first wall cooling channels. The MHD pressure drop is directly proportional to the velocity of the coolant. In the inboard blanket of the reference design ($B=7T$), the maximum allowable pressure stress under irradiation (105 MPa @150 dpa) limits the coolant velocity to approximately 30 cm/s.

Conflicting with this requirement is the need to adequately cool the structures in order to maintain temperatures below the limits imposed by corrosion mass transport and materials properties degradation at high tempera-

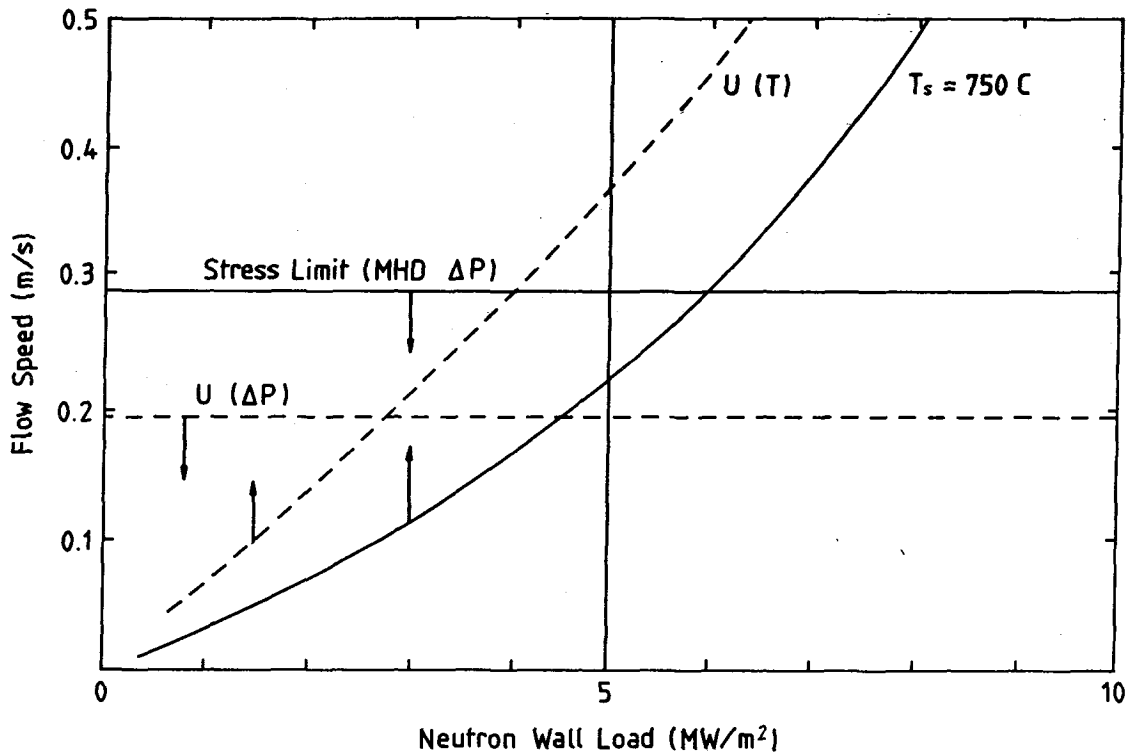


Figure 3.1-2. Design window uncertainties

ture under irradiation. For vanadium, the maximum interface and structure temperatures have both been recommended to be approximately 750°C (BCSS). (For steels, the interface temperature limit is generally lower than the structure temperature limit.) The minimum necessary flow velocity depends on the amount of energy deposited in the blanket, including both bulk heating and first wall surface heating. The heat source is roughly proportional to the neutron wall load, which must exceed a certain value governed by economic considerations. These simultaneous requirements present a very narrow design window, as indicated in Figure 3.1-1.

In Figure 3.1-2, the uncertainty in blanket behavior is plotted over the design window. The overall level of uncertainty in the temperature was estimated by assuming a 30% reduction in the heat transfer coefficient due to the effects of MHD velocity profiles. This also corresponds roughly to a reduced maximum allowable structure temperature of 650°C or a reduced maximum allowable interface temperature of 550°C. The overall level of uncertainty in

the pressure drop was estimated to be approximately 50%, due primarily to 3-dimensional MHD effects.

Any phenomenon for which the uncertainty is comparable in size to the design window is a critical feasibility issue. Therefore, MHD pressure drop, MHD fluid flow, corrosion, and materials properties under irradiation are all critical issues for the feasibility of liquid metal blankets. Tests have been identified for each of these in an attempt to reduce the uncertainties to sufficiently low values to allow for a confident determination of feasibility.

References for Section 3.1

1. D. L. Smith, et al., Blanket Comparison and Selection Study, Argonne National Laboratory, ANL/FPP-84-1, September 1984.
2. C. D. Henning, B. G. Logan, et al., "Mirror Advanced Reactor Study - Final Report," Lawrence Livermore National Laboratory, UCRL-53480 (1984).
3. M. A. Abdou, et al., "FINESSE: A Study of the Issues, Experiments, and Facilities for Fusion Nuclear Technology Research & Development (Interim Report)", UCLA, PPG-821, also UCLA-ENG-84-30 (1984).

3.2 Survey of Existing Data and Facilities

3.2.1 Survey of Existing Data

3.2.1.1 Materials Properties Data

The properties of lithium are well known, and have been assembled into the Materials Handbook for Fusion Energy Systems.^[1] Selected properties can also be found in the appendix to this chapter, including thermophysical and chemical data.

In contrast to lithium, there is a general lack of materials properties data of LiPb. Over the past two years, the material properties data base of ¹⁷Li-⁸³Pb has been built significantly, but much of the important information is still unavailable. Furthermore, the accuracies of the available data are uncertain. Those material properties which have been measured are listed in Table 3.2-1. The properties which have not been measured are listed in Table 3.2-2. For most cases, only a few scattered data points are available at best. The appendix contains data for the properties of LiPb which are known.

Table 3.2-1. Material Properties Available for LiPb

<u>Property</u>
● Phase Diagram
● Sievert's Constant
● Lithium Activity
● Density
● Thermal Expansion Coefficient
● Electrical Conductivity
● Vapor Pressure
● Neutronic Data
● Specific Heat < 300°C
● ΔH of melting

Table 3.2-2. Material Properties Unavailable for LiPb
(suggested design values are based on lead properties)

- Thermal Conductivity
 - Viscosity
 - Specific Heat > 300°C
 - Solubility of Iron, Nickel, etc.
 - Diffusivity of Tritium
 - ΔH of Reaction with Water
 - ΔH of Reaction with Air
-

3.2.1.2 Data on Liquid Metal Corrosion

Experimental data on the corrosion behavior of several austenitic and ferritic steels in liquid lithium and 17Li-83Pb environments have been obtained in static liquid-metal pots or capsules as well as in circulating systems such as thermal convection loops (TCLs) and forced-circulation loops (FCLs).²⁻²⁴ The experimental conditions for the corrosion data in liquid lithium and 17Li-83Pb are summarized in Tables 3.2-3 and -4, respectively. Relatively little data are available on corrosion in 17Li-83Pb environment. Recent experiments with static and circulating 17Li-83Pb indicate that the dissolution rates are substantially greater than those in lithium. In both environments austenitic stainless steels, e.g., Types 316 and 304 stainless steel and primary candidate alloy (PCA) develop a ferritic layer due to preferential depletion of nickel and to a lesser extent chromium from the surface; whereas, the ferritic steels, e.g., HT-9 alloy and Fe-9Cr-1Mo steel, show little or no surface degradation. Intergranular penetration of both ferritic and austenitic steels has been observed in lithium containing high (>1000 ppm) concentrations of nitrogen.

For most studies, the corrosion behavior has been evaluated in terms of weight loss per unit surface area and/or as depth of internal corrosive penetration. However, the rate of weight loss is expressed either as the average value for the entire time of exposure or as the steady-state value attained

Table 3.2-3. Summary of System and Material Conditions for Corrosion Data in Liquid Lithium

Lab. ^a	Ref.	Type ^b	Material	Velocity m/s	Impurity	Temperature °C	ΔT °C	Max. Time h	Material ^c	TMT ^d	Stress	Results ^e
ORNL	16-18	Capsule	316 SS, HT-9, 9 Cr	--	0, N < 175 ppm Li ₃ N Addition	400-700	--	10,000	Same	2 1/4	--	W, P
ORNL	19-24	TCL	316 SS, HT-9	0.03	0, N < 175 ppm	500-650	150	16,000	PCA, 316 SS, LRO	PCA	--	W/L, M, P
ORNL	25	TCL	Alloy 800	0.03	0, N < 175 ppm	500	175	3,000	Path B, Alloy 800	--	--	W, M
UW	26	FCL	316 SS	0.45-1.36	N=50-120 ppm O=275 ppm	440,490	110-195	4,000	Same	--	--	W/L
SU	27	FCL	304 SS	0.16-0.85	--	421-612	10-212	100	Same	--	--	W
ANL	28,29	FCL	304 SS	~0.03	N=50-250 ppm	427-482	70	5,000	316 SS, 304 L, PCA HT-9, 9 Cr	316 CW	Yes	W,P
WARD	30	FCL	Austenitic	1.82	--	538	150	1,000	316 SS, 304 SS 9 Cr	--	--	W/L
JAERI	31	TCL	--	0.03	--	600	100	2,500	316 SS	--	--	W
CSM	32,33	Pot	Armco Iron	--	N > 3000 ppm	565-592	--	135	Same	--	Yes	P
CSM	34	Pot	304 L	--	N > 1.2%	800	--	35	Same	--	--	P
ISPRA	35	Capsule	γ-Mn Steel	--	N=20 ppm	600	--	6,000	Same	--	--	P

^a ORNL - Oak Ridge National Laboratory
 UW - University of Wisconsin - Madison
 SU - Syracuse University
 ANL - Argonne National Laboratory
 WARD - Westinghouse Advanced Reactor Division
 JAERI - Japan Atomic Energy Research Institute
 CSM - Colorado School of Mines
 ISPRA - Commission of European Communities,
 Joint Research Centre

^b TCL - Thermal Convection Loop
 FCL - Forced Circulation Loop with Cold Trap Purification System

^c Materials other than the lithium system construction material are listed.

^d Materials tested in various thermomechanical conditions are listed.

^e W = weight loss in mg/m²-h.
 W/L = weight change as a function of loop position.
 P = depth of corrosive penetration.
 M = mass transfer/deposition.

Table 3.2-4. Summary of System and Material Conditions for Corrosion Data in Liquid Lead - 17 at.% Lithium

Lab. ^a	Ref.	Type ^b	System Conditions					Material Conditions			Results ^d
			Material	Velocity	Temp.	ΔT	Max. Time	Material	TMT ^c		
ORNL	36	Capsule	316 SS, HT-9	--	300-700	--	5,000	316 SS, HT-9	--	W, P	
ORNL	--	TCL	316 SS	0.03	500	150	4,000	316 SS, HT-9	--	W, P	
ANL	29	FCL	Carbon Steel/304 SS	0.03	427,454	150	3,500	316 SS, PCA, HT-9, 9 Cr	PCA 316 SS	W, P	
CSM	37	Pot	2 1/4 Cr	--	300-600	--	135	2 1/4 Cr	--	P	
ISPRA	38	Pot Capsule	Armco Iron 304 L	--	400-600 400	--	6,000 1,000	316 L 316 L	--	P P	

^a ORNL - Oak Ridge National Laboratory
 ANL - Argonne National Laboratory
 CSM - Colorado School of Mines
 ISPRA - Commission of European Communities, Joint Research Center

^b TCL - Thermal Convection Loop
 FCL - Forced Circulation Loop

^c Materials tested in various thermomechanical treatment are listed.

^d W - weight change in mg/m²-h
 P - depth of corrosive penetration

after the initial transient period of high dissolution rates. For austenitic stainless steels, the difference between the average and steady-state dissolution rates can be significant, particularly for long exposure times. Furthermore, the system parameters such as flow velocity, ΔT , surface area of the liquid-metal system, and liquid metal purity vary significantly for the various investigations. The existing experimental data are insufficient to accurately establish the influence of the different material and system parameters on the corrosion behavior of structural materials.

3.2.1.3 Data on MHD Effects in Liquid Metals

Recent studies indicate that local heat transfer and stress on structural members are critical issues for design. Those issues depend directly on MHD effects.

The theory for fully developed flow in circular and rectangular straight ducts is fairly well understood. Although experimental confirmation of the theory has been limited to the Hartmann Number of $M < 500$, the theory is expected to be valid to the reactor region of $M \sim 10^5$. The uncertainties of MHD are centered around three-dimensional effects. The three-dimensional effects can be caused by one or a combination of the following factors, all of which will probably be present in fusion reactors: (1) changing of B ; (2) changing of v ; (3) changing of fluid cross-section area; (4) changing of conductivity (thickness) of duct wall; and (5) interaction of eddy current.

The region of experimental data available and that required by fusion liquid metal blankets are shown in Fig. 3.2-1. The only three-dimensional data that include velocity profiles measurements have been obtained at the interaction number of $N \sim 1$ and $M \sim 10^2$, and in nonconducting ducts. No experiments have been performed with parameters and complicated configurations relevant for fusion reactor blankets.

3.2.2 Test Facilities

3.2.2.1 Corrosion Loops

There are six lithium or ^{17}Li - ^{83}Pb loops available in the U.S. These are capable of performing different functions.

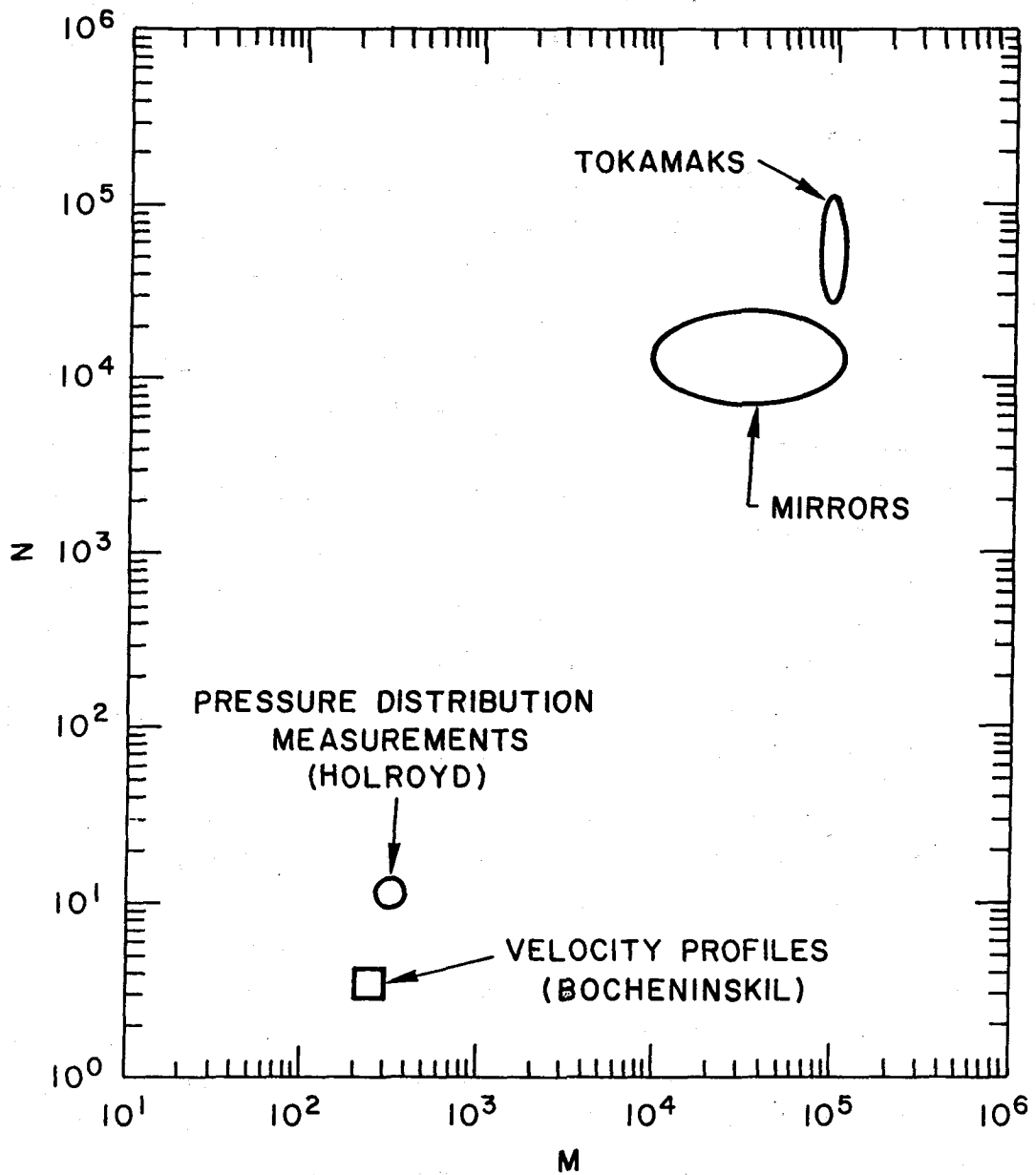


Figure 3.2-1. Hartmann number and interaction parameter ranges for proposed experiments

(a) ANL Loops

Two liquid metal loops are available at ANL. Both are forced-convection loops. The first is designed primarily for low-cycle fatigue tests in a flowing lithium environment of controlled purity. The second is designed to measure dissolution rate in flowing ^{17}Li - ^{83}Pb .

The facility for conducting fatigue tests in a flowing lithium environment consists of an MTS closed-loop servo-hydraulic fatigue machine with an associated forced-flow liquid lithium loop. A schematic diagram of the test facility is shown in Fig. 3.2-2. The lithium loop, which is constructed of Type 304 stainless steel, consists of three test vessels and a cold-trap purification system. The quantity of lithium in the loop was ~ 20 liters, and the lithium within the test vessel was recirculated at ~ 1 liter/min. The cold-trap temperature was maintained at ~ 480 K. Filtered lithium samples were obtained for analysis of nitrogen and carbon in lithium. The hydrogen concentration in lithium was established by equilibrating yttrium samples in lithium and using the reported data on the distribution of hydrogen between yttrium and lithium. During the fatigue tests, the concentration of carbon and hydrogen in lithium was ~ 8 and 120 wppm, respectively. The nitrogen concentration was maintained at ranges of 100-200, 500-700, or 1000-1500 wppm (designated low-, medium-, and high-nitrogen, respectively).

Corrosion tests were also conducted in a forced-circulation, ^{17}Li - ^{83}Pb loop consisting of a high-temperature test vessel with a heat-exchanger section and a cold leg. The eutectic alloy was prepared in a separate vessel and transferred into the loop. The total volume of the loop is ~ 2 liters. A schematic of the loop and the mixing vessel is shown in Fig. 3.2-3. Flat corrosion specimens, $\sim 70 \times 10 \times 0.3$ mm in size, of Type 316 stainless steel, prime candidate alloy (PCA), Fe-9Cr-1Mo steel, and HT-9 alloy were exposed to flowing ^{17}Li - ^{83}Pb at 727 and 700 K (454 and 427°C) for up to 3300 h. The specimens were periodically removed from the loop for weight-change measurements.

(b) ORNL Loop

The natural convection loop used by ORNL is shown in Fig. 3.2-4. The velocity of 2.5 cm/s is driven by a temperature difference of 150°C. The loop is designed to allow the coupons to be inserted and removed from the hot and

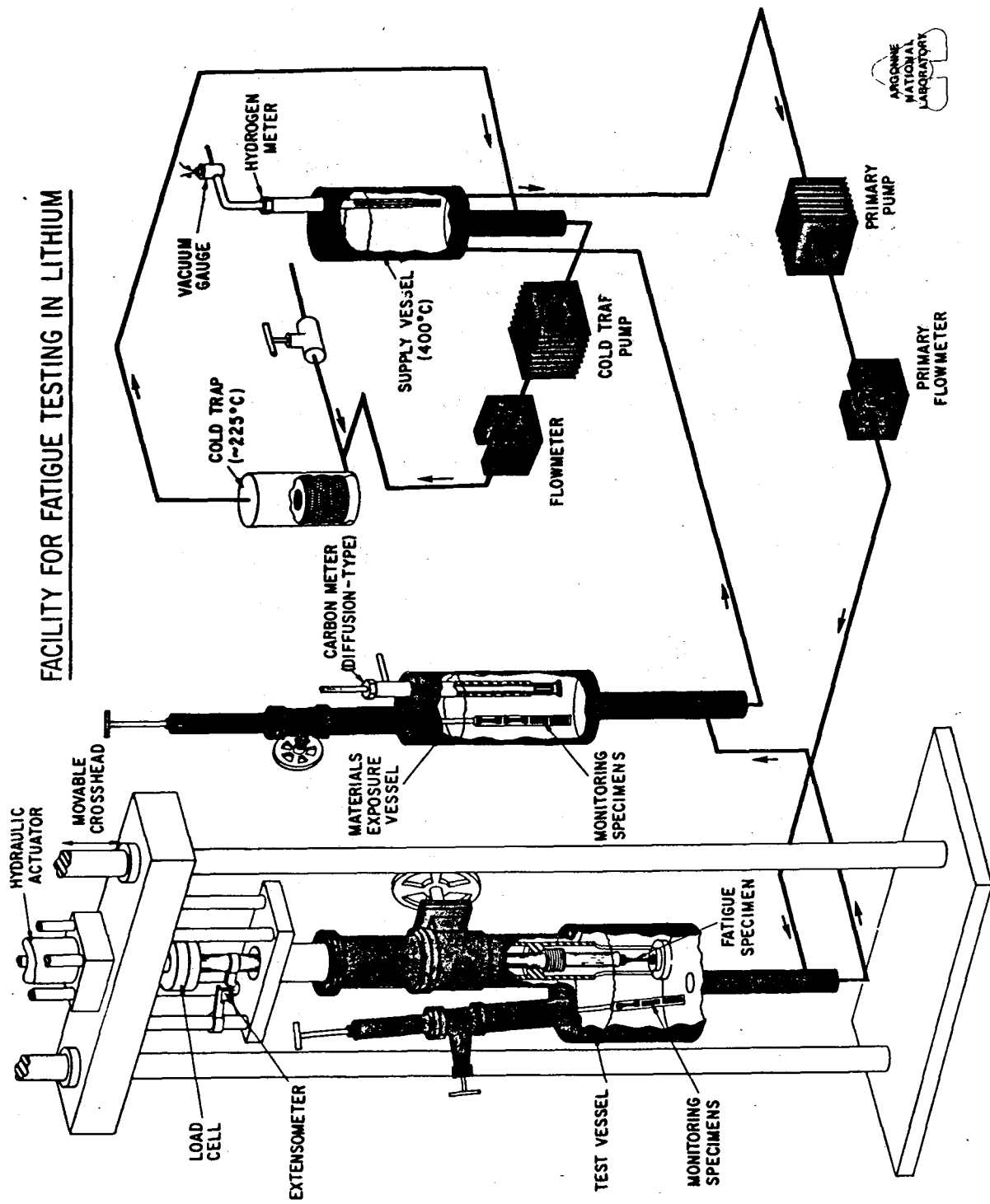


Figure 3.2-2. ANL facility for fatigue testing in lithium

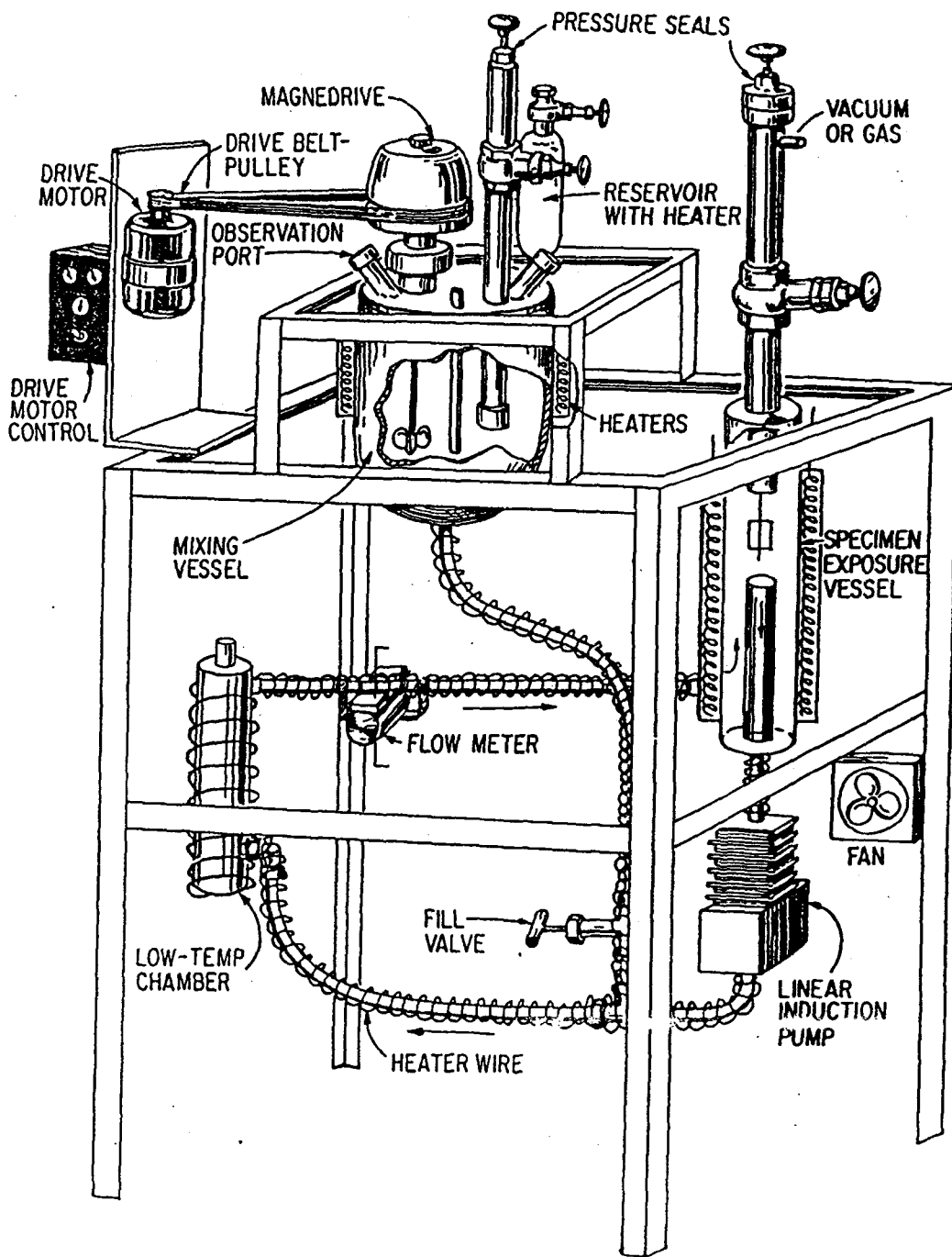


Figure 3.2-3. ANL LiPb loop

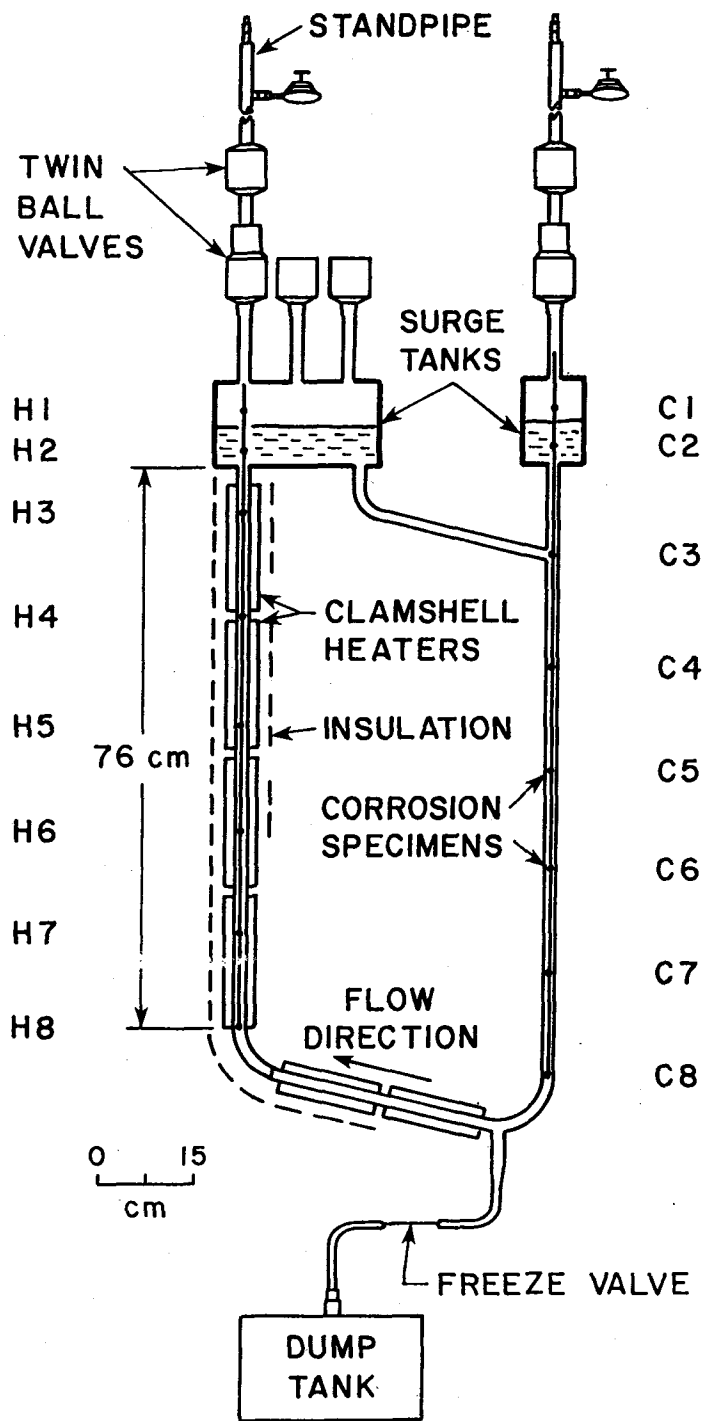


Figure 3.2-4. ORNL natural convection loop

cold legs without stopping the lithium flow. In this way specimen weight and microstructural changes can be measured as a function of exposure time. In addition, the location of specimens in both the hot and cold legs permits the measurement of any mass transfer tendencies. Samples of lithium for chemical analysis can also be taken without disrupting flow.

The lithium used in the loop was purified by cold trapping and subsequent heating at 815°C for 100 h in a titanium-lined pot containing zirconium foil.

Typical impurity concentrations of the purified lithium were 30 to 80 wt ppm of nitrogen and 30 to 130 wt ppm of oxygen as measured by a micro-Kjeldahl technique and neutron-activation analysis, respectively.

(c) Bimetallic Lithium-Pumped (BLIP) Loop of ETEC

The BLIP loop (Fig. 3.2-5) is a small, self-contained assembly mounted on a support skid. It was designed to provide a small-scale, experimental operating lithium loop for prototype testing of an electromagnetic pump, permanent magnet flowmeter, purification system plugging meter, bellows-seal globe valves, and analysis of dissimilar metal interactions. The loop was installed in the Static Sodium Test Facility of ETEC.

Construction of the skid-mounted BLIP loop was completed in 1979 and testing was initiated in FY-1981. The areas of major concern addressed by testing were:

- Efficiency of the isothermal purification tank.
- Operation of the electromagnetic pump, flowmeter, and plugging tank.
- Stability of carbides in 2-1/4 Cr-1Mo material.
- Extent of nitrogen absorption by stainless steel pipe.
- Migration of lithium into cover gas supply lines.

(d) Experimental Lithium System (ELS) Loop at Hanford

ELS contains 3800 liters of lithium in a stainless steel system, comprised of a main loop and a smaller chemistry loop. The main loop electromagnetic pump circulates lithium isothermally to 427°C, and flow rates to 38 liter/s through a jet-forming nozzle ("the target"). The chemistry loop has a cold trap, hot trap, plugging temperature indicator, sampling apparatus, and an impurity addition device. ELS is computer controlled and capable of con-

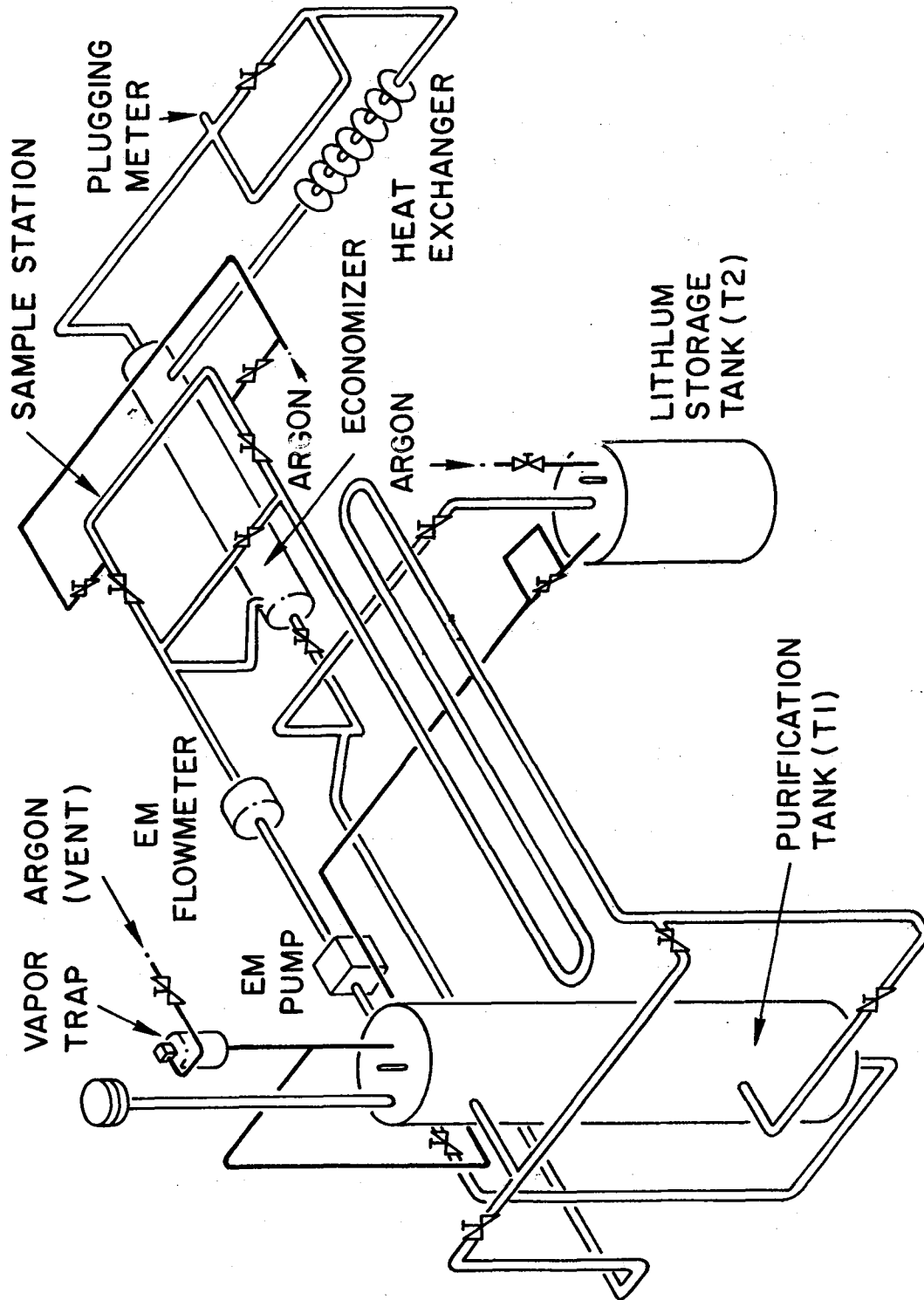


Figure 3.2-5. Isometric diagram of BLIP loop

tinuous unattended operation. A unique feature is the ability to operate with either argon cover gas or a vacuum at the free surfaces of the lithium.

An isometric view of the system is shown in Fig. 3.2-6. The main loop includes an Annular Linear Induction Pump (ALIP), throttle valve, EM flowmeter, target, surge tank, air-dump heat exchanger, and dump tank. The supply line from the pump to the target is a 10-cm (4-in.) Schedule 40 pipe, and the return line is a 15-cm (6-in.) Schedule 40 pipe. The target forms a lithium jet 10 cm wide and ~2 cm thick, with a velocity of 17 m/s. In FMIT the deuterium beam will continuously deposit 3-1/2 MW in a volume of ~5 cm³ within the jet.

A smaller insoluble side loop -- the chemistry loop -- circulates lithium through a stainless steel mesh cold trap, titanium foil hot trap, flow-through tube sampler, thief sample, and plugging temperature indicator (PTI). Characterization capability includes a resistivity meter for determining approximate lithium impurity concentrations. This side loop also has a section for testing small valves, orifices, and mechanical fittings.

(e) University of Wisconsin Lithium Loop

The flow loop, shown schematically in Fig. 3.2-7, is constructed entirely of Type 316 stainless steel. The loop is filled with "low sodium" natural lithium which was hot trapped with titanium at 600°C for one week and was then charged to the loop through a 7-micron stainless steel filter. High purity argon is used as a cover gas to protect the lithium from the atmosphere.

Four sets of coupons are tested simultaneously in parallel channels in an isothermal hot zone of the loop at a temperature up to 500°C. The 16 coupons in each test section are held together coaxially by split-tube stringers to form a continuous tubular assembly with the inner wall exposed to the lithium stream.

3.2.2.2 LMMHD Loops

In 1984, the U.S. D.O.E. Blanket Technology Program implemented experimental and analytical tasks in LMMHD. A facility is currently in preparation at Argonne National Laboratory and will consist of a NaK loop and two Tesla split-frame copper and iron magnets. Figure 3.2-8 shows a schematic of the

EXPERIMENTAL LITHIUM SYSTEM

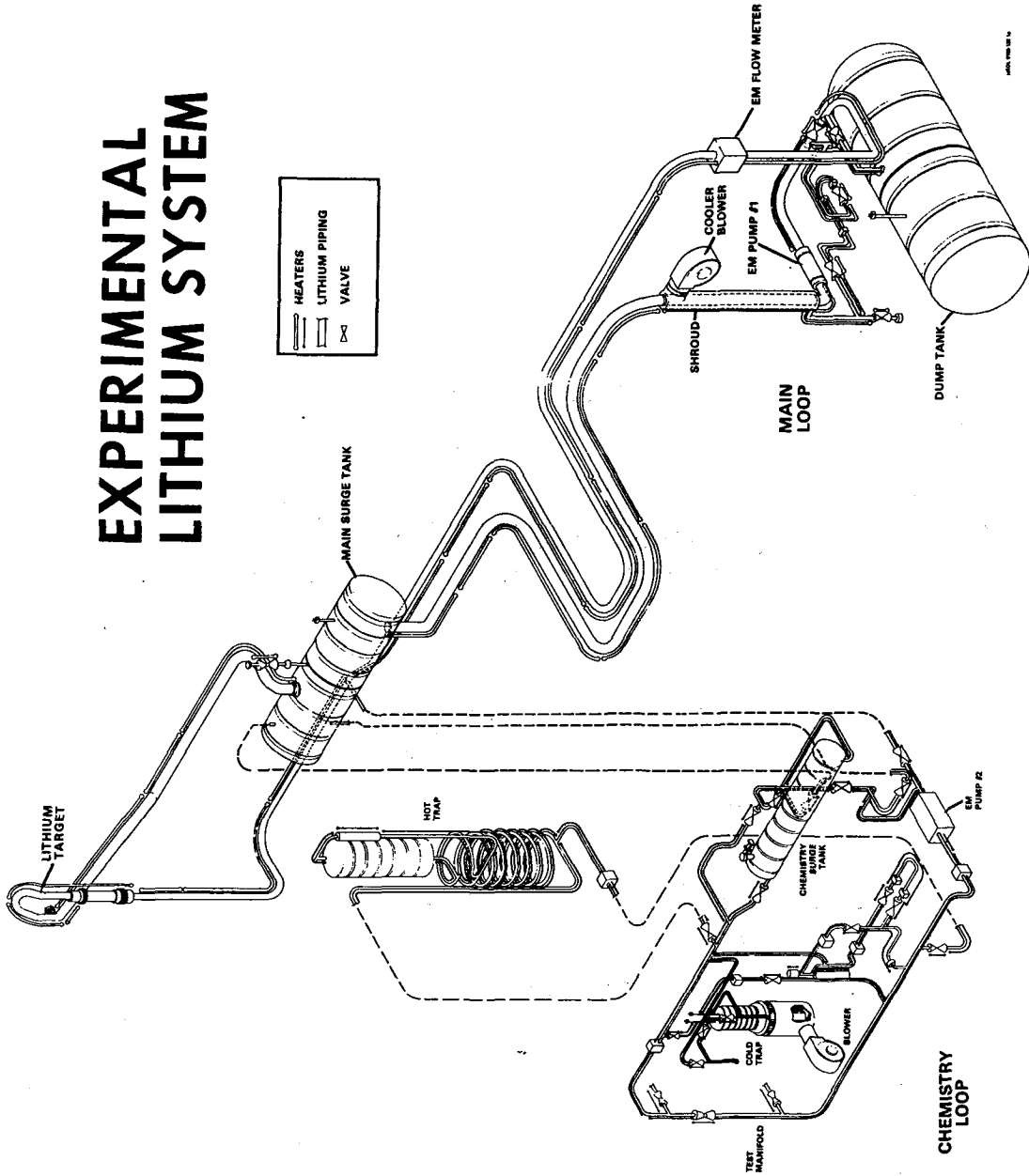


Figure 3.2-6. Experimental lithium system

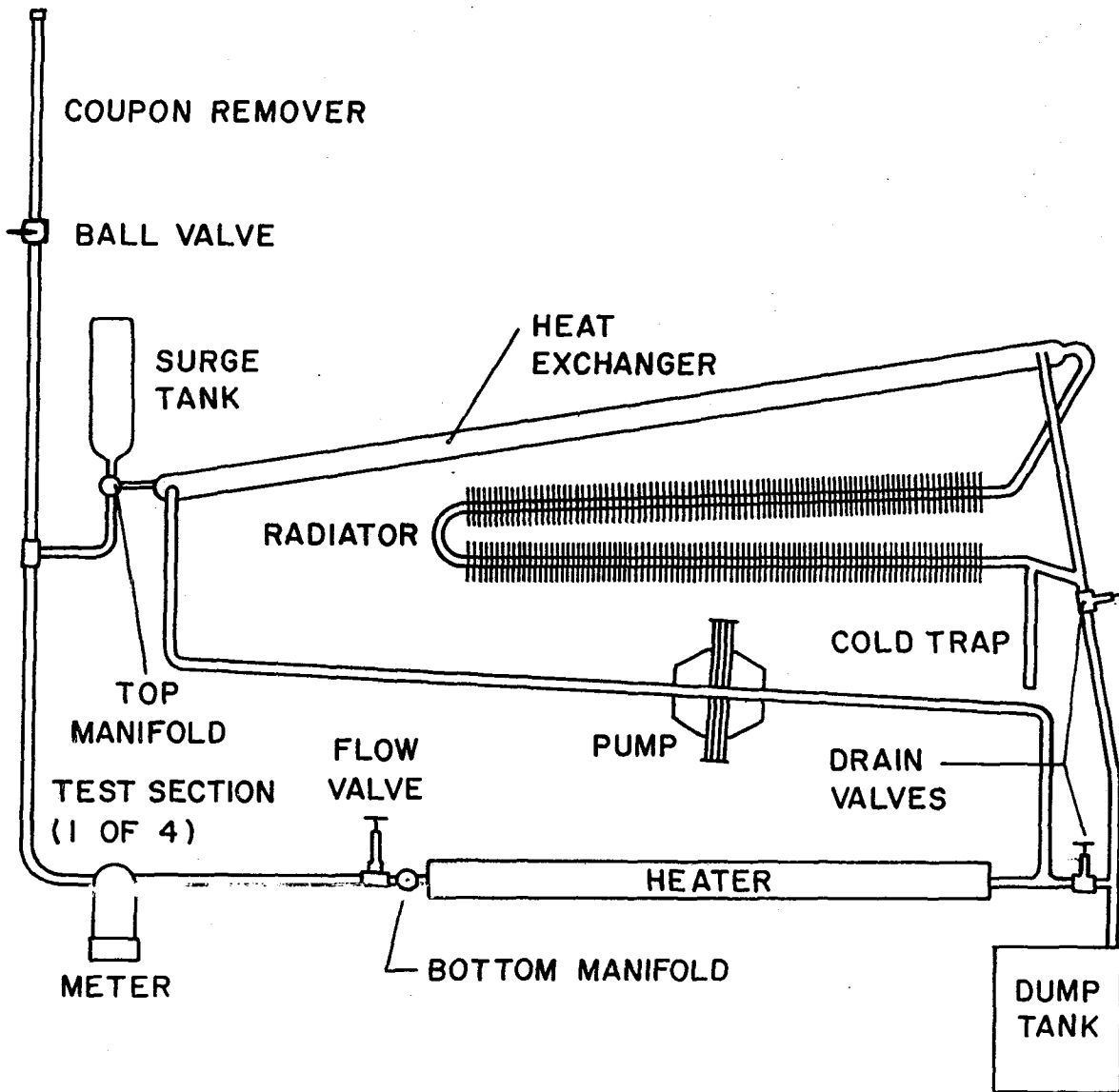


Figure 3.2-7. Lithium loop at the University of Wisconsin

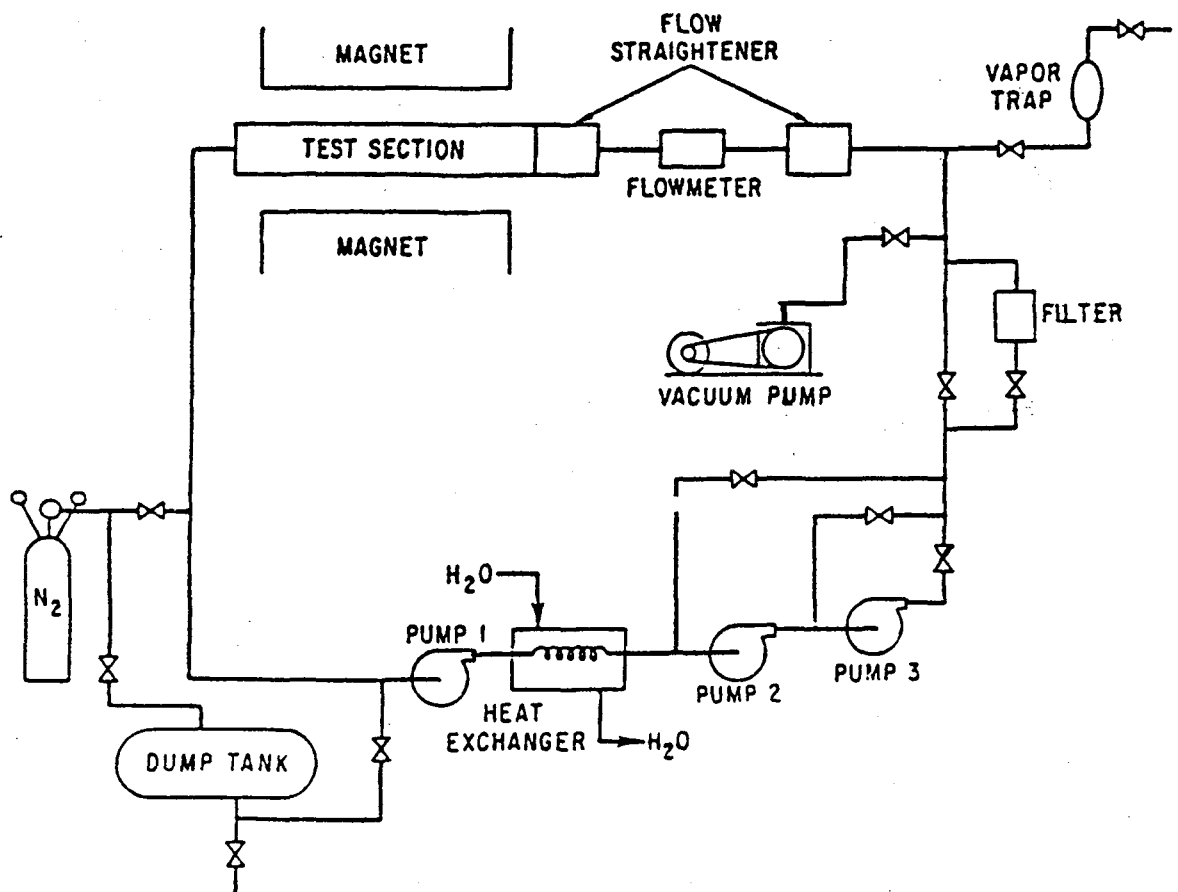


Figure 3.2-8. Schematic of facility for LMHD experiments

loop. The properties of NaK allow a good simulation of the liquid metals of interest for fusion (lithium or LiPb) under experimentally achievable conditions. NaK was favored over lithium or LiPb because operation at room temperature simplifies both the requirements for the loop and the instrumentation of the test assemblies. For example, epoxy-sealed components can be used and there is at least limited experience with hot film anemometry in NaK systems. NaK was selected over mercury because its thermophysical and electrical properties are much closer to lithium and its higher conductivity will permit magnetic interaction parameters about two orders of magnitude higher than mercury.

The facility will be completed early in 1985. General features of the loop are 300-400 gpm maximum flow, 50-100 gal of fluid volume (depends on test article), and 100-150 psi maximum pressure and magnet pole face 0.8×1.9 m with an 0.2-m separation.

Upgrading the magnet to 2.8 tesla by adding pole-face inserts and additional coils is an attractive future option. The MHD effects generally scale with the square of the field (B^2). For example, an increase from 2.0 to 2.8 Tesla would double the magnetic interaction parameters.

The loop and test articles will be instrumented to measure local pressure, flow, local velocities and voltages, and (electrical) currents.

References for Section 3.2

1. Materials Handbook for Fusion Energy Systems, Department of Energy Report, DOE/TIC-10122 (April 1980).
2. P. F. Tortorelli, J. H. DeVan, and J. E. Selle, "Effects of Nitrogen and Nitrogen Getters in Lithium on the Corrosion of Type 316 Stainless Steel," Preprint 114, NACE Corrosion/79, March 1979.
3. P. F. Tortorelli and J. H. DeVan, ADIP Quarterly Progress Report, September 30, 1979, U.S. Department of Energy Report DOE/ET-0058/7, pp. 162-169.
4. P. F. Tortorelli, J. H. DeVan, and R. M. Yonco, "Compatibility of Fe-Cr-Mo Alloys with Static Lithium", J. Mater. Energy Systems (to be issued).
5. P. F. Tortorelli and J. H. DeVan, J. Nucl. Mater. 85 & 86, 189 (1979).

6. P. F. Tortorelli, J. H. DeVan, and J. E. Selle, Proc. 2nd Intern. Conf. Liquid Metal Technology in Energy Production, U.S. Department of Energy Report CONF-800401-P2 (1980), pp. 13-44 through 13-54).
7. P. F. Tortorelli and J. H. DeVan, "Mass Transfer Deposits in Lithium - Type 316 Stainless Steel Thermal Convection Loops," Proc. 2nd Inter. Conf. Liquid Metal Technology in Energy Production, U.S. Department of Energy Report CONF-80040L-P2 (1980), pp. 13-55 through 13-63.
8. P. F. Tortorelli and J. H. DeVan, ADIP Semiannual Progress Report, March 31, 1982, U.S. Department of Energy Report DOE/ER-0045/8, pp. 482-490.
9. P. F. Tortorelli and J. H. DeVan, ADIP Semiannual Progress Report, March 31, 1983, U.S. Department of Energy.
10. P. F. Tortorelli and J. H. DeVan, "Corrosion of an Fe-12Cr-1Mo VM Steel in Thermally-Convective Lithium," Top. Conf. on Ferritic Alloys for Use in Nuclear Energy Technologies, Snowbird, June 19-23, 1983.
11. P. F. Tortorelli and J. H. DeVan, "Effect of Nickel Concentration on the Mass Transfer of Fe-Ni-Cr Alloys in Lithium," J. Nucl. Mater. 103 & 104, 633 (1981).
12. D. G. Bauer, et al., Proc. 2nd Intern. Conf. Liquid Metal Technology in Energy Production, U.S. Department of Energy Report CONF-800401-P2 (1980), pp. 13-73 through 13-81.
13. W. N. Gill, et al., AIChE J. 6, 139 (1960).
14. O. K. Chopra and D. L. Smith, ADIP Semiannual Progress Report, September 30, 1982, U.S. Department of Energy Report DOE/ER-0045/9, p. 309.
15. O. K. Chopra and D. L. Smith, ADIP Semiannual Progress Report, March 30, 1983.
16. G. A. Whitlow, et al., J. Nucl. Mater. 85 & 86, 283 (1979).
17. I. Nihei, et al., Japanese Atomic Energy Research Institute Report JAERI-M 5683 (1974).
18. W. Jordan, W. L. Bradley, and D. L. Olson, Nucl. Technol. 29, 209 (1976).
19. T. A. Whipple, et al., Nucl. Technol. 39, 75 (1978).
20. D. L. Olson, G. N. Reser, and D. K. Matlock, Corrosion (Houston) 36, 140 (1980).
21. E. Ruedl, et al., J. Nucl. Mater. 110, 28 (1982).
22. P. F. Tortorelli and J. H. DeVan, J. Mater. Energy Systems 4(2), 78 (1982).
23. B. D. Wilkinson, G. R. Edwards and N. J. Hoffman, J. Nucl. Mater. 103 & 104, 669 (1981).
24. V. Coen, et al., J. Nucl. Mater. 110, 108 (1982).

3.3 Basic Measurements

As discussed on Sec. 3.2, most of the basic information for lithium is available. An exception is the diffusivity of tritium in lithium, which may have a major impact on tritium recovery. There has been only one measurement and its accuracy is uncertain.

For ${}^{17}\text{Li}$ - ${}^{83}\text{Pb}$, the picture is completely different. Not only are many of the useful material properties not available, but the existing data cannot be confirmed either because there is only one measurement or the data are not consistent between different measurements. The total set of material data has to be carefully re-assessed and re-evaluated to ensure its accuracy. The set of material properties required include all of those given in Tables 3.2-1 and 3.2-2. The method to measure these properties is straightforward.

3.4 Separate and Multiple Effects Experiments

In this section, separate and multiple effects testing needs and associated modeling are reviewed for each class of issues. The important test conditions are considered, and scaling is explored to reduce the cost of obtaining the required information. From the testing needs, the required experiments and individual facilities are defined. The resolution of testing issues generally requires a combined program of modeling and experimentation. The ultimate goal is to develop and demonstrate the predictive capabilities needed to design blankets which can be shown with confidence to operate within acceptable safety margins.

For some issues, such as thermomechanical response and failure modes under irradiation, the safety margin can be small compared to the design requirements and the contributing uncertainties. There are many interrelated factors which determine the structural response, such as MHD-related loading conditions, materials behavior under irradiation, component fabrication technique, and even neighboring component interactions. Very integrated tests are required to satisfactorily resolve this issue.

For more specific issues, such as MHD pressure drop, the number of relevant environmental conditions is substantially less - in this case, primarily the magnetic field and geometry. It is possible that testing in separate and multiple effects non-neutron test stands alone can adequately resolve this sub-issue.

Separate and multiple effects testing are important for two reasons: first, they are the principal means to verify theory and modeling efforts to obtain predictive capabilities. Second, some of the largest uncertainties may be resolved under a limited number of environmental conditions. This allows for a cost effective means to screen candidate designs and demonstrate feasibility.

It is desirable to experimentally verify the performance of liquid metal blankets under actual reactor conditions, i.e., with reactor relevant dimensions, magnetic field strength, etc. However, it is expensive to perform experiments under full scale conditions. In separate and multiple effects testing, the number of unknowns (or variables) is generally small enough such that adequate information can be obtained under reduced test conditions. If

the conditions are reduced too much, phenomena in test stands may be quite different from those in a real blanket. In determining the size and parameter ranges of experiments, it is therefore important to explore the relevant phenomena involved and the allowed ranges of operation.

Table 3.4-1 shows the separate and multiple effects testing issues which are treated in this section. For each issue, the suggested testing scenario is defined. A test scenario considers several factors which define the usefulness of the experiments, including:

- a. required facilities
- b. the relationship between individual experiments
- c. the development requirements for executing the tests, for example, instrumentation, provision of bulk heating, etc.
- d. the relationship to theory and modeling efforts
- e. the relationship to other program elements, for example, PIC testing
- f. the nature of testing for different assumption of blanket materials and design choices
- g. different possible approaches to testing and model verification, for example, analytic, empirical, and semi-empirical methods

Generally, one or two "milestone" facilities exists for each class of issues. The features of these milestone facilities are described in sufficient detail to allow rough cost estimates and evaluation of the benefits of

Table 3.4-1. Separate and Multiple Effects Testing Issues

-
- MHD Pressure Drop
 - MHD Fluid Flow
 - Heat Transfer
 - Mass Transfer
 - Tritium Recovery
 - MHD Insulators
 - Electromagnetics
 - Tritium Breeding
-

the experiments. The major cost items, such as magnets, heaters, instrumentation, etc., and operation of the facility are described. In some cases, milestone experiments are already planned or in place.

3.4.1 MHD Flow Phenomena

3.4.1.1 Introduction

Magnetohydrodynamic (MHD) effects are recognized as being responsible for major feasibility issues for self-cooled liquid metal blankets. As a result, the design of liquid metal blankets is driven primarily by MHD considerations. The details of the designs, which seek to cool adequately the first wall, while maintaining acceptably low stresses in the pressure containing structure, depend strongly on the particular reactor parameters, most notably the neutron wall loading, the toroidal magnetic flux density, and the reactor linear dimensions. On the other hand, the geometry of the reactor imposes certain common features to all liquid metal designs. It is reasonable then to direct initial experimental and analytical investigations in MHD to such generic features and effects. The experience, data, and calculational tools obtained from such investigations will allow the development of advanced blanket designs on firmer footing than has heretofore been possible. The second round of testing can then be directed towards resolution of design issues peculiar to the advanced designs, and then finally towards designs concept verification.

Before proceeding with the development of modeling and testing needs, it is fruitful to review briefly the state of the art in MHD so that the proposed work can be put into proper perspective.

The details of any magnetohydrodynamic flow depend on the associated geometry and a number of non-dimensional parameters. These parameters, which arise naturally from the governing equations, are the magnetic Reynolds number, Re_m , the Hartmann number, M , the interaction parameter, N , and the wall conductance ratio, C . The governing equations are the Navier-Stokes equations, with the inclusion of a ponderomotive force, the conservation of mass equation, Maxwell's equations, and Ohm's law. Because in the fusion blanket environment $Re_m \ll 1$, the induced magnetic field is negligible and the problem is greatly simplified to one governed by the equations of conservation of mass, momentum, and electric charge, and Ohm's law. It is important to realize that our current inability to resolve all MHD-related issues does not result from ignorance of the basic governing laws and equations but from the difficulty of solving these equations for cases involving geometries other

than simple ones.

The general theory of flow of conducting liquids in strong magnetic fields and the exact solutions obtained so far have established the general features of such flows. The range of the parameters relevant to fusion, namely M and N larger than the order of 10^3 and C of the order of 10^{-2} or smaller, allow further simplification of the theory by placing the problems in the thin conducting wall regime. Also, in most cases, N is sufficiently large so that the non-linear inertia terms in the equations of motion can be neglected in the solution. In fact, after solutions are obtained, the neglected inertia terms are computed and the range of parameters for which such terms are indeed negligible is established. It is a fortunate coincidence that the regime of inertialess flow in thin conducting wall conduits is that which is of relevance to most fusion applications. In such a regime, the concept of characteristic surfaces, which can offer valuable qualitative information as to the character of the flow, has been established.

In summary then, the theory of inertialess flow in thin conducting wall conduits is firmly established and the general features of such flows are well understood. Based on such understanding, conceptual blanket designs can and have been developed.

Although the theory is well established, the fact remains that no firm experimental validation exists, mainly because of the difficulty of conducting experiments and obtaining local measurements in liquid metals, and the expense associated with large and powerful magnets. A rational approach to testing involving MHD-related issues would involve three steps.

a. Testing for well defined cases for which analytical solutions exist. Such testing will allow validation and increased confidence in the theory. Because analytical solutions exist for only a few cases, which do not cover the entire range of anticipated flow behavior, confining testing to these cases will not be an adequate validation of the theory. For this reason, this step should involve testing and a companion analytical effort aimed at obtaining solutions for a broad range of cases, which, although simple in geometry, are believed to encompass the range of flow phenomena relevant to fusion. This parallel approach is necessary so that analysis will guide and help plan the experiments, whereas the experimental results will provide information needed to validate and/or refine the analysis.

b. Testing for more complex cases for which analytical solutions are not feasible. The added understanding and experience gained in the first step should make it possible to arrive at a valid qualitative description of the flow phenomena in cases for which a detailed analytical solution is not possible. It is also hoped that such experience and understanding will allow the development of computer models for engineering computations of MHD flow under conditions of relevance to fusion. Testing will be aimed at validating such computational tools and/or obtaining quantitative experimental information.

c. Testing of blanket modules. Successful completion of the first two steps will enable the development of detailed blanket designs. If the resultant blanket module is more complex than the geometries explored in the first two steps, appropriate testing of the module should be carried out. Even for similar geometries, testing of a full scale blanket module, fabricated by prototypic fabrication methods, most likely will be deemed necessary.

3.4.1.2 Scaling of MHD Flow Phenomena

As explained in Section 3.4.1.1, the character of the MHD flow in a fusion blanket is determined by the magnitude of the Hartmann number, M , the interaction parameter, N , the wall conductance ratio, C , and the geometry. An experiment conducted for M , N , and C values identical to those in the blanket, and with the same geometry, will provide all the information needed to translate the results of the experiment to the prototypic blanket. Such experiments are not always practical because it is not possible to achieve prototypic M and N values without large and powerful superconducting magnets. Understanding of MHD flow phenomena, existing analyses and experimental data, and high interaction MHD flow theory can be used to relax testing requirements. For example, in fully developed laminar flows, the accelerations and the inertia terms are identically equal to zero. Therefore, the interaction parameter is irrelevant for testing of fully developed flows, provided it exceeds the rather low value required for suppression of turbulence.

The limited usefulness of achieving high prototypic values for the interaction parameter can be demonstrated by the following line of reasoning. The interaction parameter is a measure of the relative importance of the ponderomotive forces as compared to the inertia forces acting on a fluid

element. As N increases, the inertia terms become smaller. Beyond a certain value of N they become, for all practical purposes, negligible. Theoretical considerations can, for a given case, give an order of magnitude of N such that the "inertialess" regime has been reached. An experiment can verify this estimate and define it more accurately. Increasing N beyond this limit is pointless. A fluid cannot be more or less inertialess.

In general, the inertialess limit of interaction parameters depends on the case at hand, namely the geometry, the Hartmann number, and the conductance ratio. In most cases, the conditions at the blanket are expected to be such that the flow is inertialess there. The experiment should then be designed so that the estimated (by analysis) value of interaction parameter can be achieved. The precise value can be obtained experimentally by increasing the interaction parameter, with constant M and C , until an appropriate non-dimensional measured parameter (for instance, the non-dimensional pressure drop $\Delta p / \sigma V B^2 a$) does not vary with further increases in interaction parameter. In practical terms, this is achieved by varying the average velocity. Such a variation does not affect the Hartmann number.

As an example of this approach, consider the problem of a circular duct in the gradually varying transverse field that exists in the vicinity of the edge of a magnet pole face. Analytical solutions have been obtained^[1] for this problem for $1 \gg C \gg M^{-1}$ and $N \gg C^{-5/3}$, the latter condition being necessary for the inertialess regime. These conditions are evidently satisfied for the range of parameters of the fusion blanket. If testing of this case is required, all that is needed is that the above inequalities be satisfied. For an experimental test section with $C = 0.05$, the interaction parameter needs to be much larger than 150 and the Hartmann number needs to be much larger than 20. Clearly, a test with $M = N = 10^3$ will more than satisfy these conditions. Data from such a test can be used with confidence at the blanket conditions of M and N of 10^4 - 10^5 . The small possibility that as yet not known phenomena will become important and manifest themselves at M and N values higher than 10^3 cannot be strictly excluded. Such a possibility can be minimized by increasing, as much as practical, the M and N values for the testing. Indeed, this can be done with a variety of conducting fluids and reasonably sized conventional electromagnets with magnetic flux densities not in excess of the iron saturation value of about 2 T.

The aforementioned estimates of M and N values for adequate testing are not valid for all cases. A rectangular duct in the same fringing field will most likely require different values for M and N, as will the cases of abrupt variation of magnetic field, bends in planes normal to B, expansions and contractions, etc. It is because of this dependence of adequate testing values of M and N on the case at hand that it is important to carry on a parallel analytical effort to plan, conduct, and interpret the tests. For the same reason, it is important to plan the test program to include an adequately broad range of cases, so that a useful theoretical and experimental basis is formed. A basic repertoire of such cases should include uniform ducts of rectangular and circular cross sections in slowly and abruptly varying magnetic fields, rectangular and circular cross section bends in planes normal to the magnetic field, ducts with axially varying cross sectional areas, etc. Analyses for these cases either exist or can be developed. Testing of these cases will constitute the first step in the MHD test program referred to in Section 3.4.1.1. Scaling for each case will be developed as the analysis is carried out. Since experiments at M and N up to an order of 10^4 are possible, and this range is adjacent to the range of 10^4 - 10^5 in the blanket, it is expected that the scaling laws will be such that experimental results will be applicable to the blanket environment.

The second step of MHD testing will involve testing of configurations, e.g., manifolds, for which detailed analysis is not feasible. However, experience and knowledge gained during the first round of testing will be useful in establishing the qualitative features of the flow and the scaling laws. Again, since the range of 10^4 for M and N, which is easily achievable experimentally, is not too far from the prototypic range, meaningful results can be achieved.

3.4.1.3 Analysis of Minimum Test Requirements

Characteristics of MHD Flow in Blankets^[2]

a. Discrete Boundary and Shear Layers The three non-dimensional parameters mentioned above denote the ratios of forces acting on the liquid metal. The Reynolds number, Re , is the ratio of inertial force to viscous force. The interaction parameter, N , is the ratio of electromagnetic force to inertial

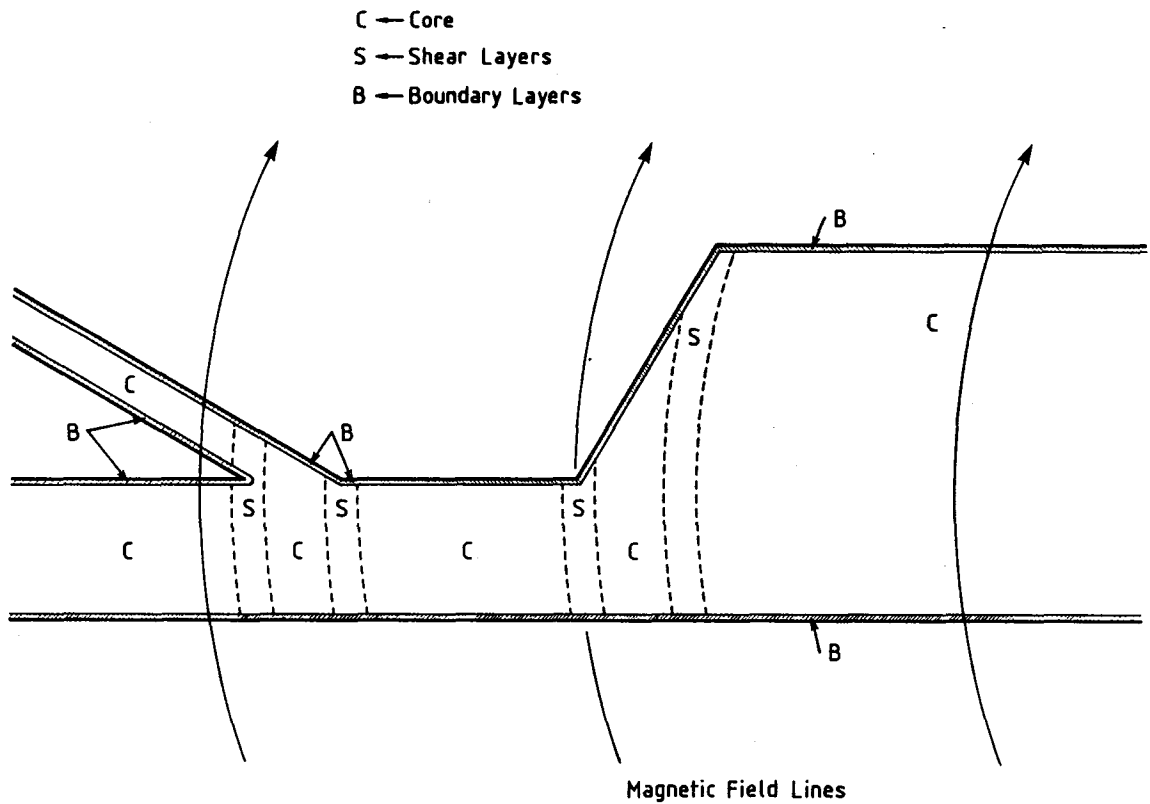


Figure 3.4-1. Prototype ducting, showing regions for analyzing the flow when Ha , N , and Re are large

force. And the Hartmann number, M , is the square root of the ratio of electromagnetic force to viscous force). In fusion reactor blankets, these parameters are usually very large.

$$Re \gg 1$$

$$N \gg 1$$

$$M \gg 1$$

(3.4-1)

Therefore, inertial and viscous forces are negligible compared with the electromagnetic force, except in boundary layers or shear layers, where large gradients and/or large velocities make them significant. Figure 3.4-1 shows these regions; inertial and viscous force free cores, boundary layers, and shear layers. The existence of discrete boundary and shear layers is a unique feature of MHD flow in fusion reactor blankets.

b. Boundary Layers In boundary layers, electromagnetic and viscous forces are both significant. Therefore, the Hartmann number is an important parameter. When the layer cuts magnetic field lines (perpendicular to the field), the boundary layer thickness δ is expressed as follows:

$$\frac{\delta}{a} \sim M^{-1} \quad (3.4-2)$$

where a is channel half width in the magnetic field direction. The thickness of boundary layers parallel to the field is greater, given by:

$$\frac{\delta}{a} \sim M^{-1/2} \quad (3.4-3)$$

Figure 3.4-2 shows the velocity profile in a layer parallel to the field. It can be seen that if the Hartmann number is larger than 100, as in a real blanket, a thin high velocity layer exists.

c. Shear Layers Abrupt changes in either the slope or electrical conductivity of any boundary surface leads to the development of large velocity gradients whose magnitudes are limited by the inertial and/or viscous forces. These discontinuities exist only in extremely thin layers - shear layers - which are parallel to the magnetic field. As long as there is flow normal to the layer, the inertial force balances with the electromagnetic force in fusion reactor blankets. The existence of discrete shear layers where the inertial force balances with the electromagnetic force requires:

$$Re > M^{1/2}, \quad (3.4-4)$$

where the shear layer thickness δ is expressed as follows:

$$\frac{\delta}{a} \sim N^{-1/3} \quad (3.4-5)$$

d. Thin Conducting Wall The ratio of wall thickness to channel half width multiplied by the conductivity ratio of the wall to the fluid is named the wall conductance ratio. The MHD pressure drop in a straight channel is usually proportional to the wall conductance ratio, C , as long as the following relation holds:

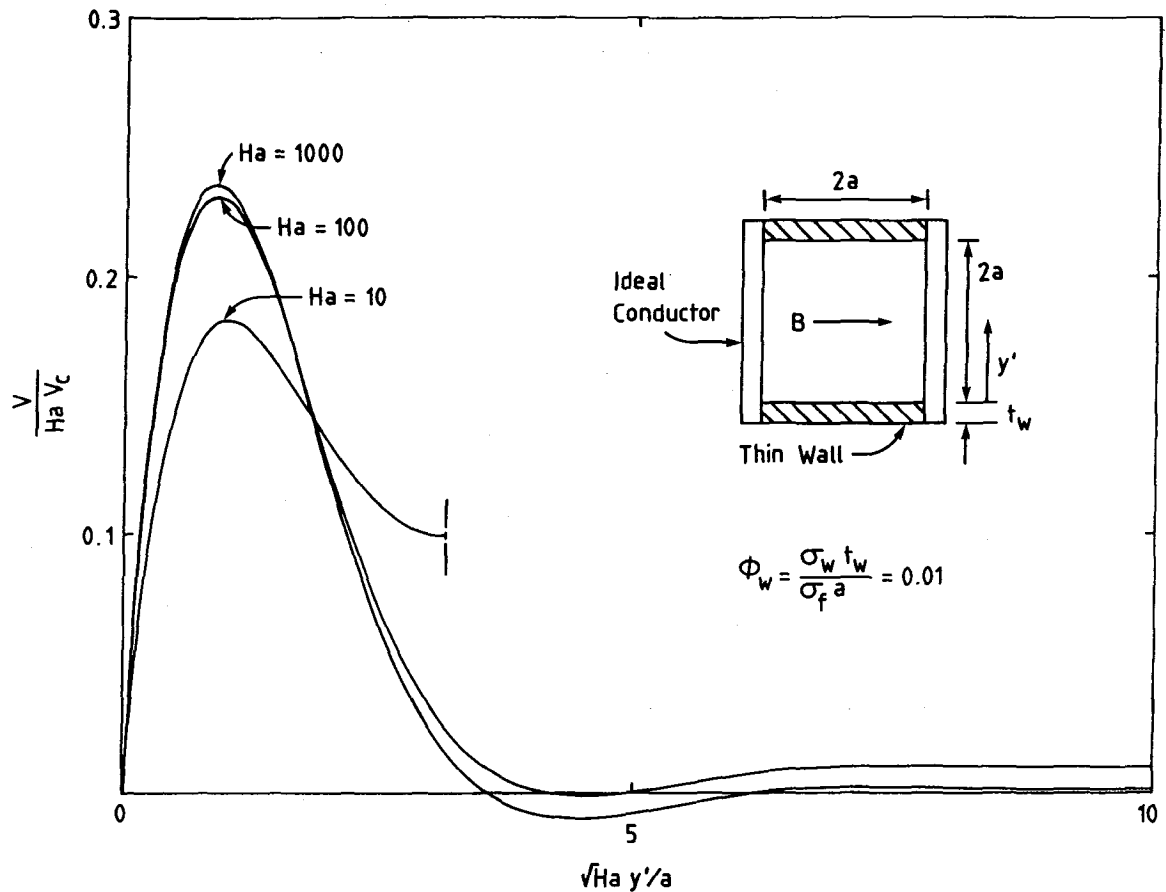


Figure 3.4-2. Velocity profiles in parallel layers

$$M^{-1} < C \ll 1 \quad (3.4-6)$$

In a fusion reactor blanket, C usually satisfies the thin conducting wall condition.

e. Flow Development Subject to Recirculating Current Spatial changes in boundary conditions of either flow or magnetic field generate currents in a plane perpendicular to the magnetic field as shown in Fig. 3.4-3. In a liquid metal blanket, it is not the inertia of the fluid but the recirculating current which affects the flow development. The recirculating current is considered to extend over the length l_e of the channel, where l_e is given by:

$$\frac{l_e}{a} \sim C^{-1/2} \quad (3.4-7)$$

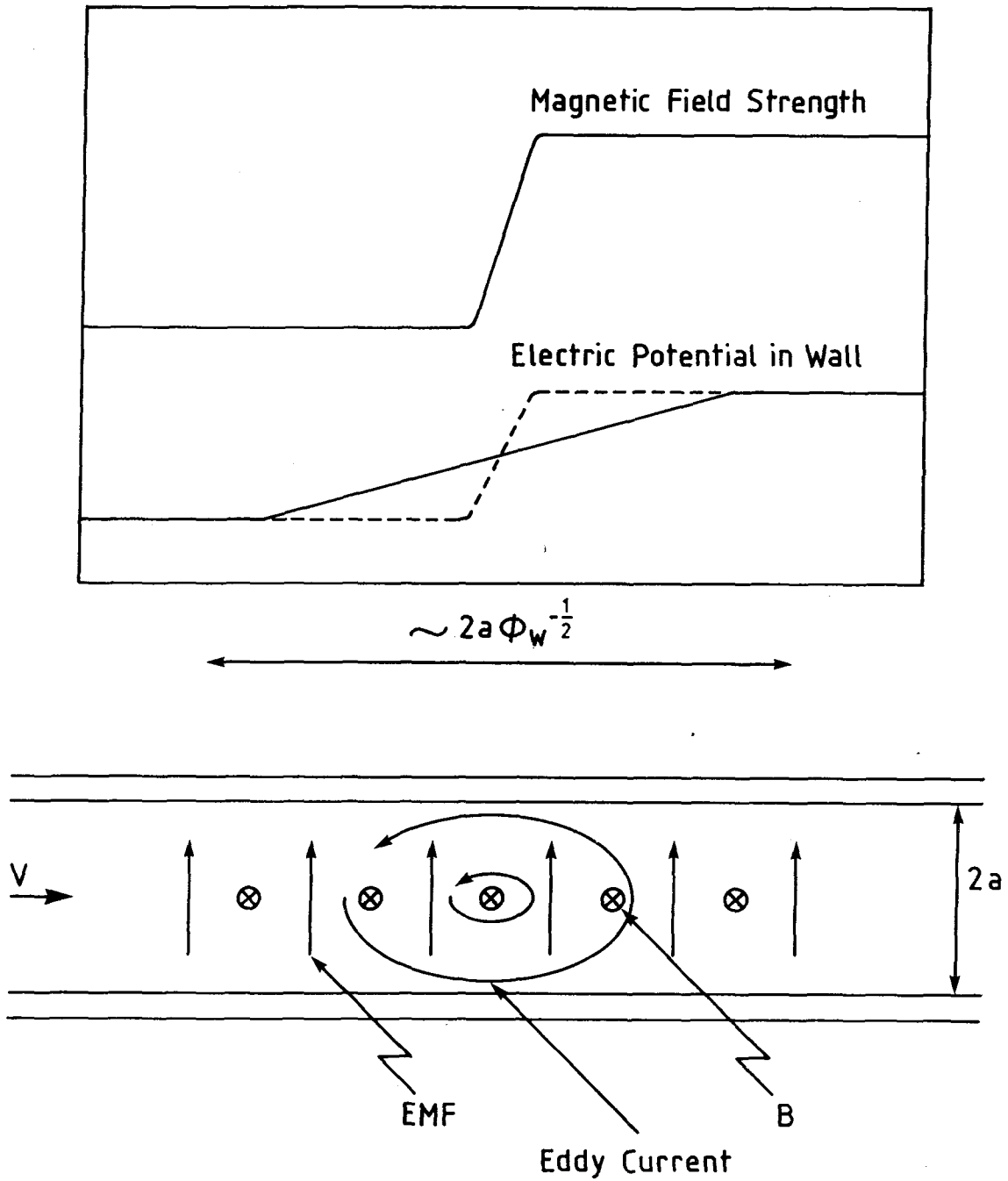


Figure 3.4-3. Eddy current induced by nonuniform potential distribution in axial direction

as long as equation (3.4-6) is valid. Usually, channels are longer than l_e in fusion reactor blankets.

f. Suppression of Turbulence^[3] Since electromagnetic forces tend to suppress turbulence, flow in a liquid metal blanket is considered to be laminar. The transition Reynolds number under parallel field is expressed by equation 3.4-8 while that under transverse field is expressed by equation 3.4-9.

$$Re_t \sim 60 M \quad (3.4-8)$$

$$Re_t \sim 500 M \quad (3.4-9)$$

Experiments at relatively low values of M and N indicate a small level of residual turbulence (1-2%) sometimes exists inside the magnetic field. It has recently been suggested that larger fluctuations can be generated by discontinuities in the flow path, even at very high M and N values.⁴ The existence and level of turbulence at high magnetic field requires further experimental and theoretical verification.

g. Small Magnetic Reynolds Number The magnetic Reynolds number Re_m denotes the ratio of induced magnetic field strength to applied field strength. It is usually far smaller than unity in real blankets.

h. Leakage Current Effects^[5] When a channel is insulated from the remainder of the blanket, the induced currents cannot leak from the channel. But usually channels are not insulated in current fusion blankets designs. As long as there is an electric potential difference between adjacent channels, eddy currents cross the channels. The leakage currents not only affect the MHD pressure drop but also affect the velocity profile. MHD flow behavior in a channel depends on the characteristics of eddy current circuit, which may pass through the whole blanket.

Minimum Requirements - Non-Dimensional Parameter Ranges

It is desirable to build experiments with the same conditions as real blankets. However, it is usually expensive because it requires a large test section and strong magnetic field.

In the event that the exact conditions cannot be simulated, it is most important to provide that the important non-dimensional parameters, such as the Hartmann number, are all preserved. But preservation of all of the relevant non-dimensional parameters is not easy. In order to preserve the Hartmann number, the product of channel width and magnetic field strength must be kept constant. Both of them cannot be reduced.

It is possible to obtain enough information from experiments with reduced non-dimensional parameters as long as the phenomena in test stands are similar to those in real blankets. For example, if the Hartmann number is reduced, the peak velocity in a wall jet is reduced as can be seen in Fig. 3.4-2. There is a certain relation between the peak velocity and the Hartmann number. If the relation is obtained under reduced conditions, the peak velocity in a real blanket can be extrapolated. However, there is a limit to the degree to which extrapolation is possible. If the Hartmann number is reduced excessively, the wall jet disappears. It is obvious that the jet behavior in blankets cannot be extrapolated from the results without wall jets.

Experiments must be made in the parameter ranges where the phenomena are essentially the same as in blankets. In the following, the minimum required parameter ranges are discussed.

Figure 3.4-4 shows the proposed parameter ranges required for MHD fluid flow tests. An interaction parameter of more than 1000 is required to keep the shear layer thickness sufficiently thin. The value of $Re/M^{1/2}$ should be larger than 10. If it is smaller, then the electromagnetic force balances not with inertial forces but with viscous forces in shear layers, and the phenomena in the layers are different from those in blankets. The Reynolds number should be smaller than $60 M$ so that the turbulence is suppressed regardless of angle between flow and field directions.

When the above conditions of $N > 1000$, $Re/M^{1/2} > 10$ and $Re < 60 M$ are satisfied, the Hartmann number is inevitably larger than 464, hence boundary layers are sufficiently thin.

The thin wall channel condition must be preserved in experiments. The ratio of channel length L to entry length l_e must not be changed excessively. These requirements are easily satisfied by preserving aspect ratios of the channel. However, it is not always necessary to preserve the ratios. They

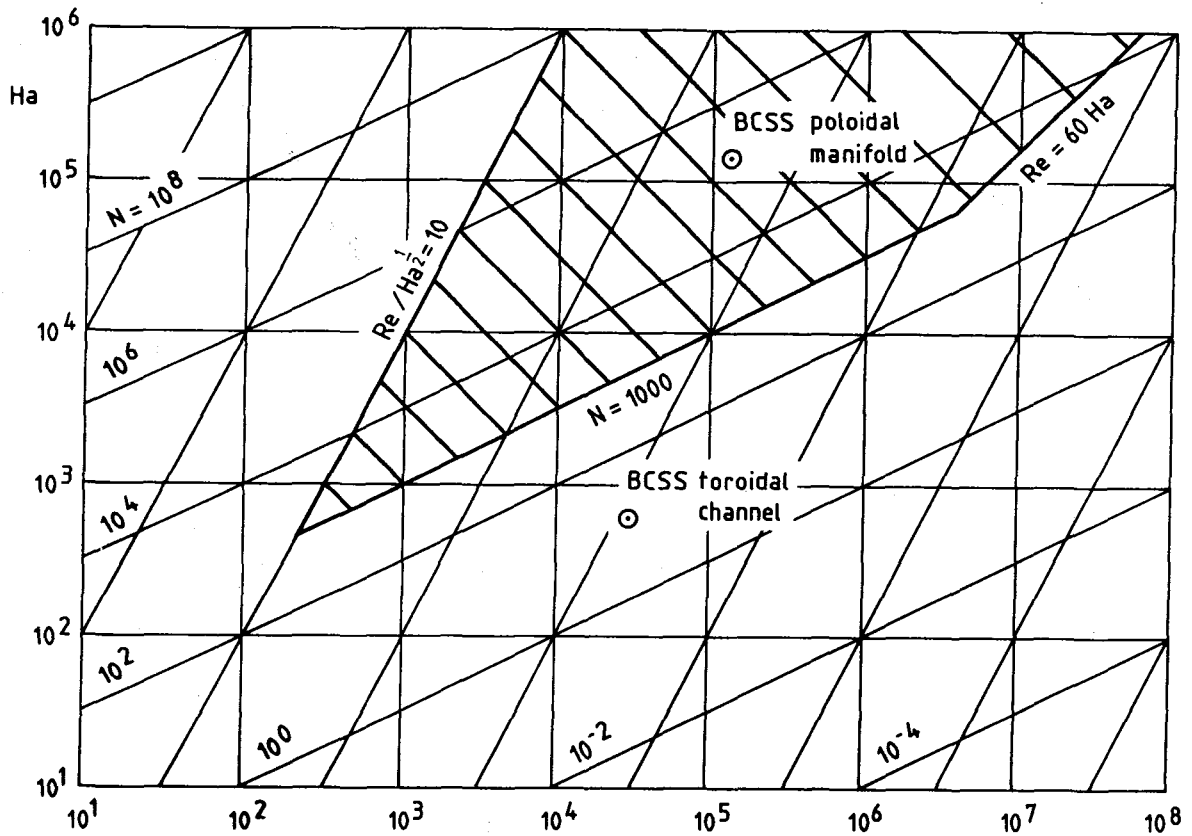


Figure 3.4-4. Required parameter range for MHD pressure drop and fluid flow

can be changed by factors, but changes by orders of magnitude are not recommended.

The aspect ratios should not be changed excessively from the viewpoint of leakage current effects. But the requirements from the viewpoint of leakage current are so severe that they cannot always be satisfied. Complete verification of the effects requires a model including an entire blanket component. This type of testing should be done using partially integrated test facilities. In single effect experiments, a single channel may be used except for special purposes.

Other Restrictions

Experiments with both a strong magnetic field and a large test section

are expensive to construct. Magnetic field strength should be reduced as much as possible. However, channel width cannot be reduced excessively, since measurements in very small channels are difficult. There is a certain range of channel width for which the experiment is effective. Measurability defines the lower limit of flow velocity. The limit depends on the measuring technique. Excessively high velocity is undesirable because it induces high MHD pressure drop which requires a large pump and strong channel walls.

Figure 3.4-5 shows the required condition of experiments with lithium plotted in a velocity vs. field strength plane. Since the non-dimensional parameters are functions of channel size, a , the required magnetic field strength and velocity ranges change with a . There is a trade-off between the field strength and the channel size. If a large channel is used, the field strength need not be very high. If a small channel is used, the field must be high.

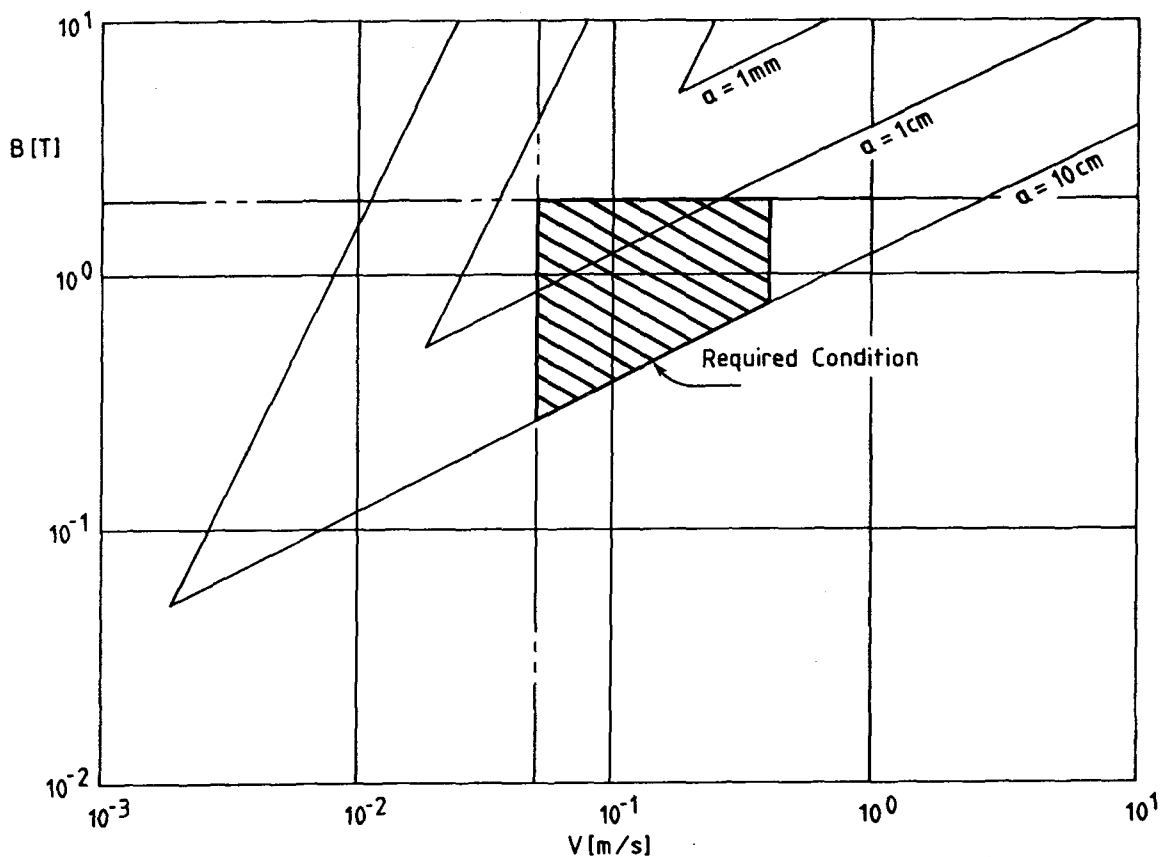


Figure 3.4-5. Required conditions for MHD flow tests with lithium

A magnetic field strength of about 2 T is considered to be the upper limit for use of normally conducting magnets. Channel half width of 1 cm ~ 10 cm is considered to be reasonable. From the viewpoint of measurement, flow velocity should be higher than 5 cm/s. It is not necessary to be higher than the velocity in a real blanket. Two types of testing condition are recommended: $B \sim 0.5$ T, $a \sim 10$ cm $V \sim 10$ cm/s and $B \sim 2$ T, $a \sim 1$ cm, $V \sim 10$ cm/s.

Experimentally required conditions for experiments with other liquid metal as a working fluid are different from that with lithium, since the properties are different. Figures 3.4-6 and 3.4-7 show the required conditions when NaK and mercury are used in experiments. Since the properties of NaK are not widely different from those of lithium, the requirements differ from those in lithium experiments only by a small factor. If other conditions are the same, magnetic field in NaK experiments should be about 50% higher than in lithium experiments. The properties of mercury are quite different.

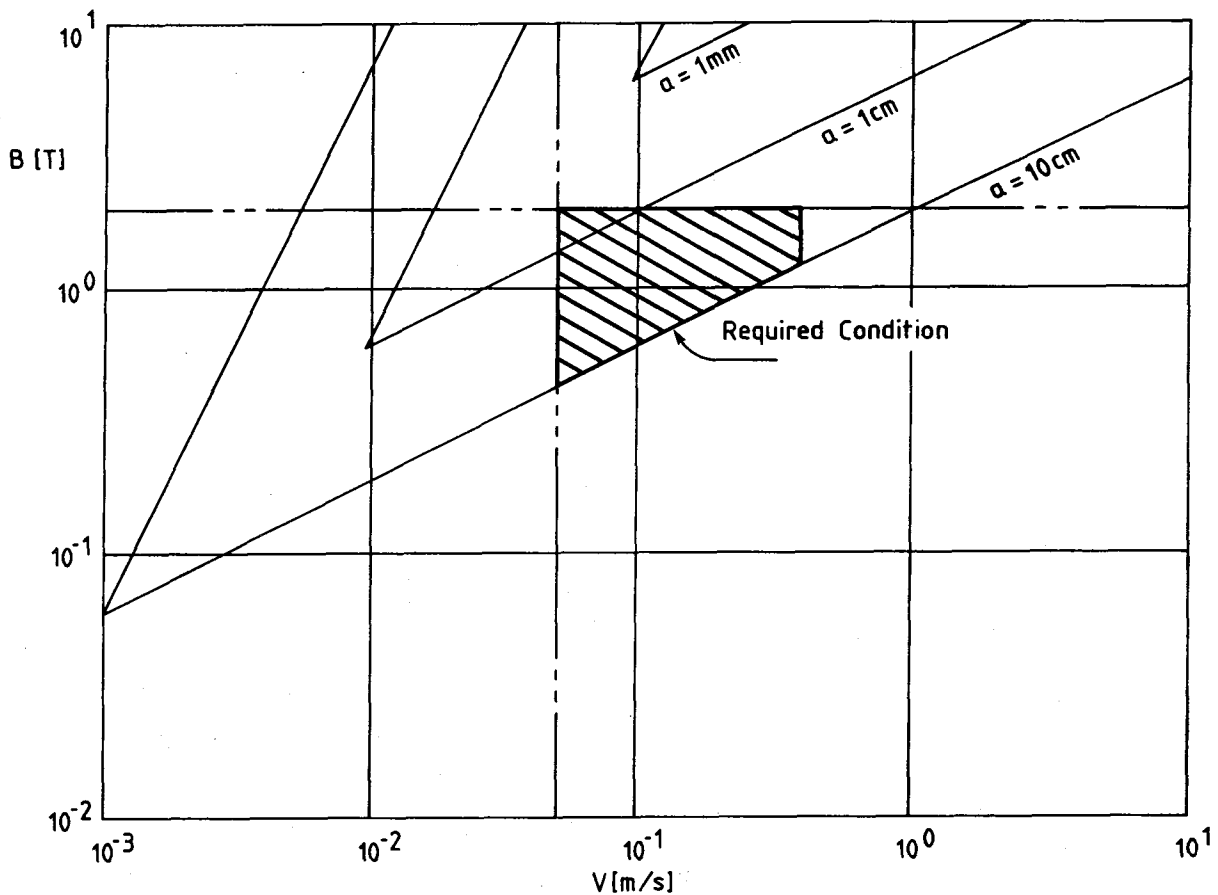


Figure 3.4-6. Required conditions for MHD flow tests with NaK

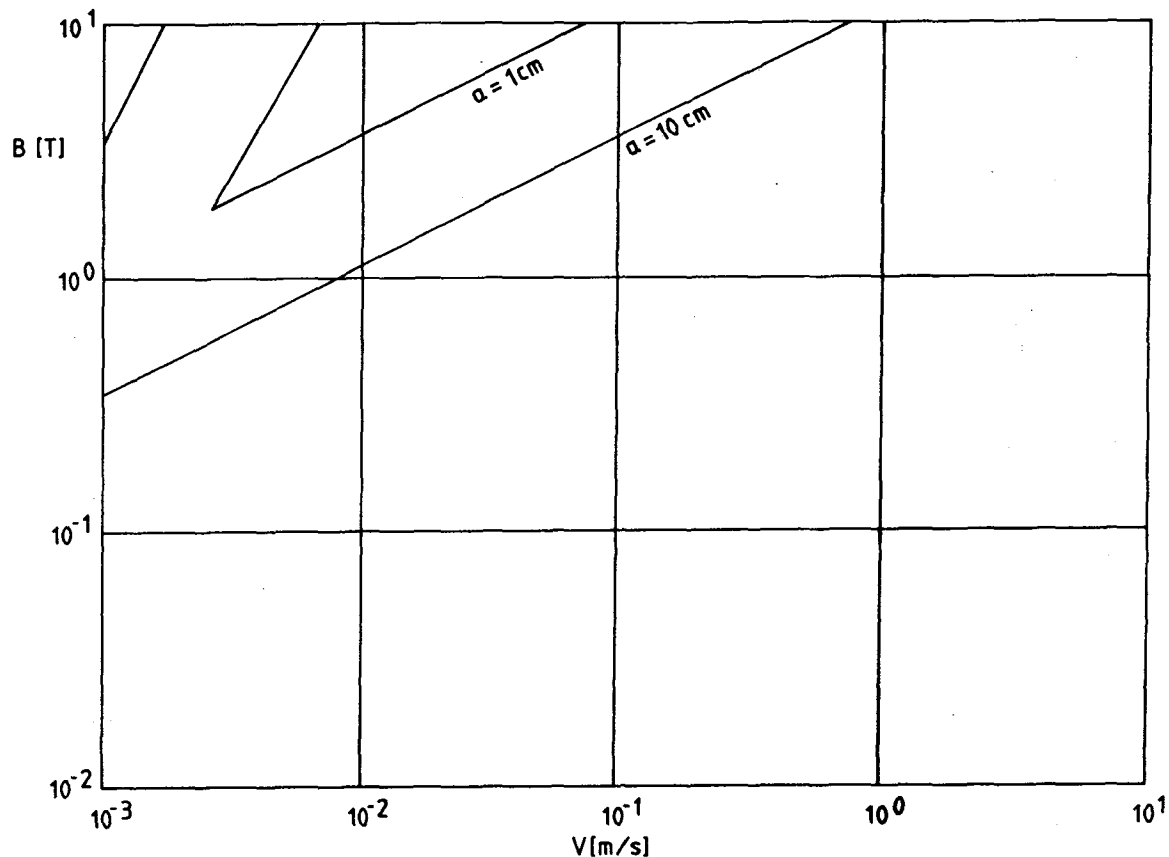


Figure 3.4-7. Required conditions for MHD flow tests with mercury

A higher field by almost an order of magnitude is necessary in mercury experiments with the same channel size and flow velocity.

3.4.1.4 Modeling Needs

As explained in previous sections, the modeling needs necessary for planning, conducting and interpreting the first round of testing will be satisfied by detailed analytical solutions for the cases to be investigated. Such analyses are painstaking and quite involved. As such, they are not suitable for the routine engineering calculations needed for the design development process. On the other hand, the current prevailing view is that straightforward numerical solution of the governing equations is not at present feasible. This is because the three-dimensional nature of the prob-

lem, coupled with the large number of unknown variables (velocity and electric current components, pressure, and voltage), and the fine mesh sizes dictated by the thin boundary and shear layers, will impose extraordinary memory size on the computer. A different approach is clearly needed.

The alternative is suggested by the fact that the amount of information needed for engineering evaluation need not be as extensive as that provided by analytical solutions or detailed numerical computations. Because the boundary and shear layers are very thin in high interactive and high Hartmann number cases, what matters for pressure drop, heat transfer, and corrosion calculations is not the detailed structure of flow and current within the layers, but rather the integral values of current and volumetric flow rate in the layer. For these reasons, approximate semianalytic schemes, where a set of trial functions with undetermined coefficients is assumed for the velocity, current, pressure, and voltage distributions, and the coefficients are determined by some error minimization requirements, appear to be adequate and appropriate. It is hoped that, as the analytical and experimental work needed for the first round of testing progresses, certain common features and properties of the flow, voltage, and current distributions will emerge to facilitate the development of a model based on such a semianalytic scheme. Subsequent testing of more complex cases can be used to validate and/or refine the model.

3.4.1.5 Facility Requirements

Ideally, test conditions should be at the same values of M , N , and C as those which prevail in the blanket to exclude any possibility of the existence of phenomena, as yet unknown, which manifest themselves only at very high M and N . Given the current understanding of MHD phenomena, it can be argued that the possibility of substantial differences in the character of the flow between M and N of the order of 10^4 and M and N of the order of 10^5 is very small (provided, of course, the inequalities which determine the prevailing regime are satisfied in both cases). On the other hand, the saturation magnetic field of iron and the economics of conventional and superconducting magnets make experiments at a Hartmann number of 10^4 much cheaper than experiments at M of 10^5 . It seems that the price of eliminating an improbable event is very high. It makes good economic and technical sense to carry out testing at M of 10^4 , particularly so because some of the proposed tokamak^[6] and all of

the mirror devices have Hartmann numbers not exceeding this order of magnitude.

Experiments at $M \sim 10^4$ can be conducted with conventional electromagnets of flux density of 2 T and pole face separation of 10-20 cm. The length of the pole face should be 1-2 m to accommodate the entrance lengths in the magnetic field, with the longer lengths being more desirable. The estimate for the required length of the magnet arises from an estimate of the extent of three-dimensional disturbances corresponding to abrupt variations of transverse magnetic field in circular ducts. This estimate is $kaC^{1/2}$, where k is an undetermined constant of order one and a is the duct radius. Although the value of k is not known, it is very likely that it will be smaller than one for the gradually changing fringing field at the ends of the magnet. Practically achievable values of $C = 0.03$ and $a = 5$ cm will then yield entrance lengths smaller than 30 cm. The pole face width should be sufficient to provide room for the instrumentation of the test section.

Some attention should be given to magnetic flux uniformity throughout the cross section of the test section. Uniformity of magnetic flux density is desirable not because such uniformity is prototypic but because it will simplify the companion analyses and will make the interpretation of the test results unambiguous. The required uniforming varies with the particular test section and the test objectives. A field uniformity of $\pm 1\%$ over the test article cross sectional area is believed to be adequate and desirable.

The interaction parameter which can be achieved depends to a large extent on the low limit for measurable velocities and the density of the working fluid. Alkali metals, Li, Na, K, and the eutectic alloys of Na and K hold a 35 to 75-fold advantage in achievable interaction parameters over mercury. Of the former candidates, the eutectic alloys offer the advantage of testing at room temperature with a penalty in achievable interaction parameters of a factor of 2. If NaK is used as a working fluid with the aforementioned 2 T electromagnet, an interaction parameter of 10^4 can be achieved at an average velocity of about 5 cm/s.

In summary, a 2 T conventional electromagnet, a test section with $C \sim 0.03-0.05$ and transverse dimension of 10 cm, and a loop with NaK as a working fluid with capacity of 0.5-100 l/s, can provide a room temperature test capability with $M \sim 10^4$ and $N \sim 5 \times 10^2-10^4$. Other alkali metals (Li,

Na, K) can also be used with a small improvement in maximum interaction parameter. Such an improvement will come with the added complication in loop cost and operation and difficulty in conducting local velocity measurements that comes with the high operating temperatures for such working fluids.

The aforementioned testing needs refer to the first two steps in the MHD testing program. For the third step, which involves full scale testing of blanket modules, different testing needs will arise. Such needs depend heavily on the proposed blanket designs. A design like the liquid metal design proposed in the BCSS^[7] requires a very large testing volume. Because concerns about interchannel current loops have been raised for such a design, it will be necessary to test a large portion of a blanket sector to address these concerns. This will require available dimensions in the direction of the magnetic field vector in excess of 2 m. A solenoidal magnet then will be much more suitable than a dipole one. On the other hand, if designs like those proposed in the TPSS^[6] which utilize simple poloidal coolant channels are to be tested, the required dipole magnets need not be much bigger than the ones described earlier in this section (although they will most probably be required to have flux densities at or near prototypic values).

Testing will involve measurement of pressures, voltages, and velocities throughout the test section. The measurement limits are responsible for the limitation in interaction parameter than can be achieved in the test section. For the 2 T magnet and NaK loop discussed above, the interaction parameter is given by $N = 6 \times 10^4/V$, where V is the average velocity in cm/s. To achieve $N \sim 10^4$, a minimum velocity of 6 cm/s is required. For this velocity, the transverse induced voltage is of the order of 0.01 volts and the pressure gradient is of the order of 2-3 psi/m. These values are certainly measurable with good accuracy. Measuring local velocities of 5 cm/s will be more difficult. A liquid metal electromagnetic velocimeter can be used, provided its output, which is 0.2 mV at this velocity, can be read with good accuracy and low noise level. The theory of MHD flow at high M and N indicates that there is a simple correlation between velocity distributions within the duct and voltage distributions on the surface of the duct. This aspect of the theory can be confirmed at higher velocities, where local velocity measurement is easier, and can then be used to deduce velocity distributions at low velocity levels. Since at lower velocities the interaction parameter is higher, the

voltage distribution/velocity distribution correlation will be all the more valid. This correlation, properly confirmed, can be used extensively in future tests to minimize penetrations into the test vehicle and to obtain flow distribution information during testing at high temperatures, where direct local velocity measurement will be much more challenging.

References for Section 3.4.1

1. J. S. Walker, "Liquid Metal Flow in a Thin Walled Pipe Near the End of a Strong Magnet," submitted for publication to the Journal of Fluid Mechanics.
2. J. C. R. Hunt and R. J. Holroyd, "Application of Laboratory and Theoretical MHD Duct Flow Studies in Fusion Reactor Technology", CLM-R169, Culham (1977).
3. M. A. Hoffman and G. A. Carlson, "Calculation Techniques for Estimating the Pressure Losses for Conducting Fluid Flows in Magnetic Fields", TID-4500, UC-20, Lawrence Radiation Laboratory.
4. S. Sukuriansky, I. Zilberman, and H. Branover, "Experiments in Duct Flows with Reversed Turbulent Cascade," Ben Gurion University, Beer Sheva, Israel.
5. M. A. Abdou, et al., "FINESSE: A Study of the Issues, Experiments, and Facilities for Fusion Nuclear Technology Research & Development (Interim Report)", UCLA, PPG-821, also UCLA-ENG-84-30 (1984).
6. C. C. Baker, et al., "Tokamak Power Systems Studies-Fiscal Year 1985," Argonne National Laboratory, ANL/FPP/TM-202 (October 1985).
7. D. L. Smith, et al., "Blanket Comparison and Selection Study-Final Report," Argonne National Laboratory, ANL/FPP-84-1 (September 1984).

3.4.2 Heat Transfer

The objectives of the heat transfer experiments are (1) to obtain proper understanding of the relationship between temperature profiles and the relevant dimensionless parameters, and (2) to discover phenomena which are not anticipated that may have significant impact on the components.

This section addresses heat transfer related issues for the liquid metal blanket with particular emphasis on the scaling relationships required in order to obtain meaningful results from the experiments.

3.4.2.1 Testing Needs

For non-neutron testing, the testing needs for heat transfer are similar to that of MHD tests. The various basic geometries described in the previous section for momentum transfer are certainly needed for heat transfer. In addition to velocity distributions, measurements of temperature distributions are needed for heat transfer experiments. It is particularly important to obtain detailed three-dimensional temperature distribution in the component in order to ensure that there are no unexpected phenomena which resulted in local hot spot with unacceptable temperatures. The number of data collected must be large enough to adequately verify the analytical or numerical model.

In addition to the basic (simple) geometries that need to be tested, there is also a need to test various manifolds in a blanket. This is of paramount importance since poor flow distribution could cause local hot and cold spots and could result in unacceptably high structural temperature or high thermal stress. Manifold geometry depends on the particular design, and at present time, no detailed manifold geometry has been identified. When blanket design becomes better defined, it may be possible to identify several basic manifold geometries for flow distribution testing.

Transient testing is also essential to verify the performance of a given blanket. This includes normal operation (start-up and shutdown) and off-normal operation (accidental conditions, such as loss of flow). At present, there is very little data on the transient behaviors of liquid metal flow and heat transfer. Again transient behavior depends strongly on blanket design. However, transient phenomena exploration using the simple geometries described in Section 3.4.2 will be useful in discovering unexpected phenomena and the

data obtained can be used to calibrate the computer model.

3.4.2.2 Modeling Needs

If a liquid metal blanket is going to be built, there is a definite need for a general purpose, thermal hydraulic design code. Large scale experiments are extremely expensive and therefore are feasible only for verifying the final design. During the design stage, computer modeling and small scale experiments are used iteratively to improve our understanding. The range of applicability of closed-form analytical solutions is limited and not flexible enough as a design tool. Currently, there is a lack of design tools which are flexible enough to address many of the critical feasibility and design issues of liquid metal blankets.

The general purpose, thermal hydraulic, design tool should be flexible enough to include the following capabilities:

- Geometry effect.
- Three-dimensional effect on velocity and temperature distributions.
- Effect of internal structure on fluid flow and heat transfer.
- Effect of property variations with temperature.
- Steady-state and transient analyses.

To develop a design code which include all these capabilities is a long term (5-10 years) and formidable undertaking. With proper planning, different capability can be implemented at different stage of the development program.

3.4.2.3 Analysis and Scaling for Heat Transfer Tests

Heat transfer related issues for liquid metal blanket include not only the liquid metal itself, but also the structural materials (particularly the first wall). The maximum structural temperature (usually at the first wall) determines the temperature level at which the blanket can operate, while the

temperature gradient in the bulk structure determines the thermal stress. In the following sections, the scaling relationships are described for the first wall and blanket under steady-state conditions. Scaling relationships under transient conditions are not discussed here as a result of lack of understanding of unsteady state liquid metal flow in a magnetic field.

Heat Transfer in First Wall

Axial Conduction

The heat transfer mechanism in the first wall is through conduction only and can usually be approximated by considering conduction in the radial direction (the direction of the thickness of the first wall). Axial conduction is negligible provided that the first wall is thin compared to the axial length of coolant channel,

$$\frac{t}{l} \ll 1 \quad (3.4-10)$$

where t is the thickness of the first wall and l is the axial length of the coolant channel.

Nuclear Heating

For tokamaks, the effect of nuclear heating is usually small compared to the effect of surface heat flux on the first wall. Nuclear heating is negligible provided that

$$\frac{Qt}{2q} \ll 1 \quad (3.4-11)$$

where Q is nuclear (volumetric) heat rate in the first wall, and q is the surface heat flux. If (3.4-11) is satisfied, then the scaling relationship for the first wall become

$$\frac{k \Delta T_{fw}}{q t} \approx 1 \quad (3.4-12)$$

where k is the thermal conductivity of the structural material, and ΔT_{fw} is the temperature rise across the first wall over a thickness of t .

For a tandem mirror, the surface heating level is usually very small, and the heat transfer problem in the first wall is not critical.

Effect of Temperature on Property Values

When either q or t becomes large, the temperature variation across the first wall becomes significant and the effect of temperature on the thermal conductivity has to be taken into consideration. Equation (3.4-12) can be rewritten into an integral form. This is a particular concern for a component (such as the limiter) exposed to high surface heat flux and with a relatively thick coating.

Heat Transfer in Liquid Metal Blanket

Dependence on Velocity Profile

In liquid metal blankets, flow is laminarized by MHD effects. Since heat is transmitted in the direction perpendicular to the flow only by conduction, temperature distribution in the fluid depends strongly on the velocity profile. There may be a large temperature gradient perpendicular to the flow direction, though thermal conductivity of liquid metal is high. Dependence of heat transfer on the velocity profile is greater in MHD flow than in turbulent flow. Thus, the scaling considerations described in Section 3.4.2 for MHD flow must be satisfied. Therefore the Hartman number, the interaction parameter, the Reynolds number, the wall conductivity ratio, etc., all must satisfy certain requirements described previously in Section 3.4.2.

Long Thermal Entry Region

In laminar flow, the temperature distribution develops very slowly, since heat is transmitted only by conduction. The thermal entry length as follows:

$$\ell_t \sim \frac{Va^2}{\alpha} \quad (3.4-13)$$

where α is the thermal diffusivity of the fluid, a is the channel width, and V is the velocity. Usually channels in liquid metal blankets are shorter than ℓ_t ; therefore, the temperature profile will not be fully developed.

Natural Convection

The ratio of buoyant force to electromagnetic force is written as follows:

$$\frac{f_b}{f_{EM}} = \frac{\rho g \beta \Delta T}{\sigma_f B^2 V \phi} \quad (3.4-14)$$

where g is the acceleration of gravity, ρ , β and σ_f are the density, the volume expansion coefficient and the electrical conductivity of the fluid, respectively. B is the field strength and ΔT is the temperature difference that drives the natural convection. The ratio is usually very small in blankets, hence natural convection is suppressed there.

Axial Conduction

Though the velocity of coolant is low in blankets, heat conduction in the flow direction is negligible compared with heat carried by convection. The ratio is written as follows:

$$\frac{q_{cond.}}{q_{conv.}} = \frac{\alpha}{VL} \quad (3.4-15)$$

where L is the channel length. The nominal value for this dimensionless group is $\sim 10^{-5}$ in a typical blanket.

Thermoelectric Effects

There is usually a large radial temperature gradient in fusion reactor blankets. Liquid metal coolant is surrounded by hot and cold walls. If the temperature difference is large and the thermoelectric power of the wall is different from that of the liquid metal, electric currents will circulate. The intensity ratio of thermoelectric current to MHD current can be written as follows:

$$\frac{i_{TE}}{i_{MHD}} = \frac{(S_f - S_w) \Delta T}{BVa} \quad (3.4-16)$$

where S_f and S_w are the thermoelectric powers for the fluid and the wall. ΔT is the temperature difference between the hot and cold walls. The ratio is about .01 in blankets.

Effects of Bulk Heating

The heat transfer characteristics in liquid metal blanket are affected by bulk heating in the coolant. If the velocity profile and bulk heating are symmetric, the temperature difference between hot and cold walls is not affected by bulk heating. If the velocity profile is skewed toward the hot or cold wall, bulk heating will reduce or increase the temperature difference, respectively.

Nuclear heating affects the average coolant temperature rise through the blanket. This plus the nuclear heating in the structure material determines the average temperature of the bulk structure. The average bulk structure temperature is often needed in order to determine the thermal stress of the structure in the blanket. Therefore, nuclear heating (or volumetric heating) will be important if thermal stress is to be modeled correctly.

Minimum Requirements for Model Testing

Table 3.4-2 summarizes the requirements and the non-dimensional parameter ranges for designing heat transfer tests of a liquid metal first wall/blanket. The parameter ranges listed in Table 3.4-2 should be maintained in the model tests so that the physical phenomena are similar between the model and the actual blanket.

It is apparent that heat transfer testing is more demanding than the MHD testing since there are additional requirements to be satisfied. It is desirable to use lower heat flux from economic consideration. This can be accomplished by increasing the first wall thickness while reducing the surface heat flux (maintain $q \cdot t$ the same between model and actual blanket) in the model test. However, in order to obtain the correct temperature and temperature gradient in the first wall of the model, the wall thickness cannot be increased. The surface heat flux can be reduced by using a structural material with a thermal conductivity smaller than that of the actual material. To maintain the correct temperature distribution in the liquid metal blanket, the parameter for thermal entrance length (which is equivalent to the dimensionless residence time) should be kept approximately the same between the model and the prototype blanket.

Table 3.4-2. Requirements for Non-Nuclear Heat Transfer Tests
of a Liquid Metal First Wall/Blanket

1. First Wall

- Negligible Axial Conduction

$$\frac{t}{\ell} \ll 1$$

- Negligible Nuclear Heating

$$\frac{Qt}{2q} \ll 1$$

or

$$\frac{k \Delta T_{fw}}{q t} \approx 1$$

2. Liquid Metal Blanket

- Correct Velocity Distribution

$$M \approx 10^4 \sim 10^5$$

$$N > 10^3$$

$$1 \gg \phi \gg M^{-1}$$

- Suppression of Turbulence

$$Re < 60 M$$

- Flow Developing Length

$$\frac{\ell \phi^{1/2}}{a} \approx 1$$

- Thermal Entrance Length

$$\frac{\ell \alpha}{va^2} \approx 10^{-2}$$

- Suppression of Natural Convection

$$\frac{\rho g \beta \Delta T}{v \sigma B^2 \phi} \ll 1$$

- Negligible Axial Conduction

$$\frac{\alpha}{v \ell} \ll 1$$

The ratio of buoyant force to electromagnetic force should be as small in test stands as it is in a real blanket. The ratio of the quantity of heat conducted in the flow direction to that carried by convection to MHD current is usually small, but not always negligible in a real blanket. This is especially true at the channel inlet, where large axial temperature gradients may exist. It is not necessary to preserve this ratio in a test stand, but some attention should be given it. The effect of viscous heating in the boundary layer is usually small compared to that of surface heat flux. Joule heating in the liquid metal is usually small compared to the nuclear heating.

In addition to the desirable feature of lower surface heat flux in the model testing, it is also desirable to reduce channel length since a long channel requires a long magnet. The channel length is restricted by the requirements of flow development and thermal entrance lengths shown in Table 3.4-2.

Table 3.4-3 lists the values of the variables and the materials proposed for the heat transfer tests and the corresponding conditions in a fusion blanket. Based on these values, the scaling parameters listed in Table 3.4-2 can be calculated and the results are shown in Table 3.4-4. Comparison between Table 3.4-2 and Table 3.4-4 indicate that all the requirements are satisfied. Thus, relevant results can be expected from the proposed model tests.

If other liquid metal is used in heat transfer experiments, the difference in the properties must be considered. In NaK experiments, a little higher magnetic field is necessary to attain a high interaction parameter as discussed previously. The thermal diffusivity of NaK is about 40% higher than that of lithium, which makes thermal entry length shorter. These facts are not desirable, but may be acceptable, since the differences are not so large.

3.4.2.4 Test Scenarios

Heat transfer tests can be conducted in the sequence and schedule shown in Table 3.4-5. Initial emphasis is given to steady-state and transient tests of simple geometries, such as single pipe, bend, etc., described in Section 3.4.3.1. At later stage of the program, a few promising manifold geometries will be selected for testing. It should be noted here that the word manifold includes not only the inlet and outlet of the blanket, but also flow distribu-

tion system inside the blanket, such as the manifold/first wall channel geometry of the toroidal/poloidal flow blanket of the BCSS project.

3.4.2.5 Facility Descriptions

The test facility will be a liquid lithium loop that has the characteristics given in Table 3.4-6. A heat source must be provided to satisfy the surface heat flux requirement. Depending on the geometry of the magnet and the test section, additional space may be needed to insert the heating element between the test section and the magnet. The pressure drop of the system must satisfy the velocity requirement in the test section.

Table 3.4-3. Comparison of Parameters Between Proposed Experiments and Actual Fusion Environment

	Experiments (Heat Transfer)	Fusion
Structural Materials	stainless steel	HT-9/V-alloy
Geometry	circular/ rectangular	circular/ rectangular
Axial Length (ℓ)	2-3 m	3-5 m
Radius ^a (a)	0.05 m	0.05 - 0.50 m
Wall Thickness (t)	5-10 mm	2-5 mm
Magnetic Flux Density (B)	0-3T	4-7T
Velocity (V)	0.1-0.5 m/s	0.1-1.0 m/s
Surface Heat Flux (q)	$0.3-0.7 \times 10^6$ W/m ² (from one side only)	1.0×10^6 W/m ²
Coolant	lithium	lithium
T _{min}	250°C	300°C

^aExtra space required for heater.

Table 3.4-4. Comparison of Dimensionless Parameters Between Proposed Experiments and Actual Fusion First Wall/Blanket

	Experiments	Fusion
$M = Ba \sqrt{\sigma/\mu}$	10^4	$10^4 - 10^5$
$R_e = \rho Vd/\mu$	6×10^4	$10^4 - 10^5$
$N = M^2/R_e$	10^3-10^4	$10^4 - 10^5$
$\phi = \frac{\sigma_w t}{\sigma a}$	0.035 ($\ll 1$)	$10^{-2} - 10^{-3}$
$\rho g \beta \Delta T / V \sigma B^2$	10^{-4}	$\ll 1$
$\ell \phi^{1/2} / a$	10	10
t/ℓ	0.005 ($\ll 1$)	0.005
$\frac{k \Delta T_{fw}}{qt}$	1	1
$\alpha \ell / Va^2$	2×10^{-2}	$10^{-2} - 10^{-3}$
$M\phi$	3×10^2	10^2
60M	$6 \times 10^5 > R_e$	$10^5 - 10^6 > R_e$
$\frac{\alpha}{V\ell}$	10^{-5}	$10^{-4} - 10^{-5}$

Table 3.4-5. Sequence and Schedule of Heat Transfer Experiments

	Time (years)								
	0	1	2	3	4	5	6	7	
1. Design and Construction of Test Loop	-----								
2. Steady-State Tests of Simple Geometries				-----					
3. Transient Tests of Simple Geometries			-----						
4. Manifold Tests							-----		

Table 3.4-6. Major Characteristics of the MHD Heat Transfer Facility

Test Section Length	2 m
Magnetic Flux Density	2 T
Liquid Velocity in Test Section	0.5 m/s
Test Section Radius	0.05 m
Surface Heat Flux (on one side of test section)	0.5 MW/m ²

References for Section 3.4.2

1. J. A. Shercliff, "Thermoelectric Magnetohydrodynamics", J. Fluid Mech., 91-2, p. 231 (1979).
2. M. A. Abdou, et al., "FINESSE: A Study of the Issues, Experiments, and Facilities for Fusion Nuclear Technology Research & Development (Interim Report)", UCLA, PPG-821, also UCLA-ENG-84-30 (1984).

3.4.3 Materials Interactions and Mass Transfer

3.4.3.1 Testing Needs for Materials Interactions and Mass Transfer

Introduction

Materials interactions place restrictions on the blanket operating temperature, on primary coolant system impurity levels, and on acceptable materials combinations. The processes associated with mass transport and materials interactions are complex and vary from one materials combination to the next. For this reason, a large number of separate issues exist, many of which can have substantial impact on the feasibility of certain designs and materials combinations.

The resolution of materials interactions issues in liquid metal blankets will require a large amount of testing, both to verify theoretical models and, in cases which prove to be theoretically intractable, to establish empirical correlations. This extensive need for testing stems from the complexity of the basic corrosion processes and the dependence on many system parameters. Existing test results are in general piecemeal. Most of the existing test information in liquid metal systems has been developed for fast breeder reactor materials with sodium coolant, making the results only partially applicable. Frequently the only available fusion-relevant information is qualitative observation under a very limited range of conditions.

Table 3.4-7 summarizes the corrosion-related concerns in liquid metal blankets. The two main categories of effects are (1) mass transport issues and (2) structural properties degradation.

Mass transport involves the entire primary coolant system, including the primary heat exchanger, impurity control system, and to some extent the tritium extraction system. The most critical mass transport issue perceived today (for steel structural materials) is the concern over redeposition in the colder regions of the primary coolant system, leading to flow restrictions. Redeposition rates limit the allowable operating temperature of many current designs. Transport of activation products from the blanket is also a serious concern, but it is generally conceded that hands-on maintenance will not be practical for any liquid metal cooled system. Remote maintenance complicates the system design, but is not considered a feasibility issue.

Table 3.4-7. Materials Interactions Issues

- A. Mass Transport
 - 1. Wall thinning
 - a. uniform dissolution
 - b. localized dissolution
 - c. spalling and non-dissolutive processes
 - 2. Corrosion/redeposition phenomena
 - a. localized deposition
 - b. activation product transport and maintenance procedures

 - B. Structural Properties Degradation
 - 1. Liquid metal embrittlement
 - 2. Effects of removing alloying elements (decrease in strength, etc.)
 - 3. Embrittlement due to interstitial element transport
 - a. Effects on surface chemistry
 - b. Effects on structural properties
 - 4. Stress-corrosion interactions
 - 5. Radiation-corrosion interactions
-

Structural properties under the combined influence of radiation and corrosion limit the lifetime of the blanket and the allowable operating conditions - both temperature and impurity levels. In addition, failure modes will be closely tied to the blanket materials properties. This subject area includes several effects which are highly dependent on the material. In addition to the type of material (e.g., ferritic steel, austenitic steel, refractory alloys), corrosion phenomena also depend on changes in alloying elements, impurity levels, or manufacturing techniques. The dominant corrosion effect for austenitic steels is selective dissolution of alloying elements, with subsequent formation of a weak ferrite layer. This surface layer is porous and can spall off in macroscopic pieces. For refractory alloys, dissolution is slow and the primary concern is interstitial element transport. The effects of hydrogen, oxygen, carbon, and nitrogen on the DBTT

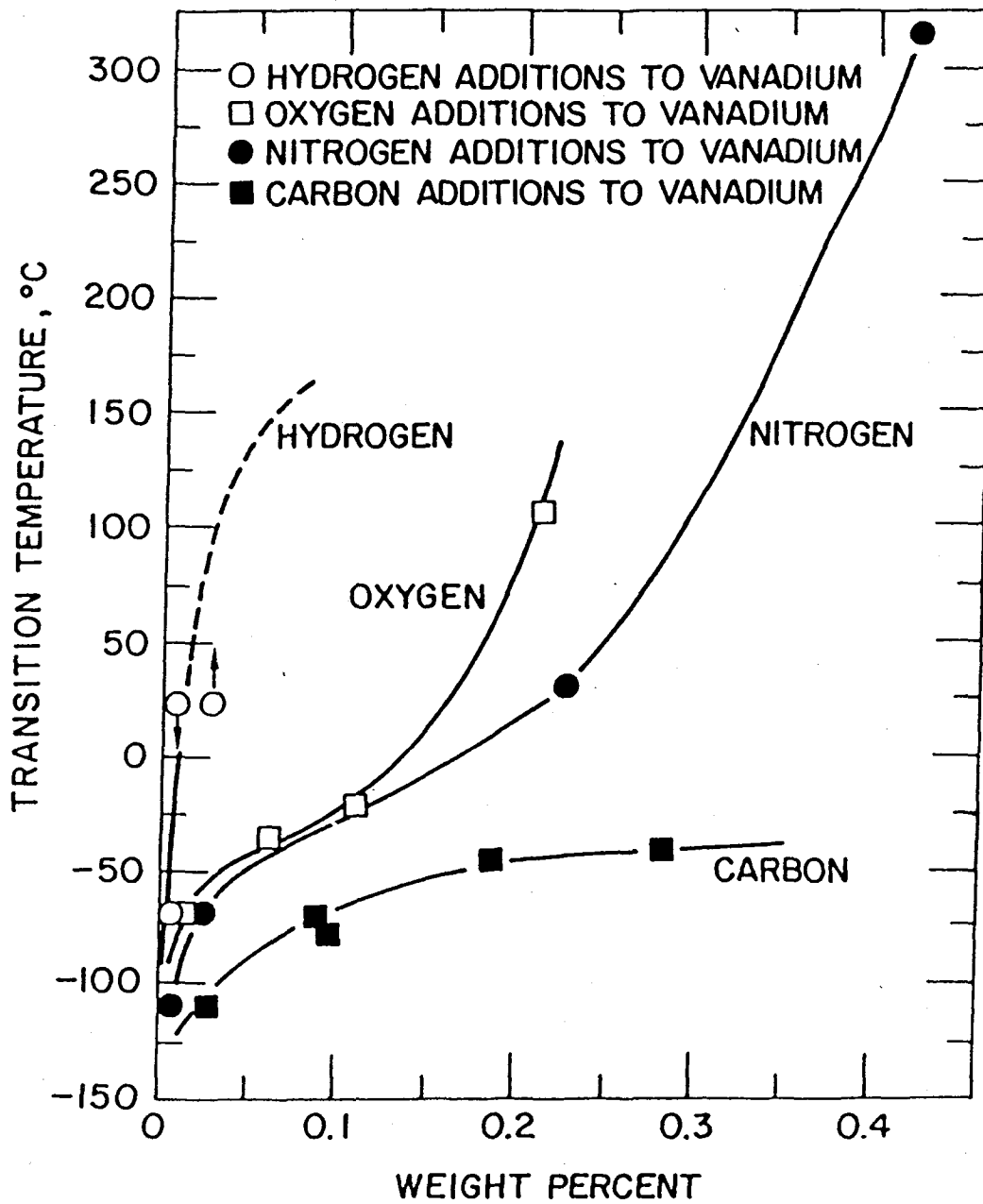


Figure 3.4-8. The effect of impurities on the DBTT of unalloyed vanadium

of unalloyed vanadium is shown in Figure 3.4-8. It suggests that the presence of interstitial impurities may raise the DBTT significantly.^[1]

Synergistic effects due to the combined influence of corrosion, radiation, and the stress field may enhance the rate of materials properties degradation beyond the simple sum of the effects. Whereas the radiation/corrosion interaction is not observed in sodium-steel systems, insufficient data exists to indicate that other alkali liquid metals are immune. Stress/corrosion enhancement of embrittlement has been demonstrated in non-stress-relieved iron, but little is known for the steels and refractory alloys considered for fusion. Due to a general lack of data on synergistic effects, the seriousness of this issue is difficult to assess currently.

List of Testing Needs

Because of the scarcity of existing data for relevant materials combinations under reactor-relevant conditions, the need for further testing is obvious. However, it is important not to assume that a perfect understanding or a complete ability to calculate materials interaction phenomena is required in order to satisfactorily resolve the issues and construct a workable blanket.

The following list presents the testing needs, in roughly increasing levels of integration, which are felt to be necessary to demonstrate the feasibility and attractiveness of the blanket with respect to corrosion issues. Table 3.4-8 summarizes these testing needs.

1. Corrosion rate basic phenomena and temperature limits. There are several different phenomena associated with corrosion. For different materials combinations and under different conditions, the most critical corrosion issue may change. A clear example is the difference between stainless steels and refractory alloys. In general, stainless steel corrosion is dominated by dissolution, whereas refractory alloys have very low solubilities and tend to be dominated by interstitial element transport. It is important to determine the nature of the basic phenomena for materials combinations of interest in order to improve our understanding of the issues and to limit the amount of data which must be gathered.

Table 3.4-8. Materials Interactions Testing Needs

1. Corrosion rate basic phenomena and temperature limits
 2. Materials development and screening
 3. Temporal dependence of corrosion processes
 4. Effects of velocity magnitude and profile
 5. Changes in materials (structural) properties
 6. Magnetic field interactive effects
 7. Stress-corrosion interactions
 8. Radiation-corrosion interactions
 9. Out-of-blanket loop effects
 10. Limits on maximum allowable impurity levels and ability to control them
 11. Corrosion and re-deposition inhibition techniques
-

In order to determine the suitability of the various materials combinations in fusion reactor applications, the most important parameter is the maximum allowable temperature which corrosion processes dictate. After identifying the controlling processes, accurate estimates of maximum allowable temperature must be found. In some liquid metal designs, the temperature window of operation is very narrow (less than 50°C), making accurate knowledge of corrosion rates essential.

2. Materials development and screening. New materials are being developed for fusion applications in order to reduce the amount of induced radioactivity and to improve structural properties under irradiation. New candidate alloys and coolants must be screened to verify chemical compatibility in the fusion system. In addition, materials compatibility should be a cornerstone in the development of new materials. Alloy tailoring (for example stabilized SS 321 in a vanadium system^[2]) can be an effective means to control corrosion problems.

3. Temporal dependence of corrosion processes. Most corrosion data has been accumulated over periods of exposure that are far shorter than the expect-

ted service life of some nuclear components. It is known that some chemical processes undergo transitions in behavior, after which the time dependence of the corrosion rate and the nature of the processes themselves change. An example is the "burn-in" period of 1500-3000 hr. for stainless steels, during which a depleted surface layer is produced. The burn-in phase is controlled by nickel and chromium diffusion through the near-surface matrix. After burn-in, the dissolution (including spalling) of the ferrite layer controls corrosion.^[3] Another observed phenomenon which occurs after a delay period is the penetration of lithium at grain boundaries.^[4]

4. Hydrodynamic effects. Mass transport rates and processes vary with both the magnitude of the fluid velocity and the spatial profile. For example, with materials combinations that are normally rate-controlled at low velocity by the liquid phase can change to solid phase rate-controlled at high velocities. The greatest influence of the velocity profile occurs near the walls. Boundary layer velocity profiles and geometric effects leading to boundary layer disruptions can control the overall mass transport phenomena in the primary cooling system.

5. Changes in structural properties. Chemical interactions will alter the properties of in-blanket structure, out-of-blanket materials, and the coolant. The greatest concern lies with structural properties changes, such as embrittlement (loss of ductility), loss of strength, changes in ductile-to-brittle transition temperature (DBTT) and fatigue properties. However, other changes in materials properties may also be important to some extent, for example surface electrical resistivity, which is important for MHD effects.

6. Magnetic field interactive effects. The primary impact of the magnetic field is to affect mass transport through effects on the flow characteristics and on heat transfer. It is well known that MHD forces cause very narrow boundary layers, streaming flows, laminarization, etc. The flow profile dominates liquid-phase transport and therefore can be a controlling factor in corrosion rates and in the chemical processes themselves. Other effects, such as increased particle formation, may also be affected by the magnetic field. To date, corrosion test information in a magnetic field has not been published; however, experimental work is on-going at CEN in MOL, Belgium.

7. Stress-corrosion interactions. Stress is known to accelerate corro-

sion in some cooling systems - most notably water-cooled steel systems. The stress-corrosion interaction may also be important in liquid metal cooled systems. For example, it has been shown in a lithium-iron system that stress accelerates grain boundary attack. The mechanism involves creep strain which disrupts the protective corrosion product layer, constantly exposing bare iron surfaces to the lithium.^[5] The danger exists primarily for non-stress-relieved portions of the material. Sufficient stress relief should be found in all blanket components, except possibly near welds.

8. Radiation-corrosion interactions. Since both corrosion and irradiation contribute to weakening of materials at grain boundaries, it is natural to expect some sort of interaction between these two effects. Sodium-stainless steel systems have not been observed to possess a strong synergism between corrosion and radiation (the whole is not substantially greater than the sum of the parts). However, it is not known whether other alkali metals will display this interaction. The degree to which a synergistic effect occurs should be measured for fusion materials, since their structural properties are a crucial parameter for blanket feasibility.

9. Stability of coatings and/or laminates. Insulating coatings or laminates can be used to significantly reduce the MHD pressure drop for liquid metal blankets. The integrity of these coatings or laminates depends on many factors, including chemical interaction with the coolant. If the insulating medium is breached or its resistivity substantially reduced, the blanket may cease to operate within its allowed temperature and pressure limits. The reliability of these coatings should also be demonstrated.

10. Out-of-blanket loop effects. The entire primary cooling system is closely tied to the corrosion processes. As the coolant travels through the various parts of the system, it encounters widely different temperatures and flow conditions. Transport and redeposition of dissolved material and impurities throughout the entire primary loop is a critical issue. This effect could be further complicated if the primary cooling system consists of more than one alloy. For example, in systems with a vanadium blanket, the out-of-blanket components (pumps, heat exchangers, piping) will probably be some form of steel. In addition, other materials such as insulators or seals may contribute to impurities in the primary coolant.

11. Impurity levels and control. Only a limited amount of information

is available on the effects of impurities on corrosion. There are two aspects of this issue: (1) the effects of impurities must be studied in order to establish impurity limits in the cooling system, and (2) techniques for controlling impurities must be developed and proven such that the maximum allowable limits can be obtained. Hot trapping and cold trapping are two such techniques which may be used in reactors to either absorb or precipitate impurities. The production and transport of impurities in the primary cooling system are important effects which require testing.

12. Corrosion and redeposition inhibition techniques Aluminum dissolved in lithium has been shown to reduce the corrosion rate of 316 SS by a factor of 5.^[6] Other techniques to treat surfaces or inject coolant impurities may be useful in controlling corrosion. The basic processes of corrosion inhibition and the inhibitor systems themselves should be further explored and tested.

3.4.3.2 Modeling Needs

Our present understanding of mass transport in liquid metal systems is very limited. Unlike heat transfer processes, which are well-characterized once the velocity field is known, corrosion mass transport depends on a large number of system parameters, including velocity, temperature, impurities, and geometry.

Most analytical modeling efforts in the past have treated stainless steel systems. These efforts have historically focussed on the dissolution of wall material into the flowing alkali coolant. The models compute diffusion through the boundary layer and bulk convection of solute in the coolant. It is common to assume that the controlling process is diffusion of alloy components through the boundary layer adjacent to the wall and that the velocity profile is hydrodynamically fully developed.

Some models consider corrosion mass transfer as a local phenomenon and model only straight channels, while other models investigate the loop as an entire system using boundary layer theory. Predictions from both local and system models are usually in error in overpredicting by factors ranging from three ^[7] to a hundred ^[8] when compared with experimental data.

The large discrepancies between theory and experiment suggest one or more

of the following explanations:

1. Boundary layer models are not sufficiently sophisticated to model the corrosion process. Other processes (solid state diffusion, surface dissolution kinetics, etc.) may be controlling, which invalidates the simple boundary layer results.

2. Data used as parameters in boundary layer models (mass diffusivity, solubility, etc.) and/or the assumed boundary conditions are in error. The discrepancies between model and experiment may be due to parameter uncertainties rather than modelling errors.

3. The experimental apparatuses used for corrosion research are usually quite complicated and include features not included in most models (cold traps, EM pumps, etc.). The geometric configurations and uncertainties in velocity profiles make accurate modeling of corrosion experiments difficult.

Analytical treatments of corrosion concentrate on the liquid side diffusion/convection processes and ignore chemical, solid-phase and kinetic processes. Several mechanisms might be important and are not currently included in modeling, including solid phase processes, interface processes, particulate kinetics and transport, and liquid phase reactions.

1. Solid phase processes. In stainless steels, the initial transient and long term steady-state behavior are attributable to the selective leaching of alloying elements from the solid phase. In vanadium alloys, impurity accumulation causes the eventual degradation of the mechanical properties of the solid phase. By neglecting the resistance to mass transport in the solid phase, corrosion models would tend to overpredict corrosion rates.

2. Interphase and interface processes. It usually has been assumed that liquid phase transport is the rate limiting step for corrosion product transport in modeling. However, dissolution kinetics can also be an important rate limiting step. Therefore, the usual assumption that the liquid is saturated at the interface (which is the boundary condition for liquid phase transport calculations) may not be valid. Additionally, the formation of compounds at the interface could greatly alter the transport rates and cause discrepancies in modeling and experimental results.

3. Particulate kinetics and transport processes. Particle kinetics and transport are most important in dissolution dominated materials (austenitic

or ferritic stainless steels) and probably less important in refractory alloy systems. Because heat transfer is much faster than mass transfer, the coolant can become super-saturated. The dissolved material, instead of depositing on surfaces, forms particulates and is carried around by the coolant. These particulates will nucleate and grow in the cold sections, deposit on selected locations, and dissolve in the hotter sections. In the cold regions, particulate formation will reduce the deposition rate. In hot regions, particulate re-solution will act to repel the driving force for wall dissolution by providing local sources of solute. At selected locations, particularly if the boundary layer is disrupted (such as the entrance region to a strong magnetic field), particulates will be deposited on the wall and cause major problems. The rate of particle nucleation is a thermodynamic function. The growth and dissolution mechanism are functions of fluid residence time and other flow parameters.

4. Liquid phase reactions and compound formation. Corrosion products and reactants are usually modeled as inert elements moving through the system of interest. The dissolved elements and the impurities may form compounds. Lack of data on the compounds formed and their thermodynamic properties makes it difficult at present to include this mechanism in present day models.

3.4.3.3 Analysis and Scaling

Materials interactions depend on a large number of environmental conditions in the blanket and primary cooling system. In general, the most critical are materials, temperature level, and impurity level. Use of the correct materials is an absolute requirement, since the phenomena change dramatically from one material combination to the next. Similarly, corrosion processes are activated by the temperature of the material: dissolution rates generally scale exponentially with temperature. The influence of impurities is not well-characterized, except to the extent that the types and level of impurities are known to be critically important.

Also important to corrosion are the thermal hydraulic conditions in the primary cooling system and the long time of exposure. Thermal-hydraulic factors include velocity magnitude and profiles, geometry, magnetic field (MHD effects), and temperature gradients, which arise due to heat sources.

Table 3.4-9. Reactor Relevant Conditions Required for Testing of Heat, Mass, and Momentum Transport Issues

	Momentum Transfer	Heat Transfer	Mass Transfer
Magnetic Field	X	X	X
Velocity	X	X	X
Geometry	X	X	X
Temperature Gradient		X	X
Temperature			X
Impurity Level			X
Material			X
Long Time Exposure			X
Geometry Outside the Magnetic Field			X

Table 3.4-9 summarizes these important environmental conditions and contrasts them with the conditions required for heat and momentum transport testing. Clearly, the number of relevant parameters is so large for mass transport that simple scaling techniques which often work with single and multiple effects phenomena are difficult to apply. Certain conditions simply cannot be scaled due to their critical and/or unknown influence on materials interactions. In section 3.4.4.5, the individual tests are described and the dominant environmental conditions are given for each.

3.4.3.4 Test Scenarios and Test Strategies

Two key decisions will have a dramatic impact on the test scenario for mass transport and materials interactions issues. These are: 1. choice of materials and 2. desired level of theoretical understanding.

Materials Selection

In liquid metal blankets, the potential coolant and/or breeder materials include lithium and $\text{Li}_{17}\text{Pb}_{83}$ for self-cooled blankets, and helium in separate-

ly cooled systems (including either separate blanket coolant or separate first-wall coolant). The possible candidate structural materials include an austenitic steel prime candidate alloy (PCA), a ferritic steel HT-9, and a vanadium-based refractory alloy V-15Cr-5Ti. A reduction in the number of breeder/coolant/structural materials combinations is crucial in order to construct an effective test strategy under a limited funding scenario.

Modifications in the alloying constituents, impurity levels, or manufacturing techniques away from the reference alloys will be considered as "innovative" materials research. Because the three reference materials represent a very broad range of issues, concentrating on their testing will provide relevant information regardless of the final choice of material. In addition to this technology carry-over, there is a recognized need for special testing of innovative materials.

The test strategy for materials interactions must be sensitive to restrictions which arise from thermomechanical, irradiation, and safety issues. The emphasis in a balanced overall test strategy should be placed on materials combinations which are most promising from an overall perspective. For self-cooled blankets operating at a neutron wall loading of 5 MW/m^2 or more, ferritic steel has a marginal design window and austenitic steel is impractical. This design window is based on a combination of thermomechanical and corrosion phenomena, including pressure drop, heat transfer, and materials dissolution. A more complete explanation is presented in section 3.1. For separately-cooled or MHD insulated blanket designs, the thermomechanical design window is broader, so austenitic steels may still be attractive. However, since self-cooled, uninsulated blankets are the primary design candidate, refractory alloys should be given increased emphasis and austenitic steels decreased emphasis.

Level of Theoretical Understanding

For every issue, there is a spectrum of testing approaches, ranging from only theoretical modeling and model verification on one extreme to only development of empirical correlations on the other extreme. A minimum level of theoretical understanding is desirable for several reasons, including:

1. to extrapolate (and scale) test results beyond the range of testing conditions,
2. to incorporate results for other materials systems and other

applications, 3. to understand failures or unexpected results when they occur, and 4. to evaluate the impact of corrosion on safety.

However, extensive modeling and testing to validate the models can be very expensive. Even in a very theoretical development scenario, experimental demonstration of the phenomena ultimately must be performed. It is conceivable to eliminate the theory effort and simply operate experiments under all anticipated conditions -- both normal and off-normal -- in order to generate empirical results for allowable temperature, impurities, materials combinations, etc.

Particularly with corrosion issues, scaling of phenomena beyond the range of conditions encountered in testing is likely to be highly risky. This is due to the large number of relevant environmental conditions and the sensitivity of corrosion processes to these conditions. Therefore, modeling and model verification may be much more difficult as compared to other issues, such as heat transfer, fluid flow, and pressure drop.

A comprehensive program of corrosion testing for fusion applications will necessarily proceed through stages, starting with the simplest possible scoping experiments which narrow the materials and design choices, and progressing to very integrated, prototypical tests which verify the compatibility of materials in a particular component design over long periods of time and in a relevant environment. The testing approach will change throughout the test sequence. By their nature, the simpler tests will be amenable to analysis and will benefit from analysis by 1. allowing materials selection without integrated testing and 2. providing insight on materials improvements and innovation. But in order to establish a "relevant" environment for verification testing, it may be necessary to include radiation damage effects, magnetic field effects, bulk heating, etc. The combination of these integrated environmental conditions probably can come only from a fusion reactor test device.

To summarize, the anticipated phases of testing and their testing approaches are:

1. early screening of individual alloys (analytic/empirical)
2. refinement of basic properties which are still poorly known (empirical)
3. critical feasibility experiments (primarily analytical)
4. primary coolant system verification (empirical)

3.4.3.5 Facility Descriptions

In this section, specific facilities are described, including the major facility components, such as loop hardware, heat sources, magnetic fields, impurity control systems, etc. In section 3.7, cost estimates for the more critical of these facilities are developed.

Table 3.4-10 summarizes the types of experiments which might be used to address the testing needs described in section 3.4.4.2, progressing from basic to integrated tests. Besides basic measurements (described in section 3.3) and the Thermomechanics Integrated Test Facility (described in section 3.5), these are all considered single and multiple effects tests.

The different tests are distinguished primarily by the environmental conditions they contain, with the more basic tests containing the fewest conditions. In Table 3.4-10, distinguishing facility characteristics are given for each class of facility. These are not the complete list of test elements and environmental conditions for each facility, but only the major additional features which make the facility unique from the previous ones.

Thermal convection tests, as with basic properties measurements, provide the three most important environments - materials, temperature, and impurities - as well as a temperature gradient and long-time exposure. Forced convection loops have all of these features and also provide relevant coolant velocity and simulation of interactions with other cooling system components, such as pumps. In systems tests, the details of corrosion in the structure become less important; exploration of cooling system operation is the primary objective. These systems tests can be viewed as forced convection loops with attached subsystems, such as a complete impurity control system (including, for example, a corrosion inhibitor subsystem). Synergistic tests fall in a separate category, since they investigate specific issues under a limited number of environmental conditions. These tests will probably be performed in a thermal convection experiment with stress or irradiation present.

There are several requirements which are shared in common with all materials interactions facilities, as summarized in Table 3.4-11. For example, the appropriate materials combinations are essential. Since both of the

Table 3.4-10. Types of Corrosion Facilities and Their Distinguishing Environmental Conditions

<u>Test Type</u>	<u>Goal of Tests</u>
1. <u>Static Capsule Measurements</u> Relevant Materials Impurities Temperature	basic properties and phenomena
2. <u>Thermal Convection Loop Tests</u> Temperature Gradient Time	mass transport under idealized conditions, scoping studies for inhibitors, impurity control, etc.
3. <u>Forced Convection Without Magnetic Field</u> Velocity magnitude and profile Cooling system components (e.g., pumps)	hydrodynamic and basic system effects
4. <u>Forced Convection With Magnetic Field</u> Magnetic field Velocity profile	MHD effects
5. <u>Systems Tests</u> Impurity control system Corrosion inhibition system Primary coolant system components	geometric and systems effects
6. <u>Synergistic Effects Tests</u> Stress field Radiation field	interactions
7. <u>Thermomechanics Integrated Tests</u> magnetic field heat source geometrically relevant design features	combined mass, heat, and momentum transport

Table 3.4-11. Shared Facilities Requirements for Most Corrosion Tests

correct materials combinations
handling of high melting temperature liquid metals
safety systems due to chemical toxicity and flammability
impurity control
unconventional fusion alloys
importance of manufacturing techniques and impurities

candidate coolant/breeder materials (lithium and LiPb) are solid at room temperature, special handling equipment must be provided for storage and transport in order to avoid problems with freezing. In addition, some liquid metals are safety hazards due to chemical toxicity or flammability. Safety systems, such as emergency room filtration systems may be needed.

Cleanliness of the liquid metals could be another very serious problem. Impurity control systems will be necessary in virtually all experiments because of the importance of impurity levels to many materials interactions. Smaller experiments generally exhibit more problems maintaining control over impurities, since the smaller volume usually implies a large surface to volume ratio. (The impurity source is usually proportional to the surface area.)

The structural alloys used as specimens or as parts of the corrosion loops will present certain common problems. Many of the alloys are unconventional, and will therefore be expensive and difficult to obtain. For example, vendors do not commonly fabricate vanadium alloys into tubing or specialized shapes. In addition, the manufacturing techniques, such as heat treatments, are important for corrosion issues and must be well controlled. The material microstructure and impurity levels should both be well-characterized.

In the following, each class of separate effect/multiple effect facility is described by giving 1. general facility features and 2. information obtained in the experiments. This set of facilities does not constitute a recommended test plan. They are significant classes of facilities which proceed through a logical sequence by gradually increasing the number of

environmental conditions and the level of integration. Any given test may or may not be included, depending on cost and time constraints, results of previous tests, etc.

a. Static capsule tests. The most basic type of corrosion test is performed in a static, isothermal capsule. Capsule tests isolate the chemical mechanisms of materials interactions (dissolution, selective leaching, interalloying, etc.) as a function of temperature. But capsule tests cannot provide information on transport mechanisms. They are generally useful only in providing a simple screening test to qualitative measure the feasibility of a particular alloy/coolant combination in terms of impurities and temperature.

b. Thermal convection loop tests. Thermal convection tests provide substantially more information for a minimal increase in cost. There are two "types" of thermal convection tests. In the simplest type of test, specimens are placed in the test section and the convection currents are used to speed the corrosion process and provide a cold area to act as a sink for mass transport. In a more sophisticated thermal convection test, the geometry is configured to resemble the actual coolant paths in a cooling system. The entire loop can be considered a kind of specimen, which models both the hot and the cold legs of a primary coolant system. The principal disadvantage of thermal convection loops is the inability to obtain a high velocity and to properly model the velocity profile.

The primary components of a thermal convection loop are shown in Figure 3.2-4, which shows a loop in existence at ORNL. It includes piping, insulation, heaters, surge tanks, and specimen extraction apparatus. Out-of-loop components include purification apparatus and diagnostic instruments for measuring weight, composition, and surface properties for the specimens and the coolant. The temperature difference in this experiment was 150°C and the flow speed 2.5 cm/s.

In the materials test program, each materials combination ideally would possess a separate test apparatus, since the phenomena are affected by the material conditions of the test facility. For more interactive types of test, this apparatus may become very complicated and expensive. Therefore, thermal convection loops provide an economical means to test a large number of candi-

date alloys for materials screening.

c. Forced convection loop tests without magnetic field. Thermal loop testing alone will not provide a complete data base for judging materials compatibility and temperature limits. Before committing to an expensive integrated test of a liquid metal blanket, it will probably be necessary to operate with full thermal-hydraulic conditions (high velocity) and to explore design and system dependent effects on the corrosion processes.

Forced convection loop tests without magnetic field will be useful in order to explore loop effects and high velocity effects without the complications of MHD velocity profiles. These loop effects include, for example, localized erosion and redeposition in the test section and the heat exchanger, impurity transport and control, and structural properties throughout the coolant loop. These tests are larger than thermal convection tests, and require substantial heat sources, heat exchangers, and economizers. Electromagnetic and/or mechanical pumps will also be required. The BLIP loop, shown in Figure 3.2-5, illustrates the added complexity and size of forced convection loops.

In some forced convection tests, impurity control systems may further complicate the loop. This includes hot traps, cold traps, and corrosion inhibition systems. Tritium recovery systems may be simulated to more accurately simulate impurity transport.

d. Forced convection loop tests with magnetic field (MHD corrosion tests). Before operating a prototypical blanket under magnetic field, simple MHD corrosion tests will be useful to explore the effect of MHD velocity profiles on corrosion under controlled conditions. It is known that the magnetic field substantially alters the velocity field from that in ordinary flow. Turbulence is suppressed at any Reynolds number of practical interest and the velocity profiles can have very thin boundary layers, high velocity jets, and other features characteristic of MHD fluid flow. These velocity profiles have been shown to be important to dissolution,^[9] and are likely to be important for any corrosion-related phenomena.

An MHD corrosion test should attempt to isolate only the effects of the magnetic field. It may be necessary to provide a fairly large field volume in

order to include geometrically relevant design features, such as bends, contractions, manifolding, etc. Since the primary emphasis is mass transport in the liquid phase, a well-characterized material which is dissolution dominated would be desirable. This test should follow MHD fluid flow tests so that the velocity profiles could be well-characterized without the need for extensive measurement. Temperature gradients throughout the test section are important in addition to the overall system temperature difference. Mass transport under magnetic field is strongly coupled to both heat and momentum transport.

e. Synergistic effects tests Synergistic effects are interactions between two phenomena whose end effect may be substantially different than the sum of the two effects alone. The primary examples of this include stress-corrosion and radiation corrosion interactions. These tests are generally carried out in thermal or forced convection loops, and are distinguished by special additional requirements. Stress-corrosion tests require a mechanism to stress specimens in the liquid metal environment. Radiation-corrosion tests can be performed in a number of ways. Corrosion specimens can be pre-irradiated or post-irradiated, but the most desirable method would involve direct irradiation of the specimen in the correct chemical and thermal environment. Small specimens could be tested this way in fission reactors.

f. Primary cooling system tests Corrosion processes are intimately connected to heat transfer and fluid flow behavior, which require prototypical modeling of components in order to fully simulate. In addition, the actual transport and control of corrosion products and impurities will depend on the design of both the blanket and the primary coolant loop system as a whole. This includes for example impurity control systems for hot trapping, cold trapping, and corrosion inhibitor chemistry. Because of these factors and because the temperature design window for some liquid metal blankets is very narrow, integrated coolant system testing will be a crucial final step in verifying materials compatibility. These tests constitute a subset of forced convection loops at a fairly high level of integration. The principal difference between this type of facility and the TMIF is in the absence of magnetic field and MHD effects. Operation of a TMIF may reduce the usefulness of this facility.

References for Section 3.4.3

1. B. Loomis and O. Carlson, Proceedings of the 3rd Annual Conference on Reactive Metals, pp. 227-243, Buffalo, NY, May 27, 1958.
2. R. L. Ammon, "Vanadium and vanadium-alloy compatibility with lithium and sodium at elevated temperatures," International Metals Reviews, Review 258 (1980) No. 5 and 6.
3. O. K. Chopra and P. F. Tortorelli, "Compatibility of Materials For Use in Liquid-Metal Blankets of Fusion Reactors," Journal of Nuclear Materials 122 & 123 (1984) 1201-1212.
4. E. Ruedl, V. Coen, T. Sasaki, and H. Kolbe, "Phase Stability and Corrosion of Cr-Mn Austenitic Steels Exposed to Pure Lithium," Journal of Nuclear Materials 122 & 123 (1984) 1247-1251.
5. T. A. Whipple, D. L. Olson, W. L. Bradley, and D. K. Matlock, "Corrosion and Mechanical Behavior of Iron in Liquid Lithium," Nuclear Technology 39 (1978) 75-83.
6. J. H. DeVan, "Compatibility of Structural Materials With Fusion Reactor Coolant and Breeder Fluids," Journal of Nuclear Materials 85 & 86 (1979) 249-256.
7. S. Malang and D. L. Smith, "Modeling of Liquid-Metal Corrosion/Deposition in a Fusion Reactor Blanket," ANL/FPP/TM-192, April 1984.
8. M. Schad, "To the Corrosion of Austentic Steel in Sodium Loops," Nuclear Technology, 50, 267 (1980).
9. M. A. Abdou, et al., "FINESSE: A Study of the Issues, Experiments, and Facilities for Fusion Nuclear Technology Research and Development (Interim Report)," University of California, Los Angeles, PPG-821, also UCLA-ENG-84-30, October 1984.

3.4.4 Tritium Recovery

3.4.4.1 Testing Needs

The tritium recovery issues depend strongly on both the breeding material and on the particular recovery method chosen. Not only are the issues for Li and ^{17}Li - ^{83}Pb completely different, but the issues for molten salt recovery or gettering to recover tritium from lithium are also completely different. The testing needs for different recovery methods are, therefore, also completely different. To identify the critical issues and testing needs to resolve these issues, a particular recovery method has to be identified.

The problems associated with tritium recovery from breeding materials are evolved around trade-offs among tritium inventory, tritium containment and tritium recovery system cost. A typical range of the parameters is listed in Table 3.4-12. A significant relaxation of any one parameter will often completely change the characteristics of the problem. The testing needs will then need to identify a process which can be scaled to a fusion reactor that satisfies the three parameters simultaneously.

Table 3.4-12. Parameter Ranges for Tritium Recovery Systems

Blanket tritium inventory	.5 to 5 kg
Tritium recovery system cost	10×10^6 to 100×10^6
Tritium leakage rate	10 to 100 curies/d

The testing needs are to determine a process which can recover tritium to an acceptable concentration and to reprocess it under an acceptable economic constraint. The tritium containment is dependent on structural material, operating temperature and power conversion systems. The process identified must reduce the tritium partial pressure to a level consistent with the power system design.

3.4.4.2 Tritium Recovery Process

Since the issues and facilities required for tritium recovery process are entirely different for different processes, it is necessary to identify the most promising process for each breeding material and develop a testing

scenario for that process. To identify the feasibility and scenarios for all the processes proposed will be clearly beyond the resources available for FINESSE. The process identified here is judged to be most promising at this time. It does not suggest, however, that this is the only recovery process to be studied in the future. The status of tritium recovery process development is such that none of the methods have been positively identified as completely satisfactory.

Tritium Recovery from Lithium: The solubility of tritium in lithium is very high. The pressure concentration relationship is

$$C = K_s \sqrt{P} \quad (3.4-17)$$

where

C is concentration in wppm,
 P is pressure in Torr, and
 K_s is Sievert's constant in wppm/ $\sqrt{\text{Torr}}$.

K_s has been measured and is

$$K_s = 39 e^{5220/T} \quad (3.4-18)$$

Current wisdom has defined $C_s = 1$ wppm, which corresponds to approximately 1 kg tritium inventory in the breeding material for a self-cooled lithium blanket. At this concentration at 500°C, the equilibrium tritium partial pressure over lithium is 9×10^{-10} Torr. Most problems associated with tritium recovery from lithium are caused by this very low pressure. Since the pressure is so low already, the tritium containment is usually not a serious problem.

Three tritium recovery methods have been experimentally studied. These are molten salt extraction,¹ permeation window² and gettering.³ The molten salt extraction system has been demonstrated to be capable of recovering tritium from lithium to a concentration relevant to fusion applications and is, therefore, chosen as the candidate method for the FINESSE study. The key problem is how to scale the system to reactor levels. The stability of the molten salt dissolved in lithium and its impact on the corrosion of lithium to structural material is also yet to be answered. However, the critical issues

are clearly identifiable and developed programs can be outlined.

The key problem associated with the tritium recovery process by gettering and permeation window is caused by the low tritium partial pressure over lithium. To recover 500 g/d of tritium at 9×10^{-10} Torr, a purge gas flow rate or vacuum pumping rate of 5×10^{10} liter/sec has to be processed. It is clearly beyond the capability from economic considerations to process such a high flow rate. For the gettering process, if gettering and regeneration occurs at the same temperature, the regenerating pressure has to be equal to or less than the gettering pressure. To reduce the flow rate to a reasonable value ($\sim 10^6$ liter/sec), the gettering will have to be at $200 \sim 250^\circ\text{C}$ and regeneration $\sim 800^\circ\text{C}$. For such a system, the gettering area acts as the cold trap and the effect of corrosion products deposited on the gettering may be large. For the permeation window process, the downstream pressure has to be equal to or less than the upstream pressure, i.e., 9×10^{-10} Torr. To reduce the problem, it is suggested that a palladium layer is used to cover the downstream side of the permeation window. The palladium will act as a catalyst to oxidation for the tritium so that the downstream tritium will be in the form of T_2O instead of T_2 . By doing so, the partial pressure of T_2O can be much higher than the upstream partial pressure of T_2 . However, the oxide layer on the downstream side of the window may have a detrimental effect on the permeation rate. The potential problems associated with the gettering and permeation window processes have to be assessed further.

Tritium Recovery from LiPb: In contrast to the lithium system, for which tritium recovery processes have been verified experimentally, no experimental work has been carried out for tritium recovery process for LiPb. Whereas the key problem for tritium recovery from lithium is tritium inventory, for LiPb the key problem is tritium containment. The Sievert's constant for LiPb is about $60 \text{ wppm/Torr}^{1/2}$ compared to $3.3 \times 10^4 \text{ wppm/Torr}^{1/2}$ for Li. Therefore, a very efficient tritium recovery system is required for LiPb to reduce the tritium partial pressure to an acceptable level.

Three different tritium recovery schemes from LiPb have been proposed. These are inert gas purging,⁴ vacuum droplets degassing,⁵ and multiple-stage counter current extraction.⁶ All the processes try to take advantage of the high tritium partial pressure to recover tritium from gas phases. The key

problem is due to the required efficiency of the recovery system. Therefore, the recovery system must handle a large stream of LiPb - probably the entire coolant stream - and the fractional recovery has to be high so that liquid phase diffusion becomes an important step. It is judged that the multiple-stage counter current extraction system is the most promising scheme due to its simplicity. A program has been developed to study the feasibility of using this process for tritium recovery.

3.4.4.3 Modeling, Analysis and Scaling

Tritium recovery from lithium: Very little work in modeling and analysis can be done in the molten salt tritium recovery system from lithium. The feasibility of the system has been demonstrated¹ to the tritium concentration level relevant to fusion applications. The key problem is the potential compatibility problem caused by the halide salt dissolved in lithium and being carried back to the blanket. Due to either radiation, EM effects or just chemical effects, the dissolved halide salt may cause problems in corrosion, structural embrittlement and activation problems. The potential problems associated with compatibility can be evaluated only by experimental methods. Modeling and analysis alone will not be sufficient to evaluate the severity of the problem.

The scaling of the system to the size of a reactor relevant system can be done and the cost of the tritium recovery system can be estimated reasonably accurately.

Tritium recovery from LiPb: If a multiple-staged tritium extraction system is used for tritium recovery from LiPb, a relatively simple mass transfer calculation can be done for modeling and analysis of the system. The key parameters required are the diffusivity of tritium in LiPb and the surface recombination constants of recombining T on the surface of LiPb to form T₂ (or HT). A straightforward mathematical model can be written for the mass transfer process within the LiPb droplet to the surface and released to the purge gas. Some initial work has started to measure the relative importance of the diffusion and surface recombination, but no definite results have been made available.

A gas to liquid counter-current extraction system has been widely in use in the chemical industry for a long time. Therefore, scaling the system to a reactor size can be done with confidence and the cost of the tritium recovery system can be estimated accurately.

3.4.4.4 Test Scenarios

Test Scenarios for Lithium: The feasibility of the molten salt extraction system has been demonstrated by the work at ANL.¹ Therefore, the next step is for system demonstration. A continuous extraction loop process, with relevant temperature and tritium concentration, and with a size extrapolatable for cost scaling purposes has to be used for the next step.

There are two key issues to be evaluated. The first is to recover a significant amount of tritium from lithium in a continuous process for a significant amount of time. The second is to investigate the possible material compatibility problem with salt dissolving in lithium and with lithium dissolved in salt. A three-step test scenario is recommended.

1. Continuous Tritium Recovery Process Loop: A mock-up blanket is used for introducing tritium and estimating the impurity level in the lithium. A continuous mixer/separators is used to intimately mix the salt and lithium and transfer the tritium to the salt. An electrolytic salt processing tank is used to recover the tritium from the salt. For system demonstration, a tritium throughput rate of ~ 10 g/d and a lithium flow rate of ~ 120 g/sec will be required. Therefore, the system can be reasonably small.
2. Corrosion Experiments: The impurity level of salt dissolved in lithium can be measured in the tritium recovery process loop. The salt level can be added to lithium as part of the corrosion experiment, as discussed in Section 3.4.3. Since corrosion will study the impact on impurity level, it is logical to study the impact of salt as a possible candidate for impurities.
3. Integrated Tritium System Loop: This facility basically integrates the continuous tritium recovery process loop and the corrosion experiments to demonstrate a continuous and self-sufficient blanket tritium system.

Test Scenarios for LiPb: Since a very efficient tritium recovery system is required for LiPb, the transport mechanism of tritium in LiPb has to be

demonstrated first. The diffusivity and recombination constant of tritium in LiPb have to be measured. With this information, the size of the recovery system, the number of stages of the recovery system, and the amount of hydrogen to the helium purge gas can be calculated. The calculation can be very accurate with the availability of this information.

A small loop can be constructed with the main component being the He/LiPb counter current extraction column. The tritium transferred to the purge can be absorbed in a Y-gettering bed and recovered periodically. Since vapor pressure for both LiPb and Y are very low, it is expected that impurity transport to LiPb can be small the remain to be within the design limits for an extended period of time. With the accumulated knowledge from either design or operation of the extraction system in the chemical industry, it is expected that scaling the reactor level is straightforward.

3.4.4.5 Facility Descriptions

Lithium System: The issues to be resolved for a molten salt extraction system are tabulated in Table 3.4-13. The issues can be separated into two categories; i.e., the separation and recovery of tritium from lithium and the impact of the tritium recovery system to the operation of the primary loop. The first category involves the operation of a continuous tritium recovery process loop and the facility required is described below. The second category involves mainly the compatibility between salt contained lithium and the structural material. The corrosion experiment will study this effect with the salt being treated as an impurity in the lithium.

The flow diagram of the continuous tritium recovery process loop is shown in Figure 3.4-9. The main components are the mixer/separator and the electrolytic salt processing tank. The system is very small, with a tritium throughput of 10 g/d and lithium flow rate of 120 g/sec.

The key function of the mixer/separator, as shown schematically in Fig. 3.4-10 is to intimately mix the tritium contained lithium and the tritium-free salt. The LiT in the lithium, being a salt-like chemical, will be preferably dissolved in salt. The impurities in the lithium, such as O, N and C will similarly be dissolved in salt. The salt and lithium can then be separated by using centrifugal force. The separating efficiency between lithium and

Table 3.4-13. Some Operational Considerations for the Molten Salt Extraction Process

1. Tritium distribution
2. Mutual solubilities
3. Phase separation
4. Perturbation on neutronics
5. Fabrication of equipment
6. Corrosion
7. Recovery of tritium from the salt

salt in a real system will be important.

The key function of the electrolytic salt processing tank is to use the electrolysis process to decompose LiT to recover tritium. The decomposition potential for LiT is ~ 1 volts while that of salt is ~ 3 volts. Therefore, a potential difference of 1 volt is to be established across the processing tank. LiT will decompose while salt will remain intact.

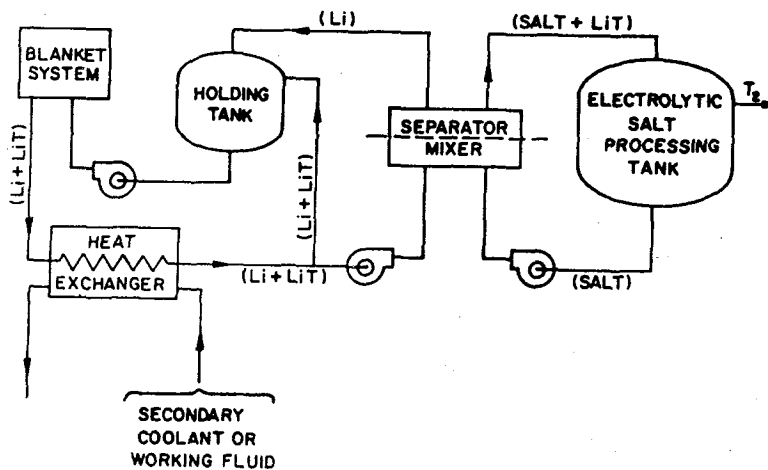


Figure 3.4-9. Flow diagram of the continuous tritium recovery process loop

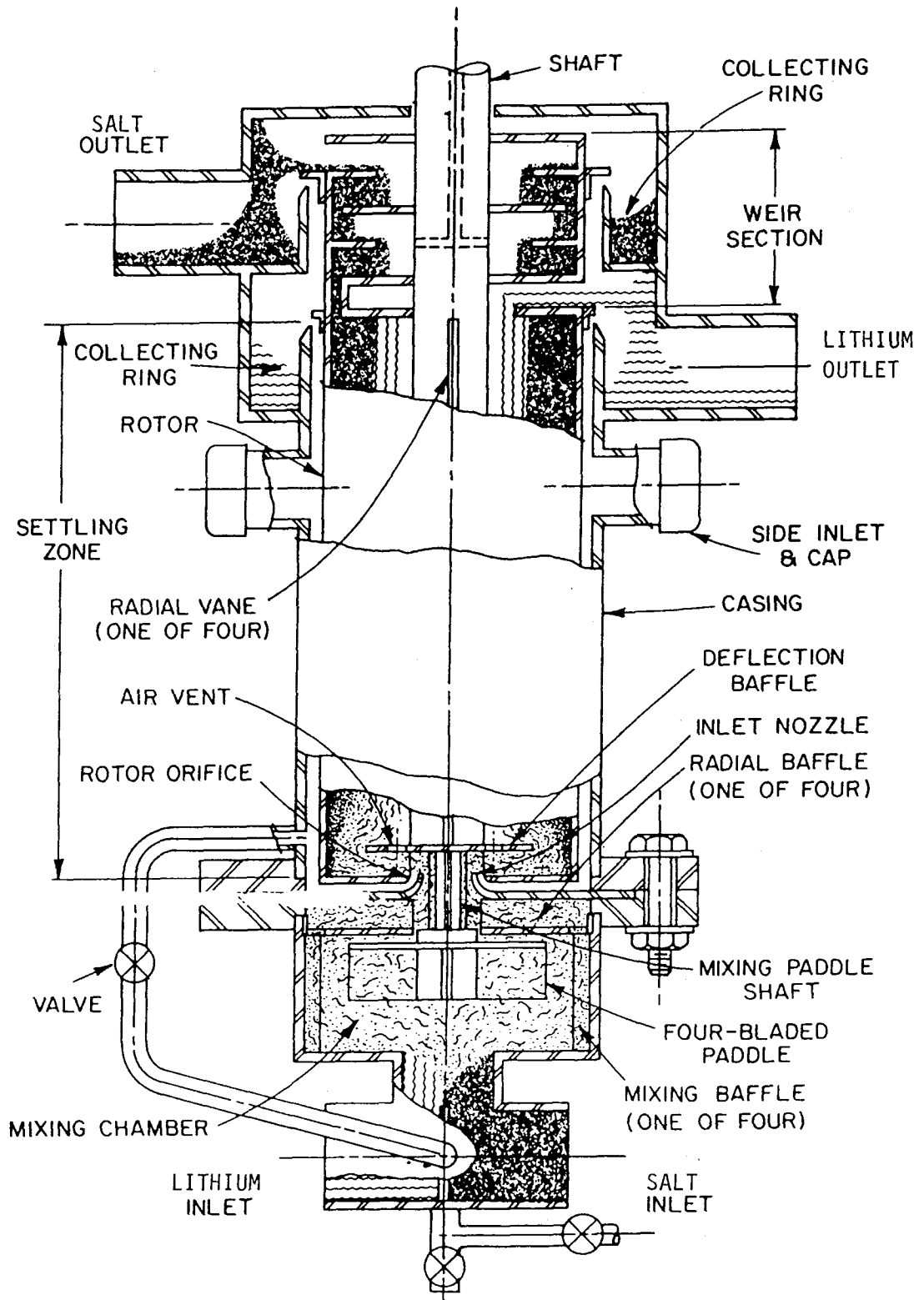


Figure 3.4-10 Conceptual design of the mixer/separator

Table 3.4-14. Summary of Analytical Methods for Impurity Measurement

SUMMARY OF ANALYTICAL METHODS

Element	Method	Specificity	Reliable Detection Limit	Remarks
Nitrogen	Micro-Kjeldahl	Nitride (Li ₃ N)	50 wppm	Cross checks with ORNL within 20%
Oxygen	Fast neutron activation (ORNL)	Nonspecific	50 wppm	Tedious, requires meticulous sample handling
Carbon	Acetylene evolution (GC detection)	Acetylide (Li ₂ C ₂)	5 wppm	CO ₂ present in GC scans, source unknown
Deuterium	Gas evolution (permeation)	Nonspecific	5 wppm	Tedious (2 weeks per sample)
Hydrogen	Gas evolution (permeation)	Nonspecific	100 wppm	Difficult to determine background correction factor
Tritium	Liquid scintil- lation counting	Nonspecific	Sub-ppb	No problem here

To verify the tritium recovery process and the cleaning up of the impurities, an analysis method has to be established for detecting the concentration. Table 3.4-14 summarizes the possible method to measure the impurity level down to the ppm region.

LiPb System: The system described here has been developed as part of the BCSS study.⁶ It is based on a multiple-stage, gas/liquid extraction system as has been used in chemical industries for decades. At each stage, openings are provided for both downward LiPb flow and upward He purge flow. The counter-current flow of LiPb and He in between any two stages is where the mass transfer mechanism occurs. To improve the recovery process, hydrogen may be added in the purge to reduce the purge gas flow rate, as well as reduce the resistance to the mass transfer due to of surface recombination.

A typical set of parameters for the tritium recovery system is summarized in Table 3.4-15. The system will be allowed to operate long enough so that steady-state process can be established. The steady-state tritium partial pressure in the He purge gas is between 10^{-5} to 10^{-6} Torr. A Y-gettering bed will be used to recover the tritium which can then be regenerated and fed to the tritium process loop, such as TSTA.

The impurity level of the proposed tritium recovery process can be controlled and should not have a major impact on the operation of the reactor. The key results to be identified are the efficiency of each recovery stage as a function of tritium concentration, hydrogen partial pressure, purge gas flow rate as well as the temperature.

Table 3.4.15. LiPb Tritium Recovery System Parameters

Extraction column cross-sectional area	1 m ²
Column height	2.5 m
Number of extraction stage	20
LiPb flow rate	100 liter/sec
Purge gas flow rate	10^3 to 10^4 liter/sec
Purge gas pressure	100 kPa
Purge gas temperature	400 to 600°C
Hydrogen partial pressure	0 to .01 kPa
Tritium concentration in LiPb	.04 to .1 wppm

References for Section 3.4.4

1. V. A. Maroni, R. D. Wolson and G. G. Staahl, "Some Preliminary Considerations of a Molten Salt Extraction Process to Remove Tritium from Liquid Fusion Reactor Blankets," Nucl. Technol. 25, 83 (1976).
2. R. E. Buxbaum, "The Use of Zirconium-Palladium Windows for the Separation of Tritium from the Liquid Metal Breeder Blanket of a Fusion Reactor," J. Separation Science and Technology, 18, 1251-73, (1983).
3. S. D. Clinton and J. S. Watson, "Tritium Removal from Liquid Metals by Absorption on Yttrium," Proceedings of the 7th Symposium on Engineering Problems of Fusion Research, Knoxville, TN, Oct. 25-28, 1977.
4. B. Badger, et. al., "WITAMIR - A University of Wisconsin Tandem Mirror Reactor Design," UWFD-400, 1980.
5. K. E. Plute, et. al., "Tritium Recovery from Lithium-Lead by Vacuum Degassing," Nuclear Technology/Fusion, Volume 4, No. 2, Part 3 (1983).
6. D. K. Sze, "Counter-Current Extraction System for Tritium Recovery from ^{17}Li - ^{83}Pb ," Fusion Technology, Volume 8, No. 1, Part 2A (July, 1985).

3.4.5 MHD Insulators

3.4.5.1 Introduction

A very effective means of eliminating most of the MHD-related issues is the use of electrical insulators to limit the amount of induced current in the liquid metal, and as a result, reduce the MHD pressure drop. Although the use of insulators can be viewed as a blanket design complexity, the resulting reduction in electromagnetic interaction can actually lead to simplified overall designs.

There are three possible methods for the reduction of MHD interaction through the use of insulators: laminated structures, insulating coatings, and resistive interfacial layers.

a. Laminated structures consist of a thin liner in contact with the liquid metal coolant and a thicker, pressure-bearing outer wall. The liner is electrically insulated from the outer wall. This approach essentially decouples the MHD pressure drop, which is proportional to the liner thickness, from the pressure-bearing wall, and allows designs with smaller conductance ratios. The reduction in pressure drop is proportional to the ratio of liner thickness (~ 0.2 mm) to the wall thickness in designs without insulators (~ 1.0 mm). Therefore, a five-fold reduction in pressure drop can be achieved. As an additional benefit, the stresses in the structural wall can be made smaller by increasing the wall thickness without any negative impact on the MHD pressure drop.

b. An insulating coating may be applied directly to the inner duct surfaces. Such coatings will change the thin conducting regime of MHD flow to an insulating wall regime. The reduction in fully developed flow MHD pressure drop is then an order of $M \cdot C$ (where M is the Hartmann number and C is the wall conductance ratio), which for most blanket designs exceeds 10^2 . Of course, such a large reduction is not necessary. Insulating coatings are attractive not so much because of the larger reduction in pressure drop that can be achieved, but because a blanket with insulating coatings will be easier to fabricate than one with a laminated structure. On the other hand, insulating coatings must satisfy a more stringent set of functional requirements than do laminated structures, including compatibility with the liquid metal coolant.

c. Submicron thick resistive interfacial layers can be formed, in principle, by proper additives to the liquid metal and/or the structural alloy. The reduction in pressure drop can be comparable to that which can be achieved through the use of insulating liners. The significant advantage of this approach is that the fabrication of the blanket will be no more difficult than that of a bare wall design. Although most compounds which can form at the interface (oxides and nitrides) have adequate resistivities for significant pressure reduction, a development effort to identify those layers which are stable and maintain their integrity under blanket operating conditions should be carried out.

3.4.5.2 Testing Needs for MHD Insulators

The general requirements of electrical insulators for blanket applications are given in Table 3.4-16. Testing will be needed to demonstrate the achievement of acceptable values in each of these categories, but resistivity before and after irradiation is the most critical parameter.

Resistivities of about 10^2 ohm-cm or larger are required for any of the applications listed above to show substantial improvement to the pressure drop (several fold reduction). Because of the absence of an internal conducting shell, coatings and resistive interfacial layers offer the potential for orders of magnitude reduction in pressure drop. This level of performance will require the achievement of resistivities greater than about 10^4 ohm-cm.

Table 3.4-17 shows a number of candidate insulators and their respective ratings with respect to the issues. Inspection of the table reveals a number

Table 3.4-16. Issues for MHD Insulators

-
- adequate electrical resistivity
 - stability in contact with the coolant and structure
 - radiation stability
 - mechanical integrity
 - fabricability
 - low activation
 - low cost
-

of promising candidates.

3.4.5.3 Test Scenarios

Because use of insulators results in significant improvement in design and performance of liquid metal cooled blankets, a development and testing effort in this area is warranted. Testing for chemical and radiation stability, mechanical integrity, and radiation induced resistivity degradation is not peculiar to insulators for blankets, and can be carried out along the same lines as similar testing which has been done for other applications.

Testing in MHD loops is not required for the laminated structure, because this case is not fundamentally different from the thin conducting wall tests which will be conducted for MHD flow phenomena, as described in section 3.4.1. The flow characteristics for fully developed flow in the presence of resistive interfacial layers are not different from those for laminated structures, and testing would not be required if only fully developed flow was of interest. However, because in three dimensional MHD situations the flow structure may be different in the presence of resistive layers than it would have been for corresponding thin wall cases, analysis and testing must be carried out for thin conducting walls with interfacial resistive layers. This effort will be identical to that suggested for the bare wall cases.

Finally, the use of insulating coatings will necessitate additional testing and analysis because the MHD regime is that of insulating walls. In the insulating wall regime, three dimensional MHD effects persist for much longer distances than they do in the thin conducting wall regime. Therefore, the design of the experimental program should accommodate this increased length. On the other hand, because in this case the MHD pressure drop is very low, coolant velocities can be increased for effective first wall cooling, and the overall blanket design can be simplified to one involving long, essentially straight ducts with bends in planes normal to the magnetic field vector. As a result, the breadth of the experimental program will be reduced to the extent necessary to address the MHD issues relevant to such simplified designs.

For both thin walls with resistive layers and walls with insulating coatings, the liquid metal/wall chemistry is important in determining the resistivity and the integrity of the interfacial layers. Therefore, such testing should be conducted at prototypical temperatures.

3.4.6 Electromagnetics

3.4.6.1 Testing Needs

Magnetic field transients generate voltages and eddy currents in the structure and coolant, which can lead to several effects, including:

1. additional stresses in the blanket
2. effects on fluid flow
3. delays in field penetration
4. arcing, leading to insulator damage and welding of structures
5. forces on the disruption melt layer, tending to enhance material losses.

In addition to transient effects, ferritic steel structures will exhibit forces at steady state due to ferromagnetism. Table 3.4-18 summarizes the electromagnetic testing issues. Transient effects on flow are absent, since they are considered as a subset of MHD effects.

Electromagnetic effects are not usually considered as feasibility issues because the stresses generated are usually controllable to less than 5-10% of the allowable design stresses. However, because the size of the design window can be very small, the inclusion of effects such as these can contribute to the elimination of a design or restriction of its acceptable operating parameter space.

Disruption effects are the most critical electromagnetics issue. The rapid time constant for disruptions, together with the potential to transfer nearly all of the plasma current, can lead to very large forces in the blanket. These forces are distributed throughout the first wall and blanket, and cause stresses in the main body of the blanket as well as stress concentrations at support points.

The interaction of the plasma current with the surrounding structures is most intense closer to the plasma. Therefore, the most serious effects are likely in the first wall and plasma interactive components. However, deep blanket penetration is possible depending on the details of the geometry and the conducting paths available. Deep penetration effects are most likely when sectors are not electrically well connected. This is particularly serious for liquid metal blankets, in which the effective blanket conductivity is tens to hundreds of times larger than for solid breeder blankets.

Table 3.4-18. Electromagnetics Issues

-
1. Stresses due to Disruptions and other Field Transients
 2. Disruption Melt Layer Stability
 3. Arcing due to Induced Voltages (and insulator breakdown)
 4. Time Constants for Control Field Penetration
 5. Stresses in Ferromagnetic Materials
 6. Effects of Ferromagnetic Fields on Plasma Stability
-

In addition to concerns over forces, electromagnetic effects also relate to plasma operation, maintainance requirements, and neutron streaming issues. Design conflicts related to electromagnetics include:

1. Neutron streaming. In order to avoid neutron streaming between blanket modules, small gaps are desired. However, small gaps will lead to the possibility of arcing and/or welding between blanket modules. Electrical insulators are not expected to work effectively close to the first wall due to their low radiation tolerance.

2. Remote maintainance. It is desirable to segment the blanket in order to make remote maintainance more proctical. However, poor conductivity between blanket modules results. This in turn can lead to large asymmetric forces from the interaction of radial and poloidal eddy currents with the toroidal field during magnetic field transients. Asymmetric radial and poloidal eddy currents will also affect plasma operation. Electrical connectors may be used, but their effectiveness in reducing radial currents and their impact on maintainance are uncertain.

3. Plasma control. Toroidal conducting paths are desirable to minimize structural effects, but time constants for field penetration increase with the conductivity. Long time constants make plasma start-up and position control difficult. Conducting and/or ferromagnetic structures near the plasma will also impact plasma stability.

In the area of electromagnetics, testing needs are strongly tied to modeling efforts, since the primary need for experiments is to test the validity of alternative models and their ranges of applicability.

The uncertainties in quantifying electromagnetics effects relates primarily to the complexity of the phenomena and not a lack of data or theoretical understanding. The theory of electromagnetics is well understood; the principal set of equations -- Maxwell's equations -- have been thoroughly understood for many years. However, the complex geometry of fusion components and the interaction with neighboring systems makes the problem difficult to solve. There are many physical assumptions which are commonly made and approximations which lead to a more tractable numerical problem.

In addition to basic electromagnetic interactions, some important phenomena may require modeling of the electromechanical coupling to the structural response of components. In this case, the complete set of equations includes both electromagnetics and structural mechanics.

There is wide acceptance of the value of numerical modeling for transient eddy current problems; however, there are a large number of alternative approaches to solving the complex set of equations. Three dimensional computer models do not currently exist which can adequately model fusion applications. This is due to the prohibitively large problems which result from direct modeling of three-dimensional structures such as a tokamak. The most common approach attempted today is to use two-dimensional codes and other simplifications to make the problem more tractable. There has been an increase in modeling activity in recent years, and experimental verification of the validity and applicability of these models is needed.

3.4.6.2 Modeling Needs

As evidenced by the proceedings of the COMPUMAG conferences^[1-4] and other workshops on electromagnetic effects,^[5] there exists a large number of computer models which have been or are currently being developed for transient eddy current calculations. The large majority of codes are two dimensional; the need for three dimensional codes will not be entirely apparent until experimental results establish the range of validity of the existing codes. If a three dimensional code does prove to be essential, then it is likely that specialized codes will be developed under different sets of simplifying assumptions.

3.4.6.3 Analysis and Scaling

Blanket Time Constants

Blanket electromagnetic time constants and levels of induced current for both liquid metal and solid breeder blankets are roughly estimated in this section. Simple modeling is used in order to demonstrate the fundamental scaling laws. Time constants are important indicators of the importance of electromagnetic effects, such as penetration of control fields, forces in the structures, and effects on the plasma. Longer time constants generally indicate better coupling of field transients into the structure, and therefore larger induced fields and larger forces.

There are two types of time constant considered here. The rate of decay of currents in the blanket is determined primarily by the self-inductance time constant, L/R , where L is the effective blanket self-inductance and R is the effective blanket resistance. The degree of coupling of the blanket to the plasma is measured by the mutual inductance, M . The total amount of current transferred can be related to both L and M in the following manner.

A simple diagram of the plasma/blanket equivalent circuit is given in Figure 3.4-11. The governing equation is:

$$M_{pb} \frac{dI_p}{dt} + L_b \frac{dI_b}{dt} + R_b I_b = 0 \quad (3.4-19)$$

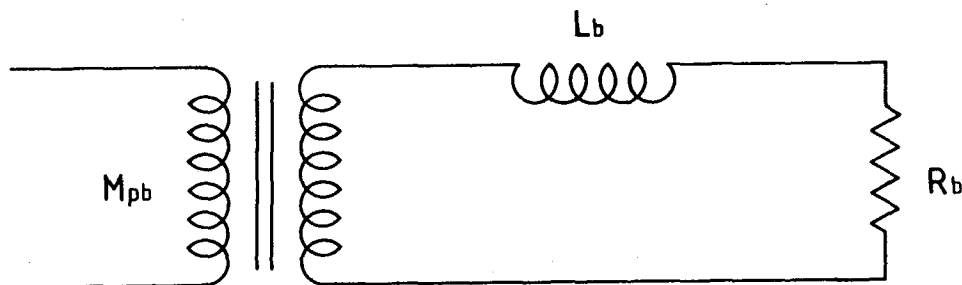


Figure 3.4-11. Plasma-blanket equivalent circuit

Fourier analysis of this equation leads to:

$$\frac{I_b}{I_p} = \frac{M/L}{\sqrt{1 + (R/\omega L)^2}} \quad (3.4-20)$$

The frequency, ω , is related to the inverse of the transient time constant. Equation 3.4-20 indicates that for a very rapid transient, the amount of current transferred to the blanket is proportional to M/L . For a slow transient, the induced current is proportional to $\omega M/R$.

In this analysis, a simplified geometry is considered as shown in Figure 3.4-12, with the following assumptions:

1. cylindrical geometry (no effects from toroidicity)
2. the blanket is segmented toroidally
3. poloidal continuity of fields (perfect coupling between poloidally neighboring blanket segments)
4. $a/R \ll 1$ ($1/R$ dependence of field is negligible)
5. $a/w \ll 1$ (negligible end effects)
6. no time dependent variations of toroidal flux (together with assumption 3, this implies that currents are confined to (r, ϕ) planes).

For a discrete circuit element, the self and mutual inductances are easily determined as constant quantities. However, for distributed structures, such as a blanket module, there is no single time constant: the time-

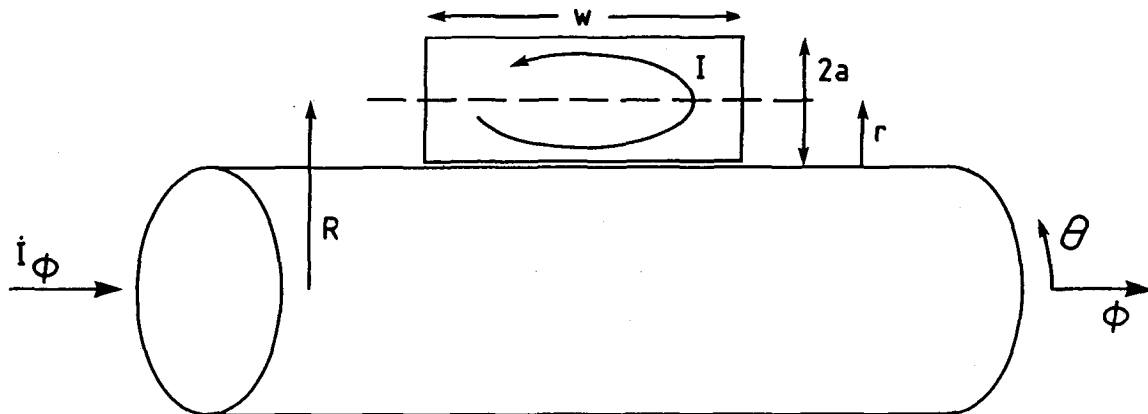


Figure 3.4-12. Geometry for calculation of blanket time constants

dependent current response depends on the current distribution throughout the structure and plasma, both of which vary in space and time. Therefore, for this analysis the time constant is approximated simply by the ratio of twice the magnetic energy to the resistive power:

$$\tau = \frac{2\varepsilon}{p} \quad (3.4-21)$$

where ε is given by

$$\varepsilon = \frac{1}{2\mu_0} \int B^2 dv \quad (3.4-22)$$

p is given by

$$p = \int \eta j^2 dv \quad (3.4-23)$$

and the integrals are performed over the entire current-containing volume. A current density spatial distribution is assumed for this calculation; it is demonstrated that the actual value of the time constant is not very sensitive to the exact choice of current density distribution. This simplified analysis then does not provide a solution for the actual current profile evolution.

Once the current distribution is specified, the magnetic field (used in the energy calculation) can be computed from Ampere's law:

$$\int B \cdot d\ell = \mu_0 I$$

or (3.4-24)

$$B = \mu_0 \int j dr$$

This equation together with the assumed current distribution allow an estimation of the blanket self-inductance. For the coupling of the plasma to the blanket, the field used in the energy calculation must be obtained from the plasma current. The current density in this case is obtained using Faraday's law:

$$\int E \cdot d\ell = - \frac{d\Phi}{dt} \quad (3.4-25)$$

When the blanket is segmented toroidally and $a/w \ll 1$, currents flow

largely in the toroidal direction but in opposite directions in the front and back of the blanket, as shown in Figure 3.4-12 (front refers to the region closest to the plasma and back refers to the region closest to the magnets). If we assume a flat current distribution for a liquid metal blanket as shown in Figure 3.4-13, then:

$$|j| = j_0 \quad (3.4-26)$$

$$B = \begin{cases} \mu_0 j_0 r & r < a \\ \mu_0 j_0 (2a - r) & r > a \end{cases} \quad (3.4-27)$$

The integrals are straightforward and yield:

$$2\epsilon = [2/3] \mu_0 j_0^2 2\pi R w a^3 \quad (3.4-28)$$

$$p = \eta j_0^2 2\pi R 2wa \quad (3.4-29)$$

and the "L/R" time is:

$$\tau = 1/3 (\mu_0/\eta) a^2 \quad (3.4-30)$$

In general, for any specified current distribution, the time constant is given by

$$\tau = c [j(r)] (\mu_0/\eta) a^2 \quad (3.4-31)$$

where c is a constant. Following the same procedure for a linearly varying current, as given in Figure 3.4-14, the current and field are given by

$$j = j_0 \frac{r-a}{a} \quad (3.4-32)$$

$$B = \mu_0 j_0 \left(\frac{r^2 - 2ar}{2a} \right) \quad (3.4-33)$$

and we obtain $c=2/5$.

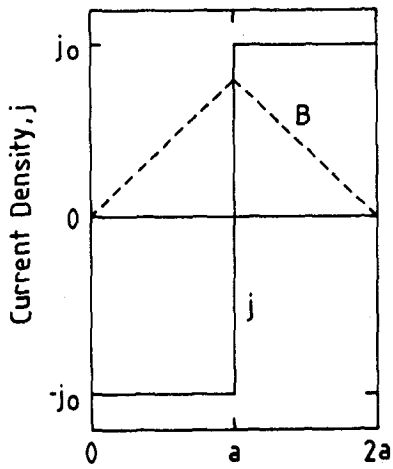


Figure 3.4-13. Flat current distribution

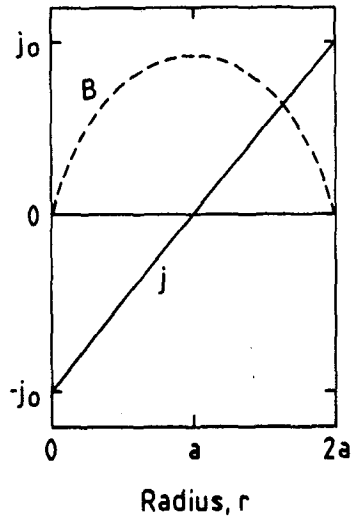


Figure 3.4-14. Linear current distribution

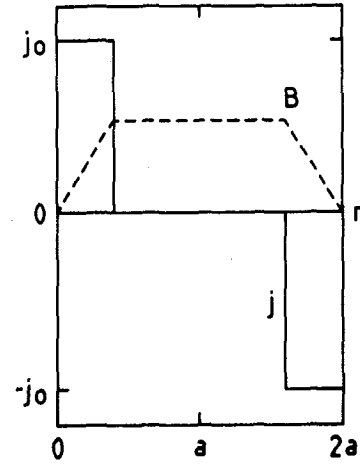


Figure 3.4-15. Surface current distribution

Shorter time constants are found in liquid metal blankets for times immediately following a rapid current transient which induces the blanket currents. This is because the blanket currents must penetrate into the bulk structure from the surface. This case is also a good approximation for solid breeder blankets, which contain the majority of the induced currents in the thin walls surrounding the blanket module. Figure 3.4-15 shows the surface current distribution of depth δ which results in an approximately uniform field (remember $a/R \ll 1$).

$$j = \begin{cases} j_0 & r < \delta \text{ or } r > 2a - \delta \\ 0 & \text{otherwise} \end{cases} \quad (3.4-34)$$

$$B = \mu_0 j_0 \delta \quad (3.4-35)$$

For this case, $c = \delta/a$ and $\tau = a\delta\mu_0/\eta$.

For the calculation of the mutual inductance between the plasma and the blanket, it is necessary to remove the assumption of an infinitely long

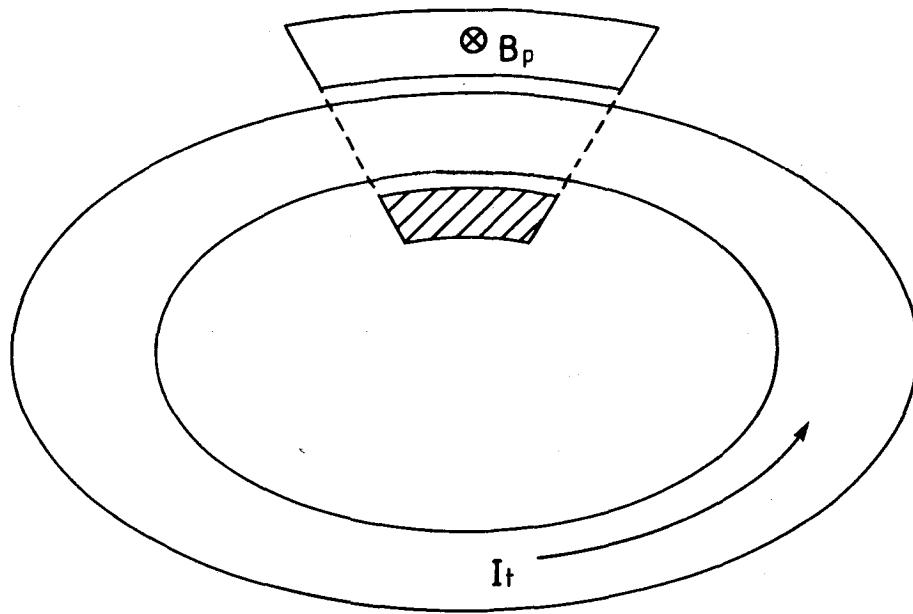


Figure 3.4-16. Coupling of blanket flux to the plasma (shaded region indicates all of the flux passes through the core of the torus)

cylinder. If the plasma is now viewed as a torus interlocking the toroidal blanket sector as shown in Figure 3.4-16, the poloidal flux through the hole in the plasma is equal to the total flux through the blanket. In other words, the plasma toroidal current is driven by the same quantity of flux which drives the blanket current. The mutual inductance M_{bp} is therefore equal to the blanket self-inductance. Hence, M_{pb} is also equal to L .

If the plasma transient is relatively slow compared to the blanket time constant, then the field penetrates freely. Under the large plasma radius assumption ($a \gg R$), the field is approximately constant throughout the blanket; the induced current by Faraday's law is a linear function of r . We can therefore use the value of c computed above, $c=2/5$, to evaluate L/R . At high frequency, the surface current distribution should be used to compute L/R .

Evaluation of Time Constants

The data in Table 3.4-19 is used to estimate the actual time constants

and coupling factors in both solid and liquid breeder blankets. For liquid lithium blankets, the ratio μ_0/η is approximately 4. The self-inductance time constant is therefore of the order $1.6-4 a^2$, or for a half meter deep blanket $\tau \approx 100$ msec. For a steel walled solid breeder blanket, $\tau \approx 2a\delta$; and for a 1/2 cm first wall $\tau \approx 2.5$ ms.

The current ratio (I_b/I_p) for a liquid metal blanket ($\tau=100$ ms) and a 25 msec plasma disruption time is approximately 97%. Longer disruption times result in poorer coupling: hence, for a 100 msec disruption time the current ratio is 70%, and for a 250 msec disruption time the current ratio is 37%.

Scaling Laws for E&M

When designing experiments, it is possible to achieve an accurate representation of electromagnetic effects under scaled conditions. Depending on the phenomenon of interest, several different scaling relations may apply. Table 3.4-20 lists the relevant dimensionless ratios which must be preserved in order to maintain electromagnetic behaviors. The most critical is generally the magnetic Reynolds number. But in cases where thermal, structural, or voltage responses are important, the other scaling laws can be equally important.

Table 3.4-19. Data for Evaluation of Time Constants (Units in mks)

$$\begin{aligned} \mu_0 &= 4\pi \times 10^{-7} \\ \eta(\text{Li}) &\approx \pi \times 10^{-7} \\ \eta(\text{SS}) &\approx 7 \times 10^{-7} \end{aligned}$$

approximate plasma resistivities: (Z=1)

100 eV	5.0×10^{-7}
1000 eV	0.158×10^{-7}
5000 eV	0.014×10^{-7}

Table 3.4-20. Scaling Relations for Electromagnetic Effects

1. Magnetic Reynolds number: ratio of magnetic diffusion time to transient time.	$Re_m = \mu \sigma d^2 / \tau, \quad (\tau = \dot{B}/B)$
2. Ratio of magnetic pressure to applied stress or yield stress.	$\frac{B_e^2 / 2\mu_o}{\sigma_a}$
3. Ratio of induced forces to applied stress or yield stress.	$\frac{JL B_e}{\sigma_a}$ or $\frac{\mu_o J^2 L^2}{\sigma_a}$ (induced field $B_i \sim \mu_o JL, J \sim \sigma \dot{B}L$)
4. Non-dimensional field gradient.	$\frac{\nabla B L}{B}$
5. Ratio of breakdown voltage to induced voltage (arcing).	$\frac{V_b}{\dot{B}L^2}$
6. Scale length ratios.	
7. Ratio of thermal diffusion time to magnetic diffusion time.	$\frac{\mu \sigma k}{\rho C_p}$
8. Ratio of thermal diffusion time to transient time.	$\frac{\rho C_p d^2}{k \tau}$
9. Ratio of magnetic to inertial forces.	$\frac{JB\tau^2}{\rho L}$ or $\frac{\sigma \dot{B}B\tau^2}{\rho}$

3.4.6.4 Electromagnetics Test Facilities

Table 3.4-21 shows the test conditions necessary to address the electromagnetics issues. These conditions can be achieved through a combination of plasma confinement devices and electromagnetic test stands.

As confinement devices become larger, many of the issues relating to electromagnetics will become more and more evident. It is expected that issues relating to plasma stability and plasma control field penetration will be resolved in next generation confinement devices.

Table 3.4-21. Test Requirements for Electromagnetics Issues

	High Field	Transient Field	Material Components	Neighboring Components	Heat Source	Simulation Mechanical Response	Simulation of Thermal Response	Field Geometry	Structure Geometry
Stresses due to Disruptions and Other Field Transients	X	X		X		X		X	X
Disruption Melt Layer Stability		X			X		X	X	X
Arcing due to Induced Voltages (and insulator breakdown)		X							X
Time Constants for Control Field Penetration				X				X	X
Stresses in Ferromagnetic Materials	X		X	X				X	X
Effects of Ferromagnetic Fields on Plasma Stability		X	X					X	X

Structural effects issues require both an electromagnetics test stand and a confinement or fusion experiment with blanket component simulation. An electromagnetics test stand is intended to provide a clean geometry in order to allow for most effective verification of computer codes and other models being developed. The fusion experiment will provide a correct simulation of the magnetic field transients as well as the structure geometry and neighboring components.

The FELIX experiment at Argonne National Laboratory is intended to provide the essential test conditions for an electromagnetics test stand.^[13] The device parameters for the initial facility configuration are listed in Table 3.4-22.

Table 3.4-22. FELIX Device Parameters

useful volume	0.9 m diameter x 1.2 m long
constant field	1.0 T
pulsed field	0.5 T
discharge time	10-100 ms (up to 50 T/s)

References for Section 3.4.6

1. COMPUMAG 76, Conference on the Computation of Magnetic Field, Oxford, March 31-April 2, 1976.
2. COMPUMAG 78 - Conference on the Computation of Magnetic Field, Grenoble, Sept. 4, 6, 1978.
3. IEEE Transactions on Magnetics, vol. MAG-18, no. 2, March 1982.
4. Fifth COMPUMAG Conference, Fort Collins, Colorado, June 3-6, 1985.
5. Workshop on Eddy Current Experiments, Argonne National Laboratory, September 8-9, 1983.

3.4.7 Tritium Breeding

The testing issues for tritium breeding, and neutronics in general, relate to uncertainties in basic cross section data and numerical models. The tests do not depend strongly on the type of breeding material. Therefore, the issues, testing needs, and facilities for tritium breeding in solid breeder blankets also apply for liquid metal breeder blankets. See section 4.4.6 for details.

3.5 Partially Integrated Experiments

The amount of separate and multiple effects testing which will take place in the blanket test program depends on many factors, including success of the experiments as well as practical constraints, such as time and money. At some point in time, it will become necessary to begin integrating several effects together, culminating in a completely integrated test facility.

FINESSE has identified possible steps between separate/multiple effects testing and fully integrated testing. The purpose of these partially integrated experiments is fundamentally different than for separate and multiple effects testing. The emphasis in partially integrated tests begins to shift away from understanding of basic phenomena and interactions, towards a more empirical demonstration of system performance under a large and complex number of environmental conditions. Partially integrated testing is useful in developing semi-empirical models from which reactor component performance can be predicted. A substantial cost savings can be accomplished by eliminating the need for every relevant environmental condition. For liquid metal blankets, the presence of neutrons is very expensive. Although neutrons influence most of the phenomena in the blanket, a great deal of information can be gathered in their absence to set the base level of performance. Partially integrated tests do not decrease the need for fully integrated fusion testing.

The issues for liquid metal blankets can be grouped into four major categories: thermomechanics, tritium breeding, tritium recovery, and safety. The nature of the test conditions required for resolution of each class of issue tends to be very different. This makes it possible to perform partially integrated testing in each issue class without missing a large influence from the omitted issues. For example, there are few expected interactions between tritium recovery and thermomechanics, or between tritium breeding and thermo-

mechanics. This has led us to consider the characteristics of partially integrated facilities for each issue category. Since the largest number of critical issues are related to thermomechanics, the facility which has received the most attention is the the TMIF, or Thermomechanics Integrated Test Facility. Characteristics of a TMIF experiment are presented in Section 3.5.1.

A facility which combines issues at an even more integrated level has also been considered. This facility would address thermomechanics, safety, and tritium issues together in the absence of neutrons. Tritium breeding issues could not possibly be accomodated without neutrons. The cost and benefit of this PITF are discussed below in Section 3.5.2

3.5.1 Non-Neutron TMIF

3.5.1.1 Purpose of TMIF and Its Role in the Test Plan

The TMIF is defined to be a thermomechanical proof of principal facility which would operate prior to fusion testing under non-neutron conditions. The principal difference between multiple effects testing with a large number of environmental conditions versus partially integrated testing is in the type of information obtained. Multiple effects tests are intended to explore phenomena, whereas partially integrated tests are to verify a component concept.

Table 3.5-1. Comparison of Testing Goals

<u>Phenomena Exploration</u>	<u>Concept Verification</u>
flexibility and variability of test conditions	known device parameter ranges
simple and variable geometries	relevant geometry
results coupled to model development	results coupled to design codes and application of models

Table 3.5-1 illustrates these differences in more detail.

As with any facility designed for operation beyond the next generation of facilities, the characteristics and even the very need for the facility can not be fully determined. The data obtained from single and multiple effects experiments may indicate that a TMIF is unnecessary, they may dramatically affect the facility characteristics, or they may even demonstrate that liquid metal blankets can not be made feasible under the required fusion conditions. In addition, blanket designs are likely to evolve through time. Since integrated and partially integrated tests are very design dependent, the TMIF can only be fully designed when candidate blanket systems have been chosen and refined.

Nevertheless, it is a worthwhile exercise to examine the general characteristics of a TMIF. In order to generate a consistent and meaningful overall test plan, the anticipated costs and required development steps must be estimated. The TMIF, if built, would be a very significant and costly element of the test program. In order to define the characteristics of TMIF in the absence of basic phenomenological information and in the absence of fixed, credible designs, a set of assumptions has been made to anticipate the future state of affairs. As time goes on, the design of TMIF must be modified according to new data and new design features.

3.5.1.2 Test Scenarios

The primary goal of the TMIF experiment is to operate at high temperature over extended period of time in order to demonstrate mechanical and materials behavior. However, TMIF may be the largest, most geometrically relevant test bed at the time of operation. As such, there will be a large amount of data desired to verify and calibrate predictions of pressure drop, fluid flow, and heat transfer characteristics. The amount of time required to accumulate these data is fairly small and can become very complicated at elevated temperature. A sensible approach to testing would include phases of operation, such as indicated in Table 3.5-2. In the early phase, at low temperature, the basic thermal hydraulic behavior would be verified in detail. Design improvements could be implemented on a fairly short turn-around time. The later phase at high temperature would focus on materials and mechanical behavior.

Table 3.5-2. TMIF Proposed Testing Sequence

Stage 1. Low Temperature Operation
high Hartmann number
high interaction parameter
low temperature
simple and complex geometries
Stage 2. High Temperature Operation
high Hartmann number
high interaction parameter
high temperature

Table 3.5-3. Parameter Range for TMIF

magnet length	3 m
magnet bore	.4 x .5 m
magnetic field strength	4-6 T
average coolant velocity	.1-.2 m/s
coolant ΔT	100-150 K
volumetric flow rate	.04 m ³ /s
total heat input (assuming no economizer)	13 MW
surface heat flux	.5-1 MW/m ²

3.5.1.3 Facility Description

The TMIF consists of a relatively large bore magnet inside of which the blanket test section is placed. The test section volume must accommodate the relevant design complexities of an actual blanket, while providing adequate thermal hydraulic entry lengths as commensurate with the anticipated entry lengths in a real blanket. In addition, the channels must be large enough to accommodate sufficient instrumentation, including velocity probes (for low temperature operation), thermocouples, strain gauges, etc. The approximate dimensions for the magnet are given in Table 3.5-3.

The quoted magnetic field strength is close to full scale. This is necessary to correctly match the velocity profiles which determine heat and mass transfer. If prior experiments determine that MHD effects are adequately simulated at lower fields, then this number could be reduced.

The coolant temperature rise is an important parameter for mass transfer. Keeping ΔT high also implies fairly large input power requirements. In order to maintain resolution in the velocity profile measurements, a minimum channel average velocity should be between 0.1-0.2 m/s, which leads to a power requirement of 13 MW.

Alternate methods of obtaining volumetric heating have been explored, including RF heating, induction heating, and direct heating of the coolant. Radio frequency waves have a very short skin depth in metals and do not penetrate far enough. Induction heating requires relatively low frequency currents in the liquid metal, which would disrupt the MHD currents and velocities. Direct heating of the coolant (for example through coolant pipes) would also disrupt the velocity profiles, as well as altering the current flow paths. Since no efficient source of bulk heating in liquid metals has been identified (other than neutrons), the heat must be supplied in the form of surface heating. Electrical resistance heaters will probably be used due to their low cost.

3.5.2 Characteristics of a Single PITF Non-Neutron Test Facility

If the TMIF is successful, then sufficient confidence should be gained in the blanket thermomechanical design such that reliable operation in the fusion test reactor can be expected. A facility similar to TMIF is being planned for

tritium recovery and processing issues. The tritium facility would consist of a simulated blanket tritium source, a tritium extraction system, and tritium processing systems. The partially integrated tritium facility is described in more detail in Chapter 5.

It is also desirable to test the entire blanket system, including the blanket, primary cooling system and tritium extraction systems, together at full or near-full scale prior to irradiation testing. This test would integrate all possible issues in the absence of neutron exposure. If problems occur, then they are much cheaper and easier to remedy in an unirradiated environment. This large scale test is called the PITF, or Partially Integrated Test Facility.

Without evaluating the cost and value of PITF in great detail, certain aspects can be qualitatively judged. Few problems are expected to occur as a result of interactions between tritium recovery systems and the blanket systems. Some notable exceptions include mass transport and effects of tritium in the primary cooling system. On the other hand, the cost of operating a large cooling system in the presence of tritium is likely to be of the order of hundreds of millions of dollars. If a TMIF and a tritium integrated facility are both built, then the added information from a PITF would be fairly small, considering its large cost.

If the role of PITF is interpreted to be a final systems demonstration before the fusion DEMO, rather than a precursor to the fusion integrated test facility, then the cost might be more acceptable. In this case, the PITF is outside the scope of FINESSE.

3.6 Integrated Experiments

3.6.1 Purpose of Integrated Testing

Fully integrated experiments contain by definition all of the relevant environmental conditions and all of the physical elements and subsystems for fusion nuclear components. An integrated experiment for a liquid metal blanket must be performed in a large volume under high magnetic field, and with a large flux and fluence of fusion neutrons. The entire primary cooling system should be in place, as well as tritium extraction, tritium processing, and safety systems. More detailed discussion of the test requirements for

integrated testing appear in section 9.3.

The primary purpose of an integrated test is to explore interactions which did not exist in previous, less integrated experiments. In addition, it will be the first component-scale experiment with neutron effects. As such, there will be a large amount of new information on how the blanket system responds to irradiation under reactor relevant conditions.

Most of the issues for liquid metal blankets (Table 3.1-4) are affected to some extent by the presence of neutrons. Thermomechanical responses under irradiation, including failure modes, are the most strongly affected and will have been the least understood at the time of integrated testing. Therefore, correct engineering scaling for thermomechanical effects should be a high priority.

3.6.2 Data Requirements

The type of data required from an integrated experiment is fundamentally different than for separate/multiple effects experiments, and even partially integrated experiments. High temperature, poor access, machine availability requirements, and irradiation will all serve to make measurements difficult. The majority of the data will necessarily represent global operating parameters. For example, the total blanket pressure drop will be measured rather than local velocity profiles. At best, there will be several pressure taps along the blanket to identify regional differences.

Radiation hardening will be a serious concern, and development of reliable instrumentation should be performed prior to operation under irradiation. For liquid metal blankets, the most important measurements include pressure, temperature, stress, and flow quantity (if possible).

As with the TMIF, it is possible that an integrated experiment would be operated in phases. In the early phases, basic confirmation measurements could be made on hydrodynamics and detailed thermal and structural behavior. In the later phases, the neutron wall loading will be increased along with the blanket temperature.

3.7 Liquid Metal Blanket Facilities Costing

It is necessary to know the approximate cost of individual facilities both for short term planning of the facilities and for long term decisions regarding the overall test plan (cost-to-benefit ratios, funding scenarios, etc.). Because of the limited amount of detail now known about future facilities, only an approximate estimate of test plan costs could be generated. The costing relied on the approximate definitions of facilities contained in the previous sections of this chapter. Only the most critical facilities were costed, as listed in Table 3.7-1.

The process of costing has resulted in a methodology for costing, ground-rules for estimates, basic cost data and a series of conclusions. These are provided in the remainder of this section.

3.7.1 Methodology for FINESSE Costing

Figure 3.7-1 represents the role of costing in the FINESSE process. In previous phases of the FINESSE process, the critical issues were used to generate testing needs and requirements for testing, which were then used to define the facilities. The cost estimates are based on the facilities definitions and will be used as one of the inputs to the test plan generation and evaluation.

Table 3.7-1. Key Liquid Metal Blanket Facilities Which Were Costed

-
1. MHD Pressure Drop/Fluid Flow
 2. Thermal Convection Corrosion Loop
 3. Forced Convection Corrosion Loop
 4. MHD Heat Transfer
 5. MHD Corrosion
 6. Tritium Extraction System
 7. Tritium Permeation and Transport Loop
 8. Thermal Hydraulic and Mechanical Safety Test
 9. Thermomechanical Integrated Test
-

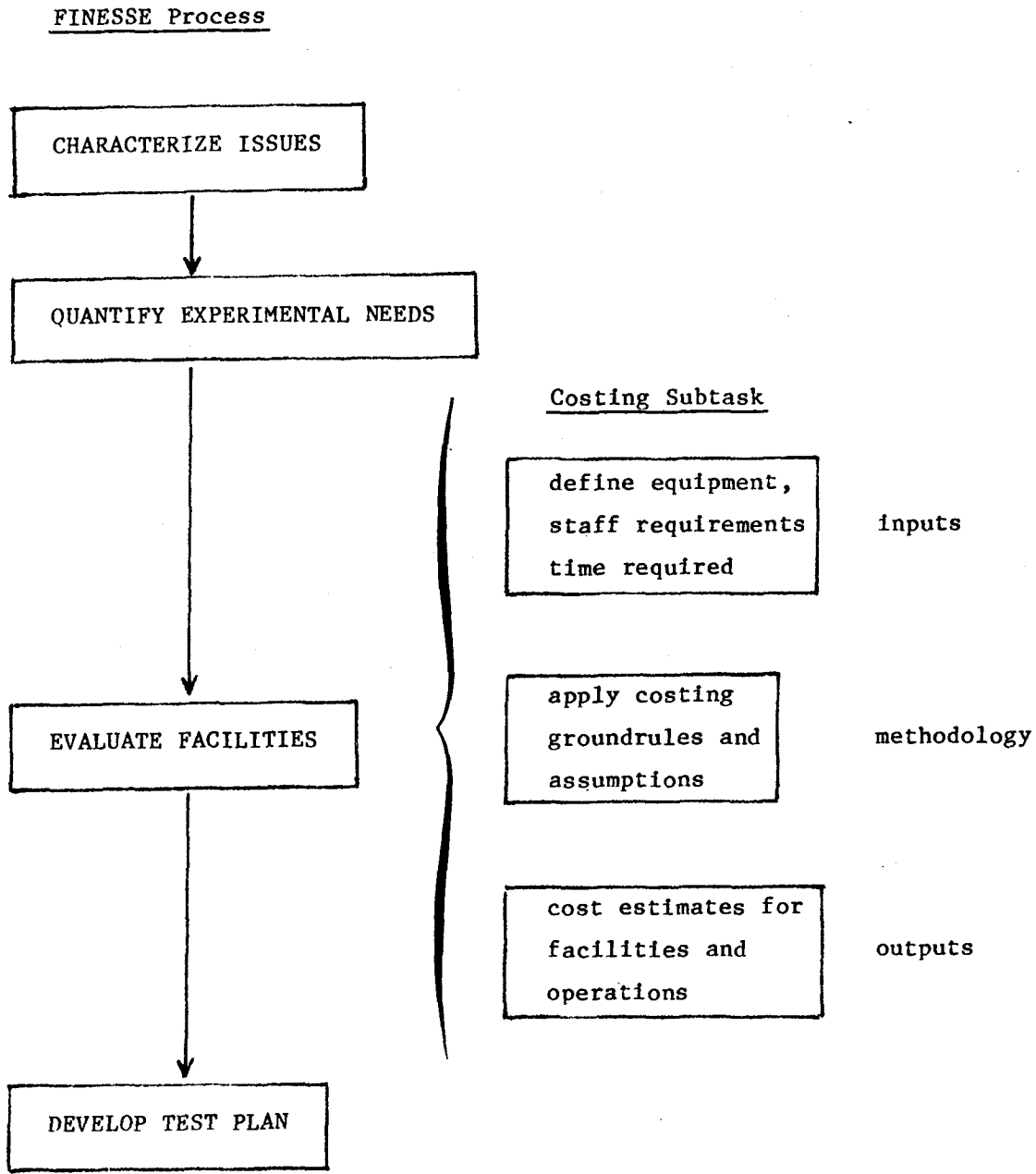


Figure 3.7-1. The relationship of the costing task to the FINESSE process

The facility requirements were provided in the form of system block diagrams, equipment listings and similarities with other systems currently utilized in the liquid metal blanket program. After refining the definitions of the required facilities, costing information was gathered relevant to the systems. Costing data sources included industry and national laboratory experience; similar equipment costs and basic equipment costs were defined through contacts with equipment/material suppliers.

Operating costs were prepared by estimating the professional, technician and support labor required for each facility on a stand alone basis and then applying an annual rate for each category of labor/skills. Cost estimates also included the building (less land) costs to house the experiment as well as provision for office, experiment and storeroom space.

The estimated direct cost of each facility includes the items listed in Table 3.7-2. In developing an overall cost for the complete test program, it

Table 3.7-2. Direct and Indirect Costs Associated with Experiments

Direct

design engineering
buildings (less land)
materials and systems
assembly and test
professional staff (experimental)
operating costs (less utilities)

Indirect

equipment and instrumentation development
scoping tests
modelling and code development
design studies
program administration
contingency

is important to include indirect as well as direct costs associated with each facility. The cost items that are classified as indirect are also listed in Table 3.7-2. Because of the difficulty in specifying indirect costs for individual experiments, they are added into the total test plan cost as a constant factor of 1.5 times the total direct costs.

Design engineering. Design engineering is the effort associated with design, specifications and procurement of the facility and equipment. As mentioned previously, each requirement is considered as a stand-alone, independent entity. Design engineering costs include staff to perform the functions of:

- project management (as necessary)
- specification preparation
- procurement of systems/equipment
- systems design
- fabrication and installation liaison

Personnel for this function would normally be engineers from various disciplines, facility designers, specification and purchasing personnel. Technicians and engineers that oversee the installation of systems are also included in this category. This cost averages 18-20% of total experiment costs.

Buildings. Since at this time, location of a particular experiment cannot be defined, we have assumed that each system defined as a requirement will have a building to house the equipment and personnel. A Butler type building is envisioned for the simple test loops whereas a facility such as the TMIF will require substantial office and experimental space. Experiments of the single purpose type such as corrosion or tritium extraction for which the purchased material and systems are less than \$0.5M assume no office or clerical space provisions. More expensive experiments are estimated at a higher cost for the buildings which were included at a maximum of 10 percent of total experiment costs.

Materials and systems. This cost category includes the experiment hardware such as magnets, power supplies, piping, heaters, pumps, etc. Also included are safety systems, heat exchanges, raw material and instrumentation and control systems. As will be shown later, this category of cost averaged 40-50% of the experiment cost.

Assembly and testing. This category of cost includes those costs associated with assembly of the experiment and performance of initial systems verification tests and operation of the facility for the 1st year after installation of the required systems. Included in this period are initial systems hookup, installation and checkout of hardware and software (if any) and the generation of any related test plan or procedures. The cost of assembly and testing varied from 8 percent on the largest devices to 25 percent of the cost on the smaller experiment. This variance is due to the 1st year operating costs and the fact that, in general, a mechanical and electrical technician is required for any experiment, regardless of the equipment involved.

Professional Staff. This category includes the theoretical support groups who define the testing requirements and parameters, provide guidance to the design engineers, specify data requirements and interpret and publish test results and provide feed back for subsequent experiments. They are assumed to be assigned to the particular experiment at its inception and are estimated against the facility cost though the first year of operation. Subsequent years would be part of the estimated operating costs. In general, this staff was minimal - in the range of 1-2 professionals for 1 to 2 years or through the 1st year of operation. The professional staff generally accounted for 15 to 20 percent of the total experiment cost.

3.7.2 Groundrules for Estimates

In preparing estimates for liquid metal and solid breeder blanket test facility costs, several groundrules and assumptions were employed, as shown in Table 3.7-3.

Stand alone facilities. During preparation of the costs for facilities, it became apparent that many possible locations/facilities can be possible for the test stands and loops required for the liquid metal blanket test program. However, the availability within the program's required time frame, staffing availability and existing or surplus equipment status could not be ascertained within the scope of this study. Therefore, the groundrule was established that all facilities and equipment would be costed on a basis that assumes no transfer of resources from existing or contemplated assets.

Table 3.7-3. Groundrules and Assumptions for Facilities Costing

1. all facilities or test stands are stand alone
(assuming no existing buildings or equipment available)
 2. constant 1985 dollars
 3. tritium costs: \$15K/gram
 4. electricity cost: 5¢ per KWHR
 5. professional yearly cost:\$130-150K
 6. technician and others: \$100K
 7. no cost for neutron (fission) sources
 8. test stands - 2 years from design start to test
 9. test stands - 4 year life
 10. contingency \$ not included
 11. no cost for land
 12. no disposal/decommissioning costs included
-

Constant 1985 dollars. Constant Dollars (1985) was chosen because at the present stage of test planning, it is believed that cost estimates are best used for comparison of facilities rather than absolute or projected total program costs. In deciding on the cost effectiveness of a facility vs. the technical risk, we felt that measuring each test requirement against constant dollars would be the most effective measure rather than to attempt projected dollar costs.

Tritium costs. A cost of \$15,000/gram was a consensus of the FINESSE team as representing the most likely cost under conditions expected during the test period.

Electricity costs. 5¢ per KWAR was selected as a consensus based up U.S. average for commercial, high volume consumers and is applicable mainly to operational costs of the large (FERF) type facilities discussed in Chapter 9 of this report.

Professional (130-150K) and technician (100K) costs. These cost estimates represent burdened industrial and governmental personnel cost used in this study and are representative of expected costs in a technology such as liquid metal blankets.

No cost for neutron (fission) sources. This groundrule applies to Solid Breeder and materials testing. FINESSE estimates have assumed that experiments are "piggy back" on existing reactors that have primary missions other than in support of fusion. Therefore other than operating staff associated with the particular experiment, no costs have been allowed for running of the reactors, maintenance or operation of the source of neutrons. Design and operation of equipment unique to the tests defined in the FINESSE plan have been included.

Test stand life and construction times. An assumption that two years from start of design to first test, with a lifetime of four years should be representative of the facilities defined in this study. These are not applicable to FERF type facilities but are representative of the type of test facility described for the liquid metal blanket and solid breeder test plans.

Contingency costing. Since the main purpose of costing the various experiments was comparison between facilities, cost vs risk assessment and an understanding of what the total program might cost, no contingency factors were applied to estimated costs.

Land cost and disposal/decommissioning costs. These costs were not considered due to the variances between geographical locations and since construction on government or public land is the most probable scenario for a fusion facility. Disposal and decommissioning were not considered due to the fact that unlike major FERF type facilities, the buildings and test stand described herein would have application to future tests and most would not be contaminated. These costs can be factored into the cost estimates should they be considered necessary for any particular study using the estimates provided herein.

3.7.3 Cost Data for the Liquid Metal Blanket Test Program

The FINESSE pricing matrix (Table 3.7-4) below represents the current

cost estimates for the major liquid metal blanket experiments. Each item Comments, estimated capital and annual operating costs complete the matrix. It should be recognized that these estimates are first-cut estimates since definition of the facilities was not performed at a very detailed level. But these estimates should be adequate for the purpose of planning a liquid metal blanket test program.

Table 3.7-5 presents a breakdown of the capital costs presented previously. The costs are shown for the following categories that were discussed in Section 3.7.1, namely:

- engineering design
- buildings
- material
- assembly and test
- professional staff

The costs shown were prepared in concert with costing groundrules and material estimates.

Figure 3.7-6 presents a breakdown of the materials & systems portion of total capital costs. This material is the necessary equipment that must be procured or fabricated to implement the particular experiment, test loop or test stand defined in column 1 of the table. Costs are catalogued by:

- magnets
- power supplies
- instrumentation and control
- safety systems
- plumbing and pumps
- blankets (or simulator)
- heat exchanger
- raw material (fluid medium or special materials)
- miscellaneous
- heating equipment

The cost of these systems was generated by analysis of the test objectives, basic schematic diagrams and costs of similar systems previously estimated or built in support of similar programs.

Table 3.7-4. Liquid Metal Blanket Facilities Costs

Item	Comments	Capital Cost Estimate (1985 \$)	Operating Costs (Per Year)
MHD Pressure Drop and Fluid Flow	Magnet Cost 1-1.5 M	2.5 M	600 k
Thermal Convection Corrosion Loop	No Magnet	750 k	400 k
Forced Convection Corrosion Loop	No Magnet, High Temp. (400-600°C) Long Run, Continuous	1.5 M	450 k
MHD Heat Transfer	Low Temperature (100°C) Relevant Geometry	4.5 M	300 k
MHD Corrosion	High Temp. (400-600°C) Long Run, High Field	7 M	600 k
Tritium Extraction	Sparged Electrode High Temp. (300-400°C)	750 k	300 k
Tritium Permeation and Transport Loop	High Temp., Long Run Complete Tritium Loop Complete Primary Loop	8 M	600 k
Thermomechanical Safety Test	Off Normal Testing High Field, Heat Flux	10 M	550 k
Thermomechanical Integrated Test (TMIF)	Complete Primary Loop (Less Tritium) Prototypical Components	15 M	1 M

Table 3.7-5. Capital Costs

Facility Name	Eng. Design	Building	Material	Assembly and Test	Prof. Staff	Total Cost
MHD	450k	100k	1.2M	300k	450k	2.5M
Thermal Convection Loop	135k	25k	255k	200k	135k	750K
Forced Convection Loop	270k	75k	535k	350k	270k	1.5M
MHD Heat Transfer	800k	100k	2.5M	300k	800k	4.5M
MHD Corrosion	800k	200k	4.7M	500k	800k	7.0M
Tritium Extraction	125k	25k	270k	200k	135k	750k
Tritium Permeation and Transport Loop	1.5k	750K	3.5M	750k	1.5M	8M
Thermal-Hydraulic-Mechanical Safety	2M	1.0M	4.3M	1.2M	1.5M	10M
Thermomechanical Integrated (TMIF)	3M	1.0M	6.8M	1.2M	3M	15M

Table 3.7-6. Materials and Systems Costs (in thousands of dollars)

Facility Name	Magnet	Power Supply	I & C	Safety	Plumb. & Pumps	Blank	Heat Exch.	Raw Material	Misc.	Heat	Total
MHD	900	200	25		75						1200
TCL			20		65		15	50	50 Coup	55	255
FCL			50	15	120		30	50		220	535
MHD Ht. Tran.	1000	300	85	115	300		150	150	150	250	2500
MHD Corrosion	2000	500	85	115	500		150	150	150	250	4700
Tritium Extr.			15		70		35	75	40	35	270
Tritium Perm.		225	100	400	800	1000	150	75	100	650	3500
Safety		400	200	485	800	1000	250	175	240	750	4300
TMIF	3000	800	80	400	400	1000	250	270	100	500	6800

3.8 Summary of Testing and Model Development Needs

Figure 3.8-1 shows a complete list of major experiments. Not all of the tests in this test matrix will necessarily be performed. The test matrix simply provides a logical progression of experiments for each class of issues, ranging from basic tests to separate effects, multiple effects, and integrated tests. For each increasing level of integration, an additional degree of geometric relevance and/or an additional environmental condition is added. As described in Chapter 2, the actual test sequence depends on the results of earlier testing, the budget, and other constraining factors.

In order to structure the list of experiments, the principal issues listed in Table 3.1-4 are grouped into three categories, each of which implies a highly interrelated set of tests, including:

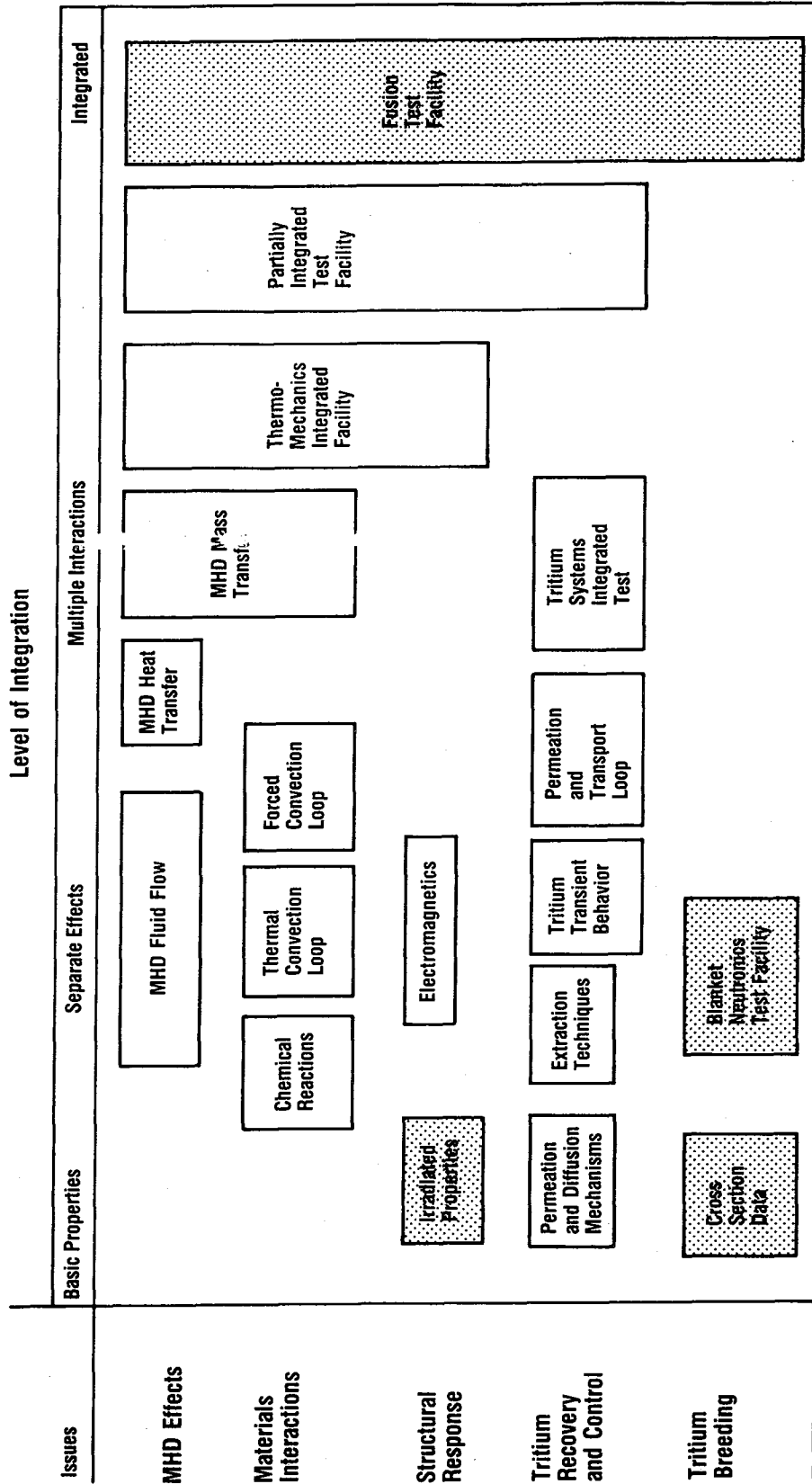
1. thermal/mechanical and materials compatibility
2. tritium recovery and control
3. tritium breeding

These testing issues do not overlap substantially for separate and multiple effects testing, but are combined only at relatively high level of integration. One reason for this is the different environmental conditions needed for the different test categories and the relative independence of the phenomena. Table 3.8-1 summarizes the dominant environmental condition required for the three test sequences. The relative independence of tritium breeding, tritium recovery, and thermomechanical issues is characteristic only of liquid metal blankets, for which tritium recovery occurs outside the boundary of the blanket and tritium breeding is usually a less critical issue.

The major liquid metal blanket experiments have been examined in detail in sections 3.4-3.5 and are briefly reviewed in the following.

3.8.1 Thermal/Mechanical and Materials Compatibility Test Sequence

The thermal/mechanical group of tests addresses the problem of maintaining the blanket within acceptable temperature and stress limits. Many of the feasibility issues for liquid metal blankets are related to this problem area. Resolution of this issue requires a determination of the acceptable limits of operation and the actual conditions in the blanket under fusion relevant conditions. The required experiments are grouped into five categories.



^a Some experiments or facilities already exist.

Figure 3.8-1. Types of experiments and facilities for liquid metal blankets^a

Table 3.8.1. Principal Facility Characteristics for the Three Test Sequences

<u>issue</u>	<u>facility characteristics</u>
thermomechanics	non-neutron, no tritium
tritium recovery	non-neutron, tritium
tritium breeding	neutrons

ries, including primarily non-neutron tests. It is assumed that a large program of materials development will occur as a supplement to the test plan described here. In addition, a small number of irradiation experiments have been identified, excluding basic properties measurements and materials characterization under irradiation. The test categories include:

1. Thermal-hydraulic
 - MHD pressure drop/fluid flow
 - MHD heat transfer
2. Materials interactions
 - Static capsule tests
 - Chemical reactions
 - Thermal convection loops
 - Forced convection loops
 - MHD corrosion
 - Stress-corrosion interactions
3. Mechanical
 - Insulator integrity without irradiation
 - Electromagnetics
4. Irradiation
 - Insulator integrity and effectiveness under irradiation
 - Radiation/corrosion interactions
5. Thermal-Hydraulic-Mechanical Safety

1. Thermal Hydraulic Tests

a. MHD Pressure Drop and Fluid Flow. Basic MHD tests are essential to determine if pressure stress limits can be maintained and to improve our

understanding of MHD flow fields in various geometries, which is critical for heat transfer. A thorough understanding of heat transfer is in turn critical for ensuring both acceptable temperatures and thermal stresses. The world program is currently in the process of constructing or operating small MHD loops, including the ALEX facility at ANL. These facilities are critical to develop understanding of MHD behavior at high magnetic field and in simple geometries. If self-cooled blanket designs continue to be developed with fairly complex geometric features, then a follow-up facility may be required with a larger field volume. Also, most experiments now planned or operating work at field strengths lower than actual fusion reactor conditions. A higher field MHD experiment may be required to verify the scaling established in smaller, lower field tests.

In parallel with MHD fluid flow and pressure drop experiments, an aggressive modeling program should be pursued. MHD effects are very design dependent, so that a sound predictive capability is required in order to transfer information gained in separate effect tests.

b. MHD Heat Transfer. The MHD heat transfer experiment is expected to be a definitive test of the ability of various blankets to maintain temperature control. This is valuable in resolving several issues and in choosing promising blankets options. It depends largely on the MHD fluid flow experiment in order to establish an understanding and predictive capability for the velocity profiles, which are so critical for heat transfer. However, even in the absence of a complete understanding of MHD fluid flow, a heat transfer experiment could be conducted in a semi-empirical mode and still provide very useful information. In this mode, correlations could be obtained for heat transfer coefficients in various geometries, similar to the technique commonly employed in the field of turbulent heat transfer. This is contrasted to a more analytic approach, which would attempt to develop and experimentally verify detailed modeling of fluid flow and heat transfer. Either choice of emphasis for this experiment results in a critical milestone experiment for determining liquid metal blanket feasibility.

2. Materials Interactions Tests

Temperature limits are usually set by materials compatibility and/or high temperature structural properties. Structural response under irradiation is a

key aspect of the latter, and will require neutron testing in point neutron sources, fission reactors, and/or fusion experiments to be fully resolved. On the other hand, corrosion issues can be more fully resolved without expensive fusion testing, allowing near term concept selection and resolution of feasibility issues.

The largest impact on corrosion is due to the environmental conditions of temperature, temperature gradient, and impurity level (which is a function of materials and primary loop sub-systems). The effect of magnetic field is less, and furthermore is geometry-dependent. It will be easier to understand the effects of magnetic field on corrosion after performing tests outside the magnetic field and after a more refined level of design selection. Testing without a magnetic field could be definitive in determining blanket feasibility.

a. Static Capsule Tests. The simplest type of corrosion test utilizes small specimens to explore the basic materials interactions. Critical unknowns include temperature dependence of corrosion phenomena, nature of the chemical reactions which take place, and surface effects in the chemical environment. In the absence of a temperature gradient, there is little or no convection; dissolution ceases when the liquid phase saturates. Application of a temperature gradient provides for circulation of the liquid and transport of material between zones of different temperature.

b. Chemical Reactions. There are two different types of safety concern over chemical reactions: coolant/breeder energy release and hydrogen evolution, and structural damage and radioactive release.

An aggressive program already exists for exploring the effects of Li and LiPb chemical reactions with air, concrete, and water. The seriousness of air and concrete reactions is considered to be small enough to make these attractiveness issues (as opposed to feasibility issues), because fairly straightforward schemes can be implemented to mitigate or eliminate the hazards. To alleviate the effects of air reactions, an inert environment could be used. To mitigate concrete reactions, a high-reliability containment structure, such as a liner, could be built.

For water reactions - particularly lithium/water - it is more difficult to isolate the reactants. Water may be present in systems with liquid metal

cooled blankets in cooling systems for the magnets, neutral beams, plasma interactive components, etc. The presence of water in plasma interactive components is most dangerous, because of the close proximity to the blanket. Water reactions are the only serious problem area which may require further testing beyond existing data. Even for these, no new facilities need be built, provided that existing facilities continue to be supported by the fission breeder reactor program.

The most serious accident consequences occur when radioactive structural materials are released. Transport of activated structural material occurs in small amounts during normal operation due to corrosion, and results in maintenance and disposal problems for the primary cooling system components. A much larger amount of material could be released under accident conditions, when air, water, or some other material reacts at high temperature with the structure. The most serious anticipated problem in this area is rapid vanadium oxidation, or volatilization. It is important to know the consequences of possible reactions, including damage to the structures, kinetics of the reactions, and production and transport of aerosols.

c. Thermal Convection Loop Tests. Thermal convection corrosion tests are suggested to establish the activation energies for relevant chemical processes, to identify the important materials and impurities which affect corrosion mechanisms and transport across the thermal gradient, and to explore the effects of corrosion on the surface of the specimen and the container. Data is particularly needed for refractory metals and for insulating coatings. In addition, mass transport in multi-component systems can be studied in thermal convection tests, for example vanadium samples in a stainless steel chamber. Current data for single component steel systems appears adequate to assess temperature limits and failure modes due to corrosion.

d. Forced Convection Loop Tests. For both steel and refractory alloy structural materials, mass transport throughout the entire primary cooling system is a critical issue. In addition, thermal/hydraulic effects may be important, such as coolant velocity, velocity profile, and temperature profile throughout the blanket. In order to correctly simulate convection in channel flow similar to blankets, a forced convection loop must be used. Without a magnetic field, forced convection loops will allow us to study velocity effects, temperature gradient effects, and impurity control methods.

e. MHD Corrosion. If the results of forced convection loop tests suggest that localized corrosion in the blanket may be a serious problem or if the design window still appears narrow, testing under a magnetic field may be needed. The magnetic field alters the velocity profile of the coolant very near the structure interface, hence the corrosion rate and even corrosion mechanisms could change. Current estimates of magnetic field effects show as much as a factor of 10 difference with vs. without magnetic field.

f. Stress-Corrosion Interactions. Enhancement of embrittlement under the combined influence of stress and corrosion has been demonstrated in non-stress-relieved iron, however data is needed for the steel and refractory alloys considered for fusion. This interaction may only be important in weld zones, where adequate stress relief may not be practical. Stress-corrosion interactions may be investigated in thermal or forced convection loops by applying an external force on specimens inside the loop.

3. Mechanical Tests

a. Insulator Integrity without Irradiation. If resistive coatings or laminates prove feasible, the impact on liquid metal blanket design would be far reaching. Design concepts would be radically altered and the critical issues would change. Because of the potential importance of insulators and the relative low cost for testing, insulator scoping tests are considered a moderately high priority. Mechanical response and lifetime issues are considered separately. Mechanical issues include fabrication techniques, bonding and delamination, and MHD effectiveness. Lifetime tests include materials compatibility and radiation effects, as described below.

b. Electromagnetics. Electromagnetic forces depend strongly on geometry and magnetic field, but very little on any other environmental conditions. Therefore, the ideal facility would have a sufficiently large magnetic field volume to accept any geometrically relevant component and high enough field to measure the effects. The FELIX facility at ANL was constructed for the purpose of electromagnetics testing. Its primary mission is to act as a source of data for verification of eddy current models which have been developed and are still in the process of being developed. Since the equations related to electromagnetic forces are well known, it is assumed that verification of the models will be sufficient to adequately predict forces in

any component configuration.

4. Irradiation Tests

a. Insulator Integrity and Effectiveness under Irradiation. Fabrication and mechanical integrity of MHD insulated structures are not expected to present serious feasibility problems for insulated blankets. The major reason that insulated blankets are not ranked higher with respect to other liquid metal blankets is concern over the behavior of the insulator under irradiation. For the two schemes to insulate blankets (coatings and laminates) the issues are significantly different.

For coatings, materials compatibility and loss of resistivity are both important concerns. Radiation may degrade the coating and lead to enhanced deterioration of the surface properties, including electrical resistivity, compatibility with the coolant, and structural properties (e.g., crack propagation).

For laminated structures, the primary concern is loss of resistivity and changes in physical properties. The insulator in a laminated structure is not required to carry structural loads, so structural properties are not a major concern. Thermal conductivity changes are not expected to be large enough to impact heat transfer. The electrical conductivity of ceramics is known to degrade significantly under irradiation, but the tolerable decrease in resistivity is large. The resistivity would have to be reduced by over 6 orders of magnitude before the MHD pressure drop was substantially altered. The degree to which these effects are negligible on MHD pressure drop, fluid flow, and heat transfer must be demonstrated experimentally.

b. Radiation/Corrosion Interactions. The synergistic effect of the combined influence of corrosion and radiation may enhance the rate of materials properties degradation beyond the simple sum of the effects. Whereas the radiation/corrosion interaction is not observed in sodium-steel systems, there is little or no data to indicate whether or not other alkali liquid metals do in fact suffer from this problem. The existence of a radiation-corrosion interaction may be demonstrated in simple thermal convection experiments in fission reactors or possibly by pre-irradiating samples in a reactor and then exposing them in a separate corrosion loop.

5. Thermal-Hydraulic-Mechanical Safety Test

In cases for which mild transients alone cannot resolve a safety issue, a specific safety test would be performed. Before building a fusion test reactor, it may be desirable to first construct a near full-scale primary cooling system, including the blanket, in order to explore possible failure modes and consequences in the absence of irradiation. Large forces and thermal hydraulic transients could be applied without the potential for catastrophic releases of tritium or activation products.

3.8.2 Tritium Recovery and Control Test Sequence

Another major class of issues involves tritium recovery and control, which includes permeation concerns. For liquid metal blankets, tritium issues are currently considered as less critical for blanket feasibility than the thermal/mechanical issues. In particular, tritium breeding is considered less of a feasibility issue than tritium extraction and control. The principal experiments for tritium recovery and control are:

1. Demonstration of Tritium Extraction Techniques
2. Permeation and Transport Loop Test
3. Tritium Transient Behavior
4. Integrated Tritium Recovery and Processing Test

1. Demonstration of Tritium Extraction Techniques. Before a blanket materials combination is selected, it will be important to determine if tritium extraction is feasible. The priority of tritium extraction experiments depends largely on a judgement as to whether or not extraction is a development issue or a feasibility issue. At the present, extraction from lithium is not considered to be a feasibility issues. However, LiPb presents a much more difficult challenge due to the high efficiency of removal required in a single pass.

2. Permeation and Transport Loop Test. There are several issues related to containment of tritium in the primary coolant loop, including tritium permeation barriers, tritium chemistry, efficiency of extraction, and others. Whereas each separate issue may be addressed in a separate effects test, this experiment is intended to demonstrate adequate tritium control in a multiple effects environment.

3. Tritium Transient Behavior. Tritium chemistry and permeation barriers may be strongly affected by thermal hydraulic transient conditions. In this case, large transient releases of tritium may occur. It is also possible that steady state tritium control may be disrupted by transients. The study of transient effects may be undertaken as a part of the base tritium program.

4. Integrated Tritium Recovery and Processing Test. The maximum anticipated test in the area of tritium recovery and control prior to fusion reactor testing consists of a large scale tritium processing system with a tritium source term (blanket mock-up) and a prototypical tritium extraction system. This test may be performed as an upgrade of the TSTA facility by attaching the simulated blanket and tritium extraction system onto the existing tritium processing systems.

3.8.3 Tritium Breeding Test Sequence

Liquid metal blanket designs usually have sufficient margin in the tritium breeding ratio to make this issue less critical. It could become more critical if testing reveals that an inboard blanket is impossible to engineer or if self-cooling is shown infeasible. In addition, the lead time to perform tritium breeding tests is not great, since long term exposure is unnecessary. Tritium breeding experiments can be carried out in point sources, since the uncertainties relate to nuclear data and accuracy of codes. Such an experiment is currently being planned in Japan. More detailed description of neutronics tests is given in Chapter 4.

3.8.4 Summary of Model Development Needs

The modeling needs for liquid metal blankets are listed in Table 3.8-3. There already exists a sizable literature on MHD fluid flow, but many of the problems of interest to fusion have not been studied. MHD is a particularly promising area for increased emphasis, since the equations which control the phenomena are well known. Materials interactions, on the other hand, are often dominated by poorly understood chemical and materials effects which strongly depend on the details of the cooling loop. Most of the modeling anticipated in this area will be empirical and more closely tied to the experiments. This is also true of tritium transport modeling.

Table 3.8-2. Summary of Model Development Needs

MHD Effects

- continued analytic modeling of velocity profiles in straight ducts and simple geometries
- 3-dimensional MHD computer codes for the solution of velocity profiles in complex geometries
- semi-empirical design codes which use characteristic surfaces to predict general fluid flow behavior in complex 3-dimensional geometries

Materials Interactions

- advanced dissolution modeling with solid phase, liquid phase, and interface transport processes
- application of more accurate boundary conditions (e.g., impurity dependence of solubility)
- kinetics of materials interaction processes
- cooling system modeling

Tritium Transport

- simple loop codes to predict transport and permeation rates in an integrated primary cooling system with extraction system
-

Appendix 3.A Materials Properties for Li and LiPb

3.A.1 Lithium Properties

Some general properties of lithium are listed in Table 3.A-1. Figures 3.A-1 through -8 show the other important properties. The enthalpies (ΔH°) and free energies (ΔG°) for various lithium reactions at 25°C are listed in Table 3.A-2.

Table 3.A-1. General Properties of Lithium

Symbol	Li
Atomic number	3
Atomic weight	6.941 a.m.u.
Isotopes/abundance	$^6\text{Li}/7.5\%$, $^7\text{Li}/92.5\%$
Crystal structure	bcc
Cubic edge length of unit	0.351 nm
Molar volume	13.1 cm ³ /gm mole
Melting point	180.54°C
Boiling point	1347°C
Heat of fusion	432.1 kJ/kg
Heat of vaporization	19595 kJ/kg

3.A.2 ^{17}Li -83Pb Properties

There is a general lack of materials properties data of LiPb. Those material properties which have been measured are presented below. For most cases, only a few scattered data points are available at best.

Phase Diagram: The phase diagram of LiPb has been well established and is shown in Fig. 3.A-9.¹ The melting points of LiPb and ^{17}Li -83Pb were confirmed by different workers.^{2,3} The accuracy of the phase diagram and, therefore, the melting temperature of LiPb in various composition appears to be accurate.

Sievert's Constant: There were basically three different measurements on Sievert's Constant of LiPb.⁴⁻⁶ The results from Veleckis and Wu appear to be in good agreement and are shown in Fig. 3.A-10. The results from Ref. 6 were measured at a hydrogen concentration that is judged to be too high.

Table 3.A-2. Enthalpies (ΔH°) and Free Energies (ΔG°) for Various Lithium Reactions at 25°C

Reaction	ΔH° (25°C) kJ/mole	ΔG° (25°C) kJ/mole
$2 \text{ Li(c)} + 1/2 \text{ O}_2 \rightarrow \text{Li}_2\text{O(c)}$	-596.85	-560.45
$2 \text{ Li(c)} + \text{O}_2\text{(g)} \rightarrow \text{Li}_2\text{O}_2\text{(c)}$	-635.55	-577.81
$\text{Li(c)} + 1/2 \text{ H}_2\text{(g)} + 1/2 \text{ O}_2\text{(g)} \rightarrow \text{LiOH(c)}$	-487.81	-442.15
$\text{Li(c)} + 3/2 \text{ H}_2\text{(g)} + \text{O}_2\text{(g)} \rightarrow \text{LiOH}\cdot\text{H}_2\text{O(c)}$	-790.47	-683.82
$\text{Li(c)} + \text{H}_2\text{O(l)} \rightarrow \text{LiOH(c)} + 1/2 \text{ H}_2\text{(g)}$	-203.76	-204.97
$\text{Li(c)} + \text{H}_2\text{O(l)} \rightarrow \text{LiOH (in H}_2\text{O)} + 1/2 \text{ H}_2\text{(g)}$	-222.35	
$\text{Li(c)} + 1/2 \text{ F}_2\text{(g)} \rightarrow \text{LiF(c)}$	-612.12	-584.30
$\text{Li(c)} + 1/2 \text{ Cl}_2\text{(g)} \rightarrow \text{LiCl(c)}$	-408.78	-387.02
$\text{Li(c)} + 1/2 \text{ I}_2\text{(g)} \rightarrow \text{LiI(c)}$	-271.08	(-260.24)
$3 \text{ Li(c)} + 1/2 \text{ N}_2\text{(g)} \rightarrow \text{Li}_3\text{N(c)}$	-198.74	-156.06
$\text{Li(c)} + 1/2 \text{ H}_2\text{(g)} \rightarrow \text{LiH(c)}$	-90.42	-69.96
$2 \text{ Li(c)} + 3/2 \text{ CO}_2\text{(g)} \rightarrow \text{Li}_2\text{CO}_3\text{(c)} + 1/2 \text{ C(c)}$	-621.74	-537.22
$2 \text{ Li(c)} + 3 \text{ CO(g)} \rightarrow \text{Li}_2\text{CO}_3\text{(c)} + 2 \text{ C(c)}$	-880.52	-717.05
$\text{Li(c)} + \text{NH}_3\text{(g)} \rightarrow \text{LiNH}_2\text{(c)} + 1/2 \text{ H}_2\text{(g)}$	-135.81	
$2 \text{ Li(c)} + 2 \text{ C(c)} \rightarrow \text{Li}_2\text{C}_2\text{(c)}$	-59.41	
$2 \text{ Li(c)} + \text{Mo(c)} + 2 \text{ O}_2\text{(g)} \rightarrow \text{Li}_2\text{MoO}_4\text{(c)}$	-1528.21	
$\text{Li(c)} + \text{Al(c)} + 2 \text{ H}_2\text{(g)} \rightarrow \text{LiAlH}_4\text{(c)}$	-103.22	
$\text{Li(c)} + \text{Sn(c)} \rightarrow \text{LiSn(c)}$	-70.29	
$\text{Li(c)} + \text{Pb(c)} \rightarrow \text{LiPb(c)}$	-61.09	
$\text{Li(c)} + \text{Tl(c)} \rightarrow \text{LiTl(c)}$	-53.56	
$\text{Li(c)} + \text{Hg(c)} \rightarrow \text{LiHg(c)}$	-87.03	
$3 \text{ Li(c)} + 2 \text{ Sb(c)} \rightarrow \text{Li}_3\text{Sb}_2\text{(c)}$	-182.00	
$3 \text{ Li(c)} + \text{Bi(c)} \rightarrow \text{Li}_3\text{Bi(c)}$	-230.96	
$2 \text{ Li(c)} + \text{H}_2\text{SO}_4\text{(l)} \rightarrow \text{Li}_2\text{SO}_4 + \text{H}_2\text{(g)}$	-623.08	
$\text{Li(c)} + \text{CH}_3\text{OH(l)} \rightarrow \text{LiOCH}_3 \text{ (in CH}_3\text{OH)} + 1/2 \text{ H}_2\text{(g)}$	-230.54	
$\text{Li(c)} + \text{C}_2\text{H}_5\text{OH(l)} \rightarrow \text{LiOC}_2\text{H}_5 \text{ (in C}_2\text{H}_5\text{OH)} + 1/2 \text{ H}_2\text{(g)}$	-215.89	

Figure 3.A-1. Heat capacity of lithium as a function of temperature

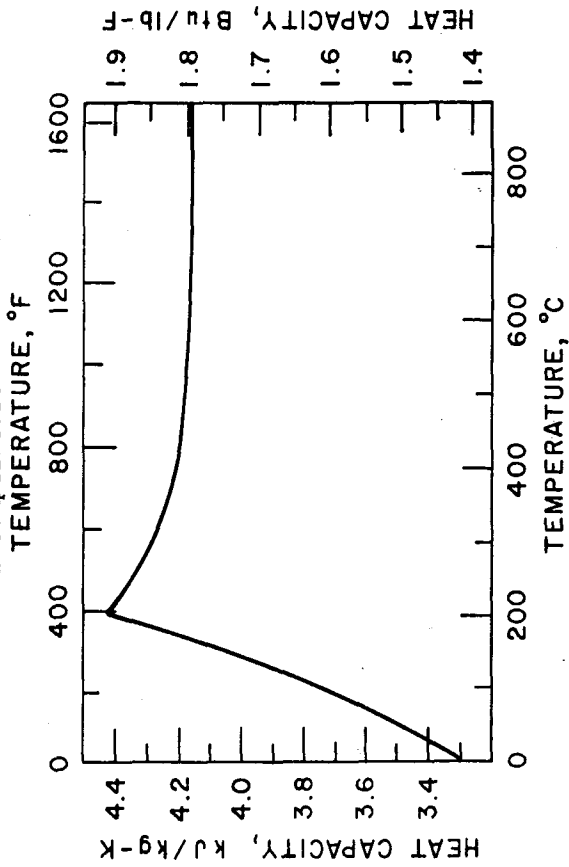


Figure 3.A-2. Thermal conductivity of lithium as a function of temperature.

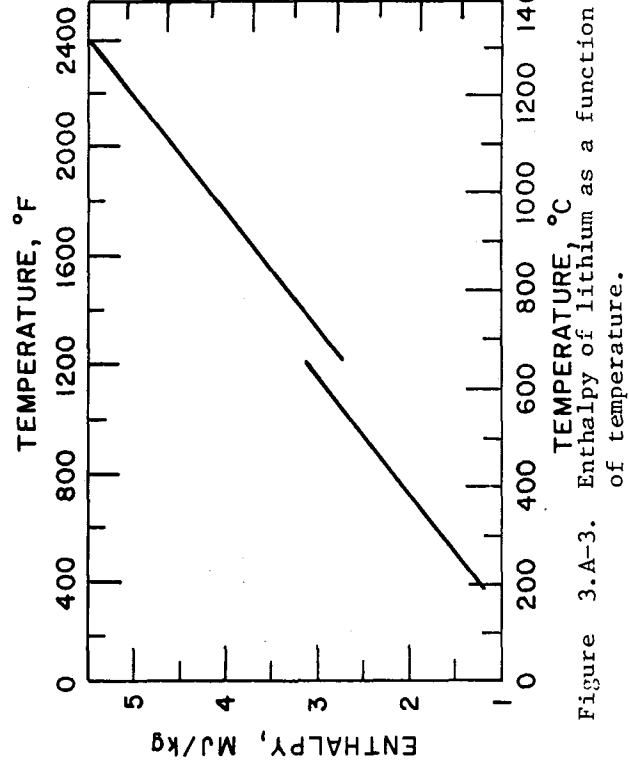
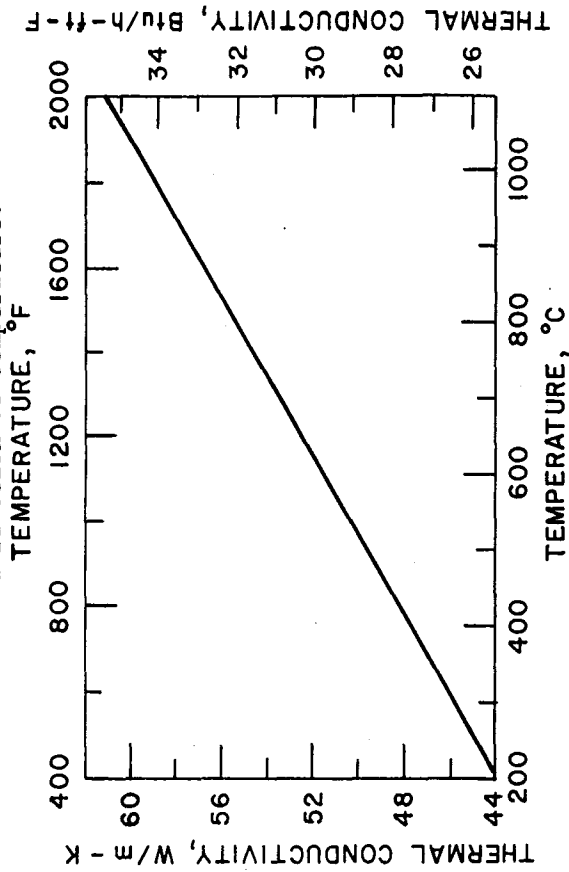


Figure 3.A-3. Enthalpy of lithium as a function of temperature.

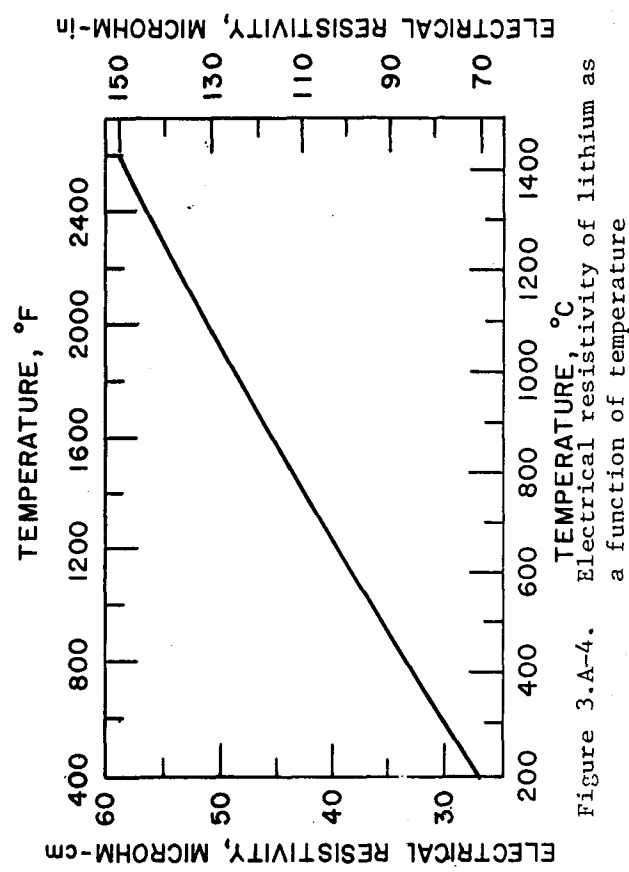


Figure 3.A-4. Electrical resistivity of lithium as a function of temperature

Figure 3.A-6. Vapor pressure of lithium as a function of temperature.

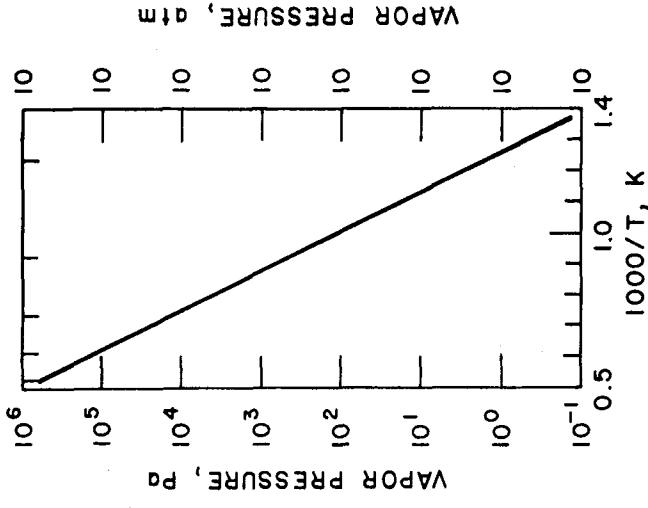


Figure 3.A-5. Surface tension of lithium as a function of temperature.

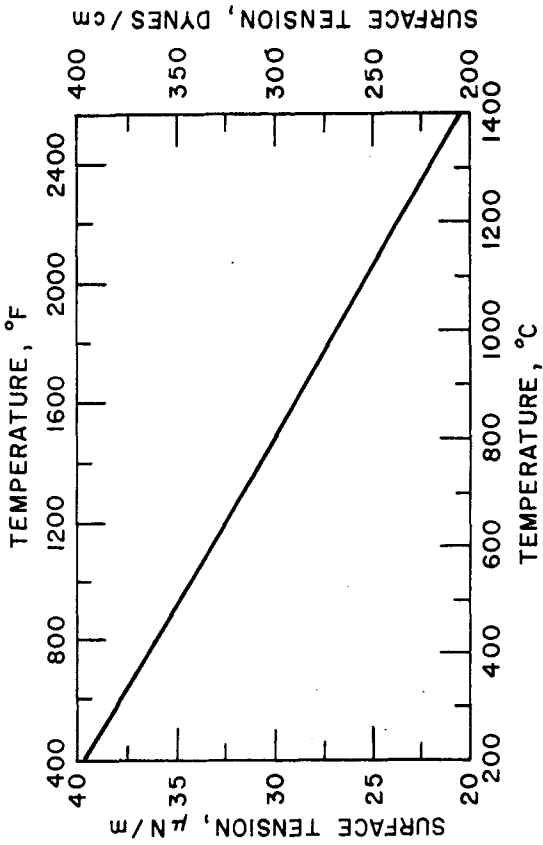


Figure 3.A-7. Viscosity of lithium as a function of temperature.

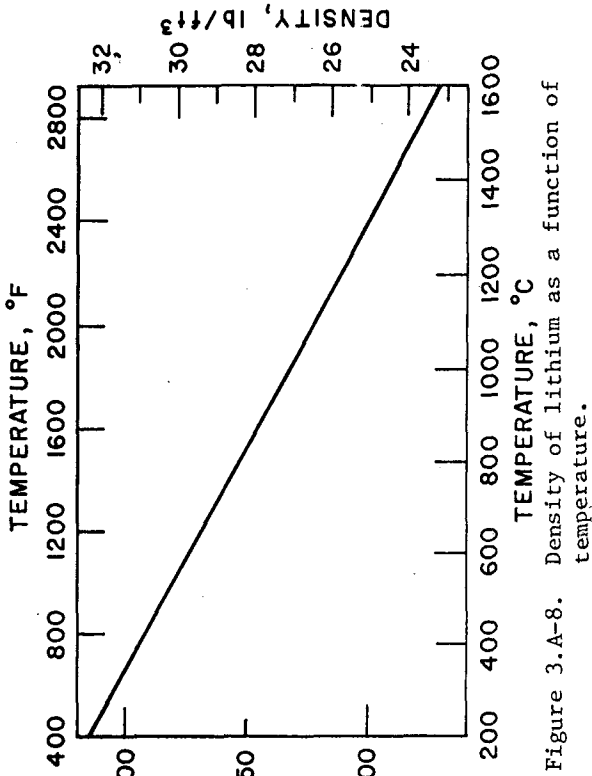
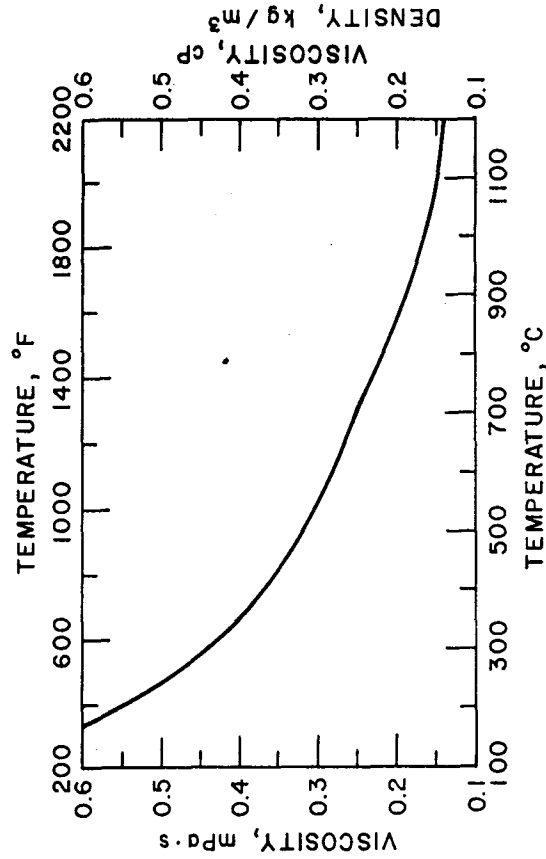


Figure 3.A-8. Density of lithium as a function of temperature.

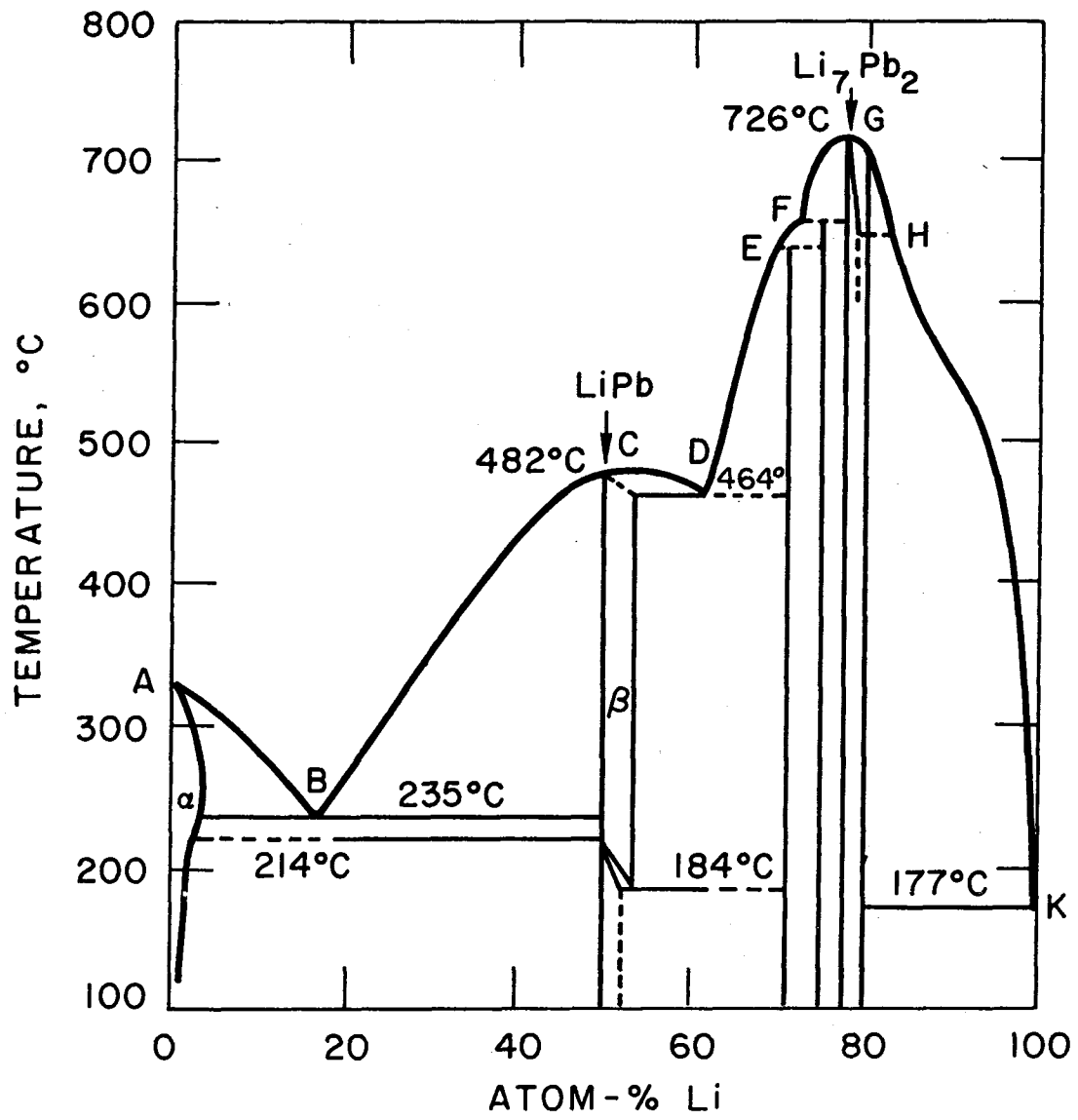


Figure 3.A-9. Phase diagram of LiPb

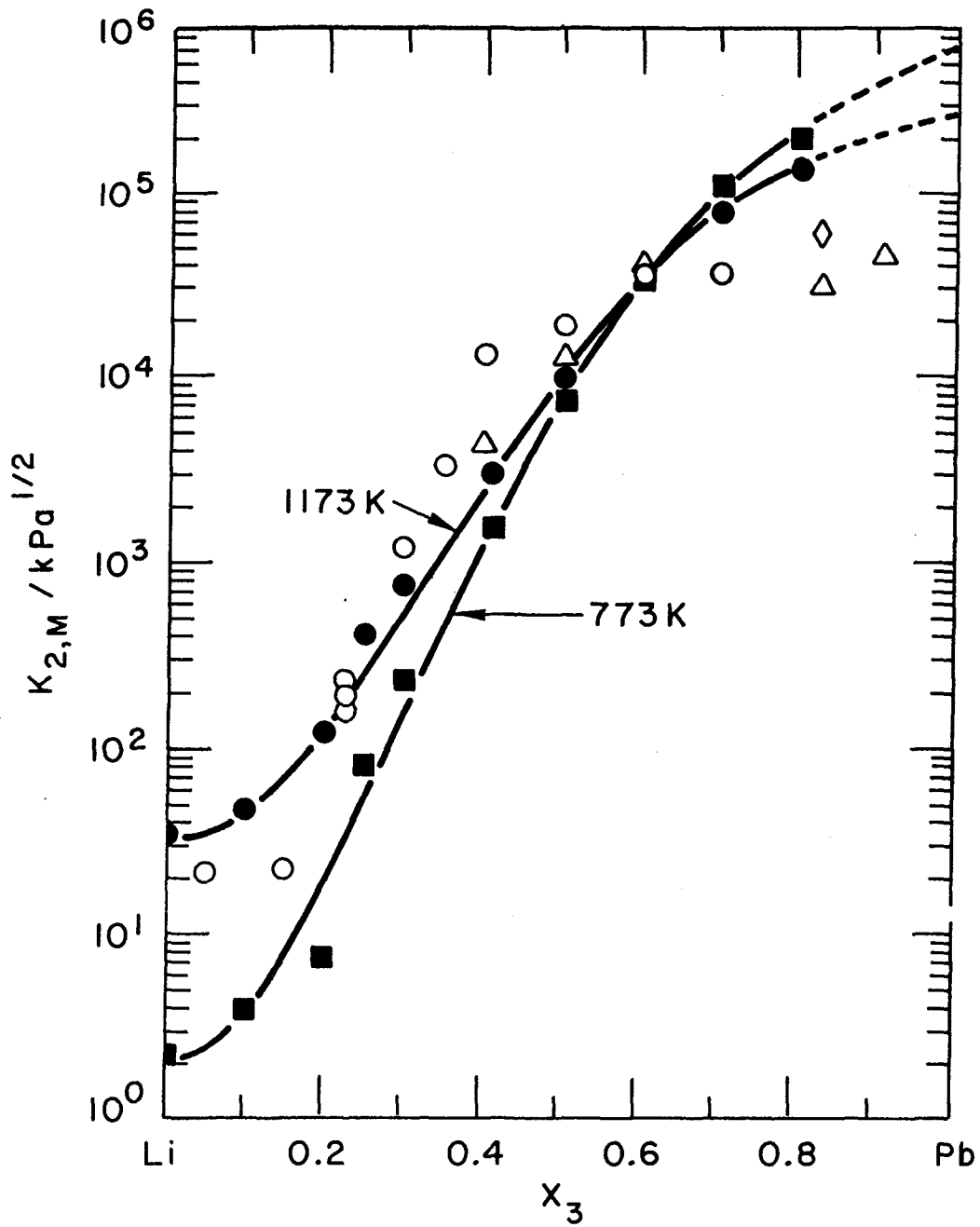


Figure 3.A-10. Sievert's constants for solutions of hydrogen isotopes in liquid LiPb alloys

Activity and Partial Pressure: The activity of lithium in the LiPb system has been measured by Knudsen diffusion mass spectrometry at 750 K and reported to continuously decrease from 4.0×10^{-3} to 2×10^{-5} as the lithium composition drops from 61 at % to 5 at %.⁷⁻¹⁰ The activity of lithium in 17Li-83Pb can be represented in the following form as a function of temperature,¹¹ i.e., $\ln a_{Li} = -6960/T + 0.0245$. Thus, the lithium activity in 17Li-83Pb can be estimated to be $\sim 1 \times 10^{-4}$ at 750 K. The activity of lead can be calculated from the activity of lithium by using the Gibbs-Duhem equation.⁸ A typical curve of activity coefficient of LiPb is reproduced from Ref. 9 and shown in Fig. 3.A-11. Since $P_n \equiv (rx)P_0 \equiv aP_0$ in which

P_n is the partial pressure of the material

r is the activity coefficient

x is the mole fraction

a is the activity

P_0 is the pressure of the pure material,

the partial pressures of lithium and lead can be calculated from the information of activity. Furthermore, on the lead-rich end of the phase diagram, the vapor phase is dominated by lead and, as a first approximation, the vapor pressure of LiPb can be taken the same as that of lead.

Density and Thermal Expansion Coefficient: The density and thermal expansion coefficient of liquid LiPb has been measured¹² and the data are shown in Fig. 3.A-12. The results appear to be accurate. The density of solid LiPb has also been reported.¹

Electrical Conductivity: The electrical conductivity of solid LiPb¹ and the electrical resistivity of liquid LiPb¹³ have been reported as shown in Figs. 3.A-13 and -14. The data accuracy is uncertain.

Thermodynamic Properties: The specific heat at constant pressure, C_p , enthalpy, and entropy of 17Li-83Pb have been measured.¹⁴ The latent heat of fusion can be obtained from these data which is 29.59 J/g. The specific heat is shown in Fig. 3.A-15. It appears that the C_p of liquid 17Li-83Pb shows a strong temperature dependence such that extrapolation to the higher temperature is not possible.

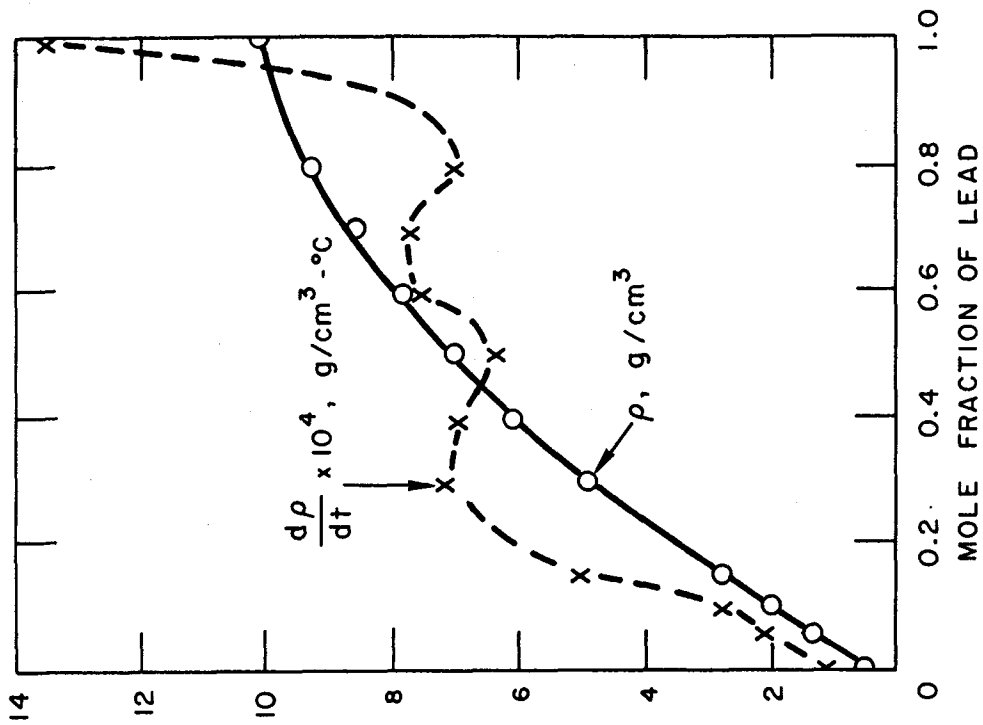


Figure 3.A-12. Density and thermal expansion coefficient of LiPb at liquidus temperature

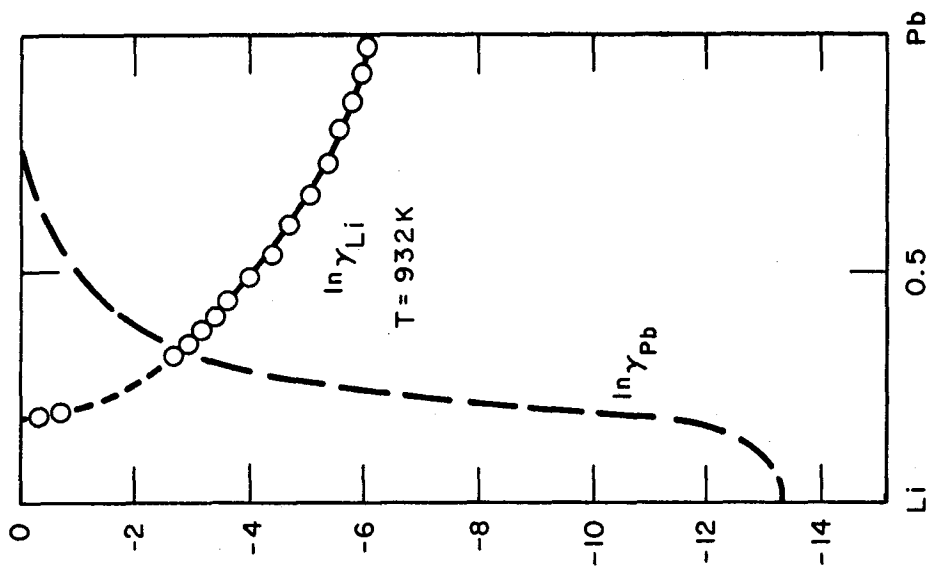


Figure 3.A-11. Activity coefficients for lithium and lead

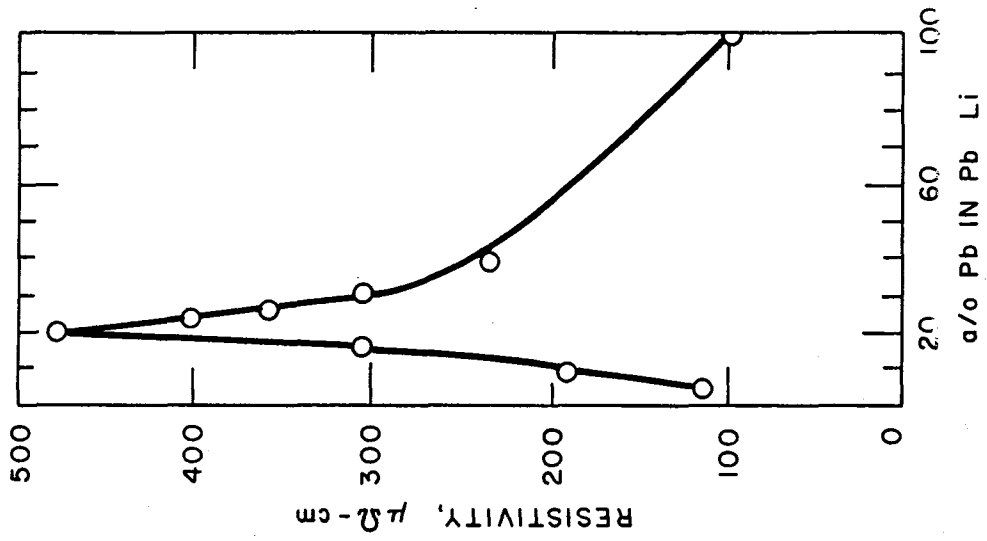


Figure 3.A-14. Electrical resistance of LiPb at 800°C

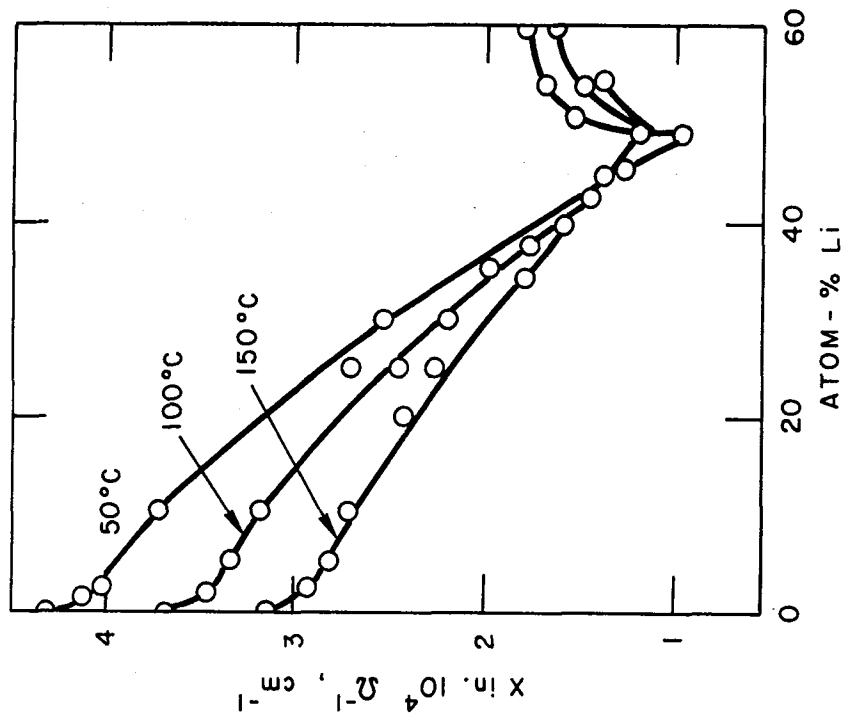


Figure 3.A-13. Electrical conductivity of LiPb

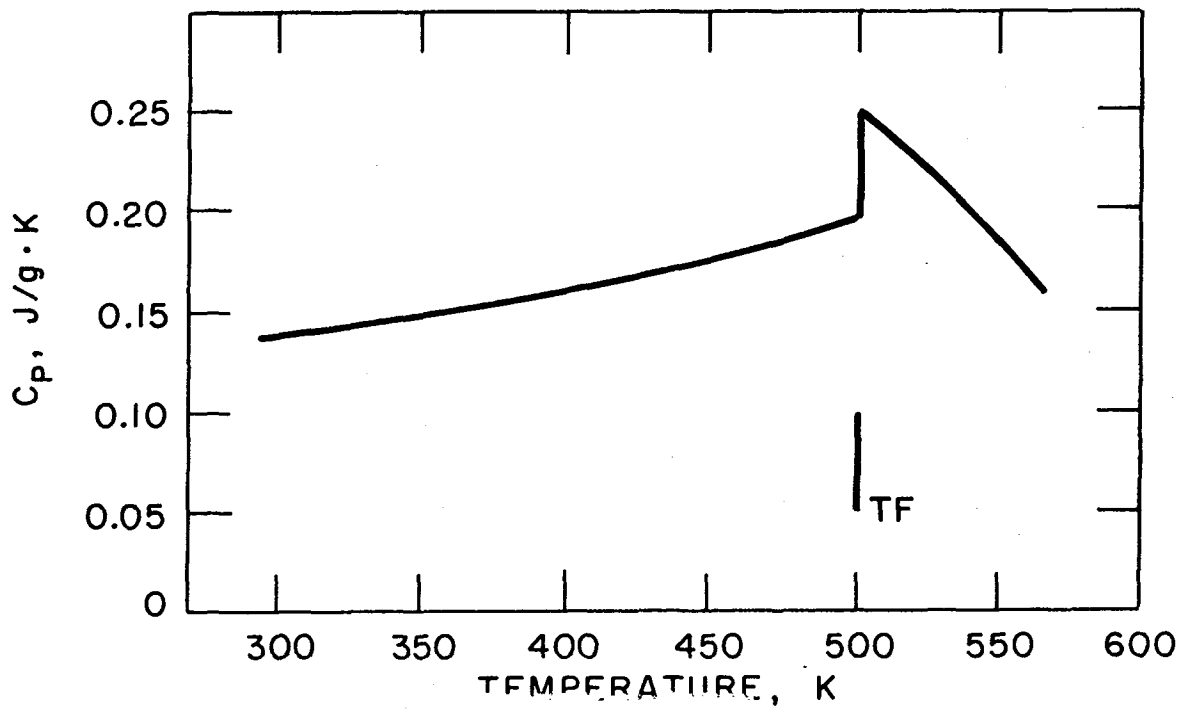


Figure 3.A-15. Specific heat at constant pressure, C_p , of ^{17}Li - ^{83}Pb

In conclusion, the material properties data base of ^{17}Li - ^{83}Pb has been built up over the past two years. However, much of the important information is still unavailable. The accuracies of the available data are uncertain.

3.A.3 Material Interaction Data

Figures 3.A-16 and -17 show the dissolution rates of austenitic and ferritic steels for flowing Li and LiPb. Figure 3.A-18 gives the solubility of hydrogen in selected metals and alloys.

References for Appendix 3.A

1. G. Grube and H. Klaiber, Z. Electrochem. 40, 745 (1934).
2. N. A. Frigerio and L. L. LaVoy, "The Preparation and Properties of LiPb, A Novel Material for Shields and Collimators," Nucl. Technol. 10, 322 (1971)
3. V. Coen, Ispra, Italy, private communication.
4. E. Veleckis, Argonne National Laboratory, private communications.
5. C. H. Wu and A. J. Blair, "A Study of the Interaction of Tritium with Liquid ^{17}Li - ^{83}Pb ," Proc. 12th Symp. on Fusion Technology, Julich, Germany, September 1982.
6. G. Pierini, et al., "Tritium Recovery from ^{17}Li - ^{83}Pb ," Proc. 12th Symp. on Fusion Technology, Julich, Germany, September 1982.
7. H. Ihle, A. Neubert and C. H. Wu, "The Activity of Lithium, and the Solubility of Deuterium in Liquid-Lead Alloys," Proc. 9th Symp. on Fusion Technology, ERATOM, Ispra, Italy, September 1978.
8. M. L. Saboungi, J. Marr and M. Blander, "Thermodynamic Properties of a Quasi-Ionic Alloy from Electromotive Force Measurements - The Li-Pb System," J. Chem. Phys. 68, 1375 (1978).
9. A. I. Demidov, A. G. Morachevskii and L. N. Gerasimenko, "Thermodynamic Properties of Liquid Lithium-Lead Alloys," Sov. Electrochem. 9, 813 (1973).
10. S. P. Yatsenko and E. A. Saltykova, "Thermodynamic Properties of Liquid Lithium-Lead Alloys," Russ. J. Phys. Chem. 50, 1278 (1976).
11. M. Ortman, University of Wisconsin, private communication.
12. H. Ruppertsburg and W. Speicher, Z. Naturforsch A 31A, 47 (1976).
13. V. T. Nguyen and J. E. Enderby, "The Electronic Structure of Lithium-Based Liquid Semiconducting Alloys," Philos. Mag. 35, (4), 1013 (1977).
14. F. Reiter, et al., "Thermodynamic Properties of ^{17}Li - ^{83}Pb ," Proc. 12th Symp. on Fusion Technology, Julich, Germany, September 1982.

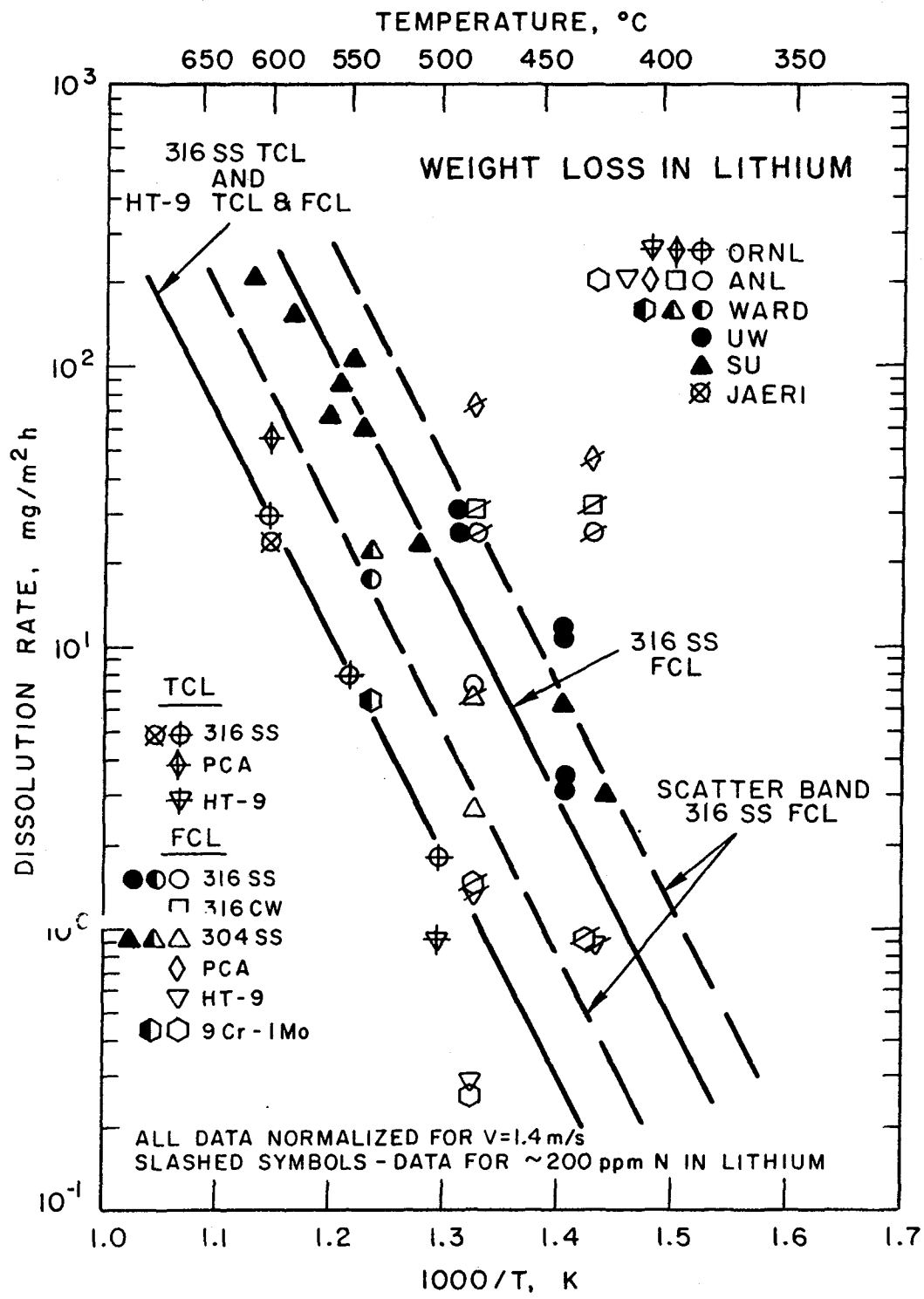


Figure 3.A-16. Arrhenius plot of corrosion rate data for types 304 and 316 stainless steel, PCA alloy, HT-9 alloy, and Fe-9Cr-1Mo steel exposed to flowing lithium

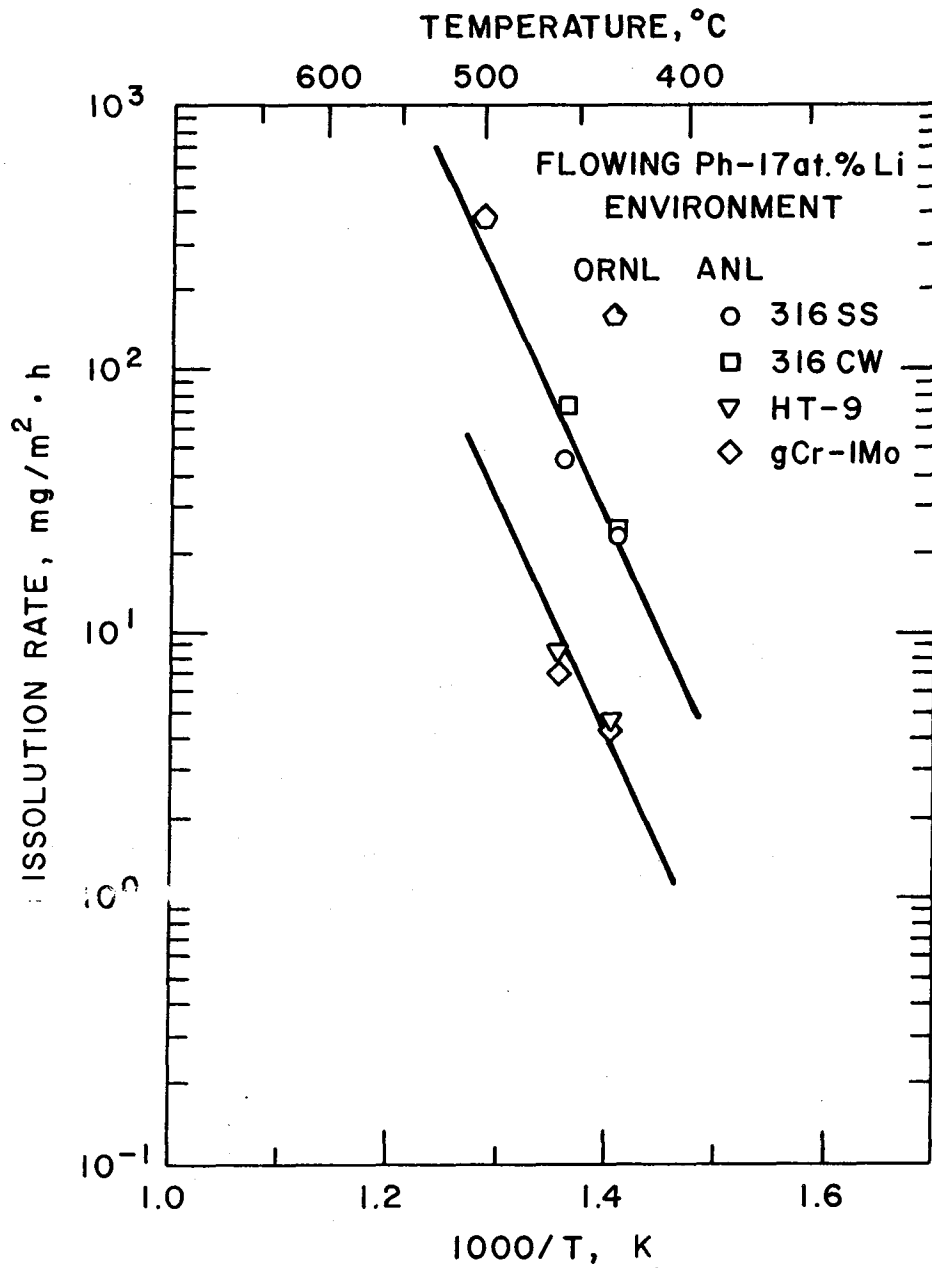


Figure 3.A-17. Arrhenius plot of dissolution rate data for austenitic and ferritic steels exposed to flowing Pb-17Li

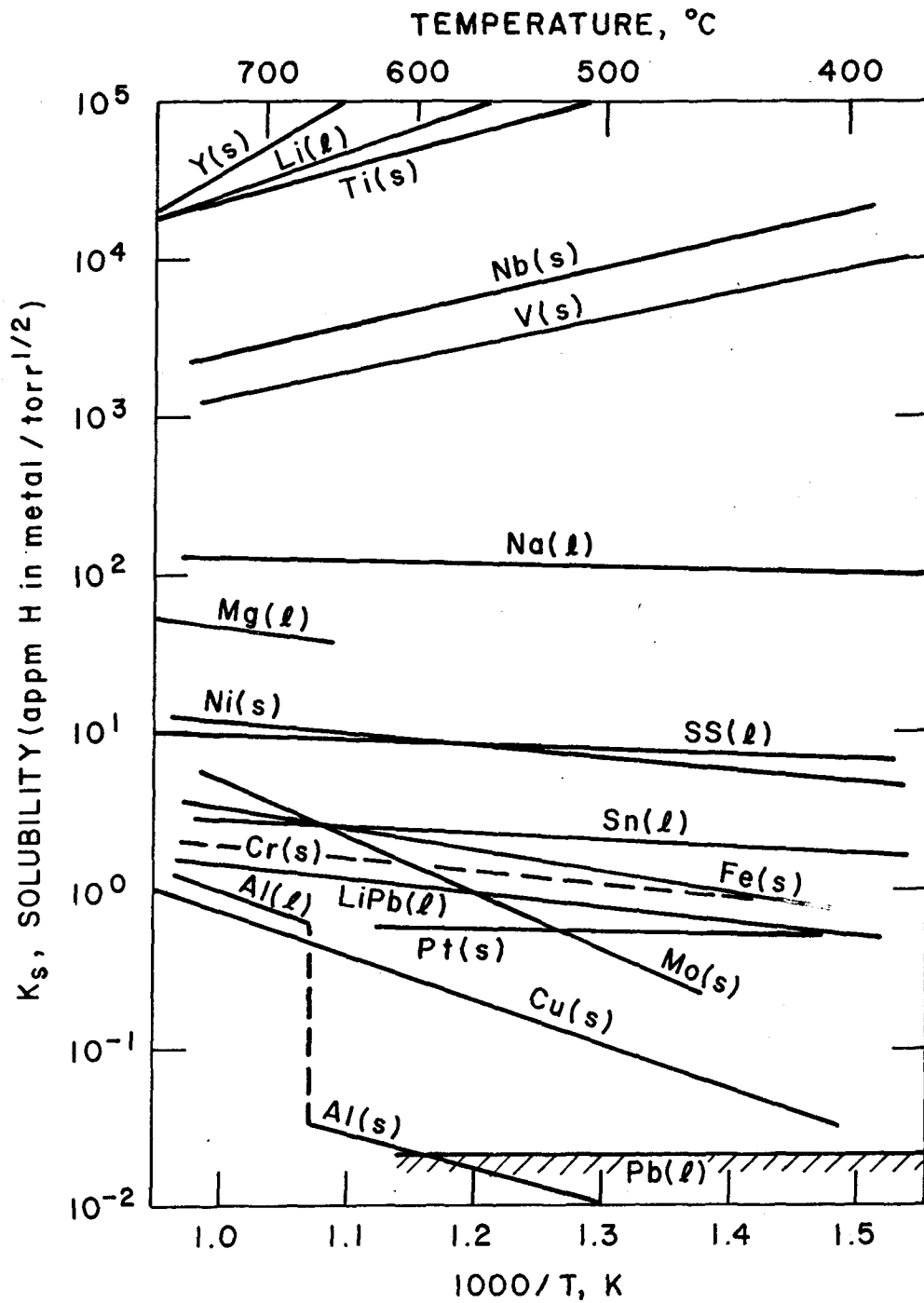


Figure 3.A-18. The solubility of hydrogen in selected metals and alloys as a function of temperature

CHAPTER 4

SOLID BREEDER BLANKETS

TABLE OF CONTENTS

4. SOLID BREEDER BLANKETS

	<u>Page</u>
4.1 Introduction and Critical Issues.....	4-1
4.2 Survey of Existing Experiments.....	4-5
4.2.1 Materials Development and Characterization.....	4-5
4.2.2 Tritium Inventory Recovery.....	4-11
4.2.3 Breeder/Multiplier/Structure Mechanical Interaction.....	4-13
4.2.4 Structure Mechanical Behavior.....	4-13
4.2.5 Corrosion and Mass Transfer.....	4-13
4.2.6 Tritium Permeation and Processing.....	4-14
4.2.7 Neutronics	4-14
4.3 Material Development and Characterization.....	4-17
4.3.1 Structure.....	4-17
4.3.2 Solid Breeder.....	4-23
4.3.3 Multiplier.....	4-29
4.4 Separate and Multiple Effect Experiments.....	4-38
4.4.1 Tritium Inventory and Recovery.....	4-38
4.4.1.1 Testing and Modelling Needs.....	4-38
4.4.1.2 Experiments and Facilities.....	4-48
4.4.1.3 Test Plan Considerations.....	4-64
4.4.2 Breeder/Multiplier/Structure Mechanical Interaction.....	4-68
4.4.2.1 Testing and Modelling Needs.....	4-68
4.4.2.2. Experiments and Facilities.....	4-71
4.4.2.3 Test Plan Considerations.....	4-77
4.4.3 Structure Mechanical Behavior.....	4-78
4.4.4 Corrosion and Mass Transfer.....	4-80
4.4.4.1 Testing and Modelling Needs.....	4-80
4.4.4.2 Experiments and Facilities.....	4-85
4.4.4.3 Test Plan Considerations.....	4-87
4.4.5 Tritium Permeation and Processing.....	4-90
4.4.6 Neutronics and Tritium Breeding.....	4-91
4.4.6.1 Uncertainty in Tritium Self-Sufficiency.....	4-91
4.4.6.2 Review of Present Status.....	4-92

TABLE OF CONTENTS (cont.)

4.4.6.3	Point Neutron Source Tests.....	4-94
4.4.6.4	Fission Reactor Tests.....	4-100
4.4.6.5	Fusion Test Facilities.....	4-101
4.5	Partially Integrated and Integrated Experiments.....	4-109
4.5.1	Non-Neutron Thermomechanical Integrity Tests.....	4-109
4.5.2	Nuclear Submodule.....	4-124
4.5.3	Fusion Experiments.....	4-140
4.5.4	Test Plan Considerations.....	4-141
4.6	Experiment Cost and Time Characteristics.....	4-143
4.7	Summary.....	4-154

LIST OF TABLES

<u>Table</u>		<u>Page</u>
4.1-1	Solid Breeder Blanket Characteristics Considered.....	4-2
4.1-2	Major Solid Breeder Blanket Issues.....	4-2
4.2-1	Solid Breeder Materials Fabricated in the United States.....	4-8
4.2-2	Representative Fabrication Capabilities Outside the United States.....	4-9
4.2-3	Solid Breeder Material Characterization Irradiations.....	4-10
4.2-4	In-situ Tritium Recovery Experiments.....	4-12
4.3-1	Material Property Needs for Solid Breeder Blankets.....	4-18
4.3-2	Structural Property Uncertainties after 15 MW-yr/m ²	4-22
4.3-3	Variation of Thermal Conductivity with Breeder Conditions.....	4-26
4.3-4	Representative Characteristics of Beryllium.....	4-30
4.3-5	Gas Production in Beryllium.....	4-33
4.4.1-1	Tritium Inventory and Transport Uncertainties.....	4-39
4.4.1-2	Contributions to Blanket Tritium Inventory.....	4-40
4.4.1-3	Contributors to Breeder Oxygen Activity.....	4-46
4.4.1-4	Typical Conditions for Present Solid Breeder Blankets.....	4-49
4.4.1-5	Influence of Experiment Parameters in Tritium Recovery.....	4-53
4.4.1-6	Characteristics of the Advanced In-Situ Tritium Recovery Experiment and Capsule Instrumentation.....	4-61
4.4.2-1	Environmental Parameter Ranges Applicable for Solid Breeder/ Multiplier/Structure Mechanical Testing.....	4-70
4.4.2-2	Solid Breeder/Structural Material Mechanical Interaction Experiment.....	4-76
4.4.4-1	Influence of Experimental Parameters on Corrosion and Mass Transfer.....	4-86
4.4.5-1	Tests to Address Tritium Permeation and Processing Issues.....	4-90
4.4.6-1	Achievable and Required Tritium Breeding Ratios and Associated Uncertainties for Leading Blanket Concepts in Tokamak Reactor in Tokamak Reactor Systems.....	4-93

LIST OF TABLES (cont.)

4.4.6-2	Experiments on Tritium Production Rate Using Point Neutron Sources.....	4-93
4.4.6-3	Estimate of the TBR Uncertainty in Various Blanket Concepts Due to Nuclear Data Uncertainties.....	4-95
4.4.6-4	Requirements for Measuring Technique Accuracy.....	4-97
4.4.6-5	Fluence Requirements for Various Measurement Techniques.....	4-103
4.5.1-1	Characteristics and Limitations of a Thermomechanical Integrity Test Facility.....	4-111
4.5.1-2	Issues Addressed by a Non-nuclear Thermomechanical Integrity Test Facility.....	4-112
4.5.1-3	Advantages and Disadvantages of Non-nuclear Heat Sources.....	4-113
4.5.1-4	Temperature Simulation of Li ₂ O/He/FS Plate Breeder.....	4-116
4.5.1-5	Characteristics of a Discrete-Source Full-Blanket TMIF.....	4-122
4.5.1-6	Possible TMIF Test Program per Blanket Concept.....	4-123
4.5.2-1	Peak Flux in Core Required to Simulate Power Density at Front of Blanket at 1 MW/m ²	4-126
4.5.2-2	Characteristics of a Representative Nuclear Submodule Assembly Experiment and Submodule Instrumentation.....	4-137
4.5.4-1	Comparison of Partially Integrated/Integrated Tests.....	4-142
4.6-1	Factors in Estimating Costs.....	4-143
4.6-2	Solid Breeder Experiment Direct Cost and Time Characteristics..	4-145
4.7-1	Major Solid Breeder Issues and Contributing Uncertainties.....	4-155
4.7-2	Material Development and Mechanical Tests.....	4-157
4.7-3	Basic Breeder Tests.....	4-158
4.7-4	Tritium Inventory and Transport Experiments.....	4-159
4.7-5	Maximum Non-fusion Device Tests.....	4-160
4.7-6	Modelling Needs.....	4-162

LIST OF FIGURES

<u>Figure</u>		<u>Page</u>
4.3-1	Range of mechanical property measurements needed and achieved for HT-9 and PCA ($15 \text{ MW/m}^2 = 180 \text{ dpa}$).....	4-20
4.3-2	Extent of irradiated data base of beryllium.....	4-32
4.3-3	Thermal creep rates for various grades of beryllium at $1000 \text{ }^\circ\text{C}$..	4-35
4.4.1-1	Experimental basis for tritium diffusivity in Li_2O and LiAlO_2 ...	4-42
4.4.1-2	Tritium surface adsorption inventory in TRIO experiment.....	4-43
4.4.1-3	Effect of oxygen activity on gas and condensed phase tritium....	4-45
4.4.1-4	Comparison of tritium generation and heating rates for solid breeder irradiation in thermal, fast and fusion reactors.....	4-50
4.4.1-5	Diagram of FUBR-1 subassembly.....	4-54
4.4.1-6	Diagram of TRIO: a) sweep gas flow path and b) capsule design...	4-56
4.4.1-7	Diagram of FFTF Materials Open Test Assembly.....	4-59
4.4.1-8	Diagram of possible Advanced In-situ Recovery experiment subassembly showing multiple capsules.....	4-60
4.4.1-9	Instrumentation and flow paths for Advanced In-Situ Recovery experiment.....	4-63
4.4.1-10	Range of temperature and burnup for Li_2O	4-65
4.4.1-11	Range of temperature and burnup for LiAlO_2 experiments.....	4-65
4.4.2-1	Fluence dependence for several of the key material properties associated with the mechanical interaction between the Li_2O and HT9 cladding.....	4-70
4.4.2-2	Schematic of subcapsule design to investigate the mechanical interaction between the solid breeder material and the structural cladding.....	4-73
4.4.2-3	Schematic of closed capsule irradiation vehicle to irradiate subcapsules designed to investigate the solid breeder/multiplier/clad mechanical interaction.....	4-74
4.4.4-1	Vapor pressure of LiOT and Li over several breeder materials...	4-84
4.4.6-1	Top view of the Phase 2 experiments at the FNS facility.....	4-98

LIST OF FIGURES (cont.)

4.4.6-2	Effect of the lithium carbonate container on the tritium production profiles.....	4-99
4.4.6-3	The R- θ geometrical model used to examine the effect of poloidal width on tritium production profiles.....	4-104
4.4.6-4	The total tritium production rate as a function of the test module poloidal width (θ_m). Also shown is the deviation from centerline values at two ^m poloidal locations within the test module ($\theta_t = 10^\circ$ and 20°).....	4-105
4.4.6-5	Total tritium production rate integrated over various spatial segments, and the overall tritium breeding rate as a function of the test module width (θ_m).....	4-107
4.5.1-1	Microwave heating profile in a γ -LiAlO ₂ block compared with 2 MW/m ² equivalent neutron wall load heating.....	4-114
4.5.1-2	Temperature profiles for Li ₂ O plate breeder, under fusion reactor and discrete-wire heating conditions.....	4-118
4.5.1-3	Temperature profiles for section LiAlO ₂ /Be BOT geometry near the first wall, under fusion reactor and discrete-wire heating.....	4-119
4.5.1-4	Block diagram of non-nuclear Thermomechanical Integrity Test Facility.....	4-121
4.5.2-1	Power density and tritium production profiles in fission slab module test for Li ₂ O/He/HT ₉ blanket.....	4-125
4.5.2-2	Microscope calculations of the tritium production rates for Li ₂ O in FFTF as a function of axial position for several core positions. These calculations assure the Li ₂ O has a density corresponding to 85% of its theoretical density and that the ⁶ Li enrichment is 2.5%.....	4-130
4.5.2-3	Microscope calculations of the neutron heating rates for Li ₂ O in FFTF as a function of axial position for several core positions. These calculations assure the Li ₂ O has a density corresponding to 85% of its theoretical density and that the ⁶ Li enrichment is 2.5%.....	4-130
4.5.2-4	Microscopic calculations indicating the decrease in the tritium production rates as a function of irradiation time. The ⁶ Li enrichments for the FFTF estimates were chosen to match the anticipated fusion tritium production rate.....	4-131

LIST OF FIGURES (cont.)

4.5.2-5	Microscopic calculations indicating the decrease in the neutron heating rates as a function of irradiation time. The ⁶ Li enrichments for the FFTF estimates were chosen to match the anticipated fusion tritium production rate.....	4-131
4.5.2-6	Simple models used to estimate self-shielding.....	4-132
4.5.2-7	Estimated in-core flux suppression as a function of solid breeder thickness and ⁶ Li enrichment.....	4-134
4.5.2-8	Estimated out-of-core flux suppression as a function of solid breeder thickness and ⁶ Li enrichment.....	4-134
4.5.2-9	Li ₂ O/He/HT9 blanket submodule.....	4-135
4.5.2-10	Instrumentation schematic for the nuclear submodule assembly test.....	4-138
4.7-1	Possible experiments for solid breeder blanket technology development.....	4-156

4. SOLID BREEDER BLANKETS

4.1 Introduction and Critical Issues

Present solid breeder blanket design concepts are based on incomplete or untested models regarding properties and phenomena. Some of the uncertainties are large enough to make the blankets potentially impractical. Consequently, the development of a feasible and attractive solid breeder blanket requires resolving these issues through experiments, modelling and innovative design. In this chapter, the issues are examined and experiments described that could address the major uncertainties in a timely and cost-effective manner.

The most important issues are tritium recovery, breeder thermomechanical behavior and tritium breeding.^(1,2) These are particularly acute for solid breeder blankets since: 1) there is limited understanding of gas transport in irradiated solids; 2) complex designs are used to keep the present low thermal conductivity solids within the temperature limits under substantial heating and neutron damage rates; and 3) the resulting designs have a significant amount of non-breeding structure, coolant and other material.

The issues and testing needs discussed here are based on the characteristics of top-ranked solid breeder concepts (Table 4.1-1) from the Blanket Comparison and Selection. Other designs (e.g., draw-salt or mobile-pebble cooled), conditions (e.g., very high neutron wall loads) and applications (e.g., synfuels production) are not expected to substantially change the major issues and experiments, but could add other issues or alter priorities. The major classes of issues are (Table 4.1-2):

Breeder/Multiplier Tritium Inventory and Recovery. Tritium recovery and control requires understanding the retention and transport of tritium within the breeder and multiplier. Uncertainties range from basic properties such as tritium intragranular diffusivity in unirradiated breeder material, to the effects of the complex breeder physical environment.

Tritium Self-Sufficiency. The tritium production rate must exceed the consumption rate. However, there are uncertainties in determining both the achievable tritium breeding rate (e.g., neutronics calculation accuracy) and in the required tritium breeding rate (e.g., blanket tritium holdup).

Table 4.1-1. Solid Breeder Blanket Characteristics Considered

Fusion-electric applications
Neutron wall loads around 5 MW/m^2
Blanket lifetimes around 15 MW-yr/m^2
Helium or water coolant
Unmultiplied and beryllium multiplied blankets
Austenitic (PCA) and ferritic (HT-9) structure
Separate purge and coolant streams
Breeder in plate, BIT or BOT geometry*

*BIT = Breeder-inside-tube; BOT = Breeder-outside-tube

Table 4.1-2. Major Solid Breeder Blanket Issues

Breeder/multiplier tritium inventory and recovery
Tritium self-sufficiency
Breeder/multiplier/structure mechanical interactions
Structural response to environmental conditions
Corrosion and mass transfer
Tritium permeation and processing from blanket
Failure modes and reliability

Breeder/Multiplier/Structure Mechanical Interactions. The interface between the breeder/multiplier and the surrounding blanket, normally through a structural cladding, can be an area where stress and heat transfer limits occur. Uncertainties include the mutual loads and responses imposed by the element on each other (e.g., swelling of clad and breeder) and their influence on the breeder thermal behavior (e.g., gap conductance).

Structural Response to Environmental Conditions. The mechanical behavior of structural elements of the blanket during blanket operation determines the physical lifetime. Uncertainties in the loading (e.g., magnitude of magnetic field transients) and response (e.g., radiation-induced creep stress relaxation, crack growth) must be accounted for by conservative designs or premature failure of the blanket may occur.

Corrosion and Mass Transfer. Material interactions uncertainties include mass transfer of the breeder within the internal porosity or out of the blanket entirely, and chemical reactions at the structure/breeder interface. These affect the configuration and operating temperature limits.

Tritium Permeation and Processing from Blanket. The permeation of tritium outside of the breeder zone is important for defining the coolant detritiation requirements, but the nature and effects of the environment and surface conditions are uncertain. Uncertainties in the recovery of tritium from the primary breeder extraction stream include the tritium form and the inventory and efficiency of the recovery process.

Failure Modes and Reliability. The mechanisms for component failure must be identified in order to determine and improve blanket lifetime and safety.

Each of these issues can be addressed by a range of experiments, from property measurements or simple scoping tests to more complex experiments as the underlying phenomena and the component design become clear. This sense of test integration is useful for identifying possible experiments and strategies. The levels adopted here include basic experiments to fabricate and characterize materials; separate-effect tests with one varying environmental condition for phenomena exploration; multiple-effect tests with several conditions applied simultaneously to explore and understand simple interactions; partially integrated tests where full component conditions are reproduced closely, but with some major factor missing (e.g., neutrons); integrated tests

to verify the concept under full conditions (although possibly scaled); and component tests to establish reliability.

It is the intent of this chapter to consider the critical issues and anticipate the type, characteristics and sequencing of the experiments needed to resolve the issues. From understanding the issues and associated experiments, it is possible to identify timely and cost-effective program plans.

The chapter begins with a brief review of existing experiments and facilities. Each of the issue categories is then examined to determine tests that could address the major uncertainties. It is important to note that all these tests need not necessarily be performed, particularly in the specific forms discussed here. Rather, experiment or facility examples are defined in order to understand their capabilities and costs, which can then be used to judge the usefulness of that type of test or facility. A large fraction of the tests are separate- or multiple-effect tests. By providing a near-term understanding of the underlying phenomena, these are cost-effective tests that can strongly influence solid breeder blanket feasibility and attractiveness. These tests can be assembled into test plans, as in Chapter 2, which identify logical sequences of major experiments that can address the majority of the uncertainties under a variety of programmatic assumptions.

References for Section 4.1

1. M.A. Abdou, et al., "FINESSE - A Study of the Issues, Experiments and Facilities for Fusion Nuclear Technology Research & Development, Interim Report", University of California, Los Angeles, PPG-821 and UCLA-ENG-84-30, October 1984.
2. D.L. Smith, et al., "Blanket Comparison and Selection Study, Final Report", Argonne National Laboratory, ANL/FPP-84-1, September 1984.

4.2 Survey of Existing Experiments

There are active experimental programs in the U.S. and abroad to develop solid breeder blanket technology. The status of the knowledge base and the remaining testing needs will be discussed in some detail in subsequent sections. A summary of the most significant completed, operating and planned experiments and facilities is provided here. Modelling and design-related activities are important but are not included.

4.2.1 Materials Development and Characterization

The development of materials for solid breeder blankets is strongly based on information from fission reactor development with respect to structural alloys, ceramic fuels and beryllium. In particular, the U.S. liquid metal reactor alloy development program has been studying the impact of neutron irradiation on mechanical properties of structural alloys for the past 25 years. This large effort led to the optimization of the titanium-modified austenitic stainless steels and more recently towards emphasis on ferritic alloys. The same general properties of high-temperature strength and radiation-resistance make these alloys of interest to the fusion program. Furthermore, fission reactor fuels are also usually solid ceramics, so much of the information and models with respect to fabrication, properties and behavior is of interest to fusion solid breeders. Finally, beryllium and other potential neutron multipliers have been considered or used in various fusion reactor applications.

The U.S. Magnetic Fusion Energy Materials Program is organized into the following major elements: Damage Analysis and Fundamental Studies (DAFS), Alloy Development for Irradiation Performance (ADIP), Special Purpose Materials, Plasma-Materials Interaction, and High Heat flux Components. The first three elements are directly relevant to solid breeder blanket technology.

Damage and Fundamental Studies (DAFS)

The scope of the DAFS program includes the development of procedures to characterize irradiation fields of test facilities and fusion reactors; theoretical and experimental investigations of the influence of irradiation variables on material damage and property changes; and the development of

damage-mechanism-based procedures to correlate material mechanical behavior changes in diverse test environments and thereby predict the corresponding behavior in relevant fusion environments.^(1,2) The effort also includes investigating the irradiation stability of simple alloys over a range of compositions.

Examples of experiments within the DAFS program include efforts to understand helium effects on mechanical properties, to investigate spectrum effects on material properties, and to look at the impact of substituting low-activation Mn for Ni in simple austenitic alloys. In one experiment, helium effects are being studied through a comparison of austenitic alloy specimens that differ only in the amount of ⁵⁹Ni. The isotopically enriched specimens will have a helium production to damage rate (He/dpa) ratio of about 10 appm, which is comparable to that in a fusion device and larger than that in the natural-enriched specimens. These specimens will be irradiated side-by-side in FFTF for up to four years (about 35 dpa) at temperatures from 360 to 600°C. In another study of the effect of neutron energy on changes in mechanical properties, tensile specimens of copper, iron, 316 SS and another steel are being irradiated in the OWR thermal fission reactor and at RTNS-II (14 MeV fusion spectrum) to a peak fluence of 10¹⁹ n/cm² (0.03 dpa in Fe). Many other recent or active experiments are described in Ref. (3).

Alloy Development and Irradiation Program (ADIP)

The scope of the ADIP program includes the development of new and innovative alloys, and experimental measurement and characterization of spectral, helium production and high neutron fluence effects on alloy properties. ADIP is organized with respect to alloy classes (referred to as paths of material development): Austenitics (Path A); Nickel-Based Alloys (Path B); Refractory Alloys (Path C); Innovative Alloys (Path D); Ferritic Alloys (Path E); and copper alloys. The development of new alloys is done in close cooperation with the DAFS program. At present, the three primary structural alloys are a titanium-modified austenitic stainless steel similar to the optimized alloy developed in the U.S. liquid metal reactor program (referred to in the fusion program as PCA or Prime Candidate Alloy, and in the fission program as a D9-type alloy), a ferritic steel such as HT-9, and a vanadium alloy such as V-15Cr-5Ti.

At this time, the irradiation experiments are predominantly being carried out in HFIR and FFTF. Earlier irradiations were also performed in EBR-II and ORR. The HFIR irradiations provide reasonable fluence data with high helium production rates in the austenitic alloys. The FFTF irradiations provide high fluence data for both alloy development and irradiation effects and are predominantly used to investigate the ferritic and vanadium based alloys.

Examples of experiments include efforts to match He/dpa ratios anticipated in the fusion first wall, to develop low activation austenitic and ferritic alloys, and to study the compatibility of solid breeder materials and liquid metals with respect to the structural material. In the ORR Spectral Tailoring Experiment, for example, a fusion first wall relevant He/dpa ratio in austenitic 316 SS and PCA is provided by changing a moderator medium surrounding the capsule to progressively decrease the thermal flux component as the quantity of ^{59}Ni increases due to nuclear reactions. Isothermal irradiations have been performed from 300 to 600°C up to a peak fluence corresponding to 15 dpa.

Special Purpose Materials - Solid Breeder

The characterization, fabrication and investigation of irradiation effects on lithium ceramics is much less advanced than for structural alloys. A number of countries have developed the capability of fabricating lithium ceramics and have embarked upon an organized effort in characterizing their physical and mechanical properties.⁽⁴⁻⁸⁾ For example, the French have undertaken a characterization program for their $\gamma\text{-LiAlO}_2$ solid breeder material which includes Young's modulus and ultimate compressive strength (as functions of porosity and grain size); thermal creep and shock (several forms); and thermal diffusivity, specific heat, and thermal conductivity (as a function of temperature). Fabrication capabilities in the U.S. are summarized in Table 4.2-1, and for the international community in Table 4.2-2.

Solid breeder materials have been irradiated in both thermal and fast reactors to investigate the impact of irradiation on stability, tritium and helium retention, and thermal conductivity (Table 4.2-3). In general, these experiments have been performed in closed capsules and have tended to be isothermal. Within the U.S., the major solid breeder materials characterization experiments were or are TULIP,⁽⁹⁾ FUBR-1A,⁽¹⁰⁾ and FUBR-1B. The TULIP

Table 4.2-1. Solid Breeder Materials Fabricated in the United States

Ceramic	LiAlO ₂	LiAlO ₂	Li ₂ O	Li ₄ SiO ₄	Li ₂ ZrO ₃	Li ₈ ZrO ₆
Crystalline Phase	Gamma (Tetragonal)	Gamma (Tetragonal)	Cubic	Monoclinic	Monoclinic	Hexagonal
Physical Form	Pellet/Monolithic	Spheres	Pellet/Monolithic	Pellet/Monolithic	Pellet/Monolithic	Pellet/Monolithic
Process	Spray dried/powder Hot pressing or uniaxial/isostatic cold pressed and sintered pellet	Plasma sprayed and Sol Gel	Lithium carbonate decomposition Hot pressing or or sintering	Alkoxide derived Hot pressing or uniaxial/isostatic cold pressed and sintered	Alkoxide derived Hot pressing or uniaxial/isostatic cold pressed and sintered	Alkoxide derived Hot pressing or uniaxial/isostatic cold pressed and sintered
Grain Size	5 μm to 3 μm	35 μm to 65 μm	3 μm to 60 μm	2 μm	2 μm	3 μm
Surface Area	1 m ² /cm ³	3 m ² /cm ³	0.17 m ² /cm ³	1 m ² /cm ³	1 m ² /cm ³	—
Density	60-99% TD	~ 100 % TD	60-99% TD	80-85% TD	85% TD	80% TD
Diameter	0.5-10 cm O.D.	—	0.5-3 cm O.D.	1 cm	1 cm	1 cm
Phase Purity	Phase pure	< 2% LiAl ₅ O ₈	Phase pure	Phase pure	Phase pure	< 2% Li ₂ ZrO ₃
Metallic Impurities	1200 μg/g	~ 5000 μg/g	500 μg/g	500 μg/g	< 500 μg/g	< μg/g
Anion Impurities (H,F,Cl)	150 μg/g	20 μg/g	15 μg/g	22 μg/g	130 μg/g	24 μg/g
Stability	Submicron LiAlO ₂ sinters above 900°C	Stable	Vaporization and grain growth	Grain growth at 900°C	Stable at 900°C	Sensitive to moisture Potential disassociation into Li ₂ O and Li ₄ ZrO ₄

Table 4.2-2. Representative Fabrication Capabilities Outside the United States

	Japan	France	Germany	Netherlands/UKAEA	CEN/SCK-MOL-Belgium	Italy
Ceramics	Li ₂ O, LiAlO ₂	LiAlO ₂	Li ₂ SiO ₃	LiAlO ₂ , Li ₂ SiO ₃ (Li ₂ O) (Li ₈ ZrO ₆)	Li ₂ SiO ₃ (Li ₈ ZrO ₆)	LiAlO ₂
Physical Forms	pellets, single crystal (Li ₂ O)	spheres, pellets	spheres, pellets	pellets, rectangular beams	pellets, granules	pellets
Grain Size	5-20 μm	0.3-30 μm	4-20 μm (spheres)	10 μm (LiAlO ₂) 20 μm (Li ₂ SiO ₃)	< 1-15 μm	1-4 μm (spheres) 0.5-1 μm (platelets)
Density	70-95% TD	60-90% TD	--	70-80% TD	80-95% TD	85-90% TD
Porosity	--	0.035-3 μm	--	1 μm (LiAlO ₂) 1-2 μm (Li ₂ SiO ₃)	< 1 μm	0.3 μm
Metallic Impurities	< 600 ppm	--	--	--	< 1000 ppm	< 2000 ppm
Anion Impurities (H, F, Cl)	--	--	--	< 100 ppm	< 100 ppm	< 100 ppm

Table 4.2-3. Solid Breeder Material Characterization Irradiations

Experiment	Ceramic	Material Characteristics				Irradiation Environment				Reactor	Time Frame
		Grain size (μm)	Density ($\% \text{TD}$)	Li-6 ($\%$)	Temperature ($^{\circ}\text{C}$)	Li burnup (Max at.%)	Container				
ORR	Li_2O	< 47	70	0.05	750,850,1000	0.05	--	ORR	--		
TULIP (US)	Li_2O	50	87	93	600	3	35% Ni, PCA	EBR-II	84		
FUBR-1A (US)	Li_2O	6	85	45	500,700,900	1.5	Ni, Ce getter	EBR-II	84/85		
	LiAlO_2	< 1	85,95	95	500,700,900	3	"	"	"		
	Li_4SiO_4	2	85	70	500,700,900	2	"	"	"		
	Li_2ZrO_3	2	85	70	500,700,900	2	"	"	"		
FUBR-1B (US)	Li_2O	< 5	60,80	56	500,700,900	5	Ni, Ce getter	EBR-II	85/89		
	LiAlO_2 (sphere-pac)	< 5	80	56	500-700/1000	9	"	"	"		
	Li_4SiO_4	< 5	80	94	400-500	9	"	"	"		
	Li_8ZrO_6	< 5	80	73	600-700	7	"	"	"		
	Li_2ZrO_3	< 5	85	70	520-620	7	"	"	"		
ALICE (France)	LiAlO_2	0.35-13	71-84	-	400,600	--	--	OSIRIS	85/86		
DELICE (Germany)	Li_2SiO_3 (Li_4SiO_4)	-	65,85,95	-	400,600,700	< 0.02	SS	OSIRIS	85/86		
EXOTIC (Neth./UK/Belgium)	Li_2SiO_3	-	80	0.05-7.5	400,600	-	-	HFR	85/86		
	Li_2O	-	-	-	-	-	-	"	"		
	LiAlO_2	-	80	0.06-7.5	-	-	-	"	"		
	Li_2ZrO_3	-	-	-	-	-	-	"	"		
CREATE (Canada)	LiAlO_2	< 1	80,90	7.5	100	-	Quartz, SS, Ni	NRU	85/86		

experiment provided information on dimensional and microstructural stability, and helium and tritium retention of Li_2O to a peak lithium burnup of 3%. The FUBR-1A experiment provided similar information on several lithium ceramics.

These experiments have been irradiated to relatively low lithium burnups when compared to present commercial designs (lithium burnups of ~ 10 at.% in unmultiplied and ~ 70 at.% in multiplied blanket designs). The FUBR-1B experiment (Table 4.2-3) is designed to investigate the effects of neutron irradiation on selected solid breeder materials to relatively high lithium burn-up (up to 9%). The irradiation has been initiated in the EBR-II with a number of U.S. ceramic materials. Several positions within the irradiation vehicles contain relative large diameter pellets (2.4 cm diameter) to investigate the impact of temperature gradients on the ceramics' response to irradiation. Other positions are capable of investigating the mechanical interaction between the solid breeder materials and surrounding cladding. New solid breeder materials supplied by international fabricators will be inserted at the first discharge of the FUBR-1B experiment as part of the BEATRIX international exchange program.

Special Purpose Materials - Beryllium Multiplier

Beryllium is the leading candidate neutron multiplier material for solid breeder blankets due to its high cross-section for the $(n, 2n)$ reaction. At present, there are no major experiments within the U.S. which are investigating irradiation effects on beryllium, although an irradiation creep experiment is being considered. The relatively modest irradiation data base has been compiled and summarized in Ref. (11).

4.2.2 Tritium Inventory Recovery

In-situ tritium recovery experiments have been or are currently being performed at several irradiation facilities around the world.⁽¹²⁻¹⁵⁾ The major participants and overall characteristics of each experimental program are summarized in Table 4.2-4. These experiments are looking at the tritium recovery behavior of Li_2O , LiAlO_2 and other ternary ceramics as a function of irradiation temperature and purge gas composition. These irradiations have tended to be isothermal and have so far investigated the lower temperature

Table 4.2-4. In-situ Tritium Recovery Experiments

Experiment	Material Characteristics				Irradiation Environment				Time Frame		
	Ceramic	Grain size (μm)	Density (ZTD) (%)	Li-6 (%)	Temperature ($^{\circ}\text{C}$)	Li burnup (Max at.%)	Sweep Gas	Flow rate ($\text{m}^3/\text{s-g}$)		Container	Reactor
TRIO (US)	LiAlO_2	0.2 (50 μm particles, 0.9 cm thick annular pellet)	65	0.55	400, ..., 700	0.2	He + H_2 He + O_2	0.01-0.1	SS	ORR	84/85
VOM-15H (Japan)	Li_2O	< 10	86	7.4	480, ..., 760	0.24	He + H_2	0.05	-	JRR-2	84
VOM 22/23 (Japan)	Li_2O	- (1.1 cm pebbles)	-	7.6	400-900	0.04	He + D_2	-	SS	JRR-2	--
	LiAlO_2	- (1.1 cm pebbles)	-	25	400-900	0.1	He + D_2	-	SS	JRR-2	--
LILA (France)	LiAlO_2	1-30 (1 cm diameter pellet)	78	7.5	375-600	< 0.02	He	-	Quartz, SS	SILOE	86
LISA (Germany)	Li_2SiO_3	- (1 cm diameter pellet)	-	-	-	-	-	-	-	SILOE	86
EXOTIC (Neth./UK/Belgium)	LiAlO_2	- (1.4 cm diameter pellet)	80, 95	0.6, 7.5	400, 600	< 0.4	He + H_2	-	SS, Ni	HFR	86
	Li_2SiO_3	- (1.4 cm diameter pellet)	50	0.6, 7.5	400, 600	< 0.4	He + H_2	-	SS, Ni	HFR	86
CRITIC (Canada)	Li_2O	- (1 cm thick annular pellet)	80	0.3	400-900	-	He + H_2 He + H_2O He + O_2	-	Inconel-600	NRU	86

limit for tritium recovery. Examination of the upper temperature limits (900°C) for Li_2O is planned in the Japanese and Canadian experiments. The lithium burnup in all experiments has been low, less than 0.4%. All experiments measure the quantity of tritium released and relative amounts of tritium forms released. Post-irradiation examination in these experiments include helium/tritium retention, dimensional stability, and microstructural characterization. Some of the experiments also provided additional information on breeder/cladding corrosion, dosimetry, and tritium permeation.

4.2.3 Breeder/Multiplier/Structure Mechanical Interaction

There has been little testing of the breeder/cladding interaction for fusion blankets. Two related experiments are measurements of heat transfer across the interface between a Li_2O pellet and a metal heat sink with a variable gap spacing,⁽¹⁶⁾ and efforts to develop a microwave heating system to test a sintered block of LiAlO_2 with internal cooling tubes under an approximately exponential internal heating profile.⁽¹⁷⁾

4.2.4 Structure Mechanical Behavior

The behavior of metals under high neutron fluence and high temperatures for fission and fusion reactors include a variety of new mechanical phenomena. Present efforts generally emphasize model development. No fusion blanket components have been tested.

First walls must also accommodate high heat fluxes and plasma bombardment. The need to develop actively-cooled components for near-term physics experiments has led to tests of small sections (single tubes, several parallel channels) under high heat flux and thermal cycling conditions.⁽¹⁸⁾

The FELIX device at ANL allows measurement of electromagnetic effects due to steady-state or pulsed magnetic fields. Experiments have been performed for several basic 2-D and 3-D geometries to provide benchmarks for present code development.⁽¹⁹⁾

4.2.5 Corrosion and Mass Transfer

Several tests of breeder and structure compatibility have been performed.^(9,21,22) Most measurements have considered Li_2O and various steels

(316SS and HT9, for example) because of the potential for formation of LiOH. Weight loss measurements for Li₂O in flowing helium with various moisture contents have been attempted at GA and ANL.^(16,22)

4.2.6 Tritium Processing and Permeation

Tritium processing and permeation experiments have been carried out in a variety of laboratories. Two of the major facilities currently performing work are TSTA (Tritium Systems Test Assembly) at LANL and TPX (Tritium Plasma Experiment) at SNLL. The TSTA experiment presently provides integrated testing of tritium processing hardware rather than specific solid breeder blanket purge processing systems. TPX is investigating issues of plasma-driven tritium permeation. Breeder-relevant tritium permeation measurements were obtained in the TRIO experiment during in-situ irradiation of LiAlO₂ pellets.⁽¹²⁾ Additional work in the U.S. on tritium permeation is underway as part of the Fusion Safety Program at INEL.

4.2.7 Neutronics

There is a large ongoing effort to improve the fusion communities capabilities with respect to neutronics calculations - tritium breeding, radiation damage, heating, shielding, and activation. This effort includes verifying and improving cross-section data and processed data libraries, as comparison of codes against benchmark experiments. Two major examples of the latter are the U.S./Japan Breeder Neutronics Program with the JAERI Fusion Neutron Source (FNS),⁽²⁶⁾ and the EPRI-sponsored TFTR Lithium Blanket Module Program.⁽²⁷⁾ Experiments with Li₂O, and more recently with beryllium, have been conducted at FNS. The Lithium Blanket Module has been constructed and analysis techniques prepared, but tests have been postponed by the delay in TFTR tritium operation.

References for Section 4.2

1. D.G. Doran, "Fundamental Radiation Effects Studies in the Fusion Materials Program," J. Nucl. Mat., 108 & 109, 1982, pp. 279-295.
2. D.G. Doran, "The Role of Radiation Damage Analysis in the Fusion Program," J. Nucl. Mat., 117, 1983, pp. 1-3.

3. "Damage Analysis and Fundamental Studies (DAFS) Quarterly Progress Report," DOE/ER-0046/21, May 1985.
4. Y.Y. Liu, M.C. Billone, A.K. Fisher, S.W. Tam, R.G. Clemmer and G.W. Hollenberg, "Solid Tritium-Breeder Materials: Li_2O and LiAlO_2 , A Data Base Review," Fusion Technology (in press).
5. "EXOTIC: Development of Ceramic Tritium Breeding Materials, Annual Progress Report 1984," EGN-167, June 1985.
6. C. Alvani, S. Casadio, L. Lorendini and G. Brambilla, "Fabrication of Porous LiAlO_2 Ceramic Breeder Material," Sixth Topical Meeting on the Technology of Fusion Energy, San Francisco, CA, March 3-7, 1985.
7. K.R. Kummerer and W. Dienst, "Selection, Characterization and Testing of Ceramic Breeder Materials," First International Conf. on Fusion Reactor Materials, Tokyo, Japan, December 3-6, 1984.
8. B. Rasneur, "Tritium Breeding Porous Ceramic $\gamma\text{-LiAlO}_2$," 13th Symp. on Fusion Technology-SOFT, Varese, France, September 24-28, 1984.
9. D.L. Porter, et al., "Neutron Irradiation and Compatibility Testing of Li_2O ," J. Nucl. Mat., 122 & 123, p. 929, 1984.
10. G.W. Hollenberg, "The Effect of Irradiation on Four Solid Breeder Materials," First International Conf. on Fusion Reactor Materials, Tokyo, Japan, December 3-6, 1984.
11. L.G. Miller, J.M. Beeston and F.J. Fulton, "Radiation Damage Experiments and Lifetime Estimates for Beryllium Components in Fusion Systems," Fusion Technology, 8, Part 2, July 1985, pp. 1152.
12. R.G. Clemmer, et al., "The TRIO Experiment," ANL-84-55, Argonne National Laboratory, September 1984.
13. T. Kurasawa, et al., "In-situ Tritium Recovery Experiment from Lithium Oxide Under High Neutron Fluence," First International Conf. on Fusion Reactor Materials, Tokyo, Japan, December 3-6, 1984.
14. E. Roth, et al., "Irradiation of Lithium Aluminate and Tritium Extraction," *ibid.*
15. H. Kwast, J.D. Elen and R. Conrad, "ENC Experiments Related to the Development of Ceramic Tritium Breeding Materials," *ibid.*
16. T. Ohkawa, et al., "Annual Report to DOE of the GA Technologies Fusion Program, Fiscal 1982," GA-A17383, GA Technologies, 1983.
17. B. Misra, et al., "Thermal-Hydraulic/Thermomechanical Testing of Solid Breeder Blanket Modules Using Microwave Energy," Fusion Technology, 8, Part 2, July 1985, pp. 927.

18. M.A. Abdou, et al., "Technical Assessment of the Critical Issues and Problem Areas in High Heat Flux Materials & Component Development," PPG-815 and UCLA-ENG-84-25, University of California at Los Angeles, June 1984.
19. L.R. Turner and W.F. Praeg, "Detailed Technical Plan for Test Program Element-III (TPE-III) of the First Wall/Blanket/Shield Engineering Test Program," ANL/FPP/TM-155, Argonne National Laboratory, March 1982.
20. L.R. Turner, et al., "The FELIX Experiments; Measurements of Electromagnetic Effects," Fusion Technology, 8, Part 2, July 1985, pp. 227.
21. R.J. Pulham, W.R. Watson and J.S. Collinson, "Chemical Compatibility Between Lithium Oxide and Transition Metals," J. of Nucl. Mat., 122 & 123, 1984, pp. 1243-1246.
22. O.K. Chopra and D.L. Smith, "Compatibility Studies of Structural Alloys with Solid Breeder Materials," in ADIP Semiannual Progress Report for Period Ending September 30, 1983," DOE/ER-0045/11, March 1984.
23. H. Maekawa, et al., "Measurements of Tritium Production-Rate Distribution in a 60 cm-Thick Li₂O Slab Assembly and its Analysis," Fusion Technology, 8, Part 2, July 1985, pp. 1460.
24. D.L. Jassby, et al., "Lithium Blanket Module Tests on the TFTR," PPPL-EPRI-9, Princeton Plasma Physics Laboratory, April 1981.

4.3 Materials Development and Characterization

A fusion reactor poses a more demanding environment than experienced by any previous nuclear application, with a high radiation flux and fluence, high temperatures, corrosive or embrittling materials, thermal cycling, magnetic fields and plasma bombardment. The behavior of existing materials is either unknown or inadequate under these conditions and the development of new materials is critical to the feasibility and attractiveness of fusion.

The materials can be roughly divided into structural materials and special purpose materials. Structural materials provide the basic framework for building and operating the entire machine, and are common to most components. The need for an appropriate structural material has long been recognized and a large effort initiated to identify, develop and characterize suitable materials. Special purpose materials are those needed for specific application in particular components. In solid breeder blankets, these are primarily the solid breeder and multiplier.

The materials needs can be divided into development (identification, production, fabrication, welding and reprocessing) and characterization (physical characteristics such as impurity content and microstructure, and unirradiated and irradiated properties). An adequate materials data base is important even in the near-term since it provides design directions, supports model development, and eliminates uncertainties in interpreting phenomena due to uncertainties in properties.

The emphasis here is on the development and characterization needs of materials specific to solid breeder blankets. Structural material development is surveyed but not described in detail. The needs for solid breeder and multiplier materials are addressed with respect to fabrication, reprocessing, and properties. A summary of the key properties is given in Table 4.3-1.

4.3.1 Structure

Present alloy development programs such as ADIP and DAFS are aimed at selecting, understanding and optimizing the properties of structural materials (Section 4.2). An analysis of the effort to develop these alloys is beyond the scope of this study. However, at some point a material will have to be

Table 4.3-1. Material Property Needs for Solid Breeder Blankets

Structure (Base and Weld Metal)

swelling
creep
ductility (primarily ferritic alloys)
DBTT (primarily ferritic alloys)
He embrittlement (primarily ferritic alloys)
tensile strength
fracture strength
crack growth

Breeder

thermal conductivity
tritium diffusivity
solubility of T_2O and T_2
surface adsorption of T_2O and T_2
equilibrium thermodynamics of solid breeder system
swelling
creep
Young's modulus
fracture strength

Multiplier

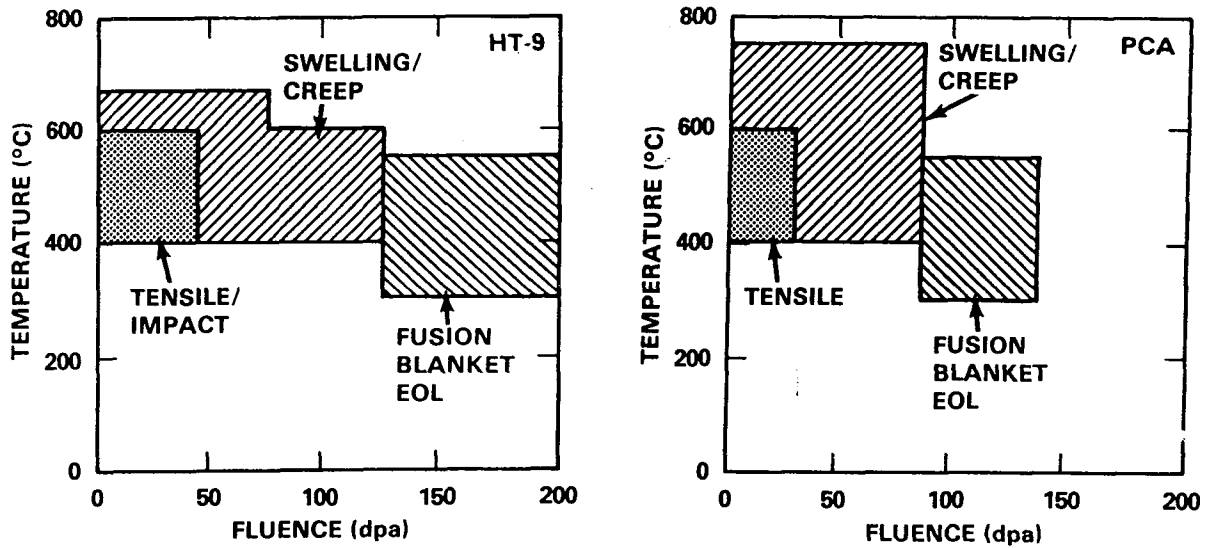
swelling
creep
ductility
tensile strength
fracture strength

selected for use in blanket experiments such as those exploring the breeder/structure mechanical interaction, even though this alloy may not be fully optimized and parallel efforts to develop better alloys can continue. The requirements on the properties of this (or any proposed) alloy are briefly considered here as illustrative of the effort required to characterize a given structural material for irradiated operation.

Due to their fairly extensive data base which indicates acceptable high-temperature strength, radiation-resistance, low cost and chemical compatibility with many solid breeder blanket materials, the most promising alloys at present are the austenitic and ferritic steels such as the PCA (Ti-modified 316 SS) and HT-9 alloys under consideration in the US. However, these are by no means established as the "best" alloys. For example, solution annealed 316L austenitic steel and quenched/tempered 1.4914 martensitic steel are being pursued as the structural materials for NET. Low activation versions of these structural materials are also of great interest. Even refractory metals such as vanadium alloys have not been ruled out since there may be ways to take advantage of their high-temperature strength and other properties while limiting chemical compatibility, ductility and DBTT problems.

The mechanical and thermophysical properties of the candidate alloys must be available over the reactor temperature and fluence range, or about 0-600°C and 0-15 MW-yr/m² based on present blanket concepts and materials. The major mechanical properties for the first wall and blanket are swelling, creep, tensile strength, ductility, fracture properties and fatigue properties.

Thermophysical properties such as heat capacity, thermal conductivity and the thermal expansion coefficient are not strongly changed from the base material over the anticipated blanket lifetime (~ 200 dpa, 2000 appm He for ferritic steel), or even within the various alloy versions. Mechanical properties, however, can change substantially. The nature of the materials data base for the two primary US alloys is indicated in Figure 4.3-1. A general description of the structural materials data base as of last year has been reported in the FINESSE Interim Report.⁽¹⁾ Within the past year, swelling and creep data for PCA have been obtained for a peak fluence corresponding to 85 dpa and similar data for HT-9 have been extended to 120 dpa. Recent Charpy impact data to 30 dpa have tended to confirm the saturation in the DBTT shift



HEDL 8510-038.3

Figure 4.3-1. Range of mechanical property measurements needed and achieved for HT-9 and PCA ($15 \text{ MW/m}^2 = 180 \text{ dpa}$).

with fluence.⁽²⁾ A series of experiments to investigate neutron irradiation effects on vanadium alloy material properties has been initiated⁽³⁾ and specimens to a neutron exposure corresponding to 57 dpa have been discharged from the FFTF reactor. Limited data at $\sim 18 \text{ dpa}$ ⁽⁴⁾ suggest that the present fusion heat of V-15Cr-5Ti may have a severe ductility reduction due to neutron irradiation.

Often the fluence dependence of many properties can be divided into two types: 1) an initial incubation period with little property change, and then a steady-state regime where the property changes directly with increasing fluence; and 2) an initial transient regime where the property changes with increasing fluence, leading to a saturation regime with little further change with fluence. Based on the present data base, models and these observations, it is possible to extrapolate property changes with fluence. However, it is important to remember that these observations are based upon material behavior

in a fission neutron environment and for neutron fluences significantly less than those anticipated in a fusion reactor. Limited data suggest that the fusion environment may alter the fluence dependence of the material behavior. For example, the tensile properties of cold worked 316SS exhibited saturation at relatively low neutron damage. However, recent data suggest that these properties are starting to change again with fluence.⁽⁵⁾

Extrapolations of the key structural material properties for PCA and HT-9 are given as a function of accumulated neutron exposure in Ref. (6), and the uncertainty range at end-of-life is summarized in Table 4.3-2. These uncertainties are clearly large and argue that further measurements are needed at higher fluences, over a broad temperature range, with fusion-relevant neutron damage (at least the cumulative dpa and He/dpa ratio, preferably with a fusion neutron spectrum), and with more specimens to improve statistics (including base and weld metal).

The He/dpa ratio is a particularly important question with respect to structural and material behavior. Helium will accumulate in the material and may impact swelling and/or embrittlement. Atomic displacements lead to rearrangement of the alloy's chemical defect structure. There may be synergistic effects at the high He, high dpa generation rates expected in a fusion spectrum. Also, the fusion neutron energy spectrum is significantly different from fission reactor testing and may alter the material property changes with neutron fluence or lead to unanticipated phenomena. Therefore, it is prudent to provide at least benchmark testing of some samples in a fusion-relevant environment.

Possible solutions include: building a high fusion fluence, large materials test volume facility such as FMIT to thoroughly develop the materials data base; using existing or modified accelerators such as LAMPF or RTNS to obtain some benchmark data; and using fission reactors with appropriately modified materials to the extent possible. For example, it is possible to produce significant He during irradiation in a thermal reactor for alloys with high nickel contents such as PCA (about 15% Ni), however the corresponding damage rate is relatively low.

Isotopically tailoring the composition of alloys with ⁵⁹Ni is one approach for obtaining fusion-relevant He/dpa ratios. This radioactive

Table 4.3-2. Structural Property Uncertainties after 15 MW-yr/m² ^a

Property	T (°C)	Uncertainty Range ^b
<u>PCA</u>		
Onset of breakaway swelling (dpa)	400-500	90 - 170
Swelling below breakaway (%)	500	-0.3 - +0.3
Irradiation-induced creep, ϵ/σ (10 ⁻⁴ /MPa)	450-500	5 - 50
Yield strength (MPa)	450-500	450 - 820
Total elongation (%)	450-550	4 - 10
Fracture toughness (MPa-m ^{0.5})	--	50 - 90
<u>HT-9</u>		
Onset of breakaway swelling (dpa)	500	> 120
Swelling below breakaway (%)	500	-0.5 - +0.5
Irradiation-induced creep, ϵ/σ (10 ⁻⁴ /MPa)	370-500	3 - 15
Yield strength (MPa)	450-550	330 - 570
Total elongation (%)	450-550	5 - 25
Fracture toughness (MPa-m ^{0.5})	--	50 - 90
Δ DBTT (°C)	370-410	80 - 160

^a15 MW-yr/m² = 180 dpa

^bUncertainty ranges represent about a 50% confidence bound

isotope (80,000 year half-life) is produced in small amounts in fission reactor irradiation of nickel. As mentioned in Section 4.2, the DAFS program has already initiated the irradiation of several austenitic alloys in FFTF to address the issue of He/dpa ratio by using isotopically enriched ⁵⁹Ni.⁽⁶⁾ Also, irradiation experiments have been suggested to investigate the impact of He/dpa ratio on simple ferritic alloys in a HFIR irradiation. Unfortunately, these experiments only investigate immediate effects on the dimensional stability and tensile properties. Larger quantities of ⁵⁹Ni are required to explore the impact of He/dpa ratio on mechanical properties such as creep, fracture toughness, DBTT, and fatigue crack growth.

At present, highly irradiated Inconel components have been processed to extract the nickel (not the ^{59}Ni specifically). The quantities which can be produced are relatively small and lead to Ni^{59} levels of at most 2.5%. While the costs for the extraction of the irradiated nickel are relatively small (~\$500/g), the deliberate irradiation of nickel to produce enough ^{59}Ni could add significantly to the overall cost. Moreover, while this low level of enrichment can be used to achieve fusion-relevant He/dpa ratios in fast fission reactor irradiation of austenitic steels, the nickel content in ferritic steels are typically too low. TRW has proposed using existing plasma separation process technology to provide ^{59}Ni enrichment up to 80%. Such concentrations would permit the investigation of fusion-relevant He/dpa ratios even in ferritic steels. The initial material would be used to investigate basic irradiation effects on swelling and tensile properties. Then, based upon the outcome of these tests and the cost for this highly enriched nickel, additional experiments using larger specimens might be performed.

4.3.2 Solid Breeder

The candidate solid breeders include Li_2O , $\gamma\text{-LiAlO}_2$, Li_4SiO_4 , Li_2SiO_3 , Li_8ZrO_6 , Li_2ZrO_3 , and possibly a few others (e.g., lithium titanates, lithium beryllates, Be/LiAlO₂ mixtures, Li_7Pb_2). The major classes of issues are fabrication, reprocessing and characterization. More details may also be found in Ref. (7).

The key properties are the physical, thermophysical, mechanical and chemical properties. Physical properties (pore and grain size and distribution, specific surface area, porosity) are needed to characterize the material. Tailoring of these properties through the fabrication process might result in improved performance. The thermophysical properties are the density, thermal conductivity, thermal sintering temperature and thermal expansion coefficient. Specific heat data is needed for thermodynamic and transient analysis. Although the breeder is not presently seen as a load-bearing member, mechanical properties are critical for predicting the interaction of the breeder with the surrounding structure. The chemical properties refer to the tritium diffusivity, solubility and adsorption properties, and the thermodynamic and phase characteristics.

The question of high burnup is important for property testing in general. No planned experiment extends beyond the 9% lithium atom burnup of the FUBR-1B experiments, although most blanket designs have regions with about 70% lithium burnup. The FUBR-1 irradiations will provide data or materials for measurement of properties for a range of burnups from 0 to 9%. If a burnup-related variation is observed, then further higher burnups would be needed. These could be achieved by longer irradiation times; matching of specimen size, neutron spectrum, neutron flux, and ^6Li enrichment for a fast burnup experiment; or possibly by fabricating specimens with high-burnup stoichiometry.

Fabrication/Processing

Fabrication uncertainties include developing processes that will yield reproducible quantities of the desired material (microstructure, purity) and form. Presently achievable forms include sintered-product (generally achievable for most materials), sphere-pac (some production for $\gamma\text{-LiAlO}_2$), single-crystal (Li_2O), and pebbles (Li_2O).

The key development questions are whether the particular characteristics desired for fusion applications can be achieved. Unfortunately, the desired characteristics are not known at this time. For example, achievable impurity levels are already fairly low with respect to neutron absorption and waste disposal, but the effects of impurities (or additives) on mechanical properties and tritium inventory are not known.

A possible approach would be the systematic variation of microstructural and compositional variables, followed by measurements of mechanical and tritium properties. This is the present approach in the French LiAlO_2 program.⁽⁸⁾ In addition, the moderate-burnup irradiation of different as-fabricated materials in the FUBR-1B experiment will provide a means to identify desired material form, microstructure and purity.

Once suitable material characteristics are identified, then fabrication methods must be available to provide enough material to support the test program and ultimately commercial production. There is experience with many solid breeder compounds in small amounts (tens of grams). Large-scale Li_2O fabrication techniques have been developed as part of the Lithium Blanket Module experiment (600 kg of sintered pellets).⁽⁸⁾ Lithium aluminate and the

ternary oxides are expected to be easier to process due to their much smaller affinity for water. In general, the extrapolation to commercial quantities will require some development but is not perceived as raising feasibility issues. One concern, however, is that material fabrication costs could be substantially reduced if a non-ideal material was acceptable, with a few percent phase impurity for example. It would need to be established whether such a material was attractive enough to justify the cost saving.

At present, enriched ${}^6\text{Li}$ is generally obtained from U.S. stockpiles of 99+% enriched Li_2CO_3 or Li metal produced until the 1960's. Most solid breeder blankets require a multiplier and substantial ${}^6\text{Li}$ enrichment (50-90%). The amount of enriched Li_2CO_3 required for a test program is estimated as under 1 kg total for the small-scale experiments, 1 kg for each submodule experiment, and about 200 kg for full-module tests (such as neutronics tests). U.S. stockpiles are sufficient to support such a test program, but methods to produce commercial reactor amounts will require development since the original Colex process involved handling large volumes of mercury and is not regarded as acceptable. Several alternate ideas exist,⁽¹⁰⁾ so the question is one of attractiveness rather than feasibility.

Reprocessing and recovery of the lithium (and ${}^6\text{Li}$) from irradiated blankets will require remote handling and mechanical/chemical processing. Although the details have not been worked out, experience in fission fuel reprocessing provides a basis for arguing that this is feasible. Furthermore, lithium resources are sufficiently large that a low-loss recycling method is not essential.

Thermal Conductivity

The most important thermophysical property uncertainty is thermal conductivity. Some information is available and models exist based on analogous materials to account for the effects of temperature, porosity, radiation, gas pressure and form.⁽¹¹⁾ However, these are large effects as illustrated in Table 4.3-3 and so the corresponding uncertainty is large. Recent measurements on $\gamma\text{-LiAlO}_2$, for example, have shown that the effect of porosity and temperature are much different than had been anticipated.⁽¹²⁾

Table 4.3-3. Variation of Thermal Conductivity with Breeder Conditions⁽¹¹⁾

Breeder Condition ^a			Thermal Conductivity ^b			
ρ (%TD)	T (C)	Form	Fluence (n/m ²)	P _{He} (MPa)	Li ₂ O (W/m-K)	γ -LiAlO ₂ (W/m-K) ²
100	700	Sintered	0	--	4.8	2.6
85	700	Sintered	0	--	<u>3.8</u>	<u>2.5^c</u>
85	400	Sintered	0	--	<u>5.2</u>	<u>2.5</u>
85	700	Sintered	10 ²⁶	--	2.6	1.6
87	700	Sphere-pac	0	0.1	1.4	1.2
87	700	Sphere-pac	0	0.6	2.2	1.7
87	700	Sphere-pac	10 ²⁶	0.1	1.2	1.1

^aDensity is % theoretical density;
Sphere-pac form is 100% TD spheres, 30-, 300- and 1200- μ m diameters.
Fluence is with respect to fast neutrons.

^bUnderlined values are measured, the rest are extrapolated.

^cFrom recent data;⁽¹²⁾ previously estimated value was 1.9 W/m-K.

To some extent, this information will be obtained from the separate and multiple effect experiments discussed later (e.g., TRIO⁽¹³⁾ and the CREATE/CRITIC series of experiments in Canada). However, these experiments are sufficiently complex that it may be difficult to clearly separate the various contributors to the observed temperature profile - for example, gap conductance or asymmetries in the heating profile. These experiments will be particularly valuable in identifying the larger scale predictability of temperature in the breeder including effects such as internal restructuring or cracking that may change the local thermal conductivity.

Thermal conductivity can be measured on well-defined specimens in a small test stand using, for example, pulsed laser techniques.⁽¹²⁾ A number of specimens would be needed to cover a range of form, porosity and impurities. Measurements of conductivity could be made at a range of temperatures and gas pressure for each specimen. Additional samples could be irradiated to high fluence and then similarly measured. This would be supported by a modelling effort to understand the influence of the environmental variables and to identify desirable breeder form and conditions for blanket designs.

Tritium Diffusivity

Intragranular diffusion is usually the rate-limiting step for tritium recovery. Some direct diffusivity data exists for single- and polycrystalline Li_2O , while the ternary oxide data is derived from polycrystalline material. Indirect measurements of polycrystalline material are also available, primarily for LiAlO_2 from the TRIO experiment. The experimental variation in diffusion coefficient in Li_2O and LiAlO_2 (the better studied materials) is almost an order of magnitude. In addition, the effects of potential trapping mechanisms such as radiation or impurities have not been systematically studied or modelled. Yet, for example, typical impurity contents are about 1000 wppm compared with tritium inventories of about 1 wppm, and large increases in hydrogen inventory have been observed in materials irradiated with ion beams.

Further measurements should be based on well-known and controlled material specimens and conditions, including crystal size, temperature and impurities. Single-crystal material is desirable for well defined measurements. Backtracking diffusivities from irradiation experiments such as TRIO is difficult since these tests are much less controlled and any measurements are a composite of many processes. However, this will require developing single crystals (e.g., 1 mm spheres at 100% TD) for LiAlO_2 and the other ternary oxides. It may be sufficient to use as-fabricated polycrystalline material for the "effective" diffusivity, but compare with some single-crystal material (Li_2O and LiAlO_2) for verification.

Ideally, initial tests would focus on the effects of temperature and then impurities (e.g., bivalent impurities such as calcium which form an electronic defect in the crystal lattice), with irradiation treated separately. Possible techniques that would avoid irradiation include soaking the specimen in D_2 or H_2 , and then either thermal anneal to recover the diffusive inventory or a measurement of the surface penetration profile. Irradiation experiments should initially concentrate on low temperature/high burnup conditions where there may be no annealing of radiation damage. With irradiation, experiments should be careful to minimize interpreting recoil of near-surface tritium as part of the diffusivity measurement.

Solubility/Surface Adsorption

Experimental results indicate that solubility and surface adsorption are also the key controlling parameters in tritium inventory and release. The dissolution of tritium in the breeder material defines a minimum inventory that was, for example, originally thought to be quite large for Li_2O until measurements indicated otherwise. The amount of surface area in typical small-grain, moderate-porosity breeders is also large enough to influence the inventory, recovery rate at startup and transient behavior. It appears that solubility is more important for Li_2O than surface adsorption, while the opposite is true for the ternary oxides. The significant influence of surface chemistry and oxygen activity were indicated by the TRIO results.

For materials such as LiAlO_2 where surface adsorption is believed more significant, measurements of the adsorption isotherms would be useful. These would measure the amount of tritium adsorbed per unit of breeder surface area as a function of H_2O and H_2 partial pressure to obtain ΔG_{abs} . These measurements should be performed at relevant temperatures and could use deuterium and hydrogen. Care must be taken to distinguish between dissolved hydrogen and surface hydrogen.

Careful measurements of solubility and surface adsorption requires several steps in addition to monitoring the adsorption and desorption. The equipment must be calibrated; samples characterized with respect to grain size and impurities; effective surface area measured and periodically rechecked; and interactions with the container material minimized.

Thermochemistry

Measurements of the equilibrium thermodynamics of the breeder system (except Li_2O) are needed to accurately model the effects of burnup, purge composition and container material on the local chemistry. The influence and potential range of oxygen activity can be large.^(12,13) In particular, these measurements should include the activities of major species, and the energy of formation of LiAl_5O_8 (in LiAlO_2) and similar reaction products.

Formation energy requires the room temperature measurement of the heat of formation through calorimetry, and the separate measurement of specific heat as a function of temperature up to peak reactor values. These measurements

require high purity (gram-sized) samples and careful technique. Specific heat properties are also needed to support analysis of transient thermal behavior.

Partial phase diagrams exist for some breeder systems, especially Li_2O , $\text{Li}_2\text{O}-\text{Al}_2\text{O}_3$ and $\text{Li}_2\text{O}-\text{silica}$.⁽¹⁴⁾ More complete phase information should be obtained, since sub-phases may show up on closer examination.

Some blanket designs have proposed mixing beryllium multiplier directly with the solid breeder to improve the neutronic, thermomechanical and tritium recovery performance. Although highly advantageous from a design viewpoint, there are thermodynamic concerns because of the strong affinity of Be for oxygen. The extent and consequences of this mixing will depend on the source of oxygen (whether the oxygen activity is maintained by the "system" or the breeder) and on the reaction kinetics (the rate might be adequately slow after an initial BeO surface layer has formed). Unirradiated, isothermal stability tests with potential breeder/multiplier mixtures could address the magnitude of this concern fairly quickly.

Mechanical Properties

The principal mechanical properties are swelling, creep, Young's modulus and tensile strength. These determine the driving force for the breeder/structure mechanical interaction and the breeder response, including cracking or deformation. The primary parameters are breeder form, temperature and burnup. Mechanical properties can be measured in standard test equipment, and should include specimens that had been preirradiated to various burnup levels. Closed capsule irradiation experiments can provide swelling and swelling-dependent creep data if the capsule boundaries allow free expansion (to measure swelling), or restrain expansion in two directions and force a creep response to swelling in the other.

4.3.3 Multiplier

Possible multipliers include lead, Zr_5Pb_3 , beryllium, beryllium oxide and Li_2BeO_2 . The preferred material is beryllium due to its excellent multiplication properties and high melting temperature. An evaluation of the resource base⁽¹⁵⁾ indicated that there is sufficient beryllium for the intermediate future (~ 50 yrs) and so resources are not considered further here. A reasonable data base for unirradiated thermophysical and mechanical

properties is available from fission and aerospace experience. The primary uncertainties are related to fabrication and reprocessing, mechanical properties, and tritium retention. Thermal conductivity is not expected to be strongly affected by irradiation since it is dominated in metals by electron rather than lattice transport. More details may be found in Refs. (7) and (15-18).

Fabrication/Processing

Beryllium can be manufactured into a variety of forms (e.g., rods) with reasonable impurity levels (Table 4.3-4). However, beryllium properties (magnitude and direction) are strongly affected by grain size, orientation and impurity content, so an important task is to determine the optimum material for fusion applications. In general it appears that fine-grained, low BeO, high purity, isotropic material is preferred. The desired porosity depends upon the application - low porosity (<5%) is preferred for mechanical strength while larger porosity (15-30%) may help limit swelling depending on the temperature range and the amount of closed pores. Specific forms for particular applications that would require development include pebbles (1 cm OD) and sphere-pac (30-1200 μm OD) with submicron-sized grains. Due to the variability of beryllium properties, it is necessary to produce at least small amounts of the relevant form for mechanical properties tests.

Development of mass-production methods for fabrication (such as a free-flowing powder); remote reprocessing (with ~1% recycle loss rates) and lower impurity content (particularly niobium and silver to meet waste disposal requirements) will be needed for commercial operation but appears feasible. The chemical toxicity of beryllium will complicate the fabrication process.

Mechanical Properties

Beryllium is a basically brittle material with high helium production in a neutron environment. Consequently, the primary mechanical properties needed for fusion are swelling, creep, strength and ductility at temperature under irradiation for the relevant beryllium form. The range of available temperature and irradiation data is summarized in Fig. 4.3-2.

Table 4.3-4. Representative Characteristics of Beryllium⁽¹⁵⁾

Characteristic	Normal ^a	Available ^b	Desirable ^c
Grain Size (μm)	25	2	0.2 for ductility and swelling
Porosity (%)	0-100	0-100	5 for fracture toughness 10-30 for swelling
Form	Normal purity powder block. High purity powder block. Fine grain powder block. High purity ingot wire and several others.		Fine-grain, high purity, low BeO, isotropic rods, pebbles and/or sphere-pac.
<u>Major Impurities (wppm)</u>			
BeO	1000	100	
C	1200	100	
Mg		80	
Al	400	90	low for fracture toughness
Si	200	60	
Fe	1200	100	
Nb	5		0.5 for waste disposal
Ag	0.5		0.1 for waste disposal

^aTypical of normal purity powder block.

^bTypical of high purity ingot wire.

^cSuggested by available data; values not necessarily self-consistent.

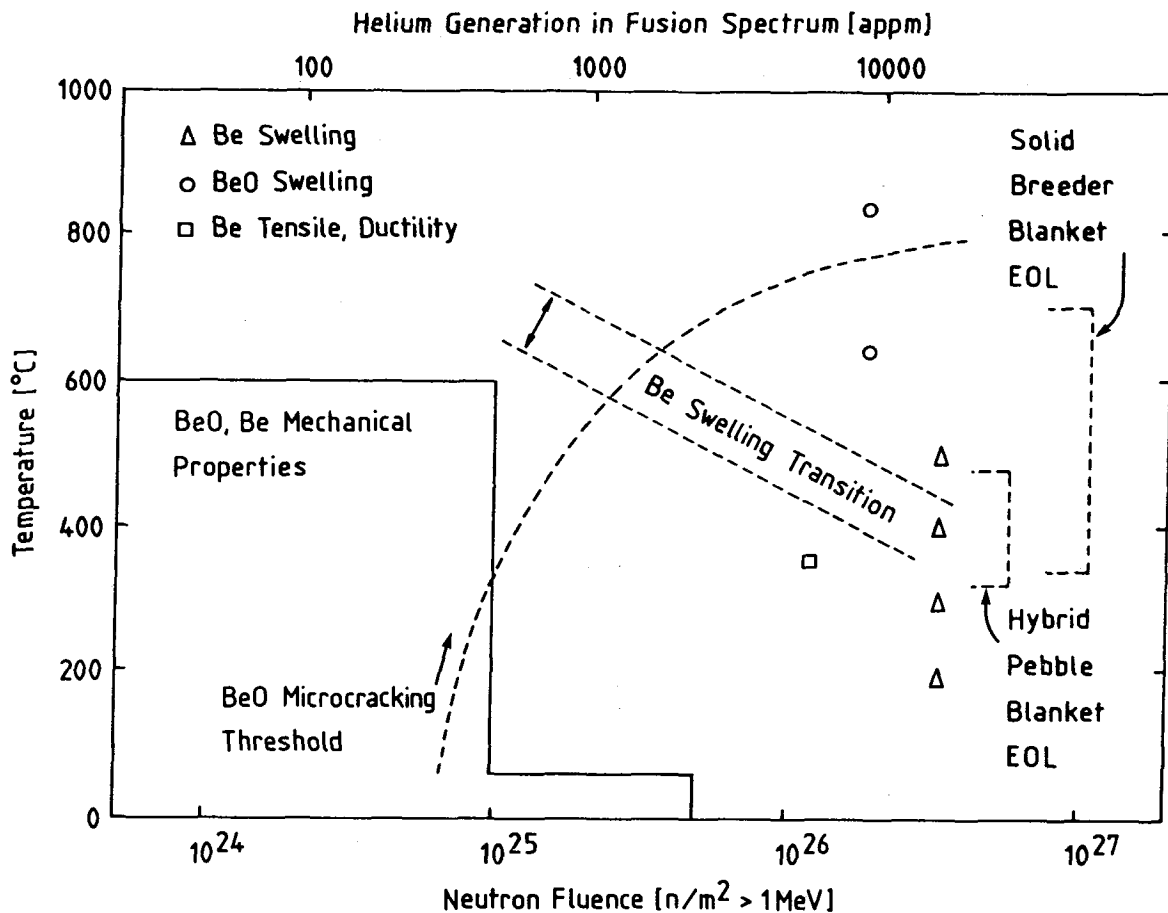


Figure 4.3-2. Extent of irradiated data base of beryllium.

Models for beryllium swelling have been developed.⁽¹⁵⁻¹⁷⁾ There appears to be a transition from equilibrium bubble swelling to a faster form when self-diffusion becomes significant.^(15,18) Additional data to confirm and extend the modelling range should include swelling during high-temperature irradiation (rather than low-temperature irradiation followed by thermal anneal), swelling in porous material (10-30% porosity) and swelling in reactor-relevant material (e.g., pebbles). Typical times to reach end-of-life helium production can be obtained from Table 4.3-5.

There is only one measurement of in-reactor creep in Be,⁽¹⁶⁾ but irradiation creep is anticipated to be small compared to thermal creep.⁽¹⁵⁾ However, thermal creep itself is a strong function of the material form and

Table 4.3-5. Gas Production in Beryllium^a

	Fast Flux (x 10 ²⁶ n/m ² -yr)	appm He/10 ²⁶ n/m ² (E > 1 MeV)	Gas Production Rate			Cumulative Helium at EOL (appm He)
			appm He/dpa	appm He/yr	appm T/yr	
Fusion breeder: ^b						
Near first wall	3.0	6800	420	20,000	--	34,000
Near back wall	0.2	5700	1570	1,100	--	12,000
Fusion electric: ^c						
Near first wall	2.1	4600	660	9,700	100	40,000
ATR thermal reactor	4.7	4500	1300	21,000	--	NA
ORR thermal reactor	1.4	4500	1300	6,300	--	NA
EBR-II fast reactor	6.3	1500	260	9,400	--	NA
FFTF fast reactor	16.0	1500 ^d	260	24,000	50-800 ^e	NA
He beam	NA	NA	1000	--	NA	NA

^aRefs. (16-18)

^bReference tandem mirror fusion breeder, Ref. (17)

^cBCSS LiAlO₂/Be/H₂O or Li₂O/Be/He blanket, 5 MW/m², Ref. (7)

^dAlso, 2000 appm He/10²⁶ n/m² for BeO in a fast reactor, Ref. (18)

^eCore mid-plane; production rate range for 1-4 yrs irradiation

purity (Fig. 4.3-3) and measurements for fusion-relevant material are needed. Both swelling and creep are expected to be important under fusion conditions, and will provide the basic mechanical loading and response.

The difficulty of slip in directions not parallel to the basal crystal plane in beryllium leads to residual microstresses in polycrystalline material under plastic deformation and consequently reduced ductility. This matters primarily if the beryllium is expected to be load-bearing (e.g., the BCSS $\text{Li}_2\text{O}/\text{He}/\text{Be}$ blanket with Be rods or fusion-breeder blankets with Be pebbles). As Fig. 4.3-2 shows, measurements of ductility, fracture toughness (below the DBTT) and tensile strength at temperatures (350-700°C), fluences (10^{27} n/m² fast neutrons) and materials of interest are almost non-existent.

Beryllium oxide may be an alternative to Be because of its increased chemical stability, although it is a much poorer multiplier. It is also fairly brittle, swells, and suffers property degradation (including thermal conductivity) during irradiation. The temperature/fluence data base as shown in Fig. 4.3-2 is similar to that for pure beryllium.

Tritium Retention

Nuclear reactions produce a small amount of tritium in beryllium relative to the production rate in the principal breeder material - about 0.03 T per DT source neutron for Be near the first wall.^(7,15) This is an inventory and safety concern if the tritium simply accumulates in the beryllium - about 1-2 kg for BCSS blankets, comparable to or larger than the blanket inventory. It is a coolant contamination concern if it can directly permeate into the coolant as in some bare Be rod or pebble designs - about 2 g/d for a BCSS-size reactor. And if the tritium is extracted by the purge system, then care must be taken with respect to chemical interactions with the breeder (e.g., effect on purge stream oxygen activity).

As with the solid breeders, careful characterization of tritium inventory and transport requires measurement of the diffusivity, solubility and surface adsorption. Some data indicates that tritium diffusion in beryllium metal is very slow at normal temperatures,⁽⁸⁾ and diffusion measurements have been reported for BeO powder.⁽¹⁹⁾ The effects of fine-grained, high-porosity forms of beryllium and the high helium generation rates are not known. A

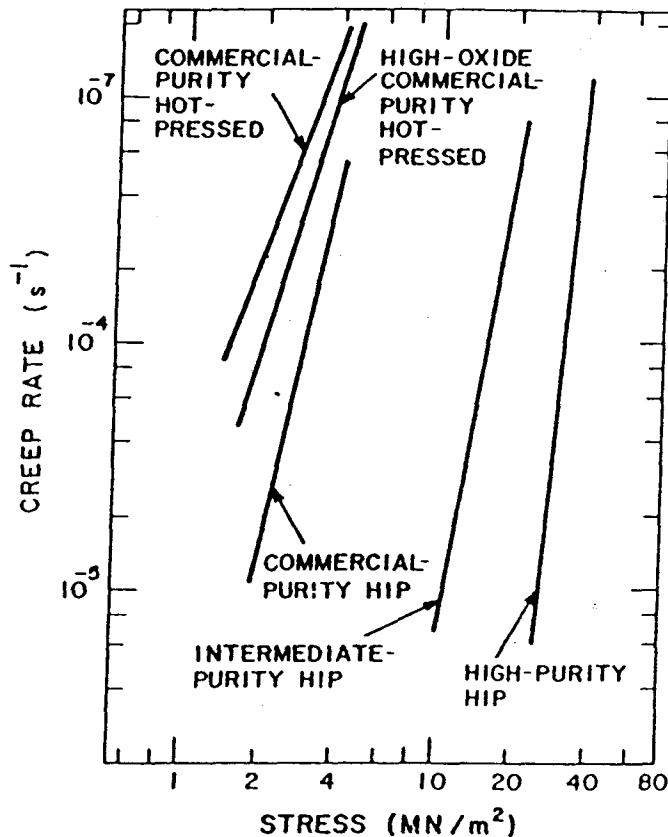


Figure 4.3-3. Thermal creep rates for various grades of beryllium at 1000°C.⁽¹⁵⁾ (HIP is hot isostatic pressed.)

suitable test would be a measurement of tritium retention and swelling similar to the closed capsule FUBR tests. The threshold energies for the $\text{Be}(n,T)$ and $\text{Be}(n,\alpha\beta)^6\text{Li}$ reactions are about 10 MeV and a few hundred keV, respectively. The latter reaction [followed by a $^6\text{Li}(n,T)$ reaction] accounts for almost 40% of the tritium production in some fusion conditions, and most of the tritium production in fission reactors.

References for Section 4.3

1. M.A. Abdou, et al., "FINESSE, A Study of the Issues, Experiments and Facilities for Fusion Nuclear Technology Research & Development, Interim Report", University of California, Los Angeles, PPG-821, also UCLA-ENG-84-30, 1984.

2. W.L. Hu, "Charpy Impact Test Results of Ferritic Alloys at a Fluence of $6 \times 10^{22} \text{ n/cm}^2$ ", ADIP Semiannual Progress Report, DOE/ER-0045/13, September 30, 1984, pp. 106-119.
3. D.N. Braski, "Vanadium Alloy Irradiation Test Matrix in FFTF", *ibid.*, pp. 63-65.
4. M.G. Grossbeck and J.A. Horak, "Tensile Properties of Helium Injected V-15Cr-5Ti After Irradiation in EBR-II", *ibid.*, pp. 99-103.
5. M.L. Hamilton, N.S. Cinnon, and G.D. Johnson, "Mechanical Properties of Highly Irradiated 20% Cold Worked Type 316 Stainless Steel", 11th Conf. Effects of Radiation on Materials, ASTM STP782, 1982, pp. 636-647.
6. R.L. Simons, "Isotopic Tailoring with Nickel-59 to Enhance Helium Production Fission Reactor Irradiation", DAFS Quarterly Progress Report, DOE/ER-0046/21, May 1985, pp. 19-22.
7. D.L. Smith, et al., "Blanket Comparison and Selection Study, Final Report", ANL/FPP-84-1, Argonne National Laboratory, September 1984.
8. B. Rasneur, "Tritium Breeding Material: $\gamma\text{-LiAlO}_2$ ", *Fusion Tech.*, 8, July 1985, p. 1909.
9. Project staff, "TFTR Lithium Blanket Module Program, Final Design Report, Vol. IV, Lithium Oxide Pellet Fabrication", GA-A17467, GA Technologies, April 1983.
10. E.A. Symons, "Lithium Isotope Separation: A Review of Possible Techniques", CFFTP-G-85036, Canadian Fusion Fuels Technology Project, February 1985.
11. Y.Y. Liu and S.W. Tam, "Thermal Conductivities for Sintered and Sphere-pac Li_2O and $\gamma\text{-LiAlO}_2$ Solid Breeders With and Without Irradiation Effects", *Fusion Tech.*, 7 399 (May 1985).
12. C.E. Johnson, et al., "Property Studies of Solid Tritium Breeding Materials", 7th Ann. Prog. Report on Special Purpose Materials for Mag. Conf. Fusion Reactors, DOE/ER-0113/4, U.S. Department of Energy, May 1985.
13. R.G. Clemmer, et al., "The TRIO Experiment", Argonne National Laboratory, ANL-84-55, September 1984.
14. D.G. Suiter, "Lithium-based Oxide Ceramics for Tritium Breeding Applications", MDC-E2677, McDonnell Douglas Astronautics Co., June 1983.
15. T.J. McCarville, et al., "Technical Issues for Beryllium Use in Fusion Blanket Applications", Lawrence Livermore National Laboratory, UCID-20319, January 1985.
16. W.G. Wolfer and T.J. McCarville, "An Assessment of Radiation Effects in Beryllium", UWFDM-632, University of Wisconsin-Madison, February 1985.

17. L.G. Miller, et al., "Special Topics Reports for the Reference Tandem Mirror Fusion Breeder: Beryllium Lifetime Assessment", UCID-20166, Vol.3, Lawrence Livermore National Laboratory, October 1984.
18. M.A. Abdou et al., "Impurity Control and First Wall Engineering", Ch. VII, FED-INTOR/ICFW/82-17.
19. A.R. Palmer, D. Roman and H.J. Whitfield, "The Diffusion of Tritium from Irradiated Beryllium Oxide Powders", Jrnl. Nucl. Mat., 14 141 (1964).

4.4 Separate and Multiple Effect Experiments

Solid breeder blankets will operate with materials and conditions where data and modelling are presently inadequate. A major class of experiments are those associated with exploring the phenomena and interactions that could occur. In order to obtain a quantitative and extrapolatable understanding, it is important that only a limited number of environmental conditions are present or varying at any given time so that only a limited number of phenomena are observed.

In this section, separate and multiple effect tests are examined based on the major classes of phenomena: tritium inventory and recovery from the blanket region; mechanical interaction between breeder, multiplier and structure; structural behavior; corrosion and mass transfer; tritium permeation and processing (from the blanket stream); and neutronics and tritium breeding. Safety-related tests are considered under the appropriate phenomena category.

4.4.1 Tritium Inventory and Recovery

4.4.1.1 Testing and Modelling Needs

Predicting tritium behavior in solid breeder blankets requires understanding tritium transport, retention and chemical form in the breeder material under the influence of the fusion environment. Transport processes include intragranular diffusion, grain boundary diffusion, porosity diffusion, and convective flow with the purge stream. Tritium retention processes include solubility, surface adsorption, collection in internal voids, trapping at radiation damage sites, and chemical trapping by impurities, burnup products or secondary phase formations. The form (gas or oxide) and behavior of tritium is influenced by the many factors that can affect the local oxygen activity, such as the purge composition, extent and oxide state of metallic surfaces (including beryllium if present), burnup and burnup rate.

Table 4.4.1-1 summarizes the important uncertainties, and Table 4.4.1-2 quantifies the contribution to the blanket tritium inventory from the various processes. The uncertainties in these processes are described below. More details may be found in Ref. (1).

Table 4.4.1-1. Tritium Inventory and Transport Uncertainties

Diffusion
* Temperature-dependent diffusivity and diffusing form
* Breeder impurity effects on diffusion
* Radiation effects on diffusion
Grain boundary transport
Solubility (T_2O and T_2)
* Surface adsorption (T_2O and T_2)
* Oxygen activity
Influence of purge, breeder, clad, burnup and flux on activity
Influence of activity on tritium inventory and transport
Porosity and purge (gas phase) transport
* Breeder restructuring effects on tritium recovery
Grain growth, pore closure, purge channel redistribution, cracking
* Breeder burnup thermochemistry
Phase diagram, thermodynamic properties (activities, c_p , ΔH_f)
Isotope swamping effects on tritium recovery
Purge stream impurity content and effects on surface desorption
Transient release of breeder tritium inventory
Thermal and chemistry (purge composition) transients
Beryllium tritium inventory and release

* Most important

Table 4.4.1-2. Contributions to Blanket Tritium Inventory^a

Contributor (g)	Li ₂ O/He	LiAlO ₂ /Be/He	LiAlO ₂ /Be/H ₂ O	LiAlO ₂ /Be/Salt	Uncertainty ^b
Diffusivity	0.04	38	2300	2000	very large
Grain boundaries	~0	~0	~0	~0	very large
Solubility	134	~0	~0	~0	moderate
Surface adsorption:					
H ₂ added	~0	~0	~0	~0	large
No H ₂ added	1200	1200	1200	1200	
Pores/purge	0.04	0.04	~0	~0	large
Beryllium ^c	0	<1500	<1500	<1500	upper bound
Coolant	0.00003	0.00001	53	900	large
First wall ^d	18.7	18.7	18.7	18.7	very large
Blanket structure ^d	1.1	1.2	9.3	42	very large

^aBCSS tokamak blankets

^bRough estimate, varies between materials: moderate (<25%), large (<100%), very large (factor of 10)

^cUpper limit refers to complete retention of tritium

^dHT-9 structural material

Intragranular Diffusion

Intragranular diffusion is generally the rate-limiting step for tritium recovery, and is much slower in the ternary oxides as compared with Li_2O . Some direct diffusivity data exists for single- and polycrystalline Li_2O , while the ternary oxide data is derived from polycrystalline material.⁽¹⁾ This data primarily addresses the strong temperature dependence of the diffusivity. As illustrated in Figure 4.4.1-1, the experimental variation in diffusion coefficient in Li_2O and LiAlO_2 (the better studied materials) is almost an order of magnitude, particularly at higher temperatures. This translates into a comparable uncertainty in breeder tritium inventory.

The effects of radiation and impurities have not been systematically addressed as noted below. The effect of grain size is reasonably well-known, but changes in grain size with operation have been largely neglected by invoking temperature constraints that should limit sintering and grain growth. There is no direct information on the form of the diffusing tritium.

Surface Adsorption

Although surface binding energies are relatively small (compared to diffusion activation energies, for example), the amount of surface area available in the breeder can be fairly large in the small-grain and high-porosity microstructures preferred for reducing intragranular and porosity related inventory. The TRIO LiAlO_2 data⁽²⁾ implied a surface inventory of 3 wppm with about a 100% uncertainty (Fig. 4.4.1-2). From Table 4.4.1-2, it can be seen that surface retention can influence the inventory, recovery rate at startup, and transient behavior. Surface adsorption can be reduced by hydrogen addition to the purge, but this can aggravate other problems such as tritium permeation and complicate the purge tritium recovery system, so it is desirable to know how much hydrogen is necessary.

Solubility

The dissolution of tritium in the breeder material defines a minimum tritium inventory. Recent data on the H_2O - Li_2O phase equilibria indicate that tritium solubility (as OT^-) in Li_2O is smaller than anticipated, and has

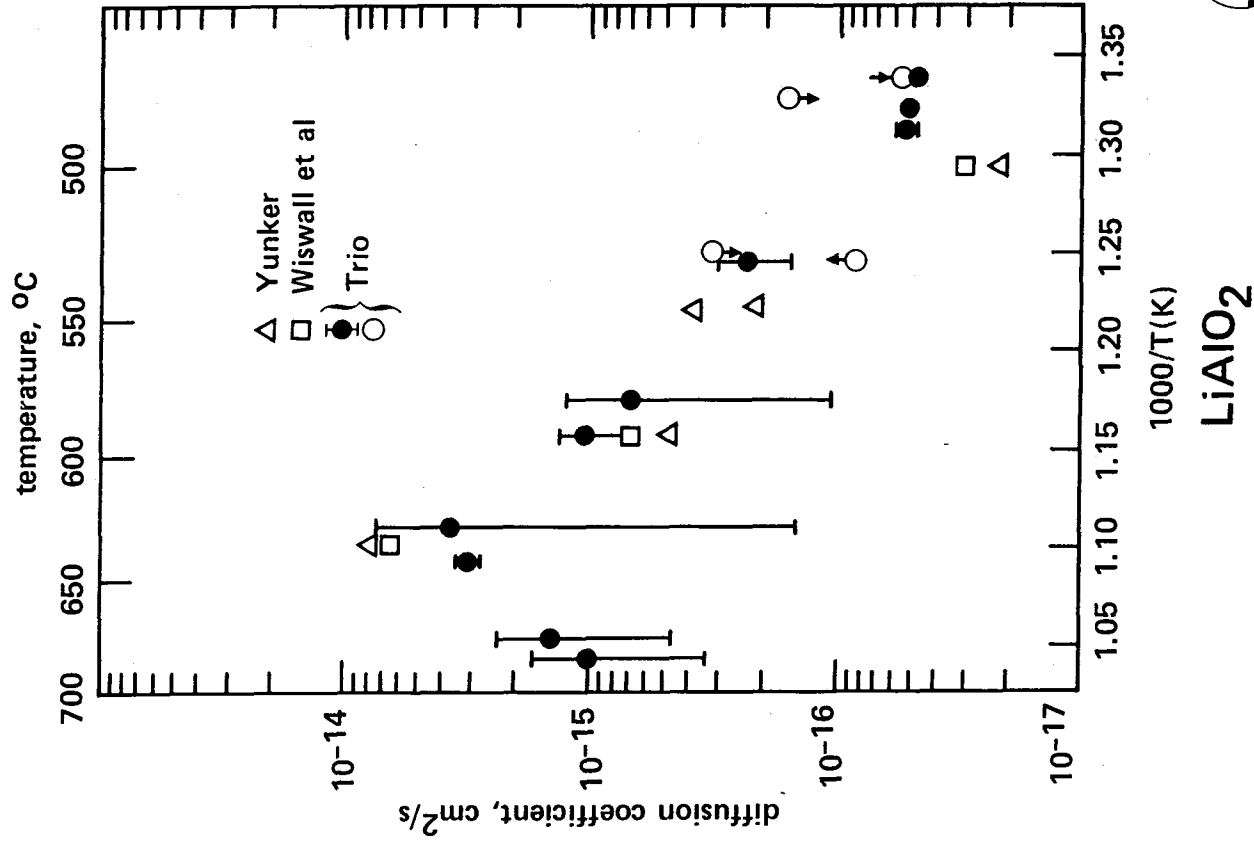
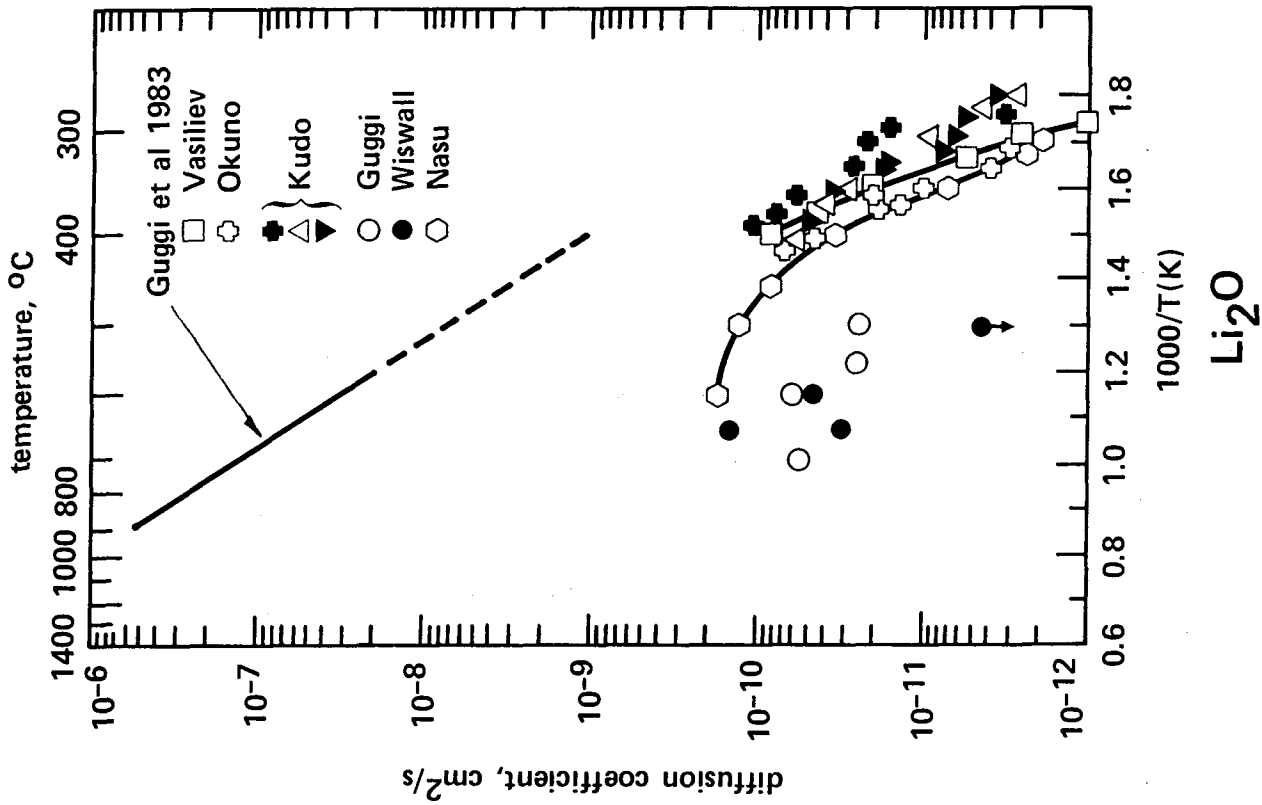


Figure 4.4.1-1. Experimental basis for tritium diffusivity in Li₂O and LiAlO₂.

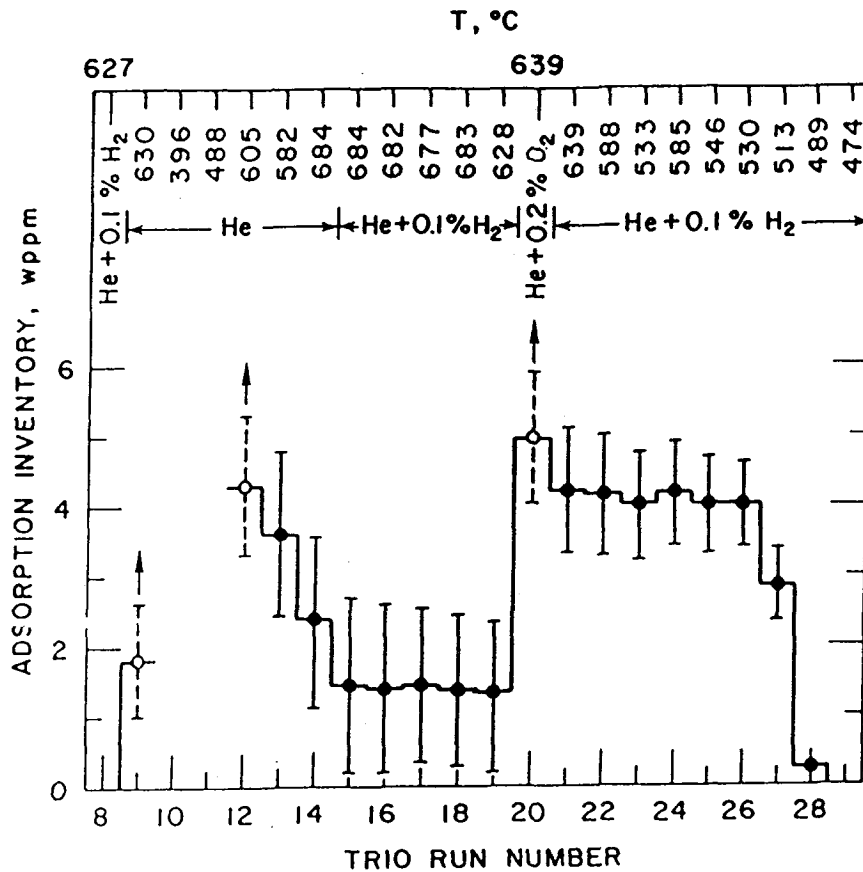


Figure 4.4.1-2. Tritium surface adsorption inventory in TRIO experiment.⁽²⁾

resulted in considerable reductions in blanket tritium inventory (to ~ 0.1 wppm T) from STARFIRE⁽³⁾ predictions based on ideal solution behavior. However, it is still the largest contributor to Li_2O blanket tritium inventory. Tritium solubility in ternary oxides is expected to be even smaller, but has not been measured. The importance of oxygen activity with respect to solubility on the gas phase form of tritium has been identified in equilibrium thermodynamic calculations.

Tritium Form

The form of tritium - T_2 , T_2O or other - can significantly impact tritium inventory within the breeder, permeation across the cladding, and extraction from the breeder stream. Although tritium was originally assumed to be primarily released in the oxidized form (e.g., STARFIRE) from the oxide breeder compounds, the VOM-15H⁽⁴⁾ and TRIO experiments indicated that

substantial fractions could be in the reduced form (T_2), particularly if H_2 was added to the purge input stream.

The actual mix of oxidized and reduced forms is primarily determined by the local oxygen concentration (i.e., oxygen activity). Figure 4.4.1-3 illustrates the importance of oxygen activity on the amount of tritium in the condensed phase for various breeder materials, and on the vapor phase concentrations of T_2 and T_2O . These calculations are based on equilibrium thermodynamic calculations, possible kinetic effects are not known.

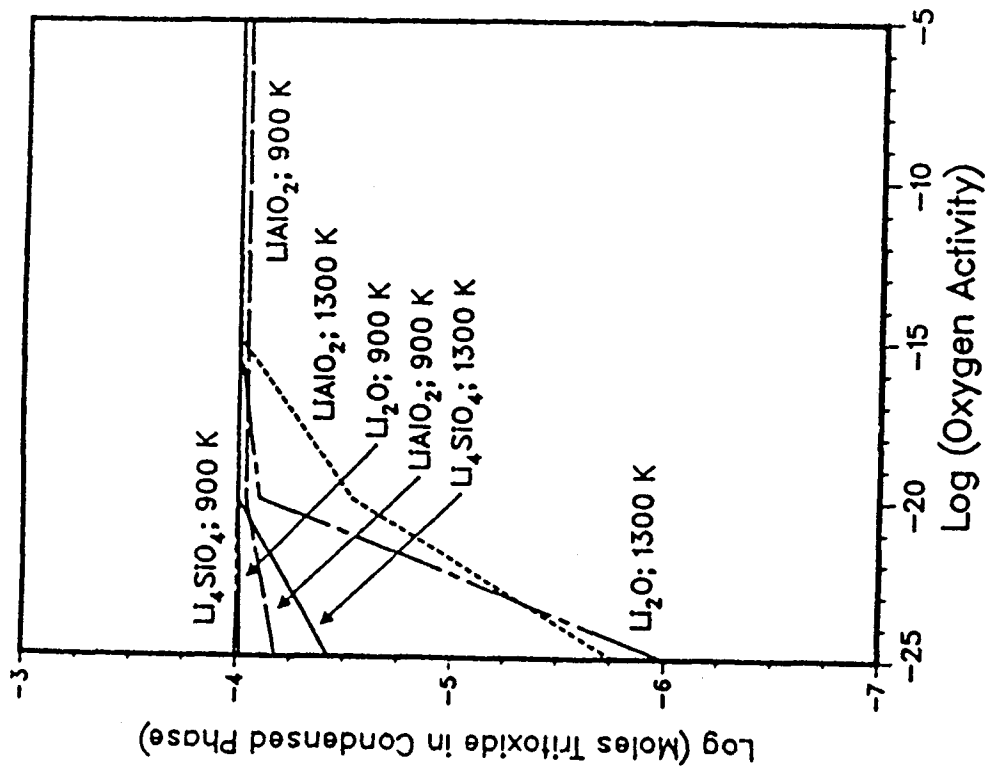
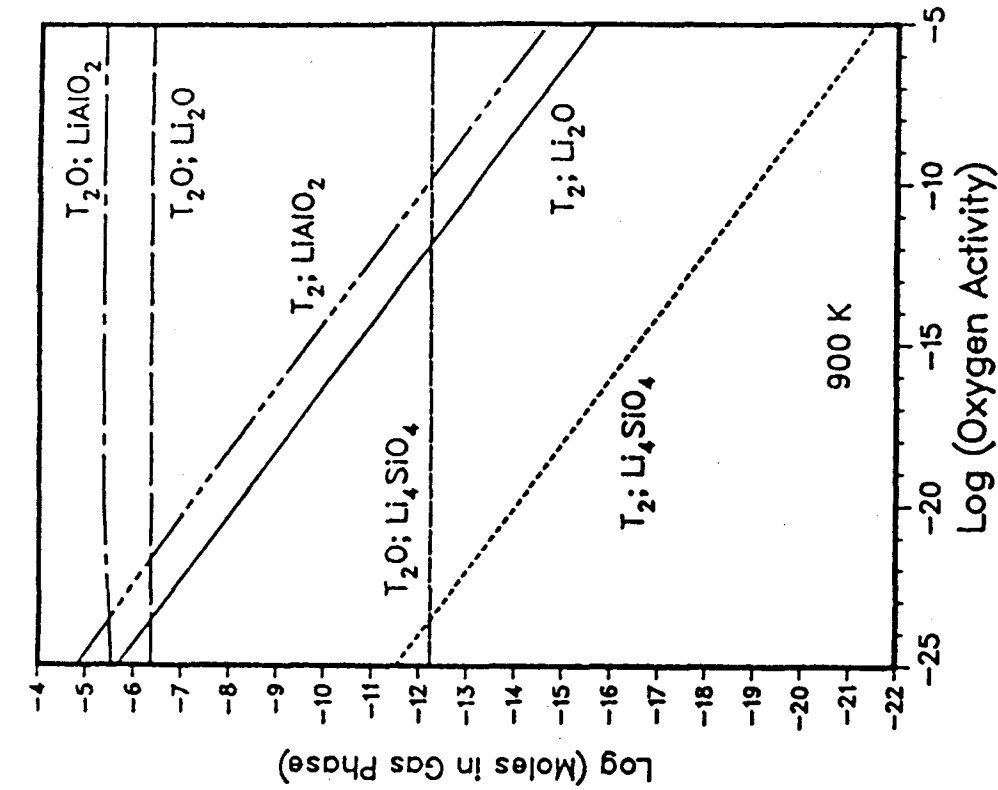
The oxygen activity itself is strongly affected by many factors as illustrated in Table 4.4.1-3. In the presence of sufficient beryllium, virtually all the oxygen will be consumed to form BeO at equilibrium. Oxygen activities could also be defined by equilibrium between H_2 and H_2O in the purge stream, between metal and metal oxide on the cladding surface, or by oxygen directly present in the purge stream as an impurity (possibly from a purge recovery system oxidizer) or an additive. In addition, it is possible that the nuclear reaction forming tritium from an oxide breeder changes the local oxide concentration. In practice, each of these processes will contribute to the global and local oxygen activity. The actual oxidation state in the breeder is not known at present, and is probably variable depending on environmental conditions and on burnup.

Isotope Exchange

Experimental results with VOM-15H and TRIO indicate that the addition of protium will reduce the tritium inventory and enhance recovery through the combined effects of isotope exchange and oxygen activity reduction. Although the effects of the thermodynamic changes are reasonably predictable, the exchange kinetics and exact impact of increased protium on overall behavior are not clear.

Trapping

Trapping of tritium atoms in radiation damage sites, internal voids (from helium production) and with impurities could inhibit diffusion. This is of concern because of the anticipated high burnup, radiation damage and helium



Molar Quantities of Gas Phase Species Over Li_2O , γ - $LiAlO_2$ and Li_4SiO_4 at 900 K

Comparison of Tritoxide Concentration in Solid Solution in Li_2O , γ - $LiAlO_2$, and Li_4SiO_4

Figure 4.4.1-3. Effect of oxygen activity on gas and condensed phase tritium.

Table 4.4.1-3. Contributors to Breeder Oxygen Activity

Controlling System	Ideal Solution Oxygen Activity (1 atm He at 1000 K)
LiAlO ₂ /Be	<< 10 ⁻³⁵
Measured Li activity in LiAlO ₂ /304 SS capsule	10 ⁻³⁵
H ₂ -H ₂ O @ 100 ppm H ₂ /1 ppm H ₂ O	10 ⁻²⁶
Iron-Iron oxide	10 ⁻²⁵
Li burnup/purge removal in Li ₂ O blanket	10 ⁻¹¹
O ₂ @ 10 ppm	10 ⁻⁵
O ₂ @ 1000 ppm	10 ⁻³

production, and appreciable breeder impurity content relative to the tritium concentrations (10-100 wppm metallic/cation impurities and ~ 1 wppm tritium).

The TRIO experiment reached 0.3% lithium burnup and FUBR-1A reached as high as 3% with no major apparent effects, although the measured tritium inventory has not been entirely explained. As noted in Ref. (2), there is otherwise no literature data to allow a qualitative evaluation of radiation-induced trapping. Measurements on radiation-induced trapping in structural materials and beryllium are underway at INEL for fluences up to 5×10^{22} (E > 1 MeV). FUBR-1B will approach 10% burnup, but no experiments are planned to reach the 70% burnup anticipated for some regions of most blanket concepts. Radiation-induced trapping is most likely to be significant at low temperatures where radiation damage is not annealed out. If it is annealed out quickly above about 400°C, then it would not be significant except in some water-cooled solid breeder blankets.

Porosity and Purge Channel (Gas Phase) Transport

A good understanding of mass transfer in porous media is generally available from the chemical engineering industry, although there are a number of semi-empirical parameters that must be defined for exact predictions, such as the pore "tortuosity." While the inventory in this phase is generally small, any pressure buildup in this phase directly influences the amount of dissolved hydrogen. Reasonable estimates indicate that this transport is

relatively fast in solid breeder blankets (large pores, over 15% porosity) and should not be a major concern. However, there are numerous uncertainties in how the porosity distribution may change with operation due to cracking, radiation or thermal-induced sintering, void swelling, hot pressing/creep, grain growth, internal mass transfer in temperature gradients, or external mass transfer of breeder material out of the blanket. The possibility of local pore closure (typically at 5% void fraction) or redistribution of the purge flow could lead to substantial local increases in inventory, while swelling and cracking might serve to keep connected pore pathways available.

Grain Boundary Transport

Grain boundary movement is anticipated to be quicker than bulk diffusion and not important for solid breeders with reasonably small grains and high porosity. However, estimates for the activation energy are about half the bulk diffusion energy, so this mechanism might be more significant if the grains grow large and if there is little connected porosity, a possibility in some blanket regions towards end-of-life or if temperatures are pushed higher than current limits in order to increase the amount of breeder relative to structure.

Transient Behavior

Transient behavior is important for predicting the initial tritium recovery rate (quantifying the required startup inventory), for determining the bounds on the tritium processing system inlet conditions allowing for normal transients (power rampup or rampdown), and for assessing the vulnerability of the tritium inventory to fault conditions. Some estimates for tritium behavior in Li_2O and LiAlO_2 are given in Ref. (5), illustrating the effect of material choice on transient response.

Generally, transient behavior is obtained from understanding the steady-state behavior and then extending it to time dependence. As such, no additional tritium-related tests would be required, although tests may be needed to identify the thermal, mechanical or chemical transients that would then affect the tritium. In practice, transient tritium response may be measured because it provides additional test data for developing even steady-state models (as in TRIO), or because some accident related conditions might

not be tested as part of assessing normal operation (particularly chemistry transients due to purge processing system failure or coolant leakage).

Modelling Needs

The present status of modelling of tritium behavior in solid breeder blankets is generally indicated by Refs. (1,2,5,6). It is typically assumed that temperatures are constrained such that diffusion and solubility limit the inventory and recovery, with allowance for pressure buildup due to gas phase transport across the open porosity. The tritium form is assumed as largely gas or oxide, depending on arguments about the local oxygen activity. Thermodynamic models are also available to calculate the nature of the various species at equilibrium. Models have not been published to predict the effects of impurities and radiation on diffusion and trapping, the local oxygen activity including the various possible contributors, and the effects of breeder restructuring

4.4.1.2 Experiments and Facilities

The basic conditions applicable to present solid breeder blankets are summarized in Table 4.4.1-4. Most of these values are straightforward to obtain in an experiment, the only question is the ability to duplicate the nuclear environment - primarily tritium generation and heating rate. Figure 4.4.1-4 shows examples of achievable heating and tritium generation rates in present fission reactors (ORR and ETR are thermal reactors, FFTF is a fast reactor). These particular results were obtained by matching the beginning-of-life (BOL) tritium generation rate by altering the ${}^6\text{Li}$ enrichment. Reasonable simulation of fusion reactor conditions is possible with present neutron sources within about a factor of two. In general, fast reactors are best for unmultiplied blankets with low ${}^6\text{Li}$ content, and thermal reactors are best for multiplied blankets with high ${}^6\text{Li}$ enrichment. An exact time-dependent match of heating and tritium generation rates is difficult for high burnups, but probably not important within the degree of matching possible.

At present, neutron spectrum effects on the breeder transmutation or damage rate are not believed to be significant for tritium recovery or breeder mechanical behavior although they are for the cladding (and so breeder/cladding interaction).

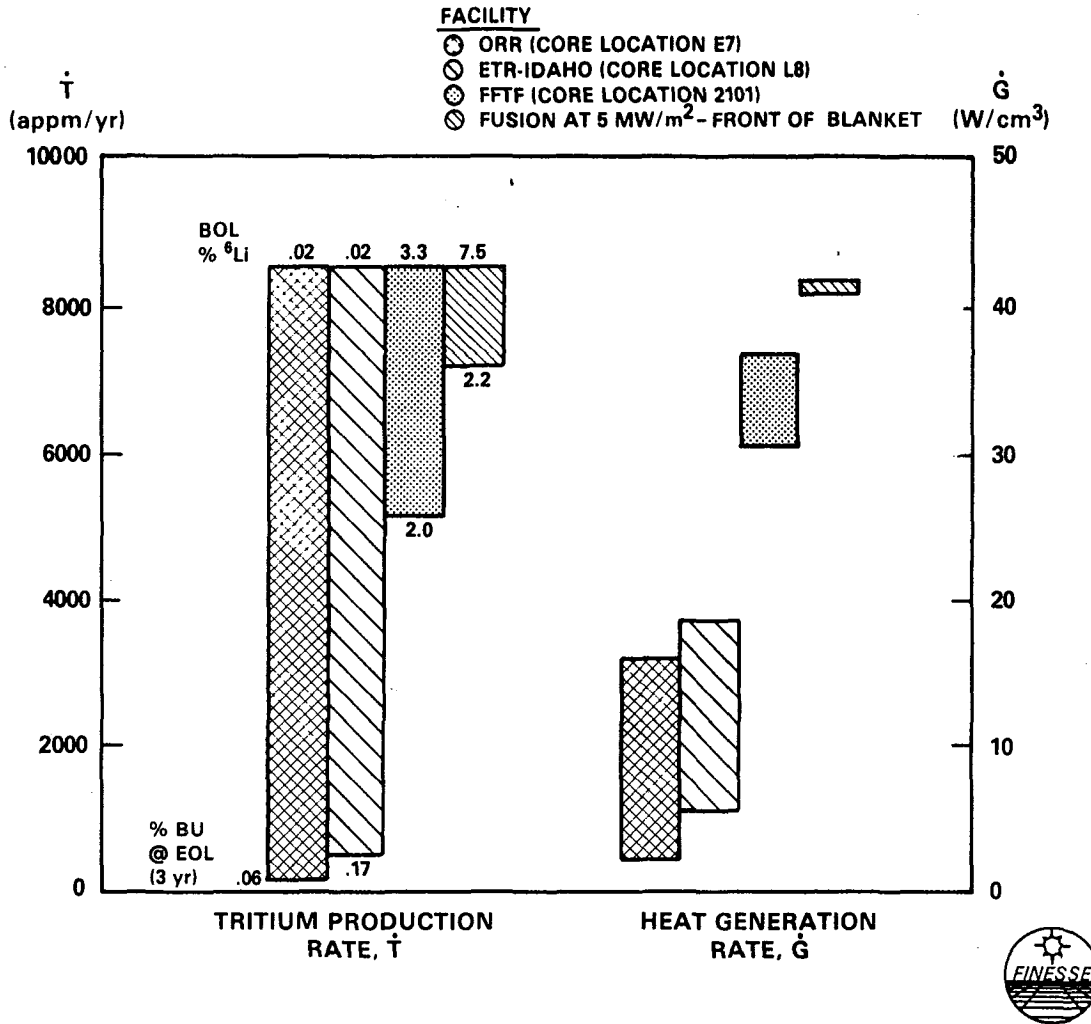
Table 4.4.1-4. Typical Conditions for Present Solid Breeder Blankets^a

Parameter	Li ₂ O	LiAlO ₂ /Be
Fabricated form	Sintered, 85%TD	Sintered 85%TD or Sphere-pac 87%TD
Grain size (μm)	3	0.2
Metallic impurities (wppm)	< 1000	< 3000
Anion impurities (wppm)	< 20	< 100
Li ⁶ enrichment (%)	7.5	90
Peak EOL burnup (% Li)	10	80
EOL time (yr)	3	3
Peak nuclear heating (MW/m ³)	50	60
T generation (T/Li-yr)	0.01	0.5
Operating temperature (°C)	410-800	350-1000
∇T (°C/m)	80,000	130,000
Breeder thickness (cm)	0.5-5	0.5-5
Clad material	HT-9, PCA	HT-9, PCA
Clad surface conditions	?	?
Purge flow rate (m ³ /s-g)	0.04	0.04
Purge composition	He @ 0.1 MPa < 1000 ppm H ₂ ? H ₂ O	He @ 0.1-0.6 MPa < 1000 ppm H ₂ ? H ₂ O
Breeder surface area (m ² /g)	0.1-1	1-10
Clad/breeder surface area	< 10 ⁻³	< 10 ⁻⁴

^aValues based on BCSS blanket designs at 5 MW/m²

FISSION/FUSION IRRADIATION COMPARISON FOR Li₂O/He/HT-9 SYSTEM

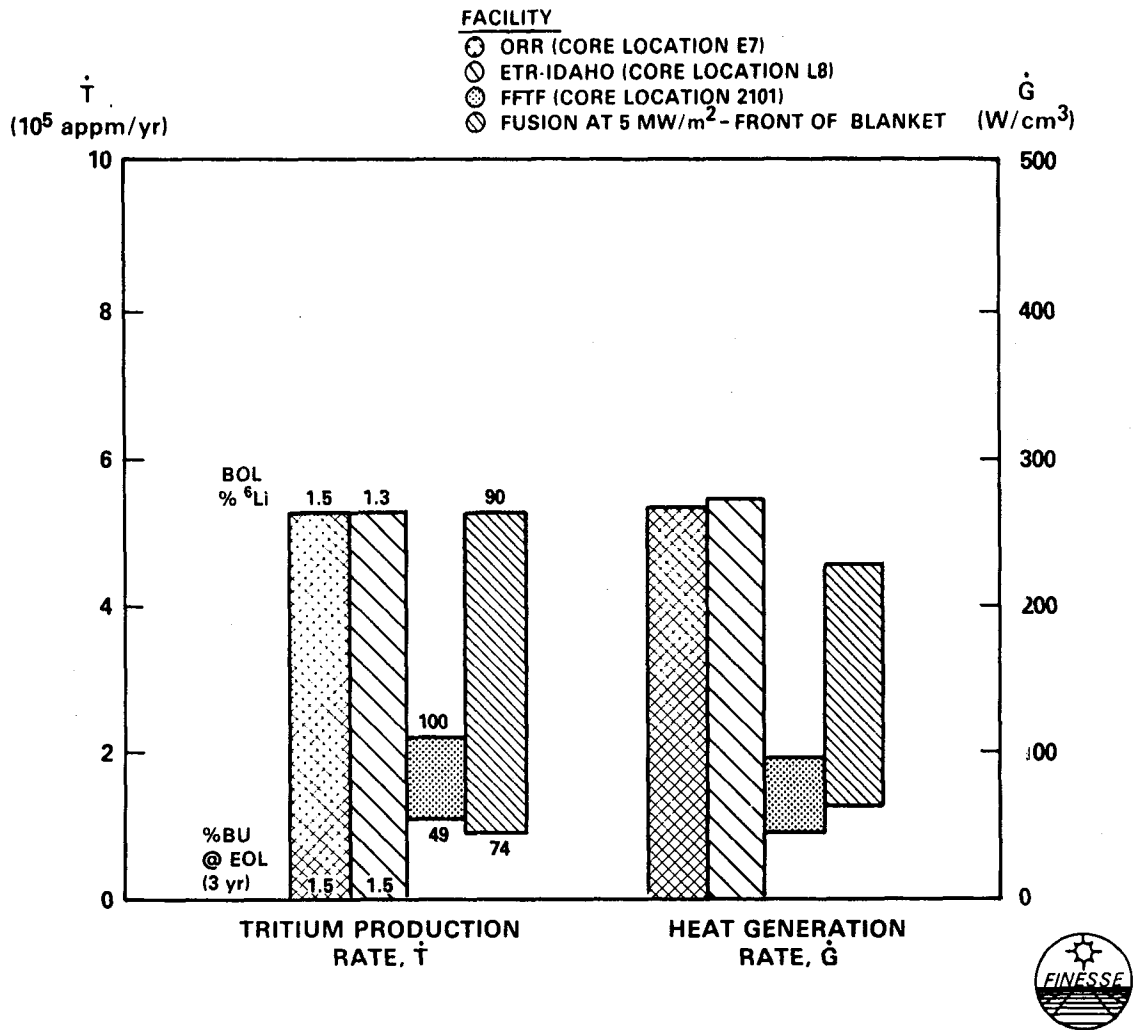
Li₂O SOLID BREEDER



(a)

Figure 4.4.1-4. Comparison of tritium generation and heating rates for solid breeder irradiation in thermal, fast and fusion reactors.

**FISSION/FUSION IRRADIATION COMPARISON FOR $\text{LiAlO}_2/\text{H}_2\text{O}/\text{HT-9}/\text{Be}$ SYSTEM
 LiAlO_2 SOLID BREEDER**



(b)

Figure 4.4.1-4. Comparison of tritium generation and heating rates for solid breeder irradiation in thermal, fast and fusion reactors.

Typical fission reactor in-core test volumes will accommodate breeder elements with 0.5-3 cm full-scale breeder spacing and reactor-relevant temperature profiles. For isothermal experiments, particularly where a tritium diffusivity is to be determined, it is desirable to maintain temperatures within about 50°C because of the exponential dependence of the processes on temperature. For typical values of 2 W/m-K thermal conductivity and 30 MW/m³ bulk heating, this implies a thickness of < 3 mm. A minimum thickness (other than fabrication limits) may be determined by lower bounds on tritium measurement accuracy or by concerns that surface effects due to the cladding material may affect the tritium response. Both these limits appear to be very small - tritium accuracies of 1 nCi/g in Li₂O have been developed for the LBM⁽⁷⁾ program compared with expected intragranular inventories of 10 mCi/g (1 wppm). And for effective breeder surface areas of 1-10 m²/g (e.g., TRIO), maintaining (area of clad/area of breeder) << 1 implies breeder thicknesses of at least 0.01 mm.

It is not clear whether these tritium recovery experiments can achieve end-of-life conditions in a reasonably short period of time (e.g., accelerated testing completed within one year). This depends on balancing heat and tritium generation rates (through lithium enrichment), specimen size (to minimize self-shielding) and neutron source conditions (flux and spectrum) over the expected test time.

The relationship between the important breeder conditions and the tritium recovery phenomena is shown in Table 4.4.1-5. The phenomena that describe tritium behavior are shown divided into four "classes" - intragranular transport and trapping, oxygen activity and effects, gas phase transport (including internal mass transfer of breeder), and mechanical effects (including breeder/clad interaction, purge flow distribution, cracking). The parameters that differentiate one class of tests from another are the presence of an active purge, temperature gradients, and geometric or mechanical effects. Of course, within any given test class, tests may vary from one another in many ways - breeder form, impurity content, burnup, etc. These test classes are subsequently referred to as Closed Capsule (e.g., FUBR-1A), In-situ Recovery (e.g., VOM-15H, TRIO), Advanced In-situ Recovery and Nuclear Submodule tests.

Table 4.4.1-5. Influence of Experiment Parameters in Tritium Recovery

Parameter	Phenomena			
	Intra-granular transport and trapping	... plus oxygen activity and effects	... plus gas phase transport (T and SB)	... plus mechanical effects
Breeder material and form	X	X	X	X
Breeder impurities	X	X	X	X
Neutron fluence and tritium generation rate	X	X	X	X
Temperature	X	X	X	X
Clad/structure material		X	X	X
Purge flow rate and composition		X	X	X
Temperature gradients			X	X
Geometry and mechanical boundary conditions				X

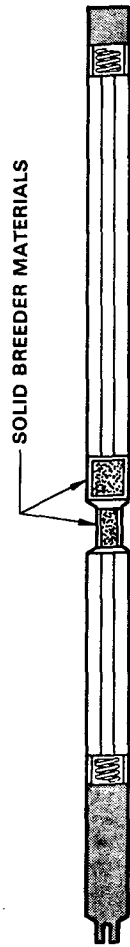
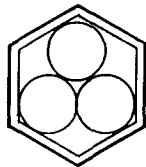
Closed Capsule

Closed capsule experiments address internal grain transport and trapping, but not surface chemistry, gas phase transport or tritium form. Surface adsorption can contribute to the measured inventory, but in blanket designs this is expected to be controlled by purge conditions so the results from closed capsule experiments are not directly applicable. Analysis of the experiments should attempt to distinguish this surface inventory from the diffusivity and trapping information (e.g., flushing the specimen with hydrogen gas).

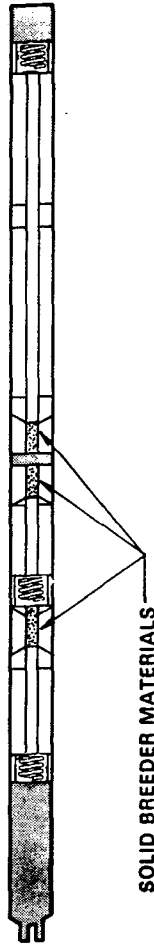
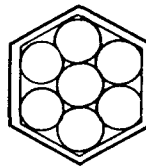
The two strategies for tritium control are to let it accumulate or to remove it. The former is the simplest, but can influence tritium retention in the breeder by the increasing concentration of tritium in the gas phase. The latter requires a tritium absorber or mechanism for permeation out of the "closed" capsule. In the FUBR-1 experiments (Fig. 4.4.1-5), a cerium oxygen getter is used to reduce T_2O vapor to T_2 , which quickly permeates through the cladding at operating temperatures into the EBR-II sodium coolant. This additional tritium load is a small increment for the primary coolant filters.

SCHEMATIC DRAWING OF FUBR-1B SUBASSEMBLIES AND PINS

S1 SUBASSEMBLY



B7A SUBASSEMBLY



HEDL 8308 004

Figure 4.4.1-5. Diagram of FUBR-1 subassembly.

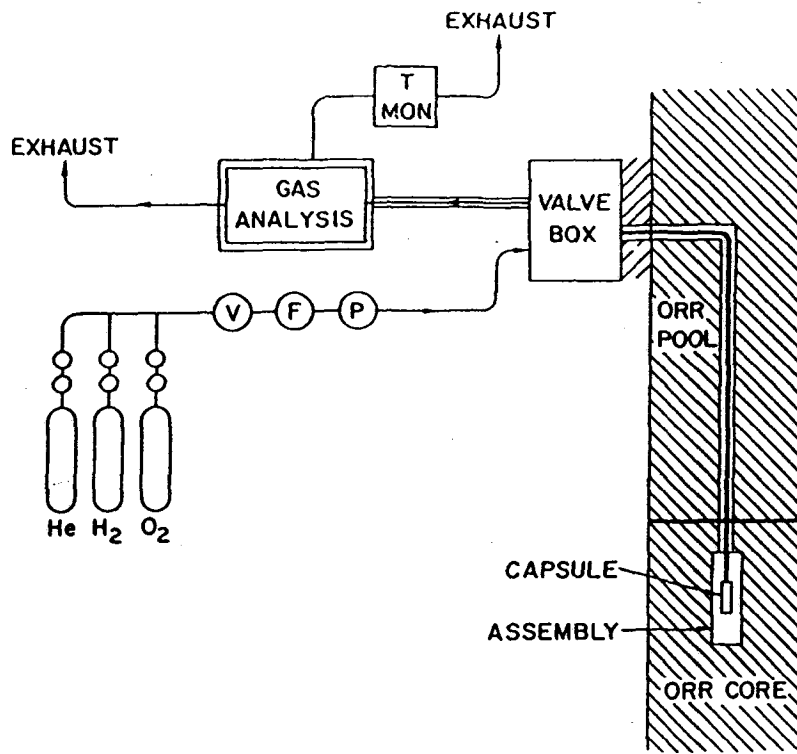
The advantage of closed capsule experiments is that they are less expensive to fabricate and operate since they are small and do not have an open connection outside of the reactor, but there is a lack of control and information during the experiment (unless actively instrumented). An appropriate gas-phase environment is difficult to maintain. Capsules must be removed at appropriate intervals for destructive analysis. Although the information is not as detailed, multiple tests and high burnup tests are relatively inexpensive compared to the other tritium tests so these are very suitable for surveying materials and parameter ranges.

These tests can also include geometric effects such as temperature gradients or breeder/cladding interaction. These could provide information on trapping due to closed porosity and internal mass transfer, but would miss important contributions from the gas composition and gas-phase transport. These would also allow tests to reach higher temperatures than might be otherwise achievable because of cladding temperature limits.

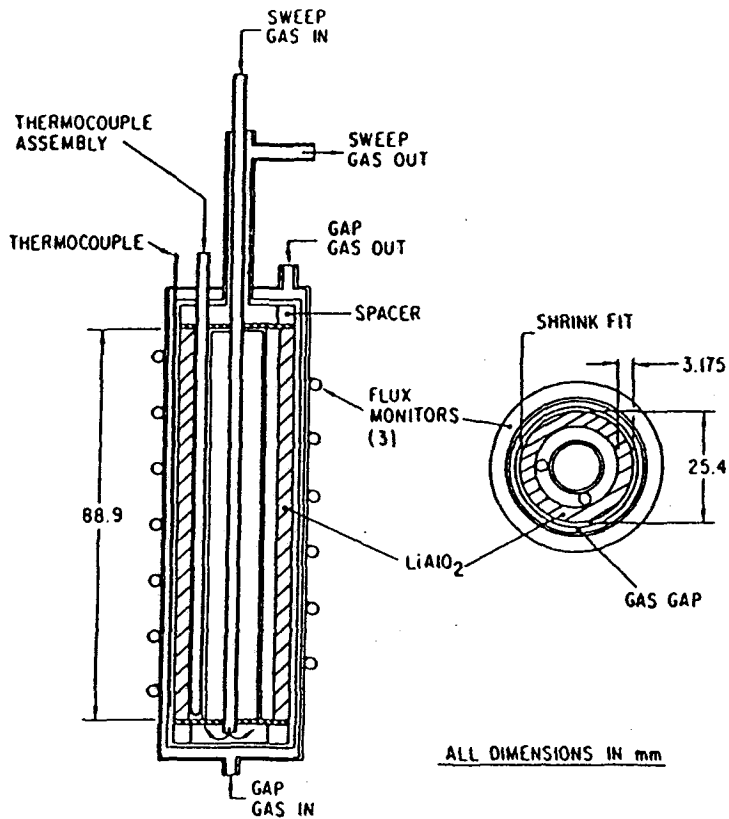
In-situ Tritium Recovery

In-situ tritium recovery experiments have an open and actively purged test capsule or test cell, and are exemplified by the VOM-15H and TRIO experiments and the many newer tests presently underway [VOM, LILA, CRITIC and others⁽⁴⁾]. The TRIO experiment is illustrated in Fig. 4.4.1-6.

As stated in the TRIO experiment recommendations,⁽²⁾ further tests should include on-line capsule monitors, thermocouples and flux monitors in the test capsule, real-time and integral monitoring of tritium (in its various chemical forms) and impurities in the purge stream and coolant. In addition, if separate diffusivity measurements are not performed, then the experiment should minimize the temperature gradient to under 50°C in order to aid the interpretation of temperature dependent phenomena such as diffusivity. Temperatures tested should span the full range of anticipated temperature limits in order to directly measure the low and upper temperature limits. The experiment should have improved monitoring of the oxygen potential in the test capsule, which requires an oxygen meter, a moisture meter and a mass analyzer. More quantitative measurements of real-time tritium response are needed. Experimental runs should go to equilibrium - i.e., from one to two weeks per run -



a



b

Figure 4.4.1-6. Diagram of TRIO: a) sweep gas flow path and b) capsule design.

to permit more quantitative measurement of release of volatile materials. More accurate gamma heating rates are needed to provide better prediction of heat transfer coefficients and thermal conductivity.

Major experimental choices are materials and temperature. In TRIO, the temperature was changed every few days, yielding a lot of information with one capsule, although this complicated the results. It is recommended that the temperature be controllable for general reasons, but only allowed to vary slowly, every one to two weeks. Similarly, the sweep gas should have variable flow and oxygen potential capabilities that would only be exercised periodically. Each capsule should have independent monitoring capability so as not to cross-influence other results. Thus the cost per capsule is expected to be somewhat, but not significantly, less for multiple capsule experiments.

Advanced In-situ Tritium Recovery

Advanced in-situ tritium recovery experiments will investigate the combined effects of several important environmental conditions that affect the breeder middle-of-life tritium release and recovery. Specifically, these will include a flowing purge gas, temperature gradients, moderate-to-high burnup, and a more reactor-relevant cladding. These may directly affect the basic tritium release and recovery phenomena observed in separate effects tests, but will also include the presence of and consequences of mechanical interactions between the multiplier, solid breeder and cladding; corrosion and mass transfer along the temperature gradient; and changes in breeder thermochemistry due to burnup. The temperature gradients within the solid breeder material can alter the tritium inventory and diffusion pathways, and can lead to mass transport within the solid breeder material. The mechanical interaction between the cladding, multiplier and solid breeder can alter diffusion and inventory by closing porosity and crack morphology. Corrosion can impact the relative oxygen content at the interface between the various materials, and this impacts tritium release. Tritium permeation may also change with time as irradiation damage accumulates within the cladding.

One design of the experimental irradiation vehicle for the advanced in-situ tritium recovery test is a series of mini-capsules designed to provide similar irradiation environments. This type of irradiation vehicle allows the experimenter to utilize several canisters and vary parameters such as solid

breeder temperature gradients, peak temperatures, or purge gas chemistry in side-by-side capsules which have nearly identical irradiation environments. In-situ monitoring allows evaluation of time-dependent effects. Thus, the tests can provide data amenable for model development with respect to: thermal performance of the solid breeder, (i.e., thermal conductivity, heat transfer coefficient); tritium retention, release, and recovery; and breeder/structure interactions.

The irradiation vehicle for the advanced in-situ tritium recovery test could be based on the Materials Open Test Assembly (MOTA), an irradiation test vehicle currently operating in FFTF (Fig. 4.4.1-7). The MOTA can irradiate materials under temperature control in capsules distributed over eight levels within and above the FFTF 91 cm core. At present, each level consists of six 3.37 cm diameter capsules 19.1 cm long. Capability exists to place three 5.08 cm diameter and ~ 13 cm long capsules in the below-core region.

This advanced in-situ tritium recovery test would modify the present MOTA by replacing one or more canisters with inner capsules (open or closed) of breeder pellets in cladding (Fig. 4.4.1-8). A gas gap containing a variable mixture of helium and argon separates the inner capsule and the outer stainless steel capsule wall. By adjusting this gas mixture, inner cladding temperatures from 400°C to over 750°C can be obtained. Radial temperature gradients within the pellets depend upon the volumetric heat generation, thermal conductivity, and geometry. For example, temperature differences up to 300°C may be obtained in a solid 2.54 cm diameter Li₂O pellet. Axial temperature gradients can be minimized by utilizing insulators, gas plenums, gas gap tailoring, and having very low or intermittent control gas flow rates. Cladding and centerline pellet temperatures can be measured with thermocouples, though care should be taken that this does not compromise the tritium release data. It is recommended that the use of thermocouples within the solid breeder material be limited, if used at all. This points to an advantage of multiple-capsule tests since side-by-side capsule tests (one with a thermocouple and one without) can be performed to isolate any thermocouple effects. A summary of the characteristics of this experiment is shown in Table 4.4.1-6.

**STRUCTURAL MATERIAL
OPEN TEST ASSEMBLY
(MOTA)**

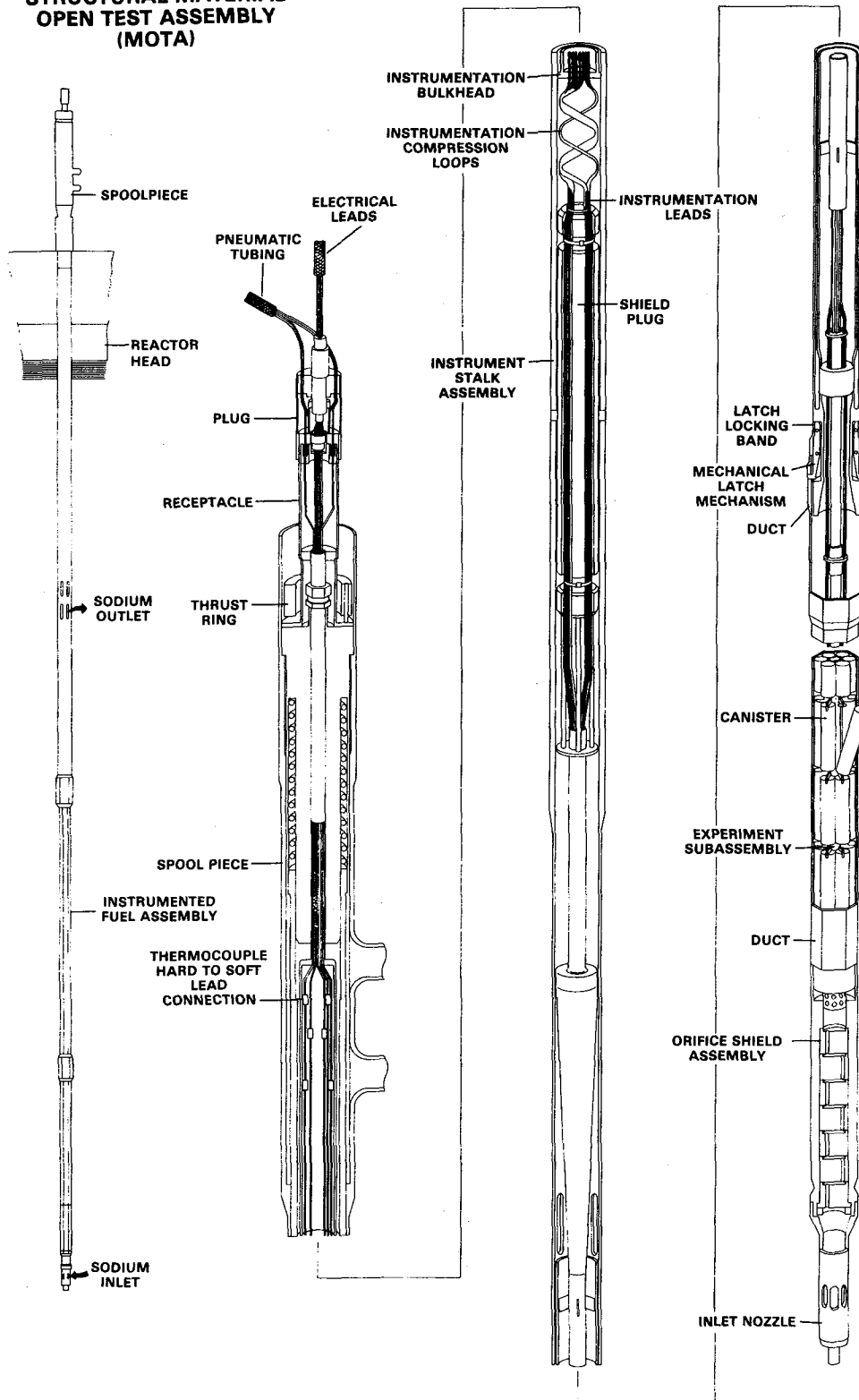


Figure 4.4.1-7. Diagram of FFTF Materials Open Test Assembly.

ADVANCED IN SITU TRITIUM RECOVERY TEST IN MOTA

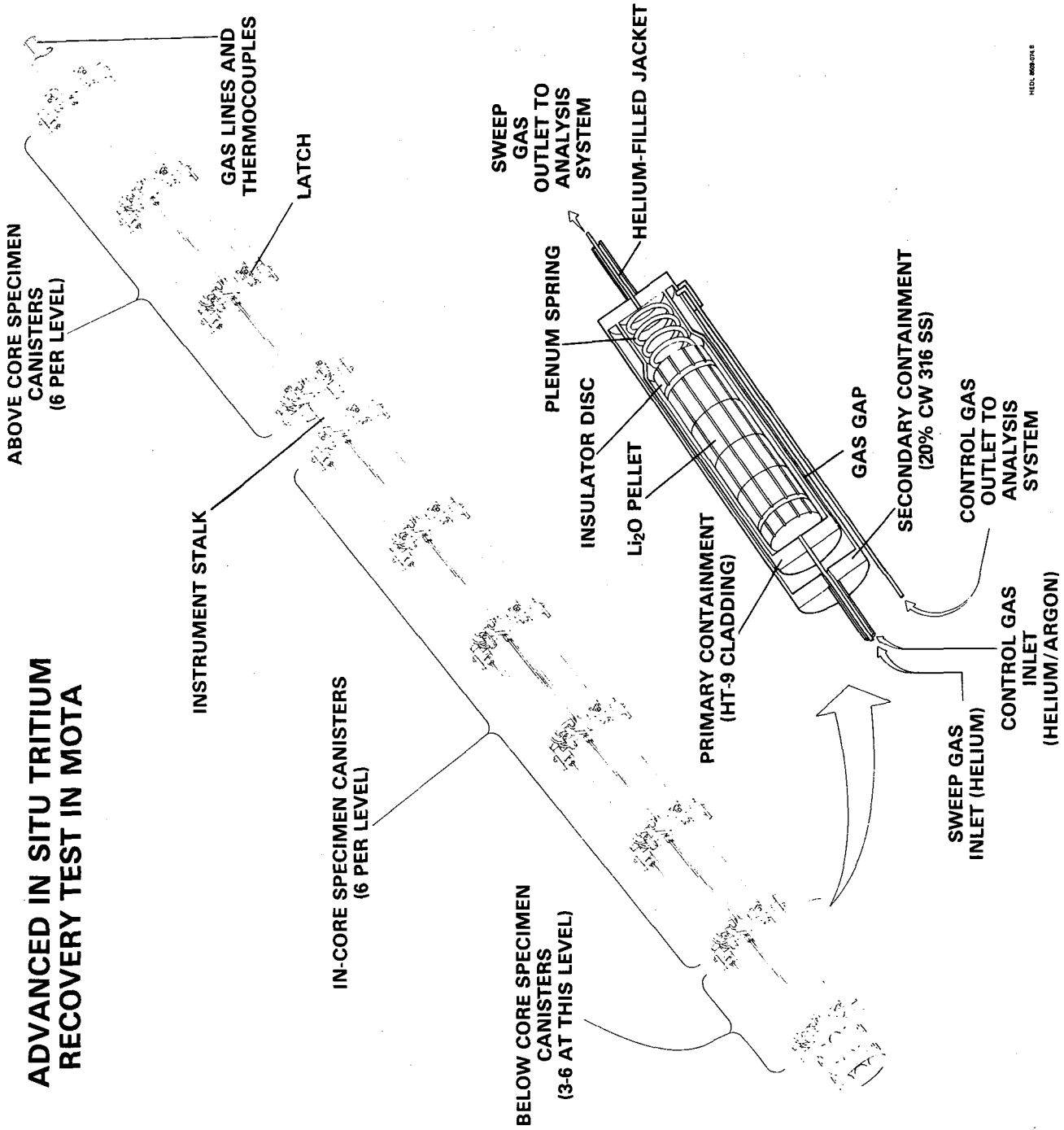


Figure 4.4.1-8. Diagram of possible Advanced In-situ Recovery experiment subassembly showing multiple capsules.

Table 4.4.1-6. Characteristics of the Advanced In-Situ Tritium Recovery Experiment and Capsule Instrumentation

Experiment Characteristics	Values	
Breeder material	Li ₂ O	
Structural material	HT-9	
Outer capsule material	20% CW 316 SS	
Structure temperature, °C	400-750	
Solid breeder temperature, °C	400-1300	
Inner capsule dimensions, mm	<u>3 Capsules</u> <u>per Level</u>	<u>6 Capsules</u> <u>per Level</u>
	Minimum wall thickness	0.25
	Inside diameter	47.30
	Outside diameter	47.80
Outer capsule dimensions, mm	Minimum wall thickness	0.89
	Inside diameter	31.90
	Outside diameter	33.68
Sodium coolant temperature, °C	365-460	
Sweep gas flow, cm ³ /min	30-300	
Sweep gas composition	He (+H ₂ or O ₂)	
Capsule instrumentation		
Temperature	Up to 2 thermocouples (single or multi-point)	
Neutron flux and fluence	Passive dosimetry (spectral sets and gradient wires)	
Sweep gas system		
Pressure and flow	Gas instrumentation	
Tritium release	SGAS ^a	
Chemistry	SGAS	
Radionuclides	SGAS	
Control gas system		
Pressure and flow	Gas instrumentation	
Tritium release	CGAS ^b	
Chemistry	CGAS	
Radionuclides	CGAS	

^aSGAS = sweep gas analysis system

^bCGAS = control gas analysis system

In-situ helium sweeping through channels in the solid breeder material provides a measure of tritium recovery but not necessarily tritium release due to permeation through the cladding wall and sweep gas outlet lines. Though metallurgical coatings and modifying sweep gas chemistry provide some control over permeation, purging of the control gas and sweep gas jacket lines may be required to quantify the amount of permeation and actual tritium released.

The instrumentation for the advanced in-situ tritium recovery test (Fig. 4.4.1-9) is similar to the TRIO test except that the system must be capable of controlling and monitoring more than one capsule simultaneously. Personnel exposure and tritium contamination of primary and secondary sodium systems are likely to limit the number of capsules. Computerized data acquisition and control systems in semiautomatic and automatic modes are undoubtedly required.

Postirradiation disassembly of the tritium recovery test capsules from the test vehicle would be performed in conjunction with the standard MOTA capsules in the Interim Examination and Maintenance cell. Special disassembly and handling procedures, however, will be required with the individual tritium-containing capsules. Capsule disassembly and component examination will be performed remotely in smaller, more manageable hot cells. Structural cladding examinations will encompass verifying overall structural integrity, measuring macroscopic swelling, mechanical testing, and microstructural analysis. Solid breeder examination will include helium, tritium, and radio-nuclide retention, lithium burnup, and microstructural and phase stability examination.

Nuclear Submodule Assembly

Nuclear submodule tests would address the effects of geometry and mechanical interactions on tritium recovery. A large breeder section, preferably a unit cell in the purge direction, should be included. Such tests would include almost all significant parameters (probably not magnetic field or the exact neutron damage effects on the structure), and would provide an opportunity for testing major interactions, including tritium behavior and also mechanical behavior, corrosion, safety, and thermal-hydraulics. Due to the more integrated nature of such tests, they are described separately in Section 4.5.2.

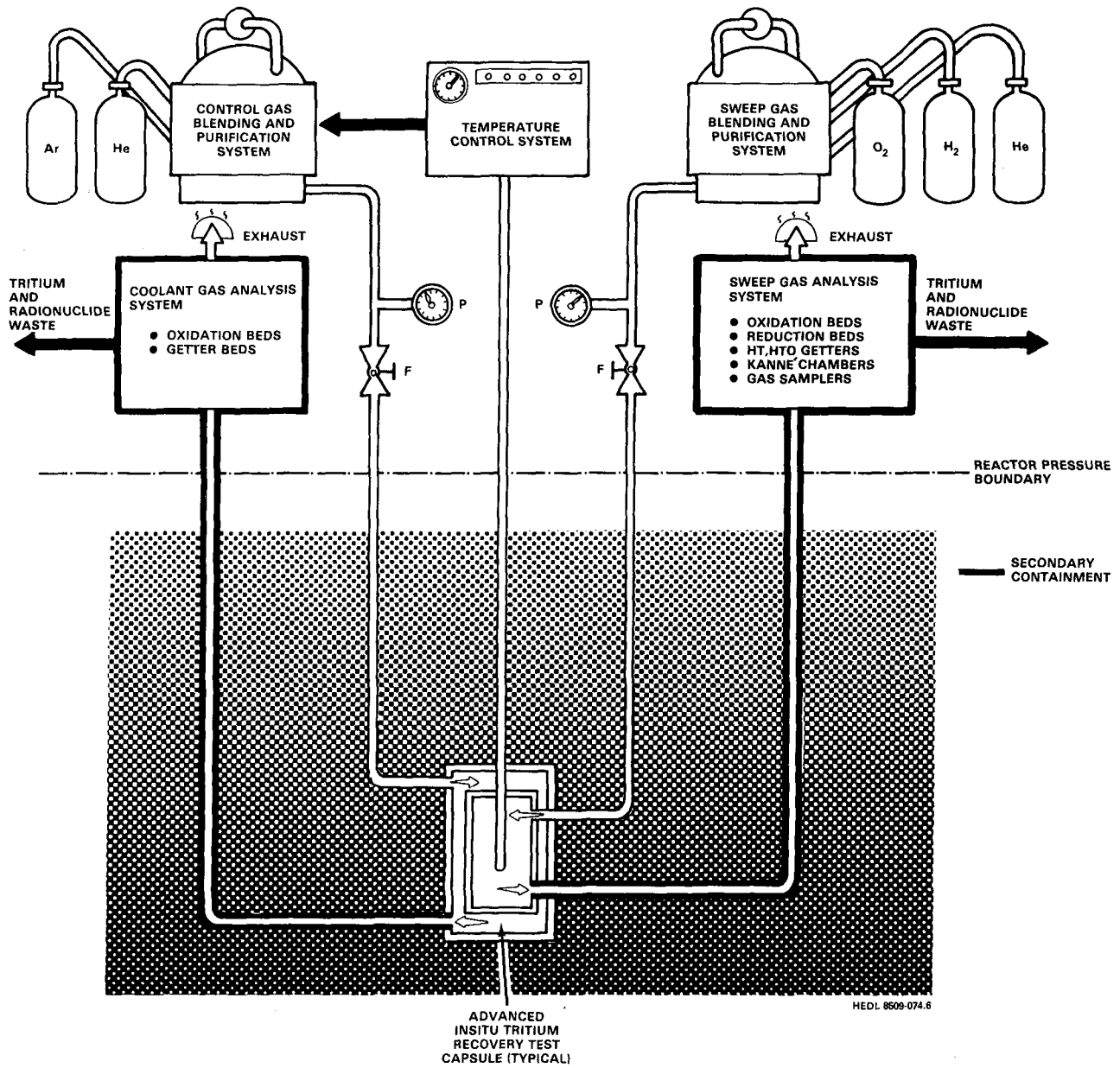


Figure 4.4.1-9. Instrumentation and flow paths for Advanced In-situ Recovery experiment.

4.4.1.3 Test Plan Considerations

The most important tritium transport related properties are diffusivity, solubility and adsorption. The particular needs are for diffusivity data for well-characterized LiAlO_2 and other ternary oxides; adsorption data for Li_2O and one ternary oxide; and data on the effects of microstructure, radiation damage and impurities on these phenomena (particularly for the ternary oxides at their lower range of temperatures).

The next most important issue is the oxygen activity in the blanket and its many effects on tritium form, inventory and transport. In-situ tests have indicated the importance of this parameter, and will be needed to address it further. This applies to all breeder materials.

Thirdly, temperature design limits must be determined. Present limits have been identified that minimize changes in breeder microstructure and maintain a predictable environment based on diffusivity, solubility, adsorption and (fast) gas phase transport. The significance of these temperature limits on blanket design, however, is large. Testing at the temperature limits, and with reactor temperature gradients, to at least middle-of-life burnup is needed to confirm present estimates. This is also applicable to all breeder materials. Perhaps the largest incentive is for Li_2O where an increase in upper temperature limit could make operation without a multiplier credible.

These uncertainties are being addressed by a number of experiments around the world (Section 4.2). Figures 4.4.1-10 and -11 illustrate the temperature and burnup ranges explored in near-term experiments for Li_2O and LiAlO_2 . Basically, closed capsule data will be available for relevant temperatures out to reasonably high burnup, some for reactor-relevant temperature gradients. A number of low-burnup in-situ recovery tests are active or planned. Measurements of some properties are also underway.

Comparing the types and parameter ranges of these experiments to the critical uncertainties, it can be seen that the present experimental program is addressing but will not resolve all the key issues. The remaining question, then, is which additional or subsequent experiments are necessary.

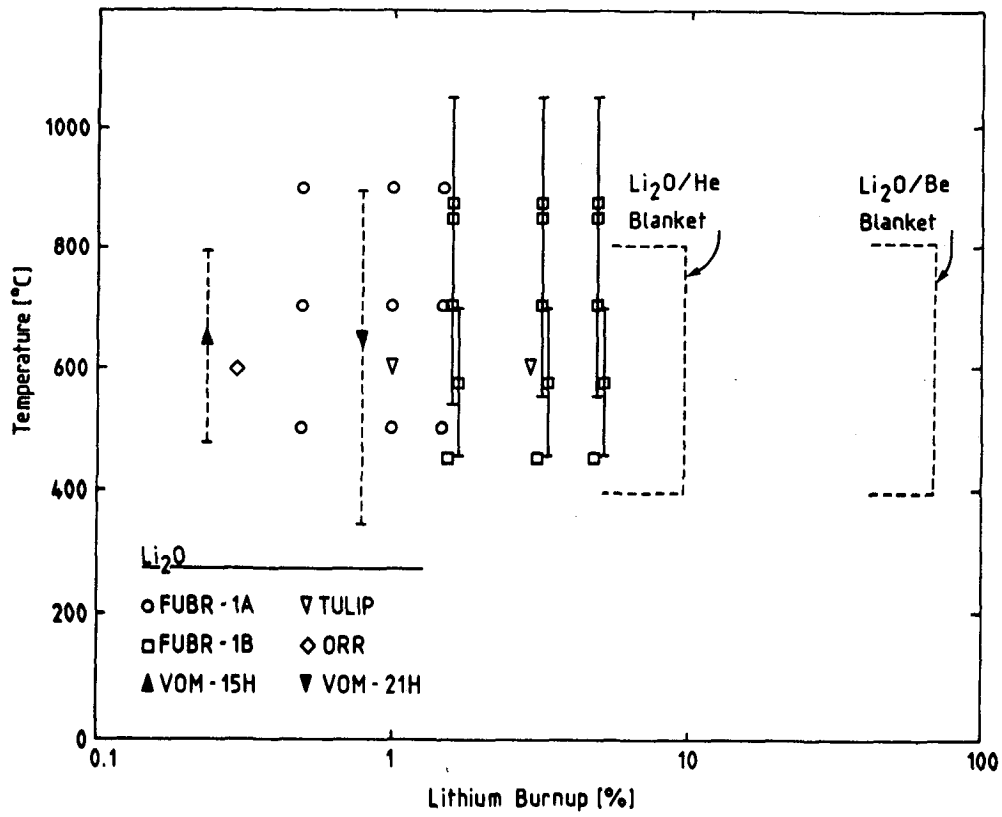


Figure 4.4.1-10. Range of temperature and burnup for Li_2O experiments.

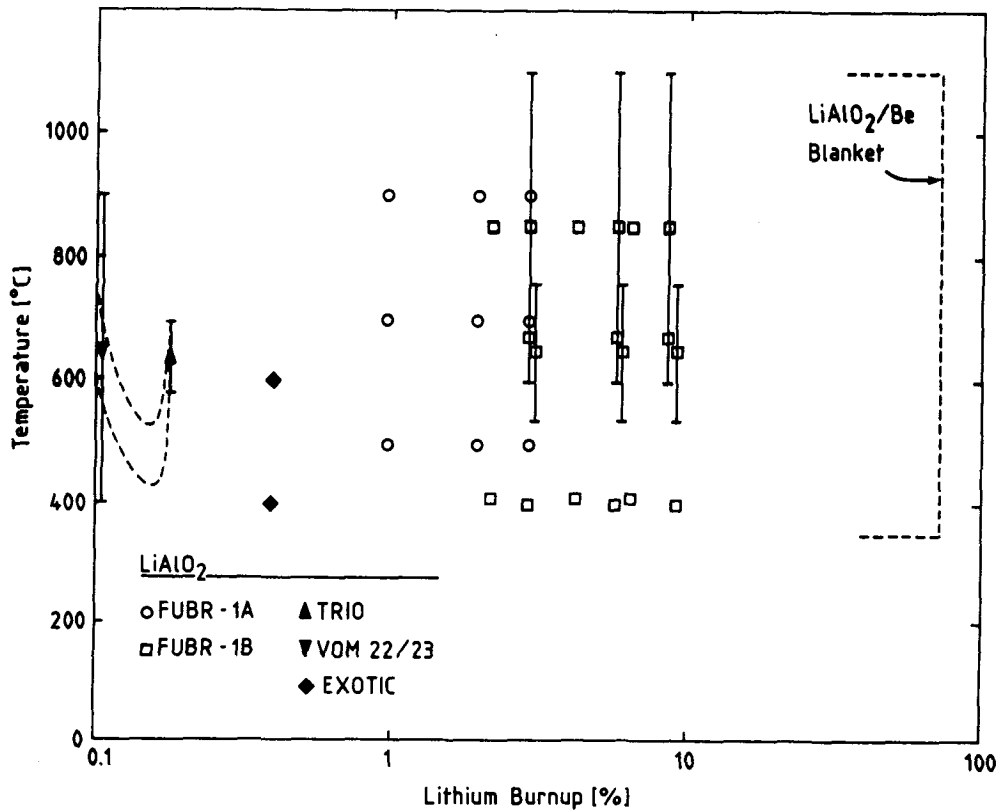


Figure 4.4.1-11. Range of temperature and burnup for LiAlO_2 experiments.

Basic measurements of diffusivity, solubility and adsorption on unirradiated material are needed, particularly for the ternary oxides. These can be inferred to varying degrees from the in-situ experiments, but their fundamental importance argues for at least some careful benchmark experiments: single-crystal diffusivity in Li_2O ; single-crystal diffusivity in a ternary oxide such as LiAlO_2 ; polycrystalline diffusivity for major candidate breeders; and surface adsorption for LiAlO_2 .

The FUBR closed capsule experiments will provide a data base for assessing burnup, material microstructure, temperature, breeder and impurity effects on tritium retention. The CREATE, ALICE, DELICE and EXOTIC closed capsule experiments will also explore these and other (e.g., cladding composition) effects and will provide irradiated materials for measurements of properties out to moderate burnups. Subject to the results of these experiments, further closed capsule experiments should be needed only for additional breeder materials or compositions, and higher burnups.

The planned in-situ recovery experiments cover a range of materials, temperatures, clad compositions and purge chemistry of interest to present blanket designs. With careful attention to oxygen activity and tritium holdup on the transfer lines, a suitable data base of basic properties, and sufficient time to achieve equilibrium with each set of conditions, a basic description of in-situ tritium behavior out to about 1% burnup should be available by 1990.

The results of all these tests will indicate desirable directions for material type, form, microstructure, purity, operating temperatures and purge chemistry. They will also support models describing local tritium transport to moderate burnups. Specific breeder configurations (breeder region geometry, breeder material and form, clad, purge channel location) would be developed from design studies.

Following FUBR, Advanced In-situ Recovery experiments will be needed to address more complex uncertainties and interactions related to tritium recovery in a representative local environment with temperature gradient, purge flow, breeder/clad interaction, and moderate burnup (> 5%). Results of these tests in turn would indicate uncertainties in basic phenomena or new directions in breeder material engineering that might suggest further tests. If suitable tritium behavior is obtained, then a large-scale fission reactor test

of a blanket section would be appropriate to verify overall behavior in a nuclear environment, with a more-representative geometry.

At any point in the test program, decisions can be made as to which materials will be pursued, or which design concepts will be pursued. Naturally, the earlier this decision is made, the greater the impact on the subsequent number of tests and program costs, but the greater the uncertainty in identifying ultimately attractive candidates. The largest impact on near-term testing comes from making material selections since the near-term experiments are not design specific. A particularly useful decision would be between Li_2O and ternary oxides like LiAlO_2 , assuming that the ternary ceramics behave at least qualitatively similar to each other but quite differently from Li_2O .

If the solid breeder program is to consider other materials such as beryllium, lithium beryllates or breeder/beryllium mixtures, then it is important that suitable scoping tests be completed quickly so that these materials can be included in the planned experiments. The basic feasibility of new breeder materials can often be addressed by relatively simple, unirradiated thermal stability tests.

References for Section 4.4.1

1. D.L. Smith, et al., "Blanket Comparison and Selection Study", Final Report," ANL/FPP-84-1, Argonne National Laboratory, September 1984.
2. R.G. Clemmer, et al., "The TRIO Experiment," ANL-84-55, Argonne National Laboratory, September 1984.
3. C.C. Baker et al., "STARFIRE - A Commercial Tokamak Fusion Power Plant Study," ANL/FPP-80-1, Argonne National Laboratory, September 1980.
4. M. Abdou, et al., (eds.), "Report on the International Workshop on Fusion Nuclear Technology Testing and Facilities," PPG-872, UCLA-ENG-85-17, UCLA-FNT-5, University of California - Los Angeles, March 10-13, 1985.
5. D.F. Holland and B.J. Merrill, "Accidental tritium release from solid breeding blankets," Proc. 10th Symp. on Eng. Prob. of Fusion Research, 1983, p. 1138.
6. M. Abdou, et al., "FINESSE: A Study of the Issues, Experiments and Facilities for Fusion Nuclear Technology Research & Development," Interim Report, PPG-821, UCLA-ENG-84-30, University of California - Los Angeles, October 1984.
7. D.L. Jassby et al., "Design of tritium breeding experiments for the Tokamak Fusion Test Reactor (TFTR)," Proc. Top. Mtg. on Trit. Tech. in Fission, Fusion and Isotope Appl., Dayton, Ohio, April 29-May 1, 1980.

4.4.2 Breeder/Multiplier/Structure Mechanical Interaction

4.4.2.1 Testing and Modelling Needs

The major issues associated with the mechanical interaction between the solid breeder, multiplier and structure are the restructuring of the solid breeder material, the deformation of the structure, and changes in the heat transfer at the interface between the solid breeder and structure.

The thermal expansion of many solid breeder materials is significantly larger than that of most structural materials. This may lead to a mechanical interaction between the structure and solid breeder material if the design gap between these two materials is small or changes with time. Also, some solid breeder materials such as Li_2O and the neutron multiplier, beryllium, do swell with neutron irradiation.^(1,2)

The response of the interacting materials to mutual loads is uncertain. It is anticipated that creep relaxation will occur to some extent, but these deformations might alter the thermal behavior and tritium recovery processes within the solid breeder material. Another complication is the anticipated cracking and/or redistribution of the solid breeder material due to cycling associated with the plasma burn cycle or transients anticipated during typical fusion reactor operations (i.e., disruptions). Such phenomena would probably lead to a significant decrease in the thermal conductivity within the solid breeder material and thereby cause the temperature within the solid breeder to rise. This may impact tritium recovery through possible grain growth, closure of open porosity and cracks leading to changes in purge channels and an increase in the surface area for adsorption associated with the solid breeder material.

Changes or uncertainties in the gap conductance also lead to uncertainty in the long-term tritium recovery characteristics. In addition to the possible impact on tritium recovery, breeder/structure interactions could lead to failure mechanisms such as breach of the structural wall between the solid breeder material and coolant due either to the deformation directly or to hot spots induced by the deformation.

The test parameters to be investigated in experiments include both environmental parameters and solid breeder material characteristics. The

important environmental parameters include temperature, neutron fluence and stress. The anticipated parameter ranges of temperature and fluence for two BCSS blanket designs⁽³⁾ are summarized in Table 4.4.2-1. Both the temperature and the temperature gradient within the solid breeder material are important since they impact the integrated thermal expansion and any cracking/redistribution which may occur within the breeder material. The neutron exposure may lead to increased swelling with increasing neutron fluence in the solid breeder/multiplier material and can be the other major driving mechanism for the interaction.

The general nature of the interaction is dependent upon the material properties responsible for the interaction and the influence dependence. The specific interaction, however, will be very design dependent. In considering the fluence dependence of the individual material properties, one can identify the major material properties which are changing with fluence and have a significant impact upon the interaction. For example, consider the mechanical interaction between the solid breeder and the HT9 cladding in the HT9/Li₂O/He blanket concept. The changes in several of the key properties with neutron exposure are given in Fig. 4.4.2-1. The swelling in Li₂O is the major material property responsible for the interaction. Thermal expansion and cracking/redistribution of the Li₂O also plays a role in this interaction, primarily in the early operation of the component (i.e., in the neutron exposure range of 0-0.2 MW-yr/m²). After a neutron exposure of ~2 MW-yr/m², most of the strength and fracture property changes have saturated, and the major properties responsible for the interaction are the balance between Li₂O swelling and the creep of Li₂O and HT9 (not shown in the figure). After a neutron exposure of 10 MW-yr/m², HT9 swelling may occur and become important. The present candidate structural materials have been fairly well characterized in irradiation experimentation and alloy development (see Section 4.2). The optimum characteristics for the solid breeder material and neutron multiplier, however, are not as well defined. For example, important characteristics for the solid breeder material such as porosity levels, grain size, and impurity levels may significantly impact the mechanical interaction and therefore should be investigated for each representative class of solid breeder material (Li₂O and one ternary breeder at a minimum).

Table 4.4.2-1. Environmental Parameter Ranges Applicable for Solid Breeder/Multiplier/Structure Mechanical Testing

	Li ₂ O/He/FS	LiAlO ₂ /H ₂ O/FS/Be
Peak Fluence	15 MW-yr/m ²	15 MW-yr/m ²
Temperature (°C)		
Structure (Cladding)	500	350
Solid Breeder (T _{min} /T _{max})	500/800	350/1000
Multiplier (T _{min} /T _{max})	---	350/650

MECHANICAL INTERACTION BETWEEN SOLID BREEDER AND STRUCTURE
HT9/Li₂O/He BLANKET CONCEPT

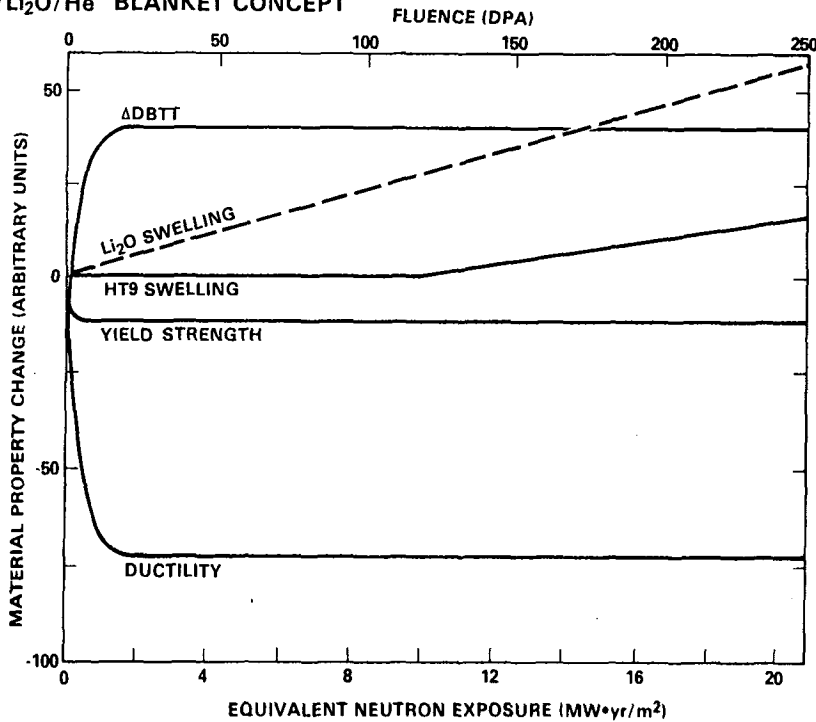


Figure 4.4.2-1. Fluence dependence for several of the key material properties associated with the mechanical interaction between the Li₂O and HT9 cladding.

To effectively design and interpret experiments which investigate this interaction will require a sufficient base material characterization and model development. Specifically, the thermal expansion, isothermal swelling, creep, and tensile properties must be known over the applicable environmental parameter space. For the solid breeder material, the thermal conductivity must also be known for the unconstrained condition. While effective design of these separate and multiple effects experiments may be possible with relatively crude models, the eventual design of blankets may require more sophisticated models if the interactions play a significant role in the overall blanket performance. At present, no models have been developed to address the mechanical interaction between the fusion solid breeder material and structure. Similar phenomena have been modeled phenomenologically in the liquid metal reactor program to describe the mechanical interaction between the fuel cladding and fuel within a pin. At present, it appears possible that such models could be adopted to describe the fusion solid breeder/clad mechanical interaction, at least for cylindrical geometries.

4.4.2.2 Experiments and Facilities

Three classes of experiments could be performed to address this mechanical interaction issue. The first class of experiment would investigate the interaction driven by differential thermal expansion. Such experiments need not initially include neutron irradiation, although a neutron flux might eventually be required to obtain relevant temperature gradients within the solid breeder material and to have the proper irradiation-assisted creep and damage in both materials. These experiments would be relatively short in duration (less than one year). They could also provide scoping information on the relative importance of various solid breeder material characteristics to the resulting mechanical interaction. The second class of experiments would investigate the interaction driven by swelling in the solid breeder material and/or neutron multiplier. These experiments require a neutron flux to drive the swelling and the neutron irradiation may be relatively long in duration (several years) if end-of-life and failure mechanisms are to be investigated. The third class of experiments would investigate the gap conductance and its changes with irradiation. These experiments will eventually require a neutron flux to obtain the proper breeder restructuring and gap morphology which are crucial to this issue. These experiments are design specific and

will be difficult to separate from the other mechanisms which lead to change in the breeder temperature with irradiation.

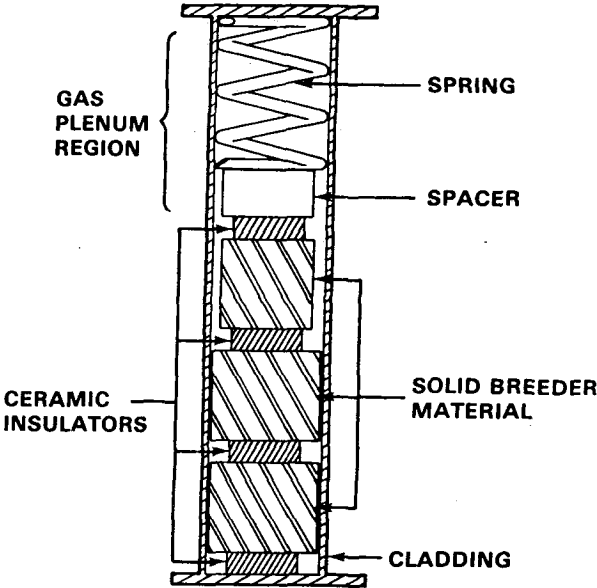
Thermal Expansion Experiments

Non-neutron experiments could address issues such as the magnitude and form of the deformation in the blanket materials due to thermal expansion-driven interactions. The difficulty is obtaining the proper temperature gradients within the solid breeder material without compromising the experiment. Simple tests where the solid breeder pellet is resistively heated within a cladding can be useful to provide basic understanding of the relative responses of the different materials to differential thermal expansion. Beyond this level of testing lies the more complicated design-specific experiments such as the proposed rf-heated LiAlO_2 block⁽⁴⁾ and those outlined in Section 4.5.

Swelling Experiments

The major environmental parameters for swelling experiments are the structural and solid breeder material temperatures, the temperature gradient within the solid breeder material, stress in both materials and the neutron fluence. As an example of a swelling experiment, consider the interaction of Li_2O with HT9 cladding. For investigating the Li_2O and ferritic steel interaction, the fast reactor neutron spectrum offers more favorable neutronics when attempting to match the anticipated fusion environment (see Section 4.5.2 and Figure 4.4.1-4). The pellet radial dimension and the lithium enrichment determine the magnitude of the heat and tritium production rates in the solid breeder material. The gap dimension determines the initial relative temperature difference between the outer circumference of the solid breeder material and the structural material and the time/fluence at which contact occurs. Finally, the cladding thickness determines the magnitude of the stress buildup in both materials. Initial experiments to investigate this phenomenon will probably be uninstrumented closed capsule experiments performed in double-walled capsules containing subcapsules similar to those shown in Fig. 4.4.2-2. Such a capsule design (Fig. 4.4.2-3) is similar to the one used in the FUBR experiments. Temperature control would probably be through the gas gap

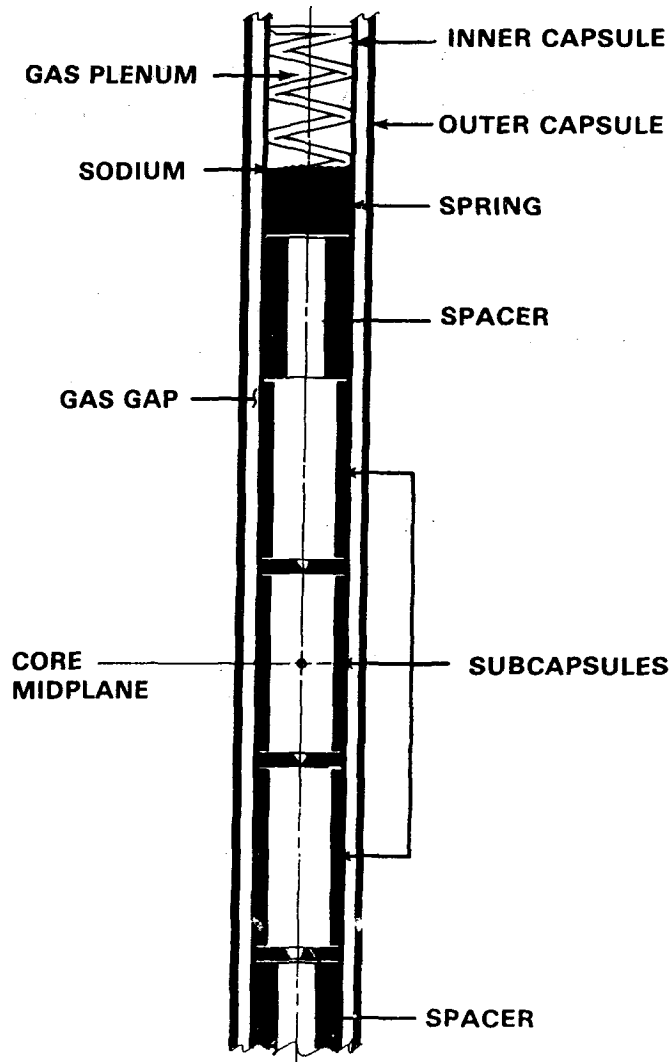
SOLID BREEDER/STRUCTURAL MECHANICAL INTERACTION SUBCAPSULE



MEDL 8509-014.5

Figure 4.4.2-2. Schematic of subcapsule design to investigate the mechanical interaction between the solid breeder material and the structural cladding.

SOLID BREEDER/STRUCTURAL MECHANICAL INTERACTION IRRADIATION VEHICLE



HEDL 8509-014 4

Figure 4.4.2-3. Schematic of closed capsule irradiation vehicle to irradiate subcapsules designed to investigate the solid breeder/multiplier/clad mechanical interaction.

in the double walled capsule to control heat flow from the subcapsule to the reactor's coolant. Each subcapsule would have a given cladding thickness and contain several cylindrical pellets, probably of the same material to avoid thermodynamic interactions between different materials. Each pellet would have a similar enrichment and vary the porosity, grain size and/or pellet diameter. Each subcapsule would be designed to have an isothermal cladding temperature and may or may not contain a tritium getter (such as cerium). Different subcapsules would investigate different solid breeder materials, cladding temperatures and/or cladding thickness. The impact of such lithium-6 enriched capsules upon reactivity would probably require that these irradiations take place on the periphery of any test fission reactor. The subcapsule(s) would be loaded in the inner capsule and the inner capsule filled with a liquid metal such as sodium or NaK for liquid metal reactor irradiations. This liquid metal serves as a thermal bonding medium. This construction permits the cladding to run at an isothermal temperature as it deforms. Interim examinations would be conducted periodically (yearly) and consist of dimensional measurements on the subcapsules and neutron radiographs to determine the dimensional stability of the solid breeder materials themselves. This swelling experiment class is summarized in Table 4.4.2-2. The maximum hardware design dimensions in this table represent an uninstrumented experiment in FFTF using a minimum of three capsules per subassembly position. The variation in the cladding wall thickness leads to a range of obtainable stresses in the solid breeder material. The range in the capsule wall temperature is due to the axial variation in the coolant temperature in FFTF. The maximum lithium burnup in such an experiment (multiplier not part of experiment) would be ~10 at.% at the end of three years of irradiation.

Final postirradiation examination of the subcapsules would include density measurements and microstructural examination of the cladding for any chemical interaction between the solid breeder material and the structural material. The final examination of the solid breeder material would include measurements for retained helium and tritium, grain size, porosity and dimensional changes and crack morphology. If the solid breeder pellets retained their geometry, then other physical property measurements such as thermal conductivity for example could also be performed.

Table 4.4.2-2. Solid Breeder/Structural Material Mechanical Interaction Experiment

Hardware Design

Subcapsule dimensions

Solid breeder pellets (diameter) < 4.5 cm
 Cladding (outside diameter/wall thickness) < 4.5 cm/0.2-0.75 mm

Capsule dimensions (outside diameter/wall thickness) < 5 cm/1.3 mm

Environment control monitoring

Temperature Gas gap dimensions
 Flux/fluence Gradient wires; spectral sets

Temperature

Capsule wall 360-460°C
 Subcapsule wall 400-750°C
 Solid breeder material
 Outside diameter 400-750°C
 Maximum gradient < 300°C

Irradiation schedule

Interim examination one/year
 Final examination 3 years
Maximum lithium burnup 10 at.%

Gap Conductance Experiments

More advanced closed capsule tests instrumented with thermocouples would be desirable. These experiments would provide direct information on both the thermal conductivity of the solid breeder material and the gap conductance as a function of neutron fluence. These experiments would use capsules of a similar design to those shown in Figs. 4.4.2-2 and 3; however, thermocouples would be placed within the solid breeder material to measure their center line temperatures. One of the major experimental issues in such experiments would be the impact of the thermocouple's presence on the solid breeder material's response. Nevertheless, these experiments would provide valuable information when conducted side-by-side with similar uninstrumented tests. More advanced

experiments would also be envisioned which incorporate cladding temperature control.

4.4.2.3 Test Plan Considerations

The overall testing required to resolve the breeder/multiplier/structure mechanical interaction uncertainties is determined by the risks imposed by this interaction. At a minimum, a number of non-neutron scoping tests should be performed to examine the impact of thermal cycling on the mechanical interaction between the solid breeder material and the structural material. These scoping experiments should be simple extensions of basic breeder materials properties testing. The need for more complex non-neutron testing to investigate the issues would depend upon the outcome of these scoping tests. The need for long term irradiation testing of the solid breeder and structural material mechanical interaction depends to a large extent upon the outcome of high burnup closed capsule tests such as FUBR-1A and FUBR-1B. If these tests indicate solid breeder dimensional stability, then mechanical interaction type experiments would not be required. On the other hand, if uninstrumented tests indicated that candidate solid breeder materials did swell, then one could envision one capsule such as the one shown in Figure 4.4.2-2 for each candidate solid breeder/ structural materials combination. More advanced (i.e., instrumented tests) may be advisable if the breeder restructuring or mechanical interaction were found to be significant. Such tests would then facilitate the understanding of results from other tests such as the advanced in-situ tritium recovery experiments.

References for Section 4.4.2

1. G.W. Hollenberg, "The Effect of Irradiation on Four Solid Breeder Materials," First International Conference on Fusion Reactor Materials, Tokyo, Japan, December 3-6, 1984.
2. L.G. Miller, J.M. Beeston and F.J. Fulton, "Radiation Damage Experiment and Lifetime Estimates for Beryllium Components in Fusion Systems," Sixth Topical Meeting on the Technology of Fusion Energy, San Francisco, CA, March 3-7, 1985.
3. D.L. Smith, et al., "Blanket Comparison and Selection Study," Argonne National Laboratory, ANL/FPP-84-1 (1984).
4. B. Misra, et al., "Thermal-Hydraulic/Thermomechanical Testing of Solid breeder Blanket Modules Using Microwave Energy," Sixth Topical Meeting on the Technology of Fusion Energy, San Francisco, CA, March 3-7, 1985.

4.4.3 Structure Mechanical Behavior

The major issues associated with the structure mechanical behavior can be divided into three categories: structure mechanical response, thermal power transient response, and electromagnetic response. The structural mechanical response to the environmental conditions includes the mechanical behavior of the various structural elements during blanket operation. The major material properties which lead to loading within the structure are differential thermal expansion and the differential dimensional stability of the material at various locations throughout the blanket. These phenomena lead to loading of the structure which is relieved by creep or crack growth. These responses are then responsible for deformation of the structure which may cause operational or maintenance problems, or may lead to failure of the structure. The thermal/power transient response of the structure must also be understood so that potential failures due to this response can be minimized through appropriate design. Normal transients associated with the periodic cycling of the plasma burn can be expected whether or not the fusion device is run in a cyclic or steady-state mode. Off-normal power transients associated with disruptions for example can also be envisioned. These phenomena can lead to failure of the structure and must be adequately explored. Finally, electromagnetic forces can also lead to loading of the structure. This loading can be either steady state or transient in nature. Of particular concern are the transients associated with plasma disruptions. These can lead to large instantaneous loads on the structure, and the magnitude of these loads must be understood. Issues associated with the magnetic field are more fully discussed in Section 3.4.7.

In order to effectively design blanket components with adequate structural lifetimes, it will be necessary to develop understanding of these phenomena in complex geometries and over applicable environments. Perhaps the largest effort for this issue will be the development of computer models which can be used to assess blanket designs. The modelling needs include relevant material properties correlations and the extension of fracture mechanics analysis to relevant geometries. Such models could then be used to develop design criteria for the structure. Much work in this area has been performed in many fields including the liquid metal reactor program. However, the present designs suggest a high degree of complexity will be associated with

fusion blanket designs, and it is this complexity (especially in geometry) which must be assessed to a large extent through models.

The experimental test parameters pertinent to structural mechanical behavior include both environmental parameter ranges and design related factors. The important environmental parameters are the maximum temperature and associated temperature gradient, and the peak fluence and associated flux gradient. The temperature gradient is the driving mechanism in the differential expansion. Both the temperature and flux gradients are responsible for the differential swelling if the material swells during its anticipated lifetime. The variation of these environmental parameters (particularly temperature and magnetic field) with time are also important when considering transient response. Examples of environmental ranges for present solid breeder blanket designs are given in the BCSS report. The major design related factors include both geometry and the joint configurations. The overall geometry leads to possible regions of stress concentrations within the structure which become potential failure sites. The joining of materials within the structure such as weldments will probably be required due to the complexity of the blanket designs. These also represent regions of dissimilar response or stress points whose responses are unknown and difficult to model.

Interactive tests could be designed to investigate selected sub-issues; however, such testing may not be required. Simple interactive tests have been designed to investigate responses such as the creep-swelling interaction, structural response to restrained swelling, and even self-welding of materials. Such limited multiple effects testing has been performed in the liquid metal reactor development program, for example. Such a testing approach could work also for the solid breeder blanket technology development. From the liquid metal reactor program, the structural response to environmental history effects was typically found to be either minor or could be modeled using the base structural material properties. Based upon this experience, it is felt that characterization of the structural response will come from experiments designed to investigate other issues. Specifically, the most stringent tests of structural response will come from the partially integrated tests which will attempt to incorporate the issues associated with the structural geometry.

4.4.4 Corrosion and Mass Transfer

4.4.4.1 Testing and Modelling Needs

The material interaction issues may be divided into interface (corrosion) and bulk (mass transfer) processes. These interactions and their uncertainties are briefly discussed below.

Coolant/Structure

For water or helium coolants and stainless steel structure, corrosion is acceptable but not negligible (e.g., $< 1 \mu\text{m}/\text{yr}$ for austenitic steel with pure hot water).⁽¹⁾ Concerns include identifying and achieving optimum coolant chemistry, corrosion product deposition and activity levels, and stress corrosion cracking.⁽²⁾ Significant discrepancies in corrosion rates exist between laboratory experiments and operating values. The optimal coolant chemistry for fusion will be different because of the different operating conditions (higher energy neutrons, neutron sputtering, magnetic fields, structural alloys). However, while further development will certainly be required for commercial reactors, it does not pose feasibility concerns.

Vanadium and refractory alloys offer high-temperature mechanical strength, but reactions with oxygen or other impurities in helium and water coolant limit operating temperatures. From Fort St. Vrain HTGR experience, levels of 10 vppm or less of oxidants in helium coolant were difficult to achieve in a power reactor environment.⁽³⁾ The limited data (mostly with unalloyed metal) indicates that alloys such as VCrTi are much more resistant than unalloyed vanadium, and may be acceptable with pressurized water up to $\sim 300^\circ\text{C}$ and helium with $< 1 \text{ ppm}$ moisture to 450°C .⁽²⁾ Corrosion measurements with the alloys is necessary to resolve the temperature and impurity limits.

The possibility of magnetic field effects on corrosion was considered in STARFIRE.⁽²⁾ Possible mechanisms were identified, but none appeared to be a major concern for steel/water systems.

Structure/Breeder

Several experiments have investigated the reactions between structural alloys (steels, transition metals) and solid breeders (Li_2O and ternary oxides).^(2,4-7) Early tests indicated severe corrosion by Li_2O within short periods of time (100 hrs). Subsequent experiments identified the importance of LiOH and have led to breeder operating limits in order to prevent LiOH formation near the cladding. Under these conditions, the reactions are fairly limited with $\sim 10 \mu\text{m}$ scales forming over ~ 1000 hrs, and a decreasing reaction rate. Very little reaction has been observed between the ternary oxides and steel (HT-9, 316SS) in sealed tube experiments.

Uncertainties include the effects of the burnup-induced stoichiometry changes, purge composition, and the corrosion rate at end-of-life ($> 20,000$ hrs). The FUBR-1A closed capsule irradiation experiments achieved up to 3% burnup over 300 full-power-days, but the cladding material was nickel-lined in order to avoid compatibility problems. Although not apparently life-limiting, understanding the extent and kinetics of the reactions defines temperature and possibly purge composition limits, and supports efforts to understand the influence of the clad surface on breeder oxygen activity and on tritium permeation through the clad.

Multiplier/Structure

Liquid lead and bismuth (melting points under 300°C) strongly corrode austenitic stainless steels at 500°C , but are more acceptable with ferritic steels and appear compatible with the refractory metals Mo, Nb, Ta and W up to 800°C .⁽²⁾ Beryllium oxide is very stable. The corrosion behavior of intermetallic compounds like Zr_5Pb_3 with structural materials is not known.⁽²⁾

Beryllium, the preferred multiplier, can react with steel to form a hard surface coating. It has an affinity for nickel, so NiBe is the most common compound with high nickel steels (FeBe_2 and BeC are also formed). Overall, however, the interaction with stainless steels should be small at the structural temperatures.⁽²⁾

Multiplier/Breeder

Some blanket designs propose a direct mixing of beryllium multiplier and solid breeder in order to enhance neutronics and tritium recovery, and simplify the thermomechanical design. However, there are thermodynamic concerns because of the affinity of Be for oxygen. The extent and consequences of this mixing will depend on the source of oxygen (whether the oxygen activity is maintained by the "system" or the breeder) and on the reaction kinetics. It is possible that the reaction rate may be acceptably slow after an initial BeO surface layer has formed. A BeO/breeder combination might be chemically acceptable if no further mixed oxides form (e.g., $\text{BeAl}_6\text{O}_{10}$), or at least do not degrade the behavior. The development of a phase diagram for the breeder/beryllium system is needed.

Multiplier/Coolant

Beryllium is reasonably compatible with many blanket coolants, and is in direct contact with the coolant in several designs.⁽⁸⁾ Significant reaction with oxygen occurs over 600-800°C, after which the reaction increases rapidly until excessive embrittlement and possibly burning occurs. The behavior with nitrogen is similar but slower.⁽²⁾

Consequently, beryllium appears compatible with reactor-grade helium up to about 700°C, with a protective oxide layer forming.⁽⁹⁾ High purity beryllium is compatible with low-temperature high-purity water, but corrosion occurs if the water is slightly ionized or if the beryllium is commercial-grade purity. There are no conclusive data with respect to high temperature water. Porous beryllium has a higher corrosion rate due to the increased surface area.^(2,9)

Beryllium and lithium are themselves compatible, but mass transfer with other metals must be considered. Data on the Be-Li-ferritic steel system indicates a temperature limit of about 450°C.⁽⁹⁾ Beryllium and nitrate molten salts (e.g., draw salt) appear compatible up to 560°C, and beryllium and flibe are compatible up to higher temperatures (> 650°C).⁽⁹⁾ Beryllium is not compatible with thorium/uranium bearing molten salts because the beryllium will react with the UF_4 to create BeF_2 and solid uranium-beryllium precipitates.⁽⁹⁾

The stability of beryllium oxide has been demonstrated for moderate times (i.e., not years) in a variety of corrosive environments including, for example, molten lithium, or hydrogen gas at 1800°C,⁽¹⁰⁾ but weight loss has been measured with water vapor.⁽¹¹⁾

Coolant/Breeder

Contact with helium coolant (either directly or through leaks) does not raise significant compatibility issues for present lithium-based oxide breeder materials which are anticipated to operate with helium purge streams in many designs.⁽⁸⁾ Contact with water can lead to formation of corrosive LiOH in Li₂O and must be avoided.

Coolant Mass Transfer

The deposition of corrosion products within the coolant stream may influence local heat transfer and flow (e.g., around spacers or other channel discontinuities) and radioactivity levels (e.g., around valves). Present reactor experience provides design guidelines for minimizing these effects.

Since some corrosion products such as Fe₂O₃ are ferromagnetic, the magnetic field could inhibit their transport and result in local deposition. This depends on the balance between the magnetic and fluid drag forces. For plausible values in water of 10 μm particles,^(12,13) magnetic field gradients of 1 T/m and ferromagnetic saturation strengths of 0.5-1 T, it appears that magnetic particles will not be significantly restrained relative to the coolant flow.⁽²⁾

Breeder Internal Mass Transfer

Experience with fission reactor fuels suggests that 10⁻⁷ MPa is a critical value for the onset of appreciable vapor phase transport in a static atmosphere. Thermodynamic calculations for the Li₂O, LiAlO₂ and Li₄SiO₄ systems indicate significant LiOT and Li vapor pressure at higher temperatures (~ 1000°C) and even at 600°C for Li₂O (Fig. 4.4.4-1).⁽¹⁴⁾ The transport of material within the breeder can lead to restructuring, grain growth and pore closure, which could significantly impact tritium recovery and breeder thermomechanical properties. Experiments indicate that even at 5% porosity, most of the volume is in closed pores.

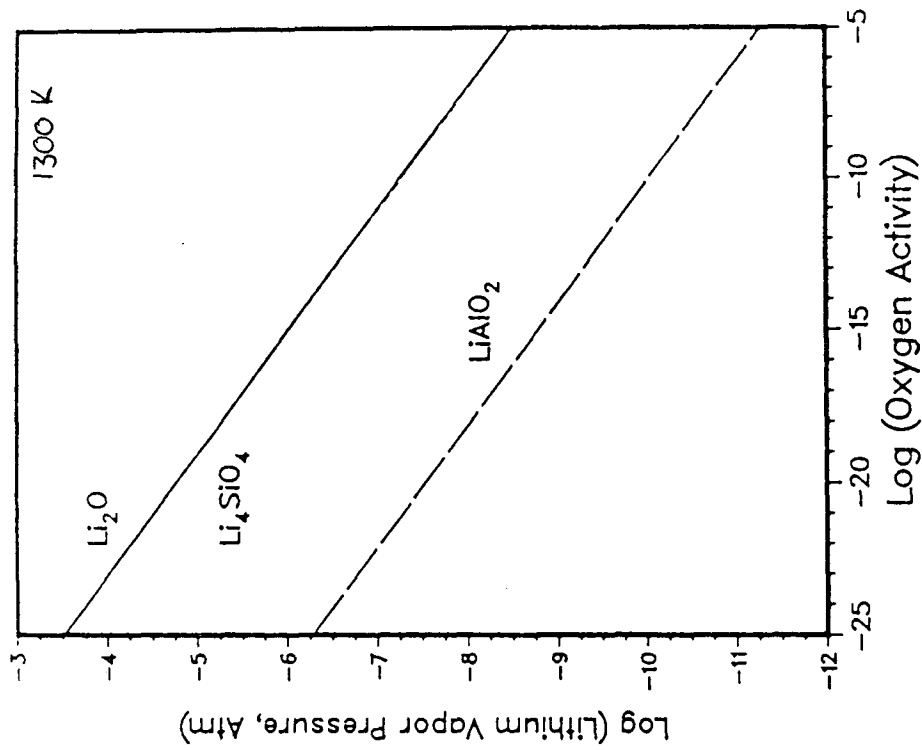
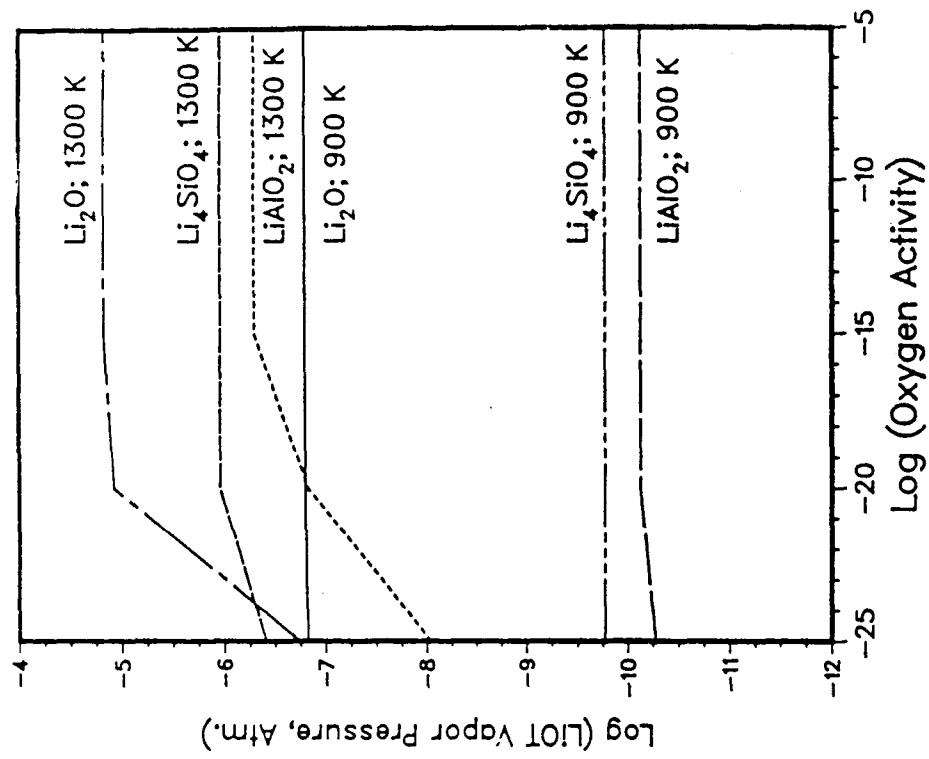


Figure 4.4.4-1: Vapor pressure of LiOT and Li over several breeder materials.

Uncertainties include the actual vapor pressure (activity coefficients have not been measured for breeders other than Li_2O), oxygen activity in the breeder, and the extent of mass transport. Some data on internal mass transfer with a reactor-relevant temperature gradient across the pellet will be obtained in the FUBR-1B experiments.⁽⁷⁾

Breeder External Mass Transfer

The loss of breeder material through removal of vapor is probably most significant for Li_2O . Measured weight loss of Li_2O in flowing He at 550°C was 12%/yr with 93 ppm H_2O in the helium, 3.8%/yr with 1 ppm H_2O , and 3.2%/yr in 1 ppm H_2O and 1 ppm H_2 .⁽⁴⁾ This is 2-3 orders of magnitude greater than those predicted from equilibrium reaction kinetics, but could be explained by a corrosion process with the container material. Further data, including measurement of vapor pressures and material removed up to high burnup, would be desirable. Other breeders may also have significant vapor pressures and scoping tests could be useful.

Modelling Needs

Published models include thermodynamic calculations of equilibrium gas species and concentrations in the breeder,⁽¹⁴⁾ and coolant corrosion product radioactivity and transport.^(2,12,15) The primary modelling needs are to quantify the internal and external mass transfer rate and redistribution in the solid breeder. Uncertainties include species and vapor pressure as a function of burnup, oxygen activity, and the possibility of liquid phase and radiation-enhanced sintering. Models should be developed to correlate the existing and upcoming (FUBR-1B) experimental data and allow extrapolation to reactor conditions (e.g., temperature limits, breeder purge system designs).

4.4.4.2 Experiments and Facilities

The primary parameters for corrosion and mass transfer are materials, impurities, time, burnup (changes in chemistry), temperature, temperature gradient, flow rate and composition, magnetic field and geometry. The influence of these on the phenomena are summarized in Table 4.4.4-1. These suggest four types of tests: thermal stability in a closed capsule; corrosion rate with active flow; internal mass transfer in the solid breeder; and external mass transfer.

Table 4.4.4-1. Influence of Experimental Parameters on Corrosion and Mass Transfer

Experimental Parameter	Phenomena				
	Chemical Reactions	Corrosion		Mass Transfer	
		Rate	Transport	Internal	External
Materials	X	X	X	X	X
Impurities	X	X	X	X	X
Temperature	X	X	X	X	X
Time	X	X	X	X	X
Burnup	(X)	(X)		(X)	(X)
Purge/coolant composition	X	X		X	X
Purge/coolant flow rate		(X)	X		X
Temperature gradient				X	
Geometry			X		(X)
Magnetic field		?	?		

() indicates that tests are useful with and without this parameter.

Thermal Stability Tests

Thermal stability tests are closed capsule, isothermal tests that need not be irradiated but should hold the material at temperature for long time periods to observe the extent of reactions and identify reaction products. Capsules need not be large, but care must be taken that the reactions observed are not undesirably affected by the capsule material itself. These can be used to provide quick scoping data on possible materials compatibility problems.

Corrosion with Flow Tests

An active flow stream is important to simulate reactor conditions (e.g., oxygen activity, dissolution and removal of elements) in order to accurately determine corrosion rates. These tests can be isothermal and unirradiated, and must be reasonably long time. A magnetic field might be included to clarify the extent of any effects. These can be scoping or detailed tests, depending on the degree of instrumentation and coolant chemistry control.

Internal Mass Transfer Tests

Internal mass transfer tests are closed capsules with temperature gradients and long test times. Initial tests should be unirradiated to develop the models for thermal transport. Subsequent irradiated tests would then add burnup and radiation-enhanced sintering effects. The proper fill gas pressure should be included since it affects the gas phase transport through the pores.

External Mass Transfer Tests

Measurements of external mass transfer require open capsules. They can be isothermal for supporting model development, or with temperature gradients to include internal mass transport. The inlet and exit conditions should be monitored for H_2O , H_2 and the appropriate vapor species ($LiOH$, Li_2O , Li). Measurements of capsule weight loss would provide an additional integral measure of mass transport. Tests could include the effects of oxygen potential (through the H_2/H_2O inlet concentration), flow velocities and breeder moisture content. Care must be taken with the container since a hot metal could complicate the behavior.

4.4.4.3 Test Plan Considerations

Corrosion and mass transfer are not considered to be feasibility issues, but present uncertainties impact temperature limits and overall design and so affect the attractiveness of solid breeder blankets. The most important uncertainties are the breeder/structure corrosion rate at high burnups (> 10%), mass transfer with temperature gradients in Li_2O , thermal stability of Be/solid breeder mixtures, and the compatibility limits for vanadium alloys with solid breeder and helium.

Separate corrosion/mass transfer tests can be largely avoided through the use of reactor-relevant cladding material in other tritium recovery or thermal-mechanical tests. For example, a 1% burnup test of tritium recovery implies about 100 reactor days or 2400 hours, certainly a reasonable corrosion time. Breeder mass transfer model development would, however, be aided by separate internal and external mass transfer tests. Furthermore, any new breeder materials should be subjected to at least scoping tests on thermal stability and on interactions with the structure.

References for Section 4.4.4

1. M.A. Abdou, et al., "A Demonstration Tokamak Power Plant Study (DEMO)," ANL/FPP-82-1, Argonne National Laboratory, September 1982.
2. C.C. Baker, et al., "STARFIRE: A Commercial Tokamak Fusion Power Plant Study," ANL/FPP-80-1, Argonne National Laboratory, September 1980.
3. H.G. Olson, H.L. Brey and F.E. Swart, "The Fort St. Vrain High Temperature Gas-cooled Reactor: Part VI, Evaluation and Removal of Primary Coolant Contaminants," Nucl. Eng. Des., 61 (3), 1980, p.315-322.
4. O.K. Chopra and D.L. Smith, "Compatibility Studies of Structural Alloys with Solid Breeder Materials," in Alloy Devel. for Irr. Perf. Semiannual Prog. Report for Period Ending Sept. 30 1983, DOE/ER-0045/11, U.S. Dept. of Energy, March 1984.
5. R.J. Pulham, W.R. Watson and J.S. Collinson, "Chemical Compatibility between Lithium Oxide and Transition Metals," Proc. 3rd Top. Mtg. on Fusion Reactor Materials, Albuquerque, New Mexico, September 12-22, 1983.
6. D.L. Porter, et al., "Neutron Irradiation and Compatibility Testing of Li_2O ," Jrnl. of Nucl. Mat., 122 & 123 (1984), p.929.
7. G.W. Hollenberg, "The Effect of Irradiation on Four Solid Breeder Materials," First Int. Conf. on Fusion Reactor Materials, Tokyo, Japan, December 3-6, 1984.
8. D.L. Smith, et al., "Blanket Comparison and Selection Study, Final Report," ANL/FPP-84-1, Argonne National Laboratory, September 1984.
9. T.J. McCarville, et al., "Technical Issues for Beryllium Use in Fusion Blanket Applications," UCID-20319, Lawrence Livermore National Laboratory, January 1985.
10. R. Brown and N. Bass, "Fabrication and Properties of Commercial Beryllia Ceramics for Nuclear Applications," Jrnl. Nucl. Mat., 14 (1964), p.341.
11. W.I. Stuart and G.H. Price, "The High Temperature Reaction between Beryllia and Water Vapour," Jrnl. Nucl. Mat., 14 (1964), p.417.
12. A.C. Klein and W.F. Vogelsang, "Radiation Hazards Due to Activated Corrosion and Neutron Sputtering Products in Fusion Reactor Coolant and Tritium Breeding Fluids," Nucl. Eng. Des./Fusion, 2 (4), 1980, p.355.
13. G.F. Schultheiss and Ch. v.Minden, "Investigations of Local Blockage Formation and Dependence on Fuel Element Spacing," Trans. 7th SMIRT Int. Conf., Vol. C., Struct. Analysis of Fuel, Cladding and Assemblies, Chicago, IL, August 22-26, 1983.
14. A.K. Fischer and C.E. Johnson, "Thermodynamics of Li_2O and Other Breeders for Fusion Reactors," J. Nucl. Mat. 133/134, 186 (1985).

15. W.E. Bickford, "Activation Product Transport in Helium Cooled Fusion Systems," 4th Top. Mtg. on Tech. of Cont. Nucl. Fusion, King of Prussia, PA, October 1980, p.1238.

4.4.5 Tritium Permeation and Processing

The tritium permeation and processing issues are distinct from those related to tritium transport in the blanket, although they are coupled by the purge composition, tritium form and concentration. Tritium permeation uncertainties affect safety (tritium loss rate to the environment), waste management (tritium imbedded in blanket structure), and maintenance (tritium levels in the primary system and reactor hall). The tritium processing system extracts tritium from the purge or coolant and concentrates it for delivery to the fuel clean-up system. Uncertainties affect the required tritium breeding rate; safety and waste management (through the residual tritium inventory and loss rate); purge chemistry (limits on levels of water, hydrogen gas, oxygen or impurities); and blanket thermal efficiency (limits on processing system temperature and throughput). The major tests to address the uncertainties are listed in Table 4.4.5-1. These concerns and experiments are described in Sections 5.3 and 5.5.

Table 4.4.5-1. Tests to Address Tritium Permeation and Processing Issues

Permeation

- Tritium diffusivity, solubility, heat of transport in structure
- Permeation measurements, with clean surfaces at blanket pressures
- Surface condition effects, with well-characterized oxide layers and permeation barriers
- Temperature gradient effect (model benchmark test)
- Neutron and gamma effects (scoping test)
- Permeation under blanket operating conditions (as part of other tests on tritium recovery and thermal-mechanical integrity)

Processing (getters or molecular sieves assumed)

- Residual tritium inventory in molecular sieves
 - Oxidizing catalyst efficiency
 - Tritium Adsorption/desorption under simulated blanket conditions (multiple cycles, a range of test complexity and purge conditions)
 - Coupled blanket/tritium processing system operation
-

4.4.6 Neutronics and Tritium Breeding

The primary uncertainties in the neutronics design of blankets are those associated with the Tritium Breeding Ratio (TBR), nuclear heating, radiation damage and induced activity. The TBR uncertainty is the most important since tritium self-sufficiency is critical for fusion feasibility, and is the most difficult to resolve since the tolerable uncertainties are small.⁽¹⁻³⁾ The testing needs for the TBR issue are directly discussed in this section. The other uncertainties can be reduced in the same or similar tests.

4.4.6.1 Uncertainty in Tritium Self-Sufficiency

Tritium self-sufficiency is attained when the achievable tritium breeding ratio (Λ_a) is greater than the required tritium breeding ratio (Λ_r). These are defined as follows.

The required TBR must exceed unity by a margin G_o , so

$$\Lambda_r = 1 + G_o + \Delta_G, \quad (1)$$

where G_o is the total loss through the fuel cycle plus a doubling time margin; and Δ_G is the uncertainty in estimating the required breeding ratio ($1 + G_o$).

The achievable TBR is a function of the reactor design, with a strong dependence on the blanket concept, and is given by

$$\Lambda_a = \Lambda_c - \Delta_a = \Lambda_c - (\Delta_s^2 + \Delta_p^2)^{0.5}, \quad (2)$$

where Λ_c is the calculated tritium breeding ratio; Δ_a is the uncertainty in calculating the achievable TBR; Δ_s is the uncertainty in TBR associated with system definition; and Δ_p is the uncertainty in TBR due to nuclear data uncertainties and modelling approximations.

The self-sufficiency condition can be written as

$$\Lambda_a > \Lambda_r, \quad (3)$$

or

$$\Lambda_c - 1 - G_o > \Delta_a + \Delta_G. \quad (4)$$

Accordingly, the uncertainty in predicting the achievable and required TBR should be less than $\Lambda_c - 1 - G_o$ (i.e., the breeding gain of tritium minus G_o).

The present uncertainties related to Λ_a and Λ_r have been estimated by Abdou, et al.,⁽²⁾ as shown in Table 4.4.6-1 for several typical blanket con-

cepts. For all the cases considered, the calculated net tritium production is not sufficiently large to cover the present uncertainties, which means that none of these designs are clearly tritium self-sufficient.

Since Δ_a includes design uncertainties Δ_g , it can be reduced by about half once detailed designs are available. Therefore, the main objective of neutronics tests is to reduce the remaining predictive uncertainty Δ_p to within about 3-5%. This requires improvements in the data base, neutronics design codes and modelling procedures. Moreover, it is possible to confirm experimentally the feasibility of design concepts using detailed partial mockups. At the final stage of neutronics tests, one can obtain bias factors (e.g., effects of an adjacent limiter port) to allow extrapolation from experimental systems to a demonstration reactor.

In neutronics testing, neutron sources naturally play a dominant role in the experimental plan. Possible sources are accelerator-based point neutron sources, fission reactors and fusion devices. As will be discussed, high-neutron-energy point sources are important for addressing uncertainties in the achievable TBR. Fission reactors are restricted in usefulness due to the soft neutron spectrum, and will be useful in reducing uncertainties in the required TBR (e.g., understanding tritium holdup in the blanket). In the long-term, fusion devices provide a relevant neutron source and more relevant geometry for addressing both the achievable and required TBR, although test facilities will probably not have full coverage blankets and so will still not be definitive tests of the achievable TBR.

4.4.6.2 Review of Present Status

There have been many experiments using 14 MeV point neutron sources. Most of them have measured neutron spectra or reaction rate distributions other than tritium production in various materials. Typical examples are the leakage spectra measurements in spherical geometries performed at LANL since 1969. Several tests using 14 MeV point sources have been done specifically to measure tritium production rates and assess the nuclear data and analytical methods in lithium-bearing materials. These physics benchmark experiments were performed in simple geometries as shown in Table 4.4.6-2. The breeder

Table 4.4.6-1. Achievable and Required Tritium Breeding Ratios and Associated Uncertainties for Leading Blanket Concepts in Tokamak Reactor in Tokamak Reactor Systems

Concept*	Achievable TBR		Required TBR		Difference $\Lambda_a - \Lambda_r$
	Λ_a		Λ_r		
	Λ_c	Δ_a	$1 + G_o$	Δ_G	
LiAlO ₂ /DS/HT9/Be	1.24	0.22	1.077	0.143	-0.20
LiPb/LiPb/V	(1.30) ⁺	0.24	1.072	0.142	-0.15
Li/Li/V	1.28	0.24	1.072	0.142	-0.17
Li ₂ O/He/HT9	1.11	0.21	1.077	0.143	-0.32
LiAlO ₂ He/HT9/Be	1.04	0.19	1.077	0.143	-0.37
Li/He/HT9	1.16	0.22	1.072	0.142	-0.27
Flibe/He/HT9/Be	1.17	0.22	1.072	0.142	-0.26
LiAlO ₂ /H ₂ O/HT9/Be	1.16	0.21	1.077	0.143	-0.27

* Concept is denoted by breeder/coolant/structure/multiplier

+ Estimated for 90% ⁶Li enrichment

Table 4.4.6-2. Experiments on Tritium Production Rate Using Point Neutron Sources*

Organization	Year	Breeder Material	Geometry (cm)
LANL	1972	LiD	Sphere, D = 60
	1979	⁶ LiD	Sphere, D = 60
Jülich	1976	Li metal	Cylinder, D = H = 120
KFK	1978	Li metal	Sphere, D = 100
FNS (JAERI)	1979	Li ₂ O-C	Sphere
	1983	Li ₂ O	Cylinder, D = H = 60
OKTAVIAN (Osaka University)	1984	Li metal	Sphere, D = 120
LOTUS (Switzerland)	1986	Li ₂ O	Block, 80 x 80 x 100

* Most of these experiments were physics benchmarks

materials include lithium oxide and lithium metal (which simulates liquid lithium). The primary measuring technique is the liquid scintillation method. Among the facilities listed in Table 4.4.6-2, the Fusion Neutron Source (FNS, Japan), OCTAVIAN (Japan), and LOTUS (Switzerland) are currently in operation. Through these experiments and analyses, significant improvements have been obtained, for example, in the tritium production cross-sections of ${}^7\text{Li}$.

At FNS, U.S.-Japan joint experiments on tritium breeding began in 1983. Most of the Phase 1 experiments (cylindrical Li_2O assemblies, stainless steel first wall, and beryllium multiplier) have been completed. The Phase 2 experiments will start in 1986. These experiments have demonstrated that point neutron sources are very useful because many neutronics issues can be addressed in a low neutron fluence. For example, the fluences at the front surface of the assemblies in the U.S.-Japan experiments are 7×10^{11} n/cm² over 50 hr of operation in Phase 1 and 7×10^{12} n/cm² over 50 hr of operation in Phase 2. These fluences correspond to 0.02-0.2 s at 1 MW/m² neutron wall load. With these fluences, ${}^6\text{Li}$ and ${}^7\text{Li}$ tritium production rates could be measured to within several percent over regions 0-60 cm from the front surface.

4.4.6.3 Point Neutron Source Tests

Cross-Section Measurements

Nuclear cross-sections are basic data needed to predict TBR and should be updated to achieve the desired accuracy. There are many reaction measurements needed for various isotopes, so it is necessary to set priorities by taking account of their uncertainties and effect on the TBR. Table 4.4.6-3 shows the uncertainty in TBR calculated by Youssef⁽⁴⁾ based on the sensitivity method and the cross-sections uncertainties and their covariance matrices compiled in the ENDF/B-V data file. The average uncertainty is about 5% for typical blanket concepts.

The required accuracies and the priorities are shown in Table 7-11 for important nuclides used in a fusion nuclear design. For TBR calculations, the highest priority are the tritium production cross-sections and the energy-angle distributions of secondary neutrons. Most cross-section measurements should be concentrated in the energy range above a few MeV.

Table 4.4.6-3. Estimate of the TBR Uncertainty in Various Blanket Concepts Due to Nuclear Data Uncertainties⁽⁴⁾

Blanket Concept	Uncertainty in TBR due to Nuclear Data Uncertainties (%)
Li ₂ O/He/PCA	4.9
LiPb/LiPb/PCA	3.9
LiAlO ₂ /H ₂ O/FS/Be*	2.1
Flibe/He/FS/Be*	3.4
Li/Li/V	6
Li/Li/FS	5.5
Li/He/FS	5
LiAlO ₂ /He/FS/Be*	2
LiAlO ₂ /DS/FS/Be*	1.9
LiPb/LiPb/V	4.4

*Based on latest unpublished evaluation for Be(n,2n) reaction by Young and Stewart, LANL

Measured data should be carefully evaluated and compiled in nuclear data files. These are processed into multi-group cross-section libraries, and the processing method itself influences the resulting accuracy. In the U.S., two cross-section processing codes, AMPX developed at ORNL and NJOY developed at LANL, are extensively used. Examples of multi-group cross-section libraries are the VITAMIN series processed by the AMPX code and the MATXS series processed by the NJOY code. These are widely used in the nuclear design of fusion reactors. These libraries should be assessed by comparing calculated values with measured ones for various integral neutronics parameters. The general nuclear data needs are being investigated in the U.S. DOE Office of Fusion Energy.⁽⁵⁾

Physics Benchmark Experiments

Benchmark measurements are performed in order to check the data and methods by comparing measured integral quantities (tritium production rate, various reaction rates, heating rate) and differential quantities (angular neutron spectrum). The geometry and materials should be simple in order to

reduce modelling approximation errors as much as possible. The materials with high priority are Li metal, Li₂O, LiAlO₂, Be, Pb, C, H₂O, and Al. The parameters required are neutron angular flux, reaction rate distributions of various threshold reactions and tritium production rate distribution. Through these experiments, improvements in nuclear data and processing methods are possible, and the discrepancies among calculational methods can be identified and minimized. Although the cross-section data for some of these materials have already been measured, more accurate and reliable data are still needed.

Instrumentation Development

The development of measuring techniques with improved accuracy is necessary to resolve some of the present experimental uncertainties. It is also necessary to develop neutronics instrumentation for use in fusion reactor diagnostics and control since the accuracy and reliability of present instrumentation is not satisfactory in a fusion environment. Table 4.4.6-4 shows the required and presently achievable accuracies for the important measuring techniques or detectors.

Blanket Material (Simple Geometry) Mockup Experiments

The objectives of mockup experiments are to provide data for the verification of design codes, modelling methods and data base, and to assist in the selection of blanket configurations and materials. These experimental systems are more complicated than physics benchmark experiments and include multiple materials such as multiplier, structure and coolant in addition to the breeding material. Effects on the TBR from the presence of these other non-breeding materials would be tested. Material configurations needed include:

<u>Breeder</u>	+	<u>Multiplier</u>	+	<u>FW & Structure</u>	+	<u>Coolant</u>
Li		Be		SUS		H ₂ O
Li + Pb		Pb		PCA		He
Li ₂ O				HT-9		
LiAlO ₂				VCrTi		

Depending on the blanket concept, enriched ⁶Li or natural enrichment may be appropriate. Solid polyethylene (C₂H₂)_n is often used for convenient

Table 4.4.6-4. Requirements for Measuring Technique Accuracy

Detector	Required Accuracy (%)	Present Accuracy (%)
Liquid scintillation method	< 3	5-10
Solid track recorder	-	Under development
NE213 Li glass scintillator	< 5	5-10
Spectrum counter (NE213 and Proton recoil)	10	10-30
Foil activation/unfolded spectrum	< 10	10-50
Foil activation/reaction rate	< 2	3-10
In-reactor neutron flux (any method)	< 3	5-20
In-operation nuclear heating rate*		
Calorimeter	< 5	> 10
TLD	< 5	30-50

*TLD's sufficiently accurate in pure γ flux;
 Calorimeters require high energy deposition rate

simulation of water. The experiments range from simple to more complex geometries. The combinations of materials should be determined based on the blanket designs. The important experimental parameters are the material volume ratios.

When a fusion environment is simulated by a point neutron source, it is necessary to adjust the incident neutron spectrum on the front "first wall" surface. In the U.S.-JAERI Phase 2 experiments, a special container of lithium carbonate will be used for this purpose. Figure 4.4.6-1 shows a top view of this experimental assembly.⁽⁶⁾ The test region consists of the lithium oxide, multiplier and/or the first wall. The container is used to reduce the flux of reflected neutrons from the concrete wall and to adjust the neutron spectrum on the front surface of the test region. Figure 4.4.6-2 shows a comparison of ^6Li and ^7Li tritium production rate distributions for the cases with and without the container. With the container, the ^6Li tritium production rate distribution is well-simulated.

These tests, including the associated cross-section and physics benchmark experiments, should be performed soon because of the importance of

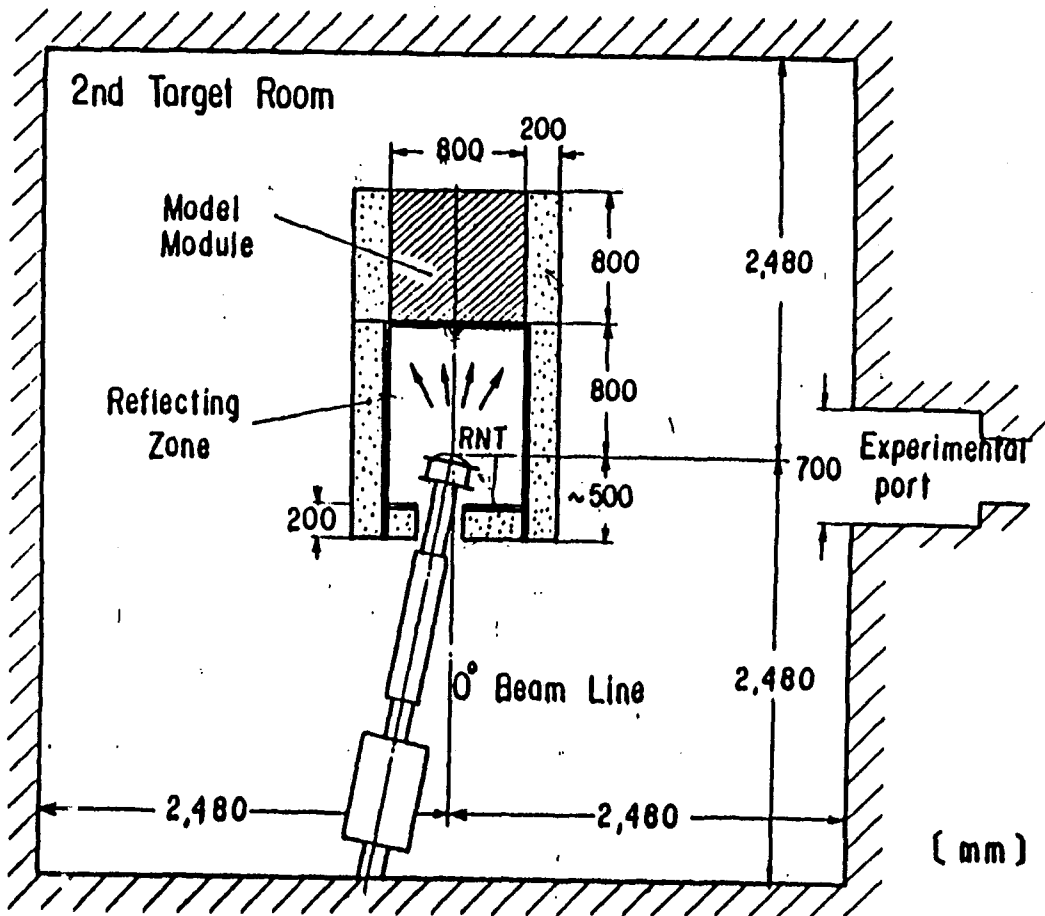


Figure 4.4.6-1. Top view of the Phase 2 experiments at the FNS facility.

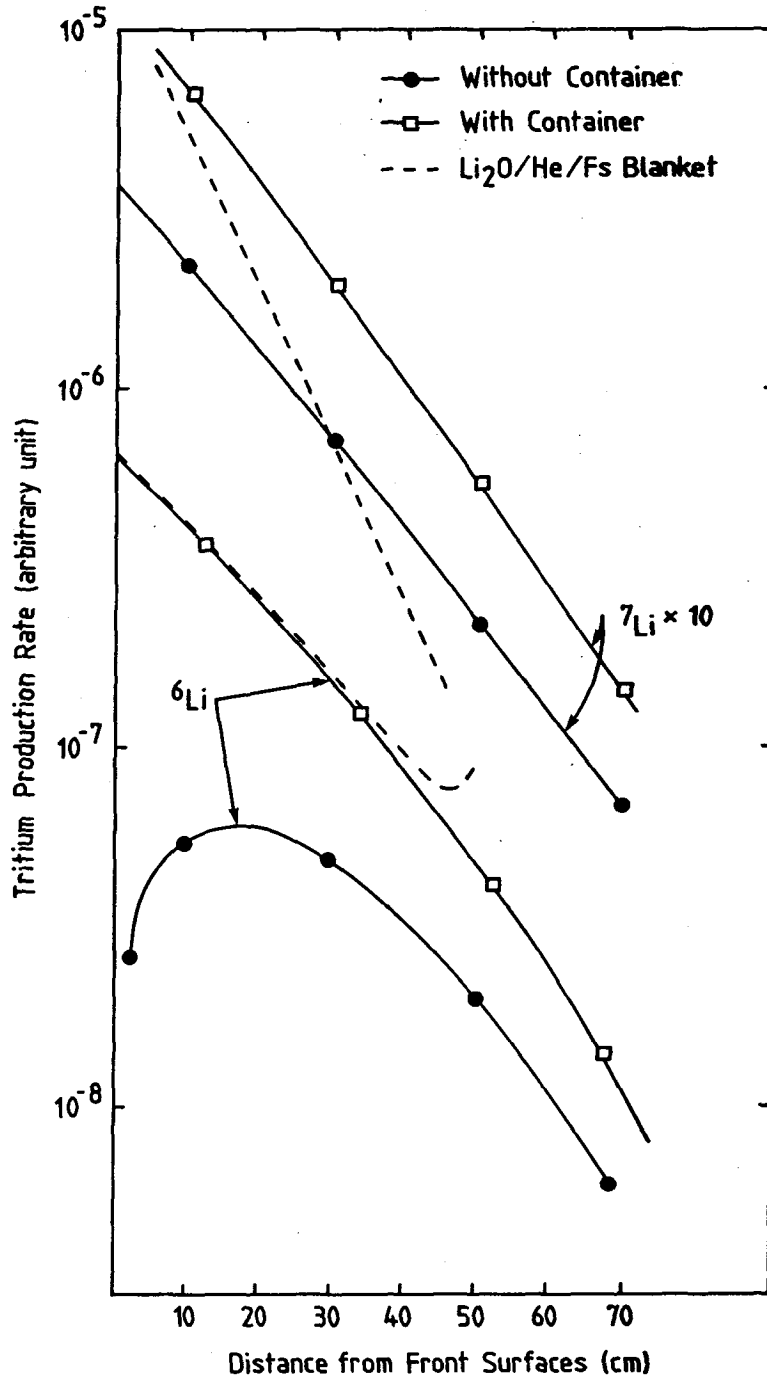


Figure 4.4.6-2. Effect of the lithium carbonate container on the tritium production profiles.

establishing the ability to breed tritium. In addition, the resolution of questions such as the need for multiplier or the need for breeding volume on a tokamak inboard side have a substantial effect on the evolution of designs and the corresponding research programs. These experiments should be completed with the goal of reducing the overall uncertainty in the achievable TBR to less than 5%.

Engineering Mockup Test

An engineering mockup test could be carried out for a reactor blanket module with a real or a slightly reduced size prior to testing in fusion test facility. The geometry and material configuration would be close to those of a real blanket. This experiment is so expensive that only one or two prototypical blanket concepts would be tested. These tests would be carried out when detailed designs have been selected.

A point neutron source is still a suitable test facility. For example, a FNS-class point source would provide fairly good accuracy in testing a FER/DEMO class blanket (2 m first wall radius, 60 cm thick, 2 m wide). However, differences (relative to full-coverage reactor blankets) in spatial dependence of incident neutrons on the first wall, test module edge effects, and the effect of local auxiliary systems (e.g., limiter or RF ports) are not easy to correct. The point-source engineering mockup test would provide the best non-fusion verification of integral neutronics parameters and models.

4.4.6.4 Fission Reactor Tests

Fission reactors are attractive neutron sources because of their high fluence, many available testing sites and moderate test volumes; but the neutron flux is predominantly less than a few MeV. Tritium production rates can be simulated both within the core and at the core side. However, the uncertainties in predicting the TBR mainly arise from the higher energy neutrons above several MeV. Therefore, fission reactors are not a proper facility to resolve uncertainties in the achievable TBR.

Nevertheless, fission reactors could be effective for special types of testing. For example, the breeder burn-up characteristics are important for a highly burnable breeder such as in LiAlO_2/Be blankets. Fission reactors can achieve the high burnup stage. Moreover, issues related to the required TBR

could be tested in fission reactors. Significant uncertainties exist in the tritium processing path such as tritium extraction efficiency. An in-core loop test could provide a good estimate for these parameters. The production rate of tritium in the core can be measured using available liquid scintillation methods. Tritium processing issues are described in Chapter 5.

4.4.6.5 Fusion Test Facilities

In order to demonstrate an adequate TBR through experiments (achievable larger than required TBR), a fusion device is needed where the blanket test module fully covers the plasma source and the geometrical arrangement duplicate the reactor in detail.

Integrated tests performed in a fusion test device and aimed specifically at verification of neutronics methods and data required specialized modules. In contrast to issues such as thermomechanical behavior, in which look-alike test modules are useful under physically-scaled conditions, neutronics verification test requires that, and are most useful when, the test module is as close to look-alike as possible.

Beside tritium production measurements, neutronics testing in a fusion test device will involve measurements of source neutron yield, neutron and gamma-ray spectra, heating rates during operation, activation and afterheat. The requirements for these tests falls within two categories: (a) test device operating conditions; and (b) test module geometrical conditions.

Test Device Operating Condition Requirements

From instrumentation considerations, all neutronics parameters except induced activation can be measured in one of two fluence modes: a low fluence mode ($\sim 1 \text{ MW}\cdot\text{s}/\text{m}^2$) or a very low fluence mode ($\sim 1 \text{ W}\cdot\text{s}/\text{m}^2$). The low fluence mode can be achieved, for example, with a wall load of $1 \text{ MW}/\text{m}^2$ and 1 s plasma burn time or, alternatively, $0.01 \text{ MW}/\text{m}^2$ and 100 s. Thus, neutronics tests impose only modest requirements on the product of the wall load and plasma burn time since the neutronics parameters, except induced activation, vary linearly with both the wall load and operating time. Notice, however, that much larger fluences than those considered here will require the use of different, less accurate, measurement techniques.

The main problem associated with the low fluence operating mode is the activation of the test module and device components which may render the test device inaccessible just after shutdown. The main problem with the very low fluence operation mode is the poor resolution and instability of measurements. Operating the test device in the very low fluence mode is most suitable for measuring tritium production from ${}^6\text{Li}$, gamma-ray heating, neutron and gamma-ray spectra. For source characterization and neutron yield, which is part of the plasma diagnostics, measurements can be undertaken in both operation modes. The operating fluence regimes for the various methods and parameters are summarized in Table 4.4.6-5.

Test Module Requirements

If the objective of the neutronics test is to verify an integrated parameter in a given blanket concept such as the tritium breeding ratio, then the test module should duplicate in detail the actual blanket module in a full coverage blanket with penetrations. This is an important requirement since extrapolating measurements of local tritium production rate in a partial coverage case to a full reactor TBR involves many uncertainties. These include uncertainties: a) in specifying the neutron source condition at the first wall of the test module; b) in predicting (by calculation or measurements) the energy-dependent angular flux at the test module boundaries; and c) in extrapolating the effects of penetrations and other configurational features of demonstration or commercial reactors that cannot be easily reproduced in a fusion test device. Since the estimated margin in TBR for candidate blanket concepts is small, very high accuracies in measurements are required, and these sources of uncertainties need to be carefully evaluated.

In a fusion test device, the test area at the first wall is limited by considerations of cost. Hence, a near-full-coverage blanket for neutronics verification tests is not practical. Therefore, a reasonable test module would partially cover the plasma source while relying on a wider but thin layer of a "reflective material" to model the effects of the full coverage geometry.

Table 4.4.6-5. Fluence Requirements for Various Measurement Techniques*

	Fluence Requirement				
	1 MW.s/m ²	1 W.s/m ²	1 kW.s/m ²	1 MW.s/m ²	
Neutron Yield		NE213 fission chamber			Multi-foil activation
Tritium Production		Li glass			Liquid scintillation (β) Gas counter (β) Mass spectrometer Proportional counter
Heating			Gas counter	TLD + Calorimeter	
Reaction Rate		Fission chamber			Activation foil Mass spectrometer
Neutron Spectrum			NE213 proton recoil		Multi-foil activation
Gamma Spectrum	NE213				

* For counter methods, the measuring time is assumed to be 10 - 100 s.

+ TLD: Thermo-luminescence dosimeter

An extensive study has been carried out to examine the usefulness of neutronics test information as a function of the test module size.^(1,7) For example, in the model shown in Fig. 4.4.6-3, the test module (and the plasma) extends over a poloidal angular width, θ_m (and indefinitely in the axial direction). The blanket module considered in this case is the BCSS⁽³⁾ Li₂O helium-cooled concept. The reflective zone shown in the figure has been optimized in material and thickness such as the incident current at the first wall of the test module is closely similar to the case where the test module fully surrounds the plasma.

Figure 4.4.6-4 shows the variation in the local tritium production rate (sum of ⁶Li and ⁷Li) as a function of the test module poloidal angular width, θ_m at three locations on the central line of the test module. The values shown are normalized to the corresponding values in the full coverage case. Also shown in this figure is the deviation of the tritium production rate at an interior position at $\theta_t/2 = 5^\circ$ and at 10° from that at the central line.

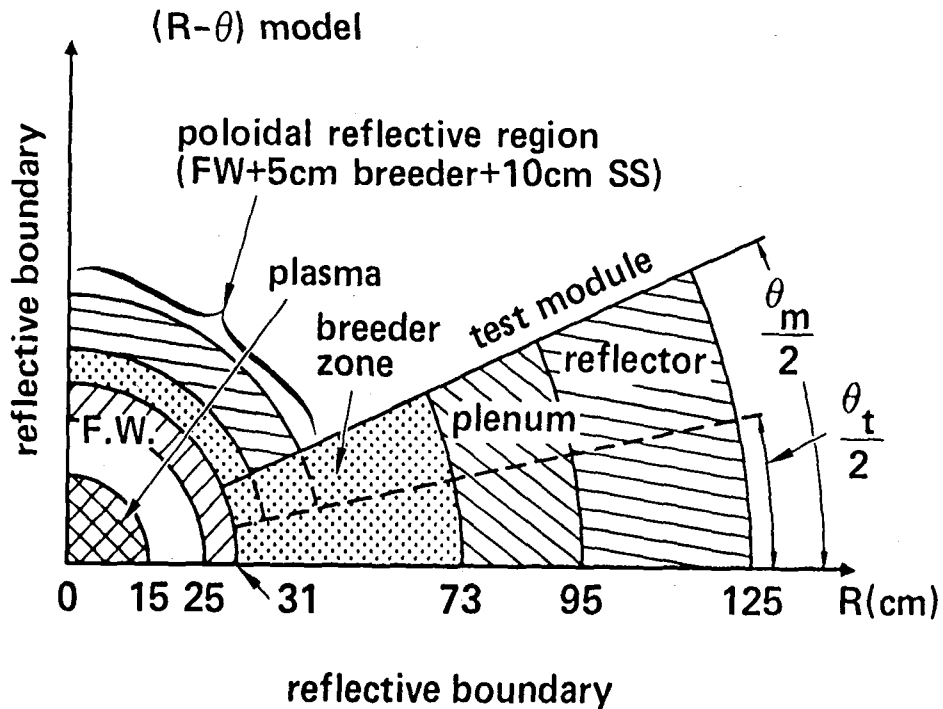


Figure 4.4.6-3. The R-θ geometrical model used to examine the effect of poloidal width on tritium production profiles.

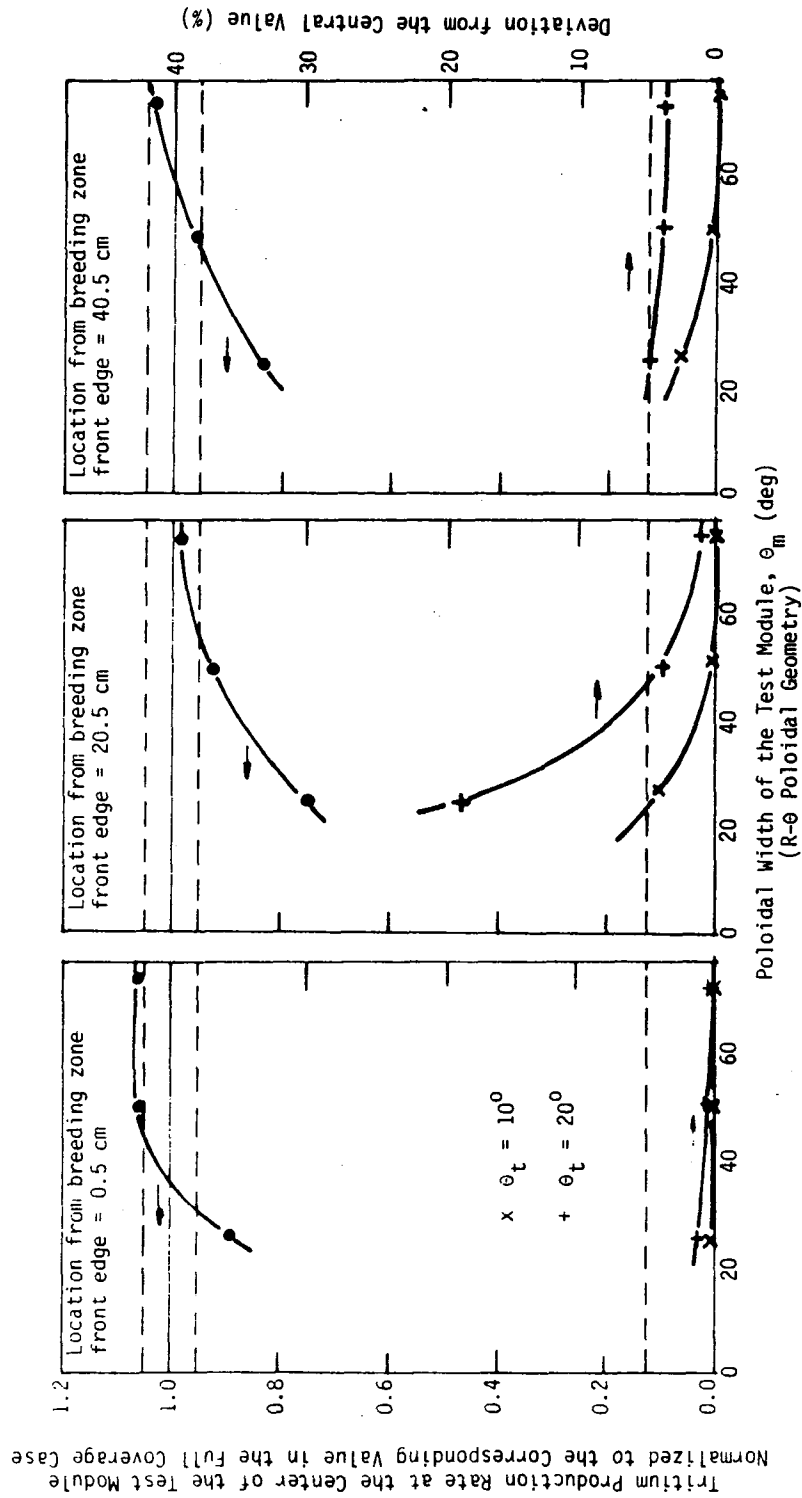


Figure 4.4.6-4. The total tritium production rate as a function of the test module poloidal width (θ_m). Also shown is the deviation from centerline values at two poloidal locations within the test module ($\theta_t = 100$ and 200).

The calculations indicate the minimum test module width that is required to match the tritium production rate at a given location inside the test module to within a desired percentage of the corresponding value in the full coverage case. For example, for a 5% agreement in the local tritium production rate at the test module centerline, the width of the test module should be either $\theta_m = 22^\circ$ (-5% deviation) or $\theta_m = 48^\circ$ (+5% deviation) for agreement at the module front, and similarly $\theta_m = 48^\circ$ or 71° for agreement at the module back.

Figure 4.4.6-5 shows the volume integrated values of tritium production rate in various segments of the test module (characterized by the thickness t_B) and the overall tritium breeding rate as function of the test module width. The values shown in this figure are normalized to the corresponding values in the equivalent volume in the full coverage case. In all the cases shown, the total tritium breeding ratio in the test module is significantly smaller than the corresponding value in the full coverage case. Note that similar effects of partial coverage in the axial direction are not included.

These results indicate the difficulty in providing a very accurate simulation of full reactor conditions without a full-coverage reactor blanket. Furthermore, the achievable tritium breeding rates in the partial coverage case are sufficiently smaller than the full-coverage case that the adequacy of tritium breeding would probably not be demonstrated. Thus, neutronics measurements by themselves do not provide strong justification for a fusion test facility, although such measurements are useful if such a test facility is available for other reasons. For example, the required tritium breeding is also an important uncertainty, and a fusion test facility would provide a good test of the flow of tritium in a closed fuel cycle that includes a tritium-producing blanket test module, plasma exhaust processing system, breeder processing system, first wall and blanket coolant processing systems, and the other systems in an integrated device.

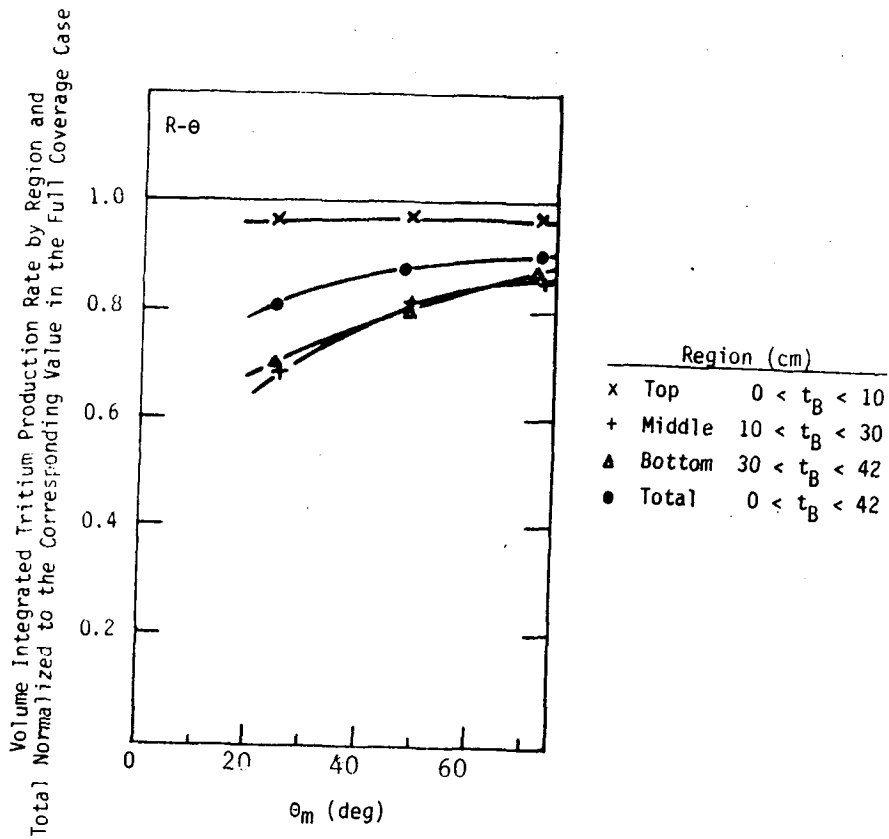


Figure 4.4.6-5. Total tritium production rate integrated over various spatial segments, and the overall tritium breeding rate as a function of the test module width (θ_m).

References for Section 4.4.6

1. M. Abdou, et al., "FINESSE: A Study of the Issues, Experiments and Facilities for Fusion Nuclear Technology Development (Interim Report)," University of California, Los Angeles, PPG-821, also UCLA ENG-84-30 (October 1984).
2. M. Abdou, et al., "DT Fuel Self-Sufficiency in Fusion Reactors," to be published in Fusion Technology.
3. D.L. Smith, et al., "Blanket Comparison and Selection Study, Final Report," Argonne National Laboratory, ANL/FPP-84-1, (October 1984).
4. M.Z. Youssef and M. Abdou, "Uncertainty in Prediction of Tritium Breeding in Various Blanket Designs due to Current Uncertainty in Nuclear Data Base," to be published in Fusion Technology.
5. E.T. Cheng, "Nuclear Data Needs for Fusion Energy Development," Fusion Technology, vol. 8, no. 1, part 2B, 1423 (July 1985).
6. T. Nakamura, "Integral Blanket Neutronics Experiments at FNS," 6th Topical Meeting on the Technology of Fusion Energy, San Francisco (1985).
7. Y. Oyama, M. Youssef and M. Abdou, "Operating and Geometrical Arrangement Requirements for Fusion Neutronics Testing," Fusion Technology, vol. 8, no. 1, part 2B, 1484, (July 1985). Also see Reference 1.

4.5 Partially Integrated and Integrated Experiments

Previous experiments focused on resolving the uncertainties in basic material behavior, phenomena and interactions. Resolving the issues requires fairly specific attention to particular phenomena or effects. Consequently, these tests had limited experimental parameters or environmental conditions, and very few variable parameters, in order to limit the number of potentially complicating factors. Instrumentation could be fairly precise and localized because the experiments were generally small.

However, there are several uncertainties that cannot be addressed in separate or multiple-effect experiments such as uncertainties associated with geometric effects or with full environmental conditions. Also, it is not always necessary to understand everything at a quantitative phenomenological level. It may be sufficient to provide semi-empirical correlations between the input and output parameters. In all these cases, the appropriate tests are more integrated than the separate and multiple-effect tests. The emphasis in integrated tests is on overall behavior and identifying unanticipated problems. Instrumentation is more limited and measurements are primarily of global or integral parameters.

At the most integrated end of their spectrum, these tests are full-scale, full-power tests of the component in an operating system. For blankets, the ideal test facility would be a fusion device, which integrates all environmental conditions, phenomena, geometrical complexities and system interactions into a single test. However, there are degrees of integration, and partially integrated tests can be considered which combine many but not all environmental conditions and geometry.

In this section, three types of partially integrated or integrated tests are considered: non-nuclear, fission reactor and fusion device tests.

4.5.1 Non-nuclear Thermomechanical Integrity Tests

Nuclear testing is critical for exploring the effects of radiation on tritium recovery and breeder/structure mechanical behavior over the lifetime of the module. However it is not necessary for addressing all issues, can be very expensive, and may not be possible with plausible irradiation facilities. For example, it is not possible to fit present full-sized breeder

blanket modules into existing fission reactors and get full (fusion reactor) power heating. Consequently, it is not possible to test important issues related to flow (distribution, instabilities, pressure drop, hot spot locations and hot spot factors), intrablanket interactions (breeder with first wall, between breeder elements) and module failure modes. Furthermore, nuclear facility safety constraints may limit the number or type of severe transient tests. For many of these issues, the key factor is a full-size (all geometric effects), full-power (all thermal effects) blanket.

In principle, many of these issues can be tested in a non-neutron test facility if a suitable heat source can be identified. This facility would:

- 1) provide a thermomechanical test of a solid breeder blanket module including normal operation, determination of design margins, and severe transient behavior; and
- 2) provide a discriminating test for design codes to be used to predict solid breeder blanket behavior under reactor heating conditions.

The characteristics and limitations of this facility are summarized in Table 4.5.1-1, and possible issues addressed are listed in Table 4.5.1-2.

Most of the uncertainties are driven by the geometry, flow conditions (pressure and flow rate) and temperature profile. The first two are easily reproduced, but the ability to simulate the important thermal effects depends to a large degree on the non-nuclear heat source used. Possible options include:⁽¹⁾ 1) Direct resistive heating, where a current is passed directly through the module; 2) Discrete-source resistive heating, where currents are passed through a distribution of resistive wires inside the module; 3) RF or microwave heating; 4) inductive heating, with a varying magnetic field; and 4) purge heating, using a hot purge flow at representative reactor breeder conditions. The advantages and disadvantages of these methods are summarized in Table 4.5.1-3.

The limitations of all the methods make it difficult for any method to duplicate the volumetric heating in a complete, full-sized blanket. For a microwave heat source, for example, the module structure and breeder cladding in some geometries would absorb the incident energy instead of the breeder. Consequently it is not possible to reproduce all geometrical, flow and thermal effects in a non-nuclear test. There are generally two possible approaches -

Table 4.5.1-1. Characteristics and Limitations of a Thermomechanical Integrity Test Facility

Characteristics

No neutrons (no radiation to complicate handling)
Full-size blanket module
Full power blanket test
Overpower testing possible
Severe transient tests possible

Limits

No in-situ radiation effects
No tritium inventory and recovery data
Temperature profiles not exactly simulated
Non-nuclear heating methods may alter blanket response

Table 4.5.1-2. Issues Addressed by a Non-nuclear Thermomechanical Integrity Test Facility

Fabrication and manufacturing of full module

Coolant behavior at full power

- blanket pressure drop
- flow distribution
- flow oscillations
- local heat transfer coefficients, hot spot factors

Structural behavior under complex high-power density conditions

- structural pressure and thermal stresses
- breeder/clad thermal expansion interaction
- steady magnetic field forces
- breeder fracturing and relocation
- thermal creep, sintering and grain growth

Thermomechanical response to off-normal conditions

- cycling effects
- operation above rated power level (design margins)
- response to LOCA, LOFA or other coolant transients
- response to power transients (surface and/or volumetric)
- response to electromagnetic transients
- response to structural failure
- operation at fractional power

Purge and hydrogen behavior under high power density conditions

- purge flow distribution and pressure drop
 - hydrogen permeation into coolant
 - effect of purge flow and hydrogen addition on mass transfer
-

Table 4.5.1-3. Advantages and Disadvantages of Non-nuclear Heat Sources

Heat Source	Advantages/Disadvantages
Direct resistive	100% efficient conversion of input to heating power Heating spread over large volume, not localized Current path, and so heating profile, is uncertain in complex blanket geometry Blanket design might have to be altered in order to provide control over current paths (e.g., insulating breaks)
Discrete-source	100% efficient conversion of input to heating power Heating localized at resistive wire locations Wire/breeder compatibility at high temperature More complex test fabrication and operation Possible altered mechanical response due to internal wires.
Microwave	Less efficient conversion of input to heating power Completely external heat source True bulk heating, penetration scale length may be similar to neutron mean free path Full module structure may reflect too much RF power, or otherwise alter heating.
Induction	Efficiency of conversion of input to heating power? Preferential heating of conducting elements, may require blanket modification to provide breeder heating Heating profile uncertain in complex blanket geometry
Purge heating	Simple, completely external heat source Very limited temperature simulation of blanket

obtain a good simulation of temperatures over a limited geometry; or a rough simulation of breeder temperature and a good simulation of structural temperature over the full geometry.

As an example of the first approach, an experiment has been designed^(2,3) to heat a $10 \times 10 \times 17 \text{ cm}^3$ block of $\gamma\text{-LiAlO}_2$ with internal coolant channels using a 10 kW klystron at 200 MHz. This models a section of a solid breeder blanket at 2 MW/m^2 equivalent nuclear heating. The microwave power profile is predicted to approximate the nuclear heating profile closely over the first 15 cm as shown in Fig. 4.5.1-1, although there are still uncertainties in the breeder dielectric properties. The result is a good simulation of breeder temperature profile over a subsection of the breeder region. Other examples of this approach are illustrated in Ref. (7). These tests provide information that could reasonably be obtained (with irradiation effects) in small-scale nuclear tests as described in Section 4.5.2, but are less expensive.

In the alternate approach, it is argued that an approximate simulation of the complex blanket temperature profile can still provide substantial and unique information at relatively low cost. In order to explore the usefulness of such a test, a representative facility design is considered.

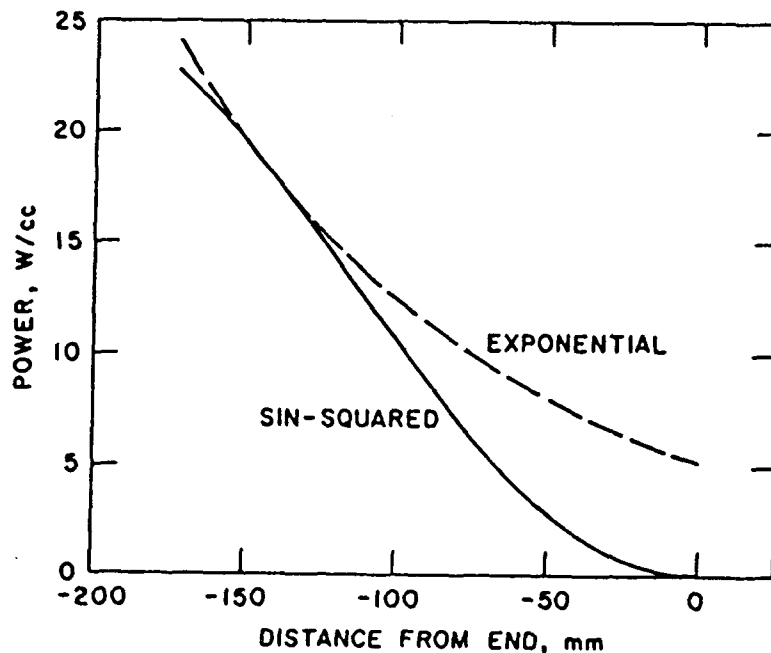


Figure 4.5.1-1. Microwave heating profile in a $\gamma\text{-LiAlO}_2$ block compared with 2 MW/m^2 equivalent neutron wall load heating.

Facility Description

There are a several possible non-nuclear test facilities depending on the heating sources (surface and volumetric) and the extent to which other environmental conditions such as magnetic fields and vacuum are included. In this description, the purpose of the facility is taken as providing a full-blanket thermomechanical test capability.

The test facility is basically a large tank, able to accommodate up to a full solid breeder blanket module, with mechanisms to provide surface and bulk heating. The tank can be evacuated to provide the differential pressure across the first wall and to minimize any oxidation or other chemical reactions between the first wall material and the chamber atmosphere at operating temperatures. It is not expected that a very high vacuum is required - about 1000 Pa would be sufficient from the module structural point of view. The chamber (and vacuum system) should be robust enough to handle module rupture and coolant leakage. More restrictive requirements on the vacuum may be provided by the heat sources. For example, 10^{-5} Pa would be necessary for electron beam surface heating as in the ASURF facility.⁽⁸⁾

The primary design difficulty is to adequately simulate bulk heating. For this example, discrete-source resistive heating is assumed. As noted in Ref. (7), this is the most suitable method, in the absence of nuclear heating, for obtaining a reasonable simulation of the thermal-hydraulic and thermal-mechanical behavior. An alternate approach that is mechanically simpler but cruder is purge heating (see Table 4.5.1-3).

A very accurate simulation of the reactor heating profile would require many wires with different currents distributed throughout the module, and consequently a large fabrication and control cost. Minimizing the number of resistive wires leads to very localized heating rates and temperatures, and possibly wire/breeder compatibility problems. A number of cases were analyzed to determine an acceptable solution that limited the number of wires consistent with providing a reasonable temperature simulation and an 800°C materials compatibility constraint on the wire operating temperature. Both the BCSS⁽⁴⁾ Li₂O/He design with plate breeder and the LiAlO₂/H₂O/Be concept with breeder-outside-tube (BOT) were considered.

Table 4.5.1-4 summarizes the cases examined with the 2-D thermal conduction code TACO-2D for the plate breeder concept. In the first cases, the resistive wires were placed along the center of the breeder. Although good coolant, clad and breeder surface temperature simulation is obtained, the maximum breeder temperature is around 1200°C unless very closely spaced wires were used. Even if 1 cm plate elements are used to minimize temperature gradients between the wires, the temperature drop to the coolant still leads to unacceptably high breeder temperatures. This would also be expected to stiffen the plates and possibly affect their mechanical response. In subsequent cases, the heating wires were split into a pair of wires offset from the center. Decreasing the wire-to-coolant distance decreased the temperature rise, and flattened the temperature distribution in the breeder interior (there is a small drop due to axial conduction).

Table 4.5.1-4. Temperature Simulation of Li₂O/He/FS Plate Breeder

Case	Wire Location	Wire Size (mm x mm)	Wire Pitch (mm)	T _{clad} (°C)	T _{ctr} (°C)	T _{max} (°C)	\dot{q}_0 (MW/m ³)
Reactor		NA	NA	415	717	717	45
1	center	2 x 2	10	446	1393	1393	50
2	center	1 x 2	6	422	1113	1113	50
3	center	10 x 1	11	443	1125	1125	45
4	offset	10 x 1	11	446	863	869	45
5	offset	1 x 1	10	438	846	960	50
6	offset	1 x 1	10	426	792	900	45
7	offset	2 x 2	10	377	566	602	45
8	offset	1 x 1	7	418	750	822	45
9	offset	1 x 1	7	420	586	622	22.5*

*Half power.

T_{clad} is the cladding temperature at the front of the breeder plate.

T_{ctr} is the breeder centerline temperature at the front of the breeder plate.

T_{max} is the breeder maximum temperature.

\dot{q}_0 is the peak nuclear heating rate assumed in determining equivalent resistive wire heating rates. [$\dot{q} = \dot{q}_0 \exp(-z/\lambda)$ where $\lambda = 0.13$ m]

In the final case analyzed, 1 mm OD resistive wires spaced every 7 mm provide reasonable reactor-like peak temperatures at full power. The peak power required per wire is 1.6 kW/m. For comparison, commercial heaters are available with 1-6 mm OD (mostly with MgO electrical insulating sheaths) and 2 kW/m.⁽⁵⁾ In order to limit the number of wires in this calculation, they are only placed in the front 20 cm of the blanket (containing 50% of the input power), leading to 30 resistive wire pairs per breeder plate. The corresponding coolant, cladding and breeder temperatures profiles are shown in Fig. 4.5.1-2, along with reactor values. An additional design possibility to reduce heating costs (particularly for long duration corrosion or mass transfer experiments) is to keep the same wire distribution, but decrease heating by a factor of two and increase the coolant inlet temperature about 50°C to compensate. This alters the temperature and heat flux simulation as also shown in Fig. 4.5.1-2.

For the BOT (breeder-outside-tube) geometry, a section of the breeder near the first wall was considered. The reference BCSS reactor temperature profiles are shown in Fig. 4.5.1-3 at the coolant outlet plane (a mixed Be/LiAlO₂ breeder is assumed with 2.5 W/m-K thermal conductivity). This geometry has a more complex temperature profile that is harder to simulate with discrete sources. The arrangement shown in Fig. 4.5.1-3 maintains structural temperatures, general breeder temperatures, and keeps peak temperatures below 800°C. Temperature gradients in the breeder are larger than in the reactor case, but are in the same direction so similar crack and mass transfer directions might be expected. These temperatures were obtained with an effective input power of 25% reactor power. Localizing the heat sources maintains the breeder temperature rise and control of coolant inlet conditions allows a reasonable structural temperature match.

First wall surface heating must also be provided. Methods include: 1) direct resistive heating, with current flowing through the structure itself; 2) radiative heating; 3) neutral or charged particle beam heating; and 4) plasma heating. Facilities capable of providing 1 MW/m² heat flux over 0.5-1 m² areas exist based on neutral beam, plasma and charged particle beam sources [e.g., NBTF, RFTF and ASURF⁽⁸⁾]. However, a simpler source might be preferred in order to allow severe transient tests where first wall rupture is possible or even expected. This suggests radiant heaters, such as the tungsten

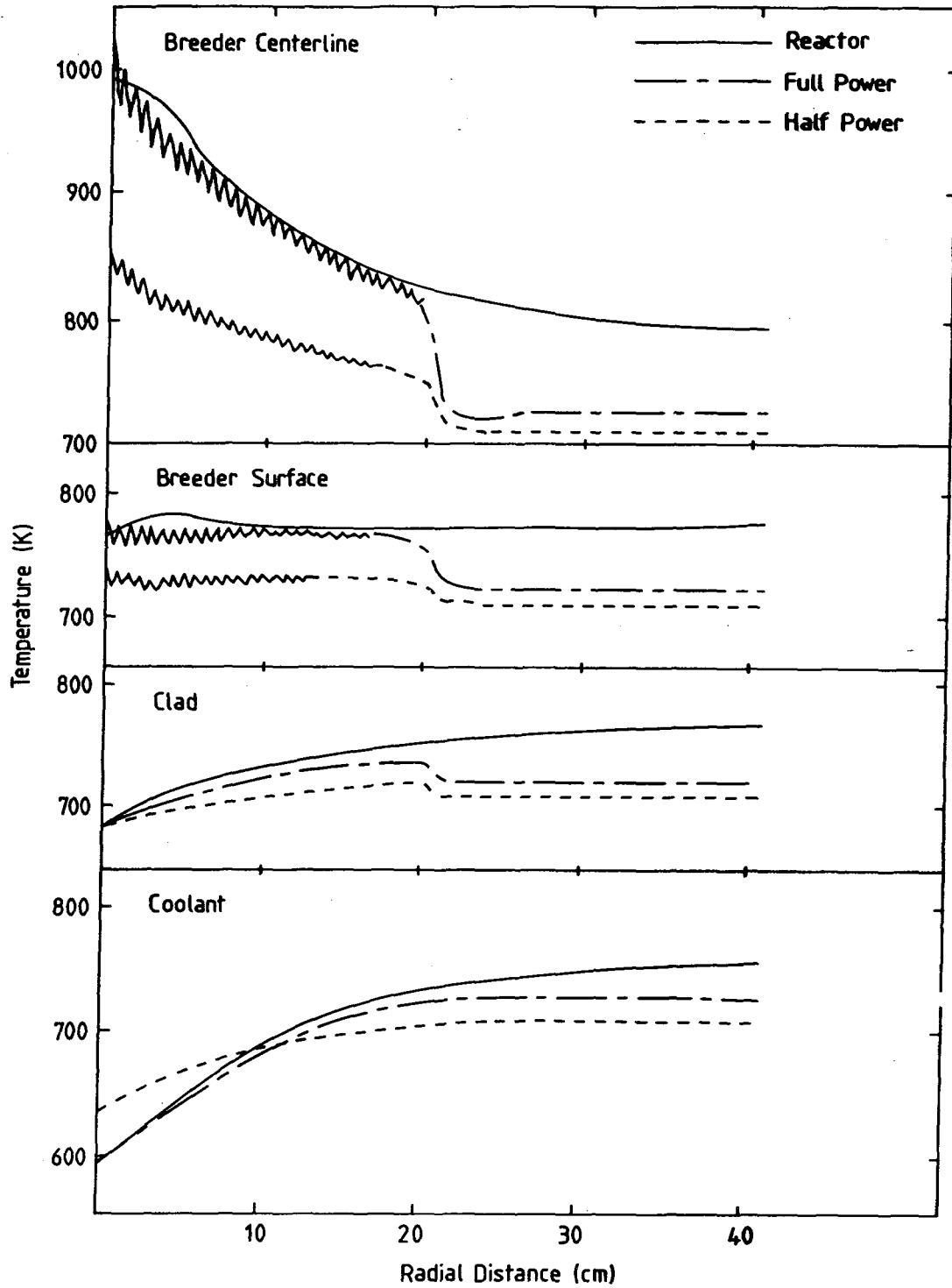
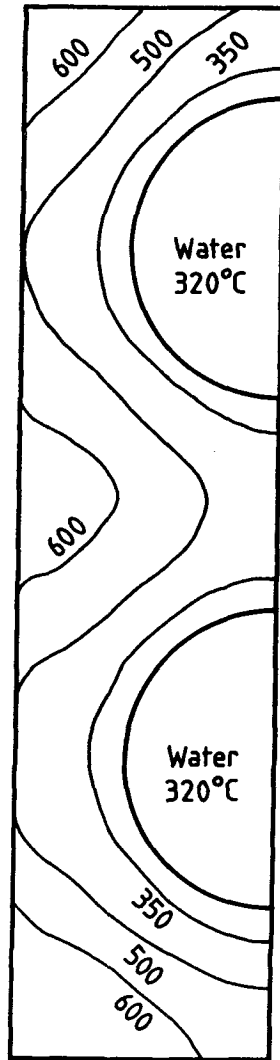
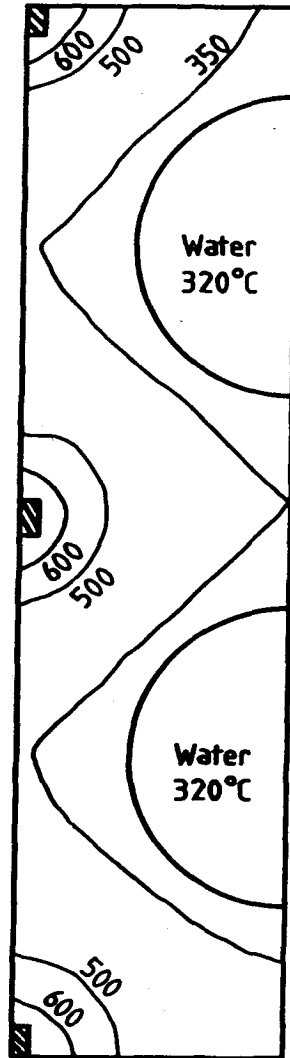


Figure 4.5.1-2. Temperature profiles for Li₂O plate breeder, under fusion reactor and discrete-wire heating conditions.



Nuclear Heating
(5 MW/m^2)



Resistive Wire Heating
(1.25 MW/m^2 equivalent)

Figure 4.5.1-3. Temperature profiles for section LiAlO_2/Be BOT geometry near the first wall, under fusion reactor and discrete-wire heating.

filaments (proposed for MFTF- α +T⁽⁶⁾ in order to provide tokamak-like surface heat fluxes) or radiant arcs [as in the Boeing High Heat Flux Facility⁽⁹⁾].

Figure 4.5.1-4 and Table 4.5.1-5 summarize the test facility as presently described. Table 4.5.1-6 suggests a possible sequence of experiments.

References for Section 4.5.1

1. G.A. Deis, et al., "Evaluation of Alternate Methods of Simulating Asymmetric Bulk Heating in Fusion Reactor Blanket/Shield Components," EGG-FT-5603, Idaho National Engineering Laboratory (1981).
2. B. Misra, R.E. Nygren, R.B. Peoppel and R.L. Kustom, "Thermal-hydraulic/Thermomechanical Testing of Solid Breeder Blanket Modules Using Microwave Energy," Proc. 6th Top. Mtg. Tech. of Fusion Energy, San Francisco, March 3-7, 1985.
3. R.L. Kustom, P. Fendley and J. Tidona, "Design of the Waveguide for Microwave Heating of Solid Lithium Ceramic Blankets," ANL/FPP/TM-198, Argonne National Laboratory (January 1985); also Proc. 6th Top. Mtg. Tech. of Fusion Energy, San Francisco, March 3-7, 1985.
4. D.L. Smith, et al., "Blanket Comparison and Selection Study, Final Report," ANL/FPP-84-1, Argonne National Laboratory (1984).
5. ARI Bulletin 5.2, "Flexible High Watt Density Electric Heaters" (October 1981).
6. M.A. Abdou, et al., "FINESSE - A Study of the Issues, Experiments and Facilities for Fusion Nuclear Technology Research & Development, Interim Report," PPG-821, also UCLA-ENG-84-30, University of California, Los Angeles (October 1984).
7. G.A. Deis, et al., "Final Report on PE-II Activities from August 1981 through September 1983," EGG-FT-6392, Idaho National Engineering Laboratory (October 1983).
8. H.D. Michael, et al., "Large Area Surface Heating Facility (ASURF) and Test Program for First Wall Design Concepts," Nucl. Tech./Fusion, 4 785 (1983).
9. A.G. Ware and G.R. Longhurst, "Test Program Element II, Blanket and Shield Thermal-hydraulic and Thermomechanical Testing, Experimental Facility Survey," EGG-FT-5626, Idaho National Engineering Laboratory (December 1981).

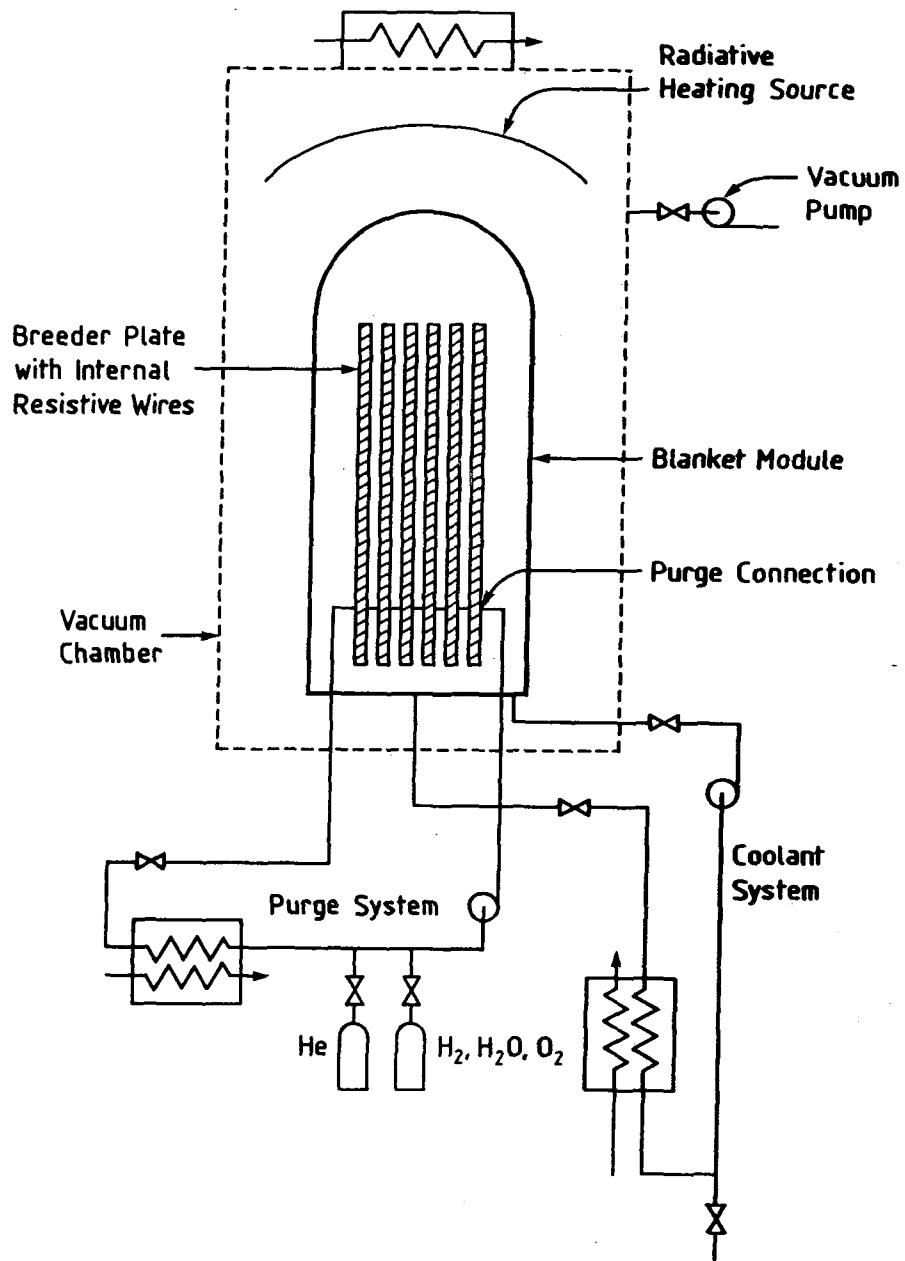


Figure 4.5.1-4. Block diagram of non-nuclear Thermomechanical Integrity Test Facility.

Table 4.5.1-5. Characteristics of a Discrete-Source Full-Blanket TMIF

Facility Parameter	Li ₂ O/He Blanket	LiAlO ₂ /H ₂ O/Be Blanket
Vacuum tank dimensions: (D x W x L m ³)	2 x 1 x 3	
Minimum vacuum pressure: (Pa)	100	
Full blanket module dimensions: (D x W x L m ³)	0.8 x 0.3 x 2	0.7 x 0.3 x 2
Surface heating	Radiant arcs or tungsten filaments	
Surface heating power:		
Flux (MW/m ²)	1	1
Total nominal/peak (MW)	0.6/0.8	0.6/0.8
Internal heating power:		
Total nominal/peak (MW)	3.5/5	3.5/5
Resistive heating elements: Nichrome wire, 1 mm OD	60 wires/plate, 21 plates/module	500 wires
Primary coolant:	He @ 5 MPa	H ₂ O @ 15 MPa
Flow rate (m ³ /s)	1 m ³ /s	--
Pumping power at 70% eff. (kW)	130	--
Helium purge:	He @ 0.1 MPa	He @ 0.6 MPa
Flow rate (m ³ /s)	0.01	0.01
Pumping power at 70% eff. (kW)	15	90
Instrumentation:	Pressure, wall temperature, leak detection	
Vacuum chamber	Thermocouples on structure, clad and	
Blanket	breeder, strain gauges	
Coolant and purge	Thermocouples, pressure gauges, flowmeter, possibly velocity or pressure probes to monitor flow distribution, gas analyzer for external mass transfer, tritium or deuterium permeation measurement	
Control:	Flow rate, purge gas composition, tritium or deuterium feed to purge for permeation measurement	
Coolant and purge	Current, voltage, power to heaters	
Power supplies		

Table 4.5.1-6. Possible TMIF Test Program per Blanket Concept

Test	Description	Test Duration		
		Nbr	Power (hrs)	Total (days)
Low power startup	System operational status check, Check module for leaks, Verify thermal-hydraulic models.	1	3	1
Full power	Blanket temperature profile, Blanket mechanical deformations, Flow distribution and vibrations, Coolant and purge pressure drop.	1	5	3
Normal transients	Startup/shutdown ramp rate effects, Overpower transients.	5	2	3
Fatigue life (slow/rapid)	Mechanical lifetime under cycling,	100	1	6
	Breeder redistribution.	1000	0.1	6
Corrosion and permeation	Coolant channel erosion, Vibrational wear, Breeder internal mass transfer and weight loss, D or T purge-to-coolant permeation.	1	1000	50
Design margin	CHF or heat transfer limits, Melting, severe deformation, loss of mechanical integrity.	1	10	3
Safety	Loss-of-flow behavior,	1	1	5
	Loss-of-coolant behavior,	1	1	5
	Rupture of vacuum/coolant boundary,	1	1	5
	Rupture of purge/coolant boundary.	1	1	5

4.5.2 Nuclear Submodule

The objective of the Nuclear Submodule Test is to obtain integral blanket performance data at conditions simulating middle and end-of-life. Issues to be addressed are: (1) integrated tritium retention, release, and recovery; (2) solid breeder thermal performance; (3) integrated breeder/structure interaction; and (4) overall structural response of the blanket submodule. The purpose of the nuclear submodule test assembly experiment is to provide a proof test of a given design concept and as such represents the most complex experiment which may be performed before full blanket testing is initiated within a fusion device. This experiment is design specific and mimics as closely as possible the anticipated environment, material selection and blanket geometry. At present, fission reactors represent the most viable neutron irradiation source for this type of environment due to their relatively large irradiation test volume and capability of attaining relevant neutron exposures.

Two types of design concepts for nuclear testing can be envisioned. One concept would use a full-scale blanket component located at the periphery of the fission reactor core. The other would use a subsection of the full blanket module and would be tested within the core region.

Designs for a full-scale experiment have been proposed and are documented in Ref. (1) and in the FINESSE Interim Report.⁽²⁾ Two solid breeder slab module test concepts, $\text{Li}_2\text{O}/\text{He}/\text{HT9}$ and $\text{LiAlO}_2/\text{Be}/\text{H}_2\text{O}/\text{PCA}$, were investigated. It was assumed that these coreside tests would require double-walled containment. Thus, for the neutron physics calculations, 2 cm of 316 SS was modeled between the core and the test module. The models used for the test modules themselves correspond exactly to those used for reference design calculations. Cases were run with and without a 0.15 cm thick Cd filter for each concept. The power density and tritium production profile calculated for the $\text{Li}_2\text{O}/\text{He}/\text{HT9}$ concept compared to reference calculations for a $1 \text{ MW}/\text{m}^2$ fusion neutron source are shown in Figure 4.5.2-1; the general similarity between the profiles is clear. However, the effect of the lower-energy fission spectrum is also obvious in the initial peaks in both power density and tritium production, as well as in the slightly steeper slope farther into the blanket. These effects are slightly less prominent in the power density

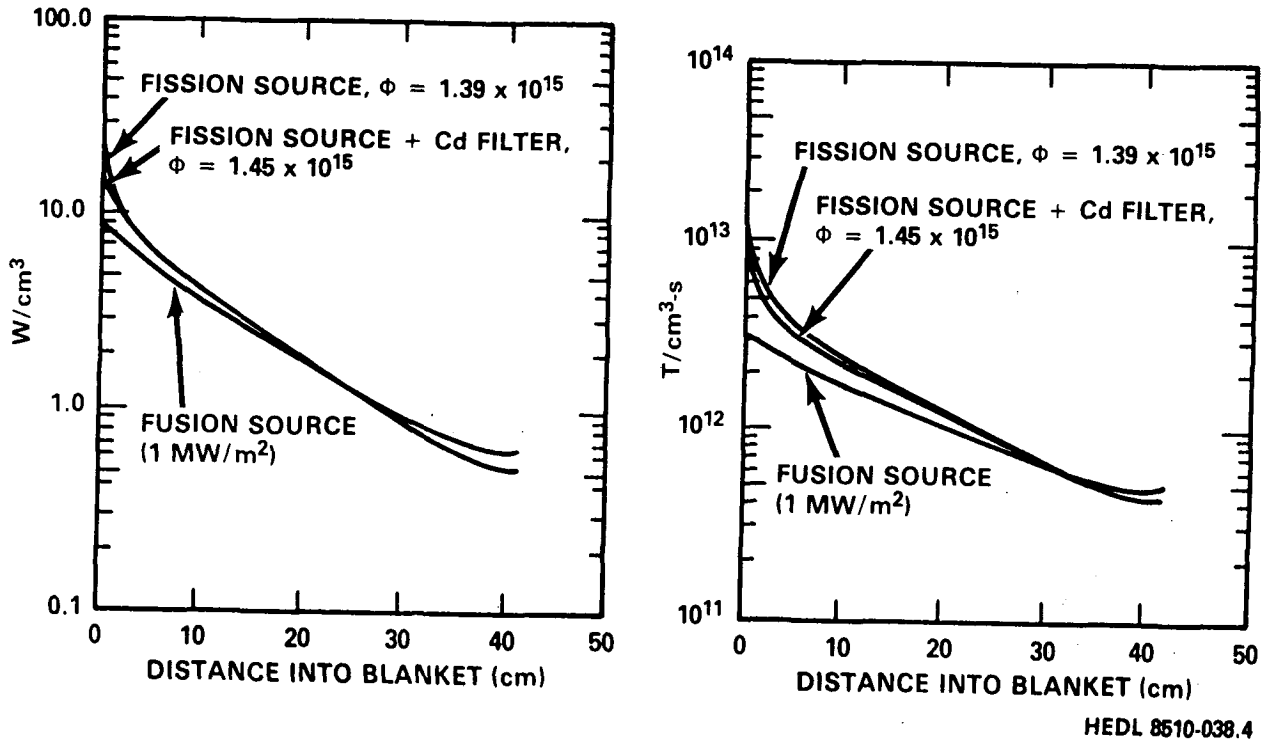


Figure 4.5.2-1. Power density (left) and tritium production (right) profiles in fission slab module test for $\text{Li}_2\text{O}/\text{He}/\text{HT9}$ blanket.

profile due to heating from fission gammas, which decays more slowly with distance into the blanket. The effect of the cadmium filter is more noticeable in the tritium breeding profiles for the same reason. In order to provide a better simulation (if this is felt necessary), a $1/v$ absorber such as boron, ^6Li , or ^3He will probably be required, in order to remove neutrons with energies above the cadmium cutoff energy. The results of calculations for the $\text{LiAlO}_2/\text{Be}/\text{H}_2\text{O}/\text{PCA}$ slab module test suggest that the power density and tritium breeding profiles in the fission test will simulate those in actual fusion operation quite closely. Table 4.5.2-1, which shows the peak flux in the core for each of the test calculations performed, normalized to $1 \text{ MW}/\text{m}^2$ equivalent power density. These values are near the limits of fission reactor heat transfer technology. It is extremely important to observe, however, that both the peak fluxes in Table 4.5.2-1 and the flux depression values depend upon the fission core configuration. In the case of the submodule calculations,

Table 4.5.2-1. Peak Flux in Core Required to Simulate Power Density at Front of Blanket at 1 MW/m²

Test Type	Blanket Concept	Filter	Peak Flux in Core ^a (n/cm ² -s)
Slab ^b	Li ₂ O/He/HT9	--	2.9 x 10 ¹⁵
Slab	LiAlO ₂ /Be/H ₂ O/PCA	-- Cd	1.4 x 10 ¹⁵ 2.2 x 10 ¹⁵
Submodule ^c	Li ₂ O/He/HT9	--	5.6 x 10 ¹⁴
Submodule	LiAlO ₂ /Be/H ₂ O/PCA	--	3.0 x 10 ¹⁴

^aWater-moderated, plate-fueled fission reactor assumed.

^bCore-side

^cIn-core

the core was assumed to be of uniform composition; the core configuration for the slab tests was nearly uniform. Actually, it is likely that elements with higher fuel loadings would be used near the test modules to help flatten the flux profile in the core edge. This would reduce the flux depression effect and thereby the peak flux required. Therefore, the information in Table 4.5.2-1 probably represents upper-limit values; both peak flux and flux depression in real tests will be less than indicated. Finally, the impact of slab tests on fission reactor reactivity must be considered. Sample 1-D calculations suggest the impact on reactivity scales as the core size with the reactivity varying from -15\$ reactivity for cores with ~ 23 cm thickness to -5\$ reactivity for cores with ~ 53 cm thickness.⁽²⁾ These calculations indicate that relatively large reactors are required to perform these slab tests.

Overall, it appears that a limited number of reactors exist or could be restarted to perform these slab tests.⁽²⁾ These tests can simulate full module response but are limited to equivalent fusion power levels of less than 1 MW/m². The disadvantages of such a test are that the corresponding neutron fluence would be relatively low and the modification to existing fission reactor facilities would be very costly if at all possible.

The other type of design concept for nuclear submodule testing would use a scaled subsection of the full blanket module and would be tested within the core region. Earlier designs for such an experiment have been proposed and documented in Refs. (2) and (3). The advantage of such a test is that the irradiation can proceed to reasonably high neutron fluences in existing fission reactors. The disadvantages with such experiments is the required scaling to fit into the existing irradiation volume. Since many of the low neutron exposure issues associated with beginning-of-life operations may be amenable to non-neutron testing and the high neutron exposure issues require neutron testing to significant fluence, in-core testing to investigate both middle-of-life and life-limiting phenomena is emphasized here.

Since this class of experiments represents a proof test for a specific design concept, the experiment must attempt to match the anticipated environment as closely as possible. The materials and geometry of the experiment are dictated by the design. Irradiation volume limitations, however, dictate appropriate scaling of the test module. The important environmental parameters include temperature, neutron fluence and their associated gradients. The gradients in the in-core test are set up by the axial variation of neutron flux within and out of the core region. The operating temperature is controlled by a balance between the heat generated within the module due to nuclear and gamma heating and the cooling system.

These desirable test parameters plus the need for adequate monitoring of the modules performance during irradiation define the irradiation facility requirements. These requirements can be categorized into the areas of instrumentation/experiment control, test volume, and neutronics. The experiment will require extensive instrumentation and experimental parameter control. The environmental parameter control for such an experiment includes coolant flow and monitoring and a purge stream flow and monitoring. Additional instrumentation could include temperature monitoring of specified regions within the module itself. These requirements must be amenable to the irradiation facility design and operation. For example, the testing of water cooled blanket concepts in liquid metal fission reactors is not possible for obvious safety reasons if water must be used as the coolant. The test volume must be adequate to obtain desirable gradients within the module and permit sufficient complexity in the geometry so as to permit a credible experiment. Finally and

most importantly, the neutron flux and spectrum must be adequate to provide both a reasonable damage rate in the structural material, and reasonable lithium burnup and heat generation rates in the solid breeder material. The optimum fission spectrum depends upon the blanket module concept being considered. For example, for the $\text{Li}_2\text{O}/\text{He}/\text{FS}$ concept, fast fission reactors appear to offer favorable neutronics. On the other hand, the mixed spectrum fission reactors such as HFIR appear to offer favorable neutronics for blanket concepts such as the $\text{LiAlO}_2/\text{Be}/\text{H}_2\text{O}/\text{FS}$ concept. Another consideration with respect to neutronics for in-core testing of submodule test assemblies is the impact of the negative reactivity associated with lithium upon the irradiation facility. This will tend to limit the size of the module, and the allowable lithium-6 enrichment will tend to shift the optimum position for the experiment to the core periphery.

The effective design and interpretation of this experiment will require extensive prior experimentation and modeling. Specifically the results of this module's performance in a non-nuclear thermomechanical integrity facility (see Section 4.5.1) would be highly recommended. Also results from the advanced tritium recovery experiments would be highly desirable for the specific material combinations to be tested. Other experiments such as those outlined in Section 4.4 would be desirable so that one could have reasonable confidence in the scaling which will be required for the in-core test.

As an example of this type of experiment, a conceptual experiment to investigate the BCSS $\text{Li}_2\text{O}/\text{He}/\text{FS}$ design is considered. This specific design was chosen since it is most amenable to testing in a fast fission reactor and is neutronically and geometrically simpler when compared to the $\text{LiAlO}_2/\text{H}_2\text{O}/\text{FS}$ concept. The FFTF reactor was chosen for the example irradiation facility because of its instrumentation capabilities, relatively large irradiation volume and its neutronics. The FFTF contains several hexagonal positions capable of providing instrumentation and environmental control to experiments located within or near the core region. The hexagonal core design permits a maximum flat-to-flat dimension of 10 cm for the irradiation vehicle without restructuring of the core region. Finally, the FFTF neutron flux and spectrum are such that reasonable testing of the $\text{Li}_2\text{O}/\text{He}/\text{FS}$ concept could be performed.

To assess the viability of the FFTF neutron spectrum and flux for testing of the $\text{Li}_2\text{O}/\text{He}/\text{FS}$ concept and to determine the optimum position within the

reactor for such a test, a series of microscopic calculations were performed. The macroscopic cross sections used in these calculations were obtained from FFTF core physics and used the ENDF-B 53-group cross sections file. The microscopic calculations assumed a typical FFTF core loading and the calculations at these specific row positions were for specific non-fueled structural assembly positions in the core. Effects such as a localized self-shielding were not explicitly included in the determination of these microscopic cross sections. The following assumptions were made.

The ${}^6\text{Li}$ enrichment was varied in order to match the initial tritium production rate anticipated for this blanket concept within the fusion environment, namely $16 \times 10^{13} \text{ T/cm}^2/\text{s}$. The theoretical density of the Li_2O was assumed to be 85%. Figure 4.5.2-2 shows the axial variation in the tritium production rate for a fixed lithium-6 enrichment of 2.5% and for several core positions. The FFTF core extends from -45 to +45 cm on these figures. The relative maximum in the production rate outside the core are due to the larger ${}^6\text{Li}(n,t)$ reaction cross sections associated with lower energy neutrons. The relative maximum near the core midplane is due to the maximum in the neutron flux. Figure 4.5.2-3 shows the neutron heating rate as a function of axial position also for 2.5% ${}^6\text{Li}$ enrichment. The contribution to the total heating rate from gamma rays within FFTF is estimated to be 10% of the nuclear heating rate. These two figures indicate that while one can match the tritium production rates with relatively modest ${}^6\text{Li}$ enrichments both within and outside the core regions, the core midplane represents a region where one can simultaneously match the anticipated tritium production heating rates.

While it is possible to approximately match both rates initially, Figs. 4.5.2-4 and 4.5.2-5 depict how these rates decrease with time. Also shown in these figures are the anticipated changes in the tritium production and nuclear heating rates for the $\text{Li}_2\text{O}/\text{He}/\text{FS}$ blanket concept near the first wall. After approximately three years (26000 hours) of irradiation in the FFTF, the tritium production rate decreases by approximately 40%. The corresponding decrease in the nuclear heating is approximately 15%. These rates are not anticipated to decrease significantly with time in the actual fusion blanket. The maximum damage rate in the structural material is 30-60 dpa/yr in FFTF which is the same magnitude as anticipated (approximately 50 dpa/yr) near the first wall in the fusion blanket design. However, the ratio

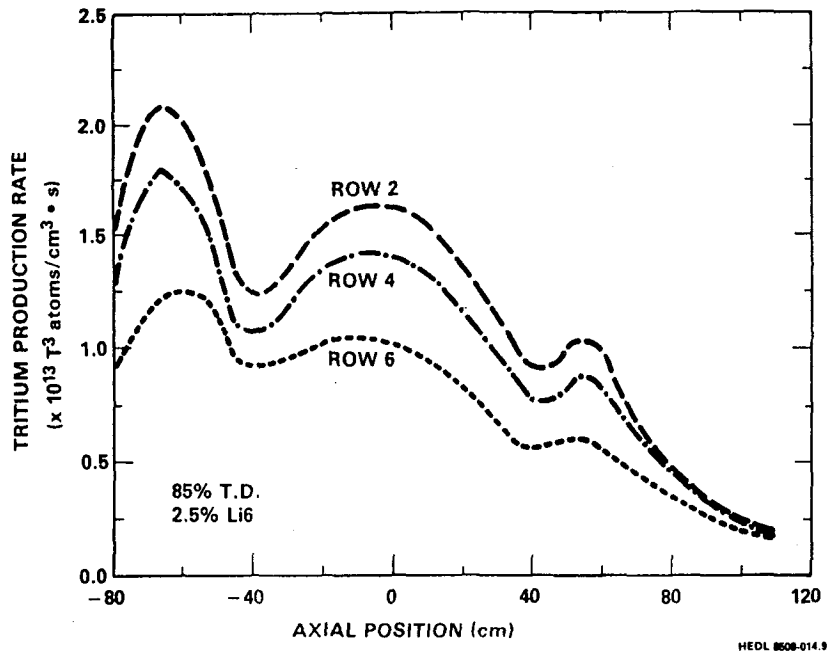


Figure 4.5.2-2. Microscope calculations of the tritium production rates for Li₂O in FFTF as a function of axial position for several core positions. These calculations assure the Li₂O has a density corresponding to 85% of its theoretical density and that the ⁶Li enrichment is 2.5%.

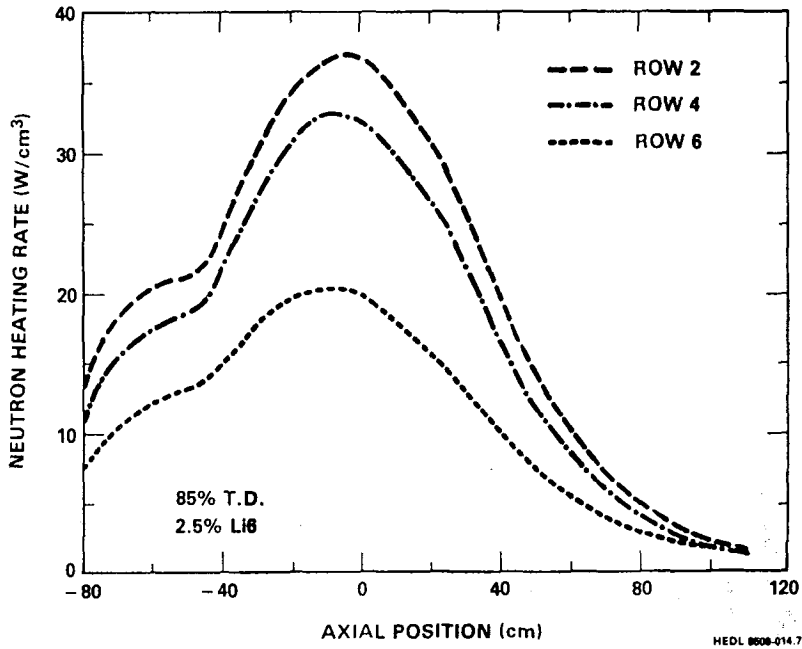


Figure 4.5.2-3. Microscope calculations of the neutron heating rates for Li₂O in FFTF as a function of axial position for several core positions. These calculations assure the Li₂O has a density corresponding to 85% of its theoretical density and that the ⁶Li enrichment is 2.5%.

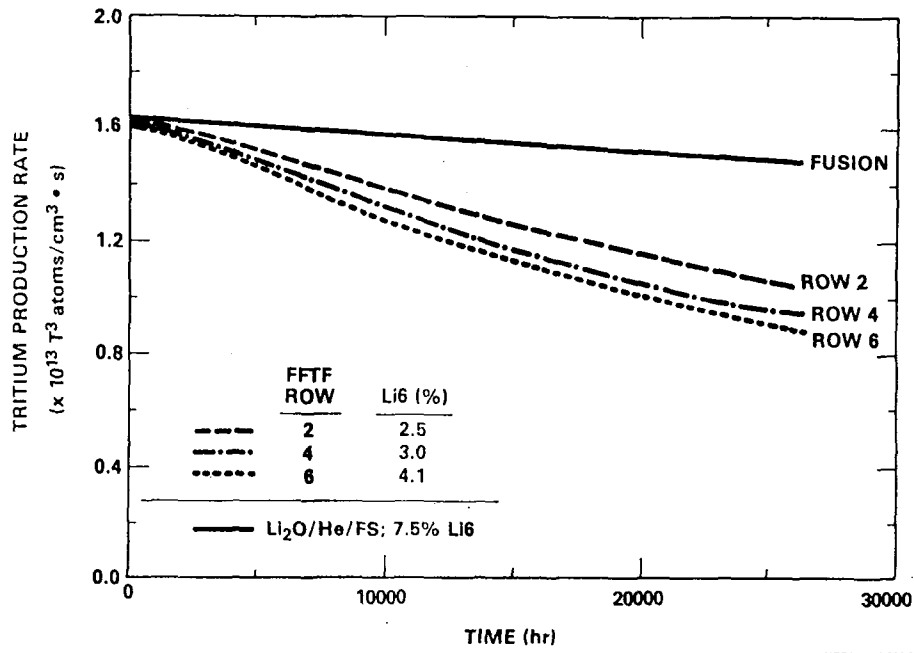


Figure 4.5.2-4. Microscopic calculations indicating the decrease in the tritium production rates as a function of irradiation time. The ⁶Li enrichments for the FFTF estimates were chosen to match the anticipated fusion tritium production rate.

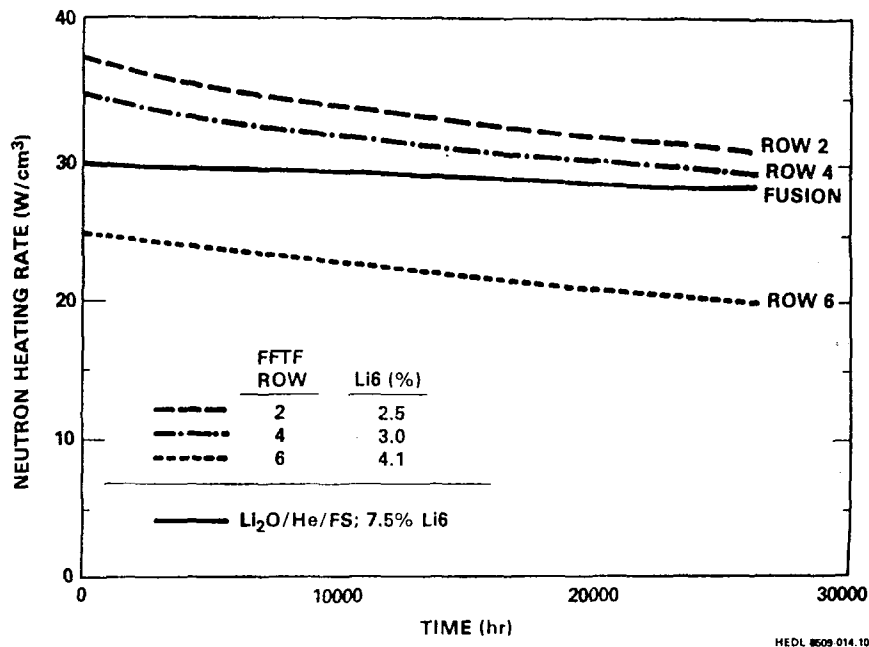


Figure 4.5.2-5. Microscopic calculations indicating the decrease in the neutron heating rates as a function of irradiation time. The ⁶Li enrichments for the FFTF estimates were chosen to match the anticipated fusion tritium production rate.

of helium production to damage production rates in the FFTF irradiation would be approximately an order of magnitude less in FFTF than compared to the anticipated ratio near the fusion first wall.

Finally, the magnitude of self-shielding was estimated to assess the impact on FFTF reactivity and gradients within the test module. Two simple one-dimensional models were assumed and are shown schematically in Figure 4.5.2-6. For the in-core position, FFTF absorber data is used to estimate the flux suppression to be anticipated for a given ${}^6\text{Li}$ enrichment and theoretical density. The flux suppression is assumed to scale as $\exp(-\alpha t)$. An absorber assembly experiences approximately 31% flux suppression for a row 5 position when comparing the flux on the flat closest to the core and the flux at the center of the assembly (5.3 cm). Therefore, $\alpha \sim 0.08/\text{cm}$ for the ${}^{10}\text{B}$ enriched absorber assembly. To convert this absorption coefficient to present experiment, one need only take the ratio of the neutron capture cross-sections and the ratio of the atom densities between the ${}^{10}\text{B}$ enriched absorber assembly

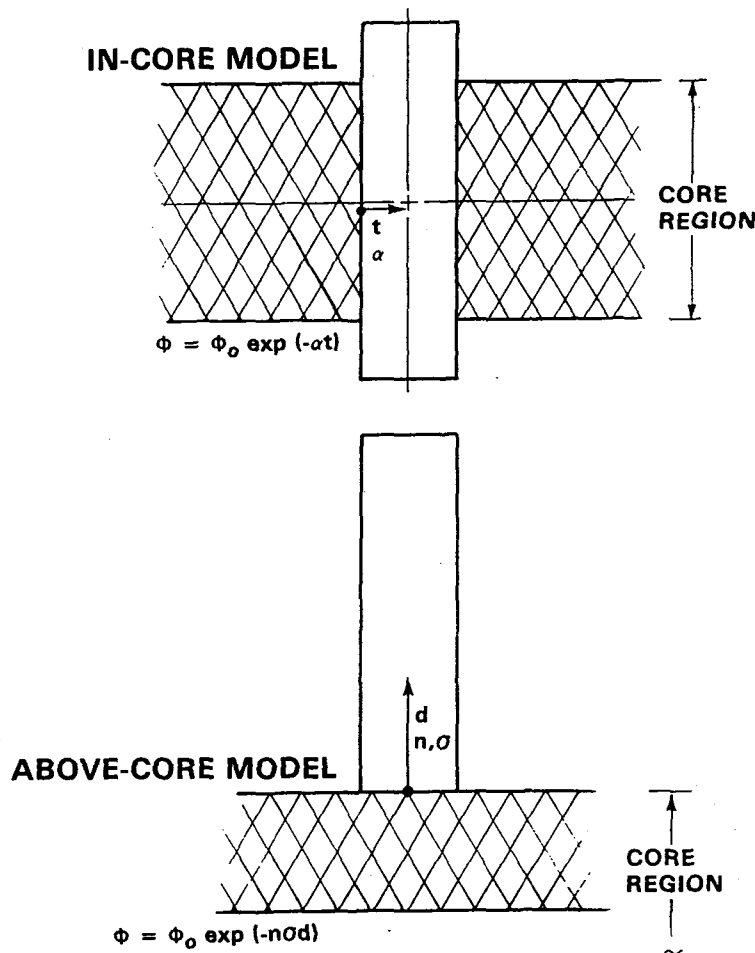


Figure 4.5.2-6. Simple models used to estimate self-shielding.

and the ${}^6\text{Li}$ enriched $\text{Li}_2\text{O}/\text{He}/\text{FS}$ submodule experiment. The value for α is then given by $0.26 \delta\beta/\text{cm}$ where δ is the fractional ${}^6\text{Li}$ enrichment and β is the fractional theoretical density. Estimates of the relative flux suppression as a function of module thickness and fractional ${}^6\text{Li}$ enrichment for 85% theoretical density are shown in Fig. 4.5.2-7. For the enrichments and geometry being considered for this experiment, the in-core flux suppression is anticipated to be small (less than 10%).

Above the core, simple linear absorption is assumed to be given by $\exp(-n\sigma t)$ where n is the ${}^6\text{Li}$ atom density, σ is the average ${}^6\text{Li}$ neutron capture cross section and t is the distance above the core. This estimate represents a lower bound since it neglects the increase in the neutron capture cross section with increasing distance from the core. Also it neglects the self-shielding of the neutron flux from directly below. Nevertheless the predicted flux suppression as a function of distance above the core, as shown in Fig. 4.5.2-8 does suggest that for lithium enrichments greater than 3% and distances greater than 10 cm above the core, self shielding starts to become significant (greater than 10%). Based upon the impact of self-shielding one would probably choose to orient the solid breeder plates within the submodule such that the widest plate dimension was oriented perpendicular to the direction towards the core center. This orientation will tend to minimize the gradient in a given canister due to self-shielding.

A conceptual design of a nuclear submodule experiment was developed to assess the capabilities, limitations and costs of such an experiment. A conceptual design of an example nuclear submodule test for FFTF is shown in Figure 4.5.2-9. The $\text{Li}_2\text{O}/\text{He}/\text{HT9}$ blanket submodule is enclosed in a 12-foot duct assembly which is mechanically attached to the bottom of a 28-foot modified Postirradiation Open Test Assembly (PIOTA) stalk. The PIOTA stalk interfaces with the reactor head and is capable of occupying any of the eight Open Test Assembly (OTA) or Closed Loop (CL) locations in core. It houses all submodule instrumentation leads and terminates out-of-reactor at electrical and pneumatic connectors. The lower duct section interfaces with the core basket which provides sodium flow through the nozzle/orifice assembly. The 360°C (inlet) sodium flows upward between the cylindrical submodule containment vessel and the hexagonal duct. The helium-cooled submodule can be axially positioned in the range of approximately -74 cm to +168 cm from core midplane

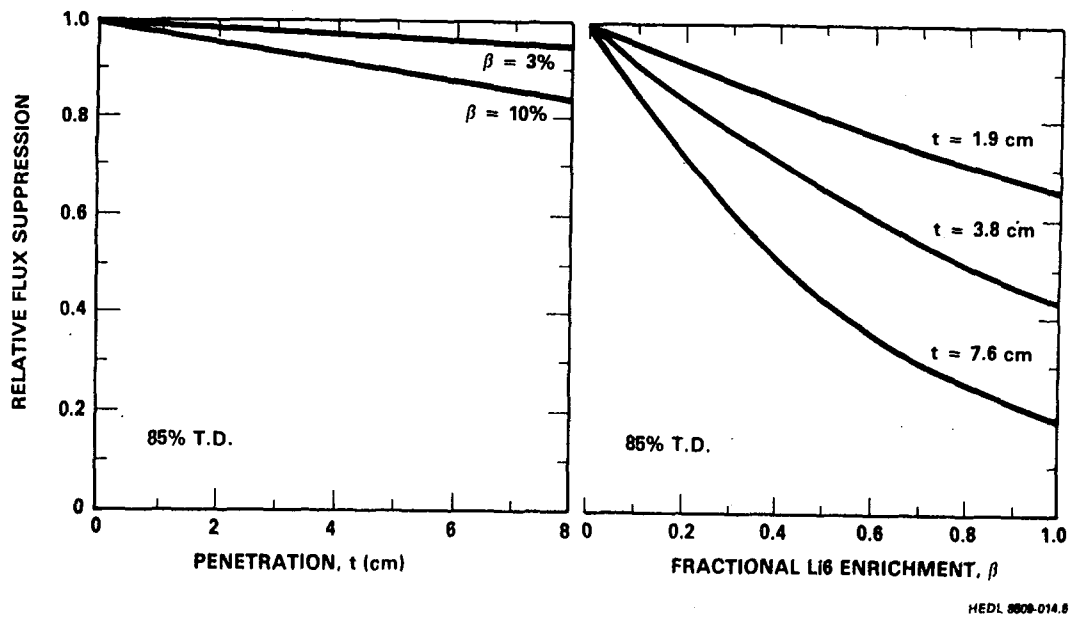


Figure 4.5.2-7. Estimated in-core flux suppression as a function of solid breeder thickness and ⁶Li enrichment.

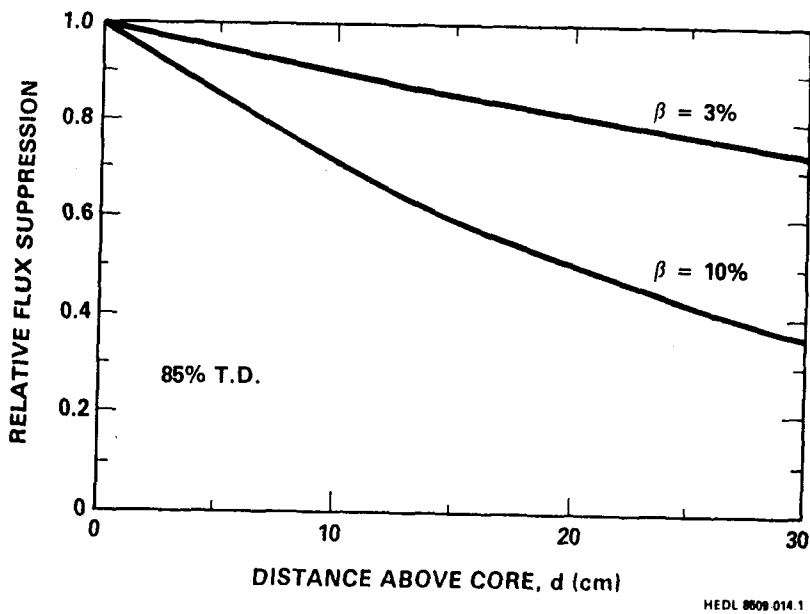
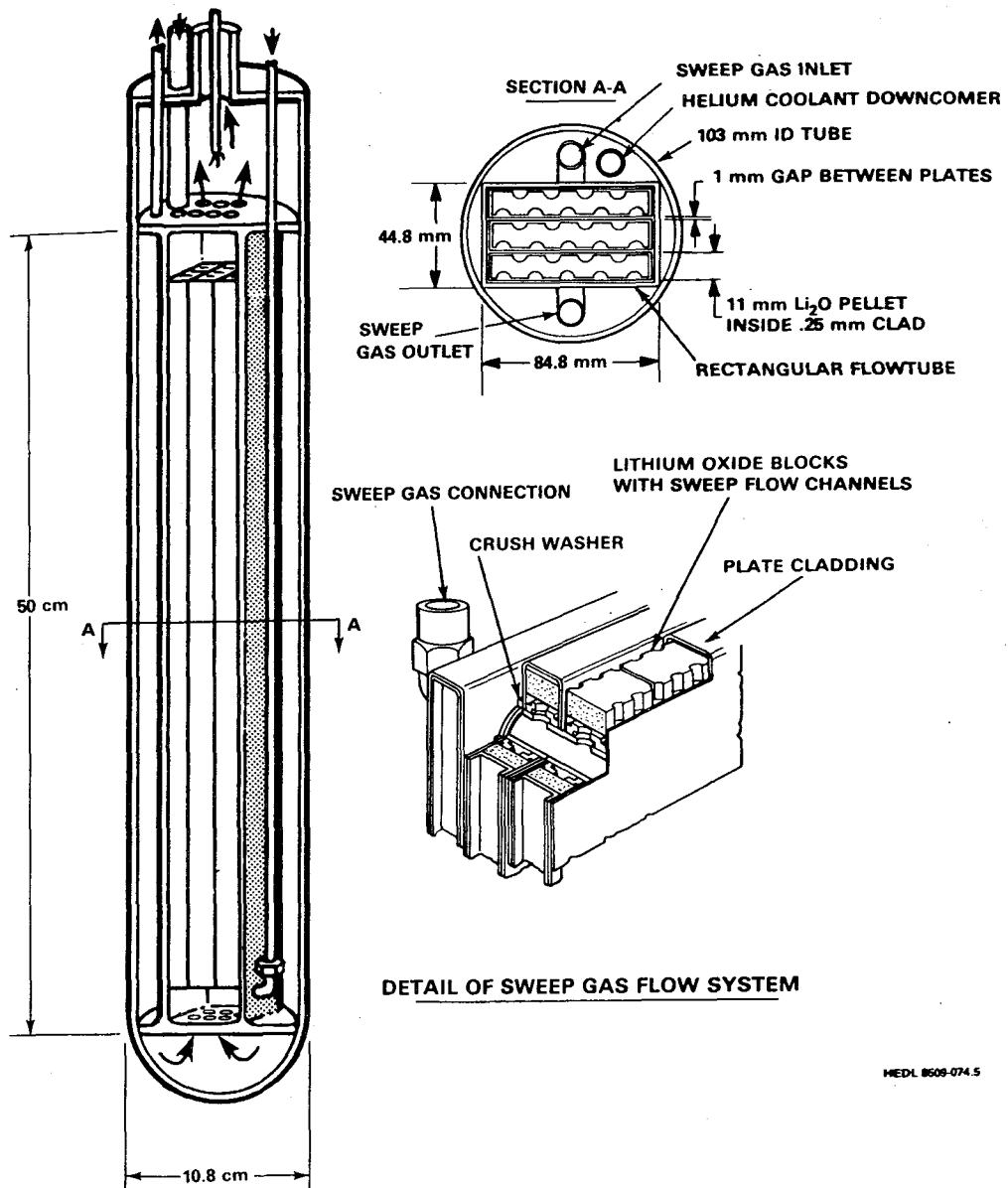


Figure 4.5.2-8. Estimated out-of-core flux suppression as a function of solid breeder thickness and ⁶Li enrichment.



MEDL 8609-074.5

Figure 4.5.2-9. $\text{Li}_2\text{O}/\text{He}/\text{HT9}$ blanket submodule.

(the FFTF active core height is 91 cm) to best simulate actual tritium production and heat generation rates. Negative reactivity effects caused by the blanket submodule must also be considered but can be minimized by locating the test assembly in a row 6 OTA position.

The $\text{Li}_2\text{O}/\text{He}/\text{HT9}$ blanket submodule is shown in Fig. 4.5.2-9. Three 1.15 cm wide plates of HT9 clad Li_2O are separated by wire wrapping to provide 1 mm wide coolant channels. The set of plates are interconnected with tritium recovery sweep lines which manifold into single inlet and outlet lines. This submodule is enclosed in a 10.8 cm diameter cylindrical vessel (with an inert gas) to isolate the submodule from reactor sodium. The large amount of heat generated within the submodule is removed by flowing helium and ex-reactor heat exchangers. High helium pressure is anticipated and maintaining relatively low structure temperatures (about 500°C) may be difficult at high total heat generation levels. A limited number of thermocouples and strain gauges are used to monitor structural cladding temperatures and deformation during irradiation. The critical locations will depend upon safety and model verification needs. Strain gauges will at least provide structural response at beginning of life; the lifetime of strain gauges under irradiation is uncertain. A summary of the operating characteristics of this experiment is shown in Table 4.5.2-2.

A simplified instrumentation schematic for the Nuclear Submodule Test is shown in Fig. 4.5.2-10. A limited number of thermocouples are used to monitor coolant temperatures (helium and sodium) and provide feedback for the gas coolant control system. The analysis and measurement systems for the coolant and purge gas loops will generally follow those used in the TRIO experiment with the recommendations given in Ref. (1). All flow meters, pressure gauges, compressors, heat exchangers, and tritium recovery and temperature control systems are ex-vessel but within FFTF containment. The recirculatory helium coolant system must have capability of monitoring and trapping any tritium and potential radionuclides that may enter the system due to either permeation or structural failure. The recirculatory sweep gas system has extensive tritium recovery and measurement instrumentation. Secondary containment in the form of purged jackets and glove boxes is required on all sweep gas outlet lines and may be required on the coolant gas outlet lines. Actual sweep and coolant gas flow rates are unknown at this time and are submodule design dependent.

Table 4.5.2-2. Characteristics of a Representative Nuclear Submodule Assembly Experiment and Submodule Instrumentation

Breeder material	Li2O
Structural material	HT9
Nominal structure temperature	500°C
Minimum/maximum breeder temperature	510/795°C
Submodule dimensions	44.8 x 84.8 mm
Number of plates	3
Cladding thickness	0.25 mm
Outer containment dimensions	
Minimum wall thickness	2.4 mm
Inside diameter	103 mm
Outside diameter	108 mm
Pressure	
Sweep gas	To be determined
Coolant gas	To be determined
Helium coolant temperature (inlet)	100-200°C
Sweep gas flow	To be determined
Sweep gas composition	He + H ₂ or O ₂
Submodule instrumentation	
Temperature	24 thermocouples
Structural deformation	12 strain gauges
Neutron flux and fluence	Passive dosimetry: spectral sets and gradient wires
Sweep gas system	
Pressure and flow	Gas instrumentation
Tritium release	SGAS ^a
Chemistry	SGAS
Radionuclides	SGAS
Coolant gas system	
Pressure and flow	Gas instrumentation
Tritium permeation	CGAS ^b
Chemistry	CGAS
Radionuclides	CGAS

^aSGAS = sweep gas analysis system

^bCGAS = coolant gas analysis system

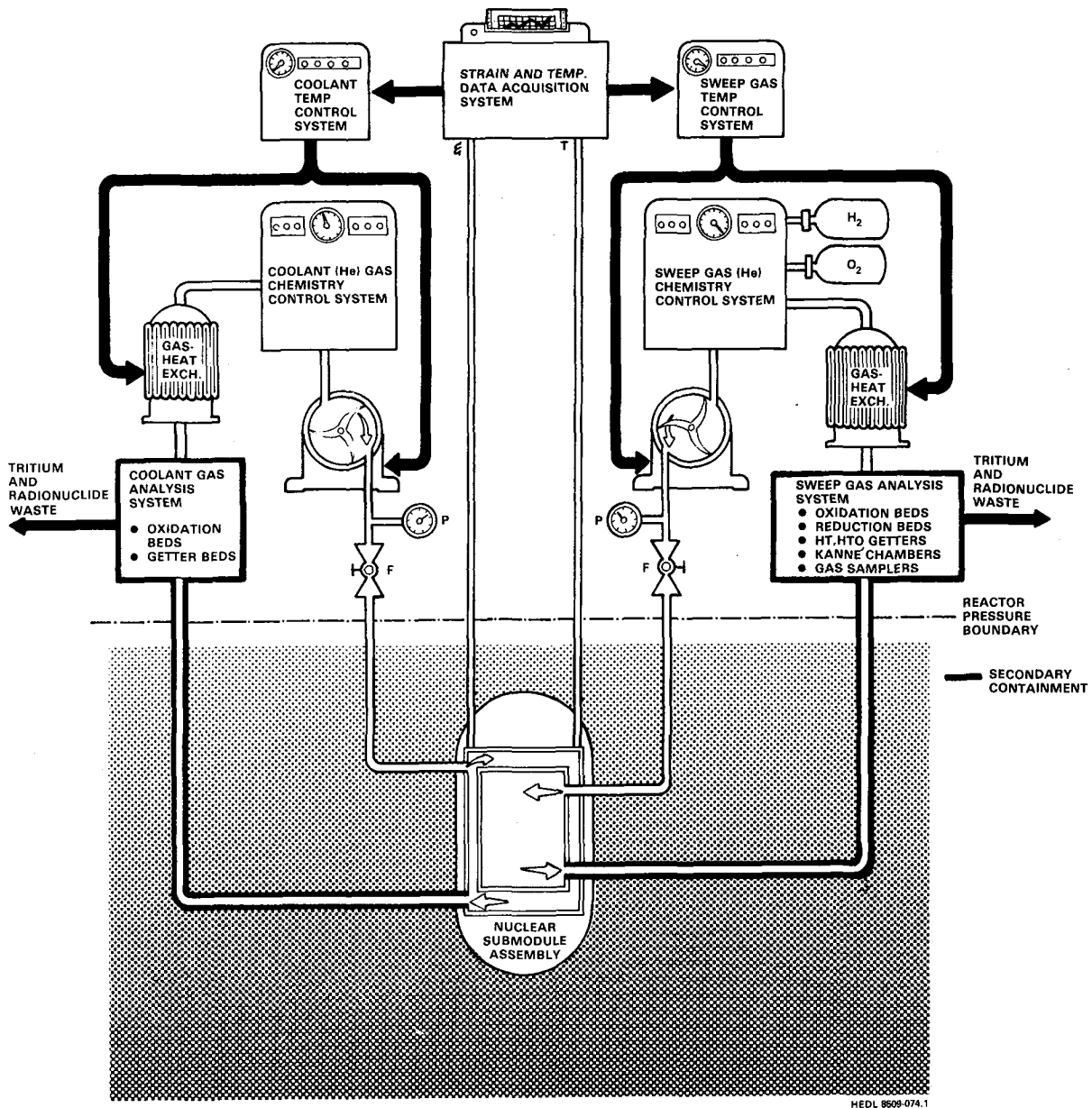


Figure 4.5.2-10. Instrumentation schematic for the nuclear submodule assembly test.

References for Section 4.5.2

1. G.A. Deis, et al., "Development of a Nuclear Test Strategy for Test Program Element V," EGG-FT-5651, Idaho National Engineering Laboratory, March 1982.
2. M.A. Abdou, et al., "FINESSE - A Study of the Issues, Experiments and Facilities for Fusion Nuclear Technology Research and Development, Interim Report," Chapter 12, PPG-821, also UCLA-ENG-84-30, University of California, Los Angeles, October 1984.
3. G.A. Deis, et al., "Development of an Engineering-Scale Nuclear Test of a Solid-Breeder Fusion Blanket Concept," EGG-FT-6111, Idaho National Engineering Laboratory, August 1983.

4.5.3 Fusion Experiments

Fusion devices provide directly relevant testing and development. Since these facilities are fairly expensive, they will be primarily relied on for tests that cannot otherwise be accomplished. Unique features of a fusion test facility include large-test-volume irradiation, fusion neutron spectrum, all environmental conditions, and all major fusion subsystems. Consequently, the key role of these tests is concept verification - to identify failure modes, unanticipated phenomena, and system interactions. Of course, if a fusion facility were available, it could also be used to address specific issues in smaller experiments.

Ideally, the fusion device would duplicate anticipated conditions in a power reactor by operating with the same major device parameters such as neutron wall load. However, it is unlikely that any fusion test device will provide reactor parameters because of cost and risk constraints. In many cases, it is possible to scale the test module design to retain the important aspects of the testing issues. However, a change in device parameters beyond certain limits often results in a change in phenomena or the inability to extrapolate to reactor conditions. In order to provide useful integrated testing, minimum requirements on the device parameters can be defined relative to reactor parameters.

For blanket concepts intended for power reactor operation at 5 MW/m^2 neutron wall load, the test device should provide at least 1 MW/m^2 . Similarly, the fusion test facility should provide at least 500 s burn to allow reaching thermal steady-state, have sufficient test volume and area to accommodate several parallel test modules, and achieve moderate fluences of $1\text{-}2 \text{ MW/m}^2$ in useful test times (less than 5 years). A more detailed analysis of these requirements is provided in Section 9.3.2. As indicated by most proposed fusion technology test devices (see Chapter 9), parameters are not expected to be substantially different from these values.

4.5.4 Test Plan Considerations

Partially integrated and integrated tests have been described that address blanket behavior under complex geometry and environmental conditions. The unique features and limitations of these tests are described in Table 4.5.4-1. Non-neutron tests can accommodate up to full blanket modules and address thermal-hydraulic and thermal-mechanical issues, especially severe transient response, but are limited by lack of irradiation effects and differences due to the non-neutron heat source simulation. Full blanket module tests are possible in fission reactors, but generally must be placed beside the core, require major modifications to existing reactors, and cannot provide over 1 MW/m^2 equivalent nuclear heating because of flux limitations. Nuclear submodule tests provide a maximum test of breeder region behavior under fission reactor irradiation, but with the limitations of partial geometry, a non-fusion spectrum, and reactor-safety related constraints on environmental conditions and transient testing. The fusion integrated tests provide all environmental conditions over a full module, but are probably limited in power level and fluence, and will require scaling to power reactor conditions.

Ideally, all these tests would be performed since none provides complete integrated testing - each provides a large but different subset of reactor-relevant parameters. However, although only a limited number of any of these experiments would be performed, they are all relatively expensive. Several alternatives can be considered.

At one extreme, it can be argued that none of these tests are necessary to assess the feasibility or attractiveness of fusion given an adequate program based on single and multiple-effect experiments, model development and design studies. (Of course, these tests would be important for the actual commercial development of fusion assuming a favorable assessment.) However, experience with other technologies repeatedly indicates the importance of integrated tests in identifying fundamental and unanticipated phenomena, and in demonstrating performance and lifetime that are not confidently predictable based on the simpler experiments.

At the other extreme, it is possible that almost the entire test program could be based on these experiments. This design/test/fix approach has been successfully utilized in other technologies. The approach relies more on empirical correlations of behavior rather than detailed understanding, and

Table 4.5.4-1. Comparison of Partially Integrated/Integrated Tests

	Non-nuclear thermomechanics integrity test	Fission full-module test	Fission breeder submodule test	Fusion integrated module test
Geometry	Full-size module	Scaled module	Submodule (breeder)	Scaled module
Neutron fluence (MW-yr/m ²)	0	1-2	> 3	1-2
Peak power density (MW/m ³)	25-60 (full)	< 10	10-25	10-25
Neutron energy	--	Fission	Fission	Fusion
Heating profile simulation	Poor/fair	Fair/good	Fair/good	Exact
Surface heating (MW/m ²)	0-1 (full)	< 0.2	NA	0-0.2
Magnetic field (T)	0-1	0	0	3
Safety (transient) tests	Severe	Some	Some	Some

focuses attention on specific phenomena rather than addressing all possible uncertainties. It requires early selection of candidate designs, and is not flexible in accommodating major design changes.

Within these positions, it is possible to consider a limited number of these experiments. Due to the relative costs of non-neutron, fission and fusion tests, a plausible approach would be limited non-neutron testing, a few nuclear submodule tests and, if available, fusion module tests. The non-neutron test facility described here represents an upper bound on the achievable non-neutron testing. These tests appears useful enough in terms of issues addressed and testing flexibility, but are still expensive in this example. Simpler or more limited approaches can be considered.

4.6 Experiment Cost and Time Characteristics

Cost and time estimates are provided here for the various experiments identified in previous sections. These costs are based on experience with similar experiments and facilities. The factors included in cost estimates are summarized in Table 4.6-1. Direct cost estimates include design, construction, operation and post-test examination associated with an experiment. A total R&D program also includes indirect costs such as modelling and code development that are not necessarily associated with specific experiments, as well as equipment or instrumentation development that may be required to support experiments. For example, some reactors do not have available instrumented or purged test assemblies. Consequently, these would have to be developed prior to inserting solid breeder test capsules.

The major assumptions for the cost estimates (see Section 3.7) are:

- no prior equipment;
- no irradiation or neutron facility charges;
- all costs in 1985 dollars;
- total indirect costs are about equal to total direct costs.

Table 4.6-1. Factors in Estimating Costs

Direct	Test design and construction
	Test operation - staff and facilities
	Post-test examination
	Test cleanup
	Direct analysis of test results
	Laboratory overhead
Indirect	Equipment and instrumentation development
	Scoping tests
	Modelling and code development
	Design studies
	Program administration
	Contingency

The direct cost and time estimates are summarized in Table 4.6-2. An equivalent annual operating cost is provided as if the experiment operated continuously for a year, and is broken down into number of staff (scientific and technical) and facility costs. The actual time required to perform a given experiment is indicated under the test time column. For example, a single-capsule in-situ tritium recovery experiment is anticipated to cost about 0.5 M\$/yr during the irradiation period. Assuming a typical irradiation test time of 1.5 years to achieve about 1% burnup, the irradiation cost would be 0.75 M\$ (excluding neutron charges). The costs can be scaled to higher or lower burnups.

In general, the tests for solid breeder blankets are fairly straightforward benchtop-class measurements or are based on irradiation in existing fission reactors. Therefore estimates are primarily based on experience with similar experiments in these facilities and not on any detailed cost breakdown. General clarifying comments are included below.

Material Development

The development of structural alloys was not considered in this chapter, although this is clearly important to the feasibility and attractiveness of fusion. However, as indicative of the type of costs needed simply to verify the properties of a developed alloy, a small but reasonable test matrix for a few alloys can be irradiated and evaluated in a single MOTA (FFTF Materials Open Test Assembly) at an estimated cost of 2.5 M\$/yr. At typical displacement rates of ≤ 30 dpa/yr for ferritic steels in fast reactors, it would take 6 years to achieve the equivalent of 15 MW-yr/m² (180 dpa).

Developing a new solid breeder material to a useful degree of availability in terms of grain size, purity (impurities and phases), form (e.g., sintered product, sphere-pac) and so on can be a substantial effort. It is estimated here as around 12 person-years. A considerable effort has already been expended on present candidate solid breeders, particularly Li₂O and LiAlO₂. It may be that new techniques developed for one ternary oxide, such as production of the sphere-pac form, can be readily adapted to the others. The costs for development of commercial production systems are not included.

An optimum form is not presently available for beryllium, although it is known that the product form has a strong influence on the properties.

Table 4.6-2. Solid Breeder Experiment Direct Cost and Time Characteristics

Experiment	Design/ Const. M\$	Annual Operating Cost			Post- Test M\$	Design Const. Time, yr	Test Time, yr	Post- Test Exam, yr
		Sci. Staff	Tech. Staff	Facil., M\$				
Breeder development:								
Fabrication	0.2	3	3	incl	0.75	incl	incl	4
Unirradiated mech. prop.	0.05	2	2	incl	0.5	incl	incl	2
Multiplier development:								
Be fabrication	0.2	3	3	incl	0.75	incl	incl	2
Unirradiated mech. prop.	0.05	2	2	incl	0.5	incl	incl	2
Closed capsule, 3% BU	0.1	0.5	incl	incl	0.08	0.1	incl	3
Diffusion coefficient measurement								
1 SB/M	0.05	1	1	incl	0.25	incl	1	2
Solubility/adsorption measurement								
1 SB/M	0.05	1	incl	incl	0.15	incl	0.5-1	1
Thermal conductivity measurement								
1 SB/M (unirradiated)	0.05	1	1	incl	0.25	incl	0.5	1
Breeder material phase diagram								
1 SB system	0.06	1	incl	incl	0.15	incl	0.5-1	1
Thermochemistry measurement								
1 SB system	0.05	1	incl	incl	0.15	incl	0.5-1	1
Corrosion/mass transfer test								
1 sample, 5000 hr, purge	0.05	0.5	incl	incl	0.08	incl	0.2	1
Thermal stability test								
1 sample, 5000 hr	0.03	0.5	incl	incl	0.08	incl	0.2	1

Table 4.6-2. Solid Breeder Experiment Direct Cost and Time Characteristics (cont.)

Experiment	Design/ Const. Cost, M\$	Annual Operating Cost			Post- Test M\$	Design Const. Time, yr	Test Time, yr	Post- Test Exam, yr
		Sci. Staff	Tech. Staff	Facil., Total, M\$				
Structure development: Development/fabrication								
Irradiated properties: 2-3 alloys, 1 FFTF MOTA	Not estimated here Values for a small but reasonable test matrix for well-defined alloys incl 3 3 1.5 2.5	incl 3	incl 3	incl 2.5	incl 4	incl 4	incl 4	incl 4
Unrestrained SB/M								
Closed capsule, 9% BU								
Subassembly, 14 tests	0.1/0.1	2	incl	0.30	0.15	1	1	3 1
Partial sub. (1 of 7 pins)	0.01/0.01	0.3	incl	0.04	0.02	1	1	3 0.15
Partially restrained SB/M								
Closed capsule, 4% BU:								
Subassembly, 10-20 tests	1/1	2	incl	0.30	1	0.5-1	0.5-1	3 0.5-1
EM effects facility								
Facility, 1 T, 50 T/s, 1 m ³	0.4/0.9					0.8	1.2	
Upgrade, 2 T, 100 T/s	+0.3/0.6					+0.3	+0.7	
Module, steady and transient	0.1/0.5	1	incl	0.25	0.2	0.2	0.8	0.5 0.5
Plasma/first wall interaction								
High particle fluence								
Thermomechanical integrity test								
Full module and power tests:								
Facility, 6 MWe	5					1	1	
Submodule, steady/transient	0.1/0.7	2	4	0.1	0.8	0.1	0.2 0.8	0.2 0.2
Limited module and power tests:								
Facility	2					0.5	0.5	
Submodule, steady/transient	0.1/0.5	2	2	0.1	0.6	0.1	0.2 0.5	0.2 0.2

[relevant tests described with Plasma Interactive Component development]

Table 4.6-2. Solid Breeder Experiment Direct Cost and Time Characteristics (cont.)

Experiment	Design/ Const. Cost, M\$	Annual Operating Cost			Post- Test Exam, M\$	Design Const. Time, yr	Test Time, yr	Exam, Time, yr	Post- Test Exam, yr
		Sci. Staff M\$	Tech. Staff M\$	Facil., Total, M\$					
Structure permeation [Basic tests described as part of Tritium system development]									
Breeder tritium extraction [Tests described as part of Tritium system development]									
In-situ tritium recovery									
Single, 0.2% BU, instrumented	0.75/0.5	3	incl	incl	0.5	1	1	0.3	0.5
Single, 1% BU, instrumented	0.75/0.5	3	incl	incl	0.5	1	1	1.5	0.5
Advanced in-situ tritium recovery									
Subassembly, 4% BU, instr.	1/2	3	incl	incl	0.5	1	2	2	1
Transient tritium release test									
Single, 1% BU, instr., large	1/2	3	incl	incl	0.5	1	2	2	1
Nuclear submodule test assembly									
Center-core position, 4% BU	2/3.5	2-3	incl	incl	0.3-0.5	1	1	3	1
Slab, side-core, 1% BU	5/53.	3	incl	incl	0.5	1	2	3	2
Blanket neutronics test facility									
DT point source, 10^{13} n/s	12						1	3	
Cross-section (10 data points)			incl	incl	1	incl	incl	incl	0.5
Blanket simple mockup									
1 flux/heating/TPR test	1-2	3	4	incl	1	0.3	0.1	0.1	0.07
(Li:1, Li ₂ O:1.5, Li ⁶ :2 M\$)									
Engineering benchmark									
1 flux/heating/TPR test	+1	3	4	incl	1	0.3	0.5	1	0.3

Consequently, further development will be needed even to identify a suitable material for the testing program. Based on the reasonably large existing data base for unirradiated beryllium, it is assumed that the further fabrication requirements will require about half of those needed to develop a new solid breeder. Beryllium toxicity should be considered in assessing costs.

Properties Measurements

It is assumed that typical properties measurements for a single solid breeder or multiplier material require about 50 k\$ worth of equipment and material (although much of the equipment is fairly standard and available at various laboratories), and about 1-2 person-years to complete a careful study of the relevant parameter ranges for a given property. The diffusivity measurements are assumed to take about 3 person-years allowing some effort towards the development of single-crystal material. These costs and times do not include providing high-burnup irradiated material. It may be noted that much of the required hardware and expertise is presently available.

Closed Capsule Irradiation

The Unrestrained Breeder/Multiplier tests are similar to the FUBR-1 experiments. A typical subassembly is assumed to contain 14 test capsules. The FUBR-1A subassembly contained 12 capsules, the FUBR-1B experiment includes 42 capsules over a few assemblies. The highly enriched material in these experiments will achieve about 9% burnup over 3 years in EBR-II. Burnup will vary with reactor flux, test location and enrichment. It is assumed that the costs for less than one subassembly can be shared down to the single pin level, or about 1/7th of the total assembly cost.

The Partially Restrained Breeder/Multiplier tests are larger in order to provide mechanical boundary conditions and temperature gradients, and more complex because there is a possibility of clad rupture. Consequently, there are fewer to a test assembly and the test is more expensive. An instrumented assembly will cost somewhat more to construct and operate than an uninstrumented one, but the more significant consequence is that the host reactor must have the capability for in-situ instrumented (and/or vented) tests. Considerable effort has been spent developing suitable assemblies for FFTF (e.g., MOTA, CLIRA) and ORR, but not for EBR-II or HFIR. Typical costs are provided

in Table 4.6-2 for a subassembly containing three capsules with several subcapsules each. Interim examinations, occurring once/year, would require about 0.2 years and 0.9 M\$.

In-situ Tritium Recovery

In-situ tritium recovery experiments require instrumentation and purge connections outside the reactor, which limits the possible reactor sites. This complexity, plus the ability to vary the capsule temperature (e.g., gap gas composition) and purge composition, plus the on-line monitoring requirements increase the cost of the experiment relative to closed capsule tests. For the simpler isothermal recovery experiments, it is possible to use a single capsule to explore the effects of a range of temperatures and purge gas compositions. Based on the TRIO experiment, about 0.2% burnup was achieved in about 100 days of irradiation.

The Advanced In-situ Recovery tests have reactor-relevant temperature gradients and possibly breeder/clad interactions, so there is less ability to vary conditions within a given capsule during irradiation. Consequently, multiple capsules may be necessary, requiring a large test volume, high fast flux reactor like FFTF where a single subassembly can accommodate several separately-purged capsules simultaneously. The incremental cost per capsule on the basic subassembly cost is small, and is mostly in the cost of the on-line instrumentation.

Nuclear Submodule Assembly

A range of large-scale fission reactor tests were considered, from full-blanket tests that would require a side-core slab position approaching 0.5 m^3 to submodule sections that would be placed into existing in-core positions. No presently operating reactors can accommodate the slab assembly without major modifications, estimated as 50 M\$, plus the cost of the test assembly itself. The submodule assemblies are estimated as about 5.5 M\$ each for design and construction. This cost reflects the fact that these are the first large-scale assemblies to be tested in a nuclear environment and must assure reactor safety, and that considerable amounts of tritium must be handled (several hundred Curies per day). The manpower requirements are predominantly engineering time during design and fabrication (5-6 person-years), with

similar amounts during the three-year irradiation and the post-test examination.

Blanket Neutronics Facility

A point source facility with a neutron strength of about 10^{13} n/s provides sufficient fluence for the most neutronics tests within 50-100 hours on continuous operation. Such facilities are presently available and there does not appear to be a need for more. However, if an additional facility is built, the facility cost is estimated as 12 M\$ (1985) based on the 1980 costs for the JAERI FNS facility (accelerator 2 M\$; building 4 M\$; instrumentation 2 M\$) and allowing for inflation (there are indications that accelerator costs have increased faster than inflation). The FNS facility took about 3 years to build, with additional design time before and during the construction phase.

The second major cost component are the blanket materials. Typical costs for material and fabrication are 600-800 \$/kg for Li_2O and Be, 200 \$/kg for Li metal, and 4 \$/kg for Li_2CO_3 . Enriched ^6Li stockpiles exist in the US, but the availability and cost for fusion testing are uncertain. Simple blanket mockups need about 1-2 Mg of blanket material to surround the source and provide a blanket-like neutronic environment. As in the US/JAERI FNS experiments, the bulk material in the test cell can often be the less expensive Li_2CO_3 , except for the blanket mockup itself ($0.25\text{-}0.5\text{ m}^3$, or 300-600 kg breeder material based on an effective density of 60%). For a multiplied LiAlO_2 blanket (90% ^6Li), this implies about 30-60 kg of ^6Li . Engineering mockups of first wall and blanket sections will require more detail in the blanket construction and more volume in the surrounding environment simulation (several Mg), increasing fabrication and materials costs.

Tests would be conducted for a given blanket mockup in a series ranging from instrument calibration, to neutron and gamma dosimetry (physics and code benchmarking), to heating and tritium production rate tests. The latter require more fluence for sufficient accuracy, which also makes the material hot. The sequence takes about 6 weeks, with 2 weeks setup, 3 weeks for the initial tests, and 1 week for the 50-100 hr exposure for the test. Including planning and analysis, each series could require up to half a year. Manpower requirements per test sequence are about 100 person-days for scientific staff,

150 person-days for technical staff, with an additional 70 person-days to analyze the instruments.

Thermomechanical Integrity Tests

Possible non-neutron thermomechanical tests range from a facility that can accommodate up to a full blanket module at full-power, to simpler tests that would investigate more limited conditions or blanket sections. Volumetric heating could be provided by RF (if possible), discrete-wire resistive heating or a hot purge stream. Surface heating, if present, could be provided by radiant arcs, particle beams or plasma. Both a full module simulation and a more limited test are considered here.

For full module test facility described here represents an upper bound on non-neutron testing. The basic facility includes vacuum chamber and pumps (about 1 Pa base pressure), surface heating source (radiant arcs for up to 1 MW/m² over 0.5 m²), power supplies for surface heaters and blanket-module heaters (6 MWe peak with 100% conversion to useful heat), cooling system (chamber walls, blanket coolant, blanket purge) and instrumentation and control (thermocouples, strain gauges, flowmeters, pressure monitors, and gas analyzers). The requirements on the vacuum chamber are simpler if discrete-wire (or hot purge) and radiant arcs are used (electron beams require 10⁻⁵ Pa vacuum), which is desirable for allowing severe transient tests. The basic facility design might resemble the electron-beam-heated ASURF⁽¹⁾ or the radiant-arc-heated Boeing High Heat Flux Test Facility.⁽²⁾ A rough cost breakdown yielded:

Engineering design (4 person-yrs)	\$600,000
Facility (brick mortar)	1,000,000
A & E (40%)	400,000
Control system	250,000
Power system (cooling, pumps, etc.)	1,400,000
Installation and testing (8 person-yrs)	<u>800,000</u>
Total	\$4,450,000

The design and construction time would be about 2 years, and the operating staff would include 2 full-time research scientists and 4 technicians providing engineering support and operations.

A fairly detailed estimate for a full test blanket module was provided based on a $\text{Li}_2\text{O}/\text{He}$ plate-type blanket with 30 resistive wire pairs per plate. This breakdown yielded, for a full blanket module:

Engineering design	\$ 78,000	1200 hrs
Tooling and manufacturing engineering	208,000	3400
Production labor and services	223,000	3800
Production material	<u>543,000</u>	<u>--</u>
Total	\$1,052,000	8400 hrs

Tooling includes design, fabrication, engineering & methods, quality control, material and management & services. Production labor and services include major equipment, conventional equipment, welding, quality control, vendor services and management & services. These costs can be compared with the Lithium Blanket Module (LBM) costs of about 2 M\$ total, including analysis.

The Li_2O material was over half of the total cost. For Li_2O , 800 \$/kg was assumed based on the LBM and JAERI FNS neutronics experiments, rather than the 40 \$/kg commercial production values assumed in BCSS. About half of this cost is for the basic high-purity Li_2O , and half is for fabricating it into the desired form. Since neutron effects and tritium production are not included in these experiments, high purity material is not necessary as long as the basic thermomechanical and thermophysical properties are not affected. Also, Li^6 enrichment is not required. Thus it may be possible to use less expensive material. Furthermore, if the module length is reduced from 2 m to 1 m, little effect on the behavior is expected but a further savings of a factor of two in materials cost is possible (design and fabrication costs would not be significantly affected). These changes could reduce the module costs as low as 0.6 M\$.

Most tests are one or two days, including test setup, bringing the module and test facility to the initial operating point, the test itself, cooldown, and module removal for examination. The time at full power is generally about 2 hours since the blanket thermal time constants are roughly 1 hour or less. However, the thermal cycle fatigue tests include 1000 0.1 hour cycles simulating rapid cycling events, and 100 1 hour cycles simulating startup/shutdown cycles that would be constrained to the blanket thermal time constant time scale in a power reactor. The thermal stability test holds the test module at reactor temperatures for 1000 hrs to observe long-time-scale changes associa-

ted with corrosion, internal and external mass transfer of breeder, permeation equilibrium, and thermal creep. It is anticipated that this latter test would run in a half-power mode, with adjusted inlet conditions to preserve structural and interface temperatures while reducing power consumption.

Less complex tests, that could still address geometry-related behavior on a larger scale than possible with a nuclear submodule test, were not explicitly considered here. An example would be the RF-heated tests of LiAlO_2 proposed by ANL. In the absence of a specific design, it is assumed that a useful experiment would cost around 2 M\$.

Electromagnetics Effects Facility

The cost and time estimates for an EM facility able to provide information on electromagnetic loading and response in steady-state or transients was based on the FELIX facility.⁽³⁾ The module tests are assumed to be dominated by fabrication costs.

References for Section 4.6

1. H.D. Michael, et al., "Large Area Surface Heating Facility (ASURF) and Test Program First Wall Design Concepts," Nucl. Tech./Fusion, 4, 785 (1983).
2. A.G. Ware and G.R. Longhurst, "Test Program Element II, Blanket and Shield Thermal-hydraulic and Thermomechanical Testing, Experimental Facility Survey," EGG-FT-5626, Idaho National Engineering Laboratory (December 1981).
3. L.R. Turner and W.F. Praeg, "Detailed Technical Plan for Test Program Element-III (TPE-III) of the First Wall/Blanket/Shield Engineering Test Program," ANL/FPP/TM-155, Argonne National Laboratory (March 1982).

4.7. Summary

Most of the critical issues for solid breeder blankets are related to the tritium and thermomechanical behavior in the breeder region. The issue categories and the most important uncertainties are listed in Table 4.7-1. At present, there is still considerable uncertainty over basic materials properties and on the definition of suitable material microstructure and form. Many of these issues require at least some level of irradiation since property changes under irradiation can be substantial. Furthermore, many of the remaining uncertainties are directly associated with nuclear effects.

A variety of experiments are needed to fully address these uncertainties. These possible tests are summarized in Fig. 4.7-1. The levels of test integration range from basic measurements of properties, to separate and multiple-effect tests to explore phenomena, and to integrated tests for concept verification.

Within each of these test categories, there are many possible specific tests with, for example, differing materials, parameter ranges and degree of instrumentation. These were described in previous sections. A brief description of each test type is given in Tables 4.7-2 to -5.

There is presently underway a fairly complete effort to characterize the materials properties and tritium transport under closed capsule and simple sweep gas experiments around the world on a few materials. Parameters under investigation include temperature, temperature gradient, burnup (0-9%), purge gas composition, clad material (SS, Ni, quartz), material form (sintered product, sphere-pac) and various microstructures and impurity contents.

These tests should be sufficient to address the known uncertainties for these materials - specifically, Li_2O , LiAlO_2 and Li_2O_3 . Further closed capsule or in-situ recovery experiments would only be necessary if these tests indicate additional effects, such as an irradiation effect that has not apparently saturated by the achieved burnup levels. In addition, any other materials would need similar attention to characterize the basic material and processes. If there is to be a selection of candidate materials within 5 years (i.e., after completion of current set of experiments), then other materials should be evaluated also. Particularly noteworthy are the lack of

Table 4.7-1. Major Solid Breeder Issues and Contributing Uncertainties

Tritium Inventory and Transport

Temperature-dependent diffusion rate and mechanism
Effect of impurities on diffusivity
Effect of irradiation on diffusivity
Solubility (T_2O and T_2)
Surface adsorption (T_2O and T_2)
Oxygen activity and effects on tritium recovery and form
Breeder restructuring effects on tritium inventory
Isotope swamping effects on tritium recovery
Burnup equilibrium thermochemistry
Impurity effects (fabrication and purge stream)
Flux effects on tritium recovery
Transient release of breeder tritium inventory

Tritium DT Self-Sufficiency

Module tritium breeding ratio

Breeder/Multiplier/Structure Mechanical Interactions

Irradiation effects on breeder/multiplier thermomechanical properties
Breeder restructuring extent
Clad deformation due to mechanical interaction
Gap conductance

Structural Response to Environmental Conditions

Irradiation effects on structural properties
Module structural strength
First wall thermal stress and fatigue life
First wall plasma interaction (erosion) lifetime
Thermomechanical response to transients

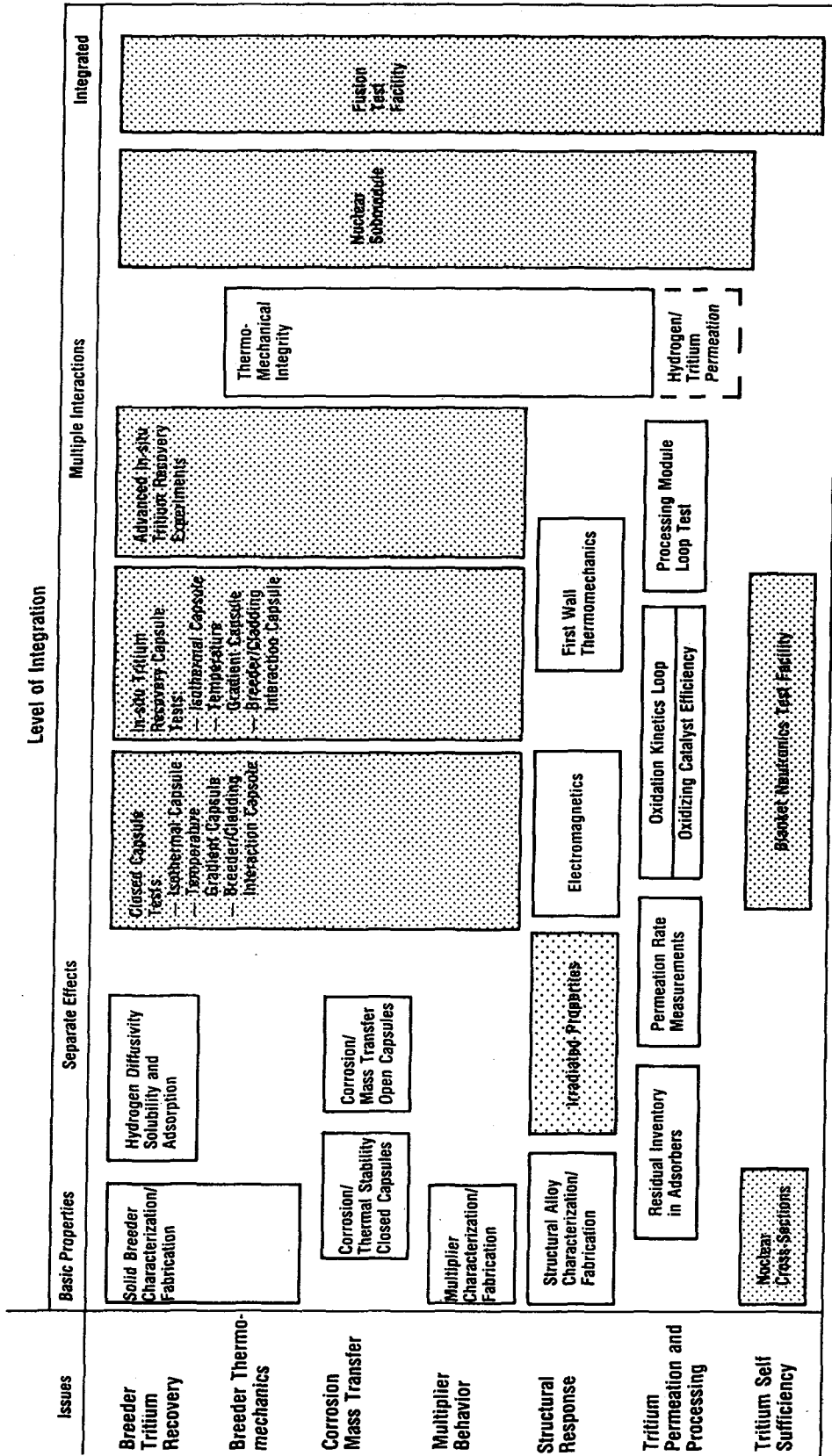
Corrosion and Mass Transfer

Internal and external breeder mass transfer
Breeder/clad corrosion

Tritium Permeation and Processing

First wall permeation rate
First wall tritium inventory with irradiation
Breeder clad permeation rate
Coolant/structure permeation barriers
Breeder/structure permeation barriers
Transient release of first wall tritium inventory
Tritium inventory in processing system

Failure Modes and Reliability



^a Some experiments or facilities already exist.

Figure 4.7-1. Possible experiments for solid breeder blanket technology development.

Table 4.7-2. Material Development and Mechanical Tests

Structural Alloy Development: Irradiation properties of HT-9 base metal and welds (especially DBTT, swelling, He embrittlement) to 15 MW-yr/m², preferably in fusion spectrum. Irradiation properties of PCA. Development and characterization of low activation ferritic and austenitic steels. Basic damage studies. Development of compatible refractory alloy.

Breeder Development: Fabrication development (single-crystal specimens, low impurity content, controlled microstructure - grain size and porosity distribution, sphere-pac); Unirradiated mechanical properties.

Multiplier Development: Beryllium fabrication development (fine grain, low impurity, low BeO, isotropic rods, pebbles and sphere-pac); fabrication and characterization of beryllium/solid breeder mixtures (thermal stability, thermal conductivity); unirradiated mechanical properties.

Unrestrained Breeder Test: Breeder or multiplier tritium and mechanical behavior; closed capsule; isothermal; high burnup, fusion spectrum if possible; uninstrumented; PIE for SB/M swelling, tritium and helium retention, grain growth (e.g., FUBR-1A or -1B subassembly to high burnup).

Partially Restrained Breeder Test: Mechanical interaction of breeder with unyielding clad (e.g., FUBR-1B) or realistic (thickness and material) clad (e.g., FUBR-II); closed capsule; some temperature measurement for thermal conductivity and gap conductance; full breeder ΔT ; thin cladding; PIE for clad/breeder deformation, tritium and helium retention; tests provide modeling data and support design of advanced in-situ tritium recovery experiments.

First Wall Erosion Life: Erosion lifetime of first wall/coating; isothermal; "relevant" plasma conditions. [Assumed treated adequately with PIC development]

Electromagnetic Tests: Effects of static magnetic field on ferritic steel structures; effects of transient magnetic fields on blanket module structure; structural elements tested to determine loading, full breeder module tested to determine response.

Table 4.7-3. Basic Breeder Tests

Diffusivity Measurements: Single-crystal breeder material; 1 mm sphere, 100%TD, small surface area to avoid surface effects; isothermal; use non-irradiated methods for inserting deuterium initially if possible to study basic temperature and impurity dependence; irradiate to provide uniform tritium generation, prefer reaching diffusion eq'm in order to avoid contributions from solubility, etc., although this may require long time; low temperature (400 °C) and high burnup in this phase since this is where diffusion is most likely to be rate-limiting (slow diffusion, no annealing of radiation damage); at low temperatures, recoil (radiation-enhanced diffusion) of tritium may be significant; PIE - thermal anneal to recovery tritium; measure diffusion coefficients of T and He, form of diffusing species if possible; some data exists for Li_2O and Al_2O_3 ; need to develop methods for making single-crystal solid breeder for other than Li_2O ; this is a precise measurement and will take time to perform accurately.

Solubility/Adsorption Measurement: Pure breeder material; isothermal; measure amount H_2O and H_2 absorbed in solid breeder, as a function of gas partial pressure, temperature, oxygen activity; measure solubility by stripping surface of H and determining remaining inventory; not a scoping test, appreciable time required for calibration and equilibration, need to limit interactions with container material; Li_2O may be a little different since probably solubility is more important, but there is also more data; experimental setup can be used for multiple materials.

Thermal Conductivity Measurement: Pure breeder material; isothermal; measure thermal conductivity as function of temperature, porosity, microstructure, burnup and gas pressure; needed at reactor conditions for all solid breeders.

Phase Diagram Measurement: Pure breeder material; isothermal; measure phases of solid breeder system (e.g., $\text{Li}_2\text{O}-\text{Al}_2\text{O}_3$ for LiAlO_2 breeder); partial phase diagrams presently available for Li_2O , LiAlO_2 and lithium-silicate systems.

Thermochemistry Measurement: High purity breeder material; isothermal; two-step process; calorimetry at room temperature to measure free energy of formation of material; separately measure specific heat of material as function of temperature over range of interest; gram quantities material; requires careful calibration and measuring.

Thermal Stability Tests: Standard purity material; isothermal; scoping test; observe reaction kinetics and end-of-blanket life form; particularly needed for Be/solid breeder and lithium beryllate compounds - will BeO surface layers sufficiently inhibit further Be reactions, what is effect of free lithium (sintering, porosity closure).

Mass Transfer Test: Standard purity breeder material; internal (with temperature gradient) and external mass transfer (with flowing purge); measure weight loss of breeder, observe redistribution of an initial Li^0 and Li^7 distribution, measure exiting gas phase species if possible; control H_2O and H_2 at inlet.

Table 4.7-4. Tritium Inventory and Transport Experiments

In-situ Tritium Recovery Experiment: Isothermal; purge flow; 2-3 weeks per test condition at least for tritium equilibrium; low to high burnup; variable temperature and purge conditions; $\Delta T < 50^\circ\text{C}$; thermocouples on clad, some in breeder (effect on local breeder?); oxygen activity control and measurement (if possible, e.g., monitor H_2 , H_2O , O_2 at inlet and exit); on-line chemistry of purge stream exit; tritium content of purge and coolant; PIE for tritium retention (e.g., TRIO-1, VOM-15H, LILA1 type tests)

Advanced In-situ Tritium Recovery Experiment: Full breeder ΔT ; purge flow and composition control; realistic clad; moderate to high burnup; thermocouples, oxygen activity (as above), on-line chemistry at purge exit and in coolant stream; PIE for tritium retention; address tritium release at moderate to high burnup, temperature limits for tritium release, corrosion and permeation.

Transient Tritium Release Experiment: Full breeder ΔT ; full breeder unit cell with high/low fluence regions, high/low temperature regions; purge flow; thermocouples, on-line chemistry in purge and coolant; PIE for tritium retention; tritium response to chemistry transients - purge or coolant interaction is most important test; tritium response to thermal transients (power or coolant); test may be performed at latter stages of Advanced In-situ Tritium Recovery or Nuclear Submodule tests.

Tritium Permeation Tests: Closed capsule; pressurized with tritium gas and other species as appropriate; probably irradiated before permeation measurements if irradiation is part of experiment; isothermal; PIE for remaining inventory; controlled coolant side conditions; includes basic structural material as well as possible permeation barrier materials; vary barrier thickness to see if surface or bulk diffusion is controlling, effects of cracking of barrier; under $10 \mu\text{Ci}$ would allow use of hoods, monitors, no special cleanup systems, may be possible to use tritium only as tracer with measurement accuracy of $\pm 10 \mu\text{Ci}$. [It is assumed that an understanding of basic permeation processes and permeation barriers is largely developed as part of Tritium processing system experiments].

Breeder Stream Extraction Tests: Development of breeder stream extraction process [Assumed developed as part of Tritium processing system experiments].

Table 4.7-5. Maximum Non-fusion Device Tests

Blanket Neutronics Facility: Calibrated 14 MeV point neutron source; tests include cross-section measurement, physics benchmark tests, development of measurement techniques, blanket tests, and engineering mockup tests; measurement of neutron flux and energy, tritium production and volumetric heating rate; very low fluence sufficient for neutronics verification.

Non-nuclear Thermomechanical Integrity Test Facility: Maximum non-nuclear test; full blanket module; full power (volumetric plus surface); surface heating sources include radiant filaments or arcs, neutral beams and plasmas; volumetric heating provided by bulk source such as RF if possible, or by discrete resistive heating; full purge and coolant flow; thermocouples, strain gauges, coolant flow conditions; post-test examination for mechanical integrity; tests of normal operating conditions, fatigue life, design power margin, severe transients.

Nuclear Submodule Test Assembly: Largest size section of breeder region that can fit into fission reactor test volume and achieve high power/high burnup levels; in principle, reactor core modifications could be made to fit a full-sized module in at a high power density; full mechanical, coolant flow and tritium recovery simulation of blanket submodule; ex-reactor measurement and control of coolant and purge conditions, limited number of in-test cladding and coolant thermocouples and strain gauges; PIE examination for tritium inventory distribution, mechanical integrity.

experiments addressing beryllium uncertainties (fabrication, form, swelling, mechanical properties, tritium transport). The general importance of a neutron multiplier also suggests that some effort should be directed towards more effective combinations of multiplier and breeder - for example, lithium beryllates, LiAlO_2/Be or BeO mixtures.

The next major series of experiments will provide more reactor-relevant information, with in-situ tritium recovery from more geometrically relevant breeder. The particular options are either an Advanced In-situ Recovery experiment with many capsules containing different materials, temperature gradients, and breeder/clad interaction in an idealized (cylindrical pellet) geometry; or a Nuclear Submodule test with more design-specific features. The choice between these would depend on whether a suitable design concept was available. If so, then a more integrated test might be appropriate in order to provide an early demonstration of solid breeder blanket feasibility and to direct subsequent research more effectively.

The number of the larger scale experiments is limited by costs, but are important for demonstrating feasibility and attractiveness. The need for them is to a large extent based on the magnitude of remaining uncertainties at that point in time. If there are still significant concerns, particularly over safety or general thermomechanical behavior, then more emphasis on these tests would be necessary, including larger-scale non-nuclear tests.

The overall program requires continuing support through model development and design studies. These are needed to support decisions on material selection, design selection, and the need for the larger-scale tests. Table 4.7-6 indicates the major modelling needs in the various technical areas.

All these experiments can generally be performed in existing facilities, from benchtop properties measurements to in-core irradiation. Fission reactors in general seem able to provide a good simulation of the most significant parameters for the critical breeder-related issues. Thus the program is not facing decisions on building major new facilities in general, although a major non-nuclear test facility would require construction. The larger part of the program cost is in the actual experiments themselves, each module, submodule, assembly or capsule is not generally reusable. The requirements imposed by fission reactor safety generally demand a high level of design and

Table 4.7-6. Modelling Needs

Material Development and Characterization

Thermal conductivity as a function of microstructure
Swelling of breeder material

Tritium Recovery

Tritium diffusion with impurities and radiation damage
Time-dependent tritium recovery with changes in temperature profile
and internal structure

Breeder/Clad Mechanical Interaction

Creep and swelling interaction between breeder and clad - effects on
breeder and on clad
Creep and swelling of beryllium elements

Structural Behavior

Inelastic fracture mechanics, plastic crack growth
Simple models for high fluence/high temperature failure-related
phenomena (e.g., creep buckling, creep/swelling)

Corrosion and Mass Transfer

Breeder internal mass transfer (vapor phase transport and liquid-phase
sintering)

Neutronics and Tritium Breeding

Improvements in 2-D and 3-D code capabilities

Tritium Processing and Permeation

--

fabrication care in each test which makes each experiment fairly time and money consuming. Thus, the major program choices are which particular experiments are needed, not which facilities or which types of experiments.

NOMENCLATURE FOR CHAPTER 4

ADIP	U.S. Alloy Development and Irradiation Program
ANL	Argonne National Laboratory
DAFS	U.S. Damage and Fundamental Studies program
DBTT	Ductile-to-brittle transition temperature
dpa	Displacements per atom
EBR-II	Experimental Breeder Reactor II (U.S. liquid metal fast reactor)
EPRI	Electric Power Research Institute
FFTF	Fast Flux Test Facility (U.S. liquid metal fast reactor)
FMIT	Fusion Materials Irradiation Test (high-flux DLi neutron source)
FNS	Fusion Neutron Source (JAERI accelerator-based DT neutron source)
FS	Ferritic steel
FUBR	U.S. closed-capsule solid breeder experiments
GA	General Atomic
HEDL	Hanford Engineering Development Laboratory
HFIR	High Flux Isotope Reactor (U.S. mixed-spectrum reactor)
HT-9	Ferritic steel alloy
INEL	Idaho National Engineering Laboratory
JAERI	Japan Atomic Energy Research Institute
LANL	Los Alamos National Laboratory
MOTA	Materials Open Test Assembly at FFTF
ORR	Oak Ridge Research Reactor (U.S. thermal reactor)
PCA	Primary Candidate Alloy (U.S. Ti-modified austenitic steel alloy)
SNLL	Sandia National Laboratory - Livermore
TBR	Tritium breeding ratio
TD	Theoretical density
TEM	Transverse Electron Microscope
TFTR	Tokamak Fusion Test Reactor at Princeton
TRIO	U.S. LiAlO ₂ in-situ tritium recovery experiment
TSTA	Tritium Systems Test Assembly at LANL
TPX	Tritium Plasma Experiment at SNLL

CHAPTER 5

TRITIUM PROCESSING AND VACUUM SYSTEMS

TABLE OF CONTENTS

5. TRITIUM PROCESSING AND VACUUM SYSTEMS

	<u>Page</u>
5.1 Introduction.....	5-1
5.2 Tritium Monitoring and Accountability.....	5-6
5.2.1 Monitor Sensitivity.....	5-6
5.2.2 Accountability.....	5-7
5.3 Tritium Permeation and Inventory.....	5-10
5.3.1 Issues.....	5-10
5.3.2 Phenomena and Key Parameters.....	5-10
5.3.3 Experiments and Facilities.....	5-12
5.4 Fuel Cleanup System.....	5-15
5.4.1 Plasma Impurity Content.....	5-15
5.4.2 Component Reliability and Inventory.....	5-18
5.5 Breeder Tritium Extraction.....	5-20
5.5.1 Issues and Key Parameters.....	5-20
5.5.2 Breeder Tritium Extraction Methods.....	5-24
5.5.3 Experiments and Facilities.....	5-33
5.6 Detritiation Systems.....	5-41
5.6.1 Air Detritiation.....	5-41
5.6.2 Water Coolant Detritiation.....	5-43
5.6.3 Helium and Liquid Metal Detritiation.....	5-45
5.7 Vacuum Pumps and Valves.....	5-46
5.7.1 Compound Cryopumps.....	5-46
5.7.2 Vacuum Valves.....	5-48
5.8 Integrated System Behavior.....	5-53
5.8.1 Operation and Control.....	5-53
5.8.2 DT Losses from System.....	5-55
References.....	5-60

LIST OF FIGURES

<u>Figure</u>	<u>Page</u>
5-1 TSTA main process loop and auxiliary systems.....	5-1
5-2 Breeder tritium processing system.....	5-22
5-3 Tritium mass flow rate and concentration operational ranges for different processing systems using gaseous tritium carriers.....	5-23
5-4 Tritium volume flow rate and concentration operational ranges for different processing systems using gaseous tritium carriers.....	5-23
5-5 Tritium concentration as a function of partial pressure for different tritium carrier fluids.....	5-25
5-6 Blanket concept with coolant processing system.....	5-25
5-7 Influence of tritium concentration at extraction unit outlet on flow rate fraction to extraction unit for Li and LiPb.....	5-29
5-8 Influence of tritium concentration at extraction unit outlet on flow rate fraction to extraction unit for He.....	5-29
5-9 Schematic representation of tritium processing schemes.....	5-31
5-10 Small scale component test set-up for tritium extraction from He streams.....	5-40
5-11 Layout of vacuum test stand.....	5-49
5-12 Major functions of vacuum test stand.....	5-50
5-13 Primary separations in DT fuel cycle for TSTA with all gaseous waste (200 Ci/yr) FCU process.....	5-57
5-14 Residual water after regeneration as a function of regeneration temperature for different purge gas dew points.....	5-59

LIST OF TABLES

<u>Table</u>	<u>Page</u>
5-1 Issues/Facilities Matrix for Tritium Systems.....	5-4
5-2 Tritium Processing and Vacuum Test Plan.....	5-5
5-3 Key Parameters for Permeation Experiments.....	5-11
5-4 FCU Inlet Quantities (Maximum).....	5-16
5-5 Range of Inlet Parameters for Tritium Extraction Systems.....	5-22
5-6 Tritium Processing Methods for Different Tritium Carrier Fluids.....	5-28
5-7 Breeder Tritium Extraction Experiments.....	5-34
5-8 Personnel and Environmental Protection Guide for Tritium Handling...	5-35
5-9 LiPb Tritium Recovery System Parameters.....	5-37
5-10 TSTA Gaseous Impurity Load and Waste Gas Flow Rates for Fuel Cleanup (FCU) Process.....	5-56

5. TRITIUM PROCESSING AND VACUUM SYSTEMS

5.1 Introduction

The path of research and development for tritium processing technology for fusion reactors looks rather different from the paths for all other technologies, with the possible exception of superconducting magnets. The reason for this is a unique set of circumstances in tritium technology that has resulted in both the need and the ability to build a "partially integrated test facility" for tritium processing relatively early in the fusion program schedule. The partially integrated test facility (PITF) for tritium is the Tritium Systems Test Assembly (TSTA) constructed at Los Alamos National Laboratory. Design and construction of TSTA began in 1977, was completed in late 1982, and was phased into tritium operations beginning in 1984.

The TSTA design exhibits three chief characteristics of a partially integrated test facility:

- TSTA is an integrated assembly of relatively complex subsystems. Figure 5-1 below is a block diagram of TSTA.

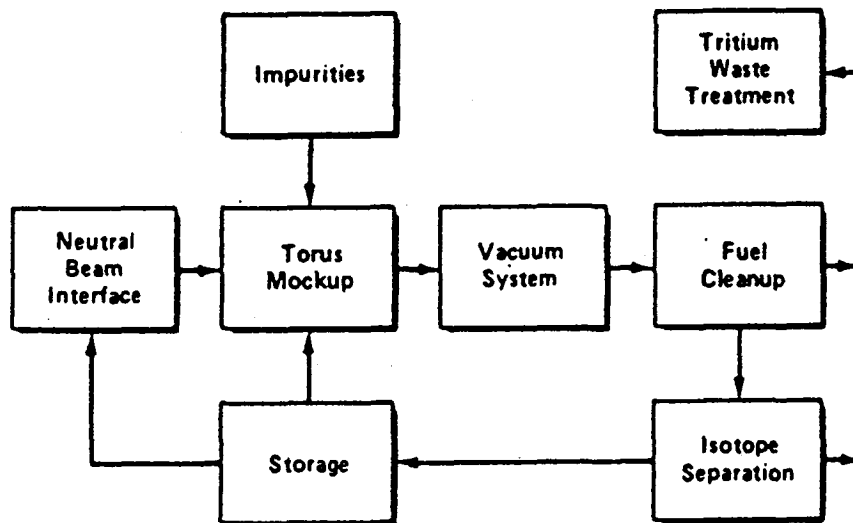


Figure 5-1. TSTA main process loop and auxiliary systems.

- TSTA is a full-scale assembly for processing 1000 g of tritium per day. This flowrate is the same order of magnitude as a commercial scale fusion reactor.
- Among the stated objectives of TSTA is the demonstration of long-term reliability of components.

The unique circumstances that prompted the construction of sophisticated PITF for tritium processing earlier than other PITF's can be summarized as follows:

- Tritium handling and treatment is needed in fusion experiments well in advance of the need for other technologies, such as tritium breeding blankets.
- A demonstration of the ability to handle tritium safely over an extended period of time is critical to the general acceptance of fusion energy.
- Even though the tritium processing systems at TSTA are full-scale systems, they are still generally of a small size (1/4-inch process lines) that makes full scale systems more practical to build than scaled down versions.

The equally unique circumstances that made the construction of a sophisticated PITF for tritium processing feasible are:

- The fusion community was able to build on a substantial base of tritium experience inherited from national security programs.
- Because tritium processing systems do not require neutrons and in most cases can be located outside of neutron environments, the complication of neutrons could be avoided in the design of TSTA.

In light of these circumstances and the resultant fact that TSTA was built and is now operating, it is not surprising that the remaining technical issues in tritium processing tend to be issues dealing with integration of tritium systems and with the interfaces between tritium systems and other systems. The existence of TSTA also necessarily influences the path of R & D in tritium processing. Other technology areas in this study have no corresponding integrated test facility and no corresponding factor to consider in laying out test plans. With an existing facility, some effort necessarily shifts from the task of shaping a test facility to the task of shaping experiments, modifications, and interactions with other technologies to realize the maximum programmatic return from the capital investment in the

facility. These factors have contributed to the directions and plans discussed in this report.

An overview or summary of the technical issues in tritium and vacuum, and the experiments and facilities needed to resolve them, is shown in Tables 5-1 and 5-2. The first lists the subject areas and indicates all of the facilities, both existing and new, that contribute to the understanding and resolution of the issues. Of the facilities listed, all but three are dictated primarily by the needs of other (non-tritium, non-vacuum) issues, but would yield information also relevant to tritium processing and vacuum. The three facilities primarily for answering tritium/vacuum issues are a vacuum facility, glovebox tests, and the flow process facility (TSTA).

Table 5-2 summarizes the sequencing, increasing complexity, and integration of experiments in the related areas. Details of the issues, experiments, and facilities are developed in the remainder of this chapter.

Table 5-1. Issues/Facilities Matrix for Tritium Systems

Issues	MAN-NEUTRON TESTS						FISSION REACTORS				POINT NEUTRON SYSTEMS				FUSION DEVICES		
	Nm-T Benchtop Tests	Vacuum Facility	Glove Box Tests	Plasma Interact. Facility	Flow Process Facility	Blanket Test with Extract.	Specimen Test	Blanket Test with Extract.	Balance of plant	Specimen Test	Blanket Test with Extract.	Balance of plant	Plasma Confinement Exp.	Existing DT Exp.	Ignition Device	FRF	
1. Monitoring & Accounting a. Monitor sensitivity b. Accountability	L L	- -	M L	- -	M M	L(1) L(1)	L -	H(1) M(1)	M L	L M(1)	M L	M L	- -	L M	H M	H H	
2. Permeation & Inventory a. Plasma driven permeation b. Pressure driven permeation c. Inventory	M M M	- - L	L H M	H L M	- L L	L(1) L(1) L(1)	L M M	L(1) L(1) M(1)	- - L	L M M	L(1) L(1) M(1)	- - L	L - M	L - H	L - H	H H H	
3. Ref. Clean-up System a. Plasma impurity content b. Component reliability & Inventory	- M	- M	- H	L -	- H	- -	- -	- -	- -	- -	- -	- -	L -	L M	H M	H H	
4. Breeder Stream Extraction a. Blanket impurity content b. Blanket processing	- M	- -	- M	- -	- M	M(2) M(2)	- -	M(1) M	- -	- -	M(1) M	- -	- -	- -	M(2) M(2)	R R	
5. Detritiation Systems a. Air b. Water coolant	M M	- -	L M	- -	H M	- -	- -	- -	M H	- -	- -	- L	- -	L L	M M	H H	
6. Vacuum Pump & Valves a. Mechanical Lifetime b. Effects of tritium	M -	H H	- -	L L	H H	- -	L -	- -	- -	- -	- -	- -	L -	H M	H H	H H	
7. Integrated System Behavior a. Operation & control b. DT losses from system	- -	- -	L L	- L	H M	L L	- -	L L	L L	L L	L L	L L	- -	L L	M M	R H	

(1) Also useful without extraction
(2) M for liquid metal blankets, L for solid breeder blankets

Ranking:

- : No particular use
- L: Low usefulness
- M: Medium usefulness
- H: High usefulness

Table 5-2. Possible Experiments and Facilities for Tritium Processing and Vacuum Systems
(Some facilities already exist)

ISSUES	LEVEL OF INTEGRATION		
	Basic Properties	Separate Effects	Multiple Interactions
Water and Air Detritiation			Detritiation of heavy water (CANDUS, 70's)
			Glove box air detritiation (60's)
Monitors			Monitor development and use (national security programs, fission reactors, 50's-80's)
			Cryogenic stills (SRL & Grenoble, 70's)
Fuel Processing			Purification for fission reactors (60's)
			Fuel processing facility (TSTA, 80's)
Tritium Permeation			Tritium plasma facility
			Ion beam implantation facility
Vacuum			Vacuum component test stand
			Permeation rate measurements
Blanket Tritium Recovery			Oxidation kinetics loop
			Development of large tritium-compatible vacuum components
			Residual inventory in adsorbers
			Oxidizing catalyst efficiency
			Permeation and diffusion mechanisms
			Liquid breeder extraction techniques
			Blanket tritium (with neutrons) recovery loop test
			Fuel processing facility with blanket interface
			Confinement experiment
			(tritium burning)
			Fusion test facility
			Blanket testing module

5.2 Tritium Monitoring and Accountability

5.2.1 Monitor Sensitivity

Issues

The subject of tritium monitoring at a fusion reactor can be divided into two parts: process monitoring and environmental monitoring. The latter includes room and stack monitoring and is primarily concerned with safety. However both are related to accountability.

Environmental monitoring of fusion reactors has been well covered in Chapter VIII of FED-INTOR/TRLJ/82-5 (pp 179-186).⁽¹⁾ The chapter may be summarized as follows.

Current state-of-the-art instruments for environmental monitoring have adequate sensitivity, response and reliability for routine monitoring without interference from extraneous radiation sources. To varying degrees, all are sensitive to external penetrating radiation although in some cases this sensitivity can be greatly lessened. To locate such an instrument within the radiation field of a reactor hall is completely unnecessary since the hall atmosphere may be readily sampled remotely. Nevertheless, the activated air produced by reactor neutrons creates an additional monitoring problem for conventional instruments. Two instruments recently developed for TFTR that can measure tritium in the presence of such activated air are currently being installed at Princeton and will be tested during the next few years. These instruments have adequate sensitivity through their slow speed of response (several minutes) is a problem for detecting releases rapidly. It is recommended therefore that continued development of such instruments be encouraged with a view to improving their performance under these conditions.

Process monitoring generally involves basically the same kind of instrumentation as that employed for environmental monitoring. Most process gas monitors employ flow-through ionization chambers which are also sensitive to external, penetrating radiation (e.g. 100 Ci/m³ equivalent per mr/h gamma or x-ray). Scintillation detectors have been used for gases as well as liquids. They are likewise sensitive to other radiation although some discrimination is possible by means of pulse shape or rise time discrimination

and by the use of coincidence/anticoincidence techniques. The high radiation fields within an inner reactor shield would probably preclude the use of most, if not all, tritium process monitors within this high radiation area. Outside of the shield, however, process monitoring may be feasible depending on the required specifications for the monitor and the local environmental radiation conditions. Thus it is not possible to say at this time what further development work is needed for process monitoring until the radiation conditions and the specific monitoring requirements are specified.

However, it should be noted that in general, tritium monitor detectors are sometimes rendered less reliable by "memory" effects produced by contamination (especially by HTO) when the tritium concentration at the detector is reduced several orders of magnitude. The background from contamination, which is generally not a problem with environmental monitors, is one that probably needs further study.

5.2.2 Accountability

Issues

Present DOE criteria may call for 100 Ci (0.01 g) accuracy in tritium processing systems. However, in a fusion reactor with 1 kg/d circulating tritium and several more kilograms in storage, this implies 0.001% accuracy. Furthermore, tritium is subject to decay, burnup, creation and permeation over a large surface area of piping, and will be present in a variety of phases and chemical compounds.

Clearly, while tritium inventory must be accountable, present criteria are technically unrealistic. Part of this issue is a regulatory issue- deciding exactly what is important to monitor and what tritium uncertainties are appropriate to meet the real concerns. For example, from the safety viewpoint, it is the vulnerable tritium inventory that must be controlled, and this may only be 10% of the total. Or it may be acceptable to treat the reactor as a black box and monitor very carefully for tritium crossing the boundaries.

The second part of this issue is technical. The requirements will always be stringent, and it is necessary to develop reliable real-time tritium monitors with good resolution even under fusion reactor conditions. This may be coupled with a comprehensive computer model of the tritium inventory. For example, tritium implanted in limiters or divertors could be as much as 1 kg, and would have to be measured or modeled. At present, periodic shutdown might be necessary to check specific inventories.

The accountability issue is really two issues that are presumably interrelated. The first issue is what will be the regulatory requirements for accounting in fusion machines. The second is what is the best accuracy in accounting that can be achieved. For now, the fusion program must work to develop the best accounting technology it can.

Description of Phenomena

Currently the best methods of accounting are off-line, batch measurements of pressure-temperature-composition in vessels of calibrated volume. The best accuracy expected is about $\pm 0.25\%$. Such accountings might be done every six months and would involve shutting down facility operations to do the accounting.

On-line accounting involves three components:

- instrumentation for measuring tritium concentration in flowing lines (e.g. ionization chambers or laser Raman spectroscopy) and for measuring flow rate;
- dynamic simulation models of the tritium processes; and
- multiple material balances and decision analysis techniques(2).

Experiments and Facilities

Development of the instrumentation for accounting is reasonably well advanced. Ion chambers, laser Raman spectroscopy, and flowmeters are available and are under continual improvement at TSTA. Improvements in ion chambers have also been made by the Canadians as a product of work for CANDU reactor sites.

The most work on accounting is needed in the development of modeling capabilities of the tritium processes. Models are needed for estimating tritium concentrations in first wall and limiter materials, in blanket materials under realistic operating conditions, and in tritium processing systems. Progress in understanding is being made in the latter area at TSTA although little modeling has yet been done. Further work at this facility should produce the necessary mathematical relationships. Similarly, experiments and analyses in conjunction with blanket tests and blanket test facilities are needed to develop the needed relationships between tritium inventory and operating conditions for blankets.

Calculations have been made for tritium inventories in first walls, but great uncertainty exists. Studies to gain understanding of permeation through the first wall also yield information on tritium inventory in the first wall (see Section 5.3).

The analytical tools other than process modeling are fully in hand. These tools are the techniques of decision analysis and material balances that are directly usable with little modification from the methods developed for use in fission fuel accounting⁽²⁾.

Modeling Requirements

Development of system tritium inventory and transport models is the major need for improving tritium accountability.

5.3 Tritium Permeation and Inventory

5.3.1 Issues

Tritium permeation through first walls, limiters, or divertors subjected to energetic tritium ion or charge-exchange neutral bombardment (plasma driven permeation, PlDP]) is a critical concern for advanced D-T reactors operating at elevated temperatures. A high concentration of tritium in the near surface region can occur by implantation of tritium atoms combined with relatively slow recombination into molecules at the plasma/wall interface. Because of the large concentration of mobile tritium near the plasma wall surface, a concentration gradient is established, causing tritium to diffuse into the bulk and to the other wall surface where it can enter the coolant.

High tritium permeation would result in larger tritium processing systems and additional shielding requirements. High tritium inventory in structures would result in access problems for maintenance, a tritium loss from the fuel cycle, and a potential safety concern during accidents.

Another critical issue is the tritium permeation through structures such as the breeder cladding (separately cooled breeders) and the heat exchanger due to different partial tritium pressures at both sides of the structure (pressure driven permeation, PrDP).

This kind of permeation determines the tritium losses to the surroundings and is therefore a substantial safety concern. The design of the tritium processing system is also sensitively dependent on pressure driven permeation.

In order to reduce tritium permeation, barriers of various types (oxide layers; sputtered or bonded layers) are provided at critical locations. The effectiveness of these barriers is uncertain.

5.3.2 Phenomena and Key Parameters

The following mechanisms, described in detail elsewhere,^(3,4) govern PlDP: penetration, desorption, reflection and recombination near the plasma-side wall; diffusion, trapping, molecular recombination in the structure; and molecular recombination and desorption at the coolant surface. The key parameters (see also Chapter 6) are the plasma-side surface conditions, which are strongly dependent on the reactor design; the tritium wall flux T_r and

energy E; the temperature T and temperature gradient $\Delta T/\Delta L$; and the neutron fluence ϕt . Neutron flux may be important in respect to recoil effects. Values for envisaged plasma edge conditions are given elsewhere.⁽³⁻⁵⁾ Table 5-3 contains minimal experiment values which allow extrapolation to reactor plasma edge conditions (e.g., the fluence at which bulk traps are created is estimated to be ≈ 0.1 dpa whereas the anticipated fluence for limiters is $\approx 20 - 50$ dpa).

Table 5-3. Key Parameters for Permeation Experiments

Key Parameters	Plasma Driven Permeation (PlDP)	Pressure Driven Permeation (PrDP)
Temperature ($^{\circ}\text{C}$)	200 - 500 ^a	200 - 500 ^a
Temperature Gradient ($^{\circ}\text{C}/\text{cm}$)	200 - 300	100 - 300
Pulse Lengths (s)	$10^2 - \infty$	$10^2 - \infty$
Neutron Fluence (dpa)	1	1
Tritium Wall Flux ($1/\text{cm}^2\text{-s}$)	10^{15}	--
Tritium Energy (eV)	$\lesssim 1000$	--
γ Radiation	Characteristic of metal under neutron irradiation	
Surface Effects	Characteristic of plasma edge	Characteristic of blanket purge and coolant system
Tritium Partial Pressure (Pa)	--	$10^{-7} - 10^1$ ^b

^aUp to 750 $^{\circ}\text{C}$ for Vanadium; higher for some coatings.

^bDependent on blanket design

In PrDP, T_2 molecules adsorb at the surface, dissociate, diffuse through the structure, recombine at the coolant surface, and desorb. At low partial tritium pressures, P_{T_2} , surface effects dominate the permeation rate \dot{m}_{perm} [$\dot{m}_{\text{perm}} (P_{\text{T}_2\text{u}} - P_{\text{T}_2\text{d}})$] where the indices u and d denote the upstream and downstream condition. At high partial pressures, diffusion is the limiting process [$\dot{m}_{\text{perm}} \propto (\sqrt{P_{\text{T}_2\text{u}}} - \sqrt{P_{\text{T}_2\text{d}}})$]. The value of P_{T_2} where the transition occurs is very uncertain and can be in the range of interest for blanket systems. PrDP is mainly of interest in combination with non-clean surfaces (oxide layers or other impurities). The permeation behavior in this case is

even less predictable due to the poorly known surface conditions (composition, integrity of layers, etc.). Typical values for key parameters for PrDP are also listed in Table 5-3.

5.3.3 Experiments and Facilities

A general view of the usefulness of various facilities to resolve the permeation issues was given in Table 5-1. Chapter 6 also notes the issues related to plasma interactive components. In the following, required experiments are described in more detail, partly based on recommendations published previously.^(4,6) A general characterization of these experiments is that a large portion of the issues can be resolved using test specimens of relative small dimensions (test specimen area $\approx 1 - 100 \text{ cm}^2$). A typical test facility for PlDP is the Tritium Plasma Experiment (TPX) at SNLL⁽⁷⁾, typical facilities for PrDP exist at, for example, KFA⁽⁸⁾ and SNLL⁽⁹⁾. The major experiments and facilities are described below in order of test complexity.

Diffusivity, Solubility, Heat of Transport: The data base for ferritic steels shows some significant variation; the data base for non-metals is extremely poor. The experiments can be performed with small specimens in a non-tritium test stand using protium or deuterium or using small amounts of tritium ($\leq 1 \text{ Ci}$) in a test facility with appropriate safety installation (hood, room monitors, etc.). For simplicity, this kind of facility is termed glove a box facility although a glove box might be required only at much higher tritium inventories (see Section 5.5.3).

Permeation; Clean Surfaces: There are considerable data available for several pure metals and ferritic steels. For many others there are either one or two measurements or ones that are unsatisfactory. For more than a dozen others, mostly rare metals, there are no data whatever. There are few data on ceramics. Data at very low partial tritium pressures are even more limited or contradictory. Again the experiments could be performed in a non-tritium or low-level glove box facility.

Influence of Surface Conditions: For PlDP, the recombination coefficient at the plasma-side wall is sensitively dependent on conditions of the surface. These experiments require either a plasma interactive facility (e.g., PISCES⁽¹⁰⁾) and a separate permeation facility, or a combined plasma tritium facility (e.g., TPX).

For PrDP the behavior of oxide layers and other sputtered or bonded coatings has to be investigated in much more detail. The tests should include thermal cycling. The surface conditions must be measurable (e.g., by Auger electron spectroscopy). A non-tritium or, preferably, glove box facility is required.

Influence of Temperature Gradient: Present tests were performed with uniformly heated probes. For code verification, some benchmark tests have to be performed with relevant temperature gradients in the wall; a TPX-like facility could be used.

Influence of Neutron and Gamma Irradiation: The effects of neutron and gamma irradiation on hydrogen trapping and release are poorly understood. Most of the data base and theory come from ion simulation of neutron damage, and not from actual neutron and gamma irradiations. No real benchmark comparisons exist between simulations and actual irradiations.

Gamma irradiation effects on hydrogen have been recently reviewed by Causey.⁽¹¹⁾ A discussion of photodesorption, as well as enhanced diffusion and detrapping by gamma radiation, can be found there. The present data base is too limited to make any definitive statements on possible gamma effects in fusion reactors. Experiments, such as those of Longhurst,⁽¹²⁾ are underway.

Only a few experiments have been conducted with neutron irradiated materials.⁽¹³⁾ Many more experiments are needed with test specimens irradiated in a fusion reactor or with a point neutron source and then used in a typical PlDP or PrDP facility.

A step further are tests where neutrons and tritium are simultaneously present (combination of fission reactor with PrDP test stand), such as the measurements of Dobrozensky.⁽¹⁴⁾ If benchmark tests have proved that neutron damage can be simulated with ions, the neutron source can be replaced by an accelerator.

Multiple Effect Tests for PlDP: Tests which simultaneously have neutrons, hydrogen ions, high temperature, and temperature differences can be carried out with fusion devices. Information may be obtained from specific exposed test articles (which may contain reactor-relevant surfaces), and from the normal plasma interactive components required to support the machine operation.

Multiple Effect Tests for PrDP: The development of blanket modules will include a range of tests as described in Chapters 3 and 4. These will include reactor-relevant conditions of temperature, stresses, thermal cycling, fluid chemistry, impurities, etc. Pressure-driven permeation may be measured as part of the normal instrumentation of these tests.

Liquid metal blanket tests generally do not include neutrons because of the emphasis on MHD and corrosion related issues. Trace amounts of tritium or larger amounts of protium or deuterium might be injected in order to provide information on pressure-driven permeation under the influence of local chemistry and geometry (which should provide representative surface conditions). Permeation is expected to be primarily a concern for separately-cooled liquid metal blankets, or those where substantial permeation back to the plasma is desired.

Solid breeder blanket tests generally emphasize nuclear testing because of the importance of internal tritium generation and radiation effects. These tests will naturally provide a realistic tritium source term for identifying tritium permeation rates. The key factors are an active purge system because of its influence on the internal chemistry (tritium form, oxide barriers), and an accurate model of the reactor cladding material. In some tests, for example, the cladding is primarily designed to firmly support the experiment and may be of a different material, thickness or mechanical support compared to the blanket cladding.

5.4 Fuel Cleanup System

5.4.1 Plasma Impurity Content

Issues

Impurity removal is the first stage in processing the tritium collected from the plasma exhaust or breeder extraction systems. The Fuel Cleanup Unit (FCU) must be able to handle a range of impurity contents (composition and concentration) and hydrogen throughputs because of variations in plant operating conditions (power level, startup/shutdown, disruptions, aging or other changes), and because of present uncertainties in the actual throughput and impurity mix. Furthermore, due to differences in flow rate, composition, impurities and isotopic abundances, the plasma exhaust and the breeder extraction flows will likely enter the FCU at different points. The output of the FCU, however, is a stream of hydrogen isotopes that are sent on to an isotope separator.

The concern is efficient handling of the known inputs, as well as allowing for their uncertainties (e.g., flow rate, impurities, T_2/T_2O ratio). Present options include combinations of uranium beds, molecular sieves, catalytic oxidation, cryogenic strippers, palladium diffusers and electrolysis cells. However, for the high tritiated vapor throughputs anticipated, uranium beds are reasonably well understood but expensive to operate, molecular sieves are less well-known, and reliable electrolysis cells are not available. TSTA is addressing many of these development and demonstration concerns. However, performance with breeder feed streams (from solid or liquid breeders) is not presently being tested, actual impurity levels are not certain until operation of a DT-burning device, inlet dust and activation product filters are not being tested, and some components need to be developed.

Description of Phenomena

A major subsystem of the Tritium Systems Test Assembly is the Fuel Cleanup System (FCU) whose functions are to: (1) remove impurities in the form of argon and tritiated methane, water, and ammonia from the reactor exhaust stream and (2) recover tritium for reuse from the tritiated impurities. To do this, a hybrid cleanup system has been designed which will test concurrently

two differing technologies--one based on disposable, hot metal (U and Ti) getter beds and a second based on regenerable cryogenic adsorption beds followed by catalytic oxidation of impurities to DTO and stackable gases, and freezout of the resultant DTO to recover essentially all tritium for reuse.

Although the species and concentrations of impurities in reactor exhaust gases are not known with certainty, the best current estimates have led to the design quantities shown in Table 5-4, corresponding to 440 mW of fusion power at a fractional burn of 5%.

Table 5-4. FCU Inlet Quantities (Maximum)

Component	Ratio to ($D_2 + DT + T_2$)	g-mols/day
Q_2^* ($D_2 + DT + T_2$)	1.0	356.
HQ (HD + HT)	0.02	7.
C (<u>CQ_4</u> + CO)	0.001	0.4
O (<u>Q_2O</u> + CO + NO + $1/2O_2$)	0.005	1.8
N (<u>NQ_3</u> + NO + $1/2N_2$)	0.001	0.4
Ar	0.05	<u>18.0</u>
TOTAL FLOW		384.

*Q = any mix of D and T atoms

Principal species underlined

No helium is shown in the feed to the FCU because helium is assumed to be separated from the impure reactor exhaust gases by operation of the compound cryopump at the reactor. This pump collects helium on one adsorbent surface at 4K and collects all other species on another surface. Experiments have shown this separation of helium is easily maintained during regeneration of the cryopump surfaces.⁽¹⁵⁾ However, additional regeneration time is required to do this. If the added time is unacceptable (or if cryopumps are not used), additional processing will be required to remove helium. Several technologies are available for removing helium if necessary.

The purity requirements for the effluent fuel stream from the FCU are determined not by the requirements of fusion fuels, but rather by the needs of the cryogenic fractional distillation system (isotope separation system) which processes the cleaned fuel stream from FCU. Experience has shown that impurity levels must be maintained below 1 ppm to ensure safe, long-term operation of such equipment without blockages or hazardous accumulation of impurities (16).

Two basic process schemes have been devised to meet the requirements of the FCU. The first is a scheme based on adsorption of impurities on molecular sieve beds at 75K, followed by catalytic oxidation of recovered impurities to form tritiated water and tritium-free compounds, freezeout of the water, and electrolysis to recover tritium. The second is based on hot uranium getter beds operated 1170 K to remove impurities as uranium oxides, carbides, and nitrides. Other alternatives are also feasible.

Experiments and Facilities

A fuel cleanup system (FCU) designed for handling what are expected to be maximum impurity concentrations, both in regard to species and amounts, has been installed and is under test at TSTA. The FCU tests both process schemes mentioned above. At every opportunity, information must be gathered about the species and concentrations of impurities (especially to reactive gases) in the plasma exhaust of operating fusion machines. This information can be definitively gained only from DT plasma machines.

In addition to the fuel cleanup system under test at TSTA, various alternative processing components to those in the system are under test and development in glovebox experiments, both with and without tritium, at a number of locations. Such work is underway in Japan (Japan Atomic Energy Research Institute), at TSTA in a joint US/Japan collaboration, in Canada, and more recently within the European Community. The most promising alternative technologies should be tested in an integrated cleanup system.

Modeling Requirements

The ability to predict impurity compositions as a function of fusion machine operating parameters would be advantageous. Such modeling efforts however must wait on initial data from operating machines.

5.4.2 Component Reliability and Inventory

Issues

Completing the information needed about the duties and performance of the fuel cleanup system is information on the reliability of FCU components during realistic system operation (including upset conditions) and information on the tritium inventory in the individual processing components during all operating modes.

The need for component reliability is obvious. Tritium inventory is important to understand for several reasons. Accurate accounting of tritium is required by DOE order (see Section 5.2.2). Knowledge of tritium inventory is also critical to determining the required tritium breeding ratio (tritium bred/tritium burned). Thirdly, knowledge of tritium inventory can help improve both process control and process safety.

Description of Phenomena

The FCU currently employed at TSTA is described in Section 5.4.1. Reliability of these components will be measured and documented in detailed failure reports from the operation of TSTA.

Inventories in the components of FCU have been calculated as part of the design phase of TSTA. These predicted estimates of tritium inventory, subject to experimental verification, indicate a maximum total tritium holdup in the FCU of approximately 34 g.

One inventory question of special concern is the amount of tritiated water adsorbed by molecular sieve beds that is not readily recovered by normal regeneration techniques. This has been further discussed in Section 5.8.2. Information on this will be available from TSTA, as well as from other studies within and without the fusion program.

Phenomena of permeation (both plasma driven and pressure driven) and blanket extraction processes both importantly affect the tritium inventory. These issues are covered in Section 5.3.

Experiments and Facilities

Questions of reliability and inventory are answered in the experiments and facilities designed for basic process and component development. Special experiments and facilities are not required. Thus these issues will be addressed at TSTA, at blanket test facilities, and in permeation tests described elsewhere.

Modeling Requirements

Modeling of reliability and inventory are both important to understanding the reliability and inventory of commercial scale machines based on tests of components. This work is under way for those components being tested at TSTA and should also be an integral part of any blanket test program.

Programs in reliability and availability modeling are under way at the University of Wisconsin's Fusion Technology Institute. An informal task force, called the "Fusion Availability Working Group," has been organized under the cognizance of the DOE Office of Fusion Energy (Reactor Systems Branch).

5.5 Breeder Tritium Extraction

5.5.1 Issues and Key Parameters

The tritium bred in the blanket must be recovered at low levels of tritium concentration and partial pressures in order to minimize tritium inventory and reduce tritium permeation to the surroundings to an acceptable level. Some extraction methods require processing large volume flows, with possible effects on the primary heat transport system (thermal and pumping power). The extraction techniques are different for different tritium carrier fluids: for liquid lithium, the scientific feasibility of achieving acceptable tritium concentrations of less than ~ 7 appm has been demonstrated, but not on an engineering scale. A concern is the effect of the extraction process on the lithium coolant loop. Extractor compounds may enhance lithium corrosion and may impose thermal penalties in self-cooled systems. For liquid LiPb, no tests have been performed, and there is some uncertainty about how to maintain the low partial pressure needed to control permeation. The tritium diffusivity in liquid metals influences strongly extraction efficiency, and is not known sufficiently for either Li or ^{17}Li -83Pb.

Concerning tritium extraction from gas (helium) purge or coolant flows, the tritium inventory in processing units may become considerable which is a safety concern and also increases the required tritium breeding ratio. Another concern is the residual tritium in materials which have to be replaced (tritium waste flow). The scientific feasibility of achieving tritium concentrations of $\sim 10^{-5}$ appm has been demonstrated in air detritiation systems but not for the specific requirements of the breeder tritium extraction systems. The influence of impurities is unclear.

Tritium extraction is a concern for all blankets; the extraction technique and the processing systems requirements are different for the different blanket concepts. Based on the present data, tritium recovery from Li or He purge gas appears feasible to regions relevant to fusion. Tritium extraction of more than a few gram/d from He coolant appears feasible to a partial pressure a few orders higher than required. There are no experimental results for tritium recovery from LiPb.

The tritium processing units are outside the neutron environment. Therefore, neutrons are possibly important only as a source of impurities through sputtering, neutron damage and production of activation products.

The inlet conditions of the processing units are not well-known due to uncertainties in the blanket in respect to

- tritium permeation rate
- hydrogen isotope form and composition
- impurity levels.

Of great importance (and uncertainty) are the effectiveness of the permeation barrier between coolant and heat exchanger and, for separately-cooled breeders, between breeder and coolant. Table 5-5 contains the range of key inlet parameters for the tritium processing systems characteristic for blanket designs discussed previously.⁽¹⁷⁾ The content of this table depends strongly on both the blanket and the tritium recovery system design.

Tritium processing methods are strongly dependent on the tritium carrier fluid. For gaseous tritium carriers, the breeder tritium processing system can be compared with the air detritiation system (ADS) and the fuel clean-up (FCU). The breeder tritium processing system consists of the blanket processing system (BPS) and the coolant processing system (CPS) as shown in Fig. 5-2. For separately-cooled blanket designs, mostly both the BPS and CPS are provided, whereas in self-cooled blanket designs all the tritium has to be processed in the CPS. Recently, separately-cooled blanket designs have been considered where the total bred tritium is only extracted from the coolant.

Figures 5-3 and 5-4 show the operational ranges of the different systems (processed tritium mass flow rate and total volume flow rate, respectively) versus the tritium concentration; the values are for a tritium production of 600 g/d. The tritium mass extracted in air detritiation systems is generally so small (about 0.01 g/d) that these systems are not optimized for tritium recovery from the absorber during the regeneration cycle. Most of the issues related to breeder tritium processing from gas flows are connected especially with the regeneration, therefore ADS experience is of limited value.

Comparing the FCU and the breeder processing system, both the volume flow rates and tritium concentrations differ by several orders of magnitudes. Again the specific issues are very different.

Table 5-5. Range of Inlet Parameters for Tritium Extraction Systems

	Tritium Carrier Fluid			
	LiPb	Li	He	
			BPS ^a	CPS ^b
T Composition:				
Fraction as HT, T ₂ (%)	100	100	1-100	0-99
Fraction as HTO, T ₂ O (%)	0	0	0-99	1-100
Tritium Partial Pressure, P _{T2} (Pa)	10 ⁻⁴ -10 ⁻⁰	10 ⁻⁷ -10 ⁻⁵	0.1-10	10 ⁻⁵ -10 ⁻²
Hydrogen Partial Pressure, P _{H2} (Pa)	0-10	0	0-100	0-10
Oxygen Partial Pressure, P _{O2} (Pa)	0	0	0	0-10
Impurity Levels (appm)	< 10	> 10	< 10	< 10
Temperatures, T (°C)	400-600	450-600	300-500	275-510
System Pressure, P (MPa)	0.1-3	0.1-3	0.1	5

^aBlanket Processing System

^bCoolant Processing System

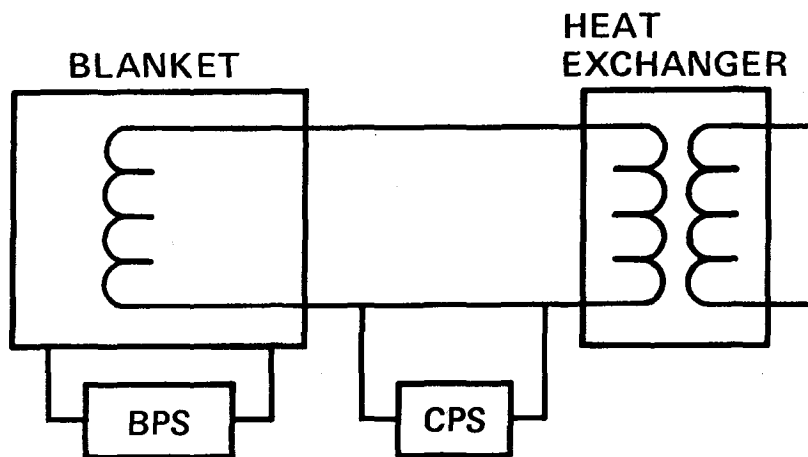


Figure 5-2. Breeder tritium processing systems.

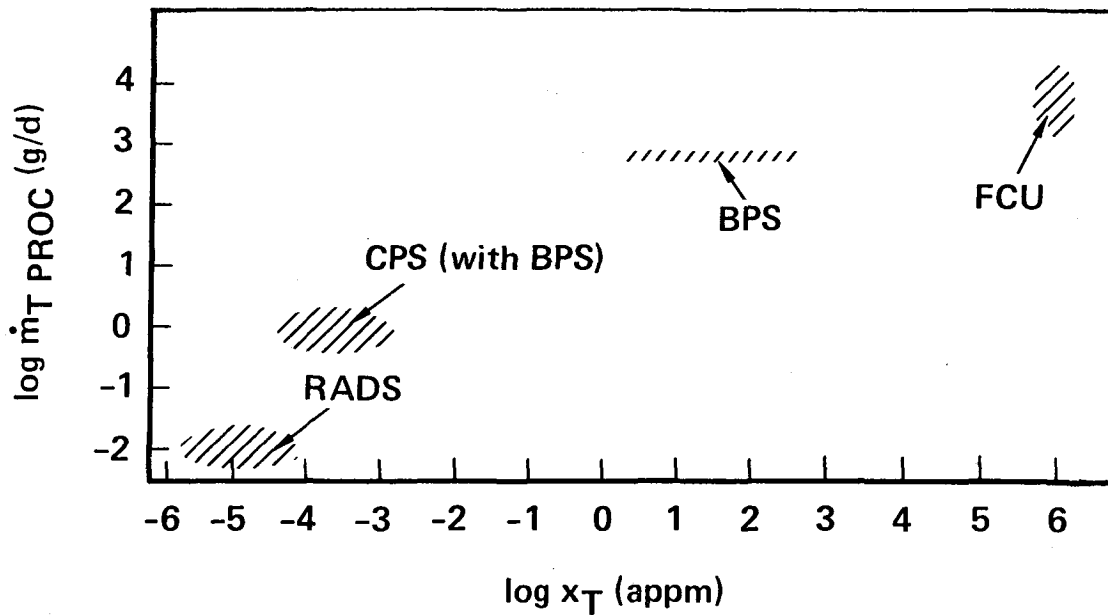


Figure 5-3. Tritium mass flow rate operational ranges of different processing systems using gaseous tritium carriers.

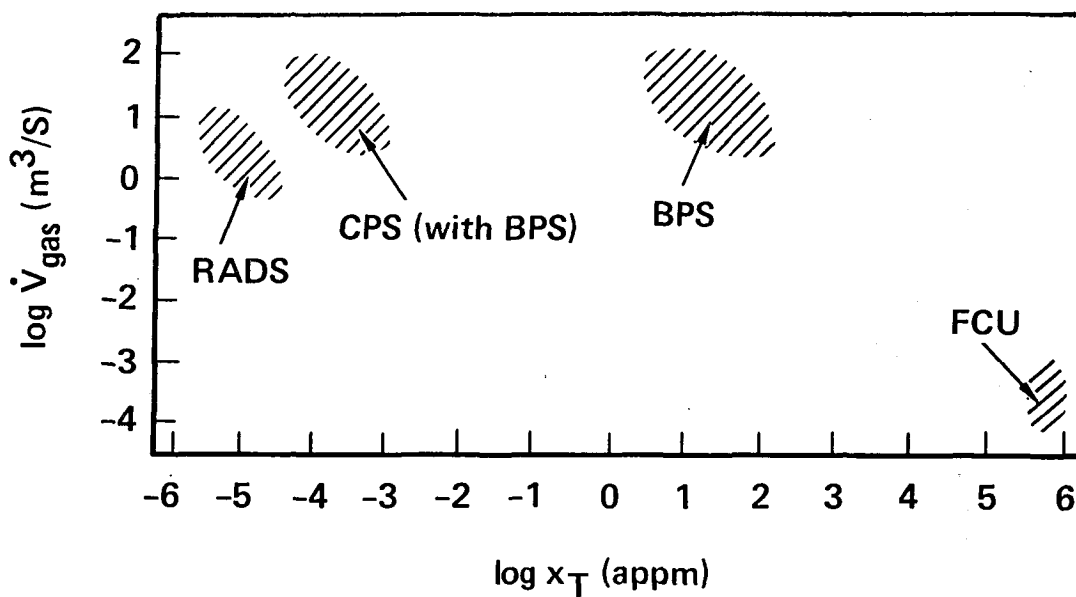


Figure 5-4. Tritium volume flow rate operational ranges of different processing systems using gaseous tritium carriers.

5.5.2 Breeder Tritium Extraction Methods

General Considerations

Tritium extraction methods are different for different tritium carrier fluids mainly due to the different tritium concentrations for a given partial pressure. For liquid metals, the relationship between tritium concentration, x , and tritium partial pressure, p_{T2} , is given by Sievert's Law:

$$x_T = K \sqrt{p_{T2}} \quad (5-1)$$

and for diluted gases by Dalton's Law:

$$x = 2p_{T2}/p_s \quad (5-2)$$

where K is the Sievert's Constant; with $K = 11000$ (appm/Pa^{1/2}) for Li and 0.546 for 17Li-83Pb, and p_s is the system pressure. Figure 5-5 shows the dependence of x on p_{T2} for Li, 17Li-83Pb and He at $p = 5$ MPa. With increasing partial pressure p_{T2} , tritium extraction becomes easier but tritium permeation and inventory increase.

For Li, permeation represents a relatively minor problem. However, the partial pressure has to be small to keep the tritium inventory small. For LiPb and He, tritium inventory is a minor problem compared to tritium permeation, and again the allowable partial pressure has to be very small.

For quantitative discussion, the system according to Fig. 5-6 is considered, typical for a liquid metal cooled or gas cooled blanket without a blanket (breeder) processing system. For simplicity, the quantities characterizing the steam generator are assumed to be the same for all three cases; the coolant mass flow rates relate to each other as do the coolant heat capacities (assuming the same coolant temperature rise, for example). The different quantities are given in Fig. 5-6, where f is the rate of the processing unit mass flow rate to the coolant mass flow rate, and the indices l , p , and HX characterize the location downstream of the blanket, downstream of the processing unit and at the heat exchanger, respectively.

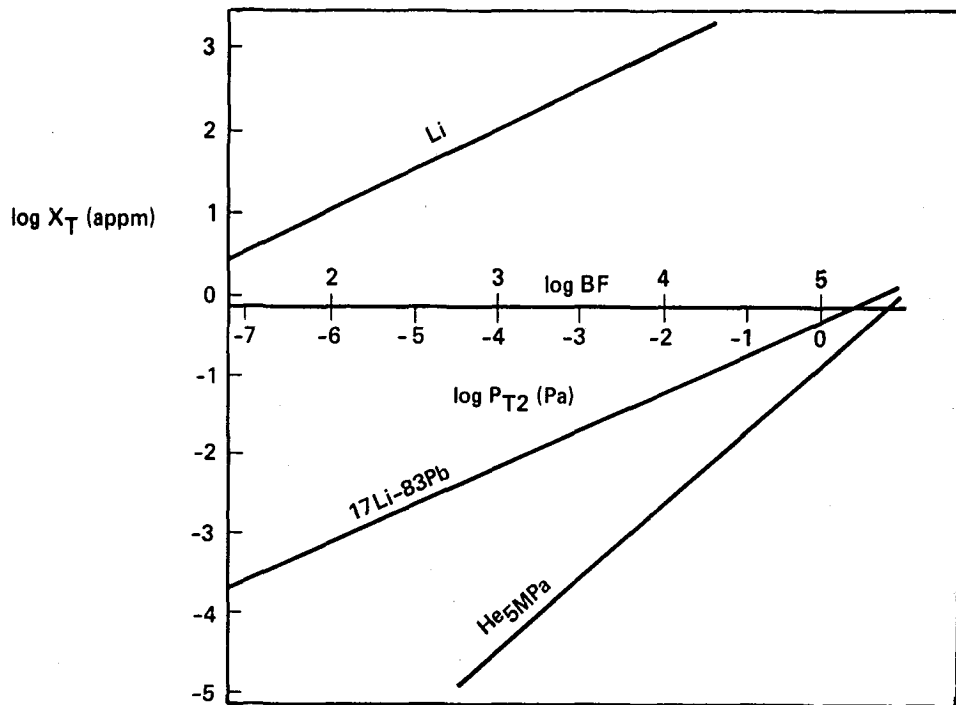


Figure 5-5. Tritium concentration as a function of partial pressure for different tritium carrier fluids.

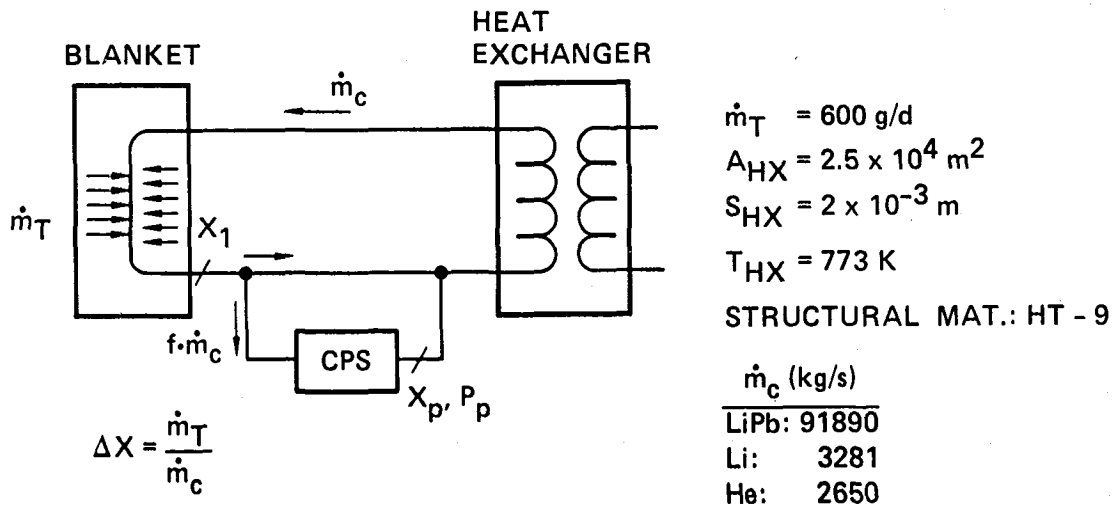


Figure 5-6. Blanket concept with coolant processing system.

Figure 5-5 also shows the required permeation barrier factor BF at the steam generator for a tritium permeation rate $\dot{m}_{\text{perm}} = 10 \text{ Ci/d}$ calculated according to

$$\dot{m}_{\text{perm}} = \frac{P}{\text{BF}} \frac{A_{\text{HX}}}{S_{\text{HX}}} \sqrt{P_{\text{T2}}} \quad (5-3)$$

where P is the permeability, $P = 2.2 \times 10^{-10} e^{(-11100/RT)} \text{ kg/m.s.Pa}^{1/2}$ for HT-9, and A_{HX} is the area and S_{HX} the wall thickness of the heat exchanger. P_{T2} and x_{T} in Fig. 5-5 correspond to the conditions at the primary side of the heat exchanger. Since a typical assumed value for the heat exchanger permeation barrier is $\text{BF} = 100$, Fig. 5.5 emphasizes the need to achieve very small concentrations especially for $^{17}\text{Li}-^{83}\text{Pb}$ and He. While the desired values of x_{p} , the tritium concentration at the outlet of the processing unit are known for reactor systems, the achievable x_{p} at an acceptable cost is presently highly speculative.

Small values are required and there are several means by which the required x_{p} can be obtained. However, these means have a strong impact on size, flow rate and power consumption, and consequently cost of the blanket tritium recovery system. Methods to achieve the required x_{p} are:

- to increase the extractor flow rate for tritium extraction from liquid metals or the extractor volume for tritium extraction from helium flows.
- to increase extraction efficiency, such as by decreasing the residual concentration in the extractor after regeneration.
- to add other hydrogen isotopes, usually protium.

The first two methods have a strong impact on the size of the extraction system. For instance the tritium concentration and volume flow rates of the countercurrent helium flow for the LiPb extraction concept may become comparable to the coolant conditions in helium-cooled blankets.

The addition of other isotopes (isotope swamping) is often used to improve the efficiency of chemical reactors. If the concentration of the sum of the isotopes at the outlet is constant, then the outlet tritium concentration with isotope swamping, x_{pis} , is

$$x_{\text{pis}} = \frac{\dot{m}_{\text{T}}}{\dot{m}_{\text{H}} + \dot{m}_{\text{T}}} x_{\text{p}}$$

where \dot{m}_T is the tritium mass flow rate to be processed and \dot{m}_H is the added protium or deuterium mass flow rate. The added isotopes have to be separated subsequently by, for example, cryodistillation. The additional effort for this process is dependent on the ratio \dot{m}_H/\dot{m}_T and is relatively small for $\dot{m}_H/\dot{m}_T = 100$. If isotope swamping is used for T₂O extraction (addition of H₂O), the processing unit to decompose hydrogen and oxygen also has a much higher load; the influence on this process step (e.g., electrolysis) is more uncertain.

Table 5-6 contains values for x_p from design studies (17Li-83Pb) and experiments (Li, He) with no isotope swamping. The values for 17Li-83Pb (not experimentally verified) represent a power reactor with high temperature operation and a 10 Ci/d leakage rate goal,⁽¹⁸⁾ and INTOR/NET with low temperature operation and higher allowed permeation into the water (the cost of water de-tritiation was considered acceptable in this design). The value $x_p = 7$ for the Li system was determined in a small-scale laboratory experiment;⁽²⁰⁾ the values for extraction using solid getters or molecular sieves are better known and were measured in TSTA, for example.

The dependency between mass flow rate ratio f and tritium concentration at the heat exchanger x_{HX} , at the processing unit outlet x_p is given by

$$f = \frac{1}{1 + (x_{HX} - x_p)/\Delta x} \quad (5-4)$$

where Δx is the tritium production rate per pass

$$\Delta x \text{ (appm)} = 2 \cdot 10^6 \frac{\dot{m}_T}{\dot{m}_C} \frac{M_C}{M_{T2}},$$

M is the molecular weight, \dot{m}_T is tritium generation rate and \dot{m}_C is the coolant mass flow rate. For the present example, Δx is 0.0049, 0.0043 and 0.0034 appm for Li, 17Li-83Pb and He.

Figures 5-7 and 5-8 show the required mass flow rate ratio f as a function of an assumed tritium outlet concentration and the partial tritium pressure at the steam generator. The required permeation barrier factor to maintain 10 Ci/d permeation across the heat exchanger is also shown. For Li, the partial tritium pressure p_{HX} is less than 10^{-6} Pa and the required barrier

Table 5-6. Tritium Processing Methods for Different Tritium Carrier Fluids

T Carrier Fluid	T Form		Extraction Method ^a	Minimum T Concentration X _p (appm) ^b	Other Application of Method
	T ₂ /HT	T ₂ O/HTO			
LiPb	X		Vacuum degassing	10 ⁻² , 5	None
	X		<u>Extraction with counter-current He flow</u>		
	X		Permeation combined with catalytic oxidation		
Li	X		Absorption with solid getters	7	None
	X		<u>Extraction with molten salt</u>		
He	X	X ^c	<u>Absorption with solid getters</u>	10 ⁻⁵	Fuel clean-up Air detritiation
	X ^d	X	<u>Adsorption with molecular sieves</u>	10 ⁻⁵	
	X ^d	X	Freezing out in cold traps		
H ₂ O		X	VPCE, LPCF, electrolysis		CANDU reactor coolant clean-up

^aPreferred method underlined.

^bTritium concentration at processing system outlet from various design studies (LiPb) and experiments (Li,He).

^cAdditional process needed to decompose T₂O, HTO.

^dAdditional process needed to oxidize T₂, HT.

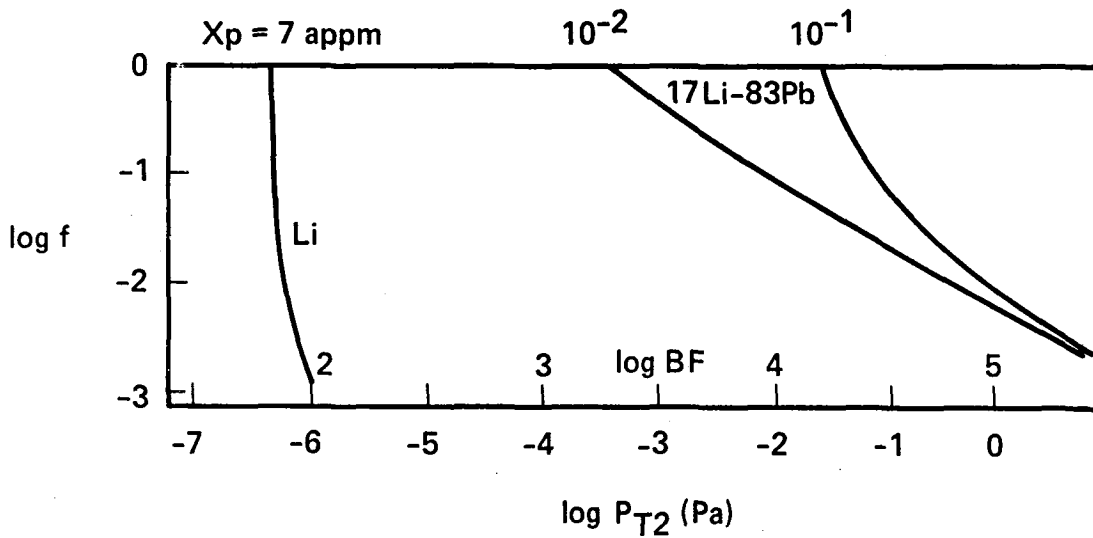


Figure 5-7. Influence of tritium concentration at extraction unit outlet on flow rate fraction to extraction unit for Li and LiPb.

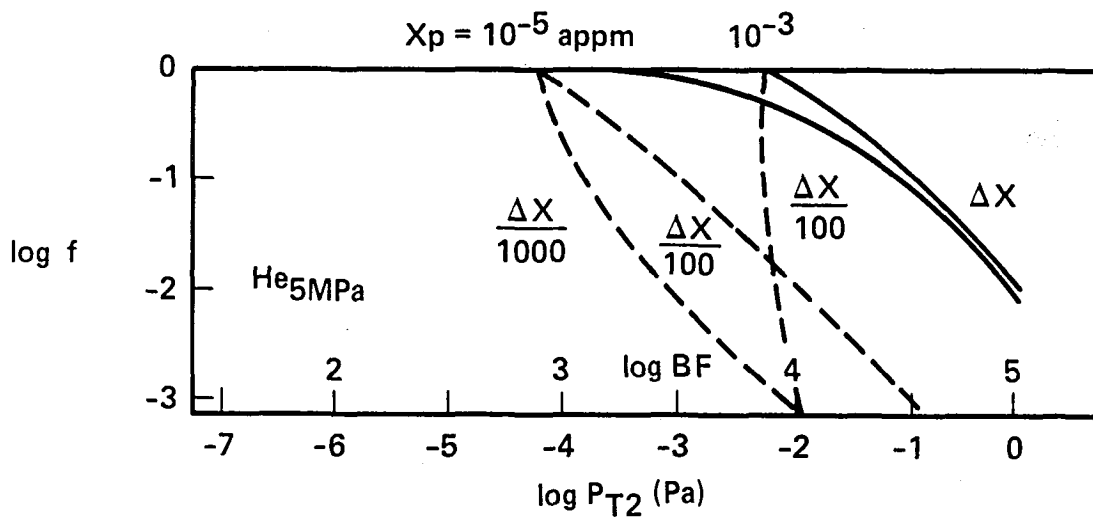


Figure 5-8. Influence of tritium concentration at extraction unit outlet on flow rate fraction to extraction unit for He.

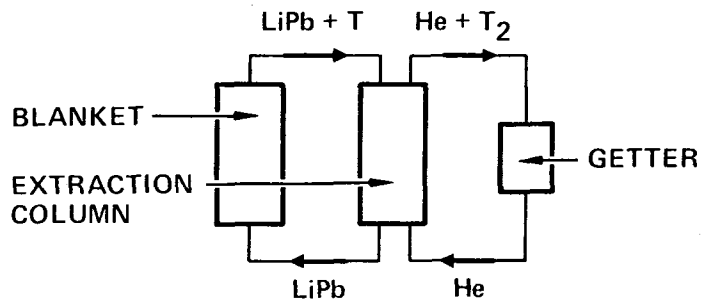
factor BF less than 10^2 , respectively, even for a small mass flow fraction to be processed ($f \sim 0.01$). For ^{17}Li - ^{83}Pb and an achievable $x_p = 10^{-2}$, then even for $f = 1$ the partial tritium pressure p_{HX} is too high with respect to tritium permeation and a more effective processing system with a lower achievable x_p is needed, possibly through isotope swamping. Details of a conceptual design of an extraction unit for LiPb ⁽¹⁸⁾ were given in Section 3.4.4.

Figure 5-8 shows the corresponding results for the helium-cooled blanket according to Fig. 5-6. Again, even for $f = 1$ (no separate blanket processing system), an achievable $x_p = 10^{-5}$ appm is not sufficiently small. However, the reduction of x_p does not have a large influence at values $f \ll 1$ ($f \approx 0.01$ is desirable from a thermal efficiency, for example). This tendency changes if the T_2 mass flow rate ($\approx \Delta x$) is decreased. This is achieved in some blanket designs by using a separate blanket processing system where tritium enters the coolant system only by permeation and the T_2 mass flow rate is typically reduced by a factor of 100-1000.⁽¹⁷⁾ Another means is to add additional oxygen to the coolant to transform T_2 to the nonpermeable form T_2O . In this case the tritium extraction system is favorably based on the adsorption of T_2O combined with a oxygen catalyst located upstream of the adsorber. Figure 5-7 can also be applied for this case if x_p is taken as the residual T_2 concentration downstream of the catalyst. The effectiveness of the preoxidation in the blanket influences again the T_2 source term ($\sim \Delta x$) and with this the required mass flow rate ratio f . Values for the effectiveness of this preoxidation do not exist. First experiments are underway.⁽²¹⁾

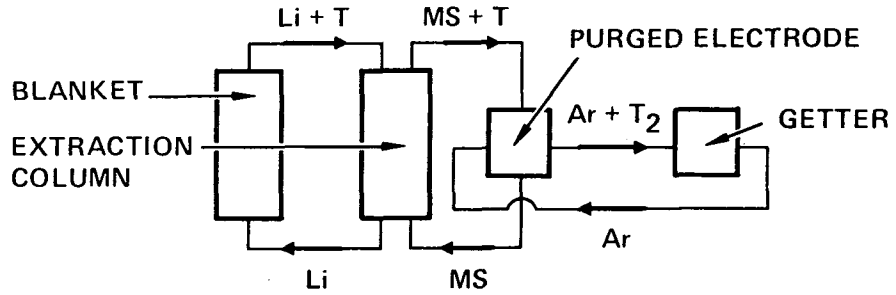
Specific Processing Methods

The general problem related to breeder tritium processing is to extract tritium with a very low concentration from a gas or liquid metal flow (tritium extraction from water is discussed in Section 5.6.2), an early overview on different techniques was given by Watson.⁽²²⁾ In subsequent process steps (e.g., during regeneration of the extractor units), tritium is highly concentrated; the further process steps are believed to represent no technical problems and will not be discussed further. Figure 5-9 shows schematically the considered processing schemes.

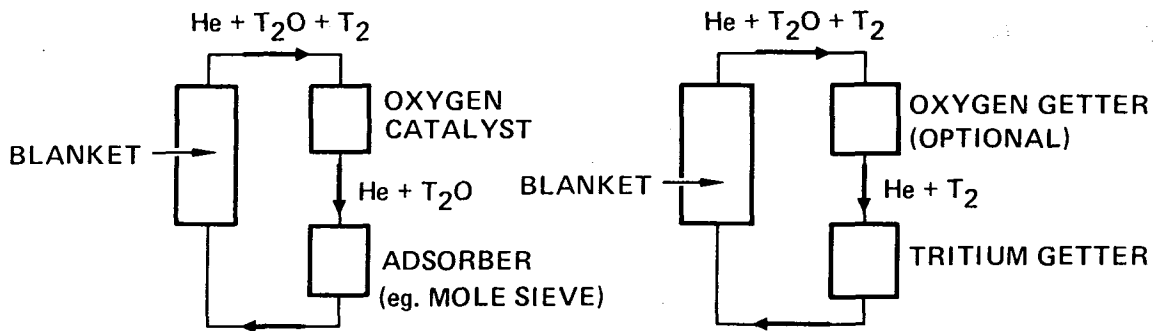
Table 5-6 shows the methods taken into consideration recently. The methods which presently appear to be most promising for BCSS-type blanket



TRITIUM EXTRACTION FROM LiPb



TRITIUM EXTRACTION FROM Li



TRITIUM EXTRACTION FROM He

Figure 5-9. Schematic representation of tritium processing schemes.

designs are underlined. The issues connected with these methods and required experiments will be described in Section 5.5.3.

In Section 3.4.4, vacuum degassing, permeation windows and countercurrent helium flow were discussed for tritium extraction from LiPb. The preferred technique, the diffusion of tritium into countercurrent flowing helium, was presented in more detail. Since tritium extraction is a critical issue for LiPb, a back-up solution should be pursued as long as the feasibility of the preferred method is not proven. This back-up solution could be a ZrPd permeation window as recently proposed.⁽²³⁾ The Pd at the downstream side (helium atmosphere with oxygen excess) acts as an oxygen catalyst to significantly reduce the partial tritium pressure P_{T_2} to produce a large partial tritium pressure difference as a driving force for permeation. The extraction of tritium from the helium flow is achieved with the help of getters or molecular sieves as discussed below.

Liquid-liquid extraction is the preferred method to extract tritium from liquid Li (as shown in Section 3.4.4). Molten salts with a higher lithium hydride solubility are used;⁽²⁴⁾ the separation of tritium from the molten salt is performed with a purged electrode.⁽²⁰⁾

The preferred extraction method for tritium extraction from He are absorption with solid getters or adsorption with molecular sieves. The first method is also proposed for the fuel clean-up system (Section 5.4) where a high hydrogen isotope concentration exists. Getters for breeder tritium extraction require elemental hydrogen isotopes for a reversible absorption-desorption cycle; many other elements, especially oxygen, are absorbed but are not desorbed at relevant temperatures. This behavior can be used to decompose tritiated water, which simplifies the total processing system compared to methods where an additional process is required (e.g., electrolysis). However, these getters become poisoned with time by these impurities and have to be replaced (raising a tritium waste stream problem). The application of getters therefore appears to be favored where the hydrogen isotopes exist mostly in the elemental form and the concentration of other elements (e.g., O, C) is low.

Molecular sieves ("mole sieves") are widely used in containment detritiation systems (compare Section 5.6). Mole sieves for breeder tritium extraction require tritium as T_2O or THO . Therefore, an additional oxygen

catalyst is generally proposed if tritium also exists in the elemental form. Compared to getters, mole sieves are much less affected by impurities. The use of mole sieves appears to be favorable where tritium is expected to exist partly as T₂O or THO and where an excess content of oxygen in the system is advantageous for other reasons. A critical issue for the use of mole sieves is, however, whether the residual inventory in mole sieves is acceptable.

5.5.3 Experiments and Facilities

In the following, experiments are described which are needed for the reliable design of a tritium processing system; the required experiments are also listed in Table 5-7. The breeder tritium extraction system is outside of the neutron environment; therefore, there is no direct need for tests in a neutron environment. Component dimensions do not usually represent an experimental limitation because the use of several identical smaller units might be preferred to the use of a single large component.

Often protium or deuterium is used in experiments instead of tritium (non-tritium benchtop tests, compare Table 5-1). Test stands with the use of tritium are denoted as glove box-type test stands, although for low tritium amounts, fume hoods are sufficient. Table 5-8 gives some information concerning personnel and environmental protection as a function of tritium inventory. The ranges of tritium inventory in the different columns are overlapping due to different requirements for different experiments (size of test section, distribution and vulnerability of tritium, site location). For the lower inventory range, the added costs for safety requirements (compared with non-tritium experiments) can be significantly compensated by the lower costs for instrumentation (e.g., no high resolution mass spectrometer needed).

Tritium Extraction from ¹⁷Li-⁸³Pb

Basic property measurements are needed such as solubility and diffusivity of tritium in ¹⁷Li-⁸³Pb. The experiments can be performed with deuterium or protium (non-tritium test) or, for increased measurements accuracy, with small amounts of tritium (< 1 Ci) in a glove box-type test stand.

The influence of diffusivity and recombination at low partial tritium pressures on the tritium transfer from LiPb into He should be determined with a simple extraction experiment with a defined phase interface (e.g., downward flowing liquid metal film on a vertical tube wall and countercurrent helium

Table 5-7. Breeder Tritium Extraction Experiments

<p><u>Test Complexity</u></p>				
<p>Integrated</p>	<p>Processing System Integration Test</p>			
<p>Partially Integrated</p>	<p>Component System Test With Simulated Blanket Impurities</p>			
<p>Multiple Effects</p>	<p>Tritium Processing in Breeder Irradiation Experiments</p>			
<p>Single effect</p>	<p>Intermediate Scale Test without and with Impurities</p>			
<p>Basic</p>	<p>Extraction in simple flow geometry (influence recombination diffusion)</p>	<p>Corrosion, He production, interdiffusion</p>	<p>Enhanced corrosion in Li due to entrained salt</p>	<p>Oxidation kinetics in gas streams with the presence of clean and oxidized walls</p>
<p>Extractor</p>	<p>Property measurements (solubility, diffusivity, etc.)</p>	<p>Pd catalyst efficiency</p>	<p>Chemical stability of salt in neutron environment</p>	<p>Adsorption and low loading, without and with impurities; influence of isotope swamping</p>
<p>Tritium Carrier Fluid</p>	<p>He</p>	<p>Permeation Window, e.g., ZrPd</p>	<p>Molten Salt</p>	<p>Selection of getter for T₂ decomposition</p>
<p>Extractor</p>	<p>He</p>	<p>Permeation Window, e.g., ZrPd</p>	<p>Molten Salt</p>	<p>Selection of getter for T₂ extraction</p>
<p>Tritium Carrier Fluid</p>	<p>Li</p>	<p>17Li-83Pb</p>	<p>Li</p>	<p>T₂ Absorbers (Solid Getters)</p>

*Preferred solution; feasibility has to be proven

Table 5-8. Personnel and Environmental Protection Guide for Tritium Handling

	Total Tritium Handled (Ci)			
	0-5	0.5-10 ⁴	10 ³ -10 ⁶	10 ⁵ -
No. of room tritium monitors (+ glovebox + stack)	1-2	2-4 (+ 1/GB) + 1 for stack	2-5 (+ 1/GB) + 1 for stack	3-8 (+ 1/GB) + 1 for stack
Bioassay program	no	yes	yes	yes
Hood + solid waste handling capability	yes	yes	yes	yes
Sec. contain. w/ glovebox cleanup + stack + storage + inventory	no	yes	yes	yes
Sec. contain. w/complex glovebox cleanup + ventilation control + breathing air + quality assurance program	no	no	yes	yes
Emergency room air detritiation	no	no	no	yes
Capital cost for protection	\$20-50K	\$80-160K	\$220K-\$1.2M	\$2-20M

flow). Again, experiments with small amounts of tritium would be preferable (glove box-type test stands).

Concerning the ZrPd-permeation window, the Pd catalyst efficiency on the downstream side has to be determined using a ZrPd pipe piece and tritium diluted in helium on the upstream side. To cover the low partial tritium pressure range of interest, the experiments should be performed with tritium in a glove-box type test stand. To investigate the influence of corrosion and other impurities on the upstream side on the permeation behavior, a small liquid metal loop with relevant impurities in a glove box facility is required. An interesting aspect is the precipitation of nickel from the blanket circuit which protects the Zr against nitrogen embrittlement.⁽²³⁾

Effects of helium production due to the tritium decay and interdiffusion of the Pd and Zr phase can be investigated without requiring LiPb on the upstream side in a small glove box. In a similar way, other materials than Zr (e.g., Ni or Nb) and Pd (e.g., Pt) should be tested.

Intermediate scale tests with relevant flow parameters (e.g., isotope swamping) are needed to demonstrate the extractor behavior without impurities and with impurities. Table 5-9 contains relevant parameters for a tritium extraction experiment using countercurrent helium flow⁽¹⁸⁾ (compare also Section 3.4.4). In this conceptual design the tritium concentration in the helium flow is very low and the helium flow rate is considerable; therefore tritium extraction from the helium on a half engineering scale is considered. The extraction from helium (T_2 absorption with getters) will be discussed later. The tritium amount in these experiments is in the order of 10^2 - 10^3 Ci, requiring safety-related capital costs in the order of \$100K. Due to the increased complexity of these tests, requiring additional facilities, the integration into a flow process facility is advantageous.

Partially integrated tests with near 1:1 scale components are desirable to determine the processing system behavior with relevant impurity levels due to corrosion and radiation, and tritium form and composition. These tests require a flow process facility (like TSTA) either connected with a blanket test facility or operating separately, supplying the processing system with the blanket output conditions obtained from other blanket tests (including neutron tests).

An integrated system demonstration is desirable to prove system performance, including plasma exhaust, vacuum system, breeder extraction system, fuel cleanup, isotope separation, tritiated waste treatment, secondary containment, and particularly overall instrumentation and control. There is a need to identify the necessary redundancy for reliability and safety. The secondary containment size and integrity must be traded off against cost and maintainability. The potential for mixing explosive amounts of hydrogen and oxygen must be assessed. These system integration tests will identify any unknown or unexpected interactions among components, as well as operating procedures, that could affect system performance. These tests require a flow

Table 5-9. LiPb Tritium Recovery System Parameters

Extraction column cross-sectional area	1 m ²
Column height	2.5 m
Number of extraction stages	20
LiPb flow rate	100 l/s
Purge gas flow rate	10 ³ -10 ⁴ l/s
Purge gas pressure	100 kPa
Purge gas temperature	400-600°C
Hydrogen partial pressure	0-0.01 kPa
Tritium concentration in LiPb	0.04-1 wppb

process facility such as TSTA or a fusion test facility combined with an appropriate partially integrated blanket test facility.

Tritium Extraction from Li with Molten Salts

Basic tests are needed to confirm the tritium distribution coefficient between Li and molten salt. The experiments can be performed with protium or deuterium in a non-tritium test stand or more accurately with tritium in a tritium glove box-type stand.

Molten salt dissolved or entrained in the Li is transported into the neutron field. Experiments to investigate the chemical stability of molten salts in a neutron field are therefore required, performed by irradiating molten salt contained in capsules with a fission reactor or point neutron source.

Corrosion experiments have to be performed with molten salt saturated with Li. For molten salts with high melting temperatures (e.g., > 415° C) redeposition can become a problem. Benchmark experiments are needed to investigate if there is an enhanced corrosion if Li is saturated with molten salt. These experiments can be performed in corrosion test stands without neutrons. Depending on the results from the irradiation experiments, mentioned above, relevant impurities have to be added.

Intermediate scale tests both in respect to the liquid-liquid extraction and the recovery of tritium from the molten salt have to be performed. These are discussed in Section 3.4.5.

Concerning partially integrated and integrated system demonstration tests, the statements made for LiPb are also valid here.

Tritium Extraction from Helium Purge or Coolant Flow

The two methods, adsorption of T_2O or absorption of T_2 , are somewhat competitive and it depends on the blanket design which method is more advantageous. There is also the possibility that both methods are applied, e.g., T_2O extraction from the helium coolant and T_2 extraction from the helium purge flow of a solid breeder blanket.

In respect to T_2O adsorption, molecular sieves are often favored compared with other adsorbers (e.g., cold traps). However, basic experiments with mole sieves are needed to investigate to what degree unregenerable tritium is bound in the mole sieve lattice. This effect can result in an unacceptably high tritium inventory. There are several methods to reduce this effect (isotope swamping, different regeneration procedures, etc.). These experiments require the use of tritium (10^2 - 10^3 Ci) and a glove box-type test stand.

If mole sieves prove to be unacceptable, the emphasis must shift to on identifying other adsorbers. One technically feasible method is the freezing out of T_2O in cold traps with liquid nitrogen as proposed for INTOR.⁽¹⁾ For BCSS-type blanket designs,⁽¹⁷⁾ this method would be economically unacceptable due to the huge heat exchanger areas and power for the refrigeration system.

Methods based on the adsorption of T_2O have to be combined with an oxygen catalyst located upstream, since T_2 is also expected in all blanket systems with T_2O . The efficiency of these catalysts at blanket relevant conditions is uncertain;⁽²⁵⁾ experiments are required, preferably with tritium (> 10 Ci, glove box-type tests).

If tritium has to be extracted from the helium flow as T_2 , then absorption with getters appears to be very favorable. There are many applications where getters are used for similar purposes (e.g., storage of tritium, fuel clean-up). For blanket processing systems, the operational conditions differ;

basic experiments are required to select an appropriate getter material which has a high hydrogen absorption efficiency at a temperature not too far below the blanket outlet temperature, does not require a high regeneration temperature (permeation problem), allows high gas volume fluxes (limited by structural integrity during absorption and desorption), decomposes well-tritiated water (reversible adsorption-desorption for hydrogen isotopes, irreversible storage of oxygen), and has a favorable behavior with time (no fast deterioration due to sticking of oxygen and other impurities at the surface). These experiments should be performed with tritium (> 10 Ci, glove box test stand).

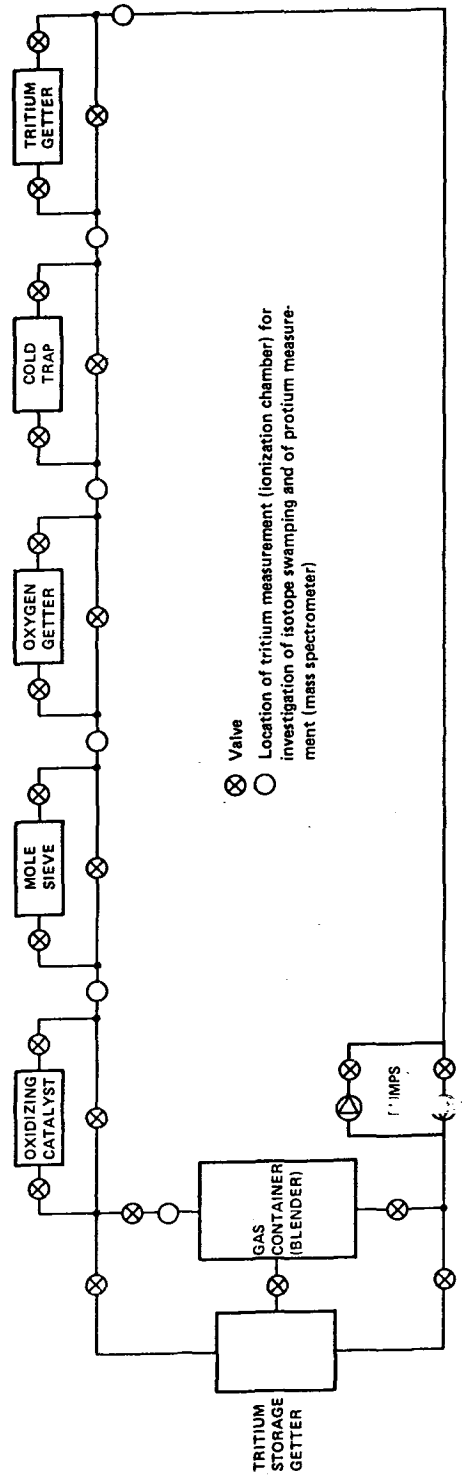
After having selected appropriate materials for T_2O adsorption and T_2 absorption, respectively, experiments are needed with larger test module dimensions to investigate the kinetics of adsorption (absorption) and desorption at low partial pressures and low loadings, including the influence of isotope swamping. Figure 5-10 shows schematically the set-up of an experiment where these effects, including the behavior of catalysts, can be investigated. By appropriate valving, different combinations of components are connected to investigate the different phenomena. These experiments can be performed in a glove box-type test stand with minimal tritium amounts of 10-100 Ci.

Intermediate scale tests are again required with relevant flow parameters (isotope swamping influence of impurities) and tritium amounts of $10^2 - 10^3$ Ci. These tests should be performed in a flow process facility.

Experiments which are important in respect to permeation but also influence the choice of the extraction method concern the oxidation of tritium. Of special interest is the case where tritium permeates through a wall with a downstream oxide layer into a helium stream containing excess oxygen. First experiments⁽²¹⁾ cover only a limited parameter range. Much more work has to follow, with special attention on the determination of the surface conditions (minimal tritium amount ≈ 10 Ci; glove box-type test stand).

Solid breeder irradiation tests can be a valuable experiment for tritium reprocessing units due to the more relevant tritium form and composition. These experiments require a neutron source and a glove box-type test stand.

In the next steps, partially integrated tests of fusion device tests are required as described for LiPb.



Minimum tritium requirement ≈ 10 Ci
 for minimum bed diameters ≈ 2 cm
 and maximal bed volume fluxes ≈ 0.5 m/s

Figure 5-10. Small scale component test set-up for tritium extraction from He streams.

5.6 Detritiation Systems

5.6.1 Air Detritiation

Issues

In the event of tritium spills into the containment building or to cope with tritium leakage and outgassing, room air detritiation systems (RADS) are needed both for personnel and environmental protection, as well as to maximize personnel access and machine availability. Because the RADS potentially is one of the two most expensive and largest of the tritium processing systems (the other being the water coolant detritiation), it is important to understand the variables in room detritiation and to optimize the RADS system design and sizing. Technical data are essential to the determination of optimum designs and sizes, but the ultimate decisions are also complicated by semi-technical judgments such as the dollar value of machine downtime, or population and worker dose.

Current RADS remove tritium from air by first catalytically oxidizing the tritium to form water (T_2O and HTO) and then capturing the water by use of refrigerated dryers (condensers) and molecular sieve drying beds. The first step (catalytic oxidation) is an undesirable step in any cleanup process because the product, tritium oxide, is some 20,000 times more hazardous than tritium in molecular form. An alternative process, such as the use of getters, would be advantageous, but to date all efforts to find an effective getter for tritium in the presence of oxygen have been unsuccessful.

A second area of concern is the potential vulnerability of the precious metal oxidation catalyst to poisoning by products of room fires (e.g., chlorides, sulfides, and smoke or soot particles) that could accompany a tritium release.

Description of Phenomena

The rate at which a tritium spill is cleaned up by a RADS depends predominantly on four parameters:

- time size (processing flowrate) of the RADS in relation to the room volume;

- The rate of oxidation of tritium in the room or the fraction of tritium in oxide form when it was spilled;
- the absorption/desorption characteristics of wall and surface coatings in the room, especially for the oxide form; and
- the degree to which room air meets or deviates from being perfectly mixed.

Note that the cleanup efficiency of the RADS itself (tritium input concentration/tritium output concentration) is relatively unimportant, assuming the efficiency is reasonably good (10^3 or higher). Measured efficiencies from experimental RADS are typically greater than 10^4 and expected values are 10^5 to 10^6 . The ideal relationship between room concentration and cleanup time assuming no absorption/desorption effects at walls and perfect mixing of room air is given by:

$$C = C_0 \exp \left[\left(\frac{F_1}{DC} - F \right) \frac{t}{V} \right]$$

where C_0 = initial concentration of tritium in room at time 0

C = concentration in room at time t

F = flowrate through room air detritiation process

F_1 , = flowrate from room air detritiation process recirculated to the room

DC = decontamination factor = tritium concentration at inlet to detritiation process/concentration at outlet

t = time

V = room volume

Experiments and Facilities

Experiments are needed to assess and evaluate the deviations from ideality in room air detritiation, including the impact of room fire combustion products.

The Tritium System Test Assembly (TSTA) has a RADS of 1400 CFM capacity and a variety of smaller test equipment, small RADS and a 1-m^3 exposure

chamber for addressing questions about oxidation rates and HTO absorption/desorption effects in various surface coating materials. Room air mixing effects can be determined in two different sized rooms. Data on room air mixing during cleanup are also available from CANDU fission reactor facilities.

Modifications to the small RADS at TSTA would permit studies of the effect of room fire products on the performance of a RADS. Test of tritium getter materials as an alternative RADS have been done at several laboratories using hydrogen. Results of these tests have not been encouraging. New ideas and materials are needed before further work in this area may be useful.

Modeling Requirements

The equations describing basic (ideal) room air detritiation are well understood. Computer codes are also available which take into account the HTO absorption/desorption effects at walls that cause deviations from ideal cleanup. However, the modeling accuracy is presently limited by the data, particularly the absorption/desorption coefficients or other parameters used in the codes that are not well quantified. Further work is also needed on how to include effects of incomplete mixing in room air.

5.6.2 Water Coolant Detritiation

Issues

The unique advantages of water as a coolant are well known. The concern is that tritium will permeate into the water within the hot breeding blanket or plasma interactive region and then transfer out of the primary loop either by leakage to the room or across a heat exchanger to the secondary water loop. This general issue embodies two subparts: one is the rate of permeation into the water (discussed in Section 5.3) and the second is the removal of tritium from the water to keep levels low (discussed here).

Besides coolant water, a second category of water that may require detritiation is the water formed by the processes used for room air and glovebox atmosphere detritiation. In these processes, tritium ends up in

water form trapped on molecular sieve drying beds. For safety or economy, detritiation of this water may be desirable.

Description of Phenomena

The issues of how much tritium may permeate into water coolant is dealt with elsewhere (Section 5.3). The issue of detritiation of the water is mainly an issue of economics. What rate of tritium extraction will be needed? What concentration of tritium can be tolerated in the water? Can less expensive detritiation process be developed?

A variety of processes, some partially industrially-proven, for the extraction of tritium from water are available⁽²⁶⁾. These are all two-step processes, first an exchange process to get tritium from the oxide into molecular gaseous form and secondly, separation of the tritium from normal hydrogen, usually by cryogenic fractional distillation. Although cheaper processes are always desirable, the available processes meet the technical requirements. Although tritium must be extracted from water at the rate at which tritium permeates into the water, the cost of extraction depends on the concentration of tritium in the stream to be detritiated. For example, must water coolant be maintained at 0.1 Ci/L or is 1-10 Ci/L acceptable? The answer depends on leakage rates of this water to the room and on transfer rates of this water across heat exchangers into secondary coolant loops. The impact of the allowable tritium concentration in water on detritiation costs has been discussed quantitatively by Rogers⁽²⁷⁾ in U. S. INTOR studies.

The most promising new, and possibly cheaper, method of water detritiation is based on laser separation. Work at Lawrence Livermore National Laboratory and at Ontario Hydro in Canada has proven the scientific principle, but much work is needed to establish the feasibility of even a small scale process. A disadvantage of the process is its use of fluorine as an intermediate reactant.

Experiments and Facilities

Much information on water detritiation on a large scale will become available from the Tritium Recovery System (TRS) now under construction at the Darlington CANDU reactor station operated by Ontario Hydro near Toronto.

Modeling Requirements

Development of models of the detritiation of water is not needed.

5.6.3 Helium and Liquid Metal Detritiation

These are described in Section 5.5.

5.7 Vacuum Pumps and Valves

5.7.1 Compound Cryopumps

Issues

A compound cryopump has two cryogenic panels; one for pumping DT and a second, a cryosorber, for pumping helium. It is the most commonly assumed pump for fusion reactor applications with low pressure, and high required throughputs of hydrogen and helium.

There are several design-related questions. In particular, should the panels for DT pumping (cryocondensing) and helium pumping (cryosorbing) be separated by a valve or conductance limiter? Helium separation capability is obtained by doing so, but is it cheaper to design this function into the Fuel Clean UP (FCU) subsystem? Also, how much tritium inventory is acceptable? What should the design goal be for the ratio of pumping to regeneration times. Should the 77K heat shield regeneration be sequenced after the DT panel warm up to prevent these pumped impurities (water, ammonia, carbon dioxide and methane) from mixing with the DT stream.

The uncertainties that must be resolved by testing include, for the various types of pumps, what is the consequence of long term thermal cycling and tritium exposure on the pump efficiency and reliability.

Description of Phenomena

For a device to be fitted with compound cryopumps, several design options are available and these require study to determine the best approach. First is the issue of configuration: in an appendage pump, the panels for T pumping and helium pumping may be placed in close proximity. Then, when one panel is regenerated, increased local pressure will cause an increased heat transfer rate to the adjacent panel and its pumped gases will come off also. This is the case unless great care is taken to warm the panel at a rate that allows the regeneration pump to maintain pressures below about 10^{-3} Torr while removing regenerated gases. Practically, to keep the DT and helium separate during regeneration requires that the surfaces be physically isolated from each other. So the first issue is whether or not to provide means, in the

form of a conductance limiter or gate valve to isolate the panels from each other during regeneration. Cost trades which weigh varying degrees of FCU complexity against additions to the compound cryopumps to provide partial gas separation are needed to resolve this design issue.

Operation is the second design issue. Specifically, how long to pump with each set of panels and how quickly and with what pumps should panel regeneration be performed? The length of pumping operation for the liquid nitrogen cooled shields and the helium cryosorber is long and may be determined by the capacity of tritium removal components downstream or the desire to limit tritium inventory. It is not necessary to regenerate all panels (LN₂ DT and helium) at the same time. The rate of heating and cooling during regeneration and sizing of the regeneration pumps need analysis to identify the best approach. Very rapid regeneration increases the availability of the panels and consequently pumping speed of the system but increases stresses on the panels. If, as mentioned above, the pumping system is used to provide partial gas separation, sequencing of the panels is an important consideration.

The major testing issue for compound cryopumps relates to the lifetime of the panels. Two factors may limit panel life-thermal cycling and tritium exposure. Both considerations apply to cryosorbing panels used for helium pumping: condensing panels (DT pumping) can be designed for infinite life. Lifetime for some cryosorbers can be determined by testing representative samples and some of this work has begun. An argon cryotrapping panel for pumping helium is not subject to limitations caused by thermal cycling or tritium exposure, however, the disadvantage of introducing argon into the fuel loop may outweigh this advantage.

Experiments and Facilities

Prior to implementing a compound cryopump configuration, a representative module should be assembled and operated. Important considerations to be duplicated are: the size should be the same as a portion of the proposed configuration; operation should match the proposed system heating and cooling rates; maintenance procedures should be verifiable; and the module should be operated with tritium. It is not essential that the torus or a segment

thereof be replicated; however, the issue of debris may have to be resolved in this facility. The module will probably require representative ducting and a torus interface capable of realistic gas loading and heat loading and, if required, a particle generator.

A vacuum test facility, suitable for the simulations described above, is shown in Figure 5-11. Included is an enclosure to contain any leaked tritium, a clean-up system and support systems to supply cryogenics, instrumentation and controls and usual utilities. Figure 5-12 shows some of the functions to be accomplished in such a facility.

These components are not expected to be exposed to substantial neutron flux. The importance of neutron effects may be determined by neutron calculations and consideration of neutron effects observed in irradiated material specimens. Some testing of specific materials (e.g. cryosorber) may be required.

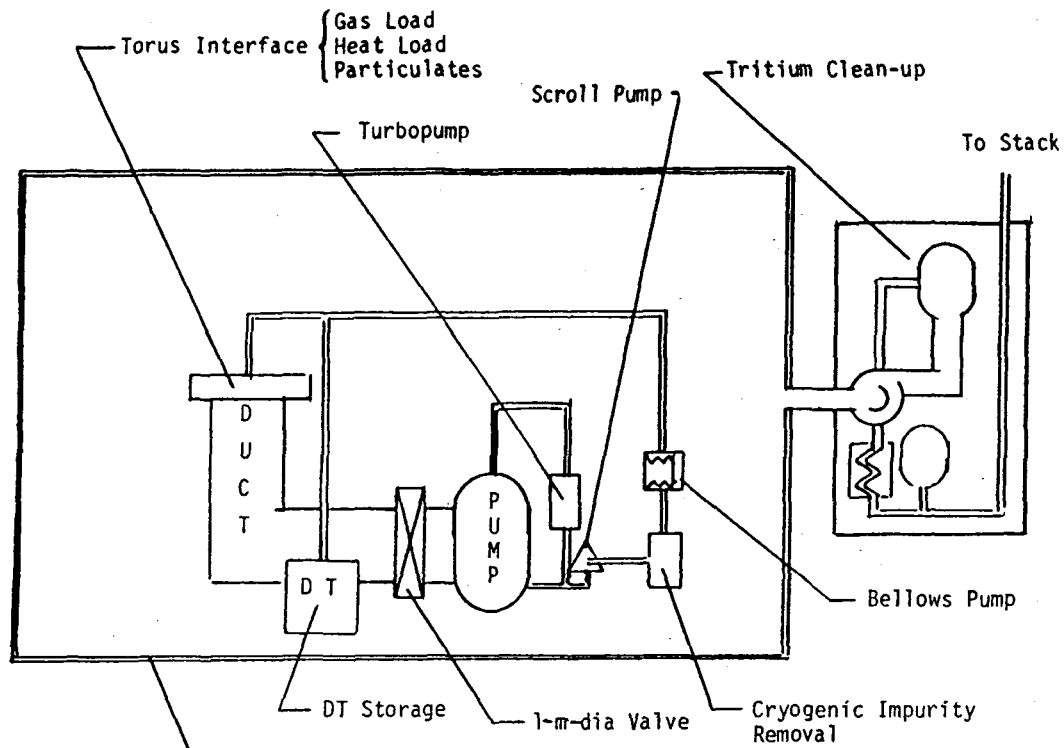
Modeling Requirements

Existing analytic techniques are adequate. Involved are calculation of neutron heating, heat and mass transfer calculations on the cryopumping surfaces and in the supply system; and gaseous conduction estimates for the specific geometries considered in both the viscous and molecular pressure ranges.

5.7.2 Vacuum Valves

Issues

Large diameter (1 meter) valves with metal seals (for tritium resistance) are often proposed for isolating pumping ducts or neutral beams from the vacuum vessel. Valves of this type require very large forces (up to 500 Kg/cm of perimeter) to effect a seal, and these forces tend to distort the valve's structure and to damage the smooth metal surfaces of seal and seat. Particles are a particular problem for a metal-sealed valve. Particles originate in the vacuum vessel and can be carried to the valve seat during periods of high pressure viscous flow. A realistic value of valve life is needed for device design purposes and for operational planning.



Secondary Containment, Area = 30 m², Volume = 200 m³
 Tritium Clean-up, Area = 10 m², Volume = 50 m³
 Support Area } Area = 20 m², Volume = 70 m³
 Cryogenics
 Instrumentation
 & Controls
 Operating Personnel - 1 Staff, 1 Tech, with 24 hour
 operation probable about 30 % of total time

Figure 5-11. Layout of vacuum test stand.

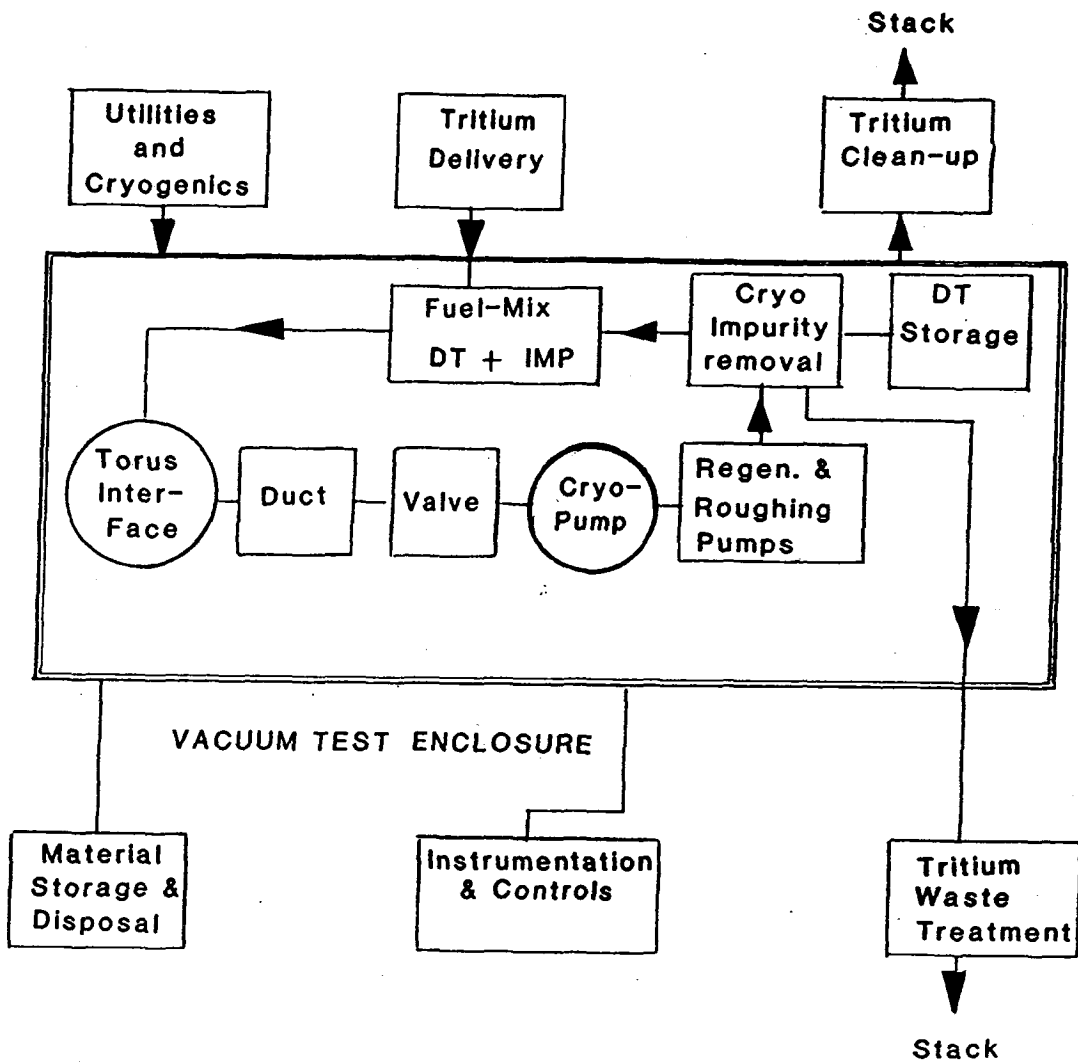


Figure 5-12. Major functions of vacuum test stand.

Tritium effects are important if metal seals are not used. Neutron radiation also will affect nonmetallic seals and may be significant for the actuator mechanism on all seal designs.

Description of Phenomena

Development of large (~1 meter) diameter metal sealed valves for fusion devices has met with limited success due to the very large sealing forces required. Metal seals are preferred because they have lower permeation rates than do elastomeric seals, because the likelihood of contaminating the torus with outgassed products is lower and because tritium degradation is eliminated.

It is not completely certain, however, that elastomeric seals will not work. Tritium degradation data for elastomers at low pressures are not available. Some radiation resistant elastomers are available and might be acceptable. Alternatively, low leakage rate valves or "conductance limiters" having a total leak rate of 10^{-3} scc/sec (scc = cubic centimeters at STP) should be considered as a fall-back position if the cost of developing leak-free ($\leq 10^{-9}$ scc/sec) becomes very high. Some back leakage into the vacuum chamber from a cryopump being regenerated is tolerable if the leakage rate is known and can be offset by increasing the capacity of the on-line pumps accordingly. For periods when a pump is out of service, leakage back into the chamber can be reduced by maintaining a vacuum on the cryopump with roughing pumps. If a pump is to be removed for repair, a blankoff plate will be sufficient to allow continued operation. Seal life is the determinant of suitability. After multiple open-close cycles, repeatability of sealing location (where the seal contacts the seat) and scuffing of the seal and seat during closure have an effect on leak rates. Baking, especially in the closed position, decreases seal life.

Experiments and Facilities

The most attractive option continues to be all-metal leak free valves. Testing of full scale prototypes in a vacuum test facility as in Figs. 5-11 and 5-12 will be the means of evaluating suitability.

Neutron radiation may have an effect on materials used in the valve. This can be resolved by specimen tests in appropriate neutron sources.

Modeling Requirements

Analysis is of limited use in predicting the performance and reliability of a large metal sealed high vacuum valve. Factors which could compromise leak rate are of the same magnitude as the uncertainties in a reasonably complete analysis. Development of large valves is likely to proceed by several iterations in design resulting from early testing of prototypes. This process will occur as part of the procurement process and need not be detailed here; however, sufficient time should be allowed and detailed testing of the hardware must be performed.

5.8 Integrated System Behavior

5.8.1 Operation and Control

Issues

An integrated system demonstration is desirable to prove system performance and safety, including plasma exhaust, vacuum system, breeder extraction system, fuel cleanup, isotope separation, tritiated waste treatment, secondary containment, and particularly overall instrumentation and control. There is a need to identify the necessary redundancy for reliability and safety. The bulk of the tritium processing system can be sufficiently far removed from the rest of the reactor that interactions are most likely to be felt through variations in the inlet conditions and these have been treated earlier as separate issues.

The secondary containment size and integrity must be traded off against cost and maintainability. Secondary containment of the basic tritium processing systems is relatively simple, straightforward, and inexpensive because the systems are generally compact and not large. This is less true for the vacuum chamber and blanket. Here tritium protection during equipment maintenance becomes more difficult because of large and complicated configurations of surface area.

Description of Phenomena

System integration incorporates at least three system aspects that cannot be properly tested in component tests. These aspects are: (1) dynamic and transient effects and interactions, and their control; (2) reliability and aging effects, especially in regard to the interactive effects of failure of one component on the reliability of a second; and (3) unforeseen effects of systems and their interconnections on each other. The latter might include the generation or transport of unexpected chemical species by one system to affect another, or might include uncovering less obvious pathways by which interactions could occur.

Two large and important parts are the development of computer control (including the software for control of process and safety systems) and the

development of written operating and maintenance procedures. These codes and documents, in a sense, represent the operational integration of subsystems into a working whole. The product of system integration tests should include verified software and procedures.

Experiments and Facilities

The Tritium Systems Test Assembly (TSTA) has as its purpose the integration and testing of the tritium processing systems. Because of budget constraints and work underway elsewhere, TSTA does not include equipment for detritiating water. Work on water detritiation has been or will be done at L'Institut Laue-Langevin in Grenoble France, at Chalk River Nuclear Laboratories in Canada, at Mound Facility, and (on a commercial scale) at the Darlington Generating Station of Ontario Hydro near Toronto. Obviously none of these integrates directly with the fusion fuel processing systems at TSTA. This interface could be added and tested.

TSTA also has no breeding blanket interface. When breeder product characteristics become available from the breeder testing program, an interface could be added at TSTA. Depending on the chemical impurities and diluents present in breeder product, it is probable that a stage of impurity removal and/or a stage of hydrogen isotope separation will be needed for the breeder product before it can be added to the main fuel processing loop. If so, these stages could be built and tested either at TSTA or at the site of breeder product extraction tests.

Modeling Requirements

The development of a dynamic simulation model of an integral tritium processing system would be beneficial. Such a code would aid the discovery and understanding of dynamic interactions among the tritium processing subsystems. Such a code is also a necessary part of any on-line tritium accounting system that ultimately will be needed for fusion fuel processing.

5.8.2 DT Losses from System

Issues

The amount of DT that is either discarded in gaseous, liquid or solid wastes, or is permanently bound up in fusion fuel processing equipment must be known since: (1) it bears on safety and environmental assessment; (2) it is necessary for accurate accounting of tritium; and (3) it is necessary in establishing the design requirements for blanket tritium breeding ratio.

Losses may be of two distinct kinds. One is recurring losses, as in routine low-level releases of tritium-bearing gaseous or liquid effluents. Considered in this category could be unrecoverable tritium diffused into periodically-discarded components, such as limiters. A second category of losses is nonrecurring losses, such as tritium that saturates the surface of process piping, or that portion of the tritiated water on molecular sieve beds that is difficult to regenerate.

Description of Phenomena

The principal function of the fusion fuel processing loop is to clean the fuel of impurities that grow into the fuel during the "burning" of plasma under the very harsh temperature conditions of the torus. The impurities are expected to deuterated and tritiated forms of methane, water, and ammonia, in addition to helium "ash". Expected amounts of impurities are shown in Table 5-10.

The amounts of impurities shown are such that the tritium bound in the impurity molecules is too much (for reasons of safety as well as economy) to discard as waste. Therefore the Fuel Cleanup System (FCU) has been carefully designed to decompose the captured impurities and recover for reuse the contained D and T to a high degree. Design values for tritium losses in waste streams from the FCU are extremely small, as shown in Figure 5-13. These values are the result of detailed process designs and have not yet been verified in actual system operation. This will be done at TSTA.

Besides the DT losses in the FCU effluent, there are additional and more significant pathways for losses. One of these is tritium that has escaped, by leaks or maintenance operations, into gloveboxes and hence to the glovebox

Table 5-10. TSTA Gaseous Impurity Load and Waste Gas Flow Rates for Fuel Cleanup (FCU) Process
 (Target: 200 Curies/Year to Tritium Waste Treatment System (TWT))

Impurity Element in Torus Exhaust	Probable Atom, %	Most Probable Impurity Molecule	Purification Process in FCU	Gas	Flow Rate, g/day	Gas Purity	Curies/Year to TWT
H	1	HD + HT	HD + HT + D ₂ + 2HD + DT plus cryogenic distillation	HD	23	$\frac{HT}{HD} = 0.2 \times 10^{-6}$	20
He	5 ^(max) ^a	He	cryogenic condensation and adsorption	He	155	$\frac{DT}{He} = 0.2 \times 10^{-6}$	80
C	0.1 ^b	C(D,T) ₄	cryotrap all impurities; oxidize them all to DTO, CO ₂ , N ₂ and Ar;	CO ₂	34	$\frac{DTO}{CO_2} = 2.5 \times 10^{-6}$	20
O	0.5	DTO		O ₂	105	$\frac{DT}{O_2} = 1.7 \times 10^{-6}$	60
N	0.1	N(D,T) ₃	separate DTO and electrolyse to recover all DT	N ₂	11	$\frac{C(D,T)_4}{N_2 + Ar} = 2.3 \times 10^{-6}$	20 - 40 ^c
Ar	.0006 - .05 ^c	Ar		Ar	0.2 - 16 ^c		

^aCorresponds to 10% burnup of DT and 1 GW(t) for TSTA throughout.

^bCan be much lower or higher depending on use of SiC liners.

^cHigher figure for removal of residual argon flush gas.

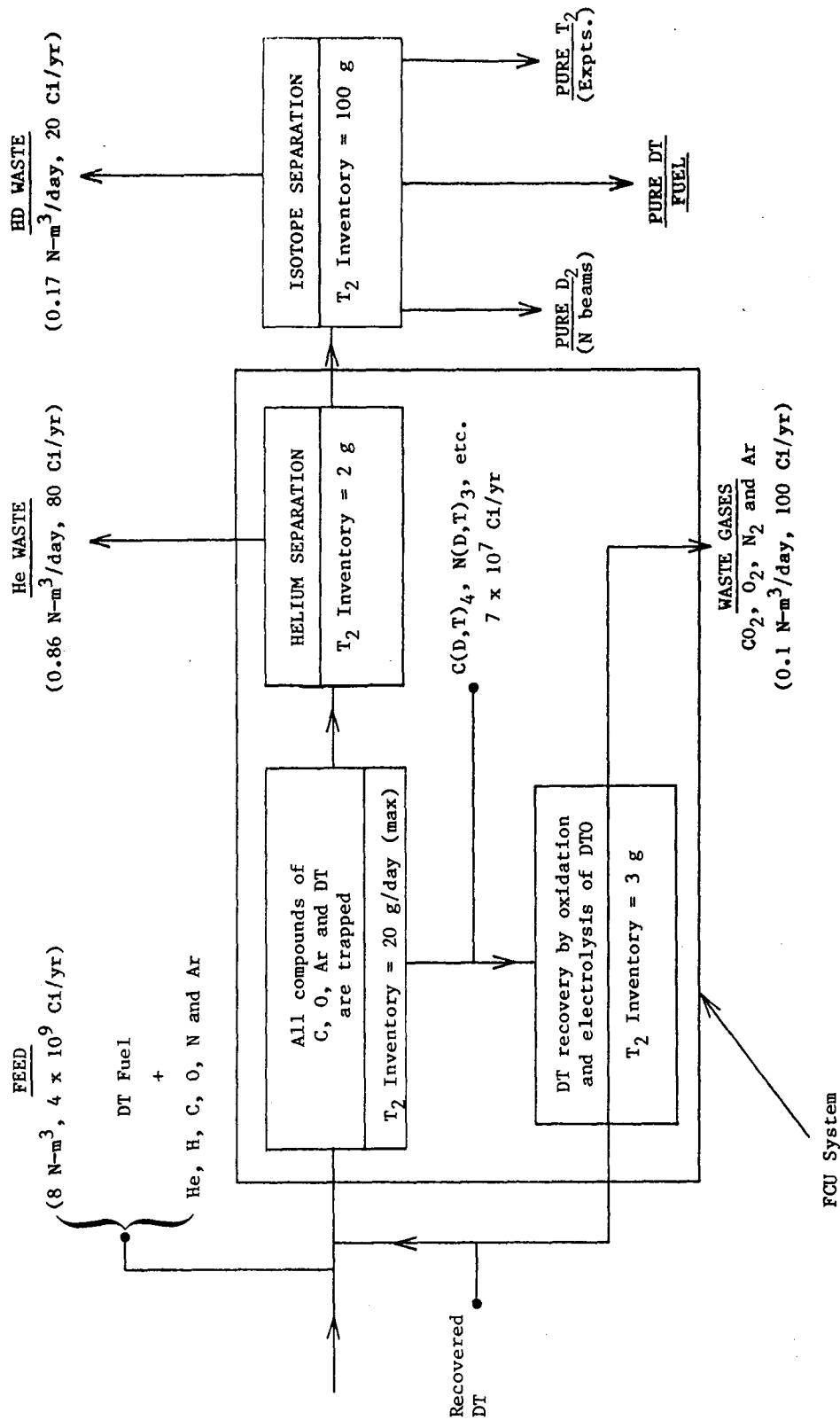


Figure 5-13. Primary separations in DT fuel cycle for TSTA with all gaseous waste (200 Ci/yr) FCU process.

atmosphere detritiation system. In current designs, this tritium is converted to oxide (water) form, captured on drying beds, and ultimately buried in doubly-contained disposal vessels. The amount of this tritium buried as a result of the first full year of tritium operations at TSTA is less than 500 curies (or 0.05 g).

If losses from this source must be reduced, two methods are available, one proved and one partially proved. The water, being small in amount, could be processed by the coolant water detritiation system. A promising new technology for detritiation gloveboxes without the formation of water is metal getters. Commercially available getters are capable of gathering tritium out of nitrogen atmosphere with high efficiency. The tritium is recoverable for reuse upon heating the getter to 500°C under vacuum.

A potential route for nonrecurring loss of DT is the portion of water absorbed on molecular sieve beds that is difficult to regenerate. The drying (regeneration) of molecular sieves is described by the curves in Fig. 5-14. It can be seen that high temperatures and very dry regeneration gas (implying large amounts of gas) are needed to extract the absorbed water completely. Therefore, a base amount of tritium will remain at all times on the molecular sieves after first use. This is a one-time loss and is not recurring unless molecular sieves are replaced often, which should not be necessary.

Limiters are components that could contain significant tritium and could also require frequent replacement, thus representing a recurring loss of DT. The DT loss in limiters could be reduced by treatment of limiters (such as cutting, heating, and/or evacuation) before disposal. More information is needed concerning plasma-driven permeation and inventory of tritium in limiters before the significance of this DT loss can be assessed. These same general comments apply as well to first wall materials.

Experiments and Facilities

Many of the questions about DT losses will be answered in the course of operations at TSTA and tritium processing systems on confinement experiments. Losses in FCU effluents will be well evaluated. Losses through glovebox detritiation will continue to be measured.

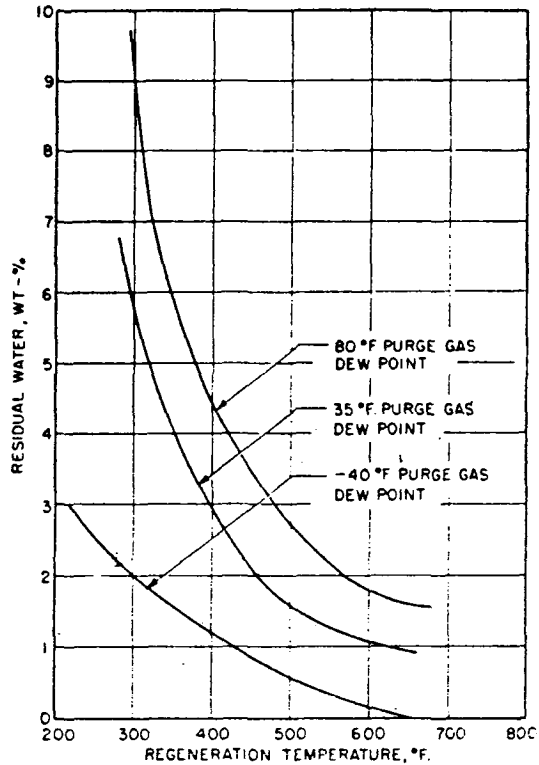


Figure 5-14. Residual water after regeneration as a function of regeneration temperature for different purge gas dew points.

Estimates of the tritium inventory in limiters will improve as results come in from experiments on plasma-driven permeation and inventory.

Modeling Requirements

More attention to overall tritium balances is needed as better data become available for making these balances. Perhaps the biggest current uncertainty is in limiters and first wall materials. Improvements are needed in modeling capability to describe plasma-driven permeation and inventory.

REFERENCES FOR CHAPTER 5

1. FED-INTOR/TRIJ/82-5, Chapter VIII, pp. 179-186.
2. D. B. Smith, D. Stripe, and J. P. Shipley, "Dynamic Materials Accounting Systems," Los Alamos Science, Los Alamos Scientific Laboratory, Los Alamos, NM, VI, No. 1, pp. 116-137 (Summer 1980).
3. K.L. Wilson, "Hydrogen Recycling Properties of Stainless Steels," J. of Nucl. Mat., 103 & 104 (1981), 453-464.
4. R.A. Kerst, W.A. Swansinger, "Plasma Driven Permeation of Tritium in Fusion Reactors," J. of Nucl. Mat., 122 & 123 (1984), 1499-1510.
5. M. Abdou, et al., "FINESSE: A Study of the Issues, Experiments and Facilities for Fusion Nuclear Technology Research & Development (Interim Report)," PPG-821, also UCLA-ENG-84-30 (October 1984), 3-115 - 3-116.
6. P.A. Finn, et al., "USA Contribution: Nuclear Data Base Assessment Group H, Tritium Systems", ETR-INTOR/DIS/NUC-2 (1984).
7. R.A. Kerst, J. Vac. Sci. Technol. 20 (1980), 1267.
8. H.P. Buchkremer, "Entwicklung und Exprobung einer Anlage zur Untersuchung der Permeation von Wasserstoffisotopen unter nuklearen Prozessgasbedingungen", KFA Julich, JUL-1111-RG, (1974)
9. W.A. Swansinger and R. Bastasz, "Influence of Thin Silicon Films on Deuterium and Tritium Permeation in Steels," Proceedings: Tritium Technology in Fission, Fusion and Isotopic Applications, American Nuclear Society National Topical Meeting, Apr. 29-May 1, 1980, Dayton, Ohio, U.S. DOE Conf-800427.
10. D.M. Goebel, G. Campbell and R.W. Conn, "Plasma Surface Interaction Experimental Facility (PISCES) for Materials and Edge Physics Studies," J. Nucl. Mater., 121 (1984) 277-282.
11. R.A. Causey, EGG-FT-5991, (1982).
12. G.R. Longhurst, G.A. Deis, P.Y. Hsu, L.G. Miller, R.A. Causey, "Gamma Radiation Effects on Tritium Permeation and Retention," Fifth Topical Meeting on the Technology of Fusion Energy, Knoxville, Tennessee, April 26-28, 1983.
13. M. Miyake, Y. Hirooka, H. Shinmura, S. Yamanaka, T. Sano, Y. Higashiguchi, "Absorption and Desorption Behavior of Hydrogen by Neutron Irradiated Titanium," J. Nucl. Mater., 103 & 104 (1981) 477-482.
14. R. Dobrozemsky, G. Schwarzinger, C. Statowa and A. Breth, "Radiation-Enhanced Permeation of H₂ in Stainless Steel," Symposium on Atomic and Surface Physics (SASP) 1980, pp.64-69, Maria Alm/Sbg Austria, Feb. 10-16, 1980; see also SASP 1982, p. 129.

15. D. O. Coffin and C. R. Walthers, "Vacuum Pumping of Tritium in Fusion Power Reactors," presented at Eighth Symp. on Engin. Problems of Fusion Res., San Francisco, CA, Nov. 13-16, 1979.
16. B. F. Dodge, "Removal of Impurities from Gases to be Processed at Low Temperatures," *Adv. Cryo. Eng.* 17, 37-55 (1970).
17. D.L. Smith, et al., "Blanket Comparison and Selection Study (Final Report)," ANL/FPP-84-1, Sept. 1984.
18. D.K. Sze, "Counter Current Extraction System for Tritium Recovery from ^{17}Li - ^{83}Pb ," Sixth Topical Mtg. on The Technology of Fusion Energy, San Francisco, March 3-7 (1985).
19. G. Pierini, A.M. Polcaro, P.F. Ricci, and A. Viola, "Tritium Recovery from Liquid $\text{Li}_{17}\text{Pb}_{83}$ Alloy Blanket Material," *Nucl. Engineering & Design/Fusion*, 1 (1984), 159-165.
20. W.F. Callaway, "Electrochemical Extraction of Hydrogen from Molten LiF-LiCe-LiBr and its Application to Liquid-Liquid Fusion Reactor Blanket Processing," *Nucl. Techn.*, 39, (1978), 63.
21. P. Finn, private communication.
22. J.S. Watson, "An Evaluation of the Methods for Recovering Tritium from the Blankets or Cooling Systems of Fusion Reactors," ORNL-TM-3794 (1972).
23. R.E. Buxbaum, "The Use of Zirconium-Palladium Windows for the Separation of Tritium from the Liquid Metal Breeder-Blanket of a Fusion Reactor," *Sep. Science and Techn.*, 18 (12 & 13) (1983), 1251-1273.
24. V.A. Maroni, R.D. Wolson, G.E. Strohl, "Some Preliminary Considerations of a Molten-Salt Extraction Process to Remove Tritium from Liquid Lithium Fusion Reactor Blankets," *Nucl. Techn.*, 25, (1975).
25. "INTOR, International Tokamak Reactor, Phase Two A Part 1", IAEA, Vienna, 1983.
26. A. Sherwood, private communication.
27. Holtslander, T. S. Drolet, and R. V. Osborne, "Recovery of Tritium from CANDU Reactors, Its Storages and Monitoring of Its Migration in the Environment," in Handling of Tritium-Bearing Wastes, Tech. Rep. Ser. No. 203, Int. At. En. Agency, Vienna (1981), 59; Also At. En. of Canada Ltd., Rep. No. 6544 (July 1979).
28. M. Rogers, "Tritium Separation Methods," pp. 2-28 to 2-36, and "Appendix C: Cost and Technology Tradeoffs for Separating Tritium from Water," FED/INTOR Tritium and Safety Issues, FED-INTOR/TRIT/B2-4 (July 1982), C-1 - C-16.

CHAPTER 6

PLASMA INTERACTIVE COMPONENTS

TABLE OF CONTENTS

6. PLASMA INTERACTIVE COMPONENTS

	<u>Page</u>
6.1 Introduction.....	6-1
6.2 Issues for Plasma Interactive Components.....	6-2
6.2.1 Particle Exhaust, Erosion and Recycling.....	6-4
6.2.2 Permeation and Retention of Hydrogen Isotopes and Helium.....	6-7
6.2.3 High Heat Flux Removal.....	6-9
6.2.4 Disruptions.....	6-12
6.2.5 Radiation Effects.....	6-13
6.2.6 System Integration.....	6-13
6.3 Parameter Ranges for Testing.....	6-14
6.4 Survey of Existing Facilities.....	6-17
6.4.1 Erosion/Redeposition and Conditioning.....	6-17
6.4.2 Tritium Permeation and Retention.....	6-19
6.4.3 High Heat Flux Removal.....	6-20
6.4.4 Disruptions.....	6-22
6.4.5 Radiation Effects.....	6-23
6.5 Testing Needs.....	6-23
References.....	6-27

LIST OF FIGURES

<u>Figure</u>	<u>Page</u>
6-1 Experiments and test facilities for plasma interactive components....	6-24

LIST OF TABLES

<u>Table</u>	<u>Page</u>
6-1 General Issues for Plasma Interactive Components.....	6-2
6-2 Specific Uncertainties for Plasma Interactive Components.....	6-3
6-3 Large Tokamak Machine Parameters.....	6-15
6-4 Operating Parameters for Plasma Interactive Components.....	6-16
6-5 Parameters of the PISCES and ICTF High Particle Flux Facilities.....	6-19
6-6 Parameters for the Tritium Plasma Experiment (TPX).....	6-20
6-7 Parameters for High Heat Flux Test Stands.....	6-21
6-8 FELIX Facility Description.....	6-22

6. PLASMA INTERACTIVE COMPONENTS

6.1 Introduction

Plasma interactive component (PIC) refers to any component inside the vacuum vessel that is in direct contact with the plasma. The components vary between magnetic confinement schemes and include pumped limiters, divertor plates, RF antennae and their associated shields, wall armor for neutral beam dumps and the entire inner surface of the vacuum vessel. Each of these components has a specific purpose such as plasma heating or particle exhaust. To perform these tasks on near-term devices, PICs must operate under very high heat fluxes. In a reactor, the environment will also include large charged particle and energetic neutron fluxes. The presence of these components in the machine influences the plasma edge and, ultimately, the particle and energy confinement times through such processes as neutral particle recycle in the edge, hydrogen permeation and release, and impurity generation and transport. The issues and testing needs considered here concentrate: 1) on the development of a data base for material response to fusion plasma edge conditions; and 2) on the testing required to assure that materials and components can withstand the harsh plasma boundary environment. The effect of PICs on core plasma behavior is a confinement issue and will be studied in confinement experiments. The development of diagnostics for use in the plasma edge region is not discussed.

In this chapter, initial experimental planning considerations are presented. These are based largely on previous studies of experimental planning and testing needs for PICs.⁽¹⁻⁵⁾ In Section 6.2, the issues associated with PIC operation are reviewed and the specific uncertainties that must be resolved through material and component testing are identified. In Section 6.3, the parameter ranges that define the testing conditions are presented. Existing test programs in the PIC area are reviewed in Section 6.4. Finally, Section 6.5 discusses additional experiments and test facilities that could address remaining uncertainties.

The strategy described here for plasma interactive components assumes that test plans must accommodate the near-term requirements of confinement experiments as well as develop components capable of extended operation in fusion reactor systems. The requirement to meet both near and long-term pro-

gram goals greatly complicates the construction and evaluation of PIC test plans. For instance, near-term tokamaks will operate with input powers in excess of 10 MW. The limiter or divertor systems for these machines requires the development of novel active cooling systems and armor attachment techniques in order to continue confinement testing. However, solutions developed to meet these near-term needs may not be viable for operation in a 14 MeV neutron flux.

In constructing a test plan for PIC, the near-term testing requirements are largely dictated by the immediate needs of the confinement program. The difficulty is then to decide at what point in time and at what level of effort to pursue long-term problems unique to reactor applications.

6.2 Issues for Plasma Interactive Components

The issues associated with PICs were divided into six general categories listed in Table 6-1. Separate effect testing in each of these categories can begin immediately or has already begun. Separate effect testing is required to qualify candidate materials and to establish a data base of fundamental information. This data base is needed to understand the interplay of all of the competing processes that take place in the complex environment of the plasma boundary layer. Note that these categories of unresolved issues are those associated with operation of components subjected to bombardment by the hot plasma. Issues related to confinement, such as the control of the plasma profiles to achieve less severe edge conditions, are not discussed.

The specific uncertainties in each of the general issue categories are discussed below and a summary table is provided in Table 6-2. Some uncertainties appear under more than one general issue category.

Table 6-1. General Issues for Plasma Interactive Components

-
- Surface Erosion/Redeposition and Conditioning
 - Permeation and Retention of Hydrogen and Helium
 - High Heat Flux Removal
 - Disruption Effects
 - Irradiation Effects
 - System Integration
-

Table 6-2 Specific Uncertainties for Plasma Interactive Components

1. Erosion/Redeposition and Conditioning
 - 1.1 Pristine, Redeposited or In-Situ Generated Coatings
 - Sputtering Rate
 - Chemical Sputtering
 - Physical Properties Measurements
 - Hydrogen Isotope Permeation and Retention
 - Neutron Irradiation Effects
 - Impurity Plating on Insulators
 - Atomic and Molecular Reaction Cross-sections
 - 1.2 Surface Conditioning
 - Conditioning Techniques
 - Heat Flux/Surface Temperature Effects
 - Isotope Exchange
 - Impurity Plating and Re-emission
 - Effects of Redeposited Surfaces
 - Neutron Irradiation Effects
2. Permeation and Retention of Hydrogen and Helium
 - 2.1 Hydrogen Isotope Permeation/Retention
 - Permeation Rate
 - Saturation Limit
 - Isotope Exchange
 - Surface Temperature Effects
 - Effects of Surface Conditioning and Treatment
 - Effects of Redeposited Surfaces
 - Neutron Irradiation Effects
 - 2.2 Hydrogen Isotope Reflection and Desorption
 - Incident Flux Characterization
 - Reflected Flux Characterization
 - Desorbed Flux Characterization
 - Effects of Surface Conditions
 - Atomic and Molecular Reaction Rates
 - 2.3 Helium Migration and Trapping
 - Implantation Rate
 - Production Rate Due to Tritium Decay
 - Migration Properties/Void Formation
 - Helium Trapping in the Redeposition Process
 - Neutron Irradiation Effects on the Above
 - Changes in Physical Properties Due to the Above
3. High Heat Flux Removal
 - 3.1 Water Coolant
 - Critical Heat Flux
 - Augmented Heat Transfer and Pressure Drop
 - Channel Erosion/Water Chemistry Control
 - Flow Distribution and Stability

- 3.2 Liquid Metal Coolants
 - Electromagnetic Effects
 - Flow Distribution and Stability
 - Augmented Heat Transfer and Pressure Drop
 - 3.3 Other Coolants
 - Heat Transfer Limits
 - 4. Disruption Effects
 - 4.1 Eddy Current Forces/Structural Response
 - Field and Current Decay Times
 - Induced Currents (Magnitude, Localization, Duration)
 - Induced Forces (Magnitude, Localization, Duration)
 - 4.2 Melt Layer Formation/Stability
 - Thermal Quench and Field Decay Times
 - Fraction of Stored Energy Deposited
 - Spatial Profiles for Energy Deposition
 - Vaporization Rates
 - Plasma-Vapor Cloud Interaction
 - Depth of Melt Layer Formation
 - Melt Layer Stability Under EM and Gravitational Forces
 - Physical Properties of the Resolidified Surface
 - 5. Neutron Flux and Fluence Effects
 - 5.1 Effects on Erosion Rates
 - Pristine Materials
 - Redepleted or In-Situ Generated Surfaces
 - 5.2 Effects on Surface Conditioning
 - 5.3 Effects on Hydrogen Isotope Transport
 - 5.4 Effects on Helium Formation and Transport
 - 5.5 Insulator Breakdown
 - 6. System Integration
 - 6.1 Remote Maintenance
 - 6.2 Safety
 - 6.3 Component Optimization for Tritium Breeding
-

6.2.1 Particle Exhaust, Erosion and Recycling

Erosion/Redeposition

Erosion/redeposition is a generic issue for all confinement systems. Energetic plasma edge particles will strike the surface of plasma interactive components and cause sputtering erosion. It is expected that the sputtered particles will enter the scrape-off region and possibly the main plasma and eventually redeposit on other exposed surfaces. Calculations predict that the redeposition process is important in reducing the impurity level in the plasma

and for extending the erosion lifetime of plasma interactive components.^(6,7) At present, there is little erosion/redeposition in plasma devices because of their short burn pulses and low availability. In addition, the plasma scrape-off conditions are different from those expected in an ignition device or a reactor where particle and energy fluxes will be much greater. Redepleted materials may exhibit properties which are inferior to those of the base material. The actual properties are unknown because redepleted surfaces of sufficient thickness have not yet been produced. For near-term devices, the primary concern is the level of impurities in the plasma. If redeposition does not occur as predicted, then the plasma impurity level will become unacceptably high in a few seconds. For long-term devices, the primary concern is the erosion lifetime of plasma interactive components, which could be only a few weeks without redeposition.

To date, only graphite, beryllium and titanium-carbide-coated graphite have been used in tokamak applications and each has problems that may prohibit its use in reactors. One notable problem for graphite is irradiation swelling and subsequent tritium retention in the porous material. For beryllium, neutron-induced helium production is a serious problem, and impurity generation through sputtering may limit the usefulness of TiC coatings. Alternative plasma side materials include B, B₄C, SiC, BeO and some higher Z options such as W and Ta. The development of plasma spray technology may allow very thick (over a few cm) surface coatings. Ceramic compounds that have a stable molten phase such as BeO, B₄C, MgO, Al₂O₃, TiB₂, TiC and VC are suitable for plasma spray. Composite coatings of ceramics and metals, cermets, such as SiC/Al and SiC/Ni, have been obtained by plasma spraying and look very promising for high heat flux applications. The physical and mechanical properties of these coatings depend strongly on the fabrication method and on the product form^(1,2); thus, extensive testing of physical properties for these coatings will have to be performed. It should also be noted that, for non-elemental and composite materials, the physical properties may be largely degraded due to surface reconfiguration during the erosion/redeposition process.

Certainly, candidate materials must undergo a large number of qualifying tests before they are used in a confinement application. Fully integrated testing, which includes all of the testing variables, may only be possible in a fusion reactor system but simpler material screening testing must be carried

out. The basic tests include measurements of physical properties, such as thermal stress limits, thermal and electrical conductivity, and physical and chemical sputtering yields. For fueling control and tritium inventory considerations, the hydrogen isotope permeation, retention and isotope exchange properties must be evaluated. This latter topic is treated in Section 6.2.2. All of these material properties may be seriously affected by the erosion and redeposition process and by neutron irradiation and other operating conditions, such as, in the case of a tokamak, strong magnetic fields, an electronegative sheath, rapid field transients and high heat and particle fluxes.

In addition to understanding the material response, testing must also be carried out to understand the plasma behavior and impurity transport in the vicinity of the neutralizing surface. Sputtering measurements can be used to estimate the impurity generation rate from a surface, but knowledge of the local plasma conditions is required to characterize the incident flux and to predict the impurity transport. Here relevant atomic and molecular reactions must be identified and their cross-sections measured.

Surface Conditioning

Surface conditioning is necessary to minimize impurity influx from thermal and particle-induced outgassing and to stabilize the hydrogen recycling properties of the surface. Conditioning is also required for neutral beam and RF heating systems to minimize high voltage breakdown.

The conditioning of plasma-interactive components involves careful pretreatment of the material to insure good vacuum qualities (i.e., low outgassing surfaces, bulk material free of large voids, defects, and cracks that can serve as leak paths). The material is usually physically and chemically cleaned to remove macroscopic contamination, and vacuum baked to degas the bulk material. Pretreatments vary in effectiveness, however, and cannot stand alone as a conditioning method. In-situ conditioning, involving baking and extensive interaction with hydrogen plasmas or atomic hydrogen, is necessary to successfully condition the walls. Successful wall conditioning is defined as the point at which low-Z impurity introduction from first-wall and limiter surfaces is negligible, the hydrogen recycling properties are well-characterized and static, and the tendency of unipolar arc formation is minimal.

In contrast to the conditioning of stainless-steel vacuum vessel surfaces, the conditioning of high flux limiter surfaces remains an open issue. As an example of the problem, graphite and carbide-coated graphite limiters have been used in many presently-operating devices (e.g., PLT, PDX, Alcator-C, ISX, TFR, TEXTOR). Much operation time has been spent in these devices to condition the limiter surfaces so that the limiter has a minimal effect on plasma operation. Yet the chemical and structural changes that occur at the surface (or near the surface) layer of the candidate limiter materials have not been quantified. Also, once the conditioning process is understood, it should be optimized to minimize impact on device operations. However, the more important surface conditioning problem for present and next generation devices will be the optimization of the conditioning process(es) required for plasma-contacting surfaces such as limiters and divertor plates. This problem represents a transition of the surface conditioning process from basically a problem in surface chemistry to a problem concerned with the response of materials to high plasma ion fluxes and high heat loads.

Looking toward reactors, the need for in-situ surface conditioning will tend to diminish as the high heat loads and much higher duty cycle will accelerate the conditioning process. However, pretreatments of materials and judicious choice of materials for plasma-contacting surfaces will become increasingly important. In-situ deposition of coatings and the possible use of binary alloys such as Cu-Li will also become increasingly important. The utility of gettering as a surface conditioning technique seems to be limited for devices beyond the present generation.

The understanding of conditioning and cleaning must be improved to the point where operation at the design level is routine. The most important elements will be rf antenna and neutral beam sources, each of which will require extensive conditioning to provide reliable high-voltage operation and negligible impurity release.

6.2.2 Permeation and Retention of Hydrogen Isotopes and Helium

Tritium

The repeated exchange of hydrogen isotopes between the plasma and surrounding walls is a dominant factor in plasma refueling in present day

devices, and it will control the critically important issues of tritium inventory and permeation in DT reactors. Tritium inventory is a near-term safety and environmental problem that must be addressed for the tritium operation of TFTR and JET and for the design of the next generation Burning Core Experiment (BCX). In advanced long-pulse/high-duty cycle reactor designs (e.g., FED, INTOR, MARS, MFTF- α +T), tritium permeation through plasma interactive components into the coolant can create a severe economic penalty.

A considerable data base has been generated for hydrogen isotope interaction with structural first wall materials such as austenitic stainless steels and Inconel alloys. However, little is known about the interaction of low-Z limiter materials, such as graphite and beryllium, with tritium. TFTR and JET have used graphite exclusively for plasma interactive components; current BCX designs (ISP, LITE, IGNITOR) all have graphite as the baseline material. Yet, graphite is a porous material with an affinity for hydrogen. Much controversy exists in the literature over fundamental tritium properties such as the surface and transgranular diffusivity, bulk solubility, and trap concentrations and binding energies. A reliable model of tritium uptake and retention for graphite in a fusion reactor environment is currently not available. The data base and understanding of tritium interaction with other candidate low atomic number materials (e.g., Be, TiC, SiC) are equally poor. For near-term devices (TFTR through BCX), experiments and theory for tritium interaction with low-Z materials and coatings are needed in order to predict and control the inventory.

In commercial reactor devices, tritium permeation through the first-wall surface and impurity control components into the coolant may lead to contamination of the coolant to unacceptable levels. Tritium inventory is a less serious issue because much larger inventories will exist in other components such as breeding blankets. Options to reduce tritium permeation must be considered including using lower permeability materials and coatings (for example on the coolant side) and coating the plasma surface with a high recycling material.

Measurements should be carried out with hydrogen/deuterium accelerators and plasma discharge devices as well as direct experiments in tritium facilities. Tritium experiments involve the complimentary techniques of gaseous (T_2), atomic (T) and ion (T^+) charging of materials. Tests using lithium

offer many advantages over protium/deuterium in detectability, as well as being a direct measurement rather than a simulation using isotopic substitution. Existing facilities for this program include H/D accelerator laboratories (e.g., Sandia, ORNL, etc.), H/D plasma devices (e.g., Plasma Simulator at ORNL; PISCES at UCLA), and tritium laboratories (e.g., the Tritium Plasma Experiment at Sandia). Extensive theory and computer modelling of tritium retention and release from these low Z materials must accompany the experimental program. The output of this program must also be benchmarked against measurement of hydrogen isotope retention (including tritium from DD reactions) in limiter materials exposed to high power, reactor grade plasmas such as those of TFTR and JET.

To define and solve the tritium permeation problem, significant progress must also be made in understanding: (1) production of trapping sites for tritium by neutron irradiation of the material; (2) changes in surface permeability and plasma side recycling due to erosion/redeposition processes; and (3) release of tritium through interfaces (e.g., from the material surface to the coolant).

Helium

For commercial reactor applications, the problem of helium exhaust from the system is complicated by helium implantation in limiter or divertor surfaces. In fact, it has been proposed that the trapping of helium under layers of redeposited material may be an effective mechanism for ash removal. Helium will also be produced in first walls and in PICs through energetic (n, α) reactions and through the decay of tritium resident in the material. Helium migration and void formation degrades the structural integrity and physical properties, such as thermal conductivity, of most materials. Consequently, all aspects of helium implantation, production and migration must be understood for materials to be used in PICs.

6.2.3 High Heat Flux Removal

Plasma interactive components provide the particle, energy and information interface between the plasma and surrounding reactor. Most of these functions require energy removal capabilities. Furthermore, since the total energy transferred can be 10-30% of the circulating power, it is also desir-

able to be able to recover as much as possible in a usable form. Energy removal is a near-term requirement, while energy recovery is an additional long-term goal. The issues and potential solutions are the same for both, except that energy recovery by standard thermodynamic power cycles requires high-temperature coolant and even less margin for heat transfer uncertainties.

Tokamaks and stellarators are presently anticipated to see peak (normal operation) heat fluxes at limiters and divertors of up to 2 kW/cm^2 , with lower values over large surface areas such as the first wall.^(8,9) Mirrors, because of rapid axial particle and energy flows in the outer radial regions, see a much lower heat flux (10 W/cm^2) on the first wall, although large removal surfaces can be incorporated into the end cell collector plates,⁽¹⁰⁾ components are not generally made larger than necessary, leading to heat fluxes on the order of $0.2\text{--}0.5 \text{ kW/cm}^2$ for direct convertor or halo scrapers. RFP's and other alternate concepts are generally high power density devices. Consequently, larger fractions of the surface area must operate at high heat fluxes (e.g., first wall at 0.5 kW/m^2). In all cases, large areas ($1\text{--}1000 \text{ m}^2$) have to be cooled in steady-state for reactor applications.

Due to its excellent heat transfer capabilities and data base, water is the preferred near-term coolant. Long-term options include other coolants such as helium, liquid metals, organics or molten salts. These alternative coolants are considered for reasons of safety, efficiency, and design simplicity. The choice of PIC coolant is closely related to the primary blanket coolant choice.

The major issues for energy removal and recovery are: 1) heat transfer limits (normal and augmented); 2) flow distribution and stability; 3) channel erosion; and 4) heat source profile. Heat transfer limits may arise for different reasons, including transition to a less efficient heat transfer mechanism (e.g., critical heat flux); limits on increasing flow velocity (e.g., pressure drop, choked flow, channel erosion, flow vibrations); or temperature limits (e.g., coolant boiling, thermal decomposition, solidification, energy recovery efficiency, mechanical strength, chemical compatibility). Normal heat transfer applies to standard laminar or turbulent flow in uniform, smooth-walled channels. Various options exist to increase or augment heat transfer, including swirl flow, roughened surfaces, subcooled boiling, and electric fields. Channel corrosion is a function of materials compatibil-

ity, interface temperature and velocity profile. Channel erosion includes physical scouring of surfaces by corrosion particles and weakening of the surface through cavitation or bubble collapse. Adequate characterization of the heat source profile is a general issue since there is usually little tolerance for unexpected local hot spots, but is not easily addressed outside of a fusion device.

The primary uncertainties in heat transfer limits are critical heat flux (water, organics, molten salts), pressure drop (liquid metals) and flow stability (all).⁽¹¹⁾ For up to about 1 kW/cm^2 , there is reasonable confidence for design predictions, although one-sided CHF (critical heat flux) measurements for liquid coolants (water) at long L/D are desirable. However, liquid metals require substantial effort to reach even these heat fluxes because of uncertainties in MHD effects especially in complex geometries. For heat fluxes above 1 kW/cm^2 , it is necessary to know the relevant CHF limits. If heat transfer augmentation is used, it will also be necessary to determine the corresponding heat transfer and pressure drop correlations.

At the higher heat fluxes and associated higher velocity flow, flow distribution, flow stability and channel erosion are principal problems. The velocities at which the onset of flow and channel erosion problems occur is not well-defined. Practical experience with water suggests 20 m/s as an upper limit for straight channels. For comparable inertial force, this suggests limits of 300 m/s for He (5 MPa), 30 m/s for Li and 20 m/s for organic coolants (higher values require particular attention to design of headers and structural support, and may not be entirely predictable). Practical helium flow limits of about 1/3 sonic speed also imply about 300 m/s at 5 MPa though higher pressures may be possible. For organic and molten salt coolants, further uncertainties include the control of fouling under high temperature or irradiation-induced decomposition (e.g., by use of smooth geometries and coolant chemistry control).

For these energy removal and recovery issues, steady-state operation of large heated surfaces at high heat flux loads must be demonstrated. Small-area tests may miss channel length effects (e.g., short lengths may be in the entry length regime), multiple channel effects (e.g., flow instabilities including stagnant and reversed flow), header effects on pressure losses and flow distribution, and mechanical rigidity (which affects flow-induced vibra-

tions) of the component. High heat flux capability is needed because it allows for more compact hardware, with associated advantages in ease of removal and in minimizing plasma contamination and parasitic neutron absorption.

6.2.4 Disruptions

Disruptions result in a rapid reduction in the plasma current accompanied by the localized deposition of much of the plasma energy on an interior surface. Disruptions are observed in all tokamaks, and the phenomena is poorly understood. Consequently, elimination of disruptions for future machines cannot be assured, and plasma interactive components must be designed to withstand the induced forces and high heat fluxes that accompany these events.

For assessing damage to in-vessel components, disruptions are presently divided into two phases, a thermal quench phase which produces localized high heat fluxes, and a current decay phase which induces large forces on the vacuum vessel and in-vessel components. For TFTR, the energy deposition time is about 0.3 ms⁽¹⁾ and is observed to be highly localized. Thus, for near-term applications, it is generally assumed that half of the stored plasma energy is deposited upon a single component, such as a single limiter module, leading to estimated heat fluxes well in excess of 10 kW/cm².

Heat fluxes of this magnitude can cause surface vaporization and melt layer formation. The interactions between the vaporized surface material and the incident plasma are not understood but are important since the outgoing vapor cloud has the potential to shield the surface and prevent more extensive damage. The difficult problem of stability analysis of the surface melt layer is compounded by the induced eddy current forces generated by the current decay. This too is an area requiring further analysis and testing as even the relative time dependence of the two phases of the disruption is not known.

The forces produced during the current decay phase determine to a large extent the structural support required for the vacuum vessel and plasma interactive components. The major forces result from the coupling of the induced eddy currents in the vessel or other plasma interactive components with the externally applied magnetic fields. The magnitude of these forces is primarily determined by the current decay time. For operating tokamaks, this

ranges from 1 to 10 ms and has been observed to increase with plasma current.(1,2)

The best hope for eliminating disruptions in tokamaks is the detection of disruption precursors followed by the activation of "soft landing" feedback systems. However, until such detection and feedback systems are available, efforts to design durable plasma interactive components must continue as future tokamaks may require frequent component replacement which would seriously impact the availability of these devices.

6.2.5 Radiation Effects

Radiation effects are generic to all fusion systems and radiation damage will affect the lifetime and operating limits of PICs. Radiation damage due to 14 MeV neutrons will affect most of the thermal and mechanical properties of materials. In the case of structural alloys, the primary concerns are the effects on the mechanical properties, including ductility (impact, tensile, and creep), strength, fatigue and crack growth behavior, and dimensional instability resulting from void or gas bubble swelling and radiation induced creep. These effects also cause concern for the plasma side materials, but the degree of concern is not as great since the plasma side materials do not carry primary loads. The integrity of bonds is expected to be degraded by radiation damage. In the case of non-metals and insulators, the thermo-physical properties, such as thermal conductivity and electrical resistance, will also be degraded.

Beyond these fundamental concerns, materials considered for use in reactor application must be evaluated in terms of the synergistic effects that neutron irradiation might have on surface conditioning, the erosion/ redeposition process, hydrogen isotope permeation and retention in the material and helium transport and void formation. Scoping tests can be accomplished by rotating samples between various separate-effect test stands or by material testing in a long-pulse, burning-core fusion experiment.

6.2.6 System Integration

The incorporation of complex plasma interactive components into the fusion machine is a difficult task. The environment to which these components

are exposed is quite severe and the performance demands on the components are very high. Certainly a great deal of material qualifying and component acceptance testing will have to be carried out before a PIC is allowed to be installed on a complex and expensive fusion experiment or reactor. Extensive testing of materials and components prior to plasma exposure reduces the risk of severe component failure, but safety precautions and procedures for remote maintenance must clearly be developed. Remote maintenance and safety issues are receiving more serious attention as confinement experiments such as TFTR move closer toward operation with tritium plasmas.

Though this is an important area, no specific test plan for system aspects of PIC testing has been considered. It is assumed that maintenance, accident and safety issues should evolve and are best addressed during the design of confinement experiments as these experiments move toward longer pulses, greater system availability and significant tritium consumption.

6.3 Parameter Ranges for Testing

The uncertainties associated with PICs have been identified in the last section; in this section, the parameter ranges for addressing these uncertainties are specified. Development of an experimental test plan for PIC is complicated by the requirement to accommodate both the near-term needs of plasma confinement experiments and the long-term needs of reactor systems. Thus, the parameter ranges for testing often change with time.

The testing environment is most easily defined by reviewing the machine parameters for confinement experiments now operating and for those planned for the future. Table 6-3 summarizes machine parameters for large tokamaks that are scheduled for operation between now and the turn of the century. The important parameters for PICs are summarized in Table 6-4, where the operating regimes for present, near-term and longer-term machines are identified.

The changing parameters from one class of devices to the next have important implications for PICs. For instance, increasing pulse lengths coupled with larger amounts of injected power require that limiters or other PICs in direct contact with the plasma be actively cooled in the next generation of devices (e.g., JET, JT-60 and Tore Supra). Thus, problems in high heat flux removal and associated thermomechanical behavior require immediate attention. However, while heat fluxes in near-term confinement experiments

Table 6-3. Large Tokamak Machine Parameters (12-22)

Device	TFTR	JET	JT-60	T-15	Doublet 3-D	Tore Supra	ISP	LITE	NET	FER
Country	USA	EC	Japan	USSR	USA	France	USA	USA	EC	Japan
First Plasma	Dec. '82	Jun. '83	Apr. '85	late '85	Jan. '86	mid '87	—	—	1992	1995
Major Radius (m)	2.55	2.96	3.0	2.4	1.67	2.42	1.62	1.76	6.4	5.5
Minor Radius (m)	0.85	1.25	0.95	0.70	0.67	0.70	0.53	3.2	1.64	1.1
Elongation	1.0	1.0-1.6	1.0	1.0	1.0-2.0	1.0	1.6	1.6	5.7	1.5
Toroidal Field (T)	5.2	3.5	4.5	3.5-4.5	2.2	4.5	8.9	9.4	—	5.7
TF Coil Conductor	Cu	Cu	Cu	Nb ₃ Sn	Cu	NbTi	Cu	Cu	—	Nb ₃ Sn/NbTi
Working Gas	H/DI(?)	H/DI	H	H	H	H/D	DT	DT	DT	DT
Plasma Current (MA)	2.5-3.0	4.8	2.7	1.4-2.0	3.5-5.0	1.7	7.8	7.0	10.0	5.3
Pulse Length (s)	1.0-3.0	10-20	5-10	5.0	2.0-5.0	30	5.0	10.0	200-1000	100
Injected Power (MW)	38	46	30-40	5.5-8	20	21	30	15	—	30
Neutral Beam	27	16	20-30	5.5-8	12-14	7	—	—	—	—
ICRH	8	30	3	—	6	6-9	—	—	—	—
LHRH	3	—	8	—	—	5-8	—	—	—	—
ECRH	—	—	—	4-6	—	—	—	—	—	—
Fueling	gas puff pellet inj	gas puff	gas puff	gas puff pellet inj	gas puff pellet inj	gas puff pellet inj	gas puff pellet inj	gas puff pellet inj	gas puff pellet inj	gas puff pellet inj
Impurity Control*	gettering	wall cond	mag lim wall cond	wall cond	pump lim stubby div	wall cond pump lim ergodic div	lim or div	pump lim	—	pol div
Fusion Power (MW)	—	—	—	—	—	—	305	420	1170	440
Wall Load (MW/m ²)	—	—	—	—	—	—	5.6	1.7	1.5	1.0

* Wall conditioning; pump limiter; stubby divertor; magnetic limiter; ergodic divertor; limiter or divertor; poloidal divertor.

Table 6-4. Operating Parameters for Plasma Interactive Components

Time Scale	Present Machines (0-3 years)	Near Term (3-8 years)	Early 1990s	Long Term (Beyond 2000)
Field Strength (T)	3-6	3-6	5-10	5-10
Plasma Current (MA)	0.5-3.0	2.0-4.0	2.0-7.0	5.0-11.0
Injected Power (MW)	5-15	15-50	15-50	15-50
Peak Heat Flux (kW/cm ²) (normal operation)	0.4-5.0	0.5-5.0	1.0-5.0	1.0-5.0
Pulse Length (s)	1-5	5-30	30-300	CW
Number of Cycles	10 ⁵	10 ⁵	10 ⁶	--
Neutron Wall Loading (MW/m ²)	--	--	1.0-5.0	1.0-5.0
Neutron Fluence (dpa)	~0	1	25	60
Fusion Power (MW)	--	--	300-500	500-1200
Surface Materials	C, TiC-coated C, Be	Re, ReO, SiC, C	Re, W, Ta	Re, W, Ta, V
Structural Materials	Stainless steels, Ni alloys	Stainless steels, Ni alloys, Cu alloys	Cu alloys, Refractory metals	Cu alloys, Refractory metals
Bonding/Attachments	Mechanical	Mechanical, bonded, plasma spray	Bonded, plasma spray	Bonded, plasma spray
Coolant Types	none	H ₂ O	H ₂ O	H ₂ O, Liquid metals, others?
<u>Disruption Characteristics</u>				
Current Decay Time (ms)	0.1-1.0	1.0-10	5.0-200	5.0-200
Thermal Quench Time (ms)	0.02-0.3	0.3-3.0	3.0-100	3.0-100
Peak Heat Flux (kW/cm ²)	80-500	500	500	500

will be quite high, ($\sim 2 \text{ kW/cm}^2$), synergistic effects of neutrons and high particle fluence will not be included. Therefore, heat removal techniques and materials devised for use in these machines can only be considered as possible but not necessarily acceptable solutions for burning core experiments or reactor applications.

Tritium may be used in both JET and TFTR, but the extent to which this experience will resolve the uncertainties identified for tritium permeation and retention is judged to be quite small since large charged particle and neutron fluences will not be realized. The problems of maintaining acceptable tritium permeation and inventories begin to manifest themselves in burning core experiments. But erosion rates and neutron fluences may still be deficient in these experiments for the purpose of fully understanding tritium behavior.

The erosion/redeposition process and the effects of 14 MeV neutrons, two very important problem areas for reactors, will also remain secondary issues on confinement experiments until pulse lengths and system availability increase to the point where large charged particle and neutron fluences can be realized. These levels of fluence will not be achieved in short-pulse burning-core experiments but will generate serious problems for systems like LITE,⁽¹⁸⁾ NET,⁽¹⁹⁾ and FER.⁽²⁰⁾

It is also important to study disruption behavior in existing and near-term tokamaks. Detection of disruption precursor signals may allow for the development of rapid feedback systems for initiating plasma soft landings. Information on how much of the plasma stored energy is deposited on what surface area must be obtained so that testing for materials and components can be carried out in the proper parameter ranges. Finally, the relative time dependence of the current decay and thermal quench phases must be determined so that the problem of induced eddy current forces acting on surface melt layers can be usefully investigated outside of the tokamak.

6.4 Survey of Existing Experiments

6.4.1 Erosion/Redeposition and Conditioning

The principal on-going work in this area is the post-plasma-exposure analysis of limiter surfaces and other PICs. Analysis techniques include Rutherford backscatter, nuclear reaction analysis and photon induced x-ray

analysis. These techniques combine to give a detailed description of near-surface composition before and after plasma exposure. This allows for measurements of surface coating erosion rates, impurity deposition and hydrogen isotope implantation depths. Such measurements have been carried out on PICs removed from PLT, PDX, TMX-U, TFTR, TEXTOR, ISX and other machines. These measurements greatly contribute to the fundamental data base, but the experiments lack the large ion fluxes needed to evaluate the redeposition process and include no neutron effects.

Experiments have been proposed that attempt to reproduce the complex environment of the plasma edge region outside of a confinement device. Most notable among these are PISCES,⁽²³⁾ which is presently operating at UCLA, and the ICF proposed by researchers at ANL.⁽²⁴⁾ The basic parameters for each of these machines are listed in Table 6-5. The technology issues that should be addressed include:

- 1) erosion/redeposition properties of candidate surfaces materials under high particle fluence;
- 2) operating limits for plasma side application of high-Z materials such as W or Ta (e.g., at what plasma temperature will runaway self-sputtering cascades be initiated);
- 3) sputtering and redeposition behavior of alloys and compounds; and
- 4) testing of self-pumped helium removal concepts.

The physics issues addressed in experiments of this type include:

- 1) investigations of high recycling regimes;
- 2) optimization of limiter and divertor geometries;
- 3) evaluation of conditioning techniques in a controlled environment; and
- 4) providing a controlled testing environment for benchmarking computational models.

The ICF experiment produces conditions much more representative of the plasma edge environment but is also a much more expensive facility (2-5 M\$). While such a facility provides valuable data, irradiation effects are still not included and the plasma edge conditions are not identical to those in a fusion reactor.

Table 6-5. Parameters of the PISCES and ICTF High Particle Flux Facilities^(23,24)

Parameter	PISCES		ICTF
	Maximum	Typical	Proposed
Gas	--	H,D,He,Ar	H,D,He,Ar
Operating Time (hr)	continuous	4-8	continuous
Ion Flux (H^+/m^2-s)	2×10^{19}	$10^{22}-10^{23}$	3×10^{22} (a)
Charge exchange / Ion flux	--	--	0.5
Energy Flux (MW/m^2)	10	--	2 (a)
Density (l/m^3)	5×10^{19}	10^{18}	10^{19}
Plasma Area (cm^2)	100	50-80	300
Electron Temperature (eV)	25	6-20	50
Ion Energy/Temperature (eV)	1	0.5	50-200
Sample Bias (V)	1000	50-500	1-3 T_e
Magnetic Field (T)	0.2	0.025-0.08	5
Base Pressure (Torr)	--	5×10^{-8}	--
Ionization	Disc cathode	10-50%	--
	Hollow cathode	40-90%	--
Hydrogen Ionization Length (cm)	--	0.5-200	--
Iron Ionization Length (cm)	--	0.1-50	--

(a) At 5° angle of magnetic field with target; angles from 5-90° possible.

6.4.2 Tritium Permeation and Retention

Some information on the behavior of hydrogen isotopes in materials is being obtained through the post-plasma-exposure analysis of PICs removed from existing confinement experiments. These samples contain hydrogen and/or deuterium and can be analyzed using nuclear reaction analysis.

The Tritium Plasma Experiment, TPX, located at Sandia National Laboratories in Livermore, is studying the interaction of various materials with a

tritium plasma.⁽²⁵⁾ In this experiment, a plasma, produced with any ratio of hydrogen isotope concentrations, can be generated and used to impact ions onto a biased sample. Incident ion energies up to 1 keV are possible at ion fluxes of $5 \times 10^7/\text{cm}^2\text{-s}$. Tritiated samples allow the use of such diagnostics as autoradiography, imaging and dissolution counting. Operating parameters for TPX are listed in Table 6-6.

Once again the facility contributes greatly to the data base but synergistic effects (e.g., neutrons) are not included.

Table 6-6. Parameters for the Tritium Plasma Experiment (TPX)⁽²⁵⁾

Gas	H/D/T/He mixtures
Operating time	continuous
Ion Flux ($\text{H}^+/\text{m}^2\text{-s}$)	5×10^{21}
Plasma density ($1/\text{m}^3$)	10^{17}
Electron temperature (eV)	7
Ion energy (eV)	10-1000
Gas pressure (mtorr)	2-10

6.4.3 High Heat Flux Removal

Existing and near-term confinement experiments are facing difficult problems in active cooling of high heat flux (HHF) components. Of immediate interest are pump-limiter front-face surfaces and leading edges, divertor neutralizer plates, rf antenna shields and neutral beam dump armors. To ensure reliable operation of these components, a considerable amount of HHF testing is being conducted. Operating test stands include a number of electron and ion beams. Some have been developed specifically for HHF testing of fusion materials and components. Others have been constructed as part of the neutral beam development program but may be converted to accommodate PIC testing.

Parameters for the major HHF test stands are listed in Table 6-7.^(1,2) Presently these facilities are being used 1) to measure the thermophysical

Table 6-7. Parameters for High Heat Flux Test Stands (1,2)

Facility	e-beam (SNLA)	e-beam (HEDL)	PMTF (SNLA)	Ion Beam (TRW)	DCTS (LLNL)	NRTS (LRL)	METF (ORNL)	HPTF (ORNL)	RFTF (ORNL)
Type	----- e-beams -----	----- ion beams -----	neutral beam test stands -----						
Particle type	e	e	H ⁺	any gas	H, He	H ⁺ , D ⁺	H ⁺	H ⁺	H, D, e, He
Energy (keV)	30	12-25	40-80	.05-2	50-100	40-80	80	120	0.01
Current (A)	1	2.5-5	20-40	10	0.2	50	60	30	--
Power (kW)	30	60	1600	20	10	--	4000	3600	1000
Pulse Length (s)	0.001-CW	0.5-CW	30	CW	CW	< 30	30	10	CW
Heat Flux ₂ (kW/cm ²)	0.3-3000	0.3-60	8	0.2	0.1-1.0	2	< 30	< 50	0.4
Test Area (cm ²)	0.01-100	1.0-200	100-200	100	10-100	--	1000	100	3000
Coolant	H ₂ O	H ₂ O	H ₂ O	H ₂ O	H ₂ O	H ₂ O	H ₂ O	H ₂ O	H ₂ O
Pressure (MPa)	2.0	0.8	6.8	--	--	--	1.7	1.7	1.7
Flow Rate (L/s)	3	1	30	--	--	--	60	60	80
Heat Removal (kW)	30	60	200	--	--	--	> 4000	> 6000	> 1000
Status*	Oper	Const	Const	Oper	Oper	Oper	Oper	Oper	Const

Oper - operating; Const - Under construction;

properties of materials for which the data base is poor, such as for Be and for novel coatings produced by plasma spray; 2) to evaluate brazing and bonding techniques; 3) to study critical heat flux onset and augmented heat transfer techniques; 4) to study melt layer formation and stability in disruption simulations; 5) to test the heat removal capacity of coolant systems designed for use in PIC applications; and 6) to study coolant channel erosion caused by flow cavitation and coolant impurities. The electron beam facility under construction at HEDL will allow HHF testing of highly irradiated specimens.

6.4.4 Disruptions

The primary concern of disruption testing is the correct simulation of the event. Correct testing parameters can be provided only by careful diagnosis of the events as they occur in tokamaks. HHF test stands are producing surface melt layers and the properties of the resolidified surface are being measured. In the area of induced currents and forces, the FELIX facility at Argonne National Laboratory, described in Table 6-8, is being used to study eddy current patterns and the magnitude and localization of the induced forces and torques.^(26,27) Development of transient electromagnetic codes is also an integral part of the FELIX program.

Table 6-8. FELIX Facility Description^(26,27)

Facility Specifications	
Solenoid Field Strength	1.0 T (4.0 T) ^a
Dipole Field Strength	0.5 T (1.0 T) ^a
Dipole Ramp Time	10 ms (3 ms)
Test Volume	0.75 m ³
Diagnostics	
Force Sensors	
Displacement/Rotation Sensors	
Rogowski Coils	
IR Thermography	

^aIndicates upgrade field levels

6.4.5 Radiation Effects

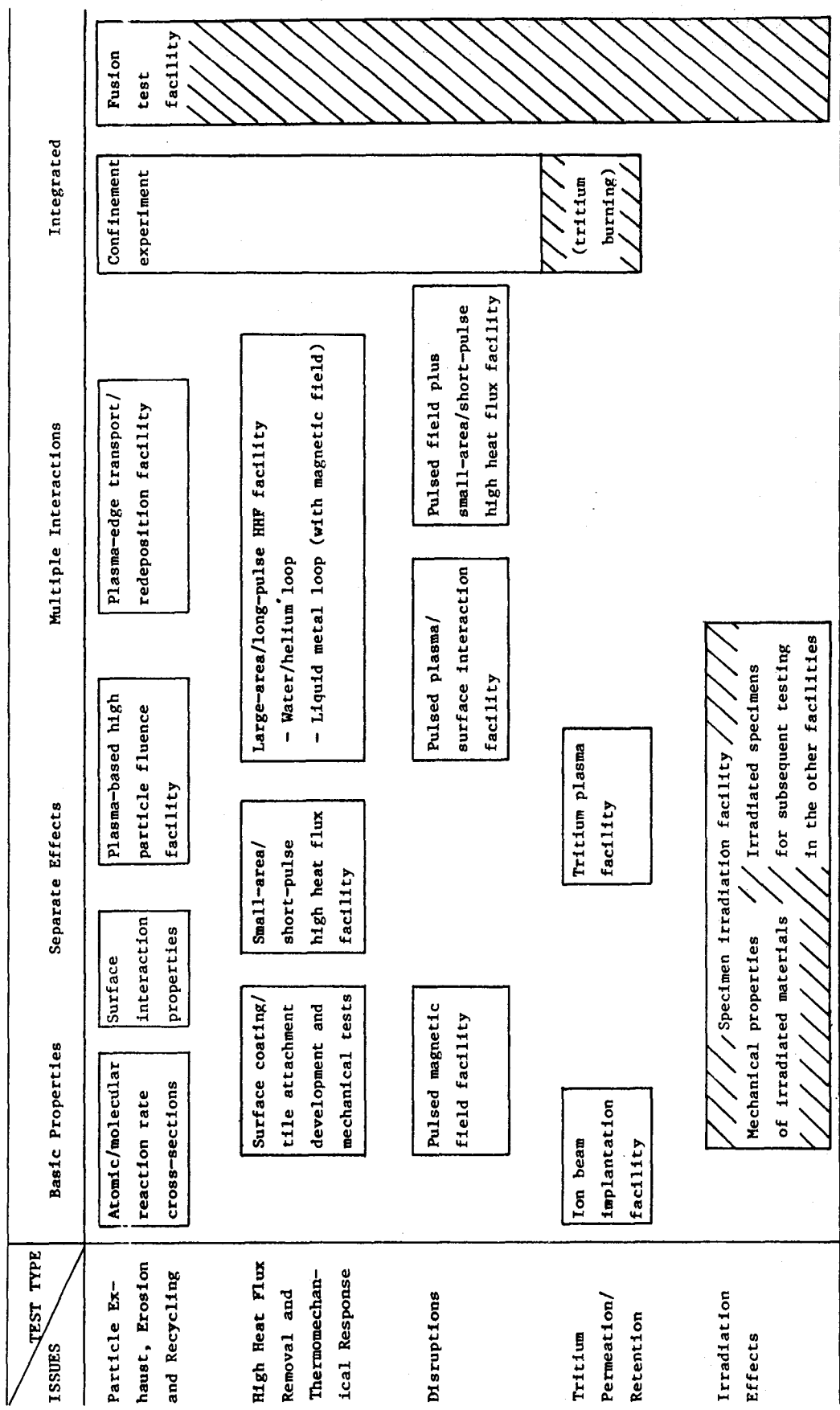
Existing facilities for neutron irradiation include EBR-II, FFTF and other fission reactors, and some point neutron sources such as RTNS-II. Their testing capabilities are discussed in Chapter 8. Of primary concern to PIC testing are the energy spectrum and fluence levels that can be achieved in the tests. Limited testing for the effects of irradiation on mechanical behavior and electrical properties of some candidate PIC materials is underway.

6.5 Testing Needs

Possible experiments and test facilities that could address major material- and technology-related uncertainties for plasma interactive components are indicated in Figure 6-1. These are organized according to the class of issues addressed, and according to the level of integration of the experiment. These experiments were not analyzed in detail here, so their parameters, costs, and relative importance for resolving the issues are not certain. However, some general comments can be made.

With respect to particle exhaust and surface effects such as erosion/redeposition and surface conditioning, there are a number of basic properties that remain uncertain for some candidate materials. These include, among others, atomic and molecular reaction rate cross-sections, sputtering yields, particle reflection coefficients at low energies, and secondary electron emission. These can be measured in well-calibrated and controlled test facilities. Sputtering yields could also be measured with redeposited and/or irradiated specimens.

The need to provide redeposited surfaces to examine surface properties, and the need to understand surface phenomena under high erosion rate conditions leads to a role for plasma-based high particle fluence facilities. As indicated in Figure 6-1, two non-fusion facilities could be considered: a smaller one able to provide high particle fluences for addressing local erosion/redeposition effects and a larger one with a more reactor-relevant edge to include effects related to the size of the plasma column with respect to recycling and ionization mean free paths, magnetic field angle, and large area redistribution of the eroded material. An example of the former is PISCES, and an example of the latter is the proposed mirror-based ICTF or a large PISCES-like plasma discharge facility. It must be noted, however, that



//// Neutron experiment

Figure 6-1. Possible experiments/facilities for plasma interactive components.

there exist doubts as to the usefulness of providing such testing in other than a truly reactor-relevant environment. The preferred test facility for a tokamak reactor, for example, would be a long-pulse tokamak.

The development of high heat flux removal techniques includes both thermal-hydraulic and thermomechanical effects. A basic program is needed to develop methods of providing the special surface materials assumed in many designs. These could include direct surface coatings (plasma spray, chemical vapor deposition), or methods to mechanically attach or bond tiles to some substrate material. The heat transfer and mechanical strength of the interface between a surface and substrate material are of considerable concern, and will require testing. Small-area and short-pulse high surface heating facilities can provide data on the thermal resistance characteristics of candidate coating materials and bonds. However, larger area and long-pulse HHF facilities will be needed to measure critical heat flux, heat transfer characteristics and stresses over useful sections of in-vessel components, and to understand the flow behavior of high heat flux coolants.

To the extent that disruptions or similar rapid electromagnetic/thermal transients are possible, a testing program will consist of measurements in confinement devices to identify the characteristics of disruptions, and of potentially non-fusion measurements to understand the complex processes related to mechanical stresses (a pulsed magnetic field facility such as FELIX), and to the effects of such phenomena as the plasma-surface interaction (e.g., vapor shielding) and melt layer stability (a combined magnetic field/HHF facility). In the latter case, the heat source need not be large or long pulse, but would have to be able to provide controlled heating in the presence of a pulsed magnetic field. Such non-fusion facilities could be used to develop models, but the characteristics of disruptions are presently poorly known and the relevance of such models to reactors is uncertain. On the other hand, the confinement experiments themselves have too complex and harsh an environment for understanding the disruption-related phenomena other than the nature of the disruption and integral "consequence" parameters (e.g., depth of melt layer).

Tritium permeation and retention can be related to plasma-driven implantation processes or pressure-driven processes. The former is of more interest

for PICs. Tests include understanding the basic properties and behavior with ion beam (charged or uncharged atoms and molecules) implantation facilities. Beyond this, measurements in plasma-based facilities could be useful to explore effects under more realistic surface bombardment conditions. In general, it may be possible to use deuterium or hydrogen and measure permeation and retention by various techniques. However, there are advantages to using tritium in that higher accuracy can be obtained with smaller amounts of tritium, and also any isotopic effects are correctly accounted for.

Irradiation effects are presently anticipated to be observed by the irradiation and associated testing (mechanical or other properties) of specimens in suitable neutron facilities. Fission reactors and some DT point sources are available, although concerns about the relevance of the environment (neutron energy spectra, flux, fluence) may limit the overall usefulness of these tests for some materials. Irradiated specimens can also be used in other facilities to measure (sequentially) synergistic effects, such as the effects of irradiation on tritium trapping.

REFERENCES FOR CHAPTER 6

1. Conn, R.W., et al., "Technical Assessment of the Critical Issues and Problem Areas in the Plasma Materials Interaction Field," UCLA, PPG-765, (1984).
2. Abdou, M., et al., "Technical Assessment of the Critical Issues and Problem Areas in the Plasma Materials Interaction Field," UCLA, PPG-815, UCLA-ENGR-84-25 (1984).
3. Stacey, W.M., Jr., et al., "US-INTOR Conceptual Design," USA INTOR/81-1, Vol. I & II, Georgia Institute of Technology (1981).
4. Abdou, M., et al., "Report on the International Workshop on Fusion Nuclear Technology Testing and Facilities," PPG-872, UCLA-ENG-85-17, (March 1985).
5. Kohzaki, Y., et al., "Systems Analysis of a Fusion Research and Development Program Based on the GERT Technique," J. Fusion Energy, vol. 3, no. 5-6, pp. 473 (1983).
6. Brooks, J.N. and McGrath, R.J., "Redeposition of the Sputtered Surface in Limiters," 9th Symposium on Engineering Problems in Fusion Research," IEEE No. 81CH1715-2 (October 1981).
7. Stadenmaier, G., "Erosion and Deposition in Tokamaks," Technical Aspects of the Joint JET-ISX-B Beryllium Limiter Experiment, pp. 1091.
8. Milora, S.L., et al., "A Numerical Model for Swirl Flow Cooling in High-Heat Flux Particle Beam Targets and the Design of a Swirl-Flow-Based Plasma Limiter," ORNL-DWG-84-2413 FED.
9. US-France Workshop on Tore Supra, Albuquerque, NM (July 1985).
10. Logan, G.B., "MARS-Mirror Advanced Reactor Study," J. Vac. Sci. & Tech.-A, vol. 3, no. 3, Part II, pp. 1129 (May/June 1985).
11. Boyd, R.D., et al., "Technical Assessment of Thermal-Hydraulics for High Heat Flux Fusion Components," SAND84-0159 (January 1984).
12. Davis, L.G. and Luxon, J.L., "The Doublet III Big Dee Project," J. Vac. Sci. & Tech.-A, vol. 3, no. 3, Part II, pp. 1161 (May/June 1985).
13. Duesing, G. and Dietz, K.J., "Construction, Operation and Enhancement of JET," J. Vac. Sci. & Tech.-A, vol. 3, no. 3, Part II, pp. 1151 (May/June 1985).
14. PPPL Design 0424, ISP.
15. Schmidt, J.A., "Summary Abstract-TFCX Design Study," J. Vac. Sci. * Tech.-A, vol. 3, no. 3, Part II, pp. 1141 (May/June 1985).

16. Scheffield, J., "The Advanced Toroidal Facility," J. Vac. Sci. & Tech.-A, vol. 3, no. 3, Part II, pp1 1134.
17. Tone, T., "The Tokamak Reactor," J. Fusion Energy, vol. 3, no. 5/6, pp. 445 (December 1983).
18. Berwald, D.H., et al., "LITE Design Study--TRW," Private Communications.
19. Toschi, R., "Summary Abstract-The Next European Torus," J. Vac. Sci. & Tech.-A, vol. 3, no. 3, Part II, pp. 1143 (May/June 1985).
20. Miyamoto, O. and Koshikawa, O., "Tokamak--Core Plasma Studies; Physics and Technology," J. Fusion Energy, vol. 3, no. 5/6, pp. 329 (December 1983).
21. Abe, T., et al., "Initial Experiments in JT-60," 12th European Conference on Cont. Fusion and Plasma Science, Budapest (September 1985).
22. Dylla, H.F., et al., "Surface Analysis of TFTR Limiter Tiles," J. Vac. Sci., & Tech.-A, vol. 3, no. 3, Part II, pp. 1105 (May/June 1985).
23. Goebel, D.M., Campbell, G., Conn, R.W., J. Nuc. Mat., 121, p. 277, 1984.
24. Goebel, D.M., Conn, R.W., J. Nuc. Mat., 128 & 129, 1984.
25. Brooks, J.N., et al., "An Impurity Control Test Facility (ICTF) for the Study of Fusion Reactor Plasma/Edge Materials Interactions," Interim Report, ANL/FPP/TM-188 (May 1984).
26. Kerst, R.A., J. Vac. Sci. & Tech., 20, pp. 1267, 1982.
27. Turner, L.R. and Cuthbertson, J.W., "Coupling Between Angular Deflection and Eddy Currents in the FELIX Plate Experiment," ANL/FPP/TM-176 (August 1983).
28. Turner, L.R., "Proposed FELIX Experiments for 1985 and Beyond," Workshop on FELIX Exp. Prog., ANL (December 7, 1984).

CHAPTER 7

RADIATION SHIELDING

TABLE OF CONTENTS

7. RADIATION SHIELDING

	<u>Page</u>
7.1 Introduction and Issues.....	7-1
7.2 Status of Experiments, Data and Methods.....	7-6
7.2.1 Required Accuracies and Status of Experiments.....	7-7
7.2.2 Status of Data Base and Methods.....	7-12
7.3 Experiments and Facilities.....	7-17
7.3.1 Experiments.....	7-19
7.3.2 Point Neutron Source Facility.....	7-26
7.3.3 Fission Neutron Source.....	7-30
7.4 Shielding Experiments in Fusion Test Facility.....	7-35
7.4.1 Operating Condition Requirements.....	7-35
7.4.2 Test Matrix Requirements.....	7-36
References.....	7-52

LIST OF FIGURES

<u>Figure</u>	<u>Page</u>
7-1 Configuration of ORNL streaming experiment (Ref. 11).....	7-11
7-2 Attenuation of neutron flux through SUS316 bulk shield (Ref. 12)....	7-11
7-3 Top view of FNS point neutron source facility.....	7-28
7-4 Nuclear heating rate calculated by 14MeV and fission spectrum sources.....	7-31
7-5 Comparison of neutron spectra in shield.....	7-33
7-6 Contribution of high energy neutron on total heating.....	7-34
7-7 Streaming experiment using TSF (ORNL).....	7-34
7-8 Nuclear heating rate distribution on radial direction.....	7-39
7-9 R- θ calculation model of shielding test matrix.....	7-40
7-10 Comparison of nuclear heating rates between the cases, full coverage, $\theta = 8^\circ$ and $\theta = 15^\circ$	7-41
7-11 Comparison of dpa rates between the cases, full coverage, $\theta = 8^\circ$ and $\theta = 15^\circ$	7-43
7-12 Comparison of gas production rates between the cases, full coverage and $\theta = 12^\circ$ with and without reflector.....	7-44
7-13 Effect of reflector on toroidal distributions of heating rates at $r = 0, 20$ and 40 cm.....	7-45
7-14 Dependence of nuclear heating rate on toroidal dimension. The relative values to the centerline ones are shown for $r = 20 \sim 80$ cm.....	7-47
7-15 r-z calculation model of shielding test matrix.....	7-48
7-16 Comparison of nuclear heating rate in the test matrices with poloidal heights 250, 120 and 102 cm.....	7-49
7-17 Dependence of nuclear heating rates on poloidal dimensions. The relative values to the centerline are shown.....	7-50

LIST OF TABLES

<u>Table</u>	<u>Page</u>
7-1 Requirements for Shielding of Some Parameters.....	7-2
7-2 Radiation Shielding Issues.....	7-3
7-3 Required Accuracies and Present Status in Nuclear Design of Fusion Reactors.....	7-8
7-4 Shielding Experiments Performed with the Use of 14 MeV Point Source.....	7-10
7-5 Summary of Material Proposed for Blanket and Shield.....	7-13
7-6 Elemental Materials of Potential Use in Fusion Reactors; A Qualitative Judgement on the Probability of Using the Material is Shown.....	7-14
7-7 Issues/Facilities Matrix for Shielding.....	7-18
7-8 Examples of Experiments.....	7-20
7-9 Types of Nuclear Data Required in Fusion Nuclear Design.....	7-21
7-10 High Priority Nuclear Data Needs for Fusion Reactors.....	7-22
7-11 Neutronics Parameters and Detectors.....	7-25
7-12 Comparison of Neutron Source Facilities for Shielding Tests.....	7-29
7-13 Contribution from High Energy Neutron (> 2.5 MeV) to Damage Parameters (%).....	7-35
7-14 Isotropic Compositions of Materials.....	7-37
7-15 Comparison of Shielding Parameters Calculated by 46 and 23 Group Cross Sections.....	7-42

7. RADIATION SHIELDING

7.1 Introduction and Issues

The role of radiation shielding is to protect the reactor components, the reactor operators and the public from intolerable levels of radiation exposure. The most sensitive components are superconducting magnets, some elements of plasma heating and exhaust systems, and instrumentation and control. Shielding must reduce the radiation damage and the nuclear heating for these components and the biological dose below the design criteria or the regulatory level. Though many shielding designs exist, the design criteria differs among themselves by factors or even an order of magnitude. Some of these design criteria are based on untested assumptions and incomplete models, and the uncertainties are not well evaluated. These uncertainties will impact the construction and operation cost, the availability, the maintainability, and the life of the reactor.

Most of the fusion neutron energy is converted into thermal energy in the blanket (more than 95%), but the flux of neutron and γ -rays exiting the blanket are still higher by several orders of magnitude than the acceptable radiation levels. For example, Table 7-1 shows typical design criteria, radiation level at the first wall, and the required shield reduction factors for the superconducting magnet (SCM) and the biological dose. For most of the parameters, the radiation level should be reduced by factor of $10^4 \sim 10^6$ as compared to values at the first wall. Since a reduction of the factor $10 \sim 10^2$ can be expected in the blanket region, shielding should add a further reduction factor of at least $10^3 \sim 10^4$ and larger reduction is required for the public. The last row shows the effectiveness of a shield composed of 1 m thick Fe1422. The design criteria are generally satisfied by the bulk shield of less than 1 m thickness. Moreover, heating, vacuum and control system penetration require additional shielding.

The key issues of radiation shielding⁽¹⁾ are categorized in Table 7-2. These are generic for the various blanket concepts and confinement systems. Although different kinds of issues may exist for a specific reactor design such as high power density systems, these issues have a lower priority in the test planning. The issues are briefly described below.

Table 7-1. Requirements for Shielding of Some Parameters

Component	Superconducting Magnet					Human	
	Nuclear Heating (Refrigerator)	Maximum Dose (Insulator)	DPA (Stabilizer)	Neutron Fluence (Critical Current)	Neutron Fluence (Occupational)	Biological Dose (Public)	
Design Criteria	10^{-3} W/cm ³ (Local)	3×10^9	5×10^{-5}	2×10^{18}	0.5	5	
	10 kw (Total)	10^9 rad	4×10^{-4} dpa/y	10^{19} n/cm ²	2.5 mrem/h	10 mrem/y	
At First Wall	10 W/cm ³		$10 \sim 12$ dpa/y	10^{14} n/cm ² · sec (14 MeV Flux)			
Required reduction from the first wall	$10^4 \sim 10^5$	$10^4 \sim 10^5$	10^6		$10^4 \sim 10^5$	$10^7 \sim 10^8$	
Reduction in Blanket			$10 \sim 10^2$				
Reduction by 1 m thick Fe1422	n: 10^5 γ: 10^4	n: 10^5 γ: 10^4	n: 10^5 H, He: 10^7	n: 10^4	n: 10^5 γ: 10^4		

Table 7-2. Radiation Shielding Issues

-
1. Design criteria of sensitive components in SCM, vacuum, NBI, RF systems and control system.
 2. Effectiveness of bulk shield
 - . composition and thickness of shield materials
 - . deep penetration of high energy neutron (14 MeV), including cross section windows
 3. Penetrations and their shield effectiveness for NBI, RF ports, and coolant pipes
 - . streaming and partial shield
 - . modeling procedure
 4. Occupational Exposure
 - . induced activity and dose distribution
 - . radioactive corrosion materials
 - . remote maintenance system
 5. Public Exposure
 - . sky shine
 - . radioactive waste of shield materials
 6. Shield compatibility with blanket and magnet including, assembly/disassembly and field penetration
-

1) The design criteria for the sensitive components are the standard ones that should be satisfied. These criteria should be determined based on the irradiation tests. The critical one among the SCM design parameters has the highest priority.

2) The bulk shield plays the principle role for the protection of magnet system and the biological exposure. Most of the effort in fusion reactor shielding research have focused on the design and analysis of the bulk shield such as was carried out in the BCSS study.⁽²⁾ Main consideration in the design of the shield involves determining the optimized compositions and thickness of the shielding. The uncertainties in data base will strongly affect evaluating the effectiveness of the bulk shield. This arises from the deep penetration of high energy neutron (14 MeV peak) and γ -rays, and/or due to the cross section windows.

3) The most difficult problems encountered in shielding of fusion reactor system are those related to radiation streaming through penetration

holes and slits. Fusion reactor system has many large penetrations of which functional requirements do not permit substantial modification in their shape. These open penetrations will directly cause a serious damage on other reactor components resulting from the leakage of neutron and γ -rays through these penetrations. Some designs adopt moving shutters to decrease the streaming, but their effectiveness and feasibility should be tested. Streaming can also occur due to unexpected malfunctions of a particular reactor component. This is one of the dominant problems in radiation shielding of fission reactors. The modeling procedure of penetrations and partial shields are not simple in the design calculations. They should be tested through experiments.

4) Issues on the occupational dose affect the maintainability and the availability of the reactor. During operation, it is impossible to have an access to the reactor component because of the very high radiation levels. Radiation exposure after shutdown is contributed by γ -rays emitted from the reactor system and building (excluding the exposure due to tritium leakage). This induced activity is due to many reaction types of isotopes for which activation data is required. At present, large discrepancy is observed among the induced activation cross section libraries. Besides the uncertainty associated with the source term prediction, the transport calculation of γ -rays has its own uncertainty in predicting streaming through penetrations.

The other possible source of radioactivity is the radioactive corrosive materials carried by coolant from the highly irradiated components (e.g. first wall) to outside of the shield. The large uncertainty exists in the amount of corrosion products, particularly in the case of liquid metal cooled blanket. Radioactive corrosive materials are one of the main contributions to the occupational exposure in fission reactors. Coolant pipes and heat exchangers with high radiation level will require additional lead shielding.

Even if the outer shield could reduce the radiation level to the normal maintenance work level, the major task of replacing the first wall and blanket would still require remote operation. If personnel access is necessary, the exposure level increases rapidly. The development of remote operation systems and robotic techniques, having a resistivity to high radiation, are needed to reduce radiation doses.

The exposure level of the public from fusion power plant is high safety concern. This is mainly caused by radiation source such as tritium release. The selection of shield material is important to decrease the long-lived radioactive waste. Radiation through sky shine will cause direct exposure to the public. This issue may not be serious for a next generation fusion facility, but will be important in power reactors.

6) Shields are set in the inboard and outboard zones between the blanket and the toroidal field coil. They must be fitted in these locations and the slit width between modules should be small enough to keep the streaming low. The design of support mechanisms for the blanket, shield and magnet must take account of the availability of space, the difference in the amount and direction of thermal expansion, the electromagnetic stresses etc. The mechanical interactions can lead to mechanical failures.

7) The design of the shield can be performed only from an integrated system design approach that involves careful trade-off studies^(3,4). Failure or extra conservatism results in large economic penalties, serious safety problem and low availability. Modification of shield modules to a fixed reactor design is often difficult and costly and sometimes even not feasible. If the shields do not work once the reactor is built, their change is quite difficult compared with the cases in fission reactors. From this viewpoint, the uncertainties in design should be decreased below the required accuracies.

The larger uncertainties due to the modeling procedure, transport and response function calculation methods and data base need the higher safety margin and conservatism. Most of the single and multiple effect testing will provide the data to be used for the improvement of these softwares.

By considering these issues in some detail, the test requirements to resolve them could be addressed. This chapter is devoted to reviewing the existing experiments, data base, methods and facilities with respect to radiation shielding and to anticipate the type and characteristics of the experiments needed to resolve the issues. For shielding experiments, providing adequate neutron source is an essential part of the planning. The performance of the neutron source facility will constrain the experimental program, and the quality and quantity of data obtained. The usefulness of a point neutron source, fission source and fusion source is described and compared. The

numerical investigation of the geometrical requirements have been performed for the shielding test matrix in a fusion test facility and the results are described in this chapter.

7.2 Status of Experiments, Data and Methods

Many shield designs have been proposed corresponding to a variety of reactor types and blankets concepts for next-generation experiments, and for demonstration and commercial reactors. There have been other shielding studies on such as the sensitivity to nuclear cross sections uncertainties and on optimization considerations. These studies provide generic issues in radiation shielding as well as the specific issues related to a particular reactor concept. Most designs, however, have no experimental verification of the accuracy and adequacy of the conclusions. Studies that are not verified experimentally may mislead the direction of research and development work. In this section, the experiments performed in U.S. and Japan are briefly reviewed. The present status of the experimental effort is too unsatisfactory to scope the overall understanding on the reliability and the accuracy of these designs and studies. Of course, this status is common among the fusion nuclear technologies and the shielding studies may rather advance more than other fields due to the experience gained from the fission program.

On the nuclear data, measurement and evaluation effort are focusing on satisfying the needs for the fusion program. Overview reports on the status and need on nuclear data are issued every year. The agreement on an international cooperation is in progress by the nuclear data communities among U.S., EC and Japan. It will be reflected in the evaluation and the compilation effort on ENDF/B-VI (U.S.), EFF (EC) and JENDL-3 (Japan) data libraries.

Many neutronics calculation codes have been developed for the fission reactor program and some of them, such as neutron and γ -transport codes and convenient shield design codes, can be used for fusion neutronics analysis upon a slight modification. New computer programs and data libraries have been developed for activation calculations although they need experimental verification on the prediction accuracy. Significant progress has been made in the Monte Carlo codes in recent years using the continuous energy and/or multi-group treatments. The former treatment has a high reliability, in principle, and can be used as a reference in evaluating other approximating

methods. The performance of supercomputer at the present generation is still unsatisfactory to fully use this method in design studies, but the future seems to be promising. Since the review works on the data and methods are found in many publications, only a brief description is given here.

7.2.1 Required Accuracy and Status of Experiments

Although adequate shielding can be provided a high degree of design conservatism could impose an unacceptably high cost on the reactor construction. Therefore, the prediction uncertainty in the shield performance is required to be as small as possible. The reduction of uncertainty, however, requires another cost for the research and development works, and hence the required accuracy in predicting the nuclear performance can be determined from a cost-benefit analysis. Abdou⁽³⁾ has investigated the cost-benefit relation and presented the required accuracies in predicting the important nuclear parameters in the blanket, shield and other reactor components where radiation is of a concern.

Conclusions from these studies are revised in the present work by taking account of recent progress in this area. The uncertainties in the nuclear responses shown in Table 7-3 consider only those due to design calculations and not including those uncertainties arising from the manufacturing process.

Radiation source is originated in the plasma region; hence the prediction accuracy of source characteristics is quite important. The uncertainty in the source prediction propagates to all other nuclear responses. The required accuracy would be a few percent. For the first wall and blanket region, good accuracies are required to predict the severe radiation damage and tritium breeding ratio. The achievable prediction accuracy generally decreases with increasing distance from the first wall, and is reflected in the required accuracies in Table 7-3.

The nuclear responses of the superconducting magnet in the toroidal field coils need a relatively high prediction accuracies because of the high radiation sensitivity. In a tokamak, the magnet is protected by the inboard bulk shield with a thickness of 60 ~ 80 cm. Since the nuclear data for neutron and gamma ray transport and response functions have ~ 10% uncertainties at least, it is very difficult to reduce the overall uncertainties below a few tens percent after such a thick shield. Therefore, the values in the original work of Abdou are modified in Table 7-3.

Table 7-3. Required Accuracies and Present Status
in Nuclear Design of Fusion Reactor*

Location/Response	Required Accuracy	Present Status
<u>First Wall/Divertor</u>		
Nuclear heating	Total 2%, local 10%	50%
Atomic displacement	10%	
Gas production	10%	
Transmutation	20%	
Induced activity	30%	50% ~ factor 3
<u>Blanket</u>		
Tritium production rate	gross 3 ~ 5%, local 10%	Gross 10%, local 20%
Nuclear heating	20%	
DPA	20%	
Gas production	20%	
Induced activity	50%	factor 2 ~ 5
<u>Bulk Shield</u>		
Nuclear heating	20%	factor 2 ~ 5
DPA	30%	
Induced activity	factor 2	factor 5 ~ 10
<u>Superconductive Magnet</u>		
Nuclear heating	gross 30%, local 50%	factor 5 ~ 10
DPA	gross 30%, local 50%	
Gas production	gross 50%, factor 2	
Dose	gross 30%, local 50%	
Induced activity	factor 2	
<u>Penetration Functional Equipment (e.g. vacuum, pump, RF, and NBI)</u>		
Nuclear heating	gross 30%, local 50%	gross factor 2, local
DPA and gas production	50%	factor 10
Induced activity	factor 2	
<u>Reactor Room</u> (outside the shield and inside the reactor bldg.)		
Biological dose during operation	factor 3	
Biological dose after shutdown	factor 2	
<u>External Biological Dose</u> (outside plant site)		
	factor 3	

* Assumed DEMO class reactor

On the biological dose, a factor of 2 ~ 3 is shown for the required accuracies. Better accuracies are, of course, desirable but they are not practically achievable because of the large radiation attenuation is required and the many possible streaming pathes involved. In fission power plants, a fairly good prediction is possible at present for the exposure dose inside the reactor building. Experiences in the construction and operation of such plants would improve the accuracy.^(34,35)

In order to achieve the accuracies cited in Table 7-3, the issues described in the preceding section should be resolved and verified through experiments. Some experimental efforts have been made using 14 MeV point neutron sources for the shielding research. They are summarized in Table 7-4. There are many other basic measurements of the nuclear cross sections, including activation cross sections, which are not shown here. The spectra measurements from the spherical materials at LLNL⁽⁵⁻⁷⁾ started in the 1960s and provided systematic data for many materials used in fusion reactors. They have been used widely to evaluate the adequacy of nuclear cross section at 14 MeV and their processing methods.⁽⁸⁾ The measured parameters are neutron and gamma energy spectra in two different angles (forward and backward against the incident deuteron beam). The radii of spheres are less than a few mean free path length. At ORNL, a series of shielding experiments⁽⁹⁻¹¹⁾ have been conducted for several years and recently the facility was shut down. The bulk shield and the streaming experiments provided the valuable data needed to know the prediction accuracies of calculations. The experimental configuration for the streaming experiment through the straight duct is illustrated in Fig. 7-1.

In Japan, two intense neutron sources have been used for the fusion neutronics experiments. Most of the machine time is devoted to the basic cross section measurements and blanket breeding neutronics. At JAERI, the bulk shield experiments⁽¹²⁾ have been performed for SUS316 with a thickness of 30 ~ 110 cm. The measured neutron spectra are shown in Fig. 7-2 for the four different thicknesses. Although the experimental accuracy is not certain, the results show that the point neutron source has enough strength to provide a measurable neutron spectrum through the thick shield. The streaming experiment has been carried out using the built-in streaming hole and the room access ports.⁽¹³⁾ A mock-up test is in progress for the NBI port of FER

Table 7-4. Shielding Experiments Performed with the Use of
14 MeV Point Source

Organization	Material	Geometry	Parameter
LLNL	^6Li , ^7Li , Be, Pb, C, O_2 , Fe, H_2O , $(\text{C}_2\text{H}_2)_n$, Cu Concrete, Nb	Sphere Radius: 0.5 ~ 5 mfp	$\phi_n(E, \mu)$ $\phi_\gamma(E, \mu)$
ORNL	SUS, BP Hevimet SUS304 Concrete	Slab, ~ 56 cm Straight duct Bent duct	$\phi_n(E)$, $\phi_\gamma(E)$
JAERI	SUS316 Graphite Concrete (building)	Cylindrical slab D = 40 cm, H = 27 ~ 112 cm D = 63, H = 61 cm Access port and streaming holes	$\phi_n(E)$, Dose Induced act. $\phi_n(E, \mu)$, Reaction rate $\phi_n(E)$, $\phi_\gamma(E)$
Osaka University	SUS Fe, Ni, Pb, C C, Pb, Fe, N_2 Concrete, SUS316, H_2O , Polyethylene Many materials (~ 20) Skyshine	NBI port and cavity Sphere (D \approx 30 cm) Slab T = 5 ~ 50 cm Small specimen Exp. room and site	$\phi_n(E)$, $\phi_\gamma(E)$, Dose $\phi_n(E, \mu)$ $\phi_n(E, \mu)$ DDX Dose

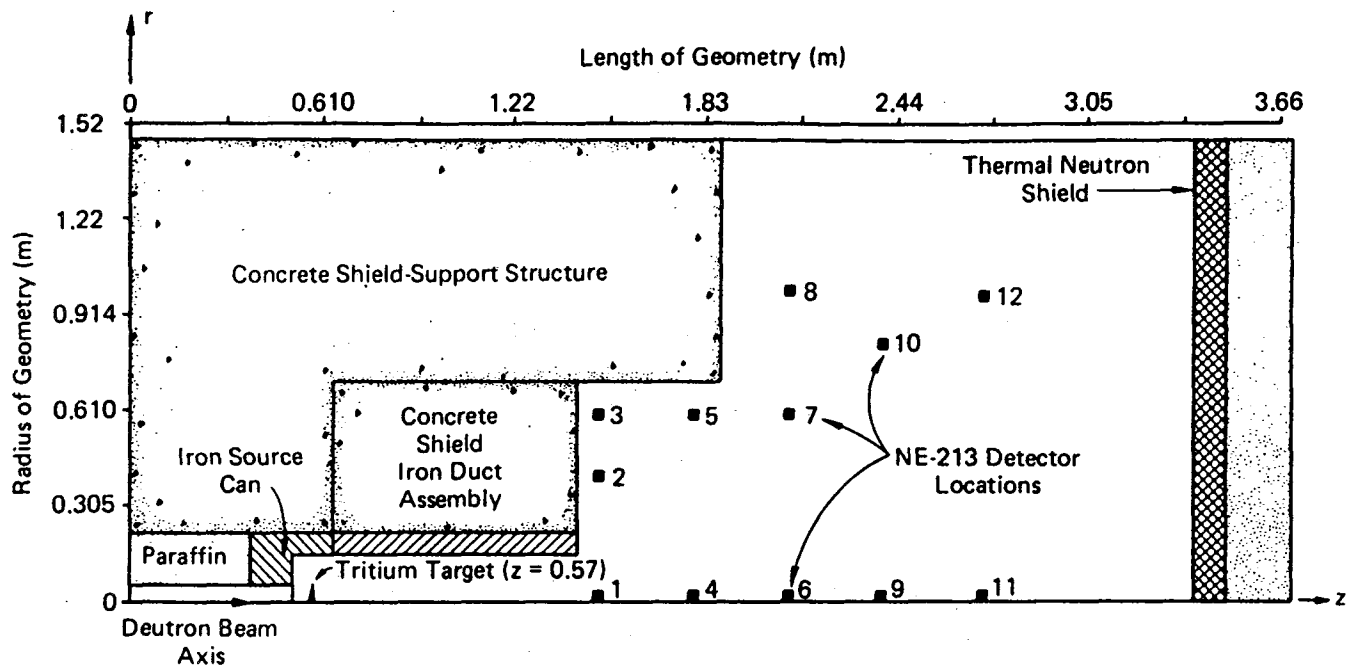


Figure 7-1. Configuration of ORNL streaming experiment (Ref. 11).

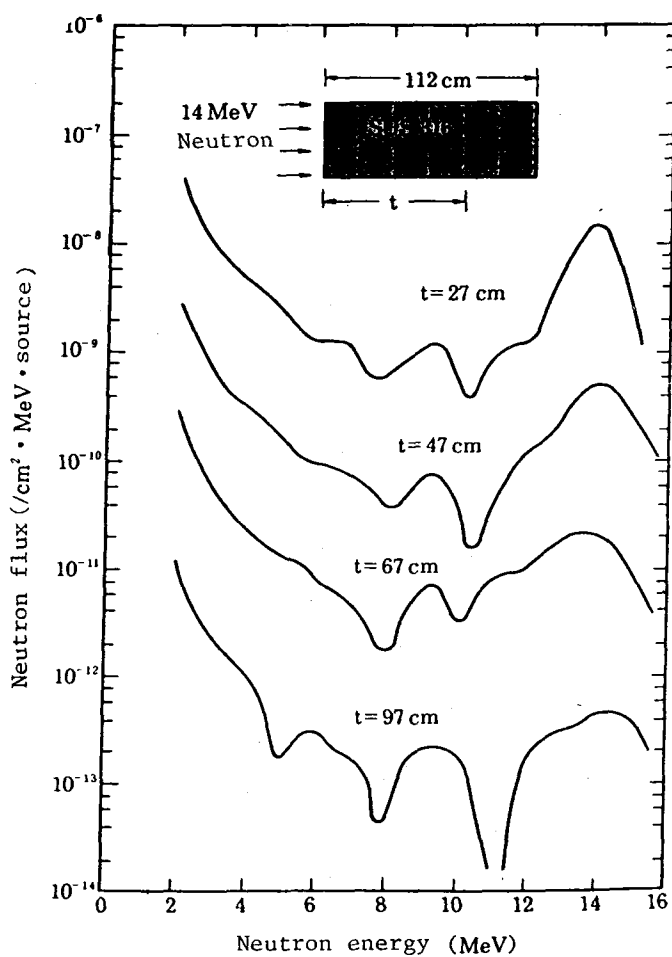


Figure 7-2. Attenuation of neutron flux through SUS316 bulk shield (Ref. 12).

(Japanese experimental fusion reactor). At Osaka University, dose rate distribution through the sky shine has been measured in the site of facility.⁽¹⁴⁾

As described above, the available experimental data is few and the kind of responses are limited. The present prediction accuracies are estimated based on comparisons between results based on the experiments and their analysis. Some results are shown in the right column of Table 7-3. No serious discrepancy has been observed except for certain induced activities. However, there is very little data to estimate the present accuracies for many nuclear responses. Since the estimated accuracies shown in the table depend largely on the constituent materials, geometries and calculation methods, these will not be appropriate for considerably different reactors and design concepts, e.g., the inboard tungsten shield.

7.2.2 Status of Data Base and Calculation Methods

Neutronics design calculations need a large amount of data and a large scale computation program. Although these are based on data and methods developed in the fission reactor program, some modifications and new developments are necessary for fusion reactors with respect to materials, energy range and reaction types. Active works have been made on the nuclear data measurements and evaluations and the modifications of conventional codes and new development of activity calculation codes.

The required data base and the priority of measurements are varied depending on the reactor design. The candidate materials proposed at the present stage for the blanket and shield are shown in Table 7-5. The elemental materials of potential use in fusion reactors are shown in Table 7-6.⁽⁴⁾ There is a diversity of elements because a number of reactor types and design concepts have been proposed that can be deployed although the materials and elements used for shielding are relatively limited in number. The data base for all these elements should be timely supplied with an appropriate accuracy. The differential nuclear data measured are compiled into evaluated nuclear data files via the evaluation work on the measured values and the theoretical model calculations. At present, evaluated nuclear data files, ENDF/B-V,⁽¹⁵⁾ ENDL(US),⁽¹⁶⁾ JENDL-2 and 3 (Japan)⁽¹⁷⁾ and EFF(EC) are

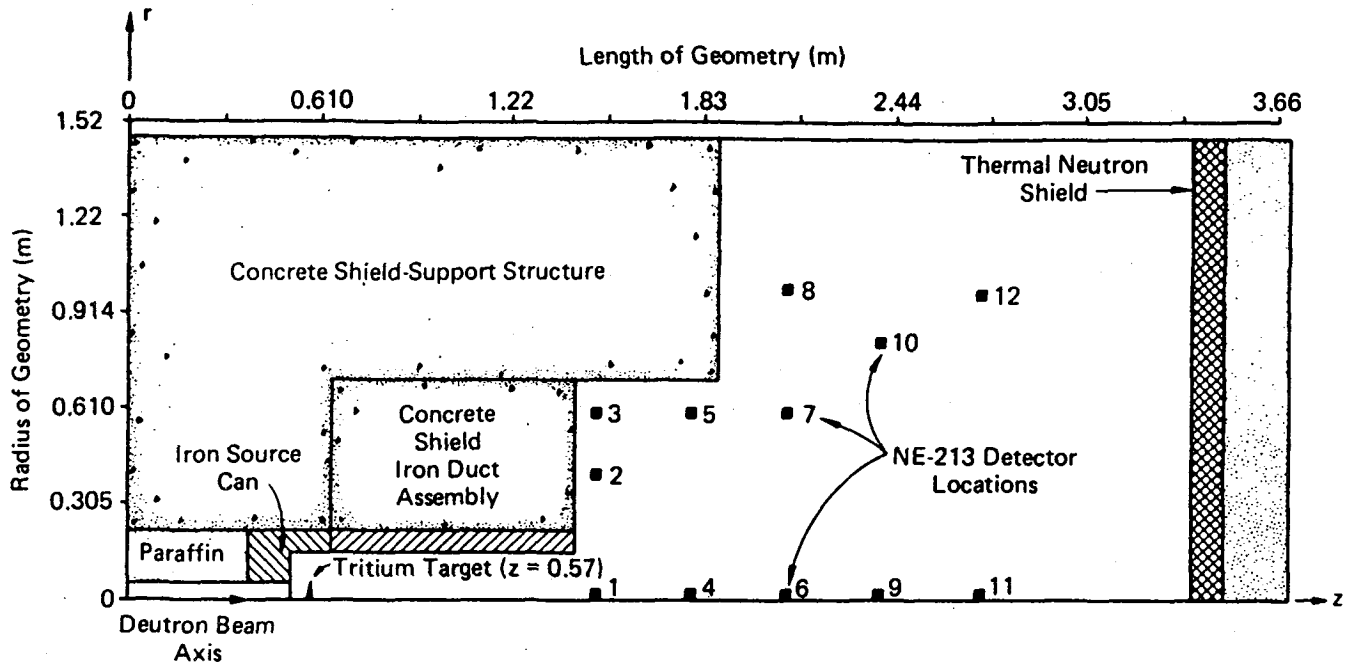


Figure 7-1. Configuration of ORNL streaming experiment (Ref. 11).

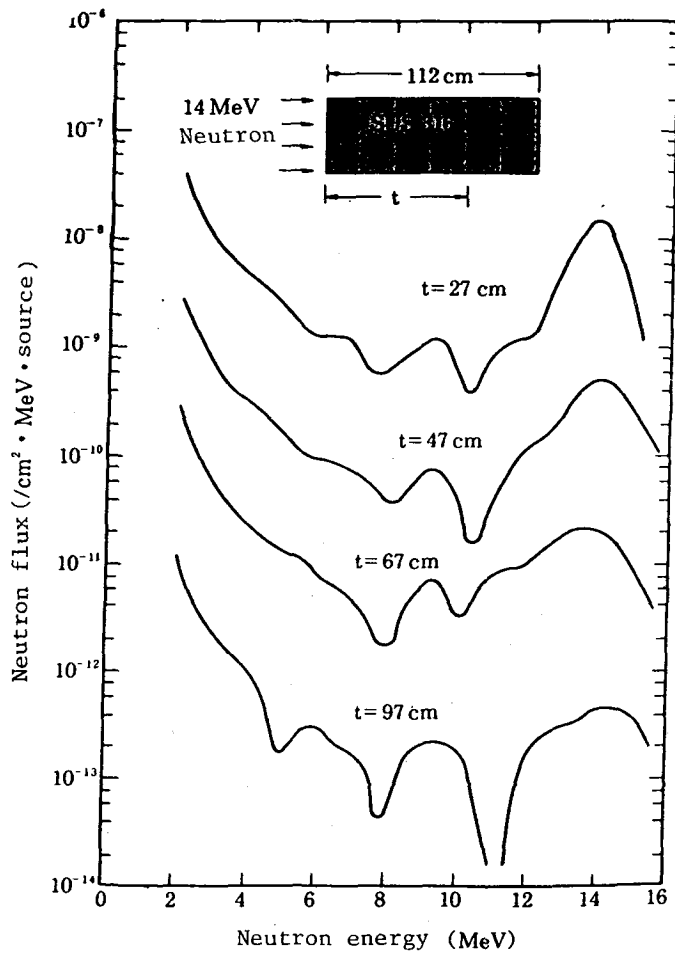


Figure 7-2. Attenuation of neutron flux through SUS316 bulk shield (Ref. 12).

(Japanese experimental fusion reactor). At Osaka University, dose rate distribution through the sky shine has been measured in the site of facility.⁽¹⁴⁾

As described above, the available experimental data is few and the kind of responses are limited. The present prediction accuracies are estimated based on comparisons between results based on the experiments and their analysis. Some results are shown in the right column of Table 7-3. No serious discrepancy has been observed except for certain induced activities. However, there is very little data to estimate the present accuracies for many nuclear responses. Since the estimated accuracies shown in the table depend largely on the constituent materials, geometries and calculation methods, these will not be appropriate for considerably different reactors and design concepts, e.g., the inboard tungsten shield.

7.2.2 Status of Data Base and Calculation Methods

Neutronics design calculations need a large amount of data and a large scale computation program. Although these are based on data and methods developed in the fission reactor program, some modifications and new developments are necessary for fusion reactors with respect to materials, energy range and reaction types. Active works have been made on the nuclear data measurements and evaluations and the modifications of conventional codes and new development of activity calculation codes.

The required data base and the priority of measurements are varied depending on the reactor design. The candidate materials proposed at the present stage for the blanket and shield are shown in Table 7-5. The elemental materials of potential use in fusion reactors are shown in Table 7-6.⁽⁴⁾ There is a diversity of elements because a number of reactor types and design concepts have been proposed that can be deployed although the materials and elements used for shielding are relatively limited in number. The data base for all these elements should be timely supplied with an appropriate accuracy. The differential nuclear data measured are compiled into evaluated nuclear data files via the evaluation work on the measured values and the theoretical model calculations. At present, evaluated nuclear data files, ENDF/B-V,⁽¹⁵⁾ ENDL(US),⁽¹⁶⁾ JENDL-2 and 3 (Japan)⁽¹⁷⁾ and EFF(EC) are

Table 7-5. Summary of Material Proposed for Blanket and Shield

Application	Material
Tritium Breeding	Liquid Lithium FLIBE Ceramic Compounds (Li_2O , LiAlO_2) Lithium-Lead Eutectic ($\text{Li}_{17}\text{Pb}_{83}$)
Structural Material	Austenitic Steel (PCA) Ferritic Steel (HT-9) Vanadium Alloy (V15Cr15Ti)
Coolant	Liquid Lithium Liquid Li - Pb Molten Salts Organic Helium, Water
Neutron Multiplication	Beryllium, Lead
Reflector	Graphite, Stainless Steel
Shield	Stainless Steel, Tungsten, Fe1422 Lead, Lead Mortar, Lead Acetate Boron Carbide (B_4C) Borated Water, Water Iron Mortar, Concrete

Table 7-6. Elemental Materials of Potential Use in Fusion Reactors; a Qualitative Judgement on the Probability of Using the Material is Shown (H = high, M = average, L = low)

Material	Demo and Commerical			Next Generation Reactors			Comments
	Blanket	Shield	Others	Blanket	Shield	Others	
Hydrogen	M	H	H	H	H	H	plasma, H ₂ O organic
Helium	H	H	H	H	M	H	coolant, also in S.C. magnets
Lithium	H	L		H			tritium breeding, coolant
Beryllium	H		H	H		H	neutron and energy multiplication
Boron		H			H		probably in B ₄ C form
Carbon	M	H	M	M	H		B ₄ C, reflector, SiC
Nitrogen			M		M	M	reactor building atmosphere
Oxygen	H	H		H	H		H ₂ O, reactor building atmosphere, Li ₂ O, LiAlO ₂
Aluminum	H	L	H	H	L	M	S.C. magnet stabilizer and structure, LiAlO ₂
Silicon	M	M	M				SiC, Stainless steel
Titanium	M	L	L	L			Structural material
Vanadium	H	L		L			Structural material
Chromium	H	H	H	H	H	H	In steel and super alloys
Manganese	H	H	H	H	H	H	In steel and super alloys
Iron	H	H	H	H	H	H	In steel and super alloys
Nickel	H	H	H	H	H	H	In steel and super alloys

Table 7.6 (cont).

Copper			H		H	Normal and superconducting magnets
Niobium	M		H		M	Structural material, also in superconductor
Molybdenum	M	L	M	M	L	HT-9, Ferritic stainless steel
Tin			M		L	In Nb ₃ Sn superconductor
Tantalum		L			L	
Tungsten		H			H	In space-restricted shield region
Lead	H	H		M	H	In lithium-lead compounds and lead shield
Zinc	L		L			Zr ₅ Pb ₃

extensive and widely used. International collaboration and data exchange are in progress. The status of individual nuclear data and response was reviewed in recent years and is not repeated here. The kinds of nuclear data required in the shield design with a high priority are the total and elastic scattering cross sections, energy and angular distribution of secondary neutron, gamma production cross sections, activation cross sections, kerma factors, and response cross sections for damage rate and diagnostics. The evaluated nuclear data files are processed into the multi-group libraries such as the MATXS and VITAMIN⁽¹⁸⁾ series by using the NJOY⁽¹⁹⁾ and AMPX⁽²⁰⁾ codes, respectively. The processing method and selected group structure influence significantly the calculation accuracy. Comparison work has been carried out between these libraries and the accurate continuous energy Monte Carlo method.^(21,39) In some cases, discrepancies in the calculated responses upon using different libraries exceeded the required overall accuracy. One of the recent developments in the group cross-section presentation methods is the use of direct presentation of energy and angular distribution of secondary neutron instead of the conventional Legendre expansion method. This new method^(22,23) can

resolve the difficulties encountered in low order Legendre expansion methods such as having negative flux or ray effects.

The calculation codes needed in shielding design are for: 1) neutron and γ -transport calculations, 2) radioactivity and response calculations, and 3) sensitivity and optimization calculations. A review of these methods and codes is given in Ref. (36). The current transport codes employ the discrete ordinates S_n , direct integration or Monte Carlo methods. The Monte Carlo methods have made great progress in recent years. The MCNP code⁽²⁵⁾ has been extensively used in the fusion neutronics calculations. The TRIPOLI code⁽²⁶⁾ has shown a reliability in the dose rate calculation in fission power plants. The VIM code⁽²⁷⁾ has been modified to apply to the fusion neutronics calculation but still improvements are needed for shielding calculations. MORSE-CG⁽²⁸⁾ has been improved to extend the capability of geometry presentation and graphic edit. Since the continuous energy M.C. method can fully simulate the real system in geometry and in physics of interaction between neutron and γ -rays, and material, detailed numerical simulation could partly replace some experiments and hence it would reduce a number of required experiments and the experimental cost. On the other hand, much remains to be improved in making the codes more accessible to non-expert users.

On the discrete ordinate S_n methods, there are good reviews,⁽²⁴⁾ so it is not mentioned here. The direct integration method is shown to be successfully applicable in the fission reactor shielding calculations.^(37, 38) Some modifications will be needed for the fusion reactor shielding calculations. Automation of linking for the discrete ordinate and Monte Carlo methods are useful for a designer.

The shield design needs the accurate evaluation of the neutron-induced component activation rate over the whole reactor lifetime in order to obtain accurate estimation of biological dose on occupancy and public. Considerable effort has been expended to produce activation data libraries and develop codes for computing activation levels. Several codes such as DKR,⁽³¹⁾ RACC,⁽³²⁾ REAC,⁽³³⁾ FORI,⁽³⁴⁾ and THIDA⁽³⁵⁾ are available together with their data files. The reliability of numerical methods and the accuracy of the data should be evaluated by comparing predictions with experimental results. There are some problems to be solved, such as the correct time dependence, the

detailed dose distribution in multi-dimensional geometries and effective algorithm to be used.

The current status of sensitivity and error analyses are described in Ref. (36). Since the sensitivity study is effective in planning the sequence, composition and geometry of experiments, it is expected to be well examined in an early stage.

7.3. Experiments and Facilities

In general, there are different kinds of experimental needs for resolving issues including:

- measuring basic data;
- understanding underlying phenomena;
- verifying integral component performance.

The planning of issue-relevant experiments should be timely, systematic and cost effective. The steps of shielding experiments can be categorized as:

- the measurements of differential nuclear data;
- neutron and gamma ray transport in bulk shield and penetration, response function of shielding parameters;
- multiple effect or integral effect on components with complex geometries.

Examples of these experiments are described in this section for each important issue.

Since neutrons are critical in all shielding experiments, the performance and specification of the neutron source facility are essential in planning the experiments. For a neutron source, there are fission reactors, accelerator-based point neutron sources and fusion sources. These are characterized on the basis of neutron spectrum, flux and fluence, available volume and geometry, and operational cost. Different experiment stages will need different conditions. Since the basic experiments usually need small specimens, the volume required is small. The multiple and partial integral experiments need larger volumes. The experiments based on transport phenomena need relatively large volumes, for example the area is several mean free path length square and the thickness should be large enough to achieve several orders of magnitude of attenuation. Table 7-7 shows the usefulness of facilities to resolve some of the important issues. Also indicated is the relative importance of

Table 7-7. Issues/Facilities Matrix for Shielding

Shield/Facilities	Non-neutron Test	Fission Reactor			Point Neutron Source			Fusion		
		Specimen Test	In Core	Side Core	Neutronics Meas. Fac.	High Fluence	Interactive	DT Exp.	Ignition	FERF
1. Criteria of design parameters for SCM vacuum system, NBI, RF, and diagnostic systems.		M	M	M		H	H		L	H
2. Bulk shield effectiveness				L	H	L	L	L	M	H
3. Penetration and its shielding effectiveness				M	H	L	L		M	H
4. Exposure on worker	L			L	L	L	L	M	H	H
5. Exposure on public					L	L	L	L	M	H
6. Compatibility with blanket including assembly and dis-assembly	M								L	H

each neutron source facility to resolve a particular issue. For the experiments concerning design criteria, the fluence has the highest priority, although the required volume may be small. The bulk shield and penetration experiments need a large volume to assemble the test pile or components. Fusion test facilities have a high potential to resolve every issue. Neutronics testing generally needs large volume, hence it is not easy to use FMIT-type facilities in common with the material irradiation tests. Therefore, the utilization of such facilities would be restricted to the irradiation-type experiments.

7.3.1 Experiments

The required experiments can be planned based on the experience in fission reactor program and will concentrate on those areas which have not been tested in that program. It is important for the fusion program to learn as much from the experience accumulated through the fission reactor development. Examples of the required experiments are shown in Table 7-8, which are analogous to those performed in a fission reactor. The experiments are categorized according to the issues but they are related to each other.

Basic Experiment

The basic experiments can be performed in the conventional accelerator or the point neutron source facilities. The number of test articles is large, hence the prioritization is necessary. The table shows the kinds of nuclear data which mainly affect the uncertainty of the issue concerned. The cross-section type used in the neutronics calculations of the fusion reactor is shown in Table 7-9. The required accuracies for the data, of course, depend on isotopes, type of reactions, energy range and required accuracies of integral quantities. Typical examples are shown in Table 7-10. They are the modified ones of Ref. (4) which are derived based on Table 7-3. The details of the nuclear data needs are discussed in Refs. (36) and (39) which include also the status of requirement to activation cross sections and the comparison study of activation data libraries.

Table 7-8. Examples of Experiments

Issues	Basic	Single Effect	Multiple and Partial Integrated Effect
Bulk Shield	Cross section of main nuclides ($\sigma_t, \sigma_e(E, \mu)$ resonance and window)	Attenuation in stainless steel, lead, tungsten, concrete copper (10 ~ 100 cm)	Optimization of bulk shield (SUS + B_4C + Pb + coolant)
Penetration	$\sigma_e(E, \mu)$	Straight duct (L/D effect, source scanning) Bent duct (shape, angle) Slit (step, width)	<ul style="list-style-type: none"> • Penetration shield • NBI port, RF port with structure • Divertor/limiter duct and exhaust • Coolant channels • Interaction of streaming holes
Induced activity and dose rate	$\sigma_{n,x}$, decay data, gamma production, $P(E_n \rightarrow E_\gamma)$	Specimen irradiation Response function	<ul style="list-style-type: none"> • γ dose through bulk shield and penetration • Shut down dose distribution in D-T burning device • γ dose from corrosion product • Sky shine
Design criteria	Damage rate	Specimen irradiation Response function	Property text
Measurement technique development			(see Table 7-11)
Data and method	Differential data base, evaluation and processing	Integral test of data base and benchmarks for method improvement	<ul style="list-style-type: none"> • Modeling of complex geometry • Interactive effect • Sensitivity study and optimization • Cost effective design method • Semi-empirical approximations

Table 7-9. Types of Nuclear Data Required in Fusion Nuclear Design

Application	Tritium Breeding	Nuclear Heating	Radiation Damage Indicators	Induced Activation	Radiation Shielding
<u>Data type</u>					
Total	X	X	X		X
Elastic	X	X	X		X
Inelastic	X	X	X		X
Neutron emission, $\sigma_{em}, P(E \rightarrow E', \mu)$	X	X	X		X
(n,2n), (n,3n)	X	X		X	X
(n, α), (n;n' α)		X	X	X	
(n,p), (n;n'p)		X	X	X	
(n,d), (n;n'd)		X	X	X	
(n,t), (n;n't)	X	X	X	X	
(n, γ), (n;n' γ), (n;x γ)		X		X	X
Gamma production $\sigma^P, d\sigma/d\Omega,$ $P(E_n \rightarrow E_\gamma)$		X			X
Decay chain and constant				X	X
Fusion reaction $t(d,n)\alpha$	X	X	X	X	X

Table 7-10. High Priority Nuclear Data Needs for Fusion Reactors

Nuclide	Type of Cross Section	Energy Range (MeV)	Accuracy Requirement (%)
${}^6\text{Li}$	$\sigma_{n,n}(E, \mu)$	2-15	10
	$\sigma_{n,n'}(E \rightarrow E', \mu)$	2-15	10
	$\sigma(\bar{n}, \alpha)t$	0.1-15	3
${}^7\text{Li}$	$\sigma_{n,nem}$	2-15	5
	$\sigma_{n,n}(E, \mu)$	2-15	5
	$\sigma_{n,n'}(E \rightarrow E', \mu)$	2-15	10
	$\sigma(\bar{n}, n't)$	5-15	3
	$\sigma_{n,nem}$	2-15	5
B	$\sigma_{n,nem}$	2-15	10
	$\sigma(\bar{n}, t)$	1-15	10
	$\sigma_{n,x\gamma}, P(E_\gamma)$	10^{-3} -15	20
C	$\sigma_{n,nem}$	5-15	10
O	$\sigma_{n,n}(E, \mu)$	2-15	5
	$\sigma_{n,n'}(E \rightarrow E', \mu)$	5-15	10
	$\sigma_{n,nem}$	2-15	5
Cr	$\sigma_{n,n'}(E \rightarrow E', \mu)$	5-15	20
	$\sigma_{n,nem}$	2-15	10
${}^{55}\text{Mn}$	$\sigma_{n,nem}$	2-15	10
Fe	$\sigma_{n,n}(E, \mu)$	2-15	10
	$\sigma_{n,n'}(E \rightarrow E', \mu)$	5-15	15
	$\sigma_{n,nem}$	2-15	10
	$\sigma_{n,\alpha}$	1-15	20
Ni	$\sigma_{n,n'}(E \rightarrow E', \mu)$	5-15	20
	$\sigma_{n,nem}$	2-15	20
V	$\sigma_{n,n}(E, \mu)$	2-15	10
	$\sigma_{n,n'}(E \rightarrow E', \mu)$	7-15	20
	$\sigma_{n,nem}$	2-15	15
Al	$\sigma_{n,n'}(E \rightarrow E', \mu)$	5-15	20
	$\sigma_{n,nem}$	2-15	10
Be	$\sigma_{n,2n}(E, \mu)$	2-15	5
	$\sigma_{n,nem}$	2-15	10
Cu	$\sigma_{n,n}(E, \mu)$	0.01-15	10
	$\sigma_{n,nem}$	2-15	10
	$\sigma_{n,x\gamma}, P(E_\gamma)$	10^{-6} -15	20
W	$\sigma_{n,n}(E, \mu)$	10^{-3} -15	10
	$\sigma_{n,n'}(E \rightarrow E', \mu)$	1.5-15	10
	$\sigma_{n,nem}$	2-15	15
	$\sigma_{n,x\gamma}, P(E_\gamma)$	10^{-6} -15	20
Pb	$\sigma_{n,2n}$	5-15	5
	$\sigma_{n,nem}$	5-15	5

Bulk Shield

The properties of bulk shield are needed as the basic design data for shielding materials shown in the table. The main constituents of bulk shield should be examined on the attenuation profile in the range of 3 ~ 7 orders of magnitude for both neutron and gamma rays because the prediction errors propagate and exponentially increase with the distance from the front surface. The measured parameters include energy spectrum, threshold reaction rates, dose rate and heating rate. The optimum shield consists of some materials which have specific purposes for shielding, i.e. absorption of thermal neutron by B_4C and gamma ray shield by lead.⁽²⁾ These optimum configurations of materials would be selected based on sensitivity analysis. The effectiveness of bulk shield should be experimentally verified together with the calculational prediction. Most of the experimental cost will depend on the material cost. The bulk shield measurements provide good benchmark problems for the transport calculation codes and nuclear data if they can be performed in the simple geometries and with well-identified source condition.

Penetrations

The penetrations in fusion reactors cause the most serious exposure on workers. Design of penetrations and associated shielding is essential and most difficult. No data is available for the verification of design accuracies. Experiments have to start from the fundamentals and then proceed systematically to understand the phenomena and to evaluate the design method. They are useful to find and examine the semi-empirical approximations. Table 7-8 shows the typical geometries required in the penetrations experiments. The streaming experiments through circular straight duct will show the fundamental aspect of penetration. The dependence on the ratio L/D (length to diameter) is a main design concern⁽⁴¹⁾. If the point neutron source is used, the dependence of dose rate distributions at the outer mouth of the duct should be measured by varying the relative position of the source to the duct entrance in order to examine the volume effect. A slit is a space between the module units of the shield and the blanket and is provided to avoid mechanical failure when the temperature rises. Although its shape varies from design to design, the width dependence would be a main variable in the experiments. The bending duct and slit are the basic considerations to reduce the streaming.

The effectiveness experiments would be carried out by varying the shape, the number of bend, the angle of bend and the distance between bend points.

Since the prediction accuracy for the streaming will not be good, (there is no data to evaluate the accuracy) even if the three dimensional Monte Carlo method is applied, partial mock-up experiments prior to detailed design are inevitable. The effectiveness of moving shutter and multi-layer slit can be tested. The local dose rate distribution is important as well as the gross exposure rate in order to protect sensitive panels components.

The penetration shield should attenuate not only the direct radiation component from the burning region during the operational phase, but also the gamma dose from the highly activated penetration components during the shutdown period. The coolant channels may cause streaming if helium gas is used or the coolant is removed after shutdown.⁽⁴²⁾ The multiple effects of these streaming holes and slits in different components could cause unexpected streaming paths, therefore, the predictable geometrical configurations for such a case should be tested prior to the final design.

Exposure from Induced Activity

Exposure dose on workers is caused by the induced activity of reactor components, building and coolant. The accurate estimation of radioactivity spatial distribution, strength, energy spectrum and time dependence is fairly difficult and the experimental verification is also not easy. The D-T burning device can provide the data for shutdown dose distribution.

The radioactive corrosion product could be estimated from the corrosion transport experiments and irradiation test of first wall and PIC materials. The distribution of deposited materials and trapping efficiency in clean-up system are not known, especially for the liquid metal coolant.⁽²⁾

The important part of public exposure dose rate may come from the sky shine in fusion power reactor. The side wall thickness of the reactor building can be increased to reduce the dose rate, but those of ceiling will affect significantly the design of reactor building. Some neutron source facilities have the potential to verify this effect.

Measurement Technique and Diagnostic Development

The experimental uncertainties should be small enough to verify the prediction accuracy of the radiation field and the response. The neutronics measurements techniques are used as the diagnostic system for the burning fusion plasma. The present reliability and accuracy of detecting system is not satisfactory for this purpose. Main measurement techniques and detectors are shown in Table 7-11 which includes the lower limits of fluences.⁽¹⁾ The required accuracies for those detectors are described in Section 4.4.6. Specifically, the measurement technique of nuclear heating rate, damage rate and multifoil activation (MFA) need further development. The effect from the magnetic field should be tested for counter type detectors.

Table 7-11. Neutronics Parameters and Detectors*

Parameter	Detector	Required Fluence
Nuclear Heating	Calorimeter	$>10^{-1}$ MW.s/m ²
	TLD	$>10^2$ W.s/m ²
Reaction Rate and Fluence	Foil	$>10^{-1}$ MW.s/m ²
Dose	Gas ionization chamber	$>10^2$ W.s/m ²
	TLD	
Neutron Spectrum	NE213	>1 W.s/m ²
	Multi-foil	$>10^{-1}$ MW.s/m ²
	Proton recoil	$>10^{-1}$ W.s/m ²
γ Spectrum	NE213	$>10^{-3}$ W.s/m ²
	Ge (Li)	
	NAI scintillator	

* FINESSE Interim Report, vol. IV, p. 7-16 (1984).

Data and Method

Since the experimental values must be compared with the predicted results obtained by calculations, all the experiments should be well identified for source characteristics, boundary conditions, and geometrical and isotropic configurations. The results from the basic experiments are compiled to produce the data base required for neutronics calculations, the single and a part of multiple effect experiments offers the differential and integral data to examine the data base, the processing method, transport and response calculation methods. Experiments in complex geometries will help in verifying the design accuracies and in providing the experimental justification of the shield design. Since the present work focuses on planning the experimental needs and some needs for improvement were briefly mentioned before, the task required in the development of data and methods are not discussed here. Improvements in modelling and method, however, are the key issues to achieve the required accuracies within a reasonable design cost.

7.3.2 Point Neutron Source Facility

There are many point neutron sources around the world which are usable for shielding experiments, although their usability is limited by their source strength or flux and fluence of 14 MeV neutrons. Present DT sources generate neutrons with the strength $10^{12} \sim 10^{13}$ n/sec, for example, they are RTNSI and RTNSII (LLNL),⁽⁴³⁾ FNS (JAERI),⁽⁴⁴⁾ OKTAVIAN (Osaka Univ.)⁽⁴⁵⁾ and LOTUS (Switzerland).⁽⁴⁶⁾ They have been used for neutronics and basic data measurements except for RTNS-II. Other available neutron sources are based on the spallation reaction with high energy protons. The neutron density is high, for example, LAMPF (LANL)⁽⁴⁷⁾ has a flux about 10^{13} n/cm².sec., although the neutron spectra is much different from the one in fusion, most neutrons having energies below 1 MeV but a significant portion having energies reaching almost 10^3 MeV. Since there is no experience in applying such a source to the neutronics experiments, the usefulness is uncertain, but may have a high potential for certain classes of experiments.

Point neutron sources having lower strengths of $10^{10} \sim 10^{11}$ n/sec can also be used in shielding experiments for neutron and gamma spectrum and dose rate measurements with several-tens cm thick bulk shield. The intensity, however, will not be high enough to measure the heating rate and foil activation rate.

An example of a point source facility is shown in Fig. 7-3. This is a top view of fusion neutron source facility FNS (JAERI, Japan). The main components of the facility are the ion generators, deuteron accelerator, beam lens system, tritium targets, assembly support, control system and instrumentations. FNS has been designed for experiments on fusion blanket neutronics, shielding, irradiation and induced activity. The estimated facility cost (1980 dollars) is \$8 M (accelerator \$2 M, instrumentation \$2 M, building \$4 M).

Although the fluence of the point neutron source is lower than the one of fusion test facility, some benefits are expected. The comparison of characteristics for both facilities is shown in Table 7-12. The benefits of a fusion facility arise from the high intense volume source having the neutron spectrum close to the one found in power reactors. On the other hand, the advantages of point neutron sources are the well-identified source characteristics, the ease of access and a large available volume. The basic and single effect experiments are suitable for the point source since the requirement on the flux and fluence are not high in the shielding experiments. Even the bulk shield experiments could be performed with a thickness more than 100 cm of stainless steel. In the following 10 ~ 15 year period, the point or small volume neutron source facility would be used mainly to resolve the issues before the construction of a fusion facility. Therefore, the options on facility are not wide. There are basically three options for point neutron sources:

- construction of new facility,
- modification of conventional point source,
- utilization of RTNS-I, RTNS-II, FNS or LOTUS.

The cost of the first option is about \$10 M and that of the second is \$2 ~ 5 M for the modification of accelerator, target system and instrumentations. These cases could provide a high intensity neutron source of 10^{13} n/sec or more. The third option is the lowest cost, but require changes in the existing programs. For example, RTNS-II is used for material irradiation tests, FNS and LOTUS are largely used for the blanket neutronics experiments. These facilities would require some small modifications to perform the shielding experiments effectively. Moreover, FNS or LOTUS facility can only be

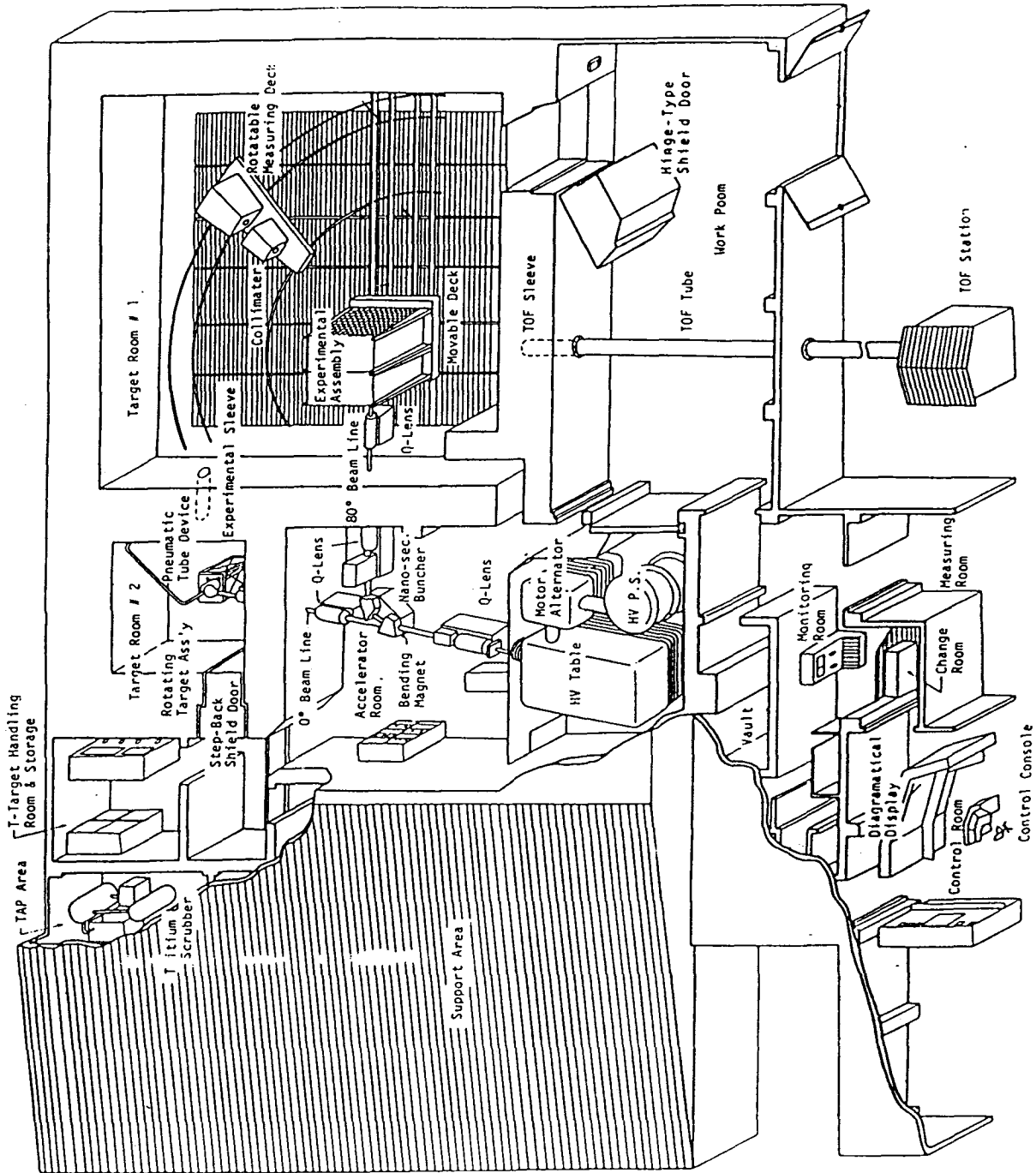


Figure 7-3. Top view of FNS point neutron source facility.

Table 7-12. Comparison of Neutron Source Facilities for Shielding Tests

Item	Point Source ^a	Fusion Test Facility ^b
Source strength	medium	high
Incident spectrum ^c	medium	good
Source characterization	good	limited
Time	medium	short
Operation cost	low	high
Volume of source	point	large
Volume of test module	large	large
Accessibility	good	medium
Parameters ^e		
cross sections	high	low
n-γ spectrum	high	medium
reaction rate	high	high
heating rate	medium	high
damage rate	low	high
induced activity	medium	high
shut down dose rate	low	high
measuring technique	high	low
Irradiation effect	low	high

^a $10^{12} \sim 10^{13}$ n/sec source

^b2 MW/m² wall loading

^cNeutron spectrum at the front surface of test module

^dAbsolute value of neutrons emitted per sec., and spatial and angular distribution, total neutron yield.

^eDegree of usefulness is shown for each parameter measurement

available based on an international cooperation similar to the ones devoted to the blanket breeding experiments in progress.

The experimental cost is estimated as

- material and manufacture ~ \$20 k,
- manpower ~ 50 person-day for scientific staff and 70 person-day for technical staff, per each series.

About four to five parameters could be measured during one series of experiments (about 3 weeks).

An additional 20 person-day is needed to analyze the data. The analytical work for pre- and post-experiments are not included in this estimation.

7.3.3 Fission Neutron Source

As an alternative to the fusion neutron source, fission reactors seem to be attractive. In the past, many fission reactors have been built and used for the shielding experiments. They should be taken into account in the planning of fusion experiments. Moreover, the reactors themselves could be used as the neutron fields. Of course, the most serious problem in using fission sources is that they do not have 14 MeV peak spectra but rather large soft components below 1 MeV. The MeV range neutron flux can be increased with the use of the convertor such as enriched uranium. If fission reactor experiments are helpful to resolve the issues, a large number of neutron sources becomes available. They have test zones with large volumes and high fluence. No systematic study has examined the possibility of using the fission neutron sources. In the following we compare some characteristics of fission and fusion sources.

Some shielding parameters have been calculated for one-dimensional cylindrical model consisting of the plasma, first wall and shield regions. The calculations were performed with ANISN⁽⁴⁸⁾ using both, a 14 MeV source and a fission source normalized to the same number of neutrons. Since the heating rate is an important parameter for the design of superconducting magnet, the attenuation profiles in the bulk shield of Fel422 are compared in Fig. 7-4.

The total and neutron heating rates distributions are shown as a function of the distance from the first wall. It can be seen that the attenuation

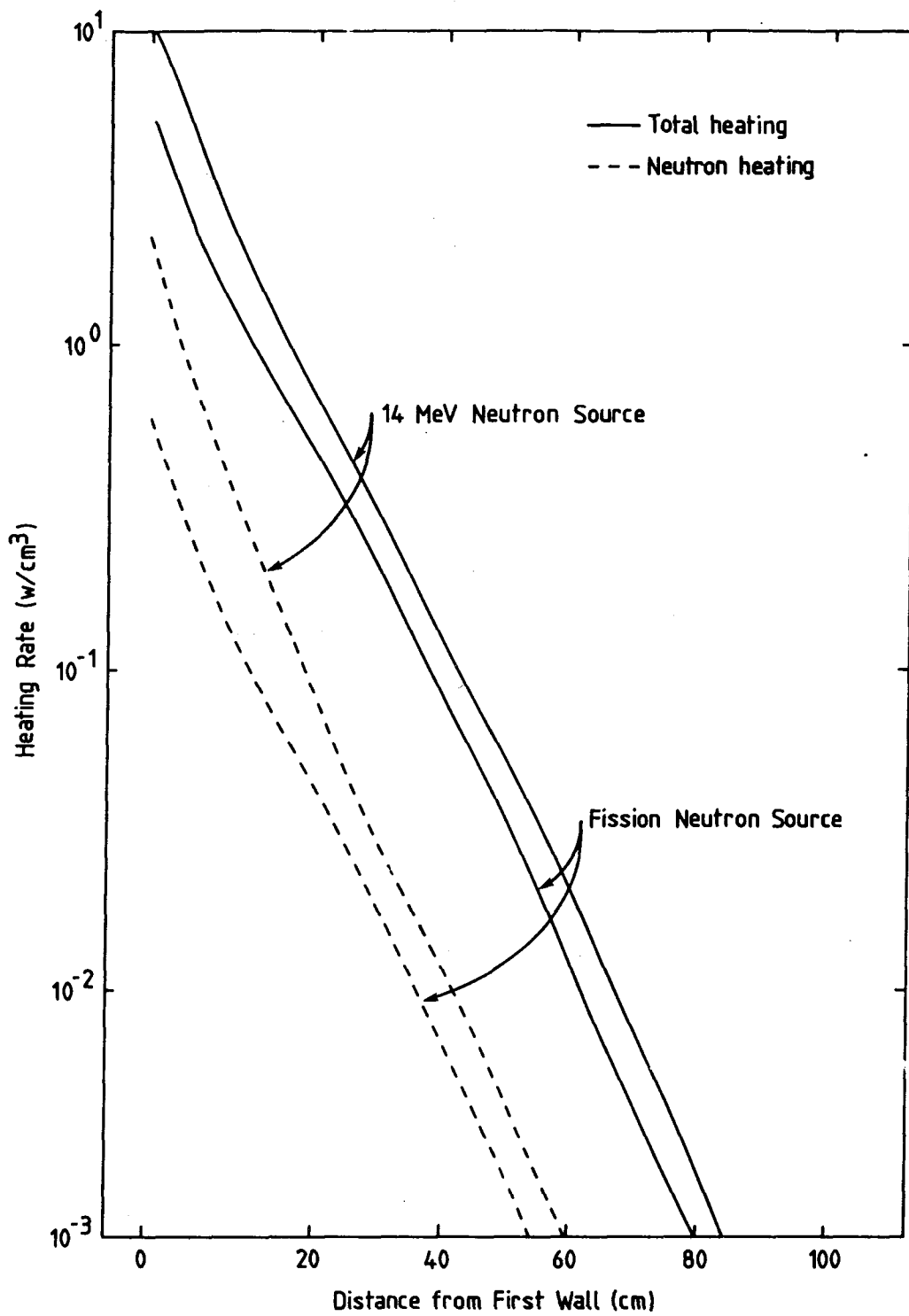


Figure 7-4. Nuclear heating rate calculated by 14 MeV and fission spectrum sources.

profiles are quite close between both sources although the absolute values are different. We could simulate well the heating rate profile in the shielding materials such as Fe422 by the fission spectrum source. The neutron spectra calculated for these cases are shown in Fig. 7-5. The upper curve shows the spectrum at a distance $r = 1$ cm from the first wall. The fission source has a low flux above 3 MeV, but agrees well with the fusion one below this energy. When the distance increases to 51 cm, the 14 MeV peak decreases by three order of magnitude, but the soft energy part decreases by two orders or less. If the high energy component above a few MeV does not play a dominant role in the total heating rate, the fission source would be satisfactory to simulate the fusion neutron source. For this purpose, the contribution from the high energy component has been examined. Figure 7-6 shows the ratios of high energy contribution in the total neutron heating for the typical fusion reactor configuration having a $\text{Li}_2\text{O}/\text{He}$ blanket + plenum + shield. The ratio drops below 20% with increasing distance from the first wall, but increases at the plenum region. Because the low energy reaction, ${}^6\text{Li}(n, \alpha)$, does not contribute outside of the blanket. Through the plenum region, the ratio decreases below 40% and in the shield it is less than 10% of the total heating rate after a few tens of cm.

On the other hand, shielding parameters with high threshold energy will not be well-simulated. For example, using the same model, the contributions of ≥ 2.5 MeV neutrons to the dpa and gas production rate are shown for each region in Table 7-13. Those of the heating rate and the dpa decrease rapidly in the shield region, but those for hydrogen and helium gas production rates do not decrease because they have high threshold energies. Although the fission source has the higher energy part than 2.5 MeV, the attenuation experiments for this energy region would be difficult to perform due to the low statistics in the deep locations of the bulk shield.

It can be said that the fission source seems to be attractive for experiments on some kinds of parameters. In particular, experiments on the streaming effect will provide useful data if they could be translated to the equivalent quantities with the fusion source spectrum. Experimental and calculational studies would be interesting on this point. Examples of fission reactors available for shielding experiments are TSF (ORNL), ASPIS (AREA) and YAYOI (Japan). Figure 7-7 shows the test zone assembled for the streaming effect in TSF having a spherical shape core.

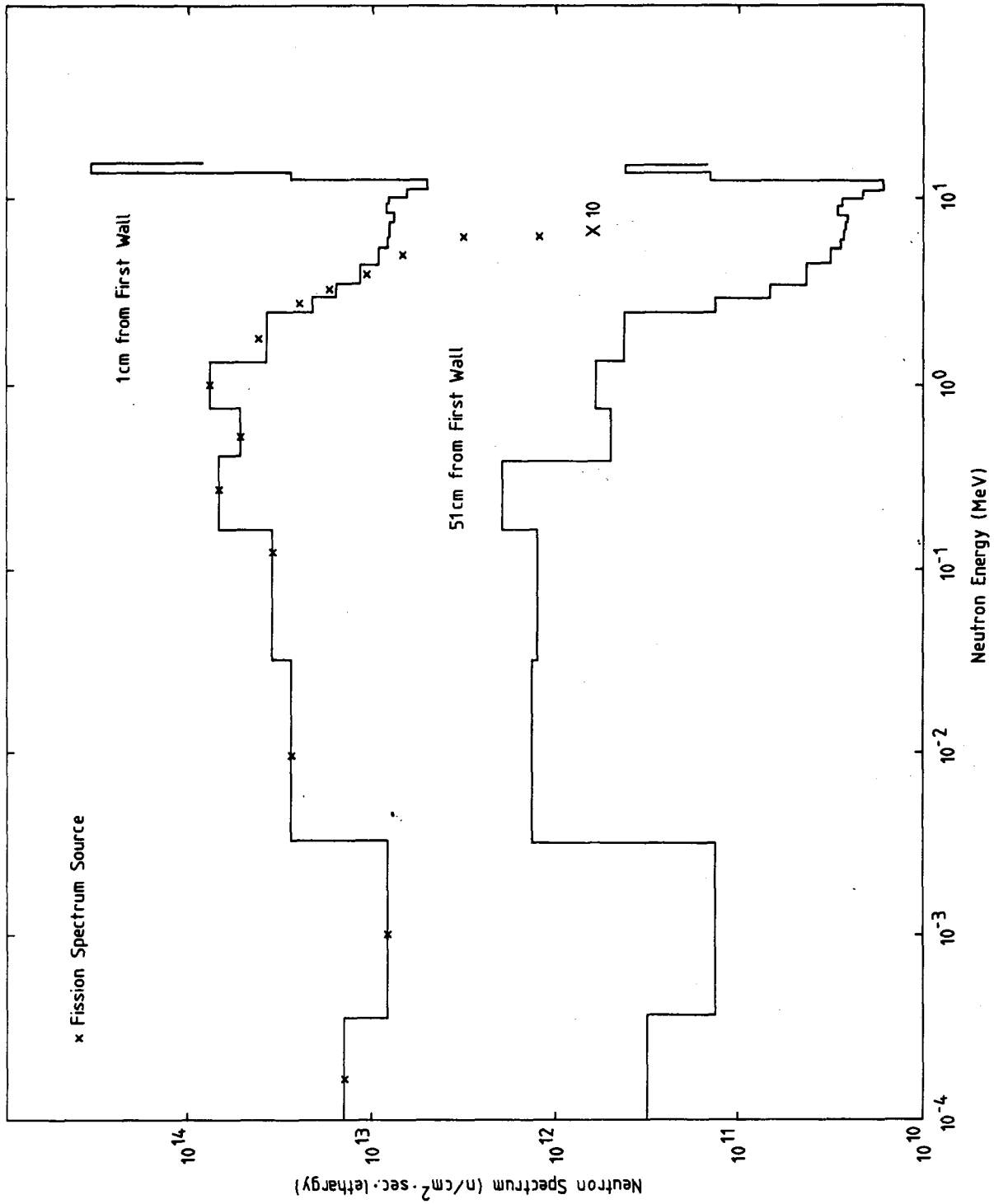


Figure 7-5. Comparison of neutron spectra in shield.

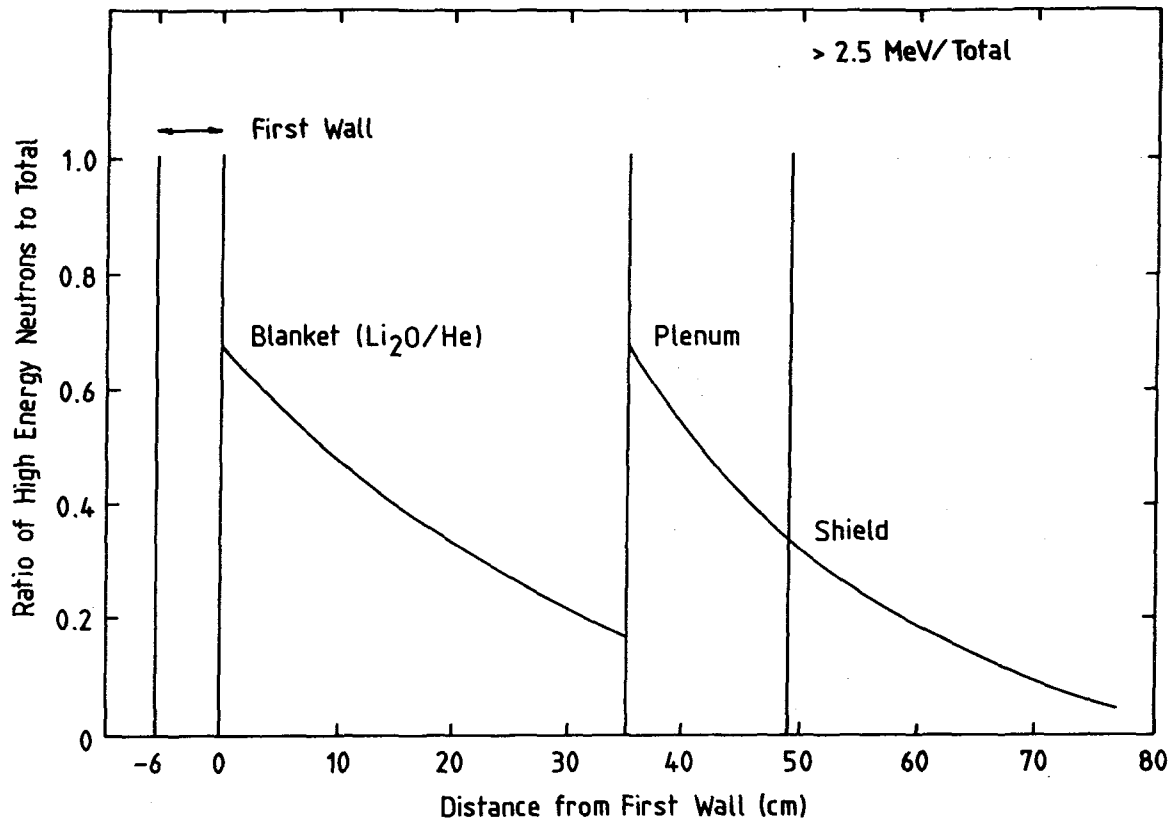


Figure 7-6. Contribution of high energy neutron on total heating.

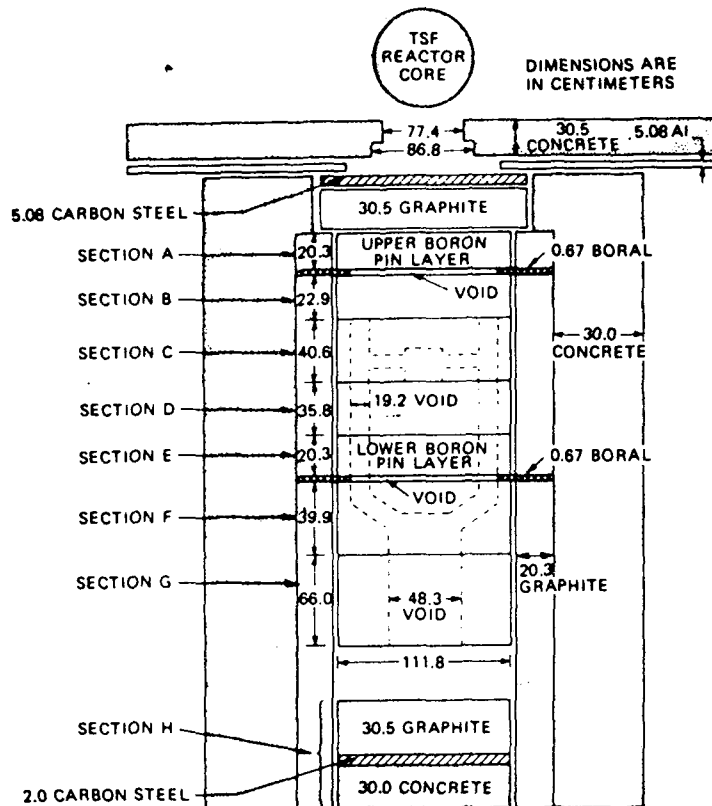


Figure 7-7. Streaming experiment using TSF (ORNL).

Table 7-13. Contribution from High Energy Neutron (> 2.5 MeV) to Damage Parameters (%)

Region	Neutron Heating	dpa	Proton Production	Helium Production
First wall	95	79	99.8	} 100
Blanket	49	67	99.7	
Plenum	57	29		
Shielding	24	7	97.9	

7.4. Shielding Experiments in Fusion Test Facility

Shielding experiments performed in a fusion test facility have many advantages with respect to the strength and volume of the source and the neutron spectrum. The fusion test facility like FERF will have many test matrixes suitable for individual experiments and be operated in various modes. Dimensions of each test matrix should be minimized to reduce the cost and to increase the number of test matrixes. This section describes the operating conditions and the test module geometry required for shielding experiments.

As an example of test facility, a tokamak type reactor is considered with the test location on the outboard regions. The minor radius of plasma is 1.1 m and the major radius is 4 m. The 5 cm thick first wall is composed of HT-9 and water with 30% volume ratio. The shielding test matrix is put adjacent to the first wall (no blanket region). The neutron wall loading is a key parameter for the accuracy or the statistic of measured values. Most neutronics test can be performed in a low fluence field, but intermediate fluence would be required if a measured position is behind the thick shield. In this study, all calculations are normalized to 1 MW/m² neutron wall loading.

7.4.1 Operating Condition Requirements

The requirements on the operating conditions are modest in the neutronics measurements as described in Ref.(1) since they can be performed in the low fluence field (~ 1MW.S/m² or less). Such a fluence can be achieved, for example, with a wall load of 0.88 MW/m² and 1.2 sec plasma burn time (e.g.,

FER)⁽⁴⁹⁾. For the irradiation tests such as induced activity measurements, higher fluence can give higher accuracy to the data. The other cases which need higher fluence are foil activation measurements at the deep zone of the shield, for example, beyond 80 cm from the first wall. Such measurements need a fluence of $\sim 100 \text{ MW} \cdot \text{S}/\text{m}^2$. Since most parameters depend linearly on the fluence, both pulse and quasi-steady operation modes are acceptable. Although the required fluence is modest the number of measured parameters is not small. Accordingly, many cycles of measurements (operation) and set-up (shutdown) will be needed. The other point to be taken into account is the activation levels of components and test modules. In high fluence tests, the modules become highly activated and render the device inaccessible after shutdown. Such an operation mode will reduce the efficiency of experiments.

Some considerations will be required to reduce interference from other test modules. If neutron and γ -ray flow into the shielding test module from others, then the source characterization and boundary conditions become complex in the analysis. The other significant point is the characterization of the neutron source from the burning plasma. Fusion neutron yield and space distribution should be measured within an uncertainty of a few percent. Shutdown dose rate measurements are better performed in the early stages of facility operations.

The spectrum and strength of incident neutron into the test matrix could be measured at the outer surface of the first wall to characterize the source, but the angular distribution could not be identified for the neutron reflected component which is amount to 70-80% of the total incident neutrons. Furthermore, the low statistical error and S/N (signal to noise ratio) value are essential to obtain data with a high accuracy. The statistics can be improved by increasing the fluence as mentioned above, but a careful set-up for the experimental environment is necessary to achieve low S/N value. The geometrical consideration is given in the following section to minimize the size of test modules within a reasonable S/N value.

7.4.2 Test Module Requirements

The requirements on the test module size for shielding experiments are examined in this section. The test module is assumed to be located on the outboard zone adjacent to the first wall. A blanket zone is excluded to maxi-

mize the neutron fluence in the test module. In a fusion device, the test area at the first wall is limited by configuration and cost considerations. Hence, it is also important to minimize the test module size. The maximum information would be obtained from the full coverage case, hence this analysis has attempted to find the minimum dimensions with the requirement that experiments at the central regions will have a reasonable area and volume, and can simulate the full coverage case within a limited deviation. The desirable size of the central test zone is about several mean free paths in width although it depends on the parameters measured and the types of experiments. Also, this size depends on the maximum deviation of measured parameters from those in the full coverage case. This is assumed to be within 20%. The basic experiments are the attenuation measurements in the radial direction, therefore, the bulk shield experiment is considered as a reference one.

The required dimensions of the test module have been examined in each direction, i.e. radial, toroidal and poloidal directions by using 1-D cylinder, 2D- $\gamma\theta$ and 2D-Z models, respectively. The calculational model is described below. The inboard and plasma region are assumed to be vacuum. The material of the test matrix and bulk shield is assumed to be 100% Fe1422. The compositions of the first wall, shield and reflector are shown in Table 7-14.

Table 7-14. Isotropic Compositions of Materials

Nuclide	First Wall	Test Matrix and Shield	Reflector
H	4.69-3*		
O	2.35-3		
Fe	2.259-2	6.953-2	5.745-2
Cr	1.848-3	1.848-3	1.600-2
Ni		1.580-3	1.179-2
Mn		3.916-4	
Mo	1.547-4		
C		2.309-3	

* Read as $4.69 \times 10^{-3} \times 10^{24}$ atoms/cm³

At first, the radial attenuation was calculated using the ANISN code⁽⁴⁸⁾ based on the ANL 46-group cross section library (25 neutron and 21 γ groups).⁽⁵⁰⁾ The calculated parameters are the nuclear heating rate (neutron and γ), dpa, and gas production (helium and hydrogen) rate. As an example, the heating rate distributions are shown in Fig. 7-8. Gamma heating is dominant in the shield. The heating rate is attenuated by more than four orders at the position $r = 100$ cm from the first wall. The requirement for bulk shield is a reduction by a factor $10^3 \sim 10^5$ as shown in Table 7-1. Hence, a thickness of 100 cm is for the test module. Further depth is necessary for some penetration experiments. Other shielding parameters attenuate also by the factors required at the position $r = 100$ cm.

The toroidal dimension is examined based on the r - θ model shown in Figure 7-9 by using the DOT 4.3 code.⁽⁵¹⁾ In the two dimensional calculations, the library with 23-group structure (neutron 13 and gamma 10 groups) was adopted to save the computation time. Both of the 46 and 23-group libraries are made from VITAMIN-C.⁽⁵²⁾ Since the difference in group structure will affect the calculated parameters, they are compared in Table 7-15, which are based on the 1-D calculations. The differences of calculated parameters by two libraries increase with the distance from the surface of first wall. At $r = 80$ cm, differences are about a factor 2~3. Accordingly, the 23 group model will not yield accurate absolute values, however, the relative values are useful.

The calculated total heating rates are compared for the cases, full coverage, toroidal angle $\theta = 8^\circ$ (the surface width at the first wall $W_F = 94$ cm) and $\theta = 15^\circ$ ($W_F = 176$ cm). The case for $\theta = 8^\circ$ shows very different attenuation profile as a function of the distance from the first wall in the deep locations with $r = 20$ cm as compared to the full toroidal coverage case and even the case for $\theta = 15^\circ$ shows a smaller gradient after several tens cm. Such differences arise from the incoming neutrons through the side walls of matrix (boundaries in the toroidal direction). To suppress this component, the whole first wall region is covered by a reflector of 10 cm thick stainless steel as shown in Fig. 7-9. Such an assumption seems to be adequate in an actual fusion test facility. The calculated heating rate for $\theta = 8^\circ$ is presented by broken line in Fig. 7-10, which shows that the attenuation profile approaches significantly the one in the full coverage case. In the

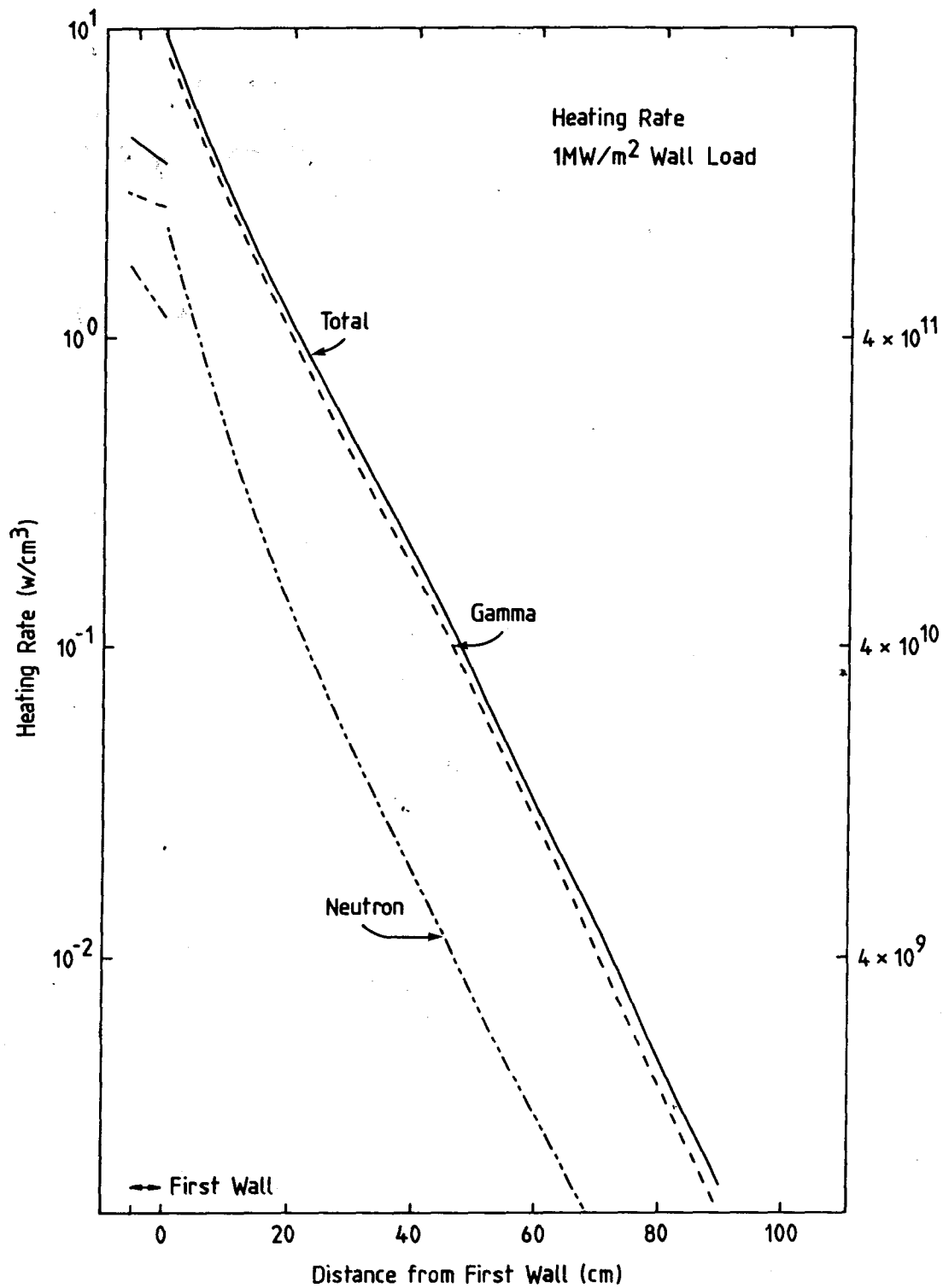


Figure 7-8. Nuclear heating rate distribution on radial direction.

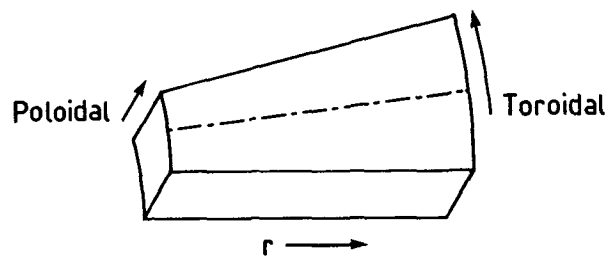
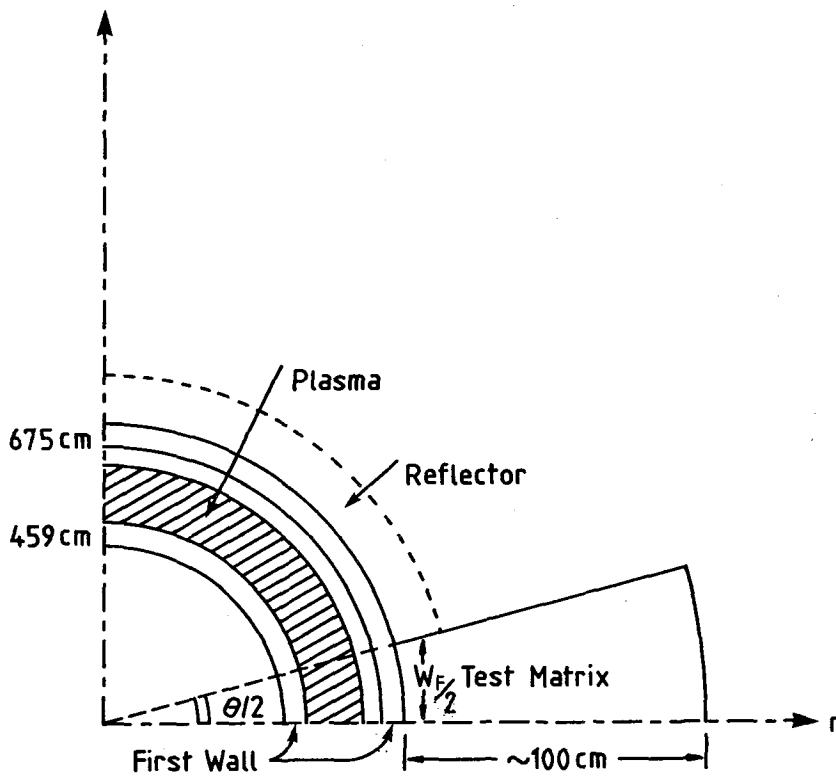


Figure 7-9. R- θ calculation model of shielding test matrix.

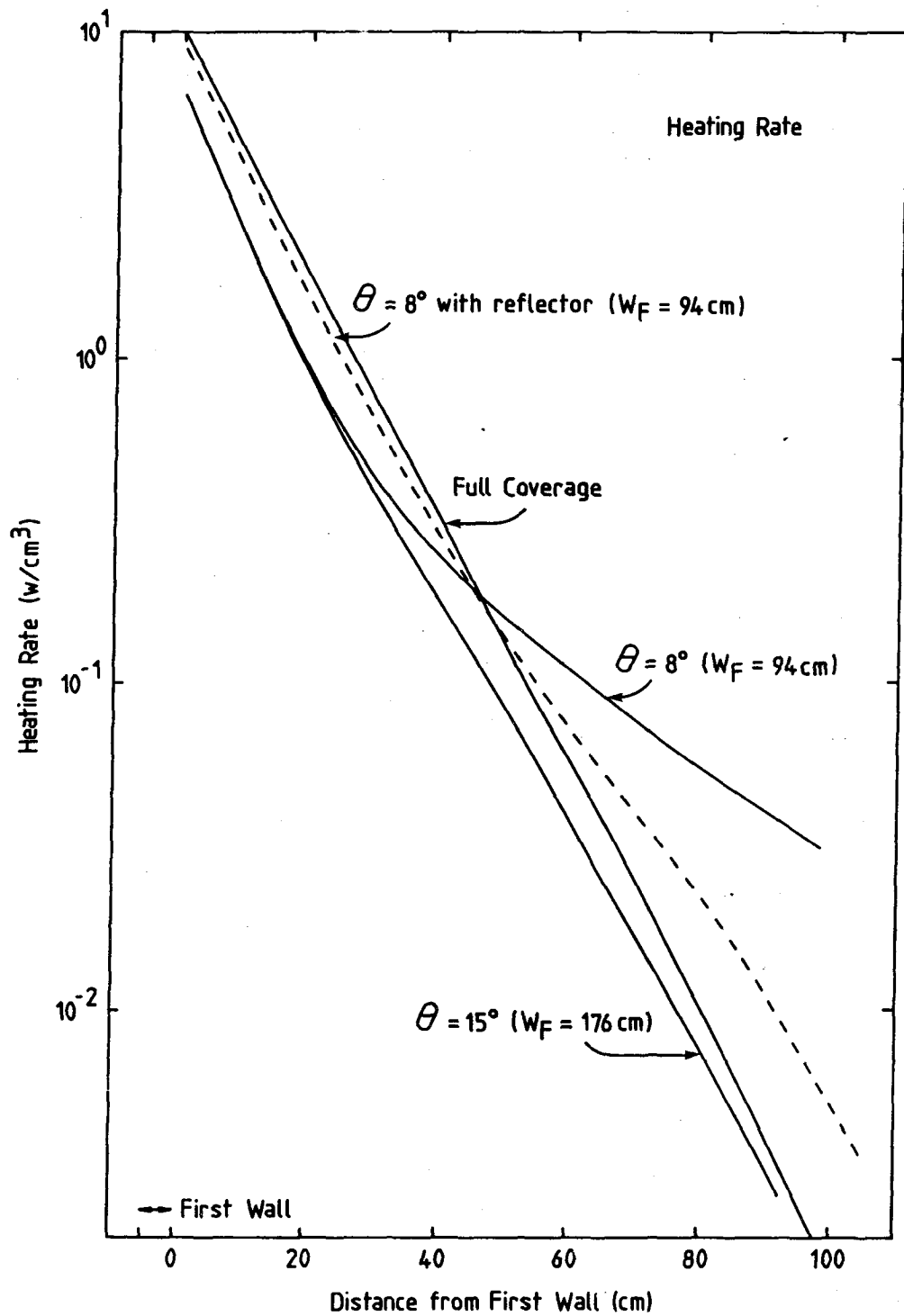


Figure 7-10. Comparison of nuclear heating rates between the the cases, full coverage, $\theta = 8^\circ$ and $\theta = 15^\circ$.

Table 7-15. Comparison of Shielding Parameters Calculated by 46 and 23 Group Cross Sections

Distance from First Wall (cm)	Total Heating Rate	dpa Rate	He Production Rate
0	0.97	1.13	1.01
20	0.99	1.40	0.96
40	1.09	1.75	0.92
60	1.34	2.29	0.89
80	1.74	3.12	0.85

* Values are normalized to the 46 group structure.

case $\theta = 12^\circ$ with the reflector gives a quite similar profile to the full coverage case. The attenuation profile for the dpa rate is shown in Fig. 7-11 for the same cases mentioned above. The case $\theta = 8^\circ$ cannot simulate the full coverage case but the case with the reflector gives better simulation. The case for $\theta = 15^\circ$ simulates well the full coverage case too. From the examination mentioned above the minimum dimension is obtained for the case $\theta = 12^\circ$ with a 10 cm thick reflector. This case can simulate the full coverage case very well for not only the heating rate and dpa rate, but also the gas production rates (hydrogen and helium production) as shown in Fig. 7-12.

The addition of reflector is also effective to flatten the toroidal distribution. The relative values of heating rate to the centerline values are compared in Fig. 7-13 between the cases for $\theta = 8^\circ$ with and without reflector. The rates are shown against the toroidal angle from the center line at the radial distances $r = 0, 20$ and 40 cm. One degree corresponds to a width of 12 cm at the first wall. At the distance $r = 20$ cm, the case without reflector deviates about 40% at the angle $\theta/2 = 3^\circ$. On the other hand the case with reflector deviates only by 10%. Moreover, when the distance increases to 40 cm, the deviation for the case without reflector is more pronounced compared with the case with reflector. Therefore, the reflector is very useful to extend the test zone, and in this case the width of available test zone is twice by adding the reflector.

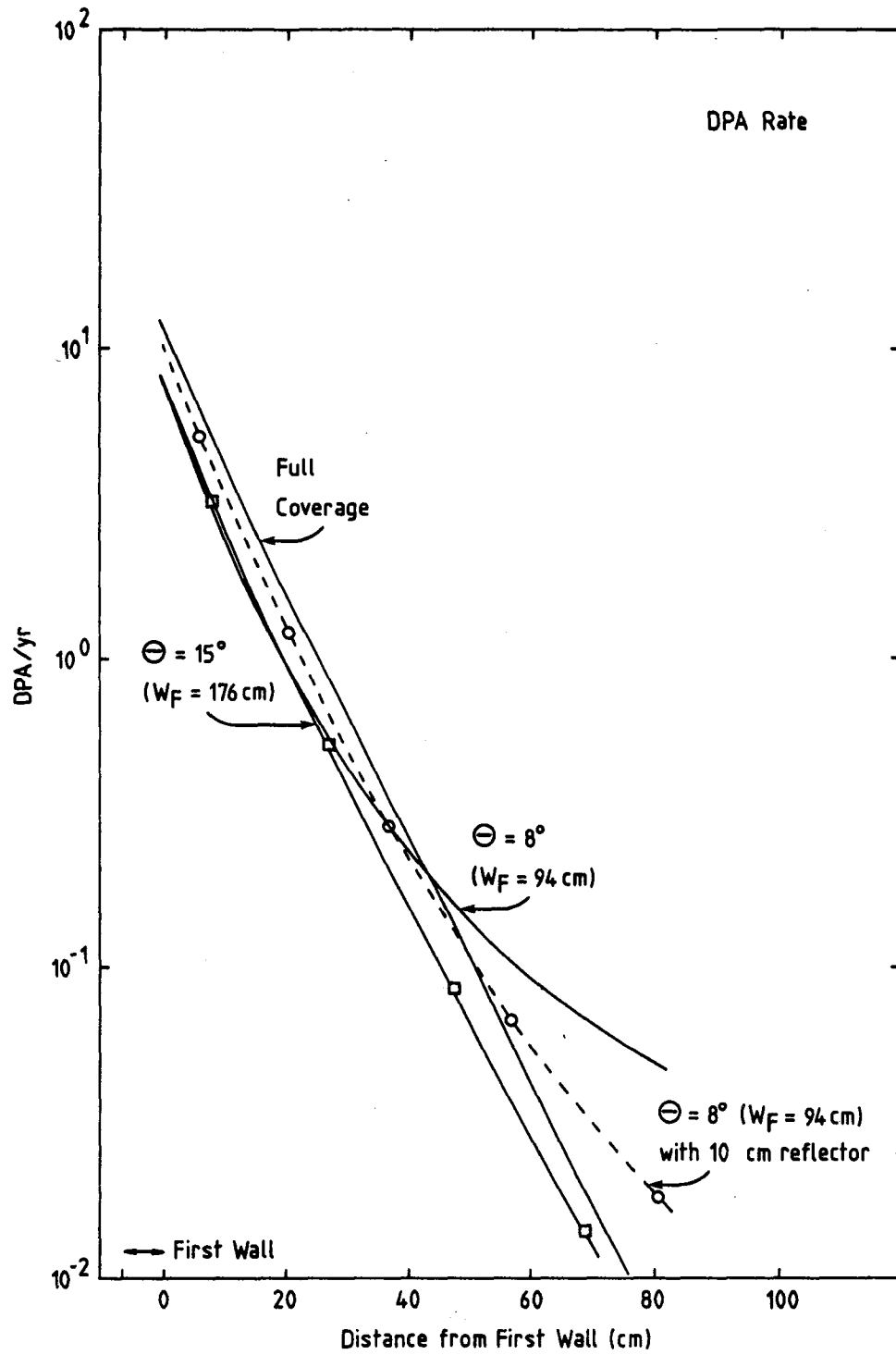


Figure 7-11. Comparison of dpa rates between the cases, full coverage, $\theta = 8^\circ$ and $\theta = 15^\circ$.

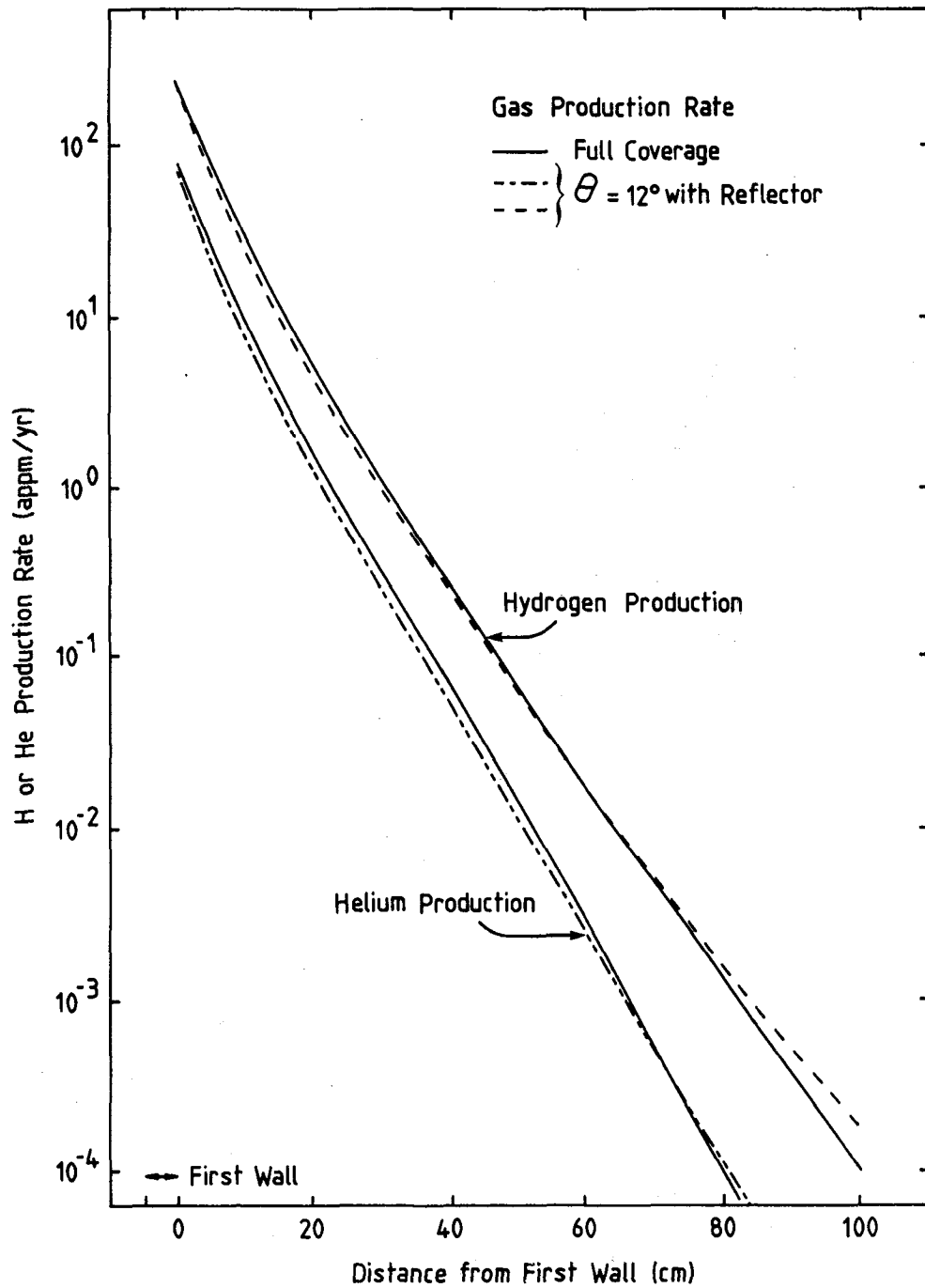


Figure 7-12. Comparison of gas production rates between the cases, full coverage and $\theta = 12^\circ$ with and without reflector.

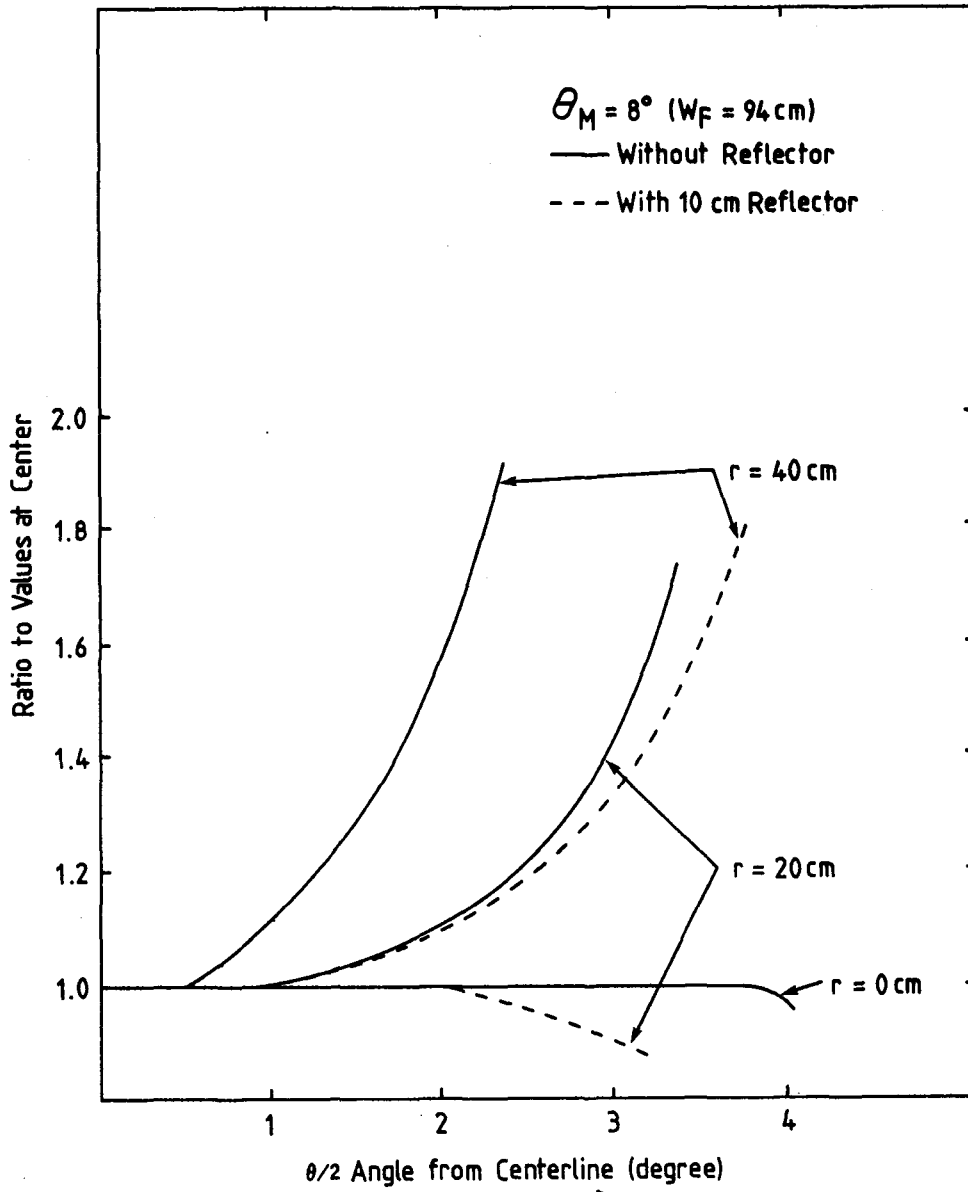


Figure 7-13. Effect of reflector on toroidal distributions of heating rates at $r = 0, 20$ and 40 cm.

In the following, the effect of toroidal dimension is compared in Fig. 7-14 for the cases $\theta = 8^\circ$ and 12° with the reflectors. The ratios of heating rates to the centerline values are shown at the same distances from the first wall. It can be found that the case for $\theta = 12^\circ$ gives the much closer values to the centerline ones than those for $\theta = 8^\circ$. At the distance $r = 60$ cm, the deviation for the case $\theta = 12^\circ$ is less than 20% up to the toroidal angle $\theta/2 = 4^\circ$, but that of the case $\theta = 8^\circ$ is more than 60%. Since the centerline value for $\theta = 12^\circ$ is quite close to the full coverage case, the central test zone equivalent to the full coverage case has the toroidal angle 4° , that is, about 50 cm width at the first wall. If this test zone has only small flat flux area, the neutronics parameters have space dependence due to the external source. In particular, in the penetration experiments, the space dependence across the holes are not desirable for the experimental set and the analysis. If the toroidal angle is $\theta = 12^\circ$ which corresponds to the 140 cm width at the first wall, the deviations from the full coverage case are less than 20% up to the distance $r = 80$ cm at the central test zone with the width of 30 cm.

The required dimension in the poloidal direction is examined using the r - z model shown in Fig. 7-15. In this model, the torous geometry is approximated by a cylinder. The poloidal dimension of the full coverage case is equivalent to that of the outer boundary of reflector, $1/2 H_F = 125$ cm. The shielding parameters have been calculated for the cases $H_F = 250$ cm, 120 cm and 102 cm. The total heating rate along the r -direction at $z = 0$ cm are compared among these cases in Fig. 7-16. The attenuation profiles are similar up to 60 cm, but beyond this distance, the case for $H_F = 102$ cm shows higher values and the case for $H_F = 120$ cm is still close to the full coverage case at $r = 90$ cm. The poloidal dependence of total heating rates are compared in Fig. 7-17. The figure shows the ratios to the centerline values at $z = 0$ cm. If the height of matrix is 250 cm, the toroidal dependence is very weak, so the large test zone can be expected, but if $H_F = 102$ cm, the heating rate increases by about 30% at $z = 30$ cm for the radial position $r = 60$ cm. If $H_F = 120$ cm, the deviation is within 20% even if the radial distance increases up to $r = 80$ cm. Accordingly, the required minimum dimension is around $H_F = 120$ cm for the poloidal direction.

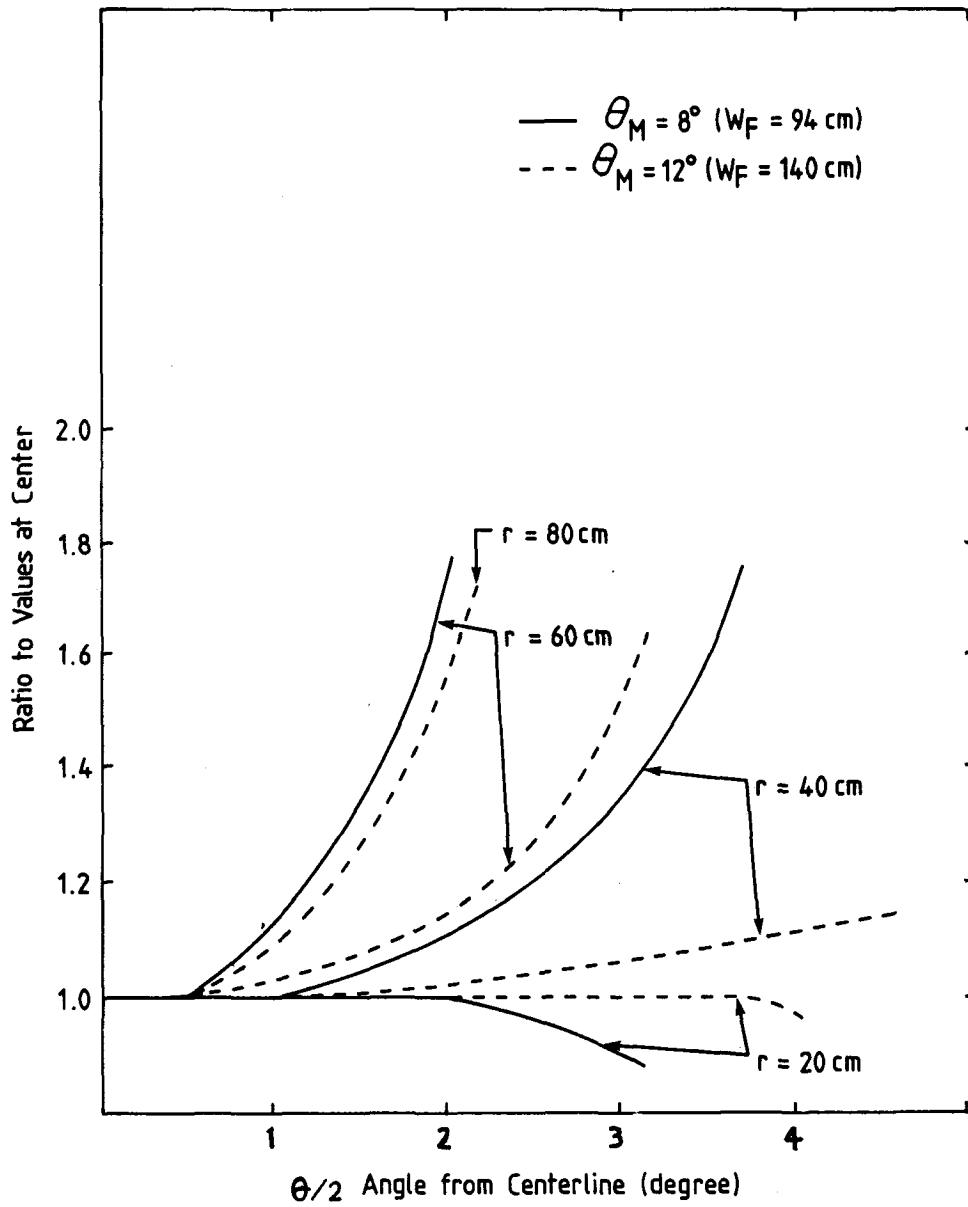


Figure 7-14. Dependence of nuclear heating rate on toroidal dimension. The relative values to the centerline ones are shown for $r = 20 \sim 80$ cm.

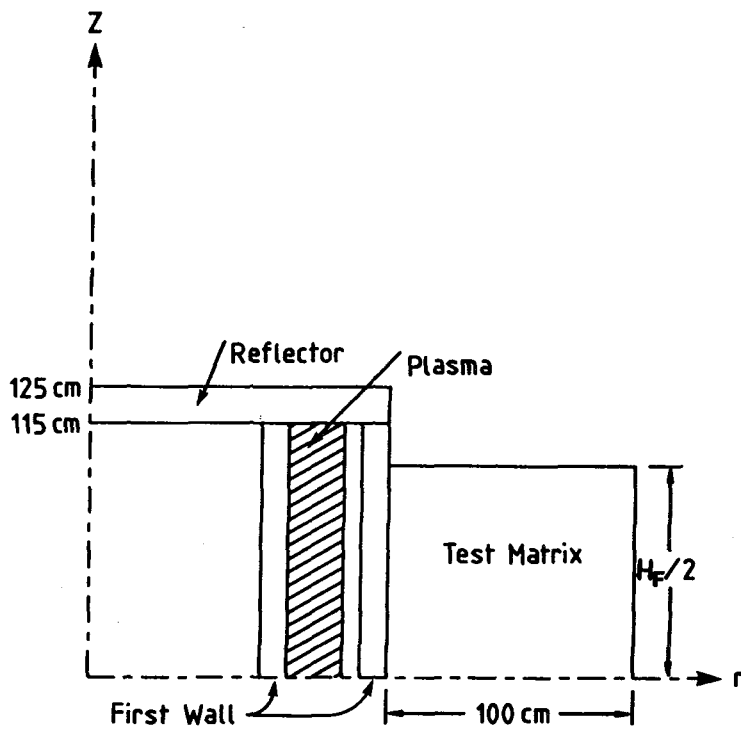


Figure 7-15. r-z calculational model of shielding test matrix.

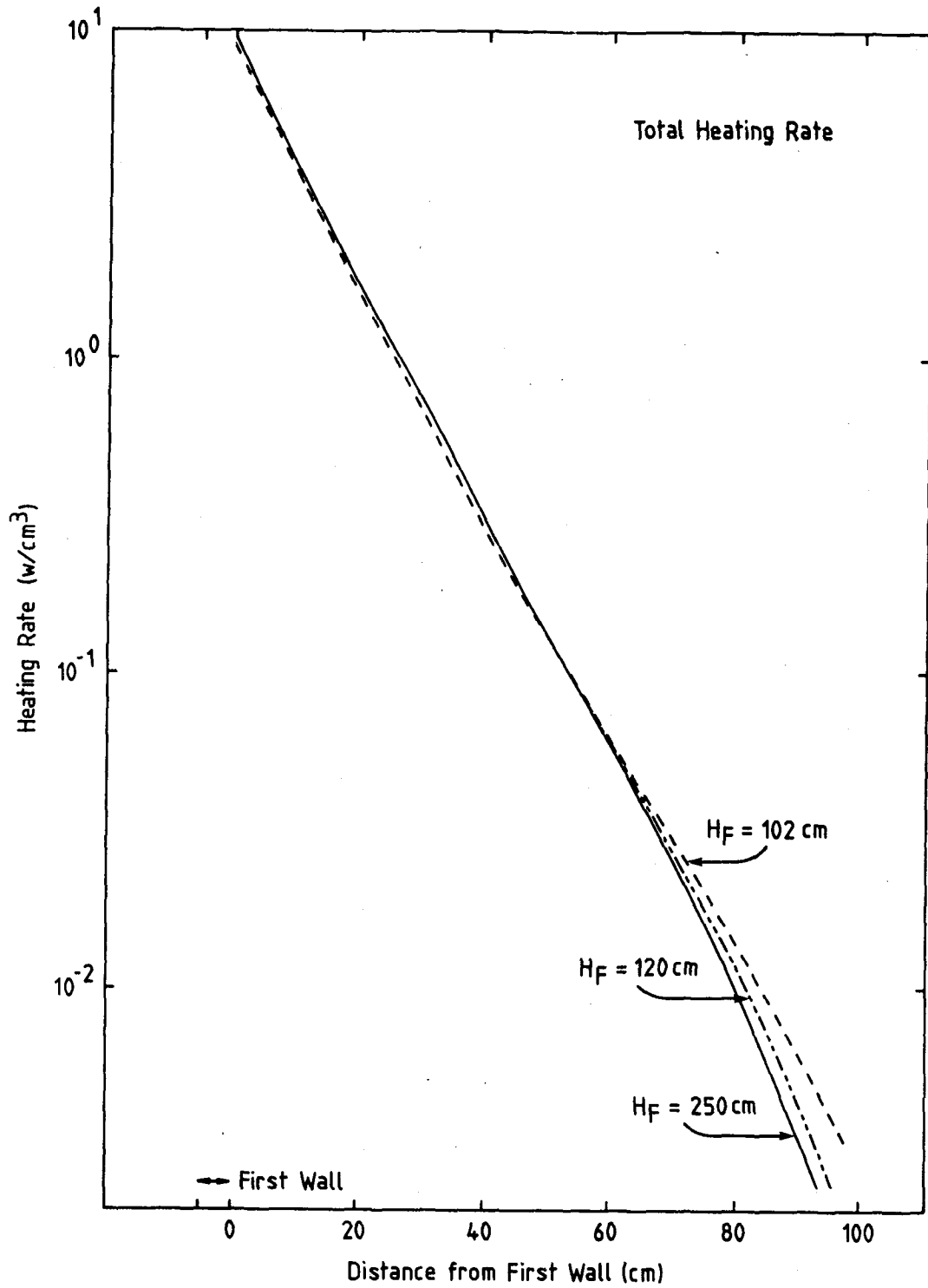


Figure 7-16. Comparison of nuclear heating rate in the test matrices with poloidal heights of 250, 120 and 102 cm.

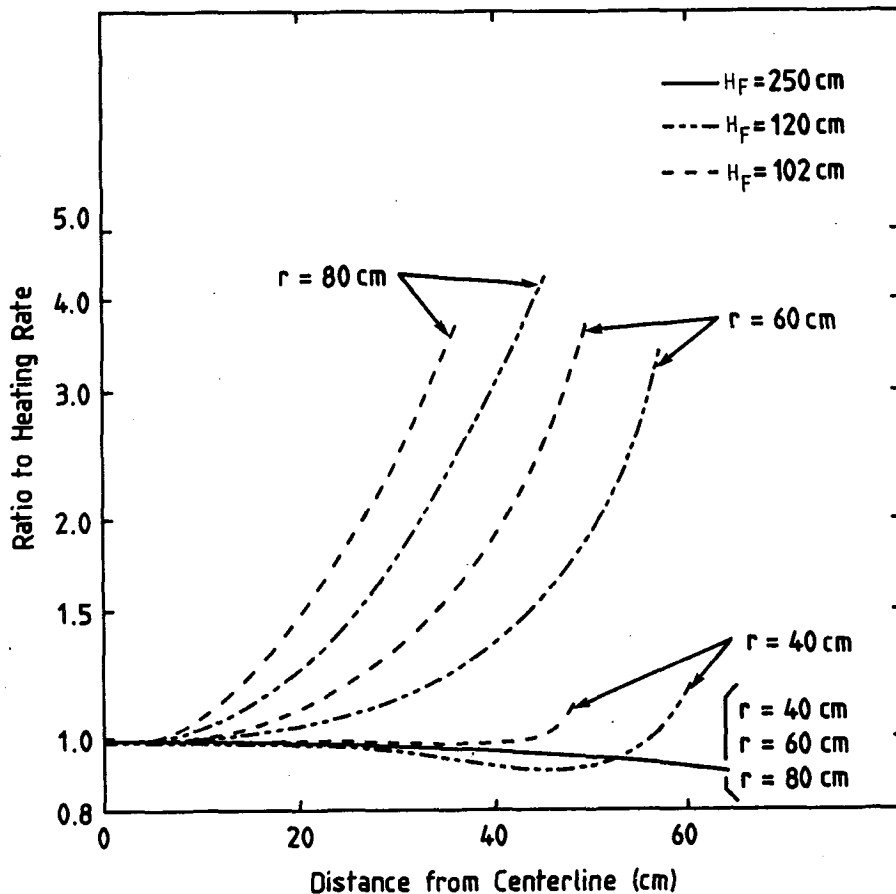


Figure 7-17. Dependence of nuclear heating rates on poloidal dimensions. The relative values to the centerline are shown.

As discussed above, the minimum dimensions are 100 cm (thickness) x 140 cm (toroidal width) x 120 cm (poloidal height). This module can provide the test zone with a 40 x 40 cm surface area at the first wall and the radial profile can simulate the full coverage case up to $r = 80$ cm within a deviation of 20% from the centerline values. It should be noted that these dimensions have been examined based on a model that the whole first wall is covered by the 10 cm thick reflector of stainless steel. If a thicker reflector is placed, the dimensions obtained above would decrease much more or the area of test zone would increase.

Besides the test module, the fusion test facility itself is a good experimental system. The heating port, control and instrumentation holes will provide useful data for the penetration measurements. The dose rate distributions in operation and after shutdown in the reactor hall would provide the useful basis for estimating the occupational exposure in the power reactor.

REFERENCES FOR CHAPTER 7

1. M.A. Abdou, et al., "FINESSE, A Study of the Issues, Experiments, and Facilities for Fusion Nuclear Technology Research & Development, Interim Report," University of California, Los Angeles, PPG-821, also UCLA-ENG-84-30 (1984).
2. D.L. Smith, et al., "Blanket Comparison and Selection Study, Final Report," Argonne National Laboratory, ANL/FPP-84-1 (1984).
3. M.A. Abdou, J. Nucl. Materials, 72, 147-167 (1978).
4. M.A. Abdou, "Nuclear Data for Fusion Reactor Technology," Proc. Advisory Group Meeting on Nuclear Data for Fusion Reactor Technology, IAEA (1979).
5. L.F. Hansen, et al., Nucl. Sci. Eng., 35, 227 (1969).
6. L.F. Hansen, et al., Nucl. Sci. Eng., 40, 262 (1970), and 60, 27 (1976).
7. C. Wong, et al., UCRL-51144 (Rev. 1 and 2), 1971.
8. M. Nakagawa, et al., "Benchmark Test of MORSE-DD Code Using Double-Differential Form Cross Sections," Japan Atomic Energy Research Institute, JAERI-M 85-009 (1985).
9. R.T. Santoro, et al., Nucl. Sci. Eng., 70, 225 (1979).
10. R.T. Santoro, et al., Nucl. Sci. Eng., 80, 586 (1982).
11. R.T. Santoro, et al., Nucl. Sci. Eng., 84, 260 (1983).
12. S. Tanaka, private communication (1985).
13. S. Tanaka, et al., "A Benchmark Experiment on D-T Neutrons and Secondary Gamma Rays Streaming Through a Concrete Bent Duct," Japan Atomic Energy Research Institute, JAERI-M 82-130 (1982).
14. T. Nakamura, private communication.
15. D. Garber (ed.), "ENDF/B-V," BNL17541 (ENDF-201), National Nuclear Data Center, BNL (1975).
16. R.J. Howerton, et al., "The LLL Evaluated Nuclear Data Library (ENDL)," UCRL-50400, vol. 15, part A (1975).
17. K. Shibata, et al., Japan Atomic Energy Research Institute JAERI-M 84-198, JAERI-M 84-204, JAERI-M 83-221, (1984).
18. C.R. Weisbin, et al., "VITAMIN-E: An ENDF/B-V Multigroup Cross Section Library for LMFBR Core and Shield, LWR Shield. Dosimetry and Fusion Blanket Technology," Oak Ridge National Laboratory, ORNL-5505 (1979).

19. R. MacFarlane, et al., "The NJOY Nuclear Data Processing System," vol. I and II (ENDF/9303-M, vol. I, LA-9303-M, vol. II (ENDF-324), Los Alamos National Laboratory (1982).
20. M.N. Green, et al., "AMPX: A Modular Code System for Generating Coupled Multigroup Neutron and Gamma Libraries from ENDF/B," Oak Ridge National Laboratory, ORNL/TM-3706 (1976), PSR-063/AMPXII.
21. M. Youssef, et al., "US/JAERI Fusion Neutronics Computational Benchmarks for Nuclear Data and Code Intercomparison," to be published in UCLA and JAERI-M (1985).
22. A. Takahashi, et al., J. Nucl. Sci. Technol., 16 (1), (1979).
23. M. Nakagawa, et al., Proc. Sixth Int. Conf. on Radiation Shielding, vol. 1, 171-179, Tokyo (1983).
24. J.D. Lee, et al., "Fusion Reactor Nucleonics: Status and Needs," UCRL-84574, Proc. 4th ANS Topical Meeting on the Technology of Controlled Nuclear Fusion (1980).
25. Los Alamos Monte Carlo Group, "MCNP--General Monte Carlo Code for Neutron and Photon Transport, Version 2B," Los Alamos National Laboratory, LA-7396-M, Rev. (1981).
26. J. Gonnard, "Overview of TRIPOLI 2," ORNL/RSIC-44, 313 (1980).
27. R.N. Blomquist, et al., ORNL/RSIC-44, 31 (1980).
28. M.B. Emmett, "The MORSE Monte Carlo Radiation Transport Code System," Oak Ridge National Laboratory, ORNL-4972 (1975).
29. K. Takeuchi, N. Sasamoto, Nucl. Sci. Eng., 80, 536 (1982).
30. N. Sasamoto, K. Takeuchi, Nucl. Sci. Eng., 80, 554 (1982).
31. T.Y. Sung, W.F. Vogelsang, "DKR: A Radioactivity Calculation Code for Fusion Reactors," University of Wisconsin, UWFD-170 (1976).
32. J. Jung, "Theory and Use of the Radioactivity Code RACC," Argonne National Laboratory, ANL/FPP/TM-122 (1979).
33. F.M. Mann, "Transmutation of Alloys in MFE Facilities as Calculated by REAC," Hanford Engineering Development Laboratory, HEDL-TME 81-37 (1982).
34. J.A. Blink, "FORIG, A Modification of ORIGEN2 Isotope-Generation and Depletion Code for Fusion Problems," Lawrence Livermore National Laboratory, UCRL-53263 (1982).
35. H. Iida, et al., JAERI-M 8019 (1978).
36. D.L. Smith, et al., "U.S.A. Contribution, Nuclear Data Base Assessment--Group H," ETR-INTOR/DIS/NUC-2 (1984).

37. G.P. Lahti, et al., (ed.), "Radiation Streaming in Power Reactors," Oak Ridge National Laboratory, ORNL/RSIC-43, ANS/SD-79/16 (1979).
38. G. Champion, et al., "Shielding Problem for PWR in France," Proc. 6th Int. Conf. on Radiation Shielding, Tokyo, vol. 1, 540 (1983).
39. E.T. Cheng, et al., "Magnetic Fusion Energy Program Nuclear Data Needs," GA Technologies, GA-A17754 (1984).
40. E.T. Cheng, "Nuclear Data Needs For Fusion Energy Development," GA Technologies, GA-A17881, (1985).
41. M.A. Abdou, "Problems of Fusion Reactor Shielding," Georgia Institute of Technology, GTR-10 (1978).
42. Y. Seki, et al., Trans. Am. Nucl. Soc., 38, 555 (1981).
43. Anonymous Experimenters Guide, Rotating Target Neutron Source II Facility, LLL M-09, (1978).
44. T. Nakamura and H. Maekawa, 9th Int. Conf. on Plasma Physics and Controlled Nuclear Fusion Research, Baltimore, IAEA-CN-41/0-4 (1982).
45. K. Sumita, et al., "Osaka University Intense 14MeV Neutron Source and its Utilization for Fusion Studies," Proc. 12th Symp. Fusion Technology, B-24, KFA (1982).
46. S. Pelloni and E.T. Cheng, 6th Topical Meeting on the Technology of Fusion Energy, 4D-5, San Francisco (1985).
47. M.S. Wechsler, W.F. Sommer, J. Nucl. Mat., 122, 1078 (1984).
48. W.W. Engle, Jr., "A User's Manual for ANISN--A One-Dimensional Discrete Ordinates Transport Code with Anisotropic Scattering," Oak Ridge Gaseous Diffusion Plant, K-1693 (1967).
49. K. Tomabechi, et al., "Concept for the Next Tokamak," Fusion Reactor Design and Technology, vol. I, IAEA, Vienna, STI/PUB/616 (1983).
50. Y. Gohar and M.A. Abdou, "MACK LIB-IV," Argonne National Laboratory, ANL/FPP/TM-106 (1978).
51. W.A. Rhoades and R.L. Childs, "An Updated Version of the DOT 4 (version 4.3) One- and Two-dimensional Neutron/Photon Transport Code," Oak Ridge National Laboratory, ORNL-5851 (1982).
52. R.W. Roussin, et al., "VITAMIN-C: The CTR Processed Multigroup Cross Section Library for Neutronics Studies," ORNL/RISC-37 (DLC-41), Oak Ridge National Laboratory, ORNL/RSIC-37 (DLC-41) (1980).

CHAPTER 8

NONFUSION IRRADIATION FACILITIES

TABLE OF CONTENTS

8. NONFUSION IRRADIATION FACILITIES

	<u>Page</u>
8.1 Introduction.....	8-1
8.2 Fission Reactors.....	8-1
8.2.1 Environmental Relevance.....	8-1
8.2.2 Facility Availability.....	8-8
8.2.3 Cost of Utilization.....	8-8
8.3 Accelerator-Based Neutron Sources.....	8-11
8.3.1 RTNS-II Facility.....	8-13
8.3.1.1 Description.....	8-13
8.3.1.2 Environmental Relevance.....	8-14
8.3.1.3 Availability.....	8-14
8.3.2 UC Davis Cyclotron Facility.....	8-16
8.3.2.1 Description.....	8-16
8.3.2.2 Environmental Relevance.....	8-16
8.3.2.3 Availability.....	8-17
8.3.3 The A-6 Radiation Effects Facility at LAMPF.....	8-17
8.3.3.1 Description.....	8-17
8.3.3.2 Environmental Relevance.....	8-19
8.3.3.3 Availability.....	8-22
8.3.4 The Fusion Materials Test (FMIT) Facility.....	8-22
8.3.4.1 Description.....	8-22
8.3.4.2 Environmental Relevance.....	8-22
8.3.4.3 Availability.....	8-29
8.3.5 Multiple Beam Facility.....	8-29
8.4 Conclusion.....	8-29
References.....	8-32

LIST OF FIGURES

<u>Figure</u>		<u>Page</u>
8-1	Fission/fusion irradiation comparison for $\text{Li}_2\text{O}/\text{He}/\text{HT-9}$ system.....	8-5
8-2	Fission/fusion irradiation comparison for $\text{Li}_2\text{O}/\text{He}/\text{HT-9}$ system.....	8-5
8-3	Fission/fusion irradiation comparison for $\text{LiAlO}_2/\text{H}_2\text{O}/\text{HT-9}/\text{Be}$ system.....	8-6
8-4	Fission/fusion irradiation comparison for $\text{LiAlO}_2/\text{H}_2\text{O}/\text{HT-9}/\text{Be}$ system.....	8-6
8-5	Schematic of RTNS target.....	8-15
8-6	LAMPF A-6 target geometry.....	8-18
8-7	LAMPF A-6 target neutron spectra.....	8-20
8-8	LAMPF beamline neutron flux profile at two RAD-II in A-6.....	8-20
8-9	Fusion Materials Irradiation Test Facility (FMIT).....	8-23
8-10	Yield of neutrons from 35 MeV deuterons on thick lithium.....	8-25
8-11	FMIT test cell perturbed flux.....	8-25
8-12	Transmutations.....	8-27
8-13	FMIT flux contours.....	8-28
8-14	Multiple beam schematic.....	8-28

LIST OF TABLES

<u>Table</u>	<u>Page</u>
8-1 Defects Produced in Type 316 Stainless Steel for One-Year Operation of Various Facilities.....	8-7
8-2 Capabilities of Selected U.S. Reactors.....	8-9
8-3 Capabilities of Selected Non-U.S. Reactors.....	8-10
8-4 Reactor Operations Costs.....	8-12
8-5 Volumes Available (cm ³) for Testing as a Function of the Minimum Neutron Flux.....	8-30

8. NONFUSION IRRADIATION FACILITIES

8.1 Introduction

Although a great deal of fusion technology testing can be completed in various test facilities in the absence of neutrons, many of the most pervasive issues can only be addressed in irradiation facilities. Radiation damage to materials and potential synergistic behavior of components in a radiation field must be understood sufficiently to permit reliable component design. To accurately characterize these phenomena, it is desirable to test in a fusion environment or one which simulates as closely as possible the environment expected in a commercially viable fusion device. Since no fusion devices will be available in the near future, it becomes necessary to use other facilities to mimic various aspects of the fusion environment. This chapter addresses the relevance of nonfusion irradiation facilities to the fusion reactor environment and the availability and cost of using those facilities.

In considering radiation effects in bulk materials and components, the irradiation environment of a fusion device can be briefly characterized as follows. The neutron spectra will consist of 14 MeV neutrons from the d,t reaction plus a large fraction (approximately 80% at the first wall) of degraded neutrons. The degraded part of the spectrum depends upon the details of the particular design and the location in the reactor. The magnitude of the total flux is approximately 2×10^{15} n/cm²-s at the first wall of a fusion device having a wall loading of 4 MW/m².

8.2 Fission Reactors

8.2.1 Environmental Relevance

In addressing the environmental relevance of fission reactors, the primary parameters to consider are neutron spectrum and flux. These determine the production rates of helium, hydrogen (including tritium), solid transmutants, displacement damage, and heat generation. Other factors are the operating temperature range and coolant type.

The objective is to simulate the important attributes of the fusion environment (which attributes are important depends on the components and the properties deemed critical). Any comparison of environments can only be made

on the basis of known or anticipated phenomena. Hence, at best, fission reactor testing cannot be considered as a complete substitute for testing in a fusion spectrum; it will be necessary to perform testing in a fusion environment to confirm correlations between the fission and fusion environments and also to identify unanticipated or "wild card" effects. The potential for the latter is increased by the fact that fission reactor irradiations may not generally achieve the highest doses expected in fusion reactors.

The principal shortcoming of fission reactor test facilities is the lack of high energy neutrons. In comparison with a fusion environment, this results in fewer displacements per neutron, possible differences in the spatial configuration of defect production ("cascade effects"), and fewer transmutations per neutron. Perhaps most important is that the ratio of transmutation rate to displacement rate is significantly lower except for a few special cases. Similarity of this ratio is currently believed to be an important general criterion for simulating radiation effects in a fusion environment.

Both actual and computer-simulated experiments suggest that high energy displacement cascades may not introduce effects (in bulk alloys) that are qualitatively different from those produced by low energy cascades. The quantitative differences in damage per neutron can be estimated from low fluence fission-fusion comparisons and from defect production models. Thus, fission reactors are believed to be useful for displacement damage studies of fusion materials.

Fission reactor studies of gaseous transmutants have concentrated on helium in metals and tritium in solid breeders. Helium is produced in nickel placed in a flux-spectrum having a substantial thermal component (as in a mixed spectrum reactor such as HFIR); He/dpa ratios can be varied somewhat by spectral tailoring. It is also produced in harder spectra if the nickel is enriched in ^{59}Ni . Thus, the study in fission reactors of the effects of helium is limited to nickel-bearing alloys. For insulators containing oxygen and nitrogen, isotopic tailoring can be exploited to produce high He/dpa and H/dpa ratios, respectively.

Solid transmutants may be produced copiously in a thermal spectrum because of high (n, γ) reaction cross sections and subsequent product decay. In general, however, the reactions are quite different from those in a fusion

environment. This phenomenon may preclude meaningful experiments to high doses in mixed-spectrum reactors for some materials.

Existing fission reactors provide sufficient test volume and flux to perform significant irradiation testing of materials and some components. In fact, the Alloy Development (ADIP) Program has many structural materials irradiations underway, and the irradiation testing of solid breeder materials is ongoing in tests such as TRIO⁽¹⁾ and FUBR⁽²⁾. The Damage Analysis and Fundamental Studies (DAFS) Program is responsible for establishing the correlations between irradiation effects in fission and fusion facilities.

The main thrust of this section is to establish the relevance of the fission environment for interactive testing. In an effort to evaluate that relevance, an analysis was performed which compared the effects of a fusion environment to those expected in typical fission facilities. There are many fission facilities available, each one with different characteristics; a few representative ones were selected for evaluation. The reactors selected were the sodium cooled fast reactor (FFTF) and two water cooled mixed spectrum reactors (ORR and ETR). These facilities were chosen because they are representative of available test reactor environments and because they have sufficient volume available for limited subcomponent testing. The ETR reactor is currently inactive, but reactivation is discussed from time to time and may be a possibility.

Beyond materials testing, the greatest utility for fission reactor testing appears to be in the solid breeder blanket area. To evaluate fission facilities, those parameters were selected which relate directly to the solid breeder blankets selected by the FINESSE committee; specifically, Li₂O/He/HT-9 with natural enrichment ⁶Li, and LiAlO₂/H₂O/HT-9/Be with 90% ⁶Li. For each of these concepts, the parameters evaluated are: helium generation rate, displacement rate, and temperature range for the structural material; and tritium production rate and heat generation rate for the solid breeder.

The expected values for these components in a fusion environment were determined assuming a neutron wall loading of 5 MW/m² at the front of the blanket. These were then compared to values calculated for the respective materials in the selected fission facilities at core mid-plane in a plausible (but not necessarily optimal) test position. The analysis was on a microscopic

basis and does not reflect the impact of the test on the fission reactor spectrum.

Figure 8-1 shows a comparison of the three test facilities and the fusion environment for the HT-9 structural material in the $\text{Li}_2\text{O}/\text{He}/\text{HT-9}$ system. The most obvious disparity is the helium production rate. Displacement damage is produced at a reasonable rate, particularly in a fast test reactor such as FFTF, but the He/dpa ratio is much lower than desired. Matching the anticipated temperatures is not a problem for unpressurized, water cooled reactors, but is more difficult in a liquid metal cooled fast reactor because of the necessity to keep the coolant molten. It is possible, however, using an insulated test position such as the Closed Loop Irradiation Assembly (CLIRA) in the FFTF to achieve these lower temperatures.

Figure 8-2 shows a similar comparison for the Li_2O solid breeder in the same facilities. The parameters of interest in this case are tritium production rates and heat generation rates. In order to achieve nearly prototypic tritium production rates, it is necessary to tailor the ^6Li enrichment to the facility. The enrichment levels were selected to give beginning-of-life tritium production rates identical to those expected in the fusion system; this also sets the heat generation rate. The lower end of the bar gives the end-of-life production rate. Shown also in the figure is the ^6Li enrichment at the beginning-of-life and the total burnup of all the lithium isotopes at the end-of-life. Note that the fast reactor environment appears to be a relatively good test bed for the Li_2O with low ^6Li enrichment, both for tritium production and heat generation.

The results for the lithium aluminate system are shown in Figures 8-3 and 8-4. For this case, thermal reactors do a much better job of simulating the tritium production and heat generation than a fast reactor except near end-of-life, but fast reactors provide high burnup effects on a similar time scale and are within a factor of two of fusion relevant tritium and heat generation rates. As would be expected for the structural material HT-9, the damage rates are nearly identical to the previous case. Again, the helium to dpa ratio is very low.

Both systems evaluated utilize HT-9, which contains only 0.5% nickel, as the structural material. Alloys which contain significant levels of nickel generate much higher levels of helium in a mixed spectrum reactor. ^{58}Ni

HT-9 STRUCTURE

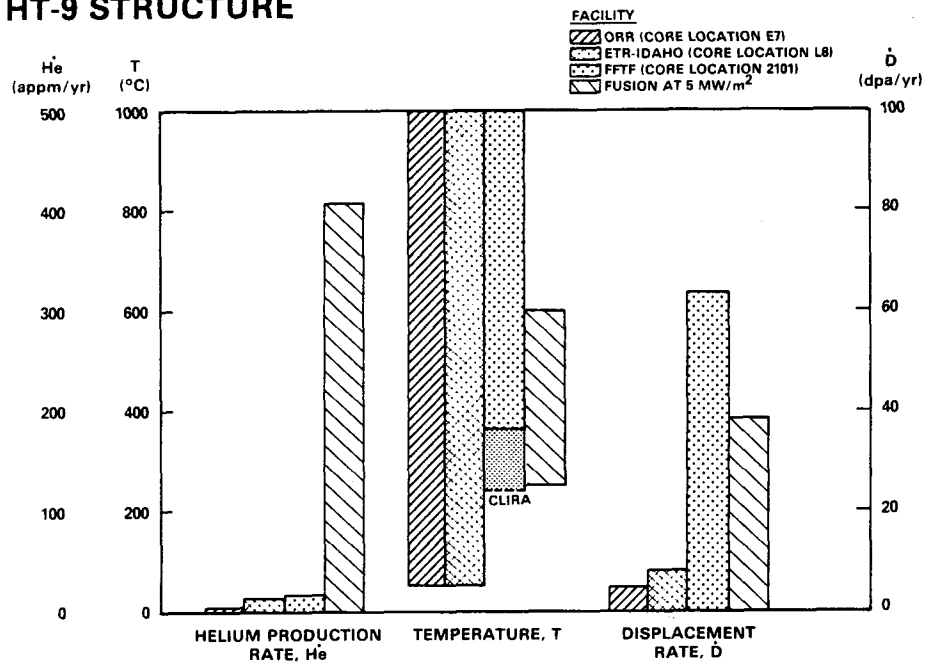


Figure 8-1: Fission/Fusion Irradiation Comparison for Li₂O/He/HT-9 System

Li₂O SOLID BREEDER

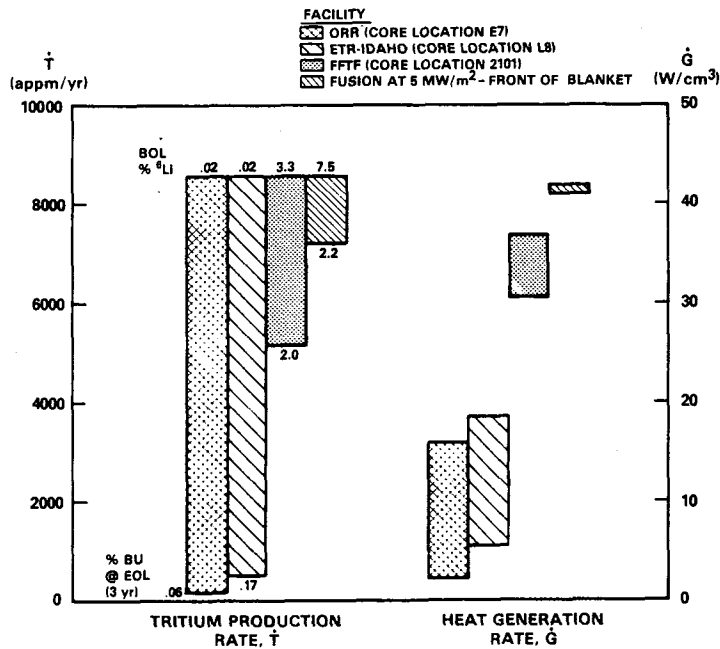


Figure 8-2: Fission/Fusion Irradiation Comparison for Li₂O/He/HT-9 System

HEDL 8511-083.2

HT-9 STRUCTURE

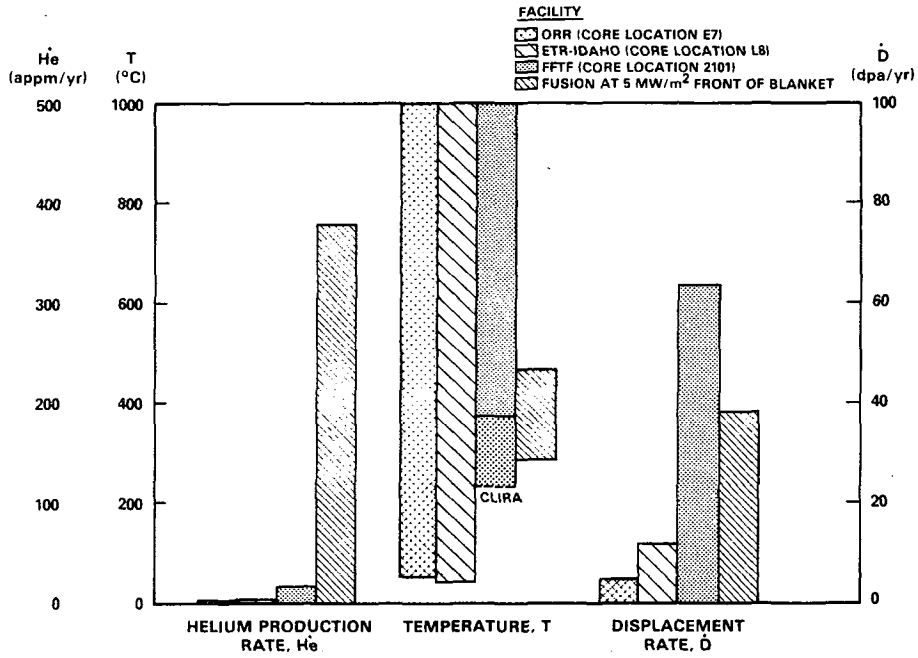


Figure 8-3: Fission/Fusion Irradiation Comparison for LiAlO₂/H₂O/HT-9/Be System

LiAlO₂ SOLID BREEDER

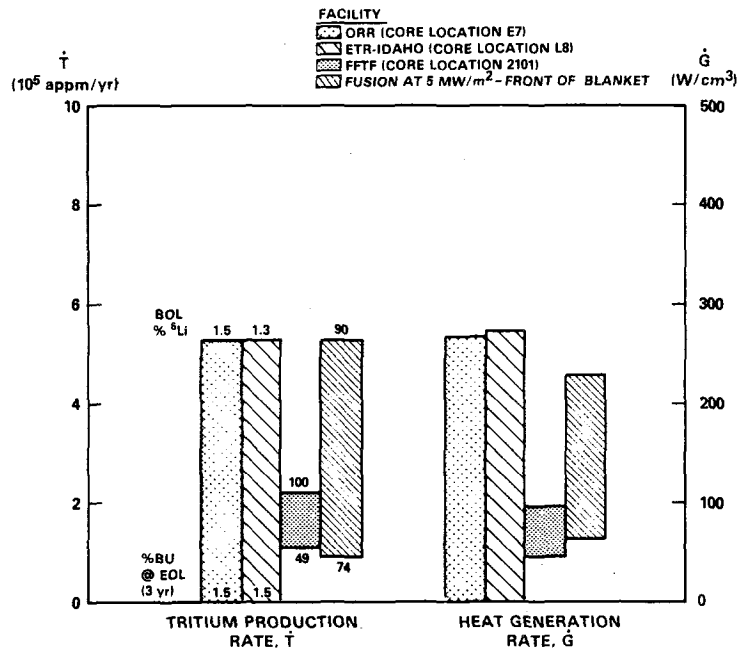


Figure 8-4: Fission/Fusion Irradiation Comparison for LiAlO₂/H₂O/HT-9/Be System

HEDL 8511-083.3

interacts with thermal neutrons and is converted to ^{59}Ni which is then converted to ^{56}Fe with the production of helium. Because the reaction occurs in two stages, the production rate of helium is nonlinear with fluence unless spectral tailoring is employed. Austenitic stainless steels (approximately 15% Ni) are one class of prime candidates; considerable testing of this class of alloys is underway in the ORR (including spectral tailoring) and the HFIR⁽³⁾. Table 8-1 shows the displacements, helium generation, and hydrogen generation in 316 stainless steels for various facilities.

Table 8-1. Defects Produced in Type 316 Stainless Steel for One-Year Operation of Various Facilities^a

Reactor ^b	Neutron Fluence ($\times 10^{26}$ n/m ²) (> 0.1 MeV)	Displacements (dpa)	Helium (at. ppm)	Hydrogen (at. ppm)
Fusion Reactor (1 MW/m ²)	0.80	11.5	144	530
EBR-II	6.9	37	Approx. 20	300
HFIR	4.4	35	1900	425
ORR	1.3	11	80 to 160	135

^aFrom: F. W. Wiffen, et al., "The Behavior of Type 316 Stainless Steel Under Simulated Fusion Reactor Irradiation," in The Metal Science of Stainless Steels, F. W. Collings and H. W. King, eds., AIME, 1979, p. 148.

^bA high flux position has been chosen. Duty factor = 1.0.

In order to achieve high helium generation rates in non or low nickel alloys, doping with natural nickel or ^{59}Ni can be employed. The latter is required to achieve the desired rate enhancement in a fast reactor. For typical austenitic stainless steels, relevant He/dpa ratios can be achieved at the periphery of the FFTF core with the relatively low enrichment of about 4% ^{59}Ni . To achieve prototypic He/dpa ratios in HT-9 (approximately 0.5% Ni) at the same location, nearly 100% enrichment of ^{59}Ni is required.

A small amount of nickel enriched to 2% ^{59}Ni has been produced, some of which has been incorporated into several austenitic alloys for irradiation testing. The enriched nickel was produced through irradiation of Inconel 600 in the ETR, followed by ion exchange separation of radioactive cobalt and recovery of the nickel by an electroplating process. The cost of producing

the enriched Ni was about \$500/gram. The cost to increase the ^{59}Ni concentration by conventional techniques has been considered prohibitively high. The possibility of using the plasma isotope separation process developed by TRW for achieving high enrichment is currently being explored. If this proves practical, it may be possible to achieve fusion development He/dpa ratios in HT-9 in a fission reactor.

8.2.2 Facility Availability

There are numerous test reactors available in the United States and abroad, but only a few can provide high damage rates or high fluence. The Interim FINESSE Report⁽⁴⁾ included a survey of existing facilities; Tables 8-2 and 8-3 are updated from that report. At this time, many fusion tests are underway or have already been completed in several of these facilities. As an example, the Materials Open Test Assembly (MOTA)⁽⁵⁾, now in FFTF, contains a large number of specimens of a wide variety materials. The MOTA facility is currently unique in having a large test volume with provisions for instrumented testing. There are discussions underway of a proposed solid breeder test in FFTF, as well as a MOTA which is dedicated solely to fusion materials irradiations. The EBR-II, another fast test reactor, has similar capability though somewhat reduced volume and flux. The HFIR and ORR reactors have also been used extensively and have fusion materials irradiations underway at this time. Usage of ORR is expected to decrease because of its low damage rate. Irradiation facilities in HFIR, on the other hand, are expected to be improved through increased test volume and provisions for instrumented testing. The increased volume will accommodate spectral tailoring but with an accompanying decrease in damage rate.

Existing facilities have sufficient volume to perform much of the needed testing although space restrictions on component testing are severe. The question of availability is primarily one of programmatic priorities.

8.2.3 Cost of Utilization

There are several types of costs associated with using the available fission facilities: operating costs; test handling, installation, and removal costs; and neutron charges. Not all of these costs are necessarily passed on to the experimenter -- facility funding from other programs often bears a

Table 8-2: Capabilities of Selected U.S. Reactors

REACTOR	LOCATION	POWER (MW)	EXP. NEUTRON FLUX $n/cm^2/sec$	EXP. SIZE (cm)	TEST POSITION EXP. VOL. (L)	NOTES	CORE SIDE FACILITY DIM.
ATR	IDAHO	250	$1.5 \times 10^{15}F$	7.6 x 122	5.6	9 FLUX TRAPS	NONE
EBR-II	IDAHO	62.5	$2 \times 10^{15}F$	7.4 x 36	1.5	Na COOLED	NONE
FFTF	WASH.	400	$5 \times 10^{15}F$	6.35 x 91 10.2 x 91	2.9 8.5	2 CLOSED LOOPS 6 INSTRUMENTED NUMEROUS NON-INSTRUMENTED	NONE
HFIR	TENN.	100	$1.3 \times 10^{15}F$ $1.5 \times 10^{14}Th$	13 x 51 7 x 51	6.8 2.0	FLUX TRAP 2 REF. POS.	NONE
ORR	TENN.	30	$4.5 \times 10^{14}F$	7.8 x 38.4	0.5	ANY CORE POS.	POOL SIDE 71 x 76 cm 5×10^{13}

HEDL 8610-158.2

Table 8-3: Capabilities of Selected Non-U.S. Reactors

REACTOR	LOCATION	POWER (MW)	EXP. NEUTRON FLUX n/cm ² /sec	EXP. SIZE (cm)	TEST POSITION EXP. VOL. (L)	NOTES	CORE SIDE FACILITY DIM.
BR-2	BELGIUM	60	1 x 10 ¹⁵ Th 6 x 10 ¹⁴ F	20 x 96	30	1 LOOP, 4 OPEN MANY POSITIONS	NONE
DIDO	U.K.	25	1.8 x 10 ¹⁴ Th 6 x 10 ¹³ F	5 x 60	1.2	D ₂ COOLED AND MODERATED	?
HFR	NETHERLAND	20	5 x 10 ¹⁴ F	14.5 x 60	9.9	INSITU TRITIUM RECOVERY EXPERIMENTS	POOL SIDE 0.8 x 10 ⁶ F 77.5 x 72 cm.
HFR	FRANCE	57	1.5 x 10 ¹⁵	?	?	D ₂ MOD.	?
JRR-2	JAPAN	10	1 x 10 ¹⁴ Th 1 x 10 ¹⁴ F	7 x 7	?	INSITU TRITIUM RECOVERY EXPERIMENTS	
KNK	WEST GERMANY	60	2 x 10 ¹⁵ F 2 x 10 ¹⁴ Th	10 x 60	4.7	SEVERAL TEMP. CONTROLLED POSITION 1 INSTRUMENTED POSITION	NONE
NRU	CANADA	200	1 x 10 ¹⁴ Th	12 x 300	33.9	INSITU TRITIUM RECOVERY EXPERIMENTS	POSSIBLE 240 x 240 cm 5 x 10 ¹³
OSIRIS	FRANCE	70	1 x 10 ¹⁴ Th 5 x 10 ¹⁴ F	8.4 x 60	3.2	SEVERAL LOOPS	? POOL SIDE
SAFARI-I	SOUTH AFRICA	20	1 x 10 ¹⁴ Th 2 x 10 ¹⁴ Th	7.6 x 61 15.2 x 61	2.8 11.2 1 x 10 ¹⁴		POOL SIDE 70 x 61 cm
SILOE	FRANCE	36	4 x 10 ¹⁴ Th 5 x 10 ¹⁴ F	8 x 60	3.0	INSITU TRITIUM RECOVERY EXPERIMENTS	POSSIBLE 48 x 63 cm ?
JMTR	JAPAN	50	3 x 10 ¹⁴ Th 3 x 10 ¹⁴ F	7 x 7	?	INCONVENIENT FOR TRITIUM RECOVERY	?

HEDL 8510-156.1

share of these costs. As an example, the FFTF which has been shown to be an excellent test bed has an annual operating budget of over \$50 M. This cost is currently funded by the LMR Program; hence, only the direct costs associated with a fusion materials experiment are funded by the Office of Fusion Energy (OFE). A private entity or foreign government would be required to pay a prorated portion of the annual operating cost; this is often referred to as neutron charges.

It would not be prudent in planning future test activities to assume that test facilities available now for little cost will remain so. It may be necessary for the fusion program to assume part or all of the operating costs of a facility if other programs are not provided with sufficient budgets to continue funding.

For the purpose of comparison, Table 8-4 gives some detail of these costs for a few representative facilities. It is important to understand that it is difficult to apply these costs directly to a program without considerable interface between the program sponsor, other users of the facility, and the facility operators. The costs listed are approximate only and are based on conversations with facility operators and DOE sponsors. Not included in the table are the costs for charging, operating, and discharging the experiment; these costs range from a few thousand dollars to several hundred thousand dollars depending on the size and complexity of the test. Also shown in Table 8-4 are neutron charges; these are a function of the plant capital cost, annual operating costs, and the relative volume of the test position. Neutron charges are not assessed when the reactor use is of benefit to the U.S. government. They are shown here because they are representative of the relative costs of performing the tests.

8.3 Accelerator-Based Neutron Sources

Another class of irradiation facilities is accelerator-based neutron sources. Their relevance to fusion technology development stems from one or more of the following attributes: 1) fusion energy neutrons (i.e., near 14 MeV or at least such as to produce effects similar to those produced by 14 MeV neutrons), 2) high flux, 3) large test volume, 4) experimental accessibility, and 5) availability.

Table 8-4. Reactor Operations Costs

Facility	Plant Costs	Neutron Charges (Annual \$/Subassembly)
FFTF	\$60 M	\$1300 M/yr (In-core position)
EBR-II	\$19 M	\$ 400 K/yr (In-core position)
ORR	\$ 4 M	\$ 375 - 450 K/yr (Depending on position)
HFIR	\$ 9.4 M	\$375 K/yr (RB position) \$140K/yr (Target position)

The main issues to be addressed with an accelerator-based neutron source are: 1) radiation damage in materials and radiation effects in components, 2) studies of tritium breeding, and 3) neutronic studies of components and systems. In this review, we will concentrate on radiation damage and radiation effects issues for which the highest fluence levels are required. Materials include structural, heat sinks, magnets, insulators, etc.

The important considerations are:

- 1) Correlations of low to high fluence effects with fusion energy neutron spectra near 14 MeV.
- 2) Correlations of fission and fusion radiation effects up to the highest fluences achieved in fission reactors (approximately 100 dpa).
- 3) Investigation of material behavior to doses of several hundred dpa (beyond the practical range of fission reactors).
- 4) Damage mechanism studies that include the effects of transmutations on microstructure and microchemistry and associated dimensional stability, mechanical behavior, and physical and electrical properties. (Helium is an especially important transmutant).
- 5) Validation and calibration of mechanistic and damage correlation models, especially for high fluence phenomena.

The number of accelerator-based neutron source facilities that can be seriously considered for radiation damage studies is small. We will concentrate here on those facilities that meet or approach certain limited characteristics. These characteristics are outlined as follows:

- 1) The facility should be capable of producing a high rate of damage, on the order of 100 dpa/year. For example, a flux of 10^{15} n/cm² of 14 MeV neutrons gives this rate for a typical metal. Currently, there are no facilities capable of this high fluence.
- 2) The spectrum should produce damage qualitatively the same as a fusion reactor. Current thinking dictates that the rate and type of transmutations produced per dpa are the best indicators for this criterion. Helium is the transmutant generally considered to be most important, and the desired He/dpa ratio is approximately 10 in steels.
- 3) Gradients in both flux and spectrum should be limited to ensure uniform damage throughout the specimen volume.
- 4) The facility should be available for extended periods.
- 5) The facility should have a test volume large enough to test large components to high fluences. Prototypic gradients would be acceptable.

Only four facilities meet at least a few of the criteria. These are RTNS-II, the UC Davis Cyclotron, the A-6 Radiation Effects facility at LAMPF, and the FMIT facility. Currently, all but the FMIT facility are operating. We include the FMIT facility because, from early in the fusion materials program, it (or its equivalent) has been an essential element in the strategy. With postponement of construction of such a facility, the available test facilities must be used creatively to infer phenomena peculiar to fusion neutrons.

8.3.1 RTNS-II Facility⁽⁶⁾

8.3.1.1 Description

The Rotating Target Neutron Source (RTNS-II) facility contains two independent sources of 14 MeV neutrons produced by the d,t reaction. Each source consists of an air-insulated Cockcroft-Walton accelerator which is typically run with a continuous beam current of 120-125 mA of 400 KeV deuterons

on target. The beam is focused onto a spot with Gaussian shape and about 2 cm in diameter on a rotating water-cooled target. Each target is 50 cm in diameter and is typically rotated at approximately 2200 rpm. It is constructed of a copper alloy coated with titanium tritide. Under intense bombardment, the tritium is gradually released and the mean lifetime of each target is only 200 hours. The major components of one of the sources are shown in Figure 8-5.

8.3.1.2 Environmental Relevance

Neutrons radiate nearly isotropically from the beam spot. Flux gradients are steep, ranging from $1/r$ in the highest flux region (about a factor of two in 2 mm) to $1/r^2$ at larger distances.

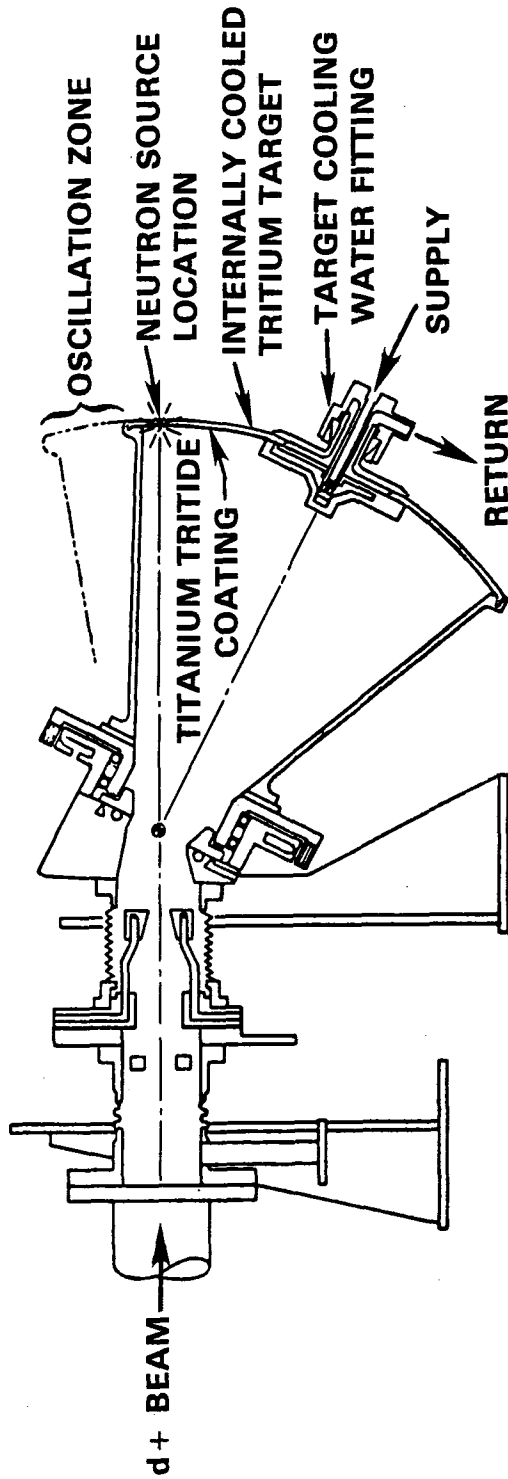
The mean source strength over the life of the target is about 2×10^{13} n/s. The highest average flux is estimated to be about 5×10^{12} n/cm²-s at a distance of about 0.35 cm. The current best evaluation for the flux profiles is given in Reference 7.

If maximum flux is to be obtained for a sample, it is very important that sample containers such as furnaces, cryostats, and other such equipment be designed with the minimum possible thickness between the neutron source and the sample. The effect of such devices upon the volume available for samples is quite large. With a furnace that is commonly used to control the temperatures of samples, there is only about 8 cm³ available with a flux greater than 10^{12} n/cm²-s and no volume with flux greater than 2×10^{12} n/cm²-s.

The maximum irradiation dose attained to date is about 10^{19} n/cm². The actual elapsed time to achieve this value at an elevated temperature (i.e., in a furnace) is about six months of irradiation for nominally 120 hours (15 shifts) each week. The maximum flux in the furnace is only about 2×10^{12} n/cm²-s. For iron or copper, the peak damage reached in this period is approximately 0.03-0.04 dpa. The helium/dpa ratio is about 14 for iron and 12 for copper. However, the maximum helium concentration is only about 0.5 appm.

8.3.1.3 Availability

Currently, the RTNS-II facility is supported jointly by the U.S. DOE and the Japanese Ministry of Education, Science and Culture (Monbusho). One source is operated 24 hours/day, 5 days/week. The other source is operated



SCHEMATIC OF SECTION OF TARGET SYSTEM. SHADED AREA SHOWS PORTION THAT ROTATES AT 5000 rpm. THE ANGLE BETWEEN THE AXIS OF ROTATION AND THE DEUTERON BEAM IS SLOWLY VARIED TO USE THE ENTIRE TRITLUM-COATED BAND ON THE INSIDE OF THE TARGET. THE NEUTRON SOURCE REMAINS STATIONARY IN THE ROOM. TO ACQUIRE MAXIMUM NEUTRON FLUX, SAMPLES ARE PLACED AS CLOSE AS REASONABLE TO THE EXTERIOR SURFACE OF THE SPINNING TARGET.

Figure 8-5: Schematic of RTNS Target (Ref. 6)

HEDL 8611-083.5

intermittently for short duration experiments. The primary (highest flux) irradiation space is dedicated to fusion materials testing. Add-on experiments in lower flux regions are performed by other programs. Operating costs for FY-85 were about \$1.9 M with about \$1.5 M expected for FY-86.

8.3.2 UC Davis Cyclotron Facility

8.3.2.1 Description

The cyclotron of the Crocker Nuclear Laboratory at the University of California at Davis was used a modest amount for radiation damage studies prior to expansion of RTNS-II operation in about 1979. The facility makes neutrons from 30 MeV deuterons stopping in a thick beryllium target.

8.3.2.2 Environmental Relevance

The principle of the neutron source is that an energetic deuteron has a significant probability of interacting with a nucleus in a thick target material. The deuterons tend to break up into a neutron and proton in such interactions. The nucleons tend to go forward with the same velocity as the incident deuteron, but with half the energy of the incident deuteron. This same principle is used in the proposed FMIT facility.

The yield of neutrons from deuterons on light elements such as beryllium and lithium is very large. For 30 MeV deuterons on thick beryllium, it is about 0.05 neutrons per incident deuteron or 8×10^{12} n/s for a 26 microamp beam⁽⁸⁾. The spectrum in the UC Davis facility peaks near 12 MeV in the forward direction, far from the target. However, it is broad and varies with emission angle relative to the beam direction. The spectra are similar to those expected in the FMIT facility.

The flux varies from about 10^{13} to 10^{12} . The maximum flux available within a furnace is estimated to be only about 5×10^{12} n/cm²-s. The volumes available with fluxes greater than 10^{13} and 10^{12} n/cm²-s are about the same as in RTNS-II but have not been evaluated quantitatively. The rates of production of dpa and He are similar to those found in RTNS-II.

8.3.2.3 Availability

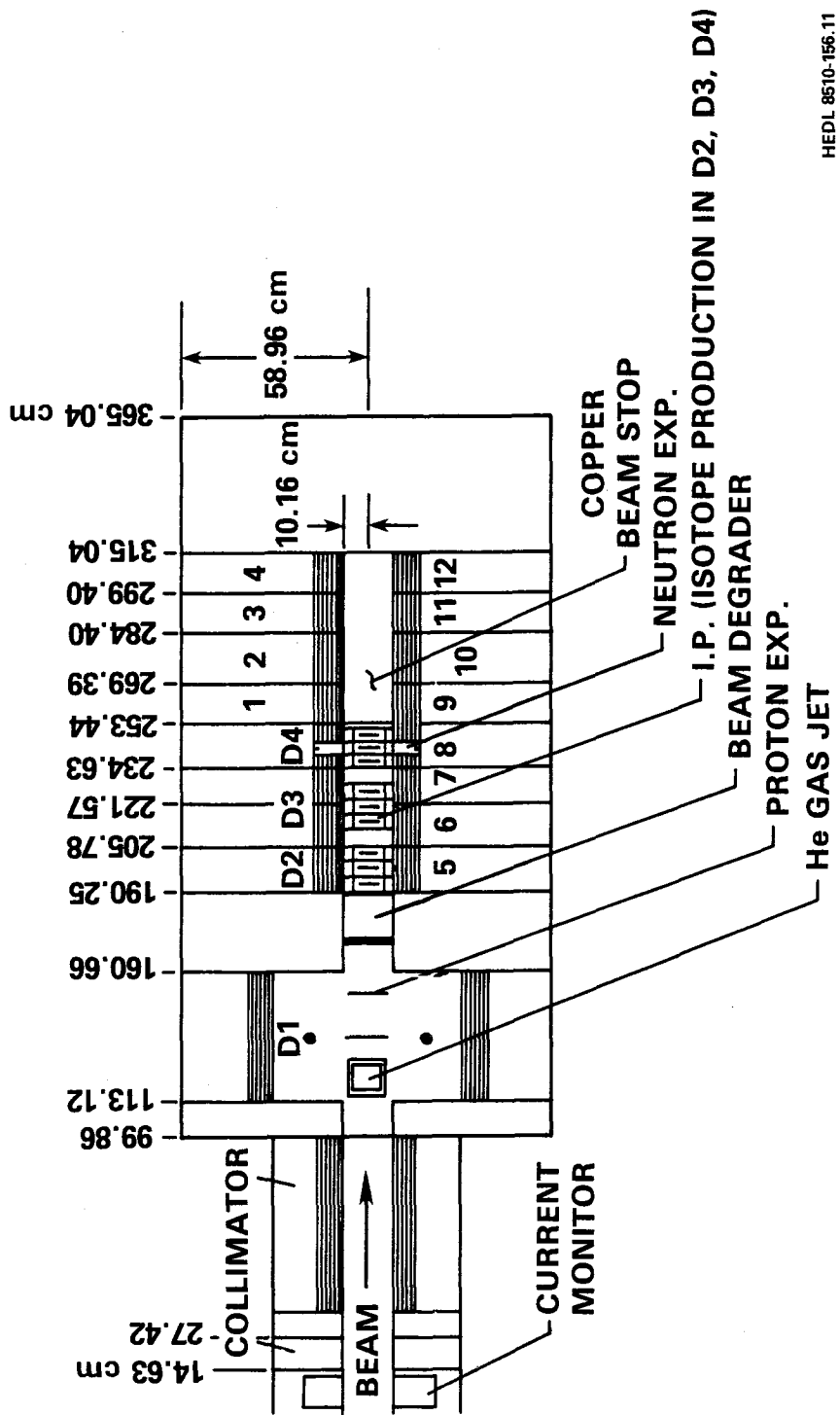
This facility has not been used much for radiation damage studies since RTNS-II went into expanded operation. Although it is associated with a university, it has for many years encouraged and supported outside use of the facilities. The availability is estimated to be 2 to 3 days/week. This would provide a large reduction in exposure compared to RTNS-II or other facilities that have higher availability. The facility is not supported by DOE/OFE, so there would be costs associated with its use.

8.3.3 The A-6 Radiation Effects Facility at LAMPF

8.3.3.1 Description

The A-6 facility is where the main beam from the Los Alamos Meson Physics Facility (LAMPF) is dumped. The beam is 800 MeV protons; however, by the time it reaches the A-6 area, it is reduced to about 760 MeV. The accelerator operates with an average beam current of about 0.75 mA. The facility can be used for radiation damage studies using either the direct proton beam or the spallation neutrons that result from interactions of the beam with the target materials. The spallation neutrons have spectra similar to a moderated fission spectrum plus a high energy tail that extends to the energy of the incident protons. The beam is pulsed with a peak current of up to 16.7 mA and pulse width of 0.5 ms occurring every 8.33 ms. A theoretical study⁽⁹⁾ indicated that this produces the same radiation damage as a steady-state source. The transverse spatial distribution of the beam on the target is Gaussian with full width at half maximum of 5.9 cm.

The target geometry is shown in Figure 8-6. This is a simplified cylindrical geometry which is used for radiation transport calculations (see Reference 10 for more details). Zones 1 through 12 are available for neutron irradiation and currently contain 16 cm thick (radially) 316 stainless steel surrounded by 33 cm of iron at 60% density. Access is available for instrumentation and cooling lines. Specimen temperature control can be controlled in the range of 20 to 800°C.



HEDL 8510-156.11

Figure 8-6: LAMPF A-6 Target Geometry

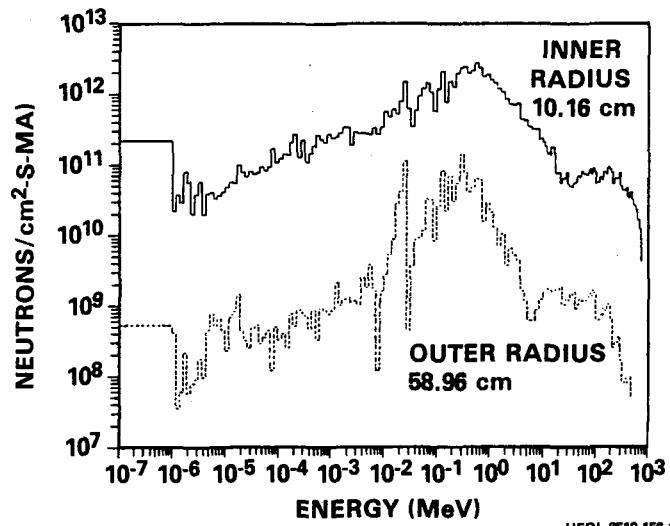
8.3.3.2 Environmental Relevance

There has been some discussion in the literature⁽¹¹⁾ of using high energy proton beams to directly simulate damage in a fusion reactor, even though specimen configurations are heavily constrained by the high rate of energy deposition. This option is not considered here because of the differences in the manner in which damage is introduced. In particular, spallation reactions introduce a large excess of helium and a wide variety of transmutant nuclei that would not be found in a fusion environment. There is also concern that neutron irradiations would lead to similar, but less pronounced, effects due to the tail of high energy neutrons in the spectrum of spallation neutrons.

The neutrons that result from the spallation phenomenon are, for the most part, considerably lower in energy than the direct protons. When an incident proton slows down in the beam stop material, it may collide with one of the nuclei. However, rather than being absorbed by the whole nucleus as would tend to happen at lower energies, it scatters off and possibly ejects a nucleon. In a thick material, this process continues until the energetic nucleus has insufficient energy to eject further nucleons and they slow down and stop in the material.

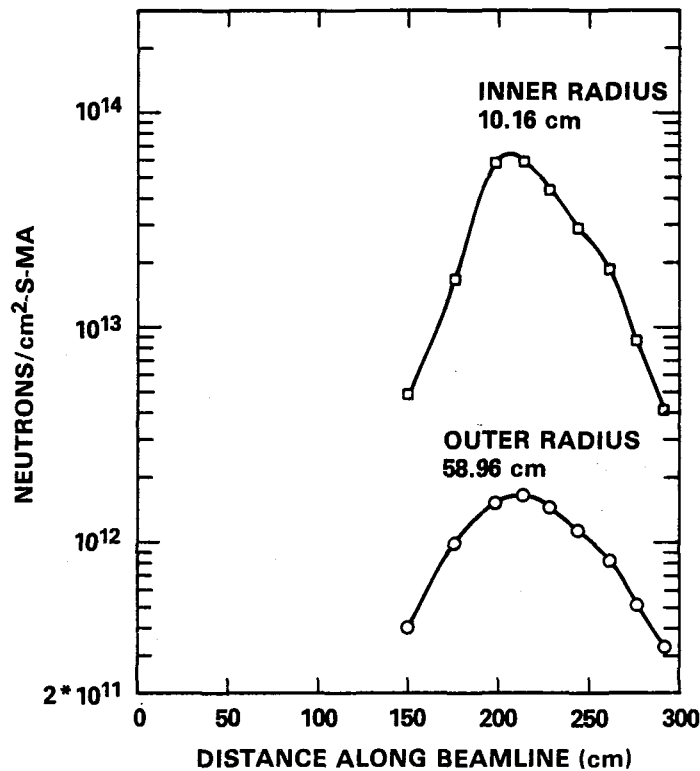
The nuclei that remain after a nucleon is ejected or spallated may have considerable residual excitation energy. Much of this energy is given off in the form of low energy neutrons which are evaporated by the hot residual nuclei. Therefore, even though the incident proton energy is nearly 800 MeV, the neutron emission spectrum is predominantly less than 1 MeV, which is characteristic of evaporation. There is also a tail of very high energy neutrons that results from the primary spallation reactions.

Figure 8-7 shows the neutron spectra calculated⁽¹⁰⁾ at the inner and outer radii of Zone 5 (see Figure 8-6) where the peak flux occurs in the axial direction. The maximum flux was about 3×10^{13} n/cm²-s per mA of beam current at a radius of 10.16 cm, dropping by a factor of 40 in 40 cm radially. The profiles of the neutron flux along the beam line for those two radii are shown in Figure 8-8. A measurement of a neutron spectrum was also made⁽¹²⁾. It agrees with calculations fairly well for neutron energies greater than about 10 KeV. For lower energy neutrons, the measured spectrum is lower than the calculation by a factor of about 5. This discrepancy is not understood but is of little consequence with respect to producing damage in most materials.



HEDL 8510-156.12

Figure 8-7: LAMPF A-6 Target Neutron Spectra



HEDL 8510-156.9

Figure 8-8: LAMPF Beamline Neutron Flux Profile at Two Radii in A-6

There are about 241 liters of total volume available for neutron irradiations in the A-6 facility. The volume available with a flux greater than 10^{13} n/cm²-s is very much less, particularly including a temperature controlled furnace. The exact volume as a function of minimum flux values has not yet been evaluated.

The maximum displacement and helium production rates have been evaluated for copper in the A-6 facility⁽¹³⁾. The uncertainties in those rates are larger than in facilities having softer spectra. This is because there are significant contributions from the high energy tail of the neutron spectrum, where the cross sections for displacement and helium production are very poorly known. For example, the production rates of helium and displacements in copper were calculated in Reference 13 for a typical LAMPF spectrum. About 95% of the helium was produced by neutrons above 20 MeV where the cross sections are poorly known. For the displacement rate, about 26% was produced by neutrons greater than 20 MeV. The calculated He/dpa ratio was about 28 which is similar to the value of 12 found in RTNS-II for copper. However, the uncertainty is significantly larger.

This illustrates the importance of the tail of high energy neutrons to the production of transmutations. It seems highly unlikely that the ratio of transmutations per dpa produced in the A-6 spectra would be similar for all important transmutants found in a fusion device. Certainly, there are some transmutations that are energetically allowed in a spallation spectrum which are below threshold in a fusion spectrum. The importance of such effects is not known.

A typical LAMPF run cycle is 9 weeks long. Three or four run cycles can be expected in a year. In 1982, the beam was available for about 3550 hours. For a comparable irradiation time and the maximum flux of 6×10^{13} n/cm²-s per mA, the maximum number of displacements for copper in the A-6 facility would be only about 0.56 dpa/calendar year. The maximum amount of helium would be about 9.8 appm He/calendar year. Placing specimens in a temperature controlled furnace will reduce the maximum damage and transmutation rates.

Near the beam where the neutron flux is largest, one also finds small contributions from charged particles. For example, at the position of the peak neutron flux, the flux of secondary protons was calculated⁽¹⁰⁾ to be about 1.2×10^{12} protons/cm²-s per mA. This is a factor of 50 less than the

neutron flux. Calculations in Reference 14 show that secondary protons contribute 6% of the dpa's produced by neutrons. Contributions to transmutations may also occur but were not mentioned. Small fluxes of energetic pions and muons were also calculated.

8.3.3.3 Availability

The LAMPF facility is supported primarily by funds for basic research in medium energy nuclear physics. Therefore, outside users would not be charged for operation of the facility if their experiments were approved. The availability was 3550 hours in 1982; however, this could be expanded somewhat(14).

8.3.4 The Fusion Materials Test (FMIT) Facility

8.3.4.1 Description

This proposed facility is based upon the intense source of neutrons that results when a 100 mA steady-state beam of 35 MeV deuterons is stopped in a thick liquid lithium jet target. The facility is described in more detail in Reference 15. A schematic of the facility is shown in Figure 8-9. The facility consists of an Alvarez-type linear accelerator, a lithium target system, and experimental facilities for irradiating and handling test specimens.

The lithium target was designed to be nominally 1.9 cm thick and flowing vertically downward in front of a 0.16 cm thick steel plate so as to rapidly carry away the 3.5 MW of heat deposited within it. It is intended that the beam spot on target will be bi-Gaussian in shape with full widths at half maximum of 3 cm horizontally by 1 cm vertically. This shape was chosen to reduce the flow requirements of the lithium and to maximize the flux in the highest flux region, while producing acceptable flux gradients.

8.3.4.2 Environmental Relevance

Neutron production in FMIT is via the same breakup reaction described for the UC Davis cyclotron in Section 8.3.2.2.

The yield of neutrons from 35 MeV deuterons on thick lithium is about 0.059 neutrons per incident deuteron or 3.7×10^{16} neutrons/s for a 100 mA

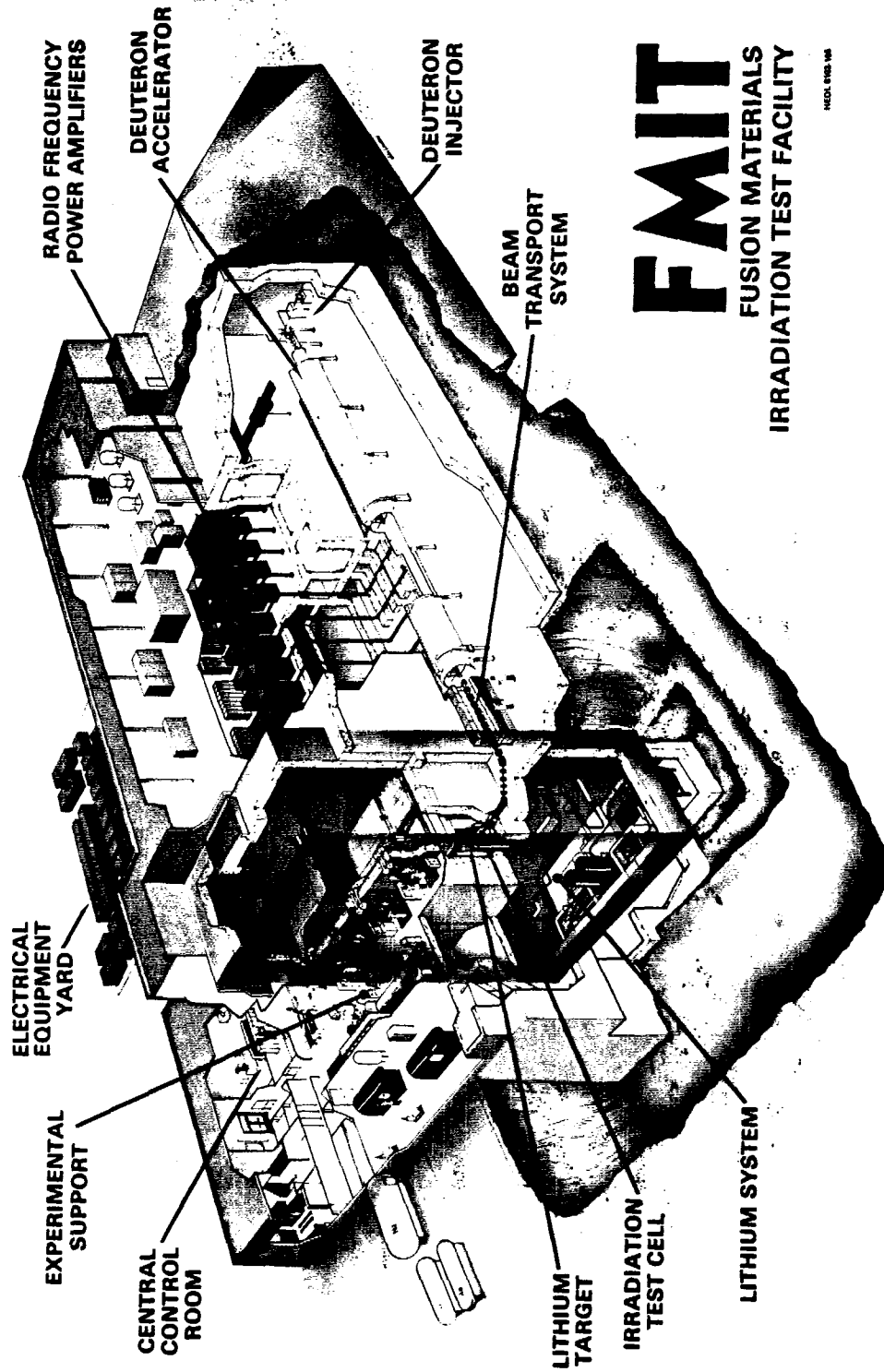


Figure 8-9: Fusion Materials Irradiation Test Facility — FMIT

beam⁽¹⁶⁾. The neutron yields and spectra were measured⁽¹⁷⁾ as a function of emission angle with respect to the beam direction. The data were observed at a large distance from the target and with a narrow beam width compared to the target thickness. Figure 8-10 shows the results, with the large yields at forward angles that peak near 14 MeV.

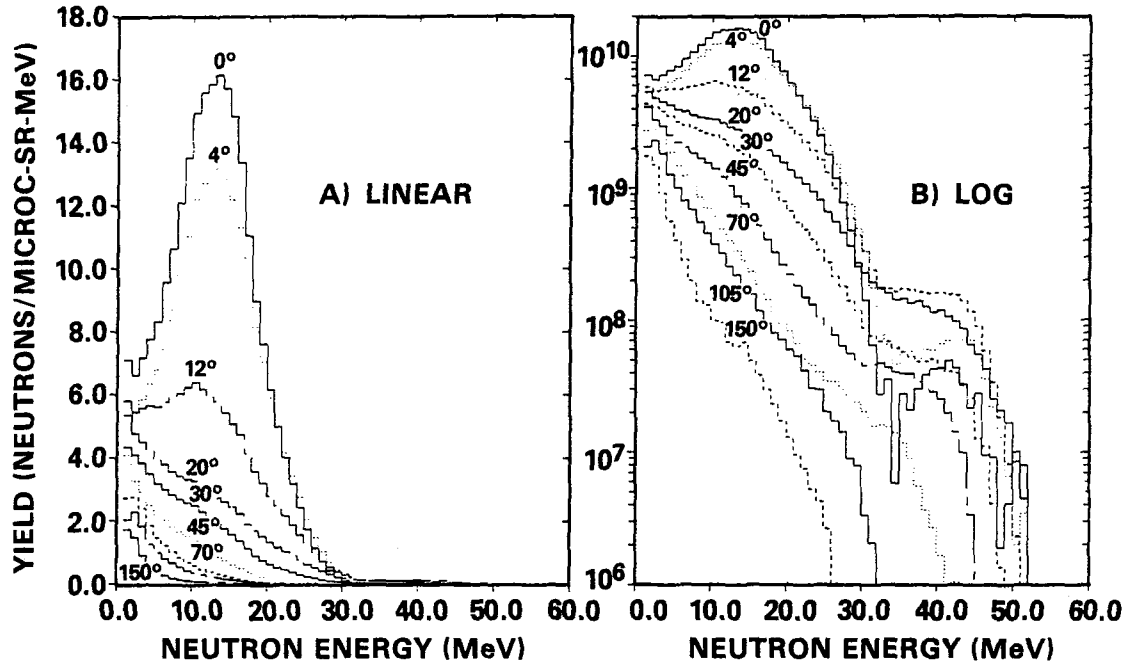
The data in Figure 8-10 were incorporated with data from measurements at other energies in order to model the differential thin target neutron yield as a function of deuteron energy and neutron emission angle. Calculations of the neutron spectra very near the target were then done using this model⁽¹⁶⁾. Such a model is necessary to allow accurate calculations of the neutron flux spectra for positions near the target that are comparable to the spatial distribution of the neutron source within the target.

D. G. Doran⁽¹⁸⁾ has shown that interpretation and application of FMIT data would not be compromised by differences between the FMIT and d,t spectra. The remainder of this section is taken from Reference 18.

Specimens would be located as close as 0.6 cm to the source. A specimen at this peak flux position (see Figure 8-11) will be exposed to neutrons from a large range of angles compared with a specimen farther from the source. The spectrum on axis far from the source is a broad peak with a maximum value at about 14 MeV. The mean neutron energy is about 12 MeV. There is a very low intensity high energy tail extending from about 32 MeV to 50 MeV; it is of significance for shielding but not for radiation damage. As one moves along the beam axis toward the source, the peak becomes less prominent and the mean neutron energy drops to about 8 MeV. Moving off axis, the spectrum softens rapidly.

The major vehicle for irradiating specimens in a high flux is the vertical test assembly, VTA-1. The hardest spectrum within this test assembly is shown in Figure 8-11. A typical first wall spectrum for the STARFIRE conceptual Tokamak reactor is also shown in Figure 8-11. For damage analysis purposes, the differences between this and the FMIT spectrum are much less important than the similarities.

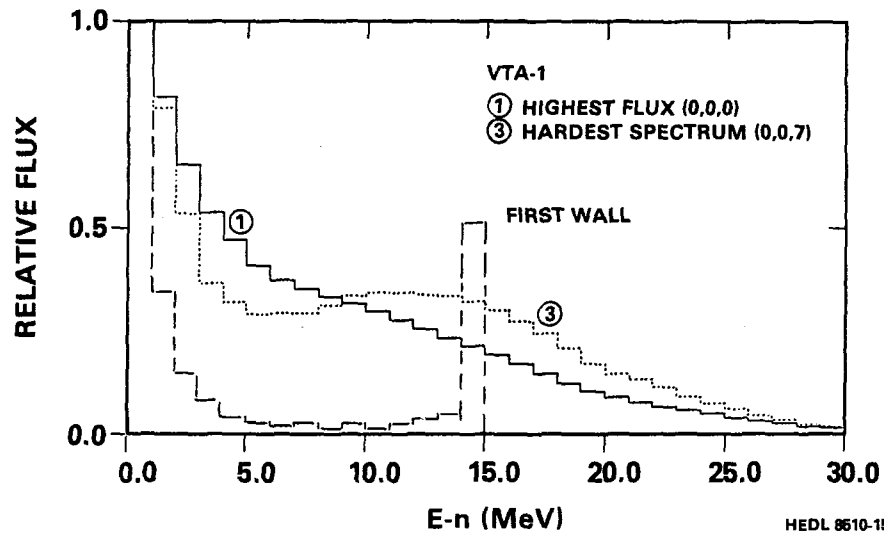
The energy dependence of displacement production for a particular material is given by the product of the displacement cross section and the flux spectrum. For stainless steel, about 50% of the displacements are produced by neutrons above 15 MeV and fewer than 3% above 30 MeV. The displacement



HEDL 8510-156.5

Figure 8-10: Yield of Neutrons from 35 MeV Deuterons on Thick Lithium

FMIT TEST CELL PERTURBED FLUX



HEDL 8510-156.8

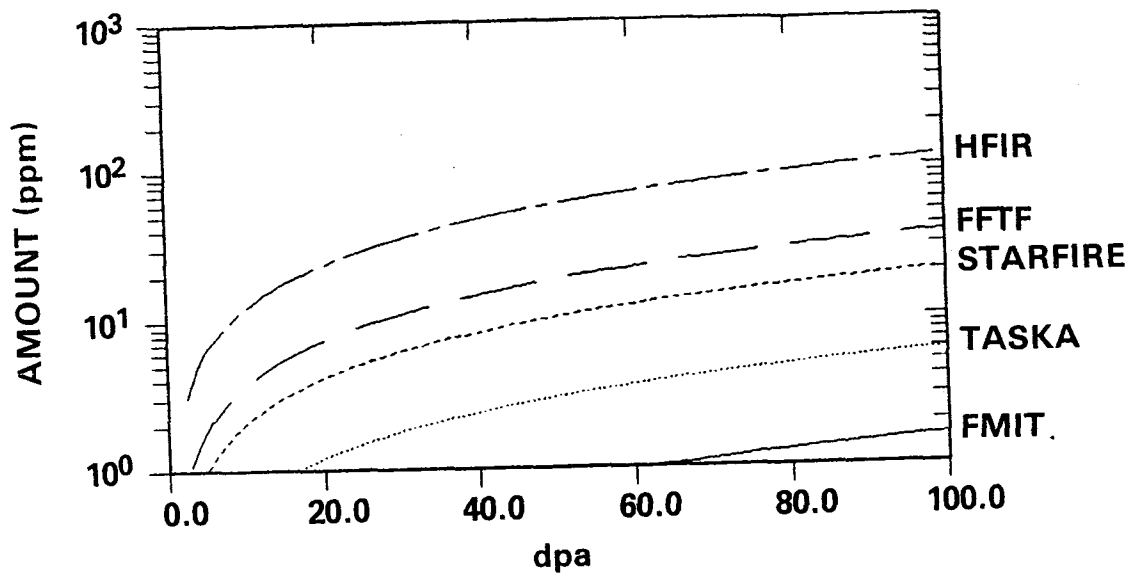
Figure 8-11: FMIT Test Cell Perturbed Flux

response for a fusion reactor first wall spectrum indicates that 40 to 50% of the displacements occur in the 14 MeV peak, and a negligible fraction below 1 MeV. Thus, the increased hardness of the FMIT spectra is, in effect, in the 20 to 30 MeV range. Both modeling and experimenting indicate that no new displacement phenomena appear at these energies (nor in the small tail above 30 MeV). To a first approximation, expressing doses in dpa (both for FMIT and the fusion device) should permit direct application of FMIT data to the fusion device. For some properties, a different defect production cross section than dpa may be more appropriate.

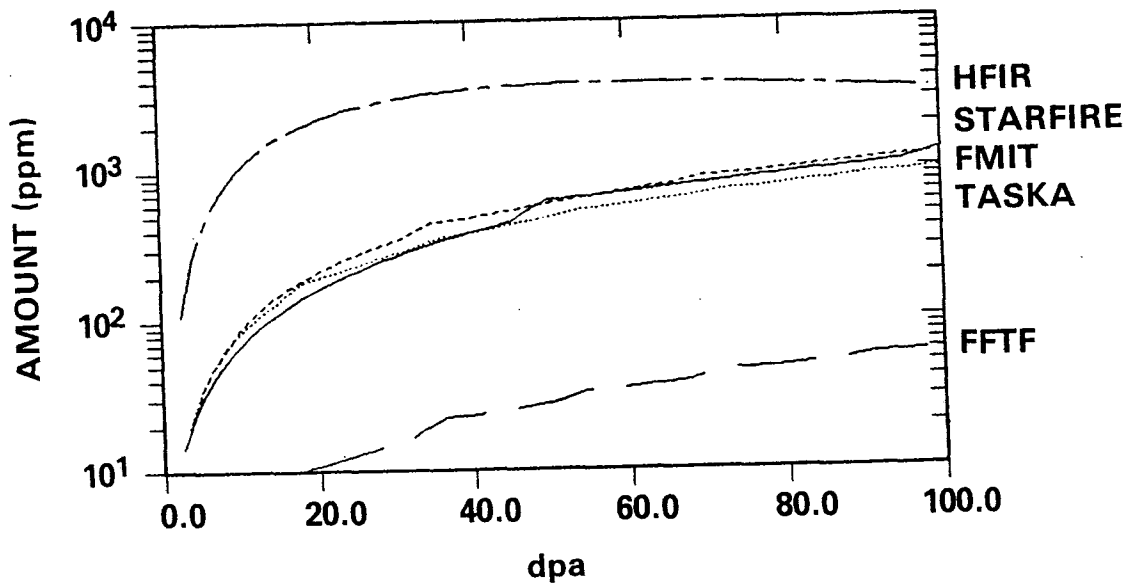
Transmutation rates in FMIT have been calculated for many elements; two typical examples are shown in Figure 8-12⁽¹⁹⁾. FMIT reproduces first wall transmutation rates (per dpa) well for threshold-type reactions, including those producing helium and hydrogen. Rates of nonthreshold-type reactions tend to be quite spectrally dependent, as illustrated in Figure 8-12 by the production of ruthenium from molybdenum contained in the prime candidate alloy (PCA, a modified 316 stainless steel). In this case, the rates in the two fusion reactor concepts differ from one another, as well as from FMIT. No cases have been identified where these differences are important.

Flux profiles unperturbed by the presence of materials are shown in Figure 8-13 compared to the vertical test assemblies used to hold the specimens. The volumes available in FMIT that have minimum (unperturbed) fluxes greater than 10^{15} , 10^{14} , and 10^{13} n/cm²-s are 7.6, 480, and 1.4×10^4 cm³, respectively. The perturbing effect of materials in the test cell increases the volume for fluxes greater than 10^{15} n/cm²-s to about 9 cm³ but has a negligible influence on the other volumes. The maximum flux is about 3×10^{15} n/cm²-s.

Calculations of the damage response and the helium production rate in copper for perturbed spectra indicate that FMIT would have a volume of about 100 cm³ in which both dpa and helium rates will be greater than produced by a wall loading of 1 MW/m² and a volume of about 8 cm³ in which the damage and helium rates will be greater than for a wall loading of 5 MW/m². The calculated ratio of helium/dpa is close to that expected from a fusion device first wall for all materials examined to date.



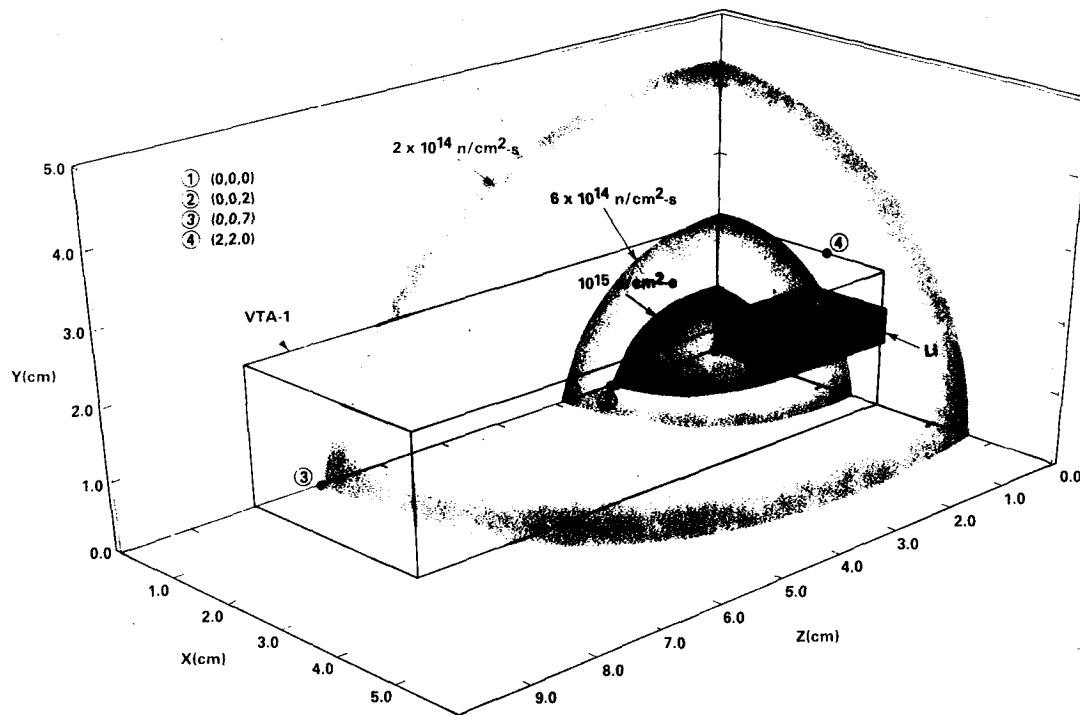
TRANSMUTATIONS IN MFE FACILITIES: RUTHENIUM — PCA



TRANSMUTATIONS IN MFE FACILITIES: VANADIUM — PCA

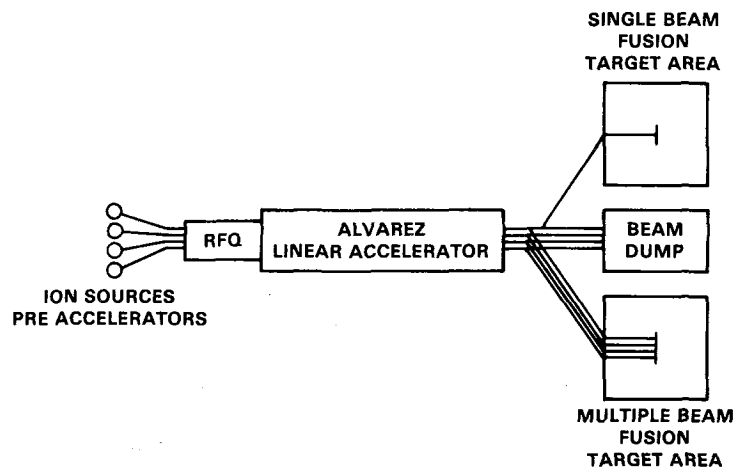
Figure 8-12: Transmutations

HEDL 8511-083.1



HEDL 8201-079.1

Figure 8-13: FMIT Flux Contours



HEDL 8510-156.10

Figure 8-14: Multiple Beam Schematic

HEDL 8511-083.4

8.3.4.3 Availability

The test cell, with dimensions of 2 x 2 x 3 meters, is large enough to accommodate component testing that is compatible with the flux-spectral contours. The availability for irradiations is projected to be about 65% with one test cell as in the current design. With two test cells (an option), the availability is projected to rise to about 85%.

The U.S. DOE/OFE has stated that international cooperation will be required to construct and operate the FMIT facility. Efforts are currently underway to investigate the possibility of such an international agreement.

8.3.5 Multiple Beam Facility

The FMIT facility design, although quite advanced, is limited by the relatively small specimen sizes that could be irradiated in flux levels above 10^{15} n/cm²-s. In order to allow testing of much larger components, an extension of the FMIT concept was proposed^(20,21).

The main technological advance is the use of multiple continuous wave (CW) beams in a common accelerator. A schematic diagram is shown in Figure 8-14. The latest concept has eight separate beam tubes, each with 0.125 amperes of deuterons accelerated to 35 MeV in a CW fashion in a common Alvarez-type linear accelerator. The current of each beam is well within the space charge limit of the FMIT design. However, the total beam of 1.0 amperes far exceeds the limitations of a single beam.

Targets would be flowing lithium as in the FMIT facility but might be larger in order to spread the neutron flux and carry away additional heat.

Fluxes up to a factor of 10 higher than in the FMIT facility could be achieved and volumes a factor of 30 larger could be obtained for the same minimum flux. A comparison of volumes available as a function of the minimum flux is shown in Table 8-5.

Testing of materials would be much like in the FMIT facility. However, large components such as sections of the first wall, shielding, and breeder blanket could be irradiated in nearly prototypic conditions including magnetic fields, high vacuum, and surface heating.

Table 8-5. Volumes Available (cm³) for Testing as a Function of the Minimum Neutron Flux

Minimum Flux (n/cm ² -s)	RTNS-II	FMIT	Multiple Beam
10 ¹⁶	--	--	7.6
10 ¹⁵	--	7.6	4.8 x 10 ²
10 ¹⁴	--	4.8 x 10 ²	1.4 x 10 ⁴
10 ¹³	--	1.4 x 10 ⁴	4.5 x 10 ⁵
10 ¹²	Approx. 8.0	4.5 x 10 ⁵	1.4 x 10 ⁷

Testing capabilities could be varied over a wide range of conditions by changing the experimental arrangement. For example, one could choose to: 1) irradiate miniature specimens simultaneously in two or more FMIT-like target areas in neutron fluxes of about 10¹⁵ n/cm²-s; 2) irradiate miniature specimens in one target area in neutron fluxes of about 10¹⁶ n/cm²-s; 3) uniformly irradiate the front surface of a component of about 30 x 30 cm with a neutron flux of about 10¹⁴ n/cm²-s; 4) irradiate a large volume (12 x 12 x 12 cm³) with a uniform spectrum and flux of neutrons of about 10¹⁵ n/cm²-s; or 5) tailor the spatial distribution of neutron flux and spectra for special cases.

8.4 Conclusion

A significant fraction of fusion technology development testing can be completed in existing nonfusion irradiation facilities. Within the United States and abroad, there exists several fission reactors which are suitable for the irradiation of fusion materials and some components or subcomponents. The primary limitations of these devices are a nonprototypic neutron energy spectrum and limited volume.

It has been shown that, though not prototypic, the fission reactor neutron environment is such that various aspects of the fusion environment can be effectively mimicked. The environment cannot be fully simulated, however; and even though high fluence testing is possible, this cannot be considered as a full substitute for testing in a fusion environment.

Though limited, fission reactor irradiation testing will play a vital role in the development of fusion technology. In particular, much information can be gained relative to the performance of solid breeder systems. Testing in support of other systems is also possible, i.e., high heat flux components,

instrumentation and control, tritium recovery system, special purpose materials, etc.

Accelerator-based sources provide another aspect of irradiation testing capability. It is possible to closely simulate the fusion neutron spectrum with these sources. They are, however, presently limited in both volume and flux. These facilities can provide the correlation between fission reactors and fusion machines but currently can only provide that correlation at a fluence level several orders of magnitude less than required.

Existing facilities can, and have, provided much information relative to neutronics, damage mechanism studies, and performance of low fluence materials and components. To provide the necessary high fluence information for development of materials and components, it will be necessary to construct the Fusion Materials Irradiation Test (FMIT) or a similar facility.

REFERENCES FOR CHAPTER 8

1. R. G. Clemmer, et al., "The TRIO Experiment," ANL 84-55, September 1984.
2. G. E. Hollenberg, "The Effect of Irradiation on Four Solid Breeder Materials," First International Conference on Fusion Reactor Materials, Tokyo, Japan, December 3-6, 1984.
3. M. L. Grossbeck, et al., "Fission Reactor Experiments for Fusion Materials Research," Proceedings of Fast, Thermal, and Fusion Reactor Experiments Conference, April 12-15, 1982.
4. M. A. Abdou, et al., "FINESSE: A Study of the Issues, Experiments, and Facilities for Fusion Nuclear Technology Research and Development (Interim Report)," UCLA-ENG-84-30, October 1984.
5. R. E. Bauer, "Materials Open Test Assembly in the Fast Flux Test Facility," HEDL-SA-2590, April 1982.
6. "Guide for Experimenters, Rotating Target Neutron Source," LLNL-M-094, Rev. 1, Lawrence Livermore National Laboratory, March 1982.
7. H. L. Heinisch, "OWR/RTNS-II Low Exposure Spectral Effects Experiments," Contribution to Quarterly Progress Report for Jan-Mar 1985, Damage Analysis and Fundamental Studies, DOE/ER-0046/21, pgs. 99-101, May 1985.
8. D. W. Kneff, et al., "Characterization of the Be (d,n) Neutron Field by Passive Dosimetry Techniques," Symposium on Neutron Cross Sections from 10 to 50 MeV, Brookhaven National Laboratory, BNL-NCS-51245, Vol. I, pgs. 113-132, May 12-14, 1980.
9. C. A. Coulter, et al., "Calculation of Radiation Damage Effects of 800 MeV Protons in a Thin Copper Target," Journal of Nuclear Materials 67, pgs. 140-154, (1977).
10. D. R. Davidson, et al., "Characterization of the LAMPF Beam Stop Area Radiation Environment," LA-UR-88-33, Los Alamos National Laboratory.
11. M. S. Wechsler and W. F. Sommer, "Spallation Radiation Damage and the Radiation Damage Facility of the LAMPF A-6 Target Station," Journal of Nuclear Materials 122 and 123, pgs. 1078-1084, (1984).
12. D. R. Davidson, et al., "Measured Radiation Environment of the LAMPF Irradiation Facility," LA-UR-84-1050, Revised, Los Alamos National Laboratory.
13. M. S. Wechsler, et al., "Calculation of Displacement and Helium Production of the LAMPF Irradiation Facility," LA-UR-84-1124, Revised, Los Alamos National Laboratory.
14. W. F. Sommer, "Private Communication," Los Alamos National Laboratory.
15. R. J. Burke, J. W. Hagen, and A. L. Trego, "FMIT: An Accelerator-Based Neutron Factory for Fusion Materials Qualification," Proceedings of the

International Ion Engineering Congress, ISIAT '84 and IPAT '83, Kyoto, Japan (Also HEDL-SA-2987, HEDL), September 12-16, 1983.

16. F. M. Mann, F. A. Schmittroth, and L. L. Carter, "Neutrons from $d + Li$ and the FMIT Irradiation Environment," HEDL-TC-1459, HEDL, November 1981.
17. D. L. Johnson, et al., "Thick Target Neutron Yields and Spectra from the $Li(d,xn)$ Reaction at 35 MeV," Brookhaven National Laboratory, BNL-NCS-51245, Vol. I, pgs. 99-109, May 12-14, 1980.
18. D. G. Doran, "Spectral Effects in FMIT," HEDL-TC-7464, HEDL, May 1984.
19. F. M. Mann, "Transmutation of Alloys in MFE Facilities Calculated by REAC (A Computer Code System for Activation and Transmutation)," HEDL-TME-81-37, HEDL, August 1982.
20. R. J. Burke, D. L. Johnson, and L. L. Carter, "Multiple Uses of an Upgraded FMIT Facility," Proceedings of the 1985 Particle Accelerator Conference, Vancouver, Canada (Also HEDL-SA-3266-FP, HEDL), May 13-16, 1985.
21. R. J. Burke, et al., "Super-FMIT, An Accelerator-Based Neutron Source for Fusion Components Irradiation Testing," Nucl. Instr. and Meth., B10/11, pgs. 483-486, (1985).

CHAPTER 9

FUSION TEST FACILITIES

TABLE OF CONTENTS

9. FUSION TEST FACILITIES

	<u>Page</u>
9.1 Introduction.....	9-1
9.2 Test Requirements.....	9-3
9.2.1 Introduction and Engineering Scaling	9-3
9.2.2 Blankets.....	9-4
9.2.3 Non-blanket Components.....	9-21
9.2.4 Summary.....	9-22
9.3 LITE Tokamak (TRW/MIT/U.Texas)	9-25
9.3.1 Concept Description.....	9-26
9.3.2 Representative Design.....	9-31
9.3.3 Development Needs.....	9-35
9.4 Demountable Toroidal Fusion Core (EASI).....	9-37
9.4.1 Concept Description.....	9-37
9.4.2 Representative Designs.....	9-39
9.4.3 Development Needs.....	9-43
9.5 Tokamak Test Facility (PPPL).....	9-44
9.5.1 Concept Description.....	9-44
9.5.2 Representative Design.....	9-44
9.5.3 Development Needs.....	9-45
9.6 Spherical Torus (FEDC).....	9-47
9.6.1 Concept Description.....	9-47
9.6.2 Representative Designs.....	9-52
9.6.3 Development Needs.....	9-52
9.7 Mirrors (LLNL).....	9-55
9.7.1 Concept Description.....	9-55
9.7.2 Representative Designs.....	9-59
9.7.3 Development Needs.....	9-61
9.8 Reverse Field Pinch (LANL/Philips Petroleum).....	9-62
9.8.1 Concept Description.....	9-62
9.8.2 Representative Design.....	9-68
9.8.3 Development Needs.....	9-74

TABLE OF CONTENTS (cont.)

9.9 Comparison of Fusion Test Facilities9-77

 9.9.1 Introduction.....9-77

 9.9.2 Performance.....9-78

 9.9.3 Cost.....9-80

 9.9.4 Risk.....9-84

 9.9.5 Summary.....9-85

9.10 Conclusions.....9-91

References.....9-93

LIST OF FIGURES

<u>Figure</u>	<u>Page</u>
9-1 Heat source effect on the BCSS $\text{Li}_2\text{O}/\text{He}_2/\text{HT-9}$ first wall temperature profile (reactor at 5 MW/m^2 neutron and 1 MW/m^2 surface heat load; scaled test module at 2.5 and 0.1 MW/m^2).....	9-8
9-2 Stress relaxation in BCSS lithium self-cooled tokamak first wall due to irradiation creep.....	9-10
9-3 Variation of key properties with fluence for $\text{Li}_2\text{O}/\text{clad}$ interaction.....	9-11
9-4 Effect of test module size versus reduction in heat load on preserving thermal and pressure stresses in lobed first walls.....	9-13
9-5 Effect of neutron wall load on temperature profile in scaled breeder test modules, for the BCSS $\text{Li}_2\text{O}/\text{He}/\text{HT-9}$ plate breeder.....	9-13
9-6 Effect of fluence gradient on swelling and creep behavior of MARS blanket at two locations along the tube.....	9-14
9-7 Burn and dwell time requirements for preserving the time-averaged temperature profile in the BCSS $\text{Li}_2\text{O}/\text{He}$ plate breeder.....	9-17
9-8 Time-dependence of tritium recovery and inventory in BCSS $\text{LiAlO}_2/\text{H}_2\text{O}/\text{Be}$ blanket.....	9-18
9-9 Magnetic field effects on diffusion-limited corrosion in Li/steel system.....	9-20
9-10 LITE vacuum vessel/TF magnet assembly.....	9-27
9-11 LITE TF coil bunch and turn arrangement.....	9-28
9-12 LITE vacuum vessel/actively cooled first wall.....	9-30
9-13 LITE FERF TF coil cross section.....	9-32
9-14 Cross-sectional view of inductively-driven Demountable Toroidal Fusion Core Tokamak.....	9-38
9-15 Partial elevation view of tokamak test facility.....	9-47
9-16 Magnetic field line contours on the $q = 2$ surfaces of a conventional tokamak and spherical torus. The portion of the field lines in the good-curvature region is dashed.....	9-49
9-17 The dependence of F and θ on q in a spherical torus configuration with $A = 1.6$ and $\kappa = 2$	9-51

LIST OF FIGURES (cont.)

9-18 (a) Elevation view and (b) plan view of an ignition spherical torus with separate first wall arrangement, internal PF coils and demountable TF coil return legs.....9-54

9-19 Cross-section of the Technology Demonstration Facility.....9-56

9-20 Plan view of MFTF- α +T (components rotated into plane).....9-57

9-21 Test module removal by simple linear motion.....9-59

9-22 Magnetic field profiles along the minor radius for the RFP and the tokamak. Solid curves show Bessel Function Model (BFM) profiles and dashed curves show Modified Bessel Function Model (MBFM) profiles.....9-63

9-23 A diagram of $F = B_{\phi}(r_p)/\langle B_{\phi} \rangle$ versus $\theta = B_{\theta}(r_p)/\langle B_{\theta} \rangle$ showing two experimental traces and the tendency for the plasma to seek and reside within the predicted⁽⁴²⁾ RFP minimum-energy state.....9-64

9-24 Scaling of plasma ohmic confinement time, τ_E , and confinement quality, $n\tau_E$, with plasma current.....9-66

9-25 Dependence of plasma current, I_{ϕ} , on plasma radius, r_p , for a range of surface heat fluxes, q_s , neutron wall loadings, q_n , ohmic power into the plasma, $P_{\Omega p}$, and fusion power, P_F . For all cases, the electron drift parameter, $\xi = 0.006$, the transport parameter, $\nu = 1$, and no anomalous ion heating was assumed. A "design triangle" is defined by $q_n \geq 1 \text{ MW/m}^2$, $P_F \geq 100 \text{ MW}$, and $q_s \leq 5 \text{ MW/m}^2$9-69

9-26 Geometry, dimensions, and notations used in preliminary engineering analysis of a RFP fusion facility.....9-70

9-27 Dependence of ohmic power losses in PF coils relative to that in the plasma as a function of the coil thickness, δ_{θ} (normalized by the conducting first wall radius), the blanket thickness Δb , and the aspect ratio A.....9-71

9-28 Lawson diagram showing projected ZT-H performance using Taylor/Connor (TC) and Diamond/An/Carreras (DAC) scaling.⁽³⁵⁾ The positions for the 1 MW/m^2 and 5 MW/m^2 neutron wall load RFP FERF designs are also shown.....9-75

9-29 Direct capital cost of various fusion test facilities relative to the total power transferred (electrical and plasma) and the fusion core size (as represented by the plasma axial length).....9-83

LIST OF TABLES

<u>Table</u>	<u>Page</u>
9-1 Candidate Fusion Engineering Test Facilities and Contributing Organizations.....	9-3
9-2 Device Parameters with Major Influence on Blanket Operation and Testing.....	9-6
9-3 Radiation Tolerance of Instrumentation and Electronics.....	9-23
9-4 Recommended Requirements on Key Parameters of a Fusion Engineering Research Facility.....	9-24
9-5 LITE FERF Nominal Parameter Overview.....	9-34
9-6 Parameters for DTFC Fusion Engineering Research Facilities.....	9-41
9-7 Representative Tokamak Nuclear Technology Test Facility.....	9-46
9-8 Summary Characteristics of Spherical Tori Test Facilities.....	9-53
9-9 Parameters for Representative Mirror Fusion Engineering Research Facilities.....	9-60
9-10 Status of Major RFP Experiments.....	9-67
9-11 Parameters for a RFP Fusion Engineering Research Facility.....	9-72
9-12 Performance Comparison of Fusion Engineering Research Facilities.....	9-79
9-13 Cost Comparison of Fusion Engineering Research Facilities.....	9-81
9-14 Risk Comparison of Fusion Engineering Research Facilities.....	9-86
9-15 Major Risk Factors for FERF Concepts.....	9-87
9-16 Summary Characteristics of Fusion Engineering Research Facilities.....	9-88

9. FUSION TEST FACILITIES

9.1 Introduction

Fusion devices are a special class of fusion technology test facilities. They are particularly useful and unique in that they can provide all fusion environmental conditions simultaneously, provide fusion spectrum neutrons, and may be the most cost-effective large-volume irradiation source.⁽¹⁾ The need for such a test facility has been recognized and reflected in many design studies (e.g., FED,⁽²⁾ MFTF- α +T,⁽³⁾ TDF,⁽⁴⁾ INTOR,⁽⁵⁾ NET,⁽⁶⁾ FER⁽⁷⁾). In some cases, the facility is viewed primarily as a reactor-relevant physics device with additional engineering testing capabilities built-in or as a later upgrade. In others, both technology and physics are comparable goals.

The primary purpose of the fusion devices considered here is to provide testing of the fusion nuclear technologies. This may change the facility characteristics and reduce costs from those usually anticipated for physics experiments. Physics information would of course be obtained, but the design is not constrained by the need to provide such data. For example, operating in a driven mode may be acceptable (perhaps preferred) for a technology facility, while ignition is a key goal of physics experiments. It is also possible for the technology test facility to be based on a different device concept than that of a reactor, although reactor (particularly tokamak) relevance is still desirable. These technology-oriented devices are generically referred to here as Fusion Engineering Research Facilities (FERFs). The concepts considered in this chapter could provide substantial physics information, but are referred to here as FERFs since it is their technology testing features that are of primary interest.

Although separating the technology and physics testing goals may reduce the cost of the individual facilities, providing a reactor nuclear environment would still be very expensive (hundreds of millions of dollars). The first section in this chapter analyzes the behavior of the nuclear technologies to determine the minimum useful requirements for a fusion test facility.

In subsequent sections, potential fusion test facilities are described that could plausibly address the nuclear technology test requirements by or around the year 2000. In particular, tokamaks, mirrors and reverse field

pinches (RFP) are major distinct device classes with a reasonable existing data base. However, within each of these device classes, there is a range of alternative approaches that depart from the conventional form and could improve the overall concept as a test facility.

For example, conventional tokamaks have moderate aspect ratios ($A \sim 3-4$) with D-shaped plasma cross-sections, such as INTOR. This tokamak is based on relatively conventional physics that has been or is being demonstrated. However, ignition is a primary physics goal, which leads to a large and high power device (600 MWth) because of the desire for relatively conventional but reactor-relevant magnets (moderate-field superconductors). Such a device would provide an excellent opportunity to test many features of fusion device operation, including blanket operation and electricity production. It also leads to high costs and potentially high technology risk due to the new and largely untested nuclear operating conditions.

Several approaches have been suggested to improve tokamak operation. Many physics improvements try to use the magnetic field more efficiently (i.e., higher beta) by altering the plasma configuration, including 'bean' cross-sections, vertical elongation (belt-pinch), very small aspect ratio and very high aspect ratio configurations. The first three changes permit moderate to large increases in plasma current compared with conventional configurations, which leads to improved energy confinement and beta limits according to current scaling laws. The bean and high aspect ratio plasma configurations are based on the possibility of a stable high-beta operating regime that may be accessed more readily by these configurations.⁽⁸⁾

Engineering improvements include pushing the magnet coil design. High-field copper coils allow higher beta and improved energy confinement with well-understood conventional tokamak physics. Demountable core designs could make the high technology risk sections of the device more replaceable. Reducing the inboard hardware to the bare minimum allows very small aspect ratios. Some small aspect ratio devices such as spherical tori depart from the conventional definition of tokamaks, and are treated separately here.

For mirrors, the confinement properties of simple axisymmetric mirror cells are well-understood. The alternatives largely refer to the treatment of the ends. Options for a test facility range from simple mirrors to complex end plugs with octupole magnets and thermal barriers. RFP physics is less

well-understood than either tokamaks or mirrors, and only the classical configuration has been examined in any detail.

In this study, several of these concepts were explored to determine their suitability as a fusion engineering research facility. Organizations familiar with the individual concepts (Table 9-1) were provided minimum device parameters (Section 9.2) and asked to generate devices that met or exceeded these requirements. Their results are summarized here on a comparative basis. It should be noted that the designs are not necessarily consistent in terms of physics, engineering and costing assumptions.

Table 9-1. Candidate Fusion Engineering Test Facilities and Contributing Organizations

Device	Example	Lead Organization(s)
Tokamak		
Moderate-field SC magnets, standard physics	INTOR	--
High-field Cu magnets, standard physics	LITE FERF	TRW/MIT/U. Texas
High-field Cu magnets, demountable core	IDT-DTFC	EASI
Moderate-field Cu magnets, 'bean' plasma	"BEAN" FERF	PPPL
Spherical Torus	ST FERF	FEDC
Tandem Mirror	TDF, MFTF- α +T	LLNL
Reverse field pinch (RFP)	RFP FERF	LANL/Philips Petroleum

9.2 Test Requirements

9.2.1 Introduction and Engineering Scaling

Resolution of the fusion technology issues requires a range of experiments from property measurements and phenomenological tests, to complex interactive and integrated tests. The simpler experiments, described in earlier chapters, require only a limited set of environmental conditions to reproduce the behavior of an operating component.

The integrated tests address the issues of interactions among effects and among physical regions, including identifying unexpected interactions or their absence, quantifying complex phenomena that must be correlated in a global sense, and verifying performance predictions. These tests can establish the basic feasibility of the design concept ("proof-of-principle"), identify failure modes, and provide operational information such as instrumentation and control needs.

Ideally, such experiments should be conducted under fusion reactor operating conditions. Otherwise there may still be unanticipated effects or failure modes when the component is placed into commercial operation. However, it is almost certain that the test device parameters (e.g., neutron wall load) will not match those of a fusion reactor because of cost constraints. Thus, these experiments raise the question of how close the test device needs to reproduce reactor parameters. For example, can testing a breeder module at a power density of 10 MW/m^3 be made to provide a reasonable simulation of reactor operation at 60 MW/m^3 ?

It is possible in many cases for which the phenomena are sufficiently well understood to modify the design (e.g., coolant flow rate) of the test module in order to recover the important aspects of the testing issues, even though the test device parameters are not the same as the commercial reactor. This process is known as engineering scaling. However, a change of device parameters beyond certain limits often results in the inability to maintain "act-alike" behavior. One of the goals of engineering scaling is to identify and determine these limits or test requirements.

This procedure is often difficult because behavior usually varies continuously as a function of the device parameters, without an abrupt change in performance. Thus, there are degrees of simulation that can be considered. The simplest requirement is to maintain the same operating regime (e.g., $Re > 2000$ for turbulent flow). The second is to maintain partial behavior (e.g., beginning-of-life stresses, but not end-of-life). Finally, for particular phenomena, it is necessary to closely duplicate the full behavior.

9.2.2 Blankets

In order to understand and quantify the scaling behavior and test requirements, analyses of blanket operation were performed, including thermal-

hydraulics, structural mechanics, tritium recovery, neutronics and corrosion.⁽¹⁾ It was not possible to treat all known issues and interactions due to resource and data limitations, nor was it possible to determine the requirements for retaining all the unexpected interactions (other than requiring operation in a fusion reactor). Instead, a limited number of specific but important issues were considered - particularly those known to be interactive or complex. If at least these effects are preserved, then their interactions should also reasonably be present. The results thus identify a minimum bound on the test requirements.

For the analyses, four specific reference blankets were chosen: the Blanket Comparison and Selection Study⁽⁹⁾ self-cooled Li/V toroidal/poloidal flow tokamak blanket, the He/Li₂O/HT-9 and H₂O/LiAlO₂/PCA solid breeder designs, and the MARS⁽¹⁰⁾ self-cooled LiPb/HT-9 mirror blanket. These blankets serve as tools to identify and quantify the problems of scaling plausible blankets, and are not necessarily the best designs for all possible reactor concepts. They cover a range of design features of general interest such as liquid versus solid breeder and, consequently, their consideration should lead to conclusions that are applicable to a large class of candidate blankets. In addition, the reactor operating conditions were assumed to correspond to a 5 MW/m² neutron wall load.

The most critical integrated testing issues for blankets are thermo-mechanical performance and failure modes, tritium inventory and recovery (especially in solid breeder blankets), and materials compatibility (especially in liquid metal blankets). The device parameters expected to have the largest effect on these issues are summarized in Table 9-2.

The uncertainties in thermomechanical performance and failure modes relate to both the complex thermal and structural loading conditions and response. While the structural behavior is clearly dependent on thermal conditions (e.g., thermal stresses, temperature dependent creep response), the thermal behavior can also be influenced by the structure (e.g., temperature profile in solid breeder changing due to cracking of breeder under stresses). Consequently it is important to preserve both thermal and structural behavior in an integrated test.

Table 9-2. Device Parameters with Major Influence on Blanket Operation and Testing

Heat Source

Surface
Nuclear (power density)

Neutron Radiation

Fluence
Flux
Spectrum

Geometry

Test port surface area and depth
Total test surface area
Test device geometry

Operating Time

Burn/dwell time
Continuous operating time
Availability

Magnetic Field

Strength
Geometry

The basic processes describing tritium inventory, recovery and permeation from solid breeders are also uncertain. These processes are very dependent on temperature, chemistry and breeder microstructure, and consequently on any interaction that affects these. Neutron radiation is anticipated to have a strong influence on all the factors. For example, swelling may cause cracking and increase the breeder temperature; burnup changes the local stoichiometry; and sintering changes the amount of porosity. Tritium recovery and permeation in self-cooled liquid metal designs are not a major blanket issue, although a tritium extraction process needs to be developed and tested.

Materials interactions depend on the chemical environment and the transport processes. The primary chemistry factors are the temperature and the basic materials. An important requirement for integrated testing is that it should reproduce impurity types and levels, which may dominate the compatibility behavior at long times. Transport processes additionally depend on

flow conditions, geometry, magnetic field and possibly temperature or concentration gradients. Nuclear radiation affects both transport (e.g., producing trap sites which slow down diffusion) and chemistry (e.g., transmutation).

Key scaling considerations for these critical issues are discussed below, according to the device parameters in Table 9-2. Quantitative test requirements are evaluated with respect to reference reactor conditions of 5 MW/m^2 neutron wall load, $15\text{-}20 \text{ MW-yr/m}^2$ blanket lifetime, long-pulse or steady-state, and 7 T magnetic field. More details are given in Ref. 1.

Heat Source

A primary device parameter is the heat source since this is the main energy input which activates most processes and interactions. A primary test requirement is to preserve the blanket temperature profiles. This is important for maintaining thermal stresses, material strength, structural response to radiation damage, transport processes and local thermochemistry.

The thermal field depends on the profile and magnitude of the heat sources. If the heating profile changes significantly (e.g., a very small plasma relative to the test module), it is difficult to retain more than local or average temperatures. If the module heat source is reduced, it is often possible to adjust dimensions and coolant flow conditions to compensate and so preserve the shape and magnitude of the temperature profile (but not the temperature gradient).

However, there are limits to even this temperature control. For example, the temperature profile along the perimeter of lobed first walls, common in high coolant pressure solid breeder blankets, has a different dependence on the surface and volumetric heating. Consequently, it is not possible to arbitrarily change the heat source and still be able to compensate by changing dimensions and coolant flow rate (Fig. 9-1). In particular, both surface and volumetric heating should be changed such that their relative contribution to the first wall temperature rise is maintained. This leads to a minimum surface heat flux requirement for testing first walls of about 0.2 MW/m^2 at 1 MW/m^2 neutron wall load relative to reactor conditions of 1 MW/m^2 surface and 5 MW/m^2 neutron heat load.

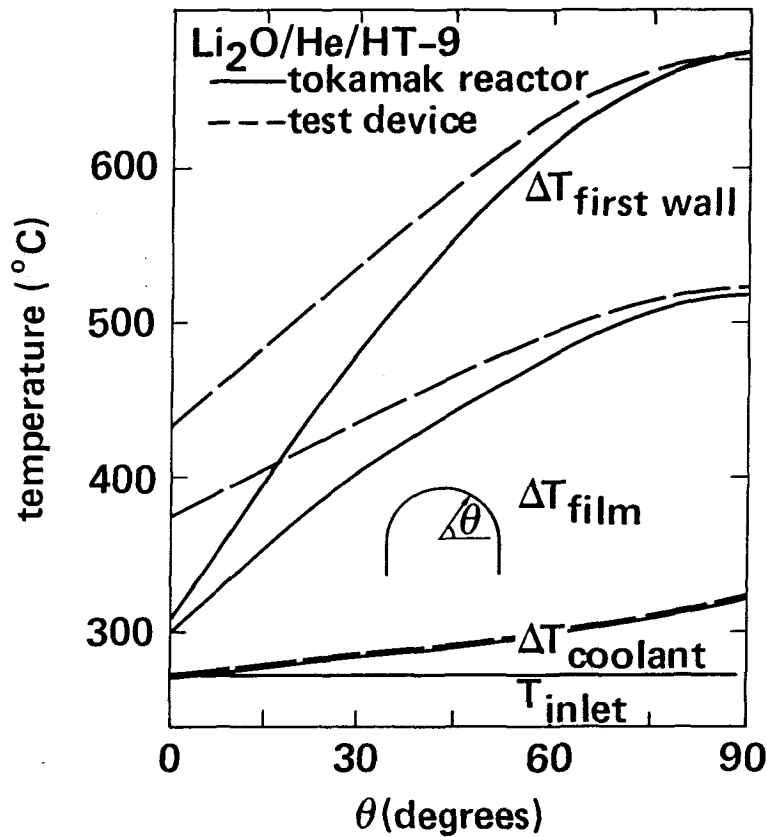


Figure 9-1. Heat source effect on the BCSS Li₂O/He/HT-9 first wall temperature profile (reactor at 5 MW/m² neutron and 1 MW/m² surface heat load; scaled test module at 2.5 and 0.1 MW/m²).

Within the solid breeder region, the temperature profile can be maintained at reasonably reduced power densities. However, as the dimensions increase to accommodate low heating rates, axial conduction and azimuthal asymmetries around coolant channels will become more significant, while the temperature gradient (and associated pore migration or segregation processes) will decrease; leading to a lower limit on the heat source of about 1 MW/m².

A possibility for enhancing nuclear heating in solid breeder blankets at low neutron wall loads is to add uranium. Calculations⁽¹¹⁾ indicate that about 1% uranium is required in order to boost the power density from 1 MW/m² effective neutron wall load to the reference 5 MW/m². This amount of material is likely to affect the tritium behavior of the breeder, if not materials compatibility.

Within liquid metal blankets like the BCSS toroidal/poloidal flow concept, it should be possible to preserve the first wall temperature differences without any nuclear heating if there is sufficient surface heating and coolant temperature control. However, uncertainties in liquid metal behavior may require appreciable bulk heating, at least in a thermal-hydraulic experiment. For other liquid metal designs such as the MARS mirror blanket, bulk heating is more important for two reasons: first, surface heating is a much less significant in mirrors (0.1 MW/m^2 rather than 1 MW/m^2); and second, the level of coolant temperature control available in the toroidal/poloidal flow design is not present in the MARS poloidal tube.

In general, a factor of more than five variation in power density or heat flux appears to lead to significant and non-compensatable changes in the temperature profile.

Neutron Radiation

Neutron radiation is both an energy source and a mechanism for change in properties and behavior. The effects of nuclear radiation include property changes, creep, swelling, sintering, transmutation and transport effects. These effects are primarily a function of the accumulated dose, and are not easily scaled to lower fluences. Test requirements can be identified based on achieving fluences where significant changes in behavior occur or saturate.

In general, the uncertainties in key properties associated with the strength and fracture behavior of the structural materials are significantly reduced after neutron testing to $1\text{-}3 \text{ MW-yr/m}^2$ (about $10\text{-}30 \text{ dpa}$).

Irradiation creep has a strong impact on the middle-of-life structural response. First wall studies including irradiation creep indicate that, as shown in Fig. 9-2, irradiation creep changes the HT-9 stresses over about $5\text{-}10 \text{ dpa}$ or $0.5\text{-}1 \text{ MW-yr/m}^2$.

Structural materials typically exhibit an incubation period of low (or zero) swelling, then change to the "breakaway" swelling regime. Based upon very limited data and theoretical considerations, it is anticipated that the incubation fluence will be $5\text{-}8 \text{ MW-yr/m}^2$ for PCA, and over 10 MW-yr/m^2 for HT-9 and V-15Cr-5Ti. Consequently, if the blanket goal fluence is $< 10 \text{ MW-yr/m}^2$, then the "breakaway" swelling behavior of HT-9 and V-15Cr-5Ti is not an

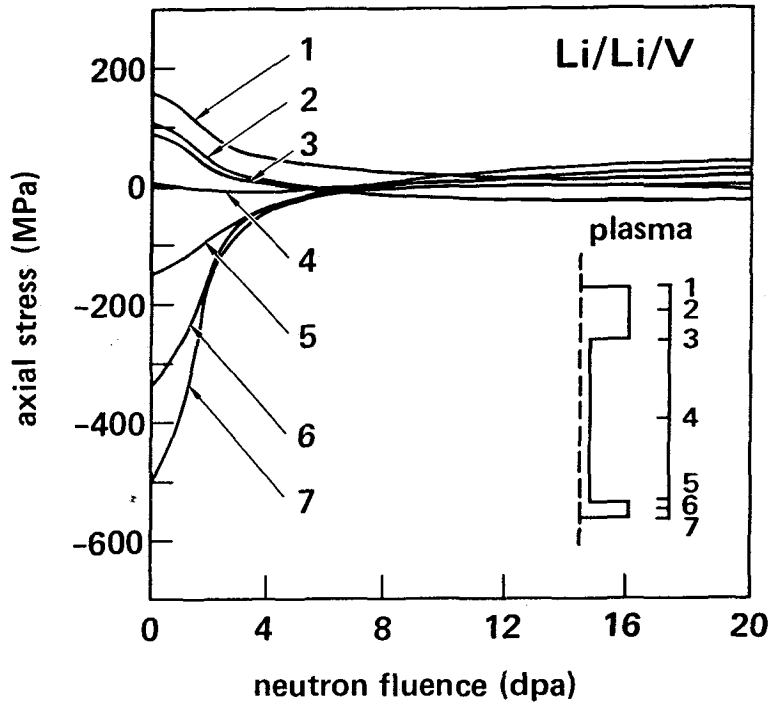


Figure 9-2. Stress relaxation in BCSS lithium self-cooled tokamak first wall due to irradiation creep.

issue. If the goal fluence is 20 MW-yr/m^2 , then the projected uncertainties for swelling and related structural behavior will remain large until measurements are performed $2\text{--}4 \text{ MW-yr/m}^2$ beyond the onset of swelling.

The solid breeder/clad interaction is another structural behavior where fluence is important. For example, the changes in several key properties with neutron exposure are given in Fig. 9-3 for the BCSS $\text{Li}_2\text{O}/\text{He}/\text{HT-9}$ blanket. Thermal expansion and cracking/redistribution of the Li_2O acts primarily in the early operation of the component ($0\text{--}0.2 \text{ MW-yr/m}^2$). After about 2 MW-yr/m^2 , most of the strength and fracture property changes have saturated, and the major properties responsible for the interaction are the balance between Li_2O swelling and the creep of Li_2O and HT-9 (not shown in the figure), until HT-9 swelling becomes important above 10 MW-yr/m^2 .

For structural materials and coolants, no significant overall transmutation is expected over the blanket lifetime. For solid breeder and multi

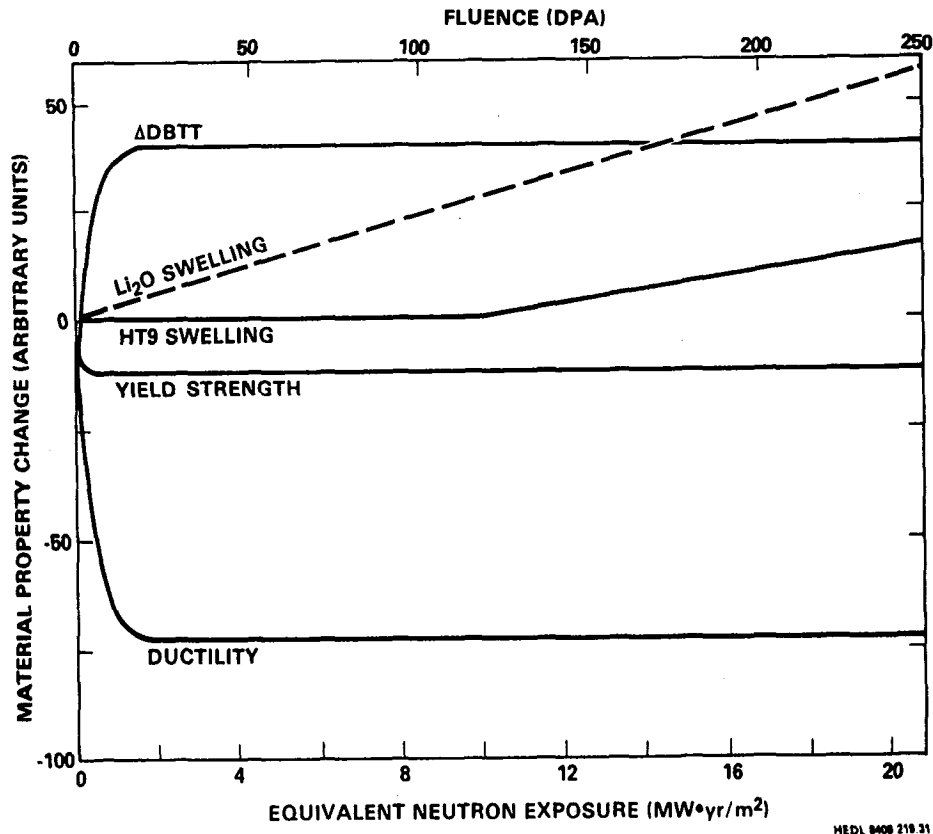


Figure 9-3. Variation of key properties with fluence for $\text{Li}_2\text{O}/\text{clad}$ interaction.

plier, however, typical end-of-life burnups are 5-10% for natural Li_2O blankets, and up to 100% (peak local burnup) in heavily multiplied blankets. For 10% burnup to establish effects due to appreciable transmutation, then solid breeder blankets should be irradiated to 1-5 $\text{MW}\cdot\text{yr}/\text{m}^2$.

In summary, fluence-related effects are not scalable but regimes can be identified where effects are expected to saturate or activate. As a minimum (and recognizing the desirability and cost of achieving high fluence), a variety of new and interactive fluence-related behaviors are expected to be observed at a fluence of 1-3 $\text{MW}\cdot\text{yr}/\text{m}^2$.

Geometry

Geometry is both a test device parameter (e.g., test volume), a way to "scale" the test module (e.g., increasing thickness to preserve temperature profile at reduced heating), and a prime factor in blanket behavior.

Structural behavior has been shown⁽¹⁾ by theory (for elastic stresses) and by example (for radiation effects) that, for the same loading conditions (temperature profile, pressure stresses, fluence profile), the structural response is similar if geometric aspect ratios are preserved. Note that cycling effects were not considered.

For solid breeder blankets, where the coolant heat transfer and pressure drop characteristics are reasonably well known, it is possible to consider scaled structural response at substantially different heating rates by increasing the member dimensions as the heat source is reduced, and correspondingly altering the coolant flow rate. For example, consider a lobed first wall under a reduced heat load. If the module first wall width is increased in proportion to the first wall thickness increase needed to maintain the temperature profile (so preserving geometric ratios), then the elastic stresses are preserved (Fig. 9-4). However, if there is limited test volume available, then it may not be possible to make the first wall as wide as desired, leading to appreciable changes in the stress profile.

Even when there is space available, increasing dimensions may alter the heat conduction paths. Figure 9-5 shows the temperature profile achievable in a solid breeder plate from the BCSS Li₂O/He blanket. At lower wall loads, the plate dimensions and coolant conditions have been changed to preserve the temperature as close as possible. However, the increased front-to-back conduction substantially reduces the peak temperature rise at the front of the blanket and affects the temperature simulation. It can also be noted that the coolant conditions may eventually change regimes from turbulent to laminar flow. In this example, 1 MW/m² is a reasonable lower limit on the test device neutron wall load.

Preserving the structural response to radiation damage depends on maintaining the temperatures, elastic loading, fluence and fluence profiles. The radiation damage profiles are difficult to scale because the neutron mean free path is relatively independent of geometry. Thus, a consequence of increasing first wall dimensions (to preserve temperature profiles at reduced power, for example) is that neutron attenuation eventually becomes significant and leads to an appreciable variation in flux, and consequently creep and swelling rate, across the first wall. For example, an increase in thickness

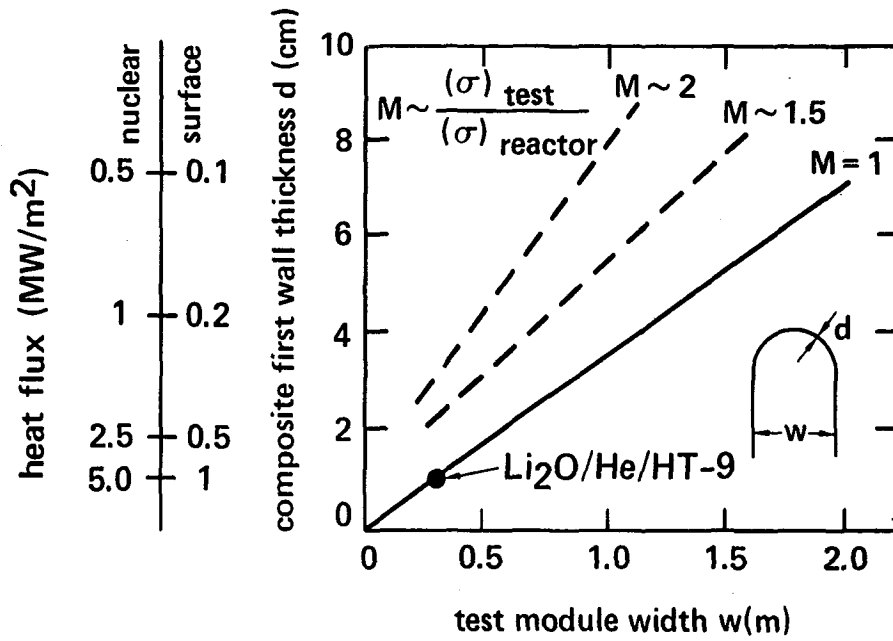


Figure 9-4. Effect of test module size versus reduction in heat load on preserving thermal and pressure stresses in lobed first walls.

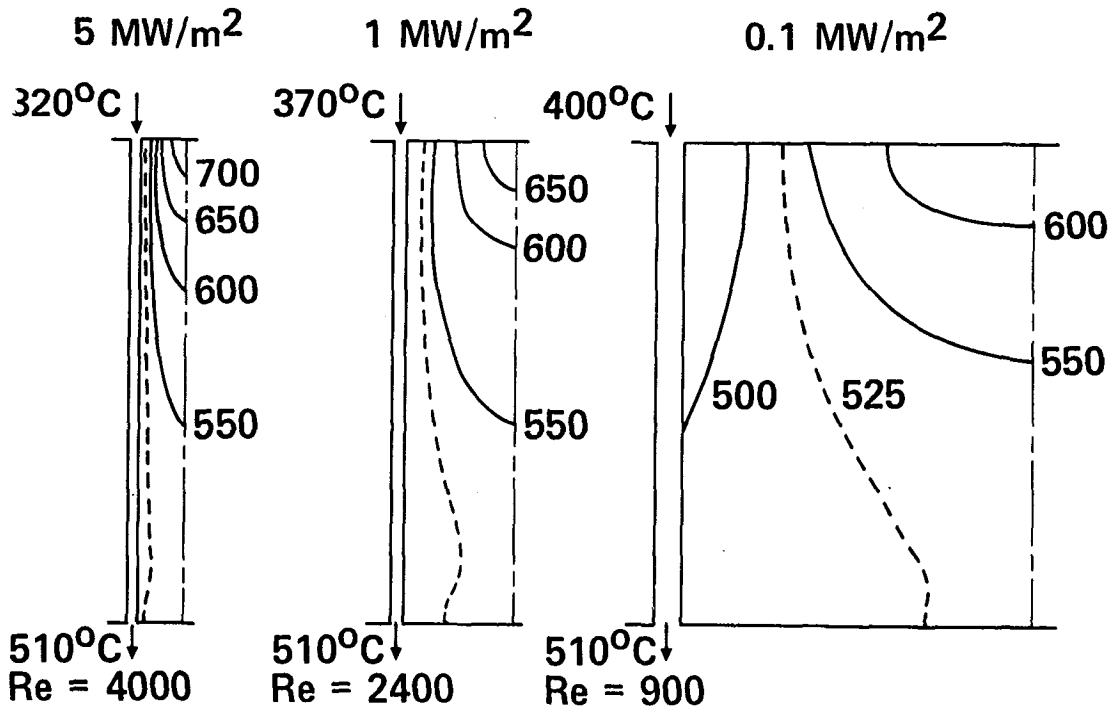


Figure 9-5. Effect of neutron wall load on temperature profile in scaled breeder test modules, for the BCSS $\text{Li}_2\text{O}/\text{He}/\text{HT-9}$ plate breeder.

by a factor of four (roughly a factor of five reduction in heat source for a tokamak first wall) leads to a factor of two variation in flux or fluence across a 1 cm composite first wall. The impact of altered fluence profiles on testing is illustrated in Fig. 9-6, which compares the MARS blanket response due to irradiation swelling with the response of a smaller test module that has the same initial stresses. The responses are quite different.

Geometry also influences thermal-hydraulic behavior, particularly in liquid metal blankets where the velocity profiles may depend not only on the immediate channel dimensions, but also on the channel wall thickness and the structure outside the channel. Thus, changing dimensions may be a less desirable scaling option.

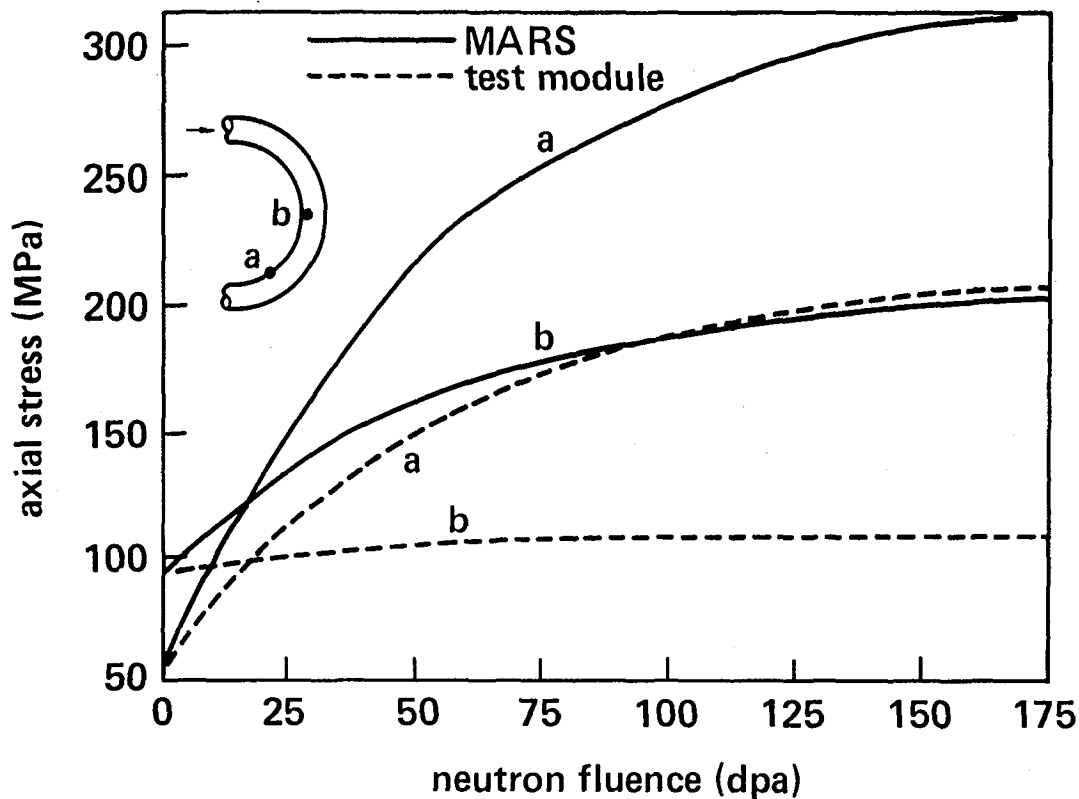


Figure 9-6. Effect of fluence gradient on swelling and creep behavior of MARS blanket at two locations along the tube.

Liquid metal flow in magnetic fields can have extremely long entry lengths - the entire blanket may be in a state of development in which heat, mass and momentum transfer coefficients are rapidly varying. (Note that it is precisely this simultaneous variation in many phenomena that is desired in integrated testing.) As a result, shortened channels may not be able to simulate the entire thermomechanical state of the blanket. Reducing the flow velocity (i.e., preserving the fluid residence time) or the channel dimensions may help to recover the entire development region for some of the important transport processes.

As another example, diffusion-limited mass transfer in liquid metal systems (i.e., at low flow rates or magnetic field strength) depends heavily on the solubility of the corrosion products, which is a very temperature-dependent property. Changes in the average temperature as well as the temperature rise along the coolant channels will affect corrosion. In order to observe the effects of changing boundary conditions beyond the channel entrance, a minimum channel length is necessary. It has been shown that, by reducing the coolant velocity in proportion to the decrease in channel length (again preserving the fluid residence time), the same dissolution rate profiles can be obtained.

Finally, consider how much space must be provided for each test module. Full blankets range from $0.3 \times 2 \text{ m}^2$ for some solid breeder designs, to $9 \times 3 \text{ m}^2$ sector-sized liquid metal blankets. If a representative subsection can be identified, then this would reduce the needed test volume. Maintaining structural and thermal-hydraulic boundary conditions is a key concern.

In an integrated test, it is important to preserve the multiple channel nature of most blankets to allow for possible interactions such as flow oscillations. At least three channels are needed to allow the center one to have representative boundary conditions, and about ten channels can be shown to have flow redistribution characteristics similar to a much larger number of channels. These considerations, plus the expanded dimensions usually needed to preserve temperatures at reduced heating rates, suggest test modules of at least 0.5 m^2 surface area. If global eddy currents strongly affect the velocity profiles in a liquid metal blanket, then modelling of the entire blanket may be required.

The depth should be sufficient to include first wall, multiplier (if any) and breeder zones, plus space for coolant manifolds. It is also desirable to have enough depth for appreciable variation in neutron flux and fluence. A 14 MeV neutron mean free path is about 10-15 cm.

The influence of test device geometry is not large for most tests, as long as the first wall radius is not smaller than the dimensions of the module first wall - in which case differences in the nuclear and surface heating profiles along the first wall, relative to the reactor, will occur.

In summary, test volume limitations suggest that the test module geometry be scaled to smaller sizes or be based on subsections of the full blanket module. However, the desire to reduce the neutron wall load leads to scaling requirements that generally seek to preserve or increase the dimensions. Thus it is not possible to significantly alter the overall dimensions, leading to test volume requirements of about 1 m² surface area by 0.8 m deep.

Operating Time

Ideally, tests should be operated under steady-state or long pulse conditions as in the reference reactor. Cycling is generally undesirable since it introduces uncertainties in interpreting experimental results and can activate processes that are not normally significant such as fatigue, crack growth or thermal ratchetting.

While long pulses may be difficult to achieve in a test device, each pulse should at least extend beyond any significant startup transients and allow the phenomena of interest to reach measurably towards equilibrium. In practice, this might be achieved by a single long burn or a series of pulses maintaining quasi-equilibrium conditions for the needed cumulative operating time. There are several time constants that must be considered: flow, thermal, tritium transport, corrosion and structural.

Flow time constants are typically 1-30 s; 1 s for solid breeder coolant, 6 s for solid breeder purge, and 30 s for liquid metal coolants. These residence times are usually preserved or increased in test modules designed to retain corrosion behavior, entry length effects, or overall temperature profiles under reduced test module size and heating.

Thermal time constants are on the order of 1 minute for most blankets (full size), except for some solid breeder designs (e.g., BCSS $\text{LiAlO}_2/\text{H}_2\text{O}/\text{Be}$) where the rearmost breeder unit cells may require close to an hour to reach thermal equilibrium. Any change in dimensions in a scaled test module will correspondingly change the thermal response time.

Pulsing is of particular concern for solid breeder blankets since it may alter the temperature profile, which in turn will strongly affect the tritium behavior. For the BCSS $\text{Li}_2\text{O}/\text{He}$ plate breeder, the resulting burn and dwell time requirements are shown in Fig. 9-7 as a function of neutron wall load. This curve is based on requiring at least three thermal time constants during the burn, and at most one thermal time constant during the dwell period, which calculations show is needed in order to preserve a quasi-steady temperature field similar to the steady-state reactor case.

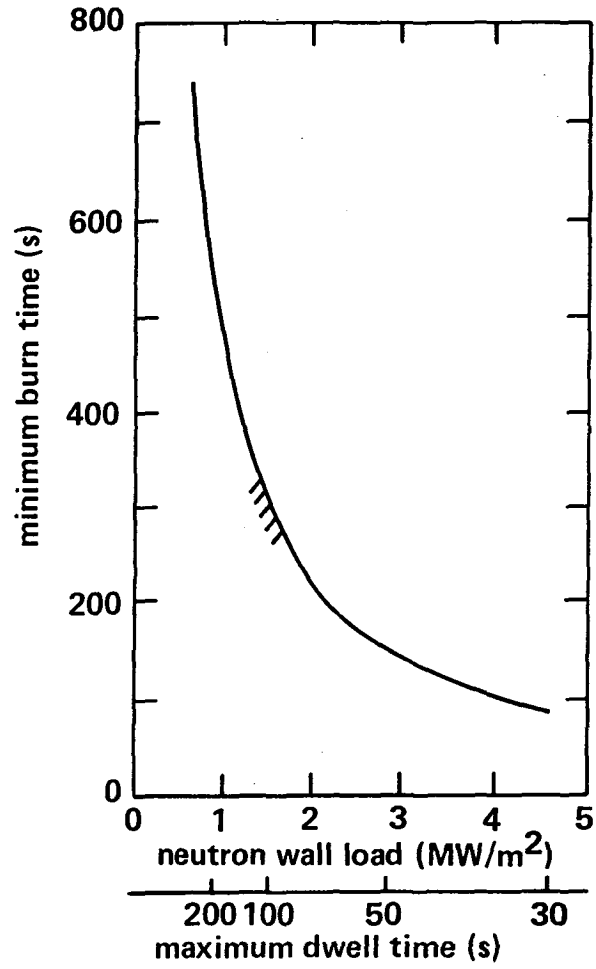


Figure 9-7. Burn and dwell time requirements for preserving the time-averaged temperature profile in the BCSS $\text{Li}_2\text{O}/\text{He}$ plate breeder.

The verification of tritium behavior is accomplished by monitoring the tritium release rate and final inventory. Generally, 67% of the equilibrium release rate occurs early in the test and can be accurately measured, but 99% recovery or inventory requires substantial operating times (Fig. 9-8).

Present calculations assuming hydrogen addition into the purge stream indicate that intragranular diffusion is the largest contributor to the total inventory. Consequently, the Li_2O and LiAlO_2 designs will probably achieve 67% of the equilibrium release rate within about one minute, independent of the neutron wall load. In order to reach inventory equilibrium, however, total operating times of minutes, days and months are needed for Li_2O , hot LiAlO_2 (over 510°C), and cold LiAlO_2 (over 350°C) breeder designs, respectively. Other processes have time scales on the order of a day (solubility, surface adsorption) or months (fluence effects), which will increase as the neutron flux and tritium generation rate decrease.

Corrosion tests typically run for 1000-10000 hours. It is desirable to achieve similar exposures in an integrated test. The influence of pulsing on such experiments was not studied.

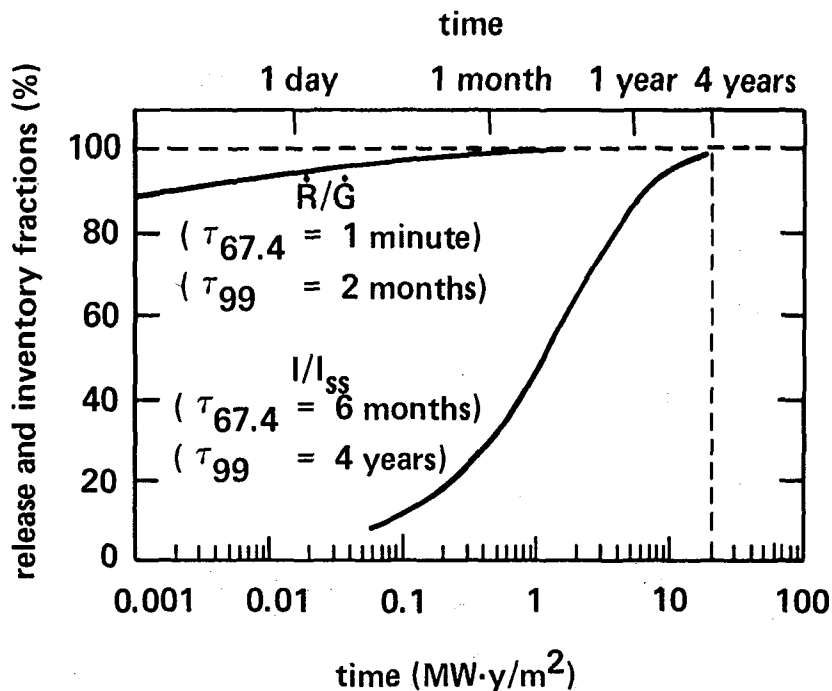


Figure 9-8. Time-dependence of tritium recovery and inventory in BCSS $\text{LiAlO}_2/\text{H}_2\text{O}/\text{Be}$ blanket.

Structural response is rapid for elastic stresses and strain, but long-term for creep, sintering, swelling and irradiation-related changes. For example, a 10 dpa goal (e.g., HT-9 irradiation creep relaxation) takes 1500 hours at 5 MW/m².

In summary, a 500 s burn and 150 s dwell at 1 MW/m² (less at higher wall loads) maintains a reasonable temperature profile in many solid breeder blankets. Liquid metal blankets have generally faster time constants and are not as sensitive. In quasi-steady operation, each test run should ideally be long enough to attain tritium, structural and corrosion equilibrium. Since these can range from minutes to years, it is difficult to specify a minimum continuous operating time. However, a run length of about 4 days (100 hours) should approach equilibrium, or at least measurable effects, for many time-dependent phenomena within 10-100 test runs.

Finally, consider the overall machine availability. Although not formally required by any particular issue, it should be as large as practical in obtain test results in a timely manner. If the test device must provide 1 MW-yr/m² within 5 calendar years or 0.2 MW-yr/m² each calendar year, then the availability (including duty cycle if pulsed) should be at least 20% at 1 MW/m² neutron wall load.

Magnetic Field

The primary effect of a magnetic field is on the MHD behavior of flowing liquid metals. The actual velocity profiles are not well known and depend on the specific design features. Thus it is somewhat arbitrary to separate magnetic field requirements from geometry since the scaling of MHD flow can be characterized by dimensionless quantities (e.g., Hartmann number, $Ha = aB\sqrt{\sigma/\mu}$) combining field intensity, dimensions and fluid properties. On the basis of presently understood scaling, magnetic field strengths under 1 T could still duplicate the MHD-dominated thermal-hydraulic behavior of present blankets. Only at much lower fields do other factors like wall friction or natural circulation affect the flow behavior.

The magnetic field has at least two effects on corrosion: laminarization of the flow resulting in a decrease in cross-flow transport compared to turbulent flow, and thinning of the boundary layer (in Hartmann or certain streaming flows) which enhances corrosion by increasing the velocity near the

wall. In Fig. 9-9, the corrosion rate in Li/steel is plotted as a function of the Hartmann number using two different assumptions for the mass diffusion coefficient.

A minimal test goal would be for a Hartmann number of 500-1000, enough to establish the test module beyond the low Hartmann flow corrosion regime. This could be obtained by increasing dimensions at lower fields, or by limiting the field to above about 0.2-0.5 T in a full-sized blanket section.

However, while this is an important device parameter for controlling blanket behavior, it is also likely to be near design values (2-3 T versus 5-7 T) in any plausible fusion test device. Consequently, the more important question is whether the magnetic field geometry is similar enough.

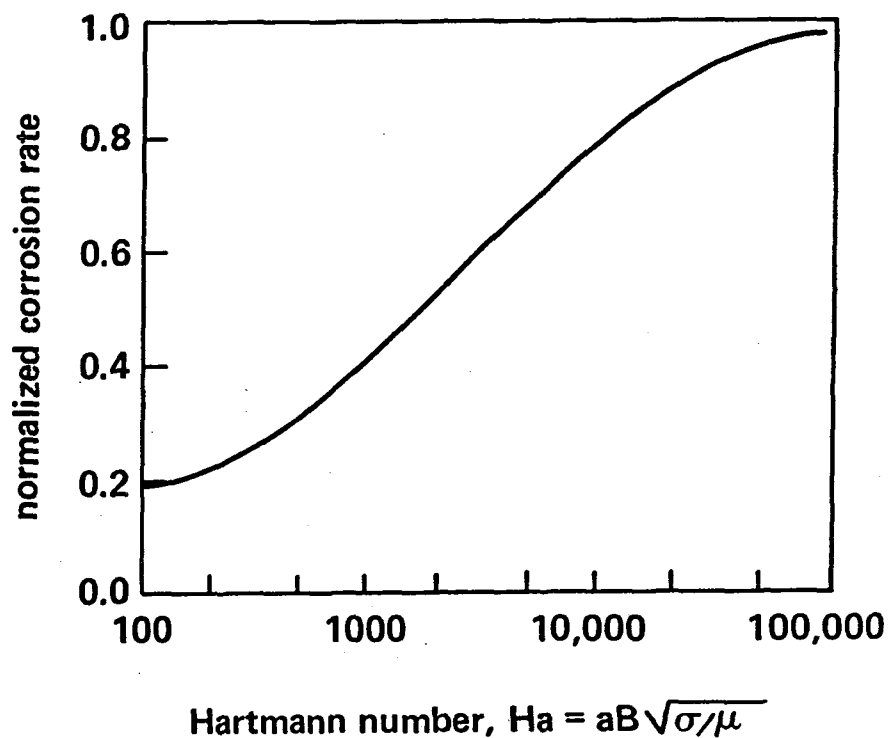


Figure 9-9. Magnetic field effects on diffusion-limited corrosion in Li/steel system.

9.2.3 Non-blanket Components

A fusion technology test facility would also provide the opportunity to test the other key nuclear technologies with full environmental conditions, a large-volume fusion neutron source, and interactions with the other components. Non-blanket components include plasma interactive components, tritium and vacuum systems, shielding and instrumentation and control.

For plasma interactive components, the opportunity to test large-area components under high heat, neutron and particle fluxes in thermal steady-state conditions can only be provided in a major fusion device. Adequate simulation of reactor conditions suggests (see the blanket analysis of heat flux scaling) that surface heat fluxes of 1-2 MW/m² over 1 m² would be desired to reasonably test 5-10 MW/m² reactor components. This is larger than required for the blanket test ports, but should be readily achievable on the actual component locations in the fusion device. The neutron fluence lifetime for plasma-interactive components is generally lower than for blankets, so a 1-2 MW/m² goal should provide adequate testing - about 10-20 dpa in steel structure, for example. An additional but unquantified requirement is for sufficient particle flux to examine the behavior of eroded/redeposited surfaces. Since the structural thickness of these components is often less than in the blanket, the 500 s blanket minimum burn time should also be sufficient to achieve flow and thermal steady-state.

Most of the tritium and vacuum system components are located away from the direct plasma and neutron environment and can be tested independently of the machine parameters. This includes machine duty cycle and fuelling rate since gas flows can be recycled as in TSTA. Major concerns that would be uniquely addressed by a fusion device are inlet conditions (chemical composition of plasma exhaust and blanket product gases) and system integration (complete cycle for tritium self-sufficiency, operations, and safety aspects). A device providing at least 1 MW/m² over 5 m² test area is probably at least 20 MW fusion power. At a 1% burnup fraction, the tritium throughput is around 10 g/h, which is sufficient to require a full tritium processing system using reactor-relevant components. Similarly, the vacuum components would be reactor-relevant, although perhaps somewhat smaller in capacity. Uncertainties related to vacuum duct impedance and particulate quantity, composition and transport could be tested in a fusion device with relevant duct geometry.

The major factor for shielding is to provide a large-volume 14-MeV neutron source with a complex geometry in terms of shielding materials, thickness and penetrations. Any fusion device that meets the minimum neutron wall load and test area requirements previously discussed should provide many opportunity to test shielding calculations, although a particular test with a "clean" geometry for deep penetration benchmarks may require a larger test port than identified for the blanket.

A fusion technology device would provide the opportunity to test instrumentation and control in reactor-relevant operation.⁽¹²⁾ For example, a magnetic field of 1-3 T and a neutron wall load of 1 MW/m² should provide a good test of electromagnetic and radiation tolerance of the signals and hardware. Fluence goals of 1-2 MW-yr/m² ($\sim 10^{25}$ n/m² @ 14 MeV) should provide an end-of-life test for many possible fusion diagnostic components (Table 9-3).⁽¹³⁾

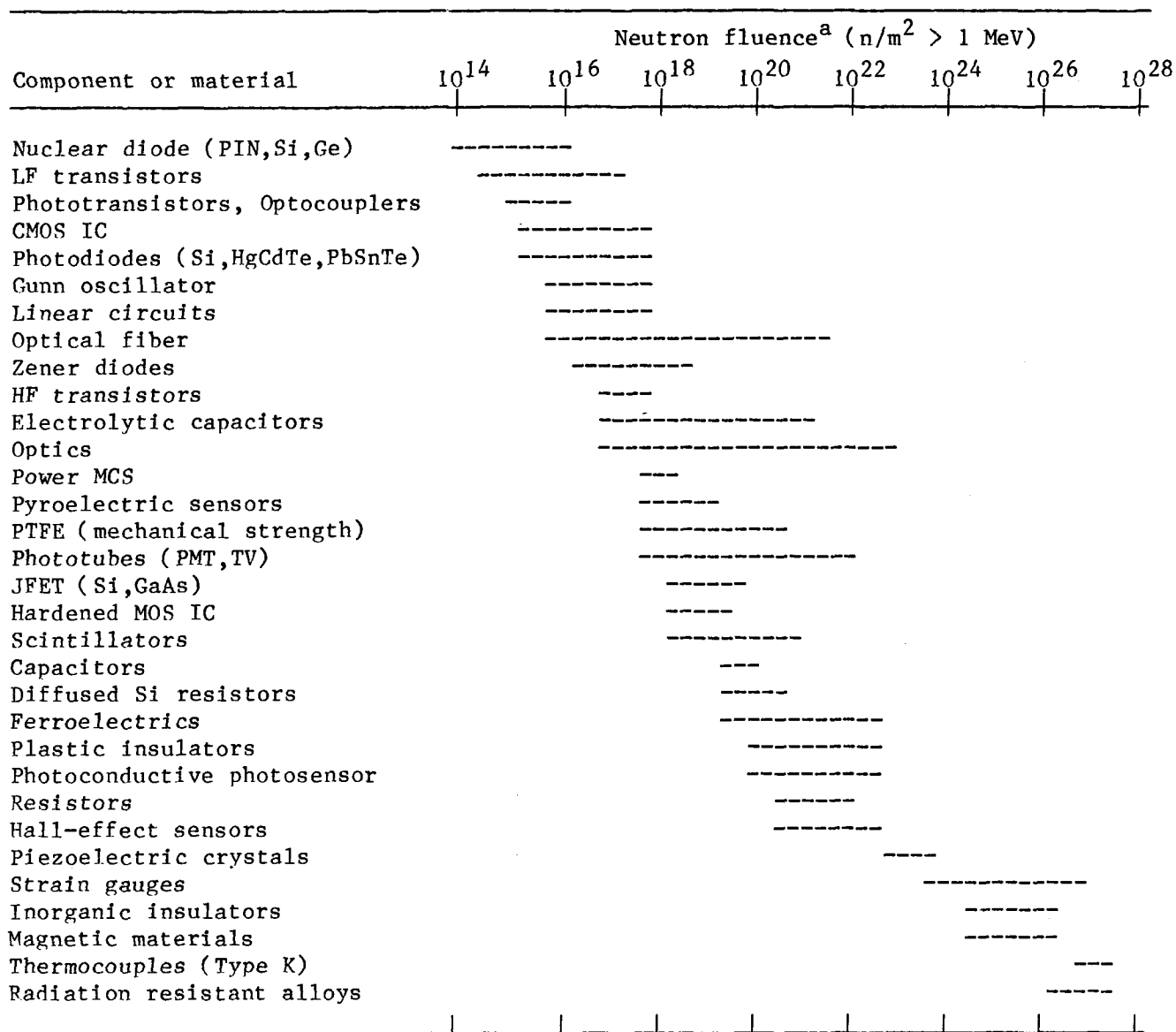
9.2.4 Summary

By modifying blanket modules and restricting the range of test device parameters, it is possible to retain key features of fusion reactor blanket operation in a less ambitious test device. While it is difficult to determine exact requirements for the test device parameters, the results of technical analyses presented here combine to suggest a reasonable compromise between the cost of high performance parameters and the reduced testing benefits of scaled down device parameters. Table 9-4 summarizes these limits for the most important parameters of a fusion test device.

Based on the blanket scaling and limited calculations for non-blanket components, it is felt that a fusion device with the parameters indicated in Table 9-4 would also serve as a good test facility for non-blanket fusion nuclear components.

The requirements indicate the importance of high power density (neutron wall load > 1 MW/m²), long plasma burn time (> 500 s) and surface area available for testing (> 0.5 m² per test module) in a fusion test device. High fluence (4-10 MW-yr/m²) is important for near end-of-life prediction, but critical information about many interactive effects can be learned at lower fluences ($\sim 1-2$ MW-yr/m²).

Table 9-3. Radiation Tolerance of Instrumentation and Electronics^(13,14)



^aBar begins and ends at fluence where most and least (respectively) sensitive components show significant degradation.

Table 9-4. Recommended Requirements on Key Parameters of a Fusion Engineering Research Facility

Parameter	Reference Reactor	Minimum	Substantial Benefit
Neutron wall load (MW/m ²)	5	1	2-3
Surface heat load (MW/m ²)			
Tokamak first wall	1	> 0.2	
Mirror first wall	< 0.1	< 0.2	
Fluence (MW-yr/m ²)	15-20	1-2 ^a	2-6 ^a
Test port size ^b	--	0.5 m ² x 0.3 m	1 m x 1 m x 0.5 m
Total test surface area (m ²)	--	5	10
Plasma burn cycle:	Steady-		Steady-
Burn time (s)	state or	> 500	state
Dwell time (s)	long-pulse	< 100	preferred
Continuous operating time	months	days	weeks
Availability (%)	70	20	50
Magnetic field strength	7	1	3

^aFor integrated testing

^bSome liquid metal blanket designs may require larger test volumes

9.3 LITE Tokamak

Currently, there are three moderate physics risk options for a tokamak next step. The first, a compact copper ignition experiment, would provide a few seconds of ignited operation to better establish the physics of plasma energy confinement scaling in the ignited regime⁽¹⁵⁾. This type of experiment would address important physics issues, but would resolve few, if any, of the engineering issues associated with the development of nuclear components for fusion reactors.

The second option for a tokamak next step is a large integrated test facility such as INTOR⁽⁵⁾. Although INTOR-class facilities would address both physics and engineering issues, such facilities will suffer from three problems. First, at an initial cost of ~ 3\$ billion, they are likely to be prohibitively expensive. Second, at a fusion power level of ~ 600 MW_f, tritium requirements are likely to exceed levels which can be provided by an external source. Third, the achievement of facility operating availabilities great enough to provide moderate neutron fluence testing will be difficult because the same components which are to be tested (e.g., blankets, plasma interactive components) must also perform reliably to achieve a high system availability. These problems are well recognized and are discussed in Chapters 15 & 16 of the 1984 FINESSE Interim Report⁽¹⁾.

A third option for a conventional tokamak next step can be a long pulse, copper coil tokamak. One such candidate has emerged as a variant to the Long Pulse Ignition Test Experiment (LITE) design developed by MIT and TRW as part of the DOE sponsored Mission I Ignition experiment studies of 1985⁽¹⁶⁾. Although a fusion engineering test reactor (FERF) based upon LITE has not been the subject of a detailed assessment, it appears that a compact LITE FERF could satisfy a two-fold ignition physics/nuclear testing mission with a life-cycle cost that is less than half that of INTOR and an initial capital cost that is about twice that of the Mission I compact ignition experiments.

An ambitious set of technology goals for a LITE FERF follows:

- Tokamak reactor relevant testing/development of fusion components
 - First wall
 - Blanket/shield
 - Primary coolant loop

- Plasma impurity control/high heat flux
 - RF heating system
 - Fueling/tritium systems
-
- Near-steady-state engineering data
 - Component lifetimes
 - Reliability
 - Remote maintenance
 - Instrumentation
-
- Engineering proof-of-principle for near and intermediate term applications
 - Medical/military isotope production
 - Production for fission reactors

Thus, with the exception of a superconducting TF coil demonstration, the LITE FERF would satisfy an engineering mission nearly as ambitious as that of INTOR.

9.3.1 LITE Technology Description

Before discussing the potential capabilities of a LITE FERF, a brief description of those features of the LITE technology which can be modified for this purpose is appropriate. The discussion which follows applies to the water cooled LITE-R3⁽¹⁶⁾ conceptual design which was developed during 1985. More recent versions of LITE (e.g., LITE-R4) would utilize liquid nitrogen cooling in an effort to increase compactness and further reduce costs. These versions maintain the central feature of the LITE technology, the use of self-supporting TF coils constructed from a high strength copper alloy (e.g., CuBeNi), but are not relevant to the FERF application because they are pulse length limited (no active cooling).

The key mechanical features of the LITE-R3 design are highlighted in Figures 9-10 and 9-11. The tokamak would have a major radius of 1.76 m, an aspect ratio of 3.2, a plasma elongation of 1.6, and a triangularity of 0.2. The water cooled copper coils would provide a field on axis of 8.4T, which would provide an ignited fusion power (at full beta) of about 300 MW.

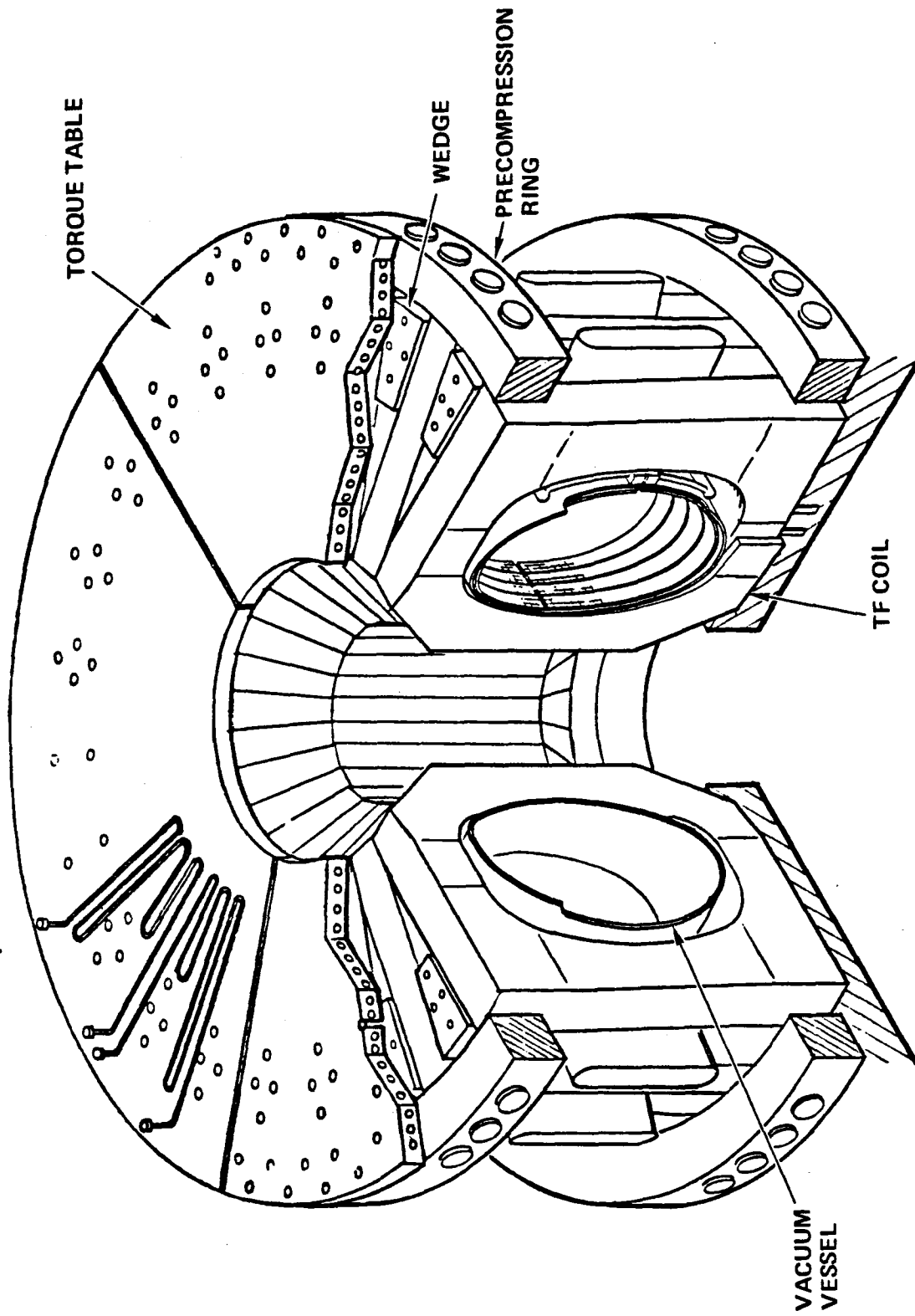


Figure 9-10. LITE vacuum vessel/TF magnet assembly.

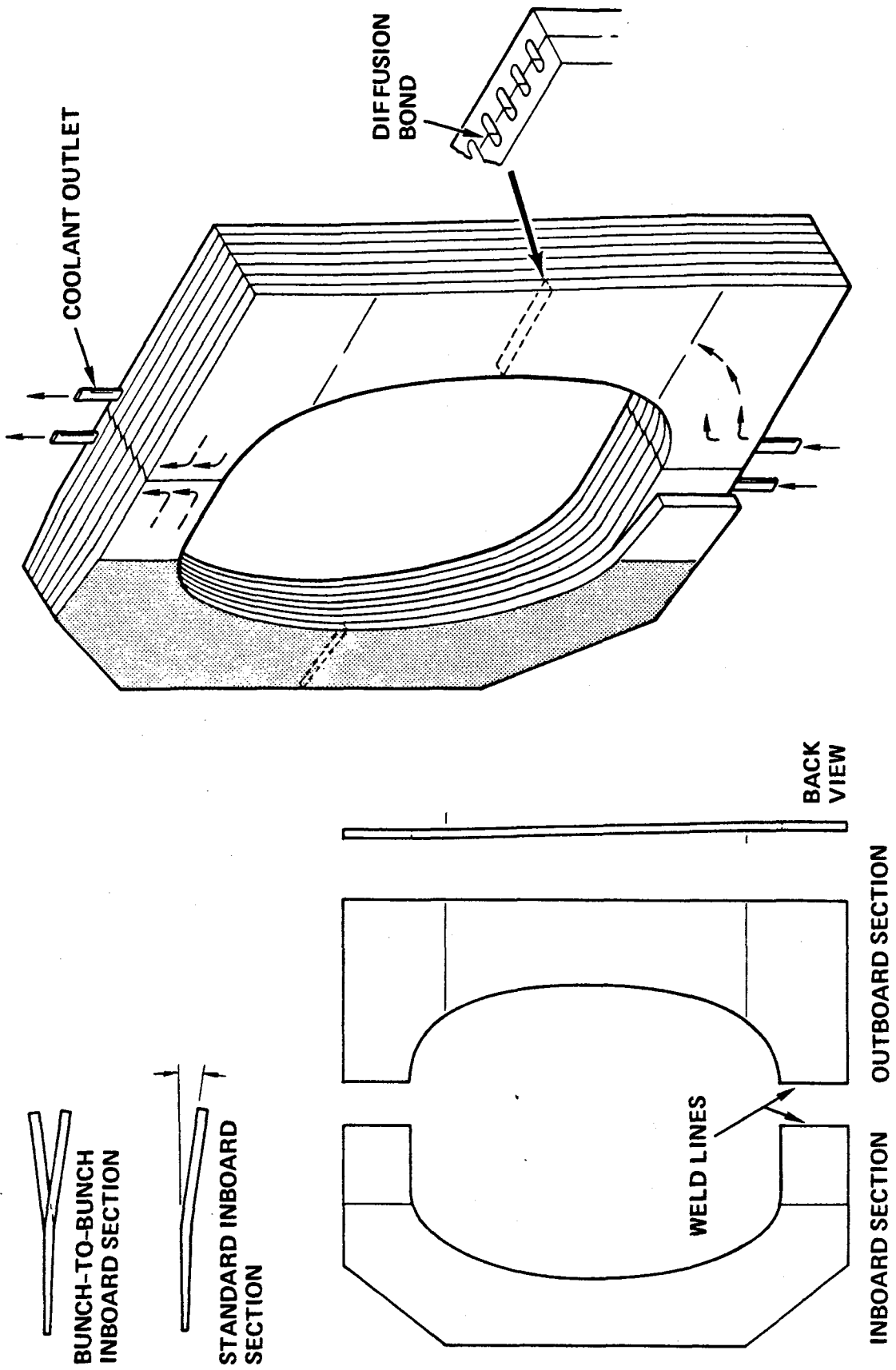


Figure 9-11. LITE TF coil bunch and turn arrangement.

The LITE-R3 design is conservative (a higher field of 10.4T appears feasible), but provides an ignition margin of at least 1.5 relative to neoclassical scaling. The figure-of-merit used to evaluate the prospects for ignition (at a fixed elongation and safety factor) is B^2a , which is 39 for LITE-R3.

As shown in Figure 9-11, the LITE-R3 TF coils would be water cooled during the pulse. Although the TF coils would be capable of indefinitely long pulses, the design pulse length is limited to 5-10 seconds to reduce the capital cost of the ignition experiment. Specifically, the high electrical consumption of the TF coils (~ 360 MW) translates to a high capital cost when the primary source of energy is rotating storage (e.g., motor-generator sets). Longer pulse operation would require that power be provided directly from the grid.

Because the pulse length is limited to only 5-10 seconds, several other design relaxations are possible for LITE-R3. Most importantly, the first wall/vacuum vessel assembly can be inertially cooled between pulses (~10 minutes). Thus, a relatively simple first wall assembly utilizing mechanically attached, but thermally decoupled, graphite tiles and water cooling from the outside of the vessel was selected. Also, an active helium ash removal and impurity control system is not needed for short pulse operation. Finally, it was decided that remote maintenance operations for all Mission I designs would be limited to external adjustments and first wall repair. Replacement of a hot TF coil/vacuum vessel sector was not a requirement for the LITE-R3 design.

Recognizing the intrinsic potential of the LITE technology for longer pulse (~20-30s) operation, the LITE-R3 design team did develop several component design concepts which would allow for longer pulse ignition experiment upgrades. These long pulse features are, in most cases, also relevant to a component copper tokamak FERF. For example, as shown in Figure 9-12, replaceable first wall coolant panels, mechanically attached to the vacuum vessel can be developed to actively cool the LITE-R3 integrated first wall/bumper limiter ($q''_{ave} = 120 \text{ W/cm}^2$, $q''_{peak} \sim 500 \text{ W/cm}^2$). These panels (96 total) can be sized for removal through the 26 cm window ports, but must be remotely connected and leak checked.

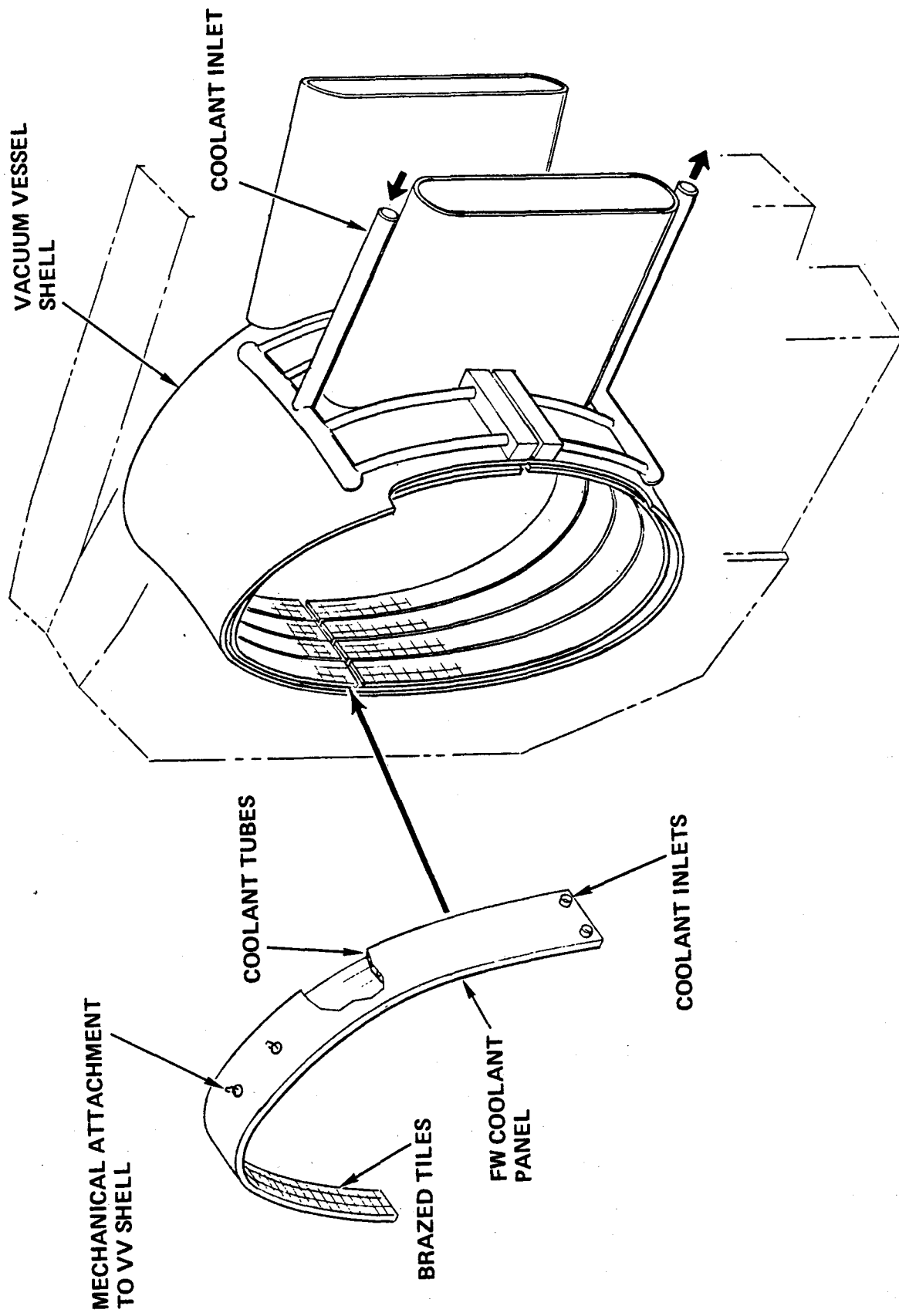


Figure 9-12. LITE vacuum vessel/actively cooled first wall.

Another FERF relevant upgrade involves provision for remote segment removal. As shown in Figure 9-10, the modular LITE-R3 machine arrangement can be designed to be remotely maintainable. Detailed design is required in this area, but sector maintenance appears feasible given sufficient attention in the initial design process.

A final FERF relevant upgrade for long pulse LITE operation involves provision for active helium ash removal and impurity control. Two options were considered for the ignition mission: A set of discontinuous, outboard-mounted pump limiters (6 total), and a continuous single-null poloidal divertor. Although both options show promise for the ignition experiment, erosion of this pump limiter leading edge is a concern and the divertor option appears to be best suited to the FERF application.

9.3.2 Representative Design

Requirements

In order to build upon the LITE-R3 upgrade design concept described above, it is of interest to further consider the specific requirements for a LITE FERF as well as those modifications to the LITE-R3 design that would be required for a FERF. The basic requirements for a LITE FERF are:⁽¹⁾

- neutron wall load 1 MW/m^2
- test area 10 m^2
- individual test section area $1 \text{ m} \times 1 \text{ m} \times 0.5 \text{ m}$
- pulse length 500 s
- neutron fluence 2 MW-yr/m^2

Mechanical Features

Given the above requirements, further modifications to the LITE-R3 design are required to increase the pulse length, prevent irradiation damage to the toroidal field coils, provide adequate test access, and to limit tritium requirements. A LITE FERF concept, sized with the above considerations in mind, is shown in Figure 9-13. In comparison with LITE-R3, the LITE FERF would have a 34 cm larger major radius, but its TF coils would be shielded

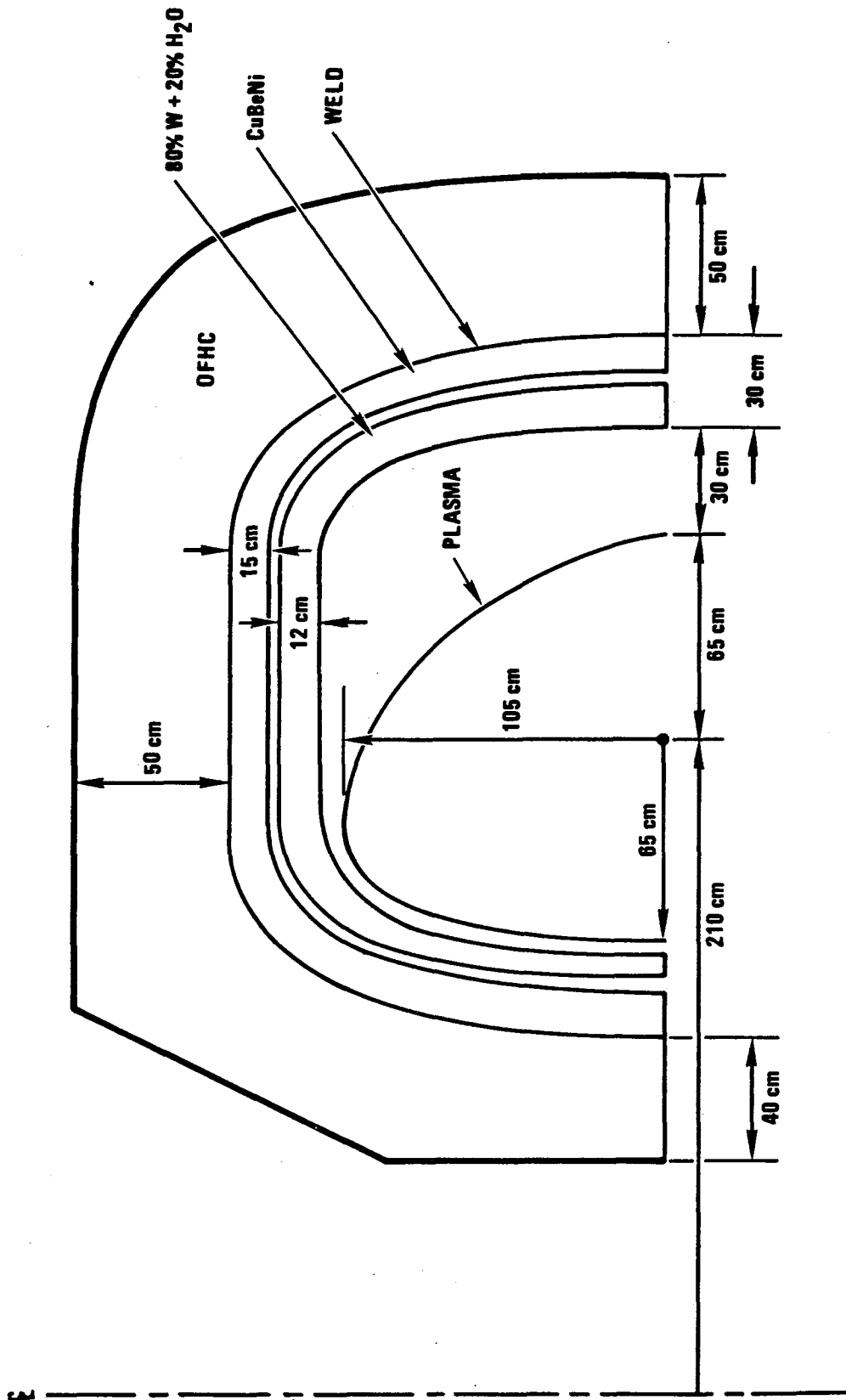


Figure 9-13. LITE FERF TF coil cross section.

using a thin, 80% tungsten - 20% water shield and its OH coil would provide enough flux to drive the plasma current for 500 seconds. The machine would continue to retain small overall dimensions; outer TF coil radius < 4 m.

A unique feature of this design concept would be the use of a composite TF coil consisting of a CuBeNi inner section welded to an OFHC copper (or Cu-Zr alloy) outer section. The stronger CuBeNi alloy is expected to be more resistant to neutron-induced displacement damage⁽¹⁷⁾, so a higher neutron flux is allowed. Stresses in the balance of the coil are low enough to use OFHC copper, with the additional benefit that resistive power consumption is reduced relative to an all CuBeNi alloy coil (CuBeNi has 60% the electrical conductivity of OFHC). Power consumption would be further reduced by use of a superconducting EF coil set.

To provide sufficient access for nuclear testing, the number of TF coil bundles would be reduced from 24 to 12. The magnetic field ripple would be limited in the new design by the increased gap between plasma and the outer leg. The number of $\sim 1 \times 1$ m² wide nuclear test ports provided by this configuration is limited only by the number of ports required for RF heating and plasma diagnostics. Based upon the Mission I ignition experiment requirements, 5 of the 12 inter-bundle parts should be adequate for these purposes, and one of the openings would be used for the TF coil electrical connections. The remaining 6 nuclear test ports would provide 6 m² of very high quality test area. Several square meters of additional test area of smaller dimensions can be provided on the outboard side of vacuum vessel (see Figure 9-13), so that a 10 m² total test area can be provided.

Operating Parameters

An overview of operating parameters for the LITE FERF is provided in Table 9-5. With a 5.5 T toroidal field on-axis, a 90 MW fusion power, providing a 1 MW/m² neutron wall loading, is expected.

In this configuration, the ignition scaling figure of merit, B^2a , is about half that of LITE-R3. If the B^2a value for LITE-R3 will be sufficient to achieve ignition, it follows that half of the ignition value will be sufficient to achieve $Q \sim 5$ operation, where Q is the fusion power divided by the ICRH RF heating power. Indeed, the B^2a value for LITE-R3 is expected to

Table 9-5. LITE FERF Nominal Parameter Overview

MAJOR RADIUS OF PLASMA	2.1
MINOR RADIUS OF PLASMA	0.66
PLASMA ELONGATION	1.6
MAGNETIC FIELD ON AXIS	5.5 T
PLASMA CURRENT	5.7 MA
SAFTEY FACTOR, q	2.6
PLASMA BETA	4.74 %
FUSION POWER	90 MW
NEUTRON WALL LOADING	1 MW/m ²
IGNITION SCALING, B^2a	20
PLASMA Q (FUSION/INJECTED POWER)	> 5

exceed ignition requirements by a margin of 1.5-2, it is possible that the LITE FERF would also ignite. Even so, it would be prudent to provide the 18 MW of continuous ICRH power for $Q = 5$ operation (plus ~ 5 MW of lower-hybrid power to start the plasma current).

Depending upon available site power levels, the LITE FERF described above would be capable of two "extended" modes of non-ignited (driven) operation, which are compared with the nominal case, below:

- Nominal case $q_n = 1 \text{ MW/M}^2$, $t_{\text{burn}} = 500 \text{ sec}$
 - $P_{\text{TF}} = 150 \text{ MW}$
 - $P_{\text{OH}} = 20 \text{ MW}$
 - $P_{\text{RF}} = 35 \text{ MW}$

- Extended burn $q_n = 1 \text{ MW/M}^2$, $t_{\text{burn}} = 1,000 \text{ sec}$
 - $P_{\text{TF}} = 150 \text{ MW}$
 - $P_{\text{OH}} = 80 \text{ MW}$
 - $P_{\text{RF}} = 35 \text{ MW}$

- Extended power $q_n = 1.5\text{-}2 \text{ MW/M}^2$, $t_{\text{burn}} = 500 \text{ sec}$
 - $P_{\text{TF}} = 210 \text{ MW}$
 - $P_{\text{OH}} = 20 \text{ MW}$
 - $P_{\text{RF}} = 35 \text{ MW}$

In the extended burn case, the OH coil power level is increased because the full positive-to-negative flux swing would be necessary, forcing a longer period of operation near the highest field that the coil can generate. This contrasts with the nominal case in which operation near the highest OH coil field occurs for only a short time during startup when ohmic heating is required.

In the extended power case, the magnetic field is increased by a factor of 1.2 and the TF coil power is increased by 40%. This mode of operation increases the TF coil stresses, making cyclic fatigue a more important concern. Consequently, a better estimate of this limit will require a more detailed design analysis.

9.3.3 LITE FERF Summary

The LITE FERF concept offers several attractive features. First, it is small and compact. Based upon the results of the Mission I studies, the cost for such a facility might be less than \$1 billion including remote maintenance and other required features.

Second, in addition to satisfying the nuclear testing requirements for blankets, a LITE FERF would also provide a very useful test bed for other tokamak-relevant fusion-nuclear technologies such as impurity control systems (poloidal divertor), plasma heating systems (ICRH, lower-hybrid, ECRH), and remote maintenance systems. This type of FERF would be capable of providing the developmental experience with these systems that will be required for the next step to be highly successful.

Third, the life cycle operating costs for such a facility are quite

reasonable considering its capabilities (see Section 9.9). Specifically, assuming a maximum 45% average capacity factor, the LITE FERF would consume only about 2 kg/yr. of tritium. This amount is believed to be available from the Canadian nuclear program in the post-1990 timeframe⁽¹⁸⁾. The overall electricity requirement, about 210 MW_e, is large, but might be available from the grid, depending upon where the facility would be sited. An initial capital cost of \$1 billion appears reasonable, and is considerably lower than that of an INTOR-class facility.

9.3.4 Development Issues

The LITE FERF is based upon relatively near term physics performance and engineering capabilities. The development issues primarily relate to the TF coil manufacture, long pulse, and irradiation effects. The main development issues for the LITE FERF are:

- Verification (scale-up) of diffusion bonding of the TF coil turns.
This may not be required if external coolant channels will be machined into the copper plates and if electroforming techniques are used to close them.
- Verification of electron beam welding (brazing) of Cu-2Be-Ni to OFHC
- Corrosion and erosion of the TF and OH coolant channels
- Irradiation effects on inorganic insulators and copper alloys and their shielding requirements
- Performance limits and lifetime of single null poloidal divertor.
This, however, is also a system which would be developed as part of the LITE FERF mission.

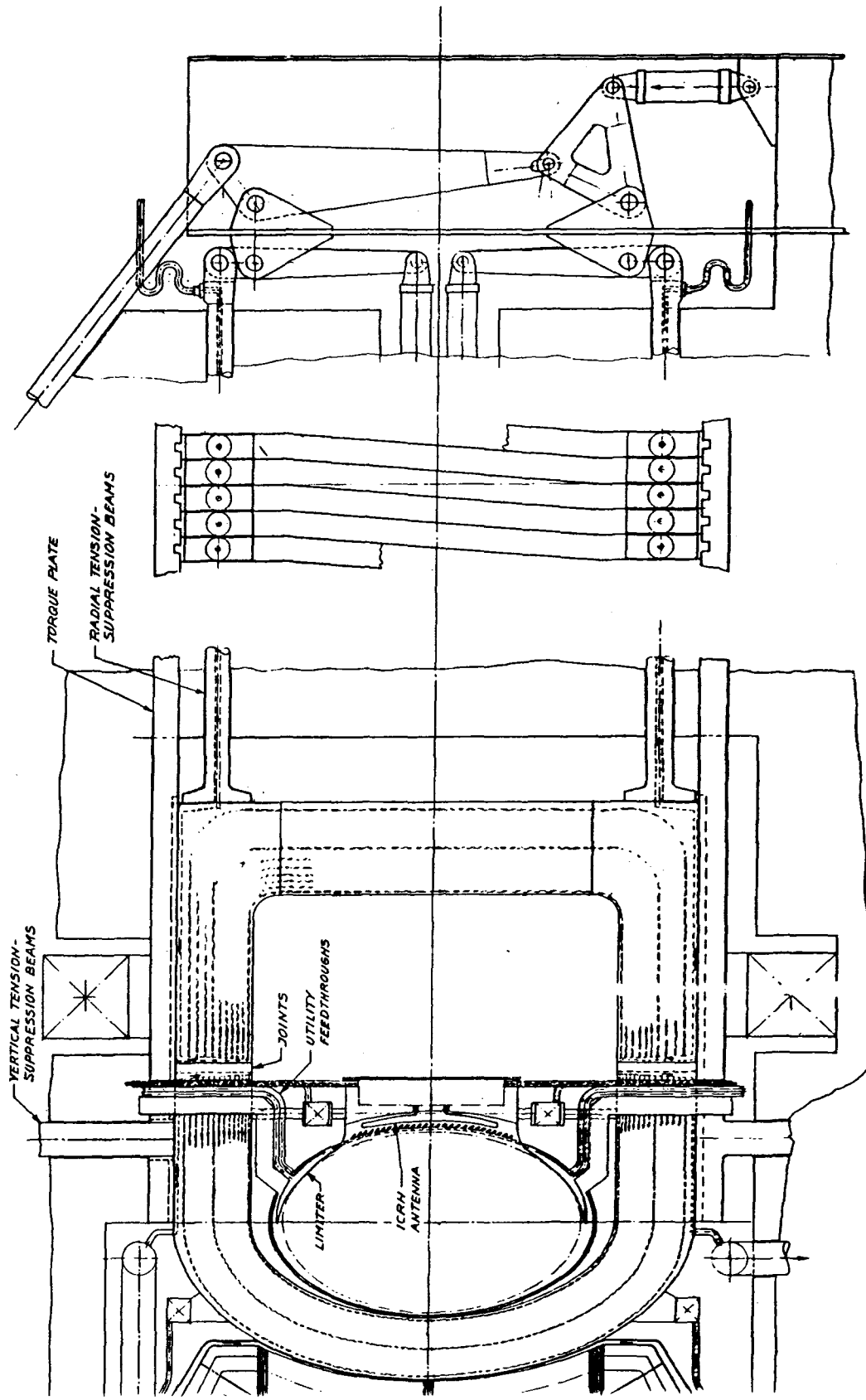
9.4 Demountable Toroidal Fusion Core (EASI)

9.4.1 Concept Description

The Demountable Toroidal Fusion Core (DTFC) concept is a small water-cooled, normally-conducting toroidal fusion device such as an inductively driven tokamak (IDT) (Fig. 9-14), a low aspect ratio tokamak, or a Reversed Field Pinch. These toroidal fusion devices can be provided with joints in the top and bottom horizontal members of the toroidal field coil turns, thus permitting the removal and replacement of the core (e.g., central OH coil, inner toroidal field coil turns, vacuum vessel, impurity control system, RF heating and current drive systems and PF trimming coils). The rest of the machine (test blanket, toroidal field current return coils, main PF coils, shields, instrumentation) remains in place.

This central feature has two important consequences. First, with attention to the design of the permanent outer toroidal subsystem, cores with a broad range of physics objectives and configurations can be tested in a single facility. Second, the DTFC concept provides for straightforward replacement of the toroidal core ($\sim 4\text{-}5$ m diameter), which is directly exposed to fusion neutron and charged particle radiation and is the subsystem that is most likely to fail. Thus, a reasonably replaceable core could increase the flexibility and availability of a DTFC fusion test facility.

Analysis to date indicates that an inductively driven tokamak DTFC concept is feasible in all of its unique areas. Using conservative scaling laws, the tokamak ignites and is capable of long (500 s) pulses, driven only by the PF/OH coil system. The joints are feasible, as is the tension-suppression system required to keep the tokamak in the desired stress state during operation. Additionally, neutronics analysis has shown that a sufficient breeding ratio is achievable for a DTFC tokamak fusion-electric power plant. A low aspect ratio RF driven DTFC also has been parametrically analysed and the results reveal an attractive option space for FERF applications although the prospects for fusion-electric power production appear dim because of the high power requirements for RF current drive for reactor-grade plasmas. Finally, preliminary analysis has suggested that a relatively low aspect ratio Reversed Field Pinch DTFC is both feasible and attractive although questions remain on the technology requirements of the central PF ohmic heating and F- θ driving coil.



VERTICAL TENSION-SUPPRESSION BEAMS

TORQUE PLATE

RADIAL TENSION-SUPPRESSION BEAMS

JOINTS
UTILITY FEEDTHROUGHS

LIMITER

ICRH ANTENNA

Figure 9-14. Cross-sectional view of inductively-driven Demountable Toroidal Fusion Core tokamak.

The experimental data base for inductively-driven tokamak is well-developed, although the ignition performance is uncertain because of the lack of knowledge of the correct electron energy confinement law. Nevertheless, Neoalculator scaling provides ignition at small geometries and relatively low toroidal magnetic fields. The low aspect ratio DTFC physics is less certain although it is not expected to radically depart from larger aspect ratio tokamaks (see Section 9.6). Finally, a Reverse Field Pinch DTFC awaits the results of a definitive hydrogen experiment.

9.4.2 Representative Designs

Inductively Driven Tokamak DTFC

The inductively driven tokamak is the reference concept for the DTFC series. This tokamak has been the most intensively investigated and has been found to be feasible in virtually all of its key features. Questions relating to non-feasibility are generic to all toroidal fusion systems - e.g., erosion of surfaces exposed to the plasma.

As a small inductively-heated and driven tokamak, both the ignition and burn phases are crucial for the establishment of the base case. For ignition, Neoalculator scaling is selected even though this results in substantially higher toroidal magnetic fields and currents than would be required for Mirnov scaling. As a consequence, high toroidal field coil power and ohmic heating coil power is characteristic of this device. However, these peak power requirements can be readily met at a variety of sites on the North American continent. Similarly, the burn phase also requires substantial power at the end of the pulse since the OH coil will have reached the end of its double swing even though the TF coil power is relatively low because of the desired modest fusion power of a test facility.

For both ignition and burn, the IDT is limited by the volt-second capability of the OH coil set. For configurations less than a minimum major radius (establishing the available flux at the magnet technological limit), the configuration will not ignite in the absence of ICRH auxiliary heating. Similarly, the availability of volt-seconds after ignition determines the pulse length at the peak plasma reactivity and highest plasma temperature.

For technology testing, the design goal was to find the smallest geometry that achieves ignition and long pulse burn, with about 100 MW of fusion power. This was found to be $R = 1.35$ m, $A = 2.3$, $\kappa = 1.5$ and $\Delta = 0.0$ with the Kruskal-Shafranov safety factor at ignition set at $q_{\text{ignition}} = 2.6$ (see Table 9-6). It is important to note that Neoalculator scaling required virtually all of the volt-second capability during ignition. At ignition, the toroidal magnetic field and plasma current are 9.87 T and 10.5 MA, respectively, considerably higher than required to sustain the fusion power level at 100 MWth. Consequently, for burn the plasma current is lowered to the minimum value necessary to confine alphas, thus allowing q_{burn} to rise to a value substantially above q_{ignition} (for the base case, $q_{\text{burn}} = 4.0$). For Troyon beta scaling, the net effect is to achieve the targeted value of fusion power while simultaneously achieving the maximum inductively driven burn time by recovering the flux difference between the ignition and burn plasma currents.

The inductively driven tokamak case was determined by parametric scans that sought the minimum DTFC geometry for Neoalculator scaling, the minimum capital and operating costs and a driven pulse length exceeding 500 seconds. The details of this case are presented in Table 9-6. This device is anticipated to have a capital cost comparable with the low aspect ratio DTFC (discussed below) but uses much higher resistive electric power (427 MWe on average). Nevertheless, this concept is based on physics and technology features that can be achieved with a high level of confidence in comparison with potentially more attractive but riskier alternative DTFC configurations.

The unique technology features of the IDT-DTFC are the joints in the TF coil and the actively-controlled tension-suppression system of the reactor that maintains the joints in a compressive state. However, stress analysis indicates that the joint region will be in a satisfactory state of (mildly) compressive stress at all times. It is felt that more risk is associated with the very highly stressed central OH coil because of the effort to make the reactor as physically small as possible while preserving the inductively driven burn time of 500 seconds. The general problem of first wall and limiter heat transfer and erosion is not unique to the DTFC concept, although the power levels are high because of the small size.

Table 9-6. Parameters for DTFC Fusion Engineering Research Facilities

Parameter	Inductively Driven	Low Aspect Ratio
Major radius (m)	1.35	1.00
Minor radius (m)	0.59	-
Aspect ratio	2.30	1.60
Elongation	1.48	2.00
Δ 0.0	0.0	
<u>Ignition</u>		
Confinement scaling	Neocalcator	Mirnov-1.5
Plasma current (MA)	10.50	8.20
Temperature (keV)	7.05	10.09
Plasma density ($1/m^3$)	4.00×10^{20}	6.83×10^{19}
$n\tau$ (s/m^3)	6.24×10^{20}	6.28×10^{19}
Safety factor at edge	2.6	2.6
β (%)	-	18.3
Ohmic heating power (MW)	7.45	1.41
Fusion power (MW)	25.0	2.4
TF coil power (MW)	402	27
OH coil power (MW)	157	0
RF current drive power (MW)	0	33
Magnetic field (T)	9.87	2.15
<u>Burn</u>		
Plasma current (MA)	4.82	9.38
Temperature (keV)	33.5	31.33
Plasma density ($1/m^3$)	1.48×10^{20}	1.01×10^{20}
$n\tau$ (s/m^3)	9.21×10^{19}	-
Safety factor at edge	4.0	4.30
β (%)	-	11.1
Fusion power (MW)	100	100
Neutron wall load (MW/m^2)	2.03	2.05
First wall heat flux (MW/m^2)	0.88	0.89
Magnetic field (T)	7.91	4.06
Burn time (s)	519	Steady-state
TF coil power (MW)	258	96
Average OH coil power (MW)	169	0
RF current drive power (MW)	0	13
Peak power (MW)	596	109
Blanket thickness (m)	1.0	1.0
Coil temperature ($^{\circ}C$)	100-150	100-150
Coolant/insulator fraction	0.100	0.100
Maximum current (MA/turn)	0.50	0.50

Low Aspect Ratio DTFC

The low aspect ratio Demountable Toroidal Fusion Core embodiment closely resembles the Spherical Torus (Section 9.6) concept in most of its key aspects except that the central TF coil turns, vacuum vessel, lower hybrid current drive launchers and field shaping coils are removed and replaced as a single DTFC unit. Similar to the inductively-driven and ohmically-heated DTFC tokamak test facility, the plasma systems and economic analysis focussed on the smallest feasible machine.

It was determined that Neoclator scaling resulted in ignited machines of reasonable size ($R = 1.5$ m) but required hundreds of megawatts of current drive to achieve ignition (in the absence of ICRH auxiliary heating). Consequently, Mirnov scaling was selected as the required electron energy confinement time. Mirnov scaling exhibits an extremely broad and forgiving ignition space (major radius, aspect ratio, elongation and triangularity). Consequently, it was decided to select the device on the basis of minimum capital and operating costs subject to the constraints of small size, and reasonable current drive power for ignition. The systems code revealed that a machine as small as $R = 0.9$ m could ignite but that the corresponding current was only barely above the plasma current required for alpha confinement (9.3 MA). Therefore, the selected core configuration has a major radius of $R = 1.0$ m, an aspect ratio of 1.6 and an elongation of 2.0. This resulted in a machine that ignited at $B = 2.15$ T and $I_{\text{plasma}} = 8.2$ MA with a current drive power of 17 MW delivered to the plasma.

Similar to the IDT-DTFC, the safety factors for both ignition and burn were varied to find the lowest cost and risk embodiment. The desired safety factor at ignition was again found to be as low as generally acceptable ($q_{\text{ignition}} = 2.6$). Similarly, the higher safety factor at burn, coupled with the highest feasible plasma temperature, was found to require the least amount of current drive power.

Table 9-6 presents the technical features of the baseline low aspect ratio DTFC fusion engineering research facility. While the capital cost is comparable with that of the IDT-DTFC, the operating cost is substantially lower because of the much lower level of site power (~ 100 MWe). However, since a relatively high value of conversion efficiency to coupled lower hybrid current drive power was assumed (50%) and the plasma densities are fairly

high, is reasonable that higher levels of current drive power would be needed. Further, there remain the questions of the physics uncertainties of Mirnov scaling and the technological feasibility of providing the current drive power (17 MW) to the plasma.

Reversed Field Pinch DTFC

A small-sized reverse field pinch based on the demountable core concept is under study, but the analysis is not complete. An alternate reverse field pinch configuration is discussed in Section 9.8.

9.4.3 Development Needs

The inductively driven tokamak DTFC is based on an ignited plasma, so requires a tokamak ignition and burn test in order to resolve the physics uncertainties prior to use as an engineering test facility. Otherwise, it is based on standard ohmically-heated and ohmically-driven tokamak theory. Any improvements in physics understanding that allow higher betas in tokamaks would also be useful in reducing the amount of electric power required for operations. The necessary technological developments include plasma edge and impurity control systems, high performance PF coil systems, and low cost power supply systems for the provision and control of high levels of inductive and resistive power. For the DTFC concept, developments are also needed in joint design and fabrication and in compact utility feed-through assemblies. Finally, since the DTFC concept as well as others with similar dimensions will have little shielding between the plasma and magnets, it is essential that radiation resistant, strong and highly conducting alloys be developed.

Both the Low Aspect Ratio and the Reversed Field Pinch DTFC concepts await proof-of-principle testing in hydrogen machines. With respect to the low aspect ratio -DTFC, efficient methods for RF current drive or some other mechanisms have to be sought and developed. The Reverse Field Pinch DTFC may require a high performance PF/OH coil system since coupling efficiency is lost at lower aspect ratios and the strength of F- θ pumping relative to inductive current drive is uncertain. The later may require the use of a half-swing OH coil in order to avoid high values of OH resistive loss after F- θ pumping is initiated for current drive (i.e. the magnetic field of the OH coil should be close to zero at ignition).

9.5 Tokamak Test Facility (PPPL)

9.5.1 Concept Description

Interest in the tokamak as a nuclear technology test facility stems mainly from its position as the most advanced laboratory fusion device. The objective of this study was to identify a device configuration and operational mode that would best utilize the tokamak concept for meeting the nuclear testing requirements while minimizing the capital and operating costs.

The requirements of small capital cost and small fusion power result in small physical size. Several trade-offs were considered for achieving the required nuclear performance and duty factor in a relatively compact device while minimizing cost and risk. The following selections were made:

1. Water-cooled copper TF coils because of the inability to shield superconducting coils in a compact device, the greater tolerance of copper coils for pulsed operation, and the lack of warmup/cooldown times.
2. Ignited operation, to minimize the electrical power required during the burn. The size penalty for an ignited device was found to be small.
3. RF heating (ion cyclotron waves), because of the difficulty of operating neutral-beam injectors in a reactor environment, as well as uncertainty in the development of injectors of the required energy and efficiency.
4. Quasi-ohmic heating to ignition, to minimize both capital cost for auxiliary heating power and degradation of plasma confinement.
5. Steady-state current drive was rejected because of its high electrical power cost. (If required at some future date, steady-state current drive could be implemented by installing RF power antennas.)
6. Location of the OH coils in the TF coil bore, to maximize the magnetic flux swing available for current startup and for driving 1000 s pulses.
7. High-beta operation during the burn to minimize TF-coil power loss. This choice required an elongated bean-shaped plasma with an elaborate system of auxiliary coils.
8. Pumped limiters, to avoid the size and complexity of magnetic divertors.

9.5.2 Representative Design

Table 9-7 and Fig. 9-15 summarize a representative tokamak test facility based on these selections. One important assumption for minimizing reactor

size is that the confinement will not degrade significantly from its ohmically-heated value, this should be valid if the externally injected power does not significantly exceed the ohmic power and the plasma density does not exceed about $5 \times 10^{20}/\text{m}^3$. Additionally, it is assumed that a stable high-beta regime can be reached and will have similar confinement characteristics to those of ohmically-heated low-beta regime tokamaks.

9.5.3 Development Needs

Experimental tokamaks have demonstrated reactor level $n\tau$ in the near-ohmic-heated regime, reactor-level temperatures at smaller $n\tau$, the effectiveness of ion cyclotron heating, and the stability of bean-shaped plasmas at relatively low beta (so far). The major plasma physics and engineering advances required relative to the expected performances of TFTR, JET, JT-60 and D-III are associated with achieving and sustaining ignited, high-beta operation over 100-s pulse lengths. Within the next few years, existing tokamaks are expected to demonstrate very high beta and 10-s pulse lengths, but no existing machine is likely to ignite.

The physics and technology areas of greatest uncertainty are:

1. While bean-shaped plasmas have been operated in the PBX device with $\langle\beta\rangle$ up to 4% for short periods, the feasibility of achieving and maintaining $\langle\beta\rangle = 20\text{-}25\%$ in tokamaks has not been demonstrated.
2. The favorable scaling of τ_E observed in the purely ohmically-heated regime is assumed to be maintained in the fusion-alpha-heated burn phase. The basis of this assumption is that in both regimes the heat input to the plasma has toroidal and poloidal symmetry.
3. The integrity of SPINEL insulation when subjected to the stresses expected in tokamak magnets, including cycling, needs to be verified.
4. The first wall lifetime under plasma erosion is only crudely estimated.
5. Maintenance of the inboard OH and shaping coils is impossible, so that their reliability (including redundancy) must ensure operation for several years. In general, remote maintenance methods, including first wall replacement, are in a primitive stage of development.
6. Feasibility of the TF coil demountable joints, particularly in coils that are repetitively pulsed to very high field.

Table 9-7. Representative Tokamak Nuclear Technology Test Facility

Parameter	Startup	Burn
<u>Geometry</u>		
Major radius, m	2.55	2.55
Minor radius, m	0.75	0.75
Aspect ratio	3.40	3.40
Plasma shape	Dee	Bean
Elongation	2.0	2.0
Inboard blanket/shield, m	0.50	0.50
Max B field at coils, T	12	6.0
<u>Plasma</u>		
Magnetic field on-axis, T	5.6	2.8
Average beta, %	4	23
Average temperature, keV	6.5	35
Average density, $1/m^3$	4.5×10^{20}	1.4×10^{20}
Plasma current, MA	7.0	5.4
$n\tau$ (Neoclator), s/m^3	1.4×10^{21}	2.1×10^{20}
Z_{eff}	1.2	1.2
Ohmic power, MW	4.9	< 1
RF power, MW	5.0	0
Pulse length, s	20	1000
<u>Magnets</u>		
TF coil bore, H x V, m	3.5 x 4.8	3.5 x 4.8
Max TF current density, kA/cm^2	0.93	0.47
TF coil power, MW	490	122
PF coil power, MW	60	45
<u>Power production</u>		
Fusion power, MW	60	185
First wall area, m^2	129	129
Outboard neutron wall load, MW/m^2	-	1.3
Surface heat flux, MW/m^2	-	0.3
Circulating power, MW	590	190

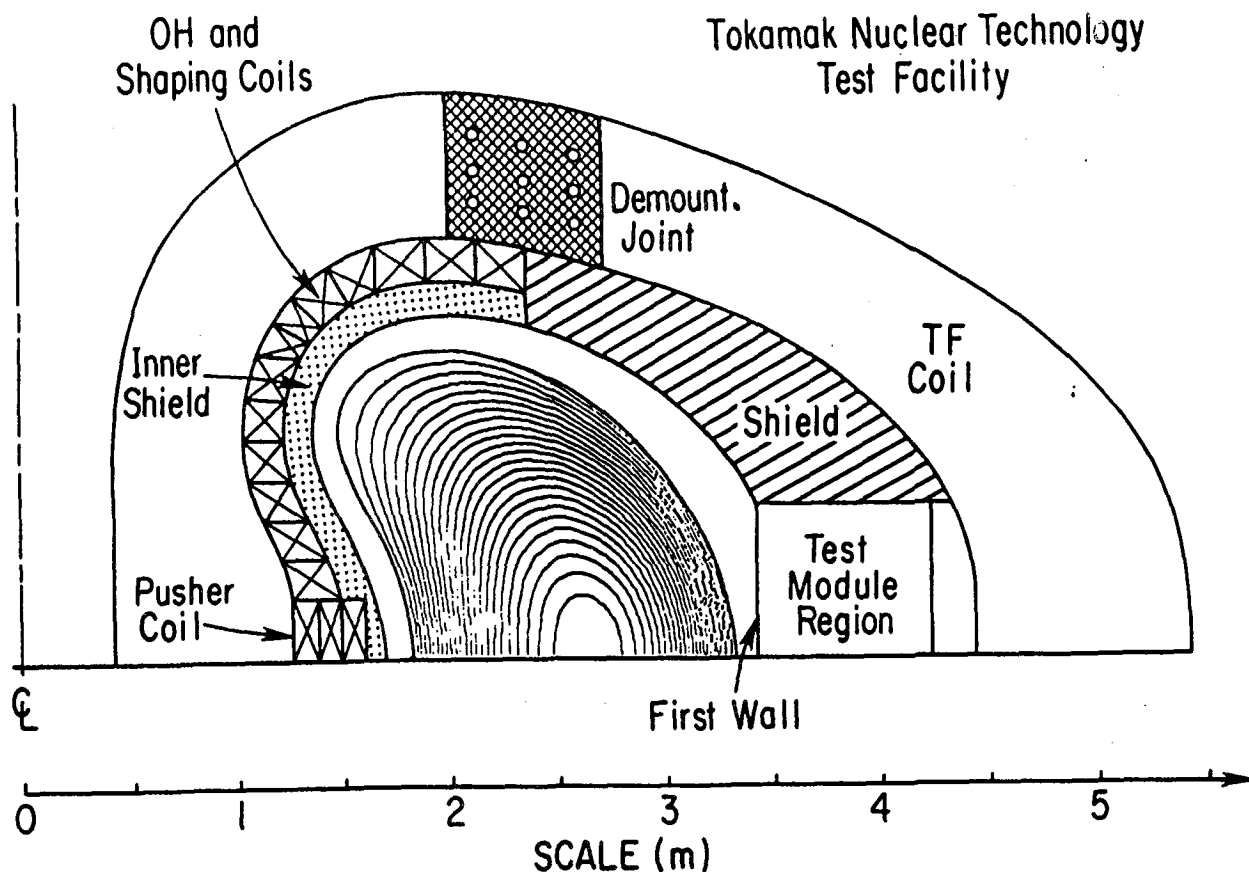


Figure 9-15. Partial elevation view of tokamak test facility.

9.6 Spherical Torus (FEDC)

9.6.1 Concept Description

Introduction

The spherical torus^(18,19) is a very small aspect ratio concept that may provide high beta, good confinement and steady-state operation in a compact configuration at modest fields. In comparison with the RFP and spheromak, a spherical torus is expected to be similar in compactness, low field and high beta; but with better, tokamak-like confinement times by more than an order of magnitude. In contrast with tokamaks, including recent small aspect ratio tokamaks^(21,22) based on conventional assumptions such as modest elongation (κ) and inductive plasma current startup, the spherical torus projects high

beta within the first stability regime through naturally large κ and plasma current at a modest poloidal beta, β_p .

The spherical torus concept is made plausible by recent progress in current drive schemes, such as initiation and ramp-up by lower hybrid waves⁽²³⁾ and maintenance by oscillating fields⁽²⁴⁾ or helicity injection⁽²⁵⁾. These current drive schemes permit compact long-pulse spherical tori with little or no solenoid and small aspect ratio, $A < 2$. The corresponding ignition spherical tori are estimated to be compact ($R = 1.0-1.6$ m) and at low fields ($B_{t0} = 3-2$ T).⁽²⁶⁾ In the case of small-size, low-field, and short-pulse experiments using pulsed high current density coils, full inductive current startup should remain feasible.

Physics Description

The primary characteristic of a spherical torus is its small aspect ratio. This has several consequences on plasma behavior, particularly elongation, current, achievable beta and confinement.

For tokamaks with $A \sim 3$, large shaping fields (quadrupole or larger) are generally needed to achieve an elongation of 1.6 with mild triangularity. In addition, with external PF coils, the total coil current is several times the plasma current. However, free-boundary MHD equilibrium studies show that $\kappa = 2$ occurs naturally in a small aspect ratio spherical torus with only a dipole vertical field. The total coil ampere-turns, relative to the plasma current, are also reduced by more than an order of magnitude when A is reduced from 4 to 1.5 for constant edge safety factor. The toroidal and poloidal coil currents become comparable, giving comparable fields.

High plasma current is also possible since the moderately pitched field lines in the inboard region of the spherical torus introduce a large toroidal rotation because of the relatively small toroidal circumference there, more than compensating for the small toroidal rotation due to the highly pitched field lines in the outboard region (Fig. 9-16). Thus for a spherical torus with $A = 1.67$, $\kappa = 2$ and $q = 2.2$, then $I_p/aB_{t0} = 7$ MA/m-T.

In conventional tokamak geometry, beta is generally observed to increase with increasing elongation κ and decreasing Aq , both of which occur in the spherical torus configuration. Recent experimental results⁽²⁷⁾ suggest that the first stability regime beta limit can be approximated by:

$$\beta_c = C_\beta I_p / a B_{t0} \quad (9-1)$$

where $C_\beta \approx 0.033$ m-T/MA. For the high currents anticipated in spherical tori, first stability regime beta limits above 20% are possible. That such a magnetic field configuration should give high beta for MHD stability can also be seen in Fig. 9-16. In comparison with a conventional tokamak, the spherical torus has a short field line length in the bad-curvature region relative to that in the good-curvature region.

In the spherical torus configuration, the poloidal beta is comparable to the toroidal beta and much less than unity, leading to essentially force-free, paramagnetic equilibrium configurations. The highly pitched magnetic field lines produce a large poloidal current that strongly enhances the toroidal field on-axis - $B_t/B_{t0} > 1.5$ is possible for $A < 2$. The enhanced B_t contributes to increasing I_p for a given q . Strong paramagnetism also introduces an large uncertainty in the application of Eq. (9-1) with respect to B_t and B_{t0} .

ORNL-DWG 85-2498A2 FED

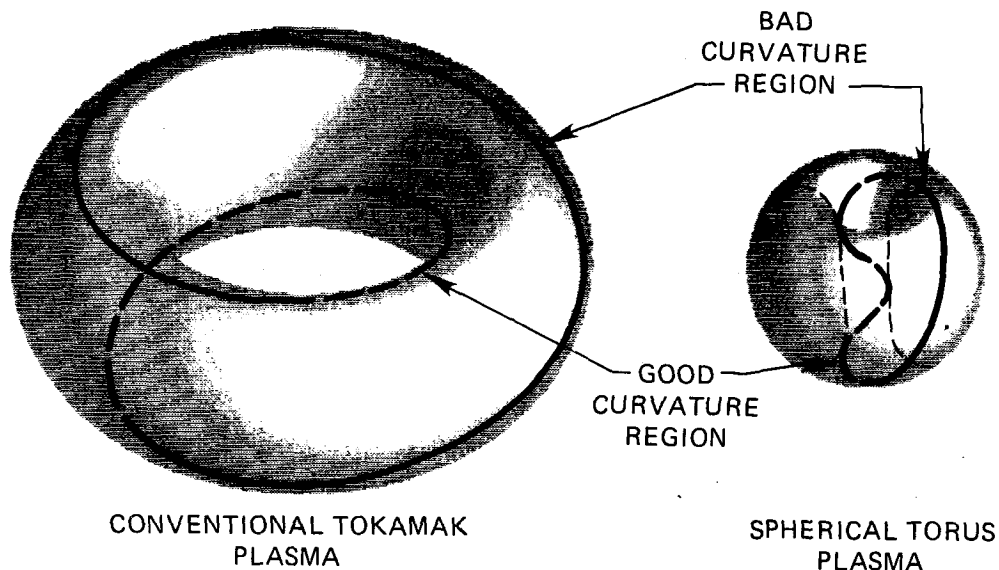


Figure 9-16. Magnetic field line contours on the $q=2$ surfaces of a conventional tokamak and spherical torus. The portion of the field lines in the good-curvature region is dashed.

A consequence of compactness is a reduced confinement time if confinement scales with the plasma size (e.g., Neoalculator scaling). However, recent experimental results indicate a strong scaling of plasma confinement with plasma current in plasmas with intense auxiliary heating (e.g., Mirnov scaling). The scaling in spherical tori is not known.

The strongly enhanced B_t at the plasma core and the large poloidal field near the plasma edge create a strong curvature of the surfaces of $|B|$, making them largely parallel to the flux surfaces at the outboard region of the plasma. In this region, the particle drift orbits coincide with the flux surfaces. This nearly omnigenous⁽²⁸⁾ region largely coincides with the region of bad curvature for MHD instability. This region is nearly free of locally trapped particles and hence has improved kinetic stability, although trapped particles still exist between the top and bottom regions of the plasma. These trapped particles have reduced "banana" width, leading to a reduced neoclassical transport.

Since internal solenoid coils are eliminated to reduce the aspect ratio, alternate current drive schemes are necessary. Small major radius and aspect ratio leads to small plasma inductance and helps current drive by reducing the flux required through external sources. Lower hybrid current drive may be possible at modest plasma densities and temperatures, but higher densities may require alternatives such as helicity injection or F- θ pumping as in RFP's.

Toroidal plasma helical pitch can be expressed by the parameter, $\theta = \langle B_p \rangle_s / \langle B_t \rangle_v$, where the subscripts indicate surface and volume averages.⁽²⁹⁾ For the spherical torus configuration ($A = 1.6$ and $\kappa = 2$), the dependence of θ on q can be plotted in F- θ space, where the pinch parameter, $F = \langle B_t \rangle_s / \langle B_t \rangle_v$, depicts averaged inverse plasma paramagnetism (Fig. 9-17). It is seen that, as the helicity increases, the spherical torus evolves from weakly paramagnetic spherical tokamak ($q = 10$), to strongly paramagnetic spherical tokamak ($q > 1$), to spherical pinch ($1 > q > 0$), to spheromak ($q = 0$), and eventually to spherical RFP ($q < 0$). In the case of spherical tokamak, $F = 0.8$ to 0.5 and $\theta = 0.8$ to 1.5 , and current maintenance via oscillating fields^(25,26) is suggested. The effectiveness of this approach is enhanced by its relatively modest stored magnetic flux.

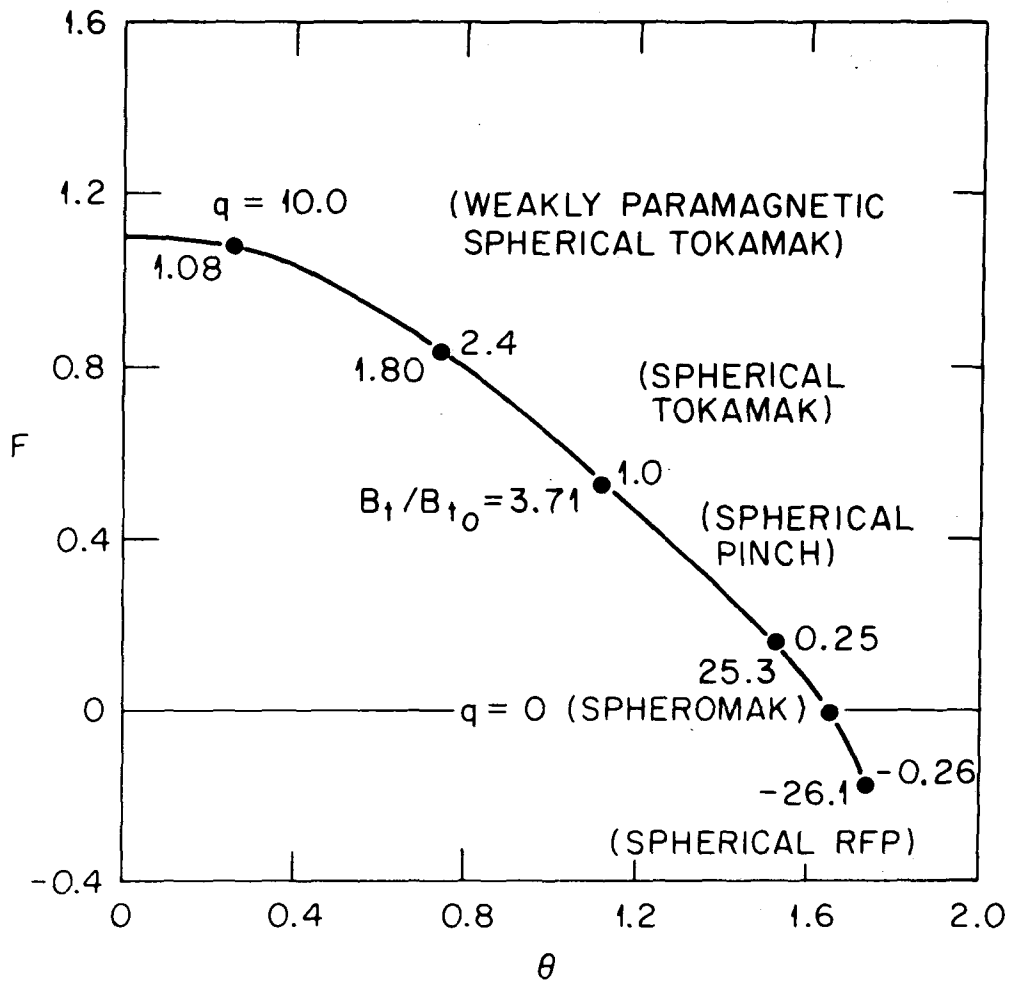


Figure 9-17. The dependence of F and θ on q in a spherical torus configuration with $A = 1.6$ and $\kappa = 2$.

Engineering Description

The spherical torus resembles the tokamak in design configuration, except that only the absolutely indispensable inboard components are retained. This is primarily a copper conductor that produces the toroidal magnetic field required by tokamak plasmas. Other components such as the solenoid, shield and organic insulator are eliminated. Inorganic insulators or separate first wall and vacuum boundary arrangements may also be eliminated in some designs.

The engineering design issues relate to the high-strength, high-current-density center conductor, the inboard shielding, the toroidal field coil configuration, and the first wall/vacuum boundary. Additionally, the need for

current drive systems and low-voltage high-current power supplies are major features of this concept.

9.6.2 Representative Designs

Typical parameters for several representative designs are given in Table 9-8.^(19,26) For an ignition spherical tokamak, the more conventional approach of a separate first wall leads to $R = 1.53$ m and $I_c = 15.3$ MA, where I_c is the coil current. Eliminating the separate first wall could save 8 cm between the plasma and center post, and reduce R by 0.2 m and I_c by 2 MA, but would require a more advanced approach to the first wall and vacuum boundary.

For high neutron production and wall load for technology development, Table 9-8 illustrates a case with $B=3$ T and $q_n'' = 1.0$ MW/m², requiring $R = 1.13$ m and $I_c = 16.9$ MA. If a modest fusion power system is desired as a low-cost prototype to a more significant fusion device, a 2 T system is also described in Table 9-8. This midget spherical torus has $R = 0.8$ m and $I_c = 7.9$ MA, requiring 2.5 MW based on Mirnov scaling and producing 4 MW of fusion power at a neutron wall load of 0.15 MW/m². (Note that the spherical torus case considered in Section 9.9 is different from these examples.)

A possible configuration for the ignition spherical torus is shown in Figure 9-18. This relatively conventional form includes a separate first wall and nuclear shield, with demountable TF coil return legs external to the shield and the PF coils. The center conductor post intercepts less than 5% of the fusion neutrons.

9.6.3 Development Needs

The features of the spherical torus plasma appear qualitatively different from conventional tokamak plasmas. These features include naturally large elongation, large plasma current, high beta in the first stability regime, low poloidal beta, comparable toroidal and poloidal fields, strong paramagnetism, near-omnigeneity, and strong helicity. In discussing the implications of these plasma features, much of the conventional wisdom of toroidal plasma physics is applied. However, there is no concrete data base for spherical tori (or for tokamaks with $A < 2$). The available tokamak data primarily covers A from 3 to 5. JET and Doublet III have A as low as 2.37 and 2.49, and will extend the data base in the next few years.

Table 9-8. Summary Characteristics of Spherical Tori Test Facilities

	Ignition	Engineering	Low power
Major radius, m	1.53	1.13	0.79
Minor radius, m	0.97	0.64	0.46
Plasma current, MA	14.1	10.3	5.1
Plasma density, $10^{20}/\text{m}^3$	0.59	1.0	0.46
Plasma temperature, keV	20	20	20
$n\tau$, s/m^3	--	--	--
Elongation, κ	2	--	--
Beta, %	24	18	18
Ignition margin	1.5 Mirnov	1.2 Mirnov	0.2 Mirnov
Fusion power, MW	60	53	4.0
Neutron wall load, MW/m^2	0.54	1.0	0.15
Magnetic field, T ^a	2	3	2
Center conductor current density, kA/cm^2	3	3	3
Center current, MA	15.3	16.9	7.9
Auxiliary power, MW	--	--	2.5
Pulse length, s	--	--	--
Current drive power, MW	--	--	--

^aOn-axis, no paramagnetic effects.

In the meantime, these discussions serve to indicate possible important directions of theoretical analysis and experimental testing. Examples include the effects of strong paramagnetism on achievable plasma beta; the effects of near-omnigeneity on plasma kinetic properties; plasma energy confinement in these configurations of small size, low aspect ratio and high current; and the effectiveness of lower hybrid wave and oscillating field current drive.

A decrease from the projected confinement would lead to larger auxiliary heating requirements; a decrease in beta to reduced fusion power and neutron wall load; and a decrease in current drive to short burn pulses. If each pulse was limited to the resistive plasma decay time, then classical

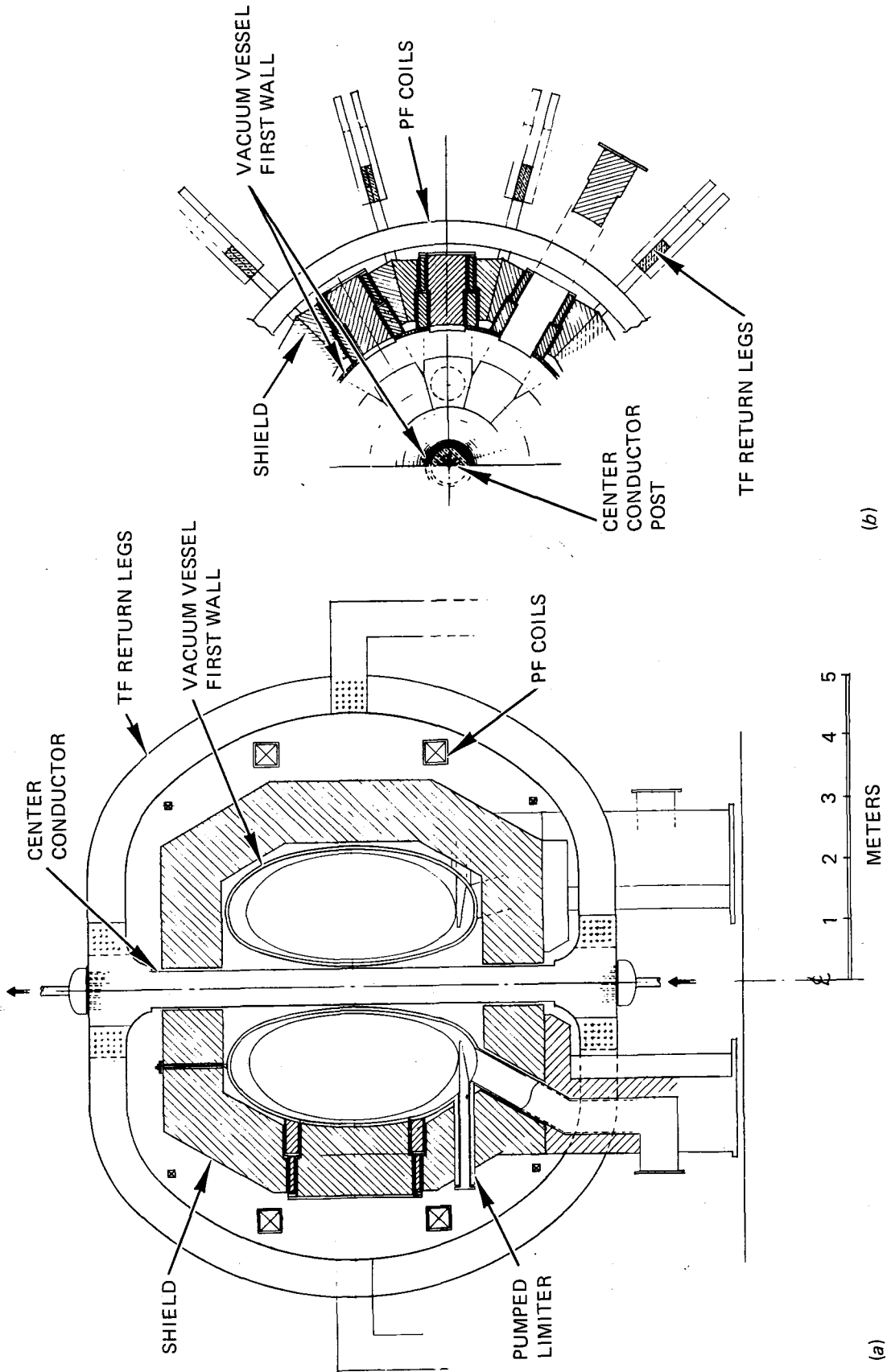


Figure 9-18. (a) Elevation view and (b) plan view of an ignition spherical torus with separate first wall arrangement, internal PF coils and demountable TF coil return legs.

resistance implies about 100 s for 90% current reduction in an ignition spherical torus.

The key engineering issues include the center conductor design and fabrication; low-voltage, high-current power supplies; and the toroidal field system structure. For the center conductor, options range from casting to explosive bonding of the single conductor post, to bonding of ceramic insulator to multiturn plate conductor that could comprise the post. For the power supplies, options range from steady-state homopolar generators to transformer rectifiers for high-duty-cycle operation, and to high current lead-based batteries for low-duty-cycle operation. For the toroidal field system structure, the options range from demountable external return legs, to combined first wall and conductor (and shield-blanket) arrangements.

The current density in the center conductor sets basic limits on the size and cost of the spherical torus. In one study of an ignition spherical torus,⁽¹⁹⁾ doubling the allowed current density to 6 kA/cm² resulted in a decrease in major radius from over 1.3 m to under 1.0 m, and an expected halving of the device weight. The technology of high-temperature copper alloys with pressurized water coolant is therefore one of the key issues of a compact high-performance DT spherical torus.

9.7 Tandem Mirrors (LLNL)

9.7.1 Concept Description

Several mirror-based fusion engineering test facilities have been studied over the past ten years including FERF,⁽³⁰⁾ TDF⁽⁴⁾ (Fig. 9-19), MFTF- α +T^(3,31) (Fig. 9-20), TASKA⁽³²⁾ and TASKA-M⁽³³⁾. These machines generally make use of the Kelley mode, with a two-component ion distribution in the central cell and the hot majority species trapped by the magnetic mirror fields. This mode is less demanding of the electric potential trapping needed in the end plugs of a tandem mirror machine. The required anisotropic plasma is generated by injecting full energy deuterium and tritium ions at angles close to normal with the magnetic field lines. Each of the mirror test facilities generates its reacting plasma by injecting a large current of neutral particles into the test cell. In all cases roughly equal currents of deuterium and tritium are injected at an energy of approximately 80 keV (the optimum for the Kelley

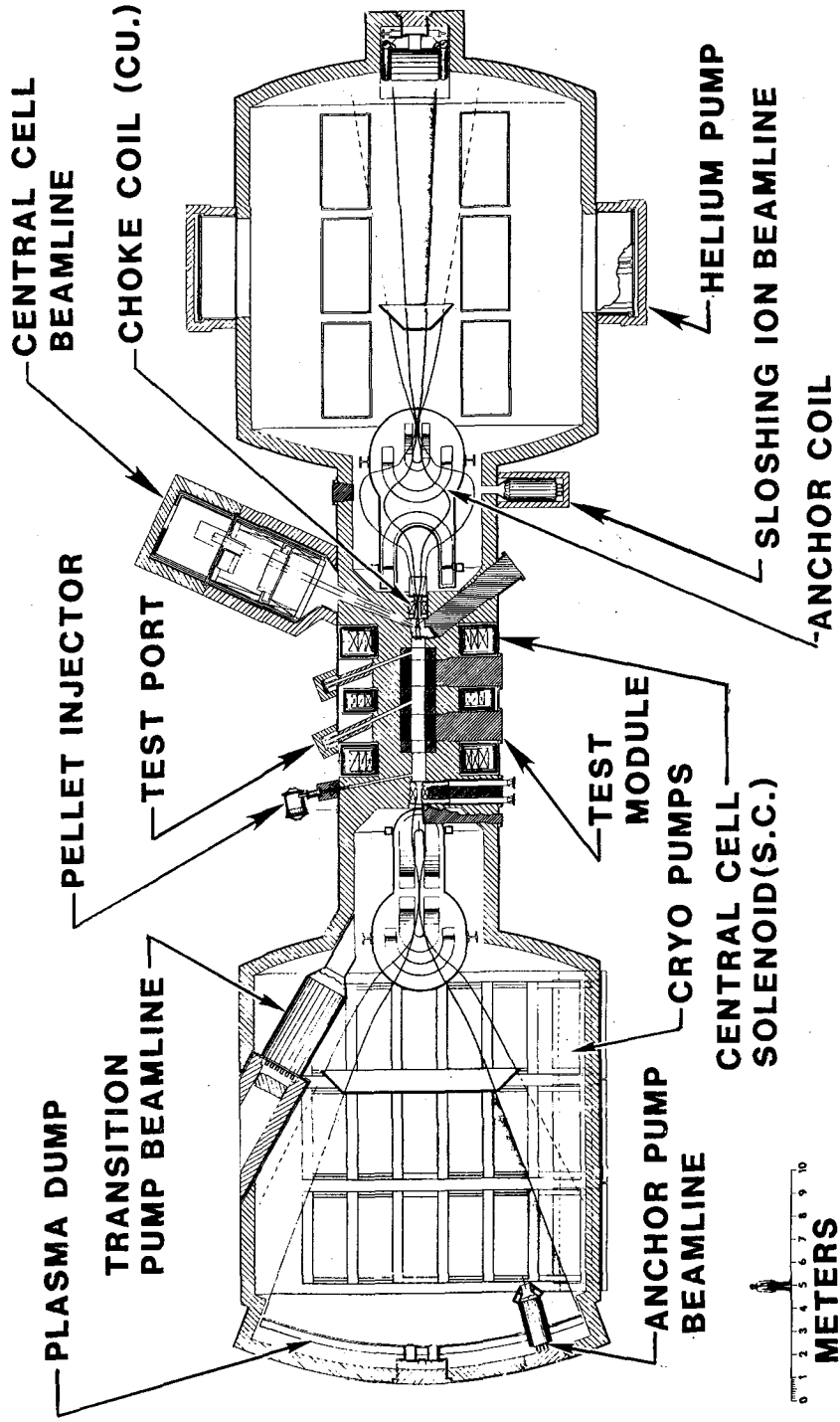


Figure 9-19. Cross-section of the Technology Demonstration Facility.

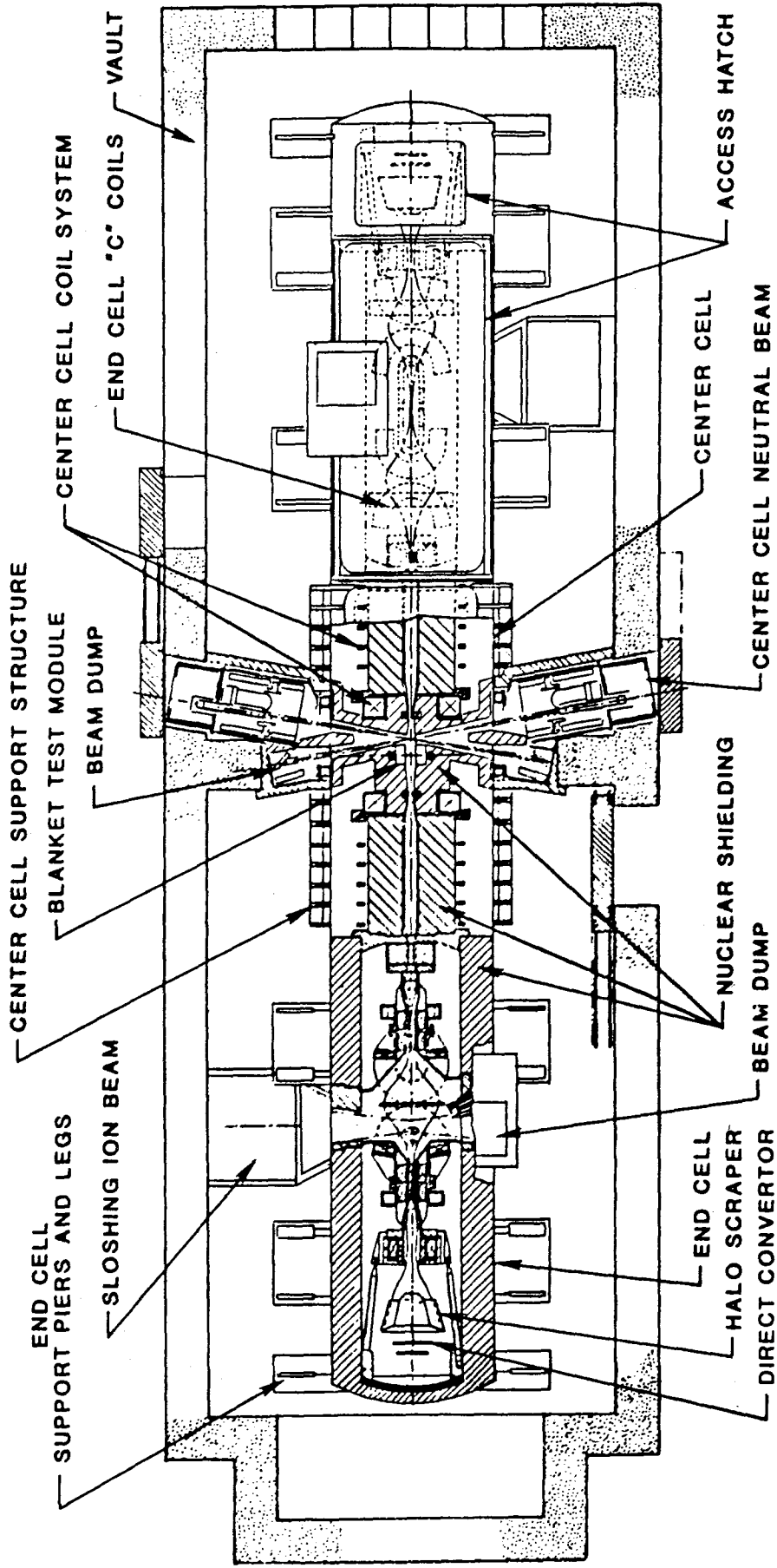


Figure 9-20. Plan view of MFTF- α T (components rotated into plane).

Mode). Kelley mode physics is well understood and its application to these devices results in conservative low-risk test cell design.

The differences among the various mirror test facilities result from the use of different end plug designs and variations in the desired first wall neutron flux and test area. Advanced plug designs have improved performance by reducing the rate of leakage, thereby making better use of the injected beams. Plug schemes have ranged from simple quadrupole single cells to octopole configurations incorporating thermal barriers.

In past designs the test areas varied from 1-10 m² (larger areas are available at the cost of more beam current and solenoid magnets). The uncollided neutron flux is also a selectable parameter with nominal values around 1-2 MW/m² and values as high as 4 MW/m² possible. In MFTF- α +T, the test cell is added to a physics experiment, modestly increasing the cost of the whole system while providing a test capability for a cost somewhat less than a combined physics/engineering facility.

The principal attributes of a mirror based FERF are:

Low fusion power	10-50 MW
Modest tritium consumption	0.07-0.3 g/hr
Modest physics requirements	Kelley mode
Good access	Linear motion
Modest power consumption	< 150 MW typical
Near term technology	
Steady state operation	~ 100 hours
Flexible test area	

One of the most important features of a mirror fusion test facility is its ability to provide a testing environment of adequate size with minimum fusion power. The ability to produce test cells over a wide range of size and wall loading allows the design of a machine with capabilities specifically tailored to the requirements of the test program. This approach allows optimization of the facility and efficient use of tritium.

All of the mirror fusion engineering research facilities are steady state devices with the capability for pulseless operation, a feature that simplifies testing and the subsequent analysis of test data. The linear nature of the test cells for a tandem mirror provides a simple right-circular cross section (Fig. 9-21) that allows introducing and extracting test articles with simple linear motion.

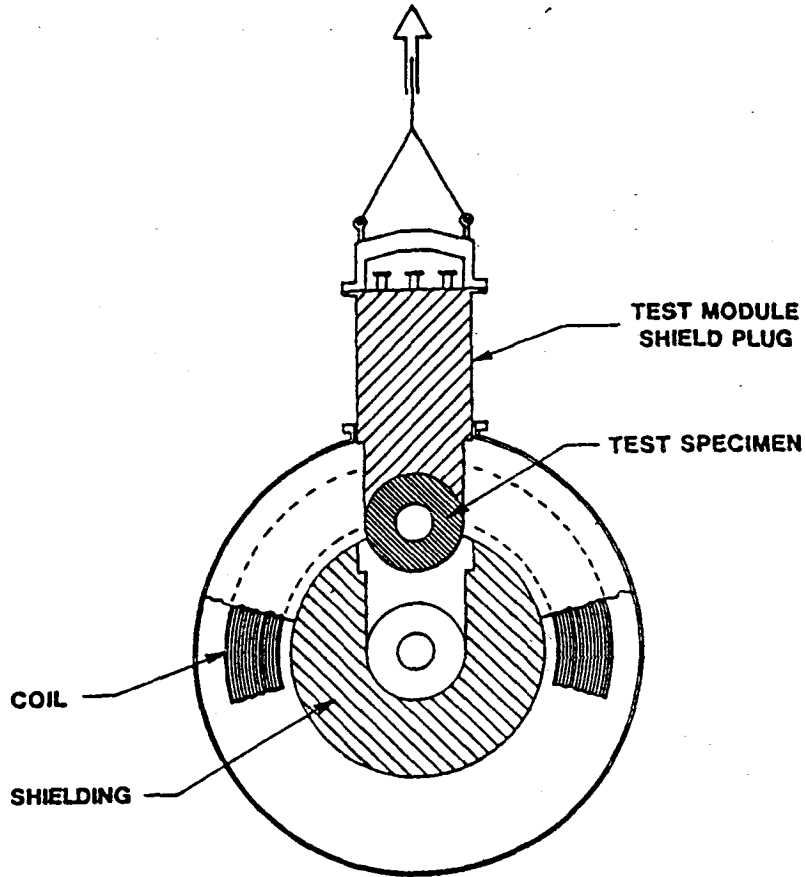


Figure 9-21. Test module removal by simple linear motion.

Power and tritium consumption are extremely important in a test facility since they can dominate the operating cost of the device. The cost of tritium is tied to the volume of the reacting plasma and, in a mirror FERT, virtually all of the reacting plasma is surrounded by useful test space.

9.7.2 Representative Design

There have been several recent detailed design studies of tandem mirror fusion test facilities. These are well-documented in the literature, especially Ref. (34). The Technology Demonstration Facility (TDF) and the MFTF-B upgrade MFTF- α +T are used here as representative of the features of these facilities. Table 9-9 summarizes their major parameters.

Table 9-9. Parameters for Representative Mirror Fusion Engineering Research Facilities

Parameters	TDF	MFTF- α +T
<u>Test cell</u>		
Test cell mode	Kelley mode	Kelley mode
Plasma radius (m)	0.15	0.15
First wall radius (m)	0.25	0.25
Test cell length (m)	4.5	4.0
Electron temperature (keV)	4.1	7
Mean hot ion energy (keV)	37	40
Hot ion density ($1/m^3$)	5.3×10^{20}	4.7×10^{20}
Warm ion density ($1/m^3$)	5.3×10^{19}	-
Hot ion lifetime (s)	0.026	0.26
$n\tau_{ion}$ (s/m^3)	-	2.0×10^{19}
Peak β potential (kV)	25	5
Peak β (%)	40	46
Magnetic field (T)	4.5	4.5
Incident beam power (MW)	65	14.4
Beam voltage (kV)	55	60
Incident current (A)	1244	240
Fusion power (MW)	20	11
Neutron wall load (MW/m^2)	2.1	2.0
Surface heat flux (MW/m^2)	~ 0.5	0.1
<u>End regions</u>		
Magnet configuration	Quadrupole	MARS quadrupole
Thermal barrier	Slushing ions	Slushing ions
Choke coil peak field (T)	15	18
Peak potential (kV)	37	69
Total slushing ion beam	11.3 A/80 kV	2.2 A/200 kV
Total transition pump beam	92 A/80 kV	0
Total barrier pump beam	14.8 A/40 kV	0
Total barrier ECRH	1 MW/35 GHz	0
Total plug ECRH	560 kW/60 GHz 1 MW/35 GHz	1.2 MW/56 GHz
Total plug drift pump	0	51 kW/1.2 MHz
Total anchor drift pump	0	0.46 MW/140 kHz
Total anchor ICRH	0 0.34 MW/50 MHz	0.8 MW/25 MHz
Total length (m)	-	65
Total electric power (MW)	260	104
Total fusion power (MW)	35.6	16.9

9.7.3 Development Needs

Technology

As with all fusion technology research facilities, the components of a mirror facility must be able to run for long periods with high availability. This is a much different requirement than that imposed on the subsystems of present physics experiments. Long pulse MFTF-B operation (30 seconds) will demonstrate thermal steady-state operation of many of the subsystems required for a mirror FERF. These include the neutral beam injectors, energetic particle dumps and RF heating systems. However, further development will still be necessary to improve their reliability and maintenance requirements. Other subsystems, such as continuous cryopumps and plasma halo pumps, are in the early stages of development but should be available in the time scale of a fusion test facility.

The development needs also include improvements in the magnet system. The high-field choke coil generally represents the most advanced magnet technology. Although coils of higher fields have been successfully built and operated, they were much smaller, operated for short times, and were not exposed to high fluxes of neutrons present in tritium-burning devices.

Physics

Although the physics of the Kelley mode central cell is well understood and an engineering test facility could be built with the single cell mirror physics of 2XIIB or the simple tandem mirror physics of TMX, the performance is greatly improved by use of the more advanced plugging concepts to be developed in TMX-U, TARA, MFTF-B and subsequent experiments. These machines use more complex magnet geometries and heating systems to enhance both the magnetic and electrostatic plugging of the central cell plasma. The physics required for a conservative mirror fusion facility is well-modelled by the experiments planned for MFTF-B, and even at the planned level of TMX-U operation a mirror fusion engineering research facility could be designed with a high level of confidence.

9.8 Reversed Field Pinch (LANL/Philips Petroleum)

Preliminary scoping studies of a fusion test facility based on a long-pulse or steady-state, ohmically-heated Reversed-Field Pinch (RFP FERF) have led to the following general features:

- Small physical size, fusion power and driver power (ZT-40M/ZT-H size)^(35,36) while maintaining high neutron wall load;
- Confinement scaling based on extrapolation of present RFP experimental results;⁽³⁶⁾
- Sub-ignition operation with the possibility of anomalous ion heating (not assumed here) to further minimize the input power and plasma size while maximizing neutron wall load, thereby minimizing the time required for significant fluence;
- State-of-the-art resistive TF and PF coils to minimize ohmic power requirements in a compact (100-200 Mg) device;
- Steady-state oscillating-field current drive (F- θ pumping)^(37,38) consistent with the experimentally observed⁽³⁶⁾ RFP plasma dynamo;
- Impurity control by toroidal field divertors;^(39,40)
- Moderate beta (5-10%), consistent with experiment.⁽³⁶⁾

9.8.1 Concept Description

The RFP is a toroidal axisymmetric device in which the primary confining field, B_θ , is poloidal and is generated by a toroidal plasma current, I_ϕ .⁽⁴¹⁾ The RFP plasma supports a toroidal bias field, B_ϕ , to stabilize sausage and elliptical distortions. Gross MHD modes with wavelengths longer than the minor radius, r_w , of an electrically conducting shell are stabilized by the shell on a short time scale and by feedback coils for longer times. If the toroidal bias field is slightly reversed near the plasma edge, the resulting magnetic shear in the plasma-edge region stabilizes local pressure- and current-driven instabilities. This stabilization occurs at reactor-relevant values of plasma beta. A sample RFP profile is illustrated in Fig. 9-22, along with a corresponding tokamak profile.

The mere existence of the RFP profiles shown in Fig. 9-22 would seem unlikely because of the probable annihilation of opposing toroidal flux at the flux surface where reversal of the toroidal magnetic field occurs. Experiments and theory have shown^(36,41), however, that a self-reversed toroidal

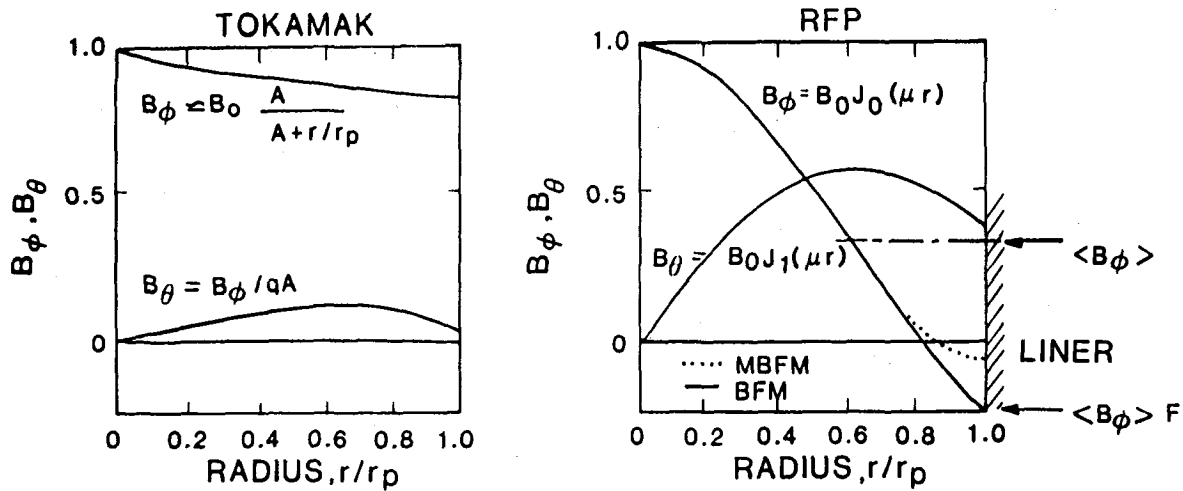


Figure 9-22. Magnetic field profiles along the minor radius for the RFP and the tokamak. Solid curves show Ressel Function Model (BFM) profiles and dashed curves show Modified Bessel Function Model (MBFM) profiles.

field and a minimum-energy state are generated even without imposing such a field externally. Given any arbitrary dissipation mechanism, the Taylor theory⁽⁴²⁾ predicts that a plasma surrounded by a flux-conserving shell will relax to a minimum-energy, force-free state. The key descriptive parameters in the Taylor theory are the pinch parameter, θ , and the reversal parameter, F , which are defined as $\theta = B_\theta(r_p) / \langle B_\phi \rangle$ and $F = B_\phi(r_p) / \langle B_\phi \rangle$, where $\langle B_\phi \rangle$ is the average toroidal field within the plasma radius.

The locus of minimum-energy states, as described in F - θ phase space, is shown in Fig. 9-23. The experimental F - θ traces show the tendency of the plasma to drift toward and reside within a specific region of F - θ space. Both the relaxation mechanism and associated time constants for the self-sustained toroidal-field reversal are not yet well explained. Nevertheless, strong experimental evidence exists for a plasma regeneration or "dynamo" mechanism that continually maintains the RFP state. Generally,^(44,45) either turbulence or resistive MHD instabilities drive this plasma dynamo action, wherein toroidal plasma currents are converted into the toroidal flux needed to maintain the toroidal-field reversal. An efficient dynamo is enforced in the plasma models during startup and burn by requiring adherence to the F - θ curve given on Fig. 9-23.

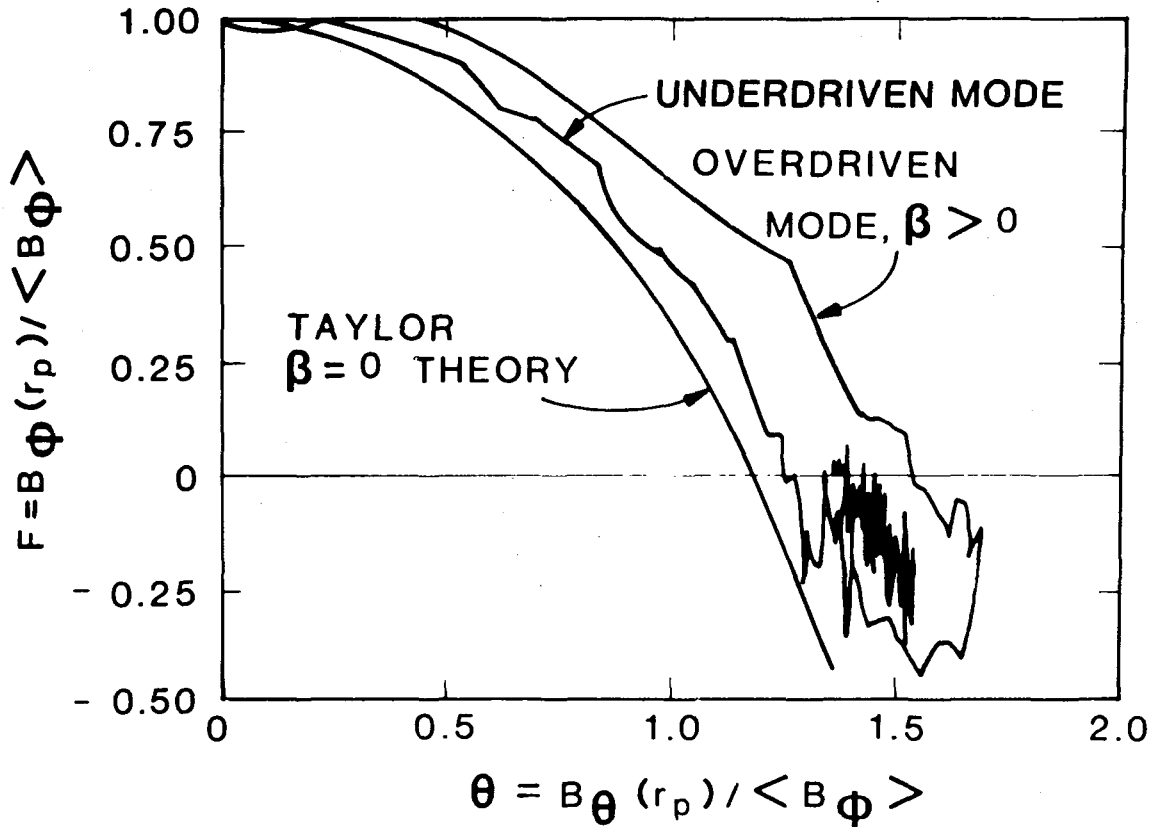


Figure 9-23. A diagram of $F = B_{\phi}(r_p) / \langle B_{\phi} \rangle$ versus $\theta = B_{\theta}(r_p) / \langle B_{\phi} \rangle$ showing two experimental traces and the tendency for the plasma to seek and reside within the predicted⁽⁴²⁾ RFP minimum-energy state.

Evidence for nearly classical resistivity in RFP plasmas exists,⁽⁴⁶⁾ giving a strong indication of an efficient plasma dynamo action. Unlike the tokamak, a close electrical coupling exists between the poloidal and toroidal circuits through the RFP plasma. This coupling also provides a means to drive toroidal current noninductively through low-frequency, low-amplitude field oscillations.^(37,38,47) Preliminary supporting experimental evidence was recently reported.^(36,37)

The relationship between F and θ , the tokamak safety factor, q , and beta points out the essential differences between an RFP and a tokamak. For either tokamak, RFP or spheromak, the total volume-averaged beta, $\langle \beta \rangle$, is related to the poloidal beta by $\beta_{\theta} / \langle \beta \rangle \approx 1 + (F/\theta)^2$. The tokamak-like state corresponds to $F \rightarrow 1$ and $\theta = F/Aq \rightarrow 1/Aq$, where A is the plasma aspect ratio. The

spheromak state corresponds to $F \rightarrow 0$ on the $F-\theta$ diagram. For the RFP state, $|F/\theta| \approx 0.13$ and $\langle \beta \rangle \approx \beta_\theta$, whereas for the tokamak $F/\theta = qA \approx 8-10$, with $\langle \beta \rangle$ being much less than $\beta_\theta \approx 1-2$. As a maximum, $\beta_\theta \lesssim A$ for the tokamak to avoid the ideal kink instability and, therefore, $\langle \beta \rangle \lesssim 1/Aq^2$. Accounting for profile effects in the RFP actually gives $\langle \beta \rangle \approx \beta_\theta/2$. The impact on the ohmic heating allowed in resistive coils for systems that can operate with low values of $|F/\theta|$, compared to those having large $|F/\theta|$ values (i.e., tokamaks), is significant. In addition, lower ohmic losses occur in the RFP poloidal-field coils for a given plasma current because of the higher aspect ratio and better inductive coupling between the coil set and plasma. Efficient use of resistive copper coils becomes practical for the RFP.

If a plasma dynamo maintains the reversed-field configuration, then the issue of enhanced plasma transport caused by the dynamo remains. Generally, the multiple-helicity, high-toroidal-mode-number field-line breaking and reconnecting that may be at the base of the RFP dynamo are expected to reduce energy confinement within internal regions of the plasma. A semi-empirical expression for the scaling of global confinement time has been obtained from small, ohmically-heated experiments of the form $\tau_E/r_p^2 = C_\nu I_\phi^\nu f(\beta_\theta)$ (Fig. 9-24). The parameters C_ν and ν have been calibrated with existing experimental results^(36,43), although direct experimental evidence for the r_p^2 and β_θ scaling remains to be generated.

Table 9-10 gives the parameters of the major RFP experiments around the world. This database has provided the foundation for the next major, mega-ampere RFPs presently under consideration by the US⁽³⁵⁾ and EEC⁽⁴⁸⁾ and supports the following generally description of "RFP performance":

- robust and efficient dynamo initiation and sustainment
- slow current ramp after low-energy formation
- constant-beta scaling ($nk_B T \propto I_\phi^2$)
- temperature increases with current
- confinement time increases with current.

For example, in ZT-40M,⁽³⁶⁾ the ease of RFP formation and dynamo sustainment have been demonstrated over a wide range of initial and machine conditions including fast-to-slow startup; high-to-low θ values; a range of field errors (including a loss of $\sim 1/3$ of the TF coils); a range of wall conditions and impurity levels; and low and high sawtooth activities.

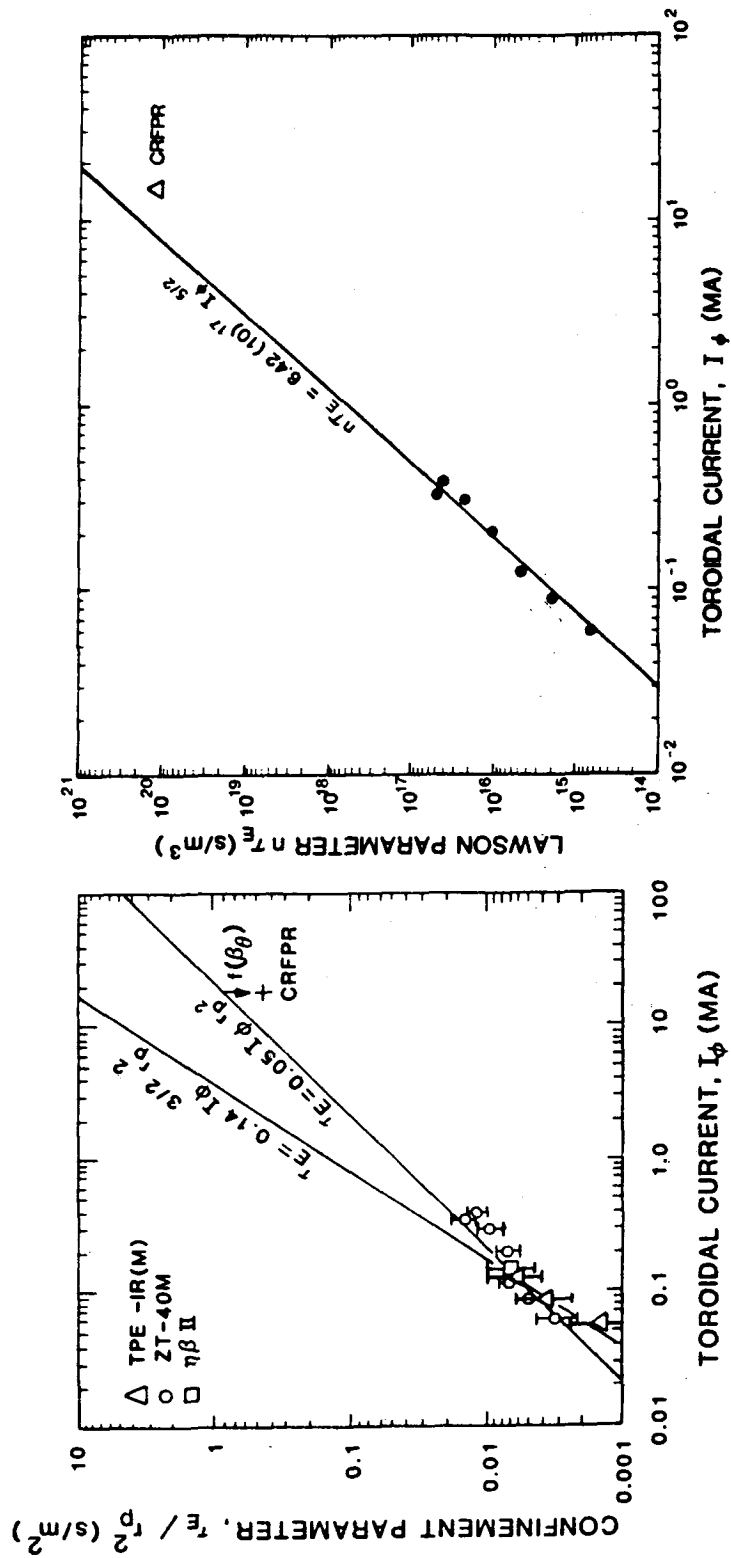


Figure 9-24. Scaling of plasma ohmic confinement time, τ_E , and confinement quality, nT_e , with plasma current.

Table 9-10. Status of Major RFP Experiments

Parameter	TPE-IR(M)	ETA-BETA-II	ZT-40M	OHTE-RFP	HBTX-1A ^a
Laboratory	Electro-Technical Laboratory (Japan)	Padova (Italy)	Los Alamos (USA)	General Atomic (USA)	Culham (UK)
Major radius, R_T (m)	0.5	0.65	1.14	1.24	0.8
Minor radius, r_p (m)	~0.09	0.125	0.2	0.2	0.26
Peak current, I_ϕ (kA)	130	150	440	500	320
Poloidal field at plasma, $B_\theta(r_p)$ (T)	0.42	0.24	0.44	0.53	0.25
Average density ($10^{20}/m^3$)	0.3	1	0.4-0.9	0.5-3.0	0.2
Current density, j_ϕ (MA/m ²)	5.1	3	3.5	4.5	1.5
Electron temperature (eV)	550	80	300-500	350-580	100
Typical pulse length (ms)	1-2	1-3	5-40	2-10	5-15
Poloidal beta, β_θ	~0.1	~0.1	0.1-0.2	0.1-0.2	~0.05
Discharge parameter, I_ϕ/N (10^{-14} A-m)	12.7	3	3-7	4.4	7.5
Energy confinement time, τ_E (ms)	~0.1	~0.1	0.3-0.7	~0.4	~0.03
Confinement parameter, $n\tau_E$ (10^{15} s/m ³)	~3	~10	12-60	~100	~0.6

^aHBTX-1A data obtained with a leak in the liner.

9.8.2 Representative Design

In principle, the coupled time-dependent plasma/first-wall circuits simulation and the systems analysis models used to select the RFP reactor design point^(40,43) could, after some modification, be used for a preliminary examination of a RFP test facility. Basic differences exist in the applied constraints, however. The resistive-coil reactor tends to minimize the fusion-power-core mass while simultaneously maximizing the engineering Q-value and plant efficiency. An optimal RFP test facility, on the other hand, would establish ceilings on total capital (fusion core size and support power) and operating (power and fuel requirements) costs for a system that maximizes neutron first-wall loading, device availability and experimental volume. Here, however, the reactor equations⁽⁴³⁾ were solved in steady state with future and more detailed study requiring time-dependent plasma/circuit simulations.

Since the objective is to maximize neutron flux (i.e., minimize time to achieve a given fluence) for a minimum total fusion power (i.e., minimize tritium consumption), a small driven RFP operating with both high plasma particle density and high current density was judged as being most appropriate; an ignited RFP would generate over 100 MW of fusion power. The effects of varying the electron streaming parameter (to assure reasonable margins on electron streaming in the high-current-density device), $\xi = (j_\phi/n_e)/v_{th}$; Z_{eff} ; plasma aspect ratio, A; scaling parameter, ν ; pinch parameter, θ ; and the amount of anomalous ion heating were explored. Both steady-state (F- θ pumping) current drive and (magnetic divertor) impurity control were assumed, but not quantitatively studied.

Representative results from the steady-state plasma simulations are shown in Fig. 9-25. A "design triangle" is defined by a minimum neutron wall load, $q_n > 1 \text{ MW/m}^2$, a maximum fusion power, $P_F < 100 \text{ MW}$, and a maximum surface heat flux, $q_s \leq 5 \text{ MW/m}^2$. Based on present ($I_\phi < 0.5 \text{ MA}$, $r_p \approx 0.15\text{-}0.2 \text{ m}$) and projected near-term experiments ($I_\phi = 2\text{-}4 \text{ MA}$, $r_p = 0.3\text{-}0.4 \text{ m}$), it was judged that $I_\phi \approx 10 \text{ MA}$ and $r_p \approx 0.3\text{-}0.4 \text{ m}$ represents a reasonable extrapolation from the next generation RFPs.

Figure 9-26 illustrates a simple model used to estimate the mass of, M_c , and power, $P_{\Omega c}$, dissipated in the coils in order to deliver a power, $P_{\Omega p}$, and current, I_ϕ , to a plasma of minor radius r_p and major radius R_T . More

$$Z_{\text{eff}} = 1.0, f_{\text{OHM}} = 0.0, A = 5.00,$$

$$\nu = 1.00, \xi = 0.006, \theta = 1.55$$

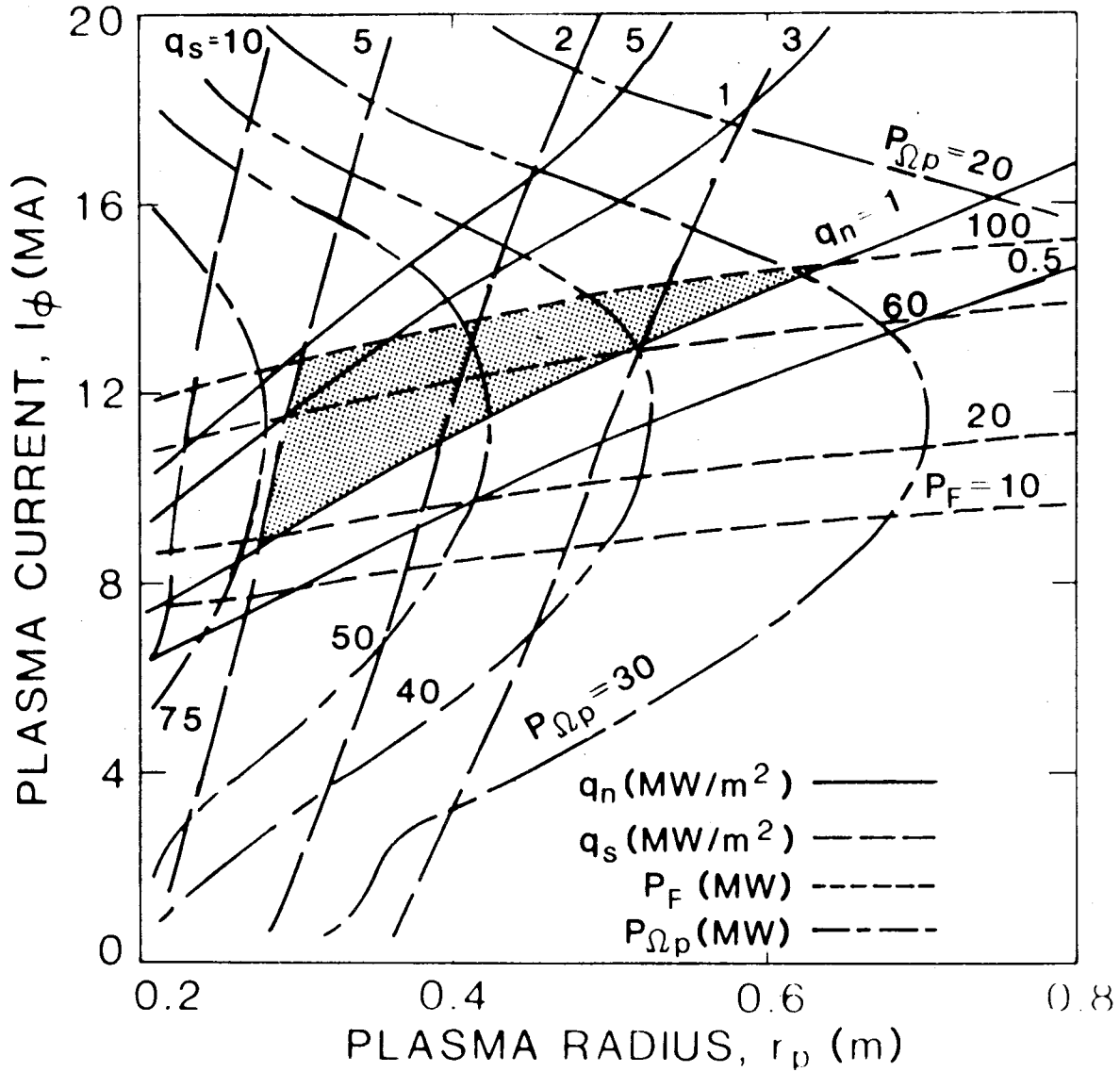


Figure 9-25. Dependence of plasma current, I_ϕ , on plasma radius, r_p , for a range of surface heat fluxes, q_s^ϕ , neutron wall loadings, q_n , ohmic power into the plasma, $P_{\Omega p}$, and fusion power, P_F . For all cases, the electron drift parameter, $\xi = 0.006$, the transport parameter, $\nu = 1$, and no anomalous ion heating was assumed. A "design triangle" is defined by $q_n > 1$ MW/m², $P_F < 100$ MW, and $q_s < 5$ MW/m².

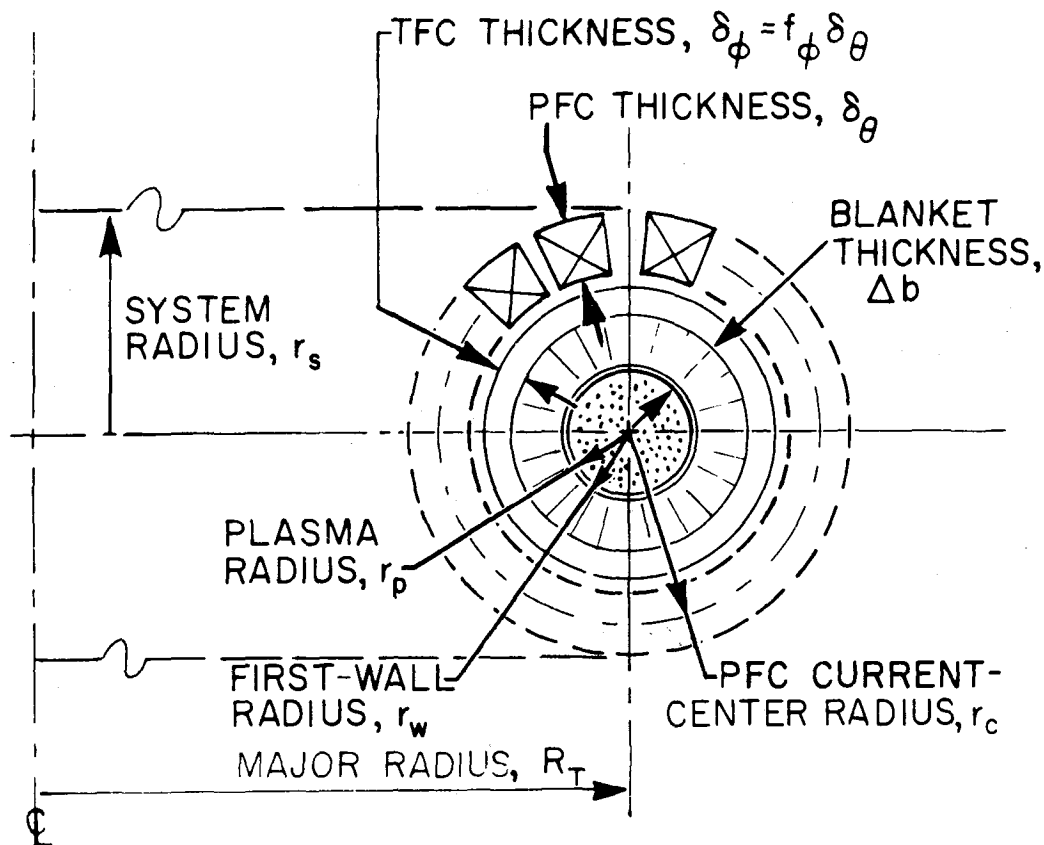


Figure 9-26. Geometry, dimensions, and notations used in preliminary engineering analysis of a RFP fusion facility.

detailed circuit and plasma equilibrium analyses are required of a final design, particularly with respect to startup scenarios, coil stresses and volt-second consumption. The tradeoff between PF coil thickness, δ_θ and plasma aspect ratio is given on Fig. 9-27. Selecting $A \approx 5$, based on near-optimal coupling of coil currents with plasma current, allows the dependence of the coil mass density and current density on the coil thickness to be displayed. The curves in Fig. 9-27 assume a blanket thickness of $\Delta b \approx r_w$. The impact of an ideally-coupled PF coil ($\Delta b = 0$) is also shown.

The coil power requirements are based on a bipolar inductive swing and peak current conditions. Preliminary estimates indicate that the inductive pulse would last for $\lesssim 10$ -20 s. Application of F- θ pumping to drive the plasma current would allow the current in the ohmic coil to be driven to zero;

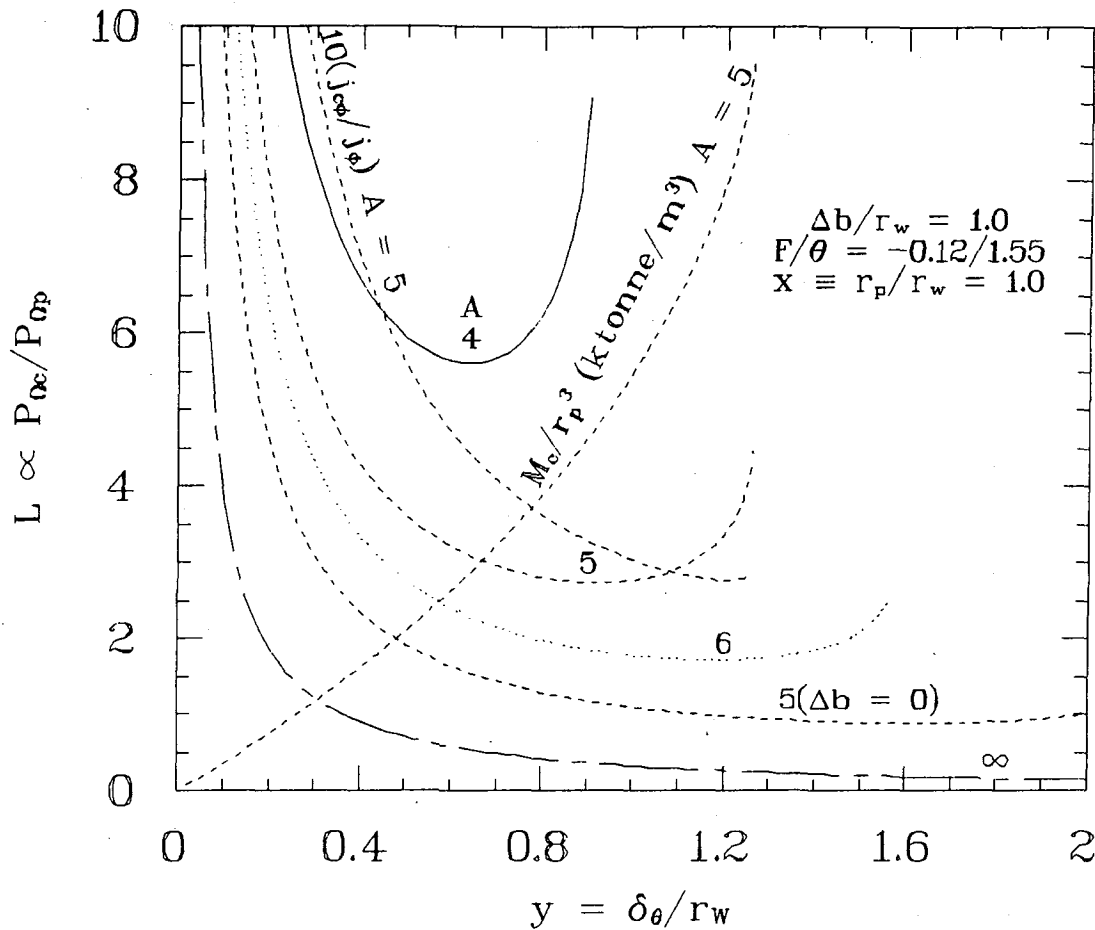


Figure 9-27. Dependence of ohmic power losses in PF coils relative to that in the plasma as a function of the coil thickness, δ_{θ} (normalized by the conducting first wall radius), the blanket thickness Δb , and the aspect ratio, A .

for the reactor case⁽⁴³⁾ the ohmic coil consumes $\sim 35\%$ of the total PF coil power. No estimates have been made of the reactive power losses in the F- θ pumping circuit for this RFP experiment, but it is assumed that the ohmic power requirements would be more than adequate if transferred to the F- θ pump current-drive system.

Table 9-11 summarizes geometric, plasma, and magnet characteristics for a single RFP fusion facility that would generate a neutron current of $1\text{--}5 \text{ MW/m}^2$ while maintaining a fusion power below 100 MW. The ohmic power delivered to the plasma is held below 75 MW, and the average surface heat flux on in-vacuum

Table 9-11. Parameters for a RFP Fusion Engineering Research Facility

Parameter	Fusion Neutron Wall Load	
	1 MW/m ²	5 MW/m ²
<u>Geometry</u>		
Plasma major radius, R_T (m)	1.50	
Plasma minor radius, r_p (m)	0.30 ^(a)	
Plasma aspect ratio, $A = R_T/r_p$	5.0	
Plasma shape	circular	
First wall area, A_{FW} (m ²)	17.77	
Blanket/shield thickness, Δb (m)	0.30 ^(b)	
Blanket/shield volume, V_{BLK} (m ³)	8.0	
<u>Plasma</u>		
Pinch parameter, $\theta = B_\theta(r_p)/\langle B_\phi \rangle$	1.55 ^(c)	
Reversal parameter, $F = B_\phi(r_p)/\langle B_\theta \rangle$	-0.12 ^(c)	
Poloidal field at plasma edge, B_θ (T)	6.27	8.67
Safety factor at plasma edge, $q(r_p)$	~0.016	
Poloidal beta, β_θ	0.072	0.065
Total beta, β	~0.04	
Average electron temperature, ^(d) T_e (keV)	3.94	6.14
Average ion temperature, ^(d) T_i (keV)	3.66	5.61
Average electron density, n_e (10 ²⁰ /m ³)	9.29	10.30
Impurity content, Z_{eff}	1.0	
Toroidal plasma current, I_ϕ (MA)	9.4	13.0
Toroidal plasma current density, j_ϕ (MA/m ²)	33.2	46.0
Lawson parameter, ^(e) $n\tau_E$ (10 ²⁰ s/m ³)	0.58	0.88
Ohmic power in plasma, $P_{\Omega p}$ (MW)	67.6	68.8
Fusion power, P_F (MW)	22.3	110.0
Plasma Q-value, $Q_p = P_F/P_{\Omega p}$	0.33	1.60
First wall average heat flux, q_s (MW/m ²)	4.1	5.1
Plasma loop voltage, V_ϕ (V)	7.19	5.29
Streaming parameter, ^(f) ξ	0.006	0.006
Plasma inductance, ^(g) L_p (10 ⁻⁶ H)	4.1	
Current drive ^(h)	F- θ pumping (to be modeled)	
Plasma resistive decay constant, L_p/R_p (s)	5.4	10.1

Magnets(i)

Total ohmic power to coils, $P_{\Omega c}$ (MW)	58.2	111.3
Toroidal field coils		
• thickness, δ_{ϕ} (m)		0.12
• current density, ^(j) $j_{c\phi}$ (MA/m ²)	10.1	13.9
• mass, M_{TF} (tonne)		44.9
Poloidal field coils		
• thickness, δ_{θ} (m)		0.30
• current density, ^(k) $j_{c\theta}$ (MA/m ²)	10.1	13.9
• mass, M_{PF} (tonne)		148.3
• PF coil inductance, ⁽ⁱ⁾ L_c (10 ⁻⁶ H)		1.18
• coil current, $I_{c\theta}$ (MA)	16.5	22.8
• solenoid flux, $L_c I_{c\theta}$ (Wb)	19.4	26.8
• coil L/R time (s)		7.2

- (a) Plasma radius taken at $T = 0$ surface and is greater than radius of reversal layer; first-wall and plasma radius taken here as equal.
- (b) Blanket/shield thickness assumed equal to first-wall radius.
- (c) Assumes reactor-like F and θ values.
- (d) Bessel-function model pressure profiles assumed, $P(r) \propto J_0^2(\mu r)$, with $n(r)$ and $T(r) \propto J_0(\mu r)$, with a consistent resistance form factor $g_{OHM} \approx 6.6$.
- (e) The experimentally calibrated scaling, $\tau_{ce} = 0.05 I_{\phi}(\text{MA}) r_p^2$, was used with $\tau_{pi} \approx 4\tau_{ce}$ and τ_E computed as the global energy confinement time. No anomalous ion heating was assumed.
- (f) The streaming parameter is $\xi = v_D/v_{th} = 3.33 \times 10^{17} j_{\phi}/n_e T_e^{1/2}$, where j_{ϕ} is in MA/m², T_e is in keV, and n_e is in 1/m³.
- (g) Taken as $L_p = \mu_0 R_T [\ln(8A) - 2 + 2\pi \ell_1/\mu_0]$, with the plasma internal inductance given by $\ell_1 \approx \mu_0/4\pi$ for the Bessel-function model.
- (h) Current drive power not estimated, but must supply at least the plasma ohmic losses (~ 70 MW). If $F-\theta$ pumping is used, $\sim 1/3$ of the PF coil power would be available after current drive is initiated.
- (i) Based on $\eta_c = 2 \times 10^{-8} \Omega\text{-m}$ and a 70% conductor fill fraction; $\Delta b = \delta_{\theta} = r_w$ assumed. Initial bipolar PF coil operation is taken over by $F-\theta$ pumping current drive once full plasma current is nearly established.
- (j) Current density in TF and PF coils equal; magnitude set by PF coil size and power consumption.
- (k) Taken as $L_c \approx \mu_0 R_T [\ln(8R_T/r_{c\theta}) - 2.0]$.

components is less than 5 MW/m^2 . The positions of these RFP FERF design points, as well as present and projected RFP devices, are shown on a Lawson diagram in Fig. 9-28.

The small size of the RFP fusion test facility designs gives L/R times for both the plasma and coil sets that are sufficiently short (7-10 and 20 s, respectively) that some form of current sustainment is even more desirable than for a reactor.^(40,43) A bipolar startup is envisaged, with the PF coils serving as an energy store used to initiate a low-current, low-energy (~ 0.5 - 1.0 keV) RFP; the inductive startup through a resistive transfer is sufficiently stressing and inefficient to preclude its use for attaining the final plasma conditions. The PF coil would be charged in reversed-bias conditions to a state not unlike the final, full-plasma-current condition. A resistive transfer in time $\tau_R = 1$ - 2 s would form an RFP that would subsequently be ramped in a time $\tau_L \gg \tau_R$ to the final steady-state plasma condition. This slow current ramp would initially be driven directly from the power grid ($< 100 \text{ MWe}$), with F- θ pumping possibly being applied prior to current flat-top once the plasma resistance becomes sufficiently low. The plasma would then be taken to the final conditions, and the F- θ pumping current drive would thereafter sustain the plasma. The ohmic coil current would then be allowed to decay slowly to zero.

Optimization of this startup and sustainment scenario to minimize power, flux, and technology requirements is a major area of future work. The devices suggested in Table 9-11 appear promising from both the viewpoints of cost (mass, energy, power) and performance, but the crucial tradeoff between coil cost and technology (i.e., voltage, power, and volt-second requirements) and the overall approach to the F- θ pumping drive coils remain to be made.

9.8.3 Development Needs

The RFP program is not yet ready to embark on a device of the class suggested in Table 9-11. The next-step RFP devices presently being proposed,⁽³⁵⁾ however, represent the necessary intermediate step to the RFP test facility (and ultimately for the RFP reactor), as these next-step devices aim for 2-4 MA plasma currents. Key technical issues in both physics and technology will be addressed. The major issues for the RFP test facility are:

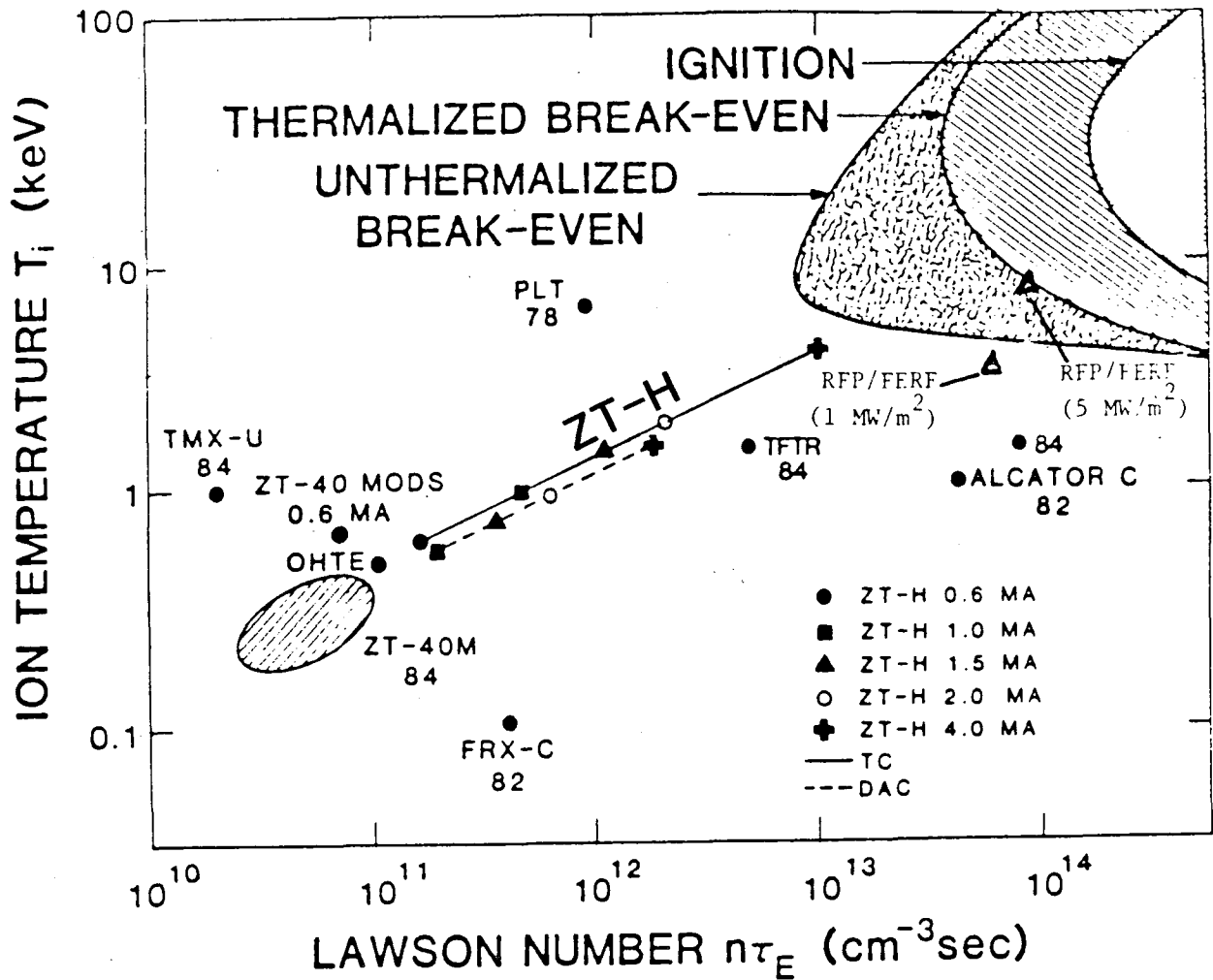


Figure 9-28. Lawson diagram showing projected ZT-H performance using Taylor/Connor (TC) and Diamond/An/Carreras (DAC) scaling.⁽³⁵⁾ The positions for the 1 MW/m^2 and 5 MW/m^2 neutron wall load RFP FERF designs are also shown.

- Extrapolation of the present RFP confinement scaling (0.1-0.5 MA experiments) to higher currents (7-10 MA) in plasmas of small to moderate size ($r_p = 0.3-0.4$, $A = 5-6$).
- The electrical (stabilizing) role of the conducting shell and the degree to which it can be segmented and the insulating gaps removed from the region of high neutron flux.

- The impact of non-axisymmetric perturbations, such as from limiters or divertors, on the toroidal-field reversal layer and associated stability and confinement.
- Feasibility and efficiency of F- θ pumping current drive, which to date has only been subjected to partial tests.
- Ability to handle high heat and particle fluxes from a small, high-power-density plasma.
- Effectiveness of pumped limiters or toroidal divertors in protecting in-vacuum components and removing impurities from the plasma, and the compatibility of both with the RFP dynamo and confinement.
- Degree to which anomalous ion heating in dense, ohmically heated discharges prevails to improve system performance within acceptable power and heat-flux limits.
- Optimal startup and sustainment of an ohmically driven RFP FERF.

Although many of these issues can be resolved only by experiments, further resolution or bounding of uncertainties and options can occur through design analysis and system modelling. Areas where more work, invention, and optimization are required include:

- Startup and control of a steady-state, subignited, ohmically-driven burn.
- Detailed tradeoff study of driven versus ignited plasma operation.
- Coil and power-supply requirements for F- θ pumping current drive.
- Startup and sustenance of poloidal flux requirements and PF coil designs for a maximum inductive pulse length.
- Design of impurity control systems, including edge-plasma phenomena, plasma-wall interaction, effect of divertor magnetics on the plasma, thermal-hydraulics and fueling.
- Fusion power core optimization, including capital versus operating costs, maintenance and other factors.

Preliminary models, estimates, and approaches for many of these issues have been suggested in Refs. 40 and 43. Application and extension of these models to describe the RFP fusion engineering research facility in more detail is warranted by the promise suggested in the designs presented here.

9.9 Comparison of Fusion Test Facilities

9.9.1 Introduction

Previous sections have defined the technical requirements for a Fusion Engineering Research Facility (FERF) and have described several candidate concepts, although these concepts have been analyzed to different levels of detail. This section will provide a comparison of their strengths and weaknesses. The approach is to characterize the concepts by a short list of distinct parameters that represent the overall attractiveness of the device.

The primary purpose of these test facilities is assumed to be technology testing. Consequently, the major parameters are those that summarize performance (as a test facility) as a function of cost and risk. Specific values were provided by the concept designers, except in several indicated situations where a consistent assumption has been applied to all designs.

The representative engineering test facilities considered here are:

(1) INTOR (1982 US FED/INTOR): A conventional reactor-relevant tokamak with ignited operation, inductively-driven current and RF heating. INTOR can provide full integrated testing of plasma and technology, including electricity production.

(2) LITE FERF: A driven version of the LITE ignition experiments. The LITE tokamaks incorporate a high-field copper magnet to achieve relatively high beta within conventional tokamak physics assumptions. This device is able to operate in normal (1 MW/m^2 and 500 s pulse), extended pulse (1000 s) and high power (2 MW/m^2) modes.

(3) "BEAN" FERF: A tokamak with moderate-field copper coils, a bean-shaped plasma to access a stable high beta regime, and quasi-ohmic heating to ignition.

(4) IDT-DTFC: A toroidal plasma configuration with joints on copper TF coils (and elsewhere) such that the entire core can be replaced in a single operation. The example considered here is a small inductively-driven tokamak with conventional ohmic heating and beta, but a correspondingly high electrical consumption.

(5) ST FERF: A representative spherical torus configuration with low fusion power, non-inductive current drive and a low magnetic field.

(6) TDF and MFTF- α +T: Relatively recent tandem mirror designs with neutral-beam driven test cells within the central cell region. The end plug magnet and thermal barriers are similar to TMX-U and MFTF-B configurations. TDF can operate in a high neutron wall load mode as considered here, plus a high plasma 0 mode. MFTF- α +T is an upgraded version of MFTF-B with the addition of a test cell, tritium burning capabilities, and (as assumed here) improved availability.

(7) RFP FERF: A representative configuration with copper coils and ohmic heating. Two RFP versions are considered, a 1 MW/m² normal and a 5 MW/m² extended version.

9.9.2 Performance

Performance is a measure of the FERF's ability to provide testing capability. The unique characteristics of fusion devices for technology are the potentially large test volume exposed to fusion-relevant neutrons and other environmental conditions. Consequently, the test performance parameters are related to geometry, neutron production, operating time, magnetic field and surface heat flux. Table 9-12 summarizes these performance characteristics for the representative FERF concepts.

These concepts generally meet or exceed the requirements defined in Section 9.2, with at least 1 MW/m² neutron wall loads, test volumes that can accommodate large test modules, and long pulse to steady-state operation. Significant magnetic field strength and surface heating are also present.

Since device availability and lifetime are important parameters that cannot be accurately predicted, consistent assumptions are adopted where possible. In particular, it is assumed that the test facilities have about a 15 year useful life, with 3 years of initial shakedown and physics testing with minimal neutron production, and the remainder with a gradually increasing availability. The effective availability for neutron operation is taken as 9 years at the ultimate availability. This availability should be as high as possible, but is unlikely to be better than 50%. For example, if the device operates on a 4 day/week, 24-hour schedule, then each run is 100 hours and the availability is 60%. With an additional 10 weeks of maintenance, experiment, and upgrading activities per year, the ultimate availability is about 45%.

Table 9-12. Performance Comparison of Fusion Engineering Research Facilities

	TOKAMAKS			SPHERICAL TORUS		TANDEM MIRRORS		REVERSE FIELD PINCH
	INTOR	LITE FERF	BEAN FERF	DTEC-IDT	FERF	TDF	MFTF- α +T	
Neutron wall loading, MW/m ²	1.3	1.0-2.0	1.3	2.0	1.0	2.1	2.0	1.0-5.0
Surface heat flux, MW/m ²	0.1	0.1	0.2	0.9	0.1	0.3	0.1	3.5-4.4
First wall radius, m	1.2	0.8	0.75	0.59	0.59	0.3	0.25	0.3
First wall area, m ²	380	72	110	40	31	8	4	18
Accessible test area, m ² (a)	38	7.2	11	4.0	3.1	4	2	3.5
Test port area/depth, m ² /m	2/1	1/1	1.5/0.8	1.2/1	1.6/0.8	1.6/0.8	0.8/0.8	1/0.3
Pulse length, s	200	500-1000	1000	520	SS	SS	SS	SS
Device duty cycle, % (a)	80	90	90	90	100	100	100	100
Run duration, h (a)	100	100	100	100	100	100	100	100
Ultimate availability, % (a)	35	45	45	45	45	45	45	45
Neutron fluence, MW-yr/m ² (b)	3.3	4.0	4.7	7.3	4.0	8.5	8.1	4.0-20
Fluence x Area/Year, MW-yr/yr	14	2.9	5.8	3.2	1.4	3.8	1.8	1.6-7.9
External field on-axis, T	5.5	5.5	3-6	8	3	4.5	4.5	7-9

(a) Consistent estimate.

(b) Assuming total equal to 9 years at ultimate availability.

This is assumed for all the devices, with the exception of INTOR. Due to its dependence on tritium breeding blankets, a reduction in availability of 10% is assumed.^(1,5) MFTF- α +T states a design availability of 10%,^(3,31) and is based on an upgrade of an existing physics experiment facility whose design and operation may or may not permit ambitious improvements in availability and lifetime. However, in the absence of specific limits, it is assumed here that levels of availability can be achieved consistent with the other test facilities.

The maximum fluence is based on the consistent lifetime and availability values adopted here. Although not particularly high, it is possible that these fluences exceed actual design limits. Note that duty cycle must be considered in addition to the availability in determining fluence.

The accessible test area is the first wall area associated with large test volumes (both in area and depth) that can be accessed from the exterior for coolant, purge and instrumentation lines and for module removal. Additional smaller test spaces may also be available. This test area is assumed to be 10% of the total first wall area in low aspect ratio toroidal devices, 25% in higher aspect ratio devices (RFP) and 50% of the central test cell area in mirrors. For example, in tokamaks, it is based on the outboard first wall area between magnet coils horizontally and about equal to the plasma height vertically, with allowance for pumping, heating and other penetrations. It is possible that the available test area may exceed that which can reasonably be used (e.g., 20 m²⁽¹⁾), but this was not considered as a factor in this comparison (only INTOR had a very high potential surface area).

9.9.3 Costs

The capital cost is probably the single most limiting parameter when considering experiments over 100 M\$. Operating costs can also require large annual commitments in some cases due to the need to supply large amounts of electricity or tritium. Table 9-13 summarizes the power, tritium consumption and electrical consumption characteristics of these devices, as well as the capital, annual and total cost (in 1985 dollars). Detailed costs were not available for many of the FERF concepts, and those that were available are not necessarily consistent even though they are based on standard accounts and

Table 9-13. Cost Comparison of Fusion Engineering Research Facilities

	TOKAMAKS			SPHERICAL TANDEM MIRRORS			REVERSE FIELD PINCH	
	INTOR	LITE FERF	BEAN FERF	DTFC-IDT	TORUS FERF	TDF		MTF-a+T
Fusion power, MW	620	90	185	100	39	36	17	22-110
Tritium consumption, kg/yr	5.8(a)	2.0	4.1	2.2	0.97	0.90	0.42	0.55-2.8
Electrical consumption, MWe	200	210-270	185	427	120	250	104	126-180
Total capital cost, M\$(b)	2800	900	1200	1200	700	1200	600	700-800
Annual operating costs:								
Electricity, M\$/yr(c)	24	37	33	76	24	49	20	25-35
Tritium supply, M\$/yr(d)	87	30	62	33	15	14	6.3	8.2-42
Operation, M\$/yr(e)	140	45	60	60	35	60	30	35-40
Total, M\$/yr	251	112	155	169	74	123	56	68-117
Total cumulative cost, M\$(f)	5500	2000	2800	2900	1500	2500	1200	1400-2000

(a) Assuming TBR=0.6

(b) Consistent estimates

(c) 0.05 \$/kWe-h

(d) 15,000 \$/g

(e) 5%/yr of total capital cost

(f) 3 yrs operation only plus 9 years at ultimate availability

algorithms similar to those used in FEDC/INTOR.⁽⁴⁹⁾ A consistent independent evaluation of the costs was not performed. However, certain rules have been adopted in order to provide a more consistent cost basis.

The capital cost includes direct and indirect costs. The total capital costs are assumed to be a factor of two larger than the direct costs, including engineering, installation and contingency (45, 15 and 40% of direct costs, respectively).⁽⁵⁾ These costs do not include those associated with test ports and test modules. The direct capital cost will vary substantially among the concepts, depending on many factors. The most important parameters are the total power handled (electrical power plus fusion power) since this reflects the size and capacity of the heat transport, magnet and electrical systems, and the plasma length since this relates to the size of the vacuum vessel, support structure and building. Figure 9-29 illustrates the total power and plasma length for several experimental fusion devices, along with direct capital cost if available. Assuming that capital cost is approximately linear in the power and length, then estimated direct capital costs can be obtained for the FERF concepts.

The annual costs are divided into electricity, tritium supply and operations. Other than INTOR, these concepts consume amounts of tritium that can in principle be obtained from external sources such as CANDUs.⁽¹⁸⁾ A tritium-producing blanket increases design complexity, and consequently tritium is assumed to be supplied by external sources at 15,000 \$/g, except for INTOR with an internal tritium breeding ratio of 0.6.⁽⁵⁾ Electricity, assumed significant only during operation, is costed at 0.05 \$/kWh.

Operating cost estimates were analyzed in some detail for INTOR, including tritium, electricity, material (~5% of direct capital cost), maintenance (~5% of direct capital cost per year), decommissioning (20% of direct capital cost), personnel (other than maintenance, about 500 people), and a 5% contingency. This led to an equivalent annual rate of ~10% of the direct capital cost per year. The TASKA and TASKA-M studies assumed 3%/year of the total cost.^(32,33) For comparison, TFTR (320 M\$ as of 12/82) is currently operating with a total budget of roughly 100 M\$/yr. Experimental fission reactor operating costs range from 60 M\$/yr for FFTF (sodium-cooled, 400 MWth), 20 M\$/yr for EBR-II (sodium-cooled, 62 MWth), and 4 M\$/yr for ORR (water-cooled,

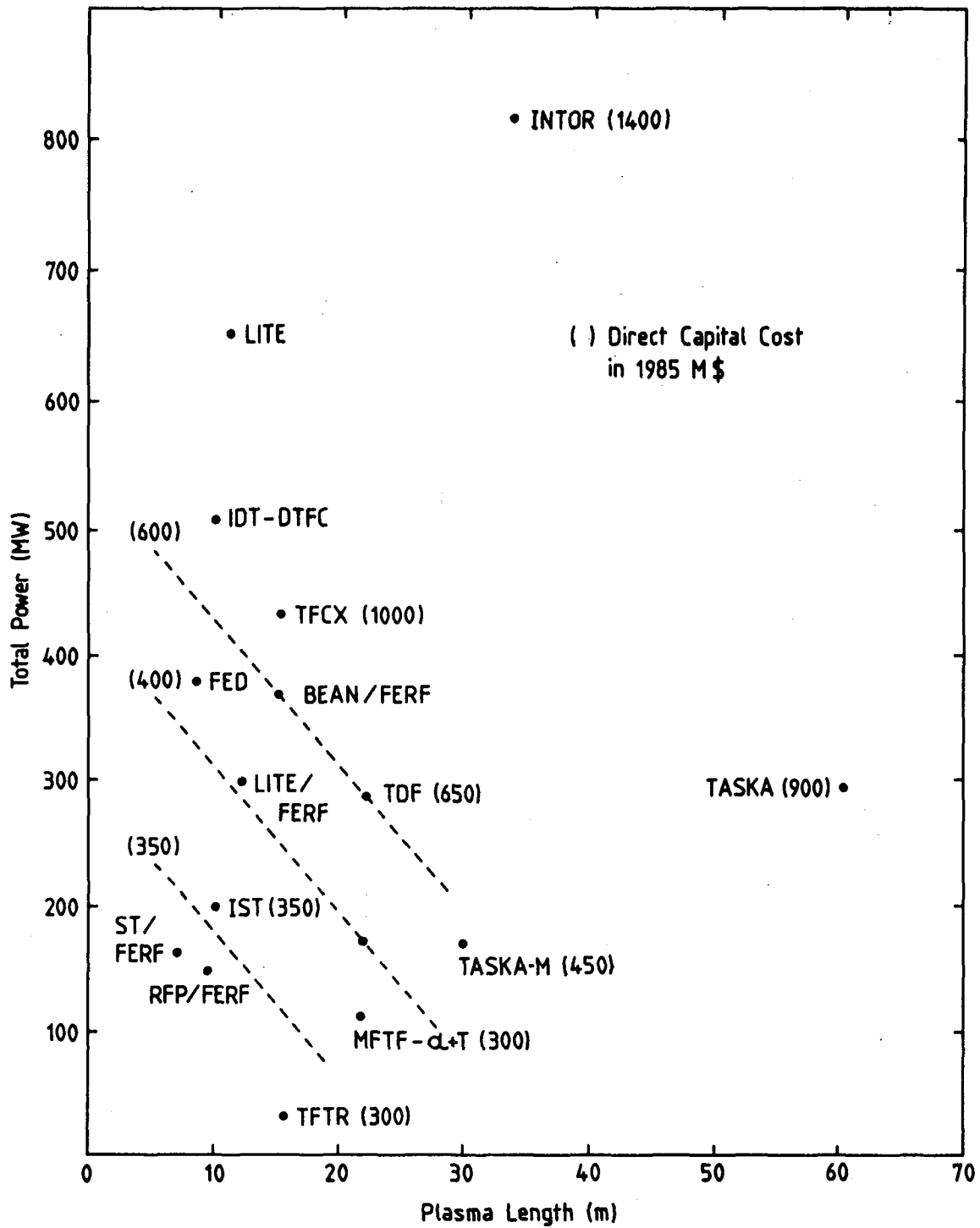


Figure 9-29. Direct capital cost of various fusion test facilities relative to the total power transferred (electrical and plasma) and the fusion core size (as represented by the plasma axial length).

30 MWth). Here, annual operating costs other than tritium and electricity are assumed to be 10% of the direct capital cost, or 5% of the total capital cost.

The total costs are based on 3 years of operating expense only (low availability during shakedown and physics testing), and 9 years at the ultimate availability including tritium and electricity (a total of 15-20 years of operation with a more realistic improvement in availability). Power consumption is neglected during the dwell part of the duty cycle and during startup.

9.9.4 Risk

These facilities will be the first test of many components in a fusion nuclear environment. Each facility (or test port) must be tolerant of possible test module failures since identifying failure modes and lifetime is a primary purpose of these tests. However, it is not desirable for the test facility itself to fail. The facility is viewed as a means to provide fusion nuclear technology testing, and is not directly the test itself. Of course, there are sufficiently few fusion nuclear devices planned that substantial information will be obtained from operating the FERF.

The risk is divided into physics and technology risk. The former relates to the ability to confine, heat and control the plasma. The latter describes the various hardware and systems.

Risk is difficult to quantify and compare since the concepts are so different and have a very limited data base. To some degree, global risk parameters with respect to existing machines may be inferred from plasma confinement characteristics (e.g., $n\tau, T$) and by device fluence or availability. Clearly, the physics data base for tokamaks is better than for the other concepts, and no device has yet operated entirely in a FERF regime. However, the relevance of the data base to some concepts is not clear (e.g., tokamak data for spherical tori). Consequently, it is not possible to unambiguously quantify the degree to which a projected device confinement exceeds the available data. Also, present devices are so far from fusion test facility fluence conditions (e.g., TFTR will achieve about 10^{-8} MW-yr/m²) that there is little basis for direct comparison of technology risk.

Nonetheless, each concept has a different level and nature of risk that can be indicated at least qualitatively (e.g., INTOR). To this end, Table 9-14 indicates the risk for each FERF concept considered here in terms of extrapolating from present experimental programs. Present experiments include, for example, TFTR and JET for tokamaks, TMX-U and TARA for mirrors, and ZT-40 for RFP's, but not TFCX, MFTF-B, or ZT-H. With respect to technology, present experiments include the Large Coil Project and TSTA, for example, but not ALT-II. The risk is assessed separately for all major physics and technology functions. Three levels of risk or extrapolation are adopted:

- Moderate: - Moderate extrapolation from existing data base;
- FERF will still meet most objectives if performance is not as good as anticipated but no worse than presently achievable;
- No additional testing beyond existing experiments is required for FERF design;
- Large: - Large extrapolation from existing data base;
- Risk can be substantially reduced by experiments in relatively small fusion devices or non-fusion test facilities;
- Very large: - Very large extrapolation from existing data base;
- FERF behavior/availability will not be acceptable if performance is no better than presently achievable;
- Major additional testing required before FERF, such as a new physics device or significant technology development program.

Table 9-15 summarizes the high risk areas and the concepts most affected. Further discussion is provided in the appropriate concept sections.

9.9.5 Summary

From the previous characterizations of possible FERF concepts with respect to performance, cost and risk, it is possible to extract a short set of key discriminating parameters as in Table 9-16.

The irradiation capability, or the ability to provide neutrons, includes the neutron wall loading, device availability and test area (which is defined to include regions with adequate depth). Clearly, the larger these device parameters are, the quicker tests can be completed. These parameters can be

Table 9-14. Risk Comparison of Fusion Engineering Research Facilities (a)

	TOKAMAKS						SPHERICAL			TANDEM MIRRORS		REVERSE	
	INTOR	LITE FERF	BEAN FERF	DTFC-IDT	TORUS FERF	TDF	MFTF- α +T	PINCH	FIELD				
Plasma operating mode ^(b)	I	D-I	I	I	D	D	D	D	D				
<u>Physics Risk</u>													
Confinement	M	M	V	L	V	L	L	V	V				
Exhaust and impurity control	L	L	L	L	L	L	L	V	V				
Fuelling	M	M	L	M	L	M	M	L	L				
Heating	M	M	L	M	L	M	M	L	L				
Burn length	M	M	M	M	V	M	M	V	V				
Plasma control	M	M	V	L	L	M	M	V	V				
<u>Technology Risk</u>													
Magnets and shielding	M	L	V	V	V	L	L	L	L				
Exhaust and impurity control	L	L	L	V	L	L	L	V	V				
Heating	L	L	L	L	L	L	L	L	L				
Tritium	V	M	M	M	M	M	M	M	M				
Burn length	M	M	M	M	V	M	M	V	V				
Maintainability	L	L	L	L	L	M	M	L	L				
Balance of plant	M	M	M	M	L	M	M	M	M				

(a) Moderate (M), Large (L) or Very large (V) extrapolation from present experiments.

(b) I - ignited, D - driven

Table 9-15. Major Risk Factors for FERF Concepts

Risk Area	Devices Affected	Comments
<u>Physics</u>		
Impurity control	RFP	$Z_{\text{eff}} \sim 2-4$ over 40 ms in present devices with bumper limiters; RFP magnetic field configuration complicates direct application of tokamak divertor and limiter data.
Second stability regime	Bean tokamaks	Existence and access to second stability high beta regime.
Transport scaling	Bean tokamaks Spherical torus Small A tokamaks	Transport in second stability regime, and transfer to this regime. Low aspect ratio scaling. FERF has $A \sim 2$, present tokamaks have $A \sim 2.4-5$.
F-0 pumping	Spherical torus RFP	No tokamak experiment, some RFP data
Plasma control	RFP	Need for close conducting shell.
Thermal barrier	Tandem mirror	End plug effectiveness in reducing losses; experiments underway in TMX-U and TARA
<u>Technology</u>		
Exhaust/impurity control	Tokamak Spherical torus RFP	Erosion of leading edges; Thermal stress and heat transfer limits; Surface coating/tile attachment.
Tritium breeding	Conventional tokamak	Large fusion power devices need to reliably provide over 50% of own tritium
High field copper magnets	High-field tokamak Spherical torus Tandem mirror RFP	Development of copper coils with high strength and conductivity; Inorganic (radiation-resistant) insulators; Improved current density and heat transfer; Improved welding/bonding methods between conductor and structure.
Current drive	Spherical torus RFP	Needed for confinement, pulse length and heating; Physics and technology needs uncertain.

Table 9-16. Summary Characteristics of Fusion Engineering Research Facilities

	TOKAMAKS				SPHERICAL		TANDEM MIRRORS		REVERSE FIELD PINCH
	LITE		BEAN		TORUS				
	INTOR	FERF	FERF	FERF	FERF	FERF	TDF	MFTF- α +T	
Neutron wall load, MW/m ²	1.3	1.0-2.0	1.3	2.0	1.0	1.0	2.1	2.0	1.0-5.0
Fluence x Area/Year, MW-yr/yr	14	2.9	5.8	3.2	1.4	1.4	3.8	1.8	1.6-7.9
Pulse length, s	200	500-1000	1000	520	360,000	360,000	360,000	360,000	360,000
Physics risk ^(a)	2	1	7	3	8	8	2	2	10
Technology risk ^(a)	5	4	5	6	8	8	3	3	7
Total capital cost, M\$	2800	900	1200	1200	700	700	1200	600	700-800
Annual operating cost, M\$	251	112	155	169	74	74	123	56	68-117
Total cost/useful neutron ^(b)	4	7	5	9	11	11	6	7	9-2
Useful neutrons/cost/"risk" ^(c)	4	3	2	1	1	1	3	3	1-2

(a) Larger values indicate higher risk; based on risk contributors in Table 9-14.

(b) (Total cost)/(Annual fluence*area) rounded to nearest leading digit.

(c) (Annual fluence*area)/(Total cost)(Physics+Technology Risk) rounded to nearest leading digit.

traded amongst each other within certain bounds without affecting overall attractiveness. For example, a lower neutron wall load but a higher device availability could still lead to the same fluence achieved per year. And a larger test area could also substitute for neutron wall load, for example, since the overall test requirements include the need for completing a variety of tests, and increased test area would allow more tests to be conducted simultaneously. Thus, the product of neutron wall load, availability and test area is used for this parameter, or the average neutron power available for testing (MW-yr/yr). This is more useful than a parameter based on total integrated fluence since the test programs are constrained in time, and devices should be preferred that achieve the same integrated fluence over shorter periods of time.

The ability to provide fusion reactor relevant conditions is expressed by the degree of required scaling. All the fusion device concepts considered possess many characteristics of a fusion reactor, and would provide unique testing of system integration aspects, instrumentation and control in a noisy environment, tritium, activation, mechanical and thermal loads, vacuum and impurities, and so on. Magnetic fields are typically at least 1 T, and more often higher. Of all the parameters, perhaps the most critical for duplicating reactor conditions is the neutron wall loading. As discussed earlier, this should be at least 1 MW/m² for simulating reactor conditions at 5 MW/m². Even at 1 MW/m², considerable but plausible extrapolation is required to predict operation at reactor levels. So there is certainly advantage in operating at higher neutron wall loads. In addition, many device parameters are at least indirectly related to neutron wall load, so larger neutron loads generally imply that all parameters are more reactor-relevant.

Finally, present fusion concepts often operate in a pulsed mode for reasons of cost or physics risk (steady-state operation has not been demonstrated for any fusion device). However, fusion reactors are anticipated to have at least long burn lengths. Since pulsing introduces thermal and mechanical variations that can lead to fatigue or other effects, it is desirable to minimize these from the point of view of simulating reactor conditions. Thus the third performance parameter is the burn length capability, or the pulse length here since the present concepts all have high duty cycle and are assumed to be able to operate for 100 hrs continuously.

Summary risk parameters are desirable to represent "overall" physics and technology extrapolation from presently active experimental programs. A crude measure of "overall" risk could be based on the sums of the subsystem extrapolations or risks identified in Table 9-14, where zero "risk" points are assigned for a moderate extrapolation, one point for a large extrapolation, and two points ("twice the risk") for a very large extrapolation. As noted earlier, it must be clearly recognized that estimates of risk, particularly "overall" risk, are difficult. A possible alternative approach to providing a quantitative risk parameter would be to estimate the cost of development and testing required to achieve a common level of understanding.

The major cost parameters are the capital and annual operating cost as given in Table 9-13. Two possible cost-benefit figure-of-merit are also included - the cost per useful neutron (based on the total cost and the annual fluence/area product), and the useful neutrons per unit cost and "risk" (where risk is based on the sum of the physics and technology risk points). These cost-benefit parameters provide some normalization of the data, but must be interpreted with due caution.

Some observations may be made from the comparison (Table 9-16). First, all concepts provide reasonable performance for technology testing - the minimum requirements identified earlier are 1 MW/m^2 neutron wall load, 1 MW of irradiation capability (e.g., 1 MW/m^2 over 5 m^2 test area at 20% availability each year), with pulse lengths over 500 s. The physics risk is lowest for driven, moderate-beta, moderate-aspect-ratio tokamaks. The technology extrapolation is lowest for tandem mirrors with moderate end plug designs. Uncertainties with respect to magnets (e.g., choke-coils versus large high-field TF coils), exhaust (e.g., erosion and heat removal from plasma interactive components) and heating (e.g., continuous neutral beams and long-pulse RF antennae) are comparable overall to tokamaks, but linear systems have some advantage in ease of maintenance. The tandem mirror also provided the lowest cost consistent with the performance requirements.

The cost per neutron figure-of-merit indicates the economy of scale - INTOR is the largest device and provides considerably more potential test area (although there are some questions as to its practical utility) without a corresponding large increase in cost. The spherical torus and reverse field pinch offered relatively low total power, but were also sufficiently small that the irradiation capability was limited.

9.10 Conclusions

There are two underlying questions in this chapter. First is the usefulness of a fusion device specifically for technology testing. The alternative strategy relying on combined physics and technology devices such as FED, INTOR, FER and NET has been or is being pursued in several countries. Several reasons to separately provide testing of nuclear components have been advanced, most recently in Ref. (1). These include the potential for lower risk and cost, higher availability leading to faster testing, and more device options. In this chapter, concepts that could provide such a test facility have been identified and evaluated to assess the plausibility of the fusion engineering test facility concept.

In this respect, it is clear that there exist a wide variety of possible Fusion Engineering Research Facility concepts. Indeed, it seems that any magnetic configuration that has unique advantages for a fusion reactor could also provide unique advantages as a test facility. On the other hand, there is at present no facility design that can easily be built under present US budget limitations without some international framework. A technology test facility may not be as costly as a combined physics/technology device, but is still an expensive proposition. This is perhaps not surprising since costs are driven by the presence of neutrons and by the overall power level handled. With present concepts, ignited fusion devices (low electrical consumption) generally require high fusion power, while driven fusion devices (low fusion power) generally require high electrical power.

The second question is whether a particularly attractive technology test facility concept can be identified for further study and/or optimization. All the devices considered would be useful test facilities. If the facility must be built in the near-term, then low risk is important and the options are either a moderate-beta moderate-field tokamak or a tandem mirror with a simple test cell and end plugs. Tokamaks have a much more extensive data base but tandem mirrors offer lower device cost because they can access the lower limits of useful testing performance. Tokamaks have the advantage in unit cost-effectiveness. A high performance RFP could provide an interesting alternative if the high physics and technology risks are acceptable or can be reduced by other experiments.

Finally, several areas for improvement in fusion test facility designs are suggested by this comparison. With respect to designs, the importance of reducing the total device power (fusion plus electrical) and maintaining a reasonable amount of test area is emphasized. Better definition and assessments of the useful test volume and of the device costs are also needed to support a useful comparison. With respect to experiments, common high risk technologies are the magnets and plasma interactive components. Development of these specific technologies could reduce these risk contributors and allow improved performance. And for many concepts, it appears that a single non-DT physics experiment could be performed that could verify the assumed physics scaling and essentially make a subsequent DT fusion engineering research facility a low-to-moderate physics risk device.

REFERENCES FOR CHAPTER 9

1. M. Abdou, et al., "FINESSE, A Study of the Issues, Experiments and Facilities for Fusion Nuclear Technology Research & Development (Interim Report)," University of California, Los Angeles, PPG-821, also UCLA-ENG-84-30 (October 1984).
2. C.A. Flanagan, D. Steiner, G.E. Smith, et al., "Initial Trade and Design Studies for the Fusion Engineering Device," ORNL/TM-7777, Oak Ridge National Laboratory, June 1981.
3. K.I. Thomassen and J.N. Doggett, "Options to Upgrade the Mirror Fusion Test Facility," UCID-19743, Lawrence Livermore National Laboratory, 1983.
4. "A Tandem Mirror Technology Demonstration Facility," UCID-19328, Lawrence Livermore National Laboratory, Livermore, 1983.
5. W.M. Stacey et al, "US FED/INTOR Critical Issues," USA FED-INTOR/82-1, October 1982.
6. R. Toschi, "Objectives and Main Features of the Next European Torus Project," Fusion Tech., 1(2), 201 (1985).
7. T. Tone, N. Fujisawa and M. Sugihara, "Status of Fusion Experimental Reactor (FER) Design," Fusion Tech., 1(2), 214 (1985).
8. G. Navratil, "Large Aspect Ratio, High-beta Tokamak Fusion Reactor," Columbia University, Report # 98, DOE/ET/53016-87, 1985.
9. D. L. Smith, et al., "Blanket Comparison and Selection Study - Final Report," Argonne National Laboratory, ANL/FPP-84-1, September 1984.
10. C. D. Henning, et al., "Mirror Advanced Reactor Study - Final Report," Lawrence Livermore National Laboratory, UCRL-53480 (1984).
11. M. Abdou, et al., "Engineering Testing," Ch. XII, FED-INTOR/TEST/82-4 (1982).
12. G.T. Sager, G.H. Miley, J.F. Baur and I. Maya, "Plasma Instrumentation for Fusion Power Reactor Control," 6th Top. on Tech. of Fusion Energy, San Francisco, California, March 3-7, 1985.
13. F. Arendt, et al., "CORIANDER: Comparison of Relevant Issues and Nuclear Development for Fusion Energy Research," KfK 3919 and FPA-84-7, Kernforschungszentrum Karlsruhe, 1984.
14. J. Grover, Hanford Engineering Development Laboratory, private communication, 1985.
15. B. Coppi, "Advanced Fusion Burning Core Experiment," Massachusetts Institute of Technology, Report PTP-84/16, August 1984.

16. L. Bromberg, et al., "Long Pulse Ignition Test Experiment, Version R3," in preparation, Massachusetts Institute of Technology, 1985.
17. N. Hoffman, Energy Technology Engineering Center, personal communication, 1984.
18. T.S. Drolet, K.Y. Wong and P.J.C. Dinner, "Canadian Experience with Tritium - The Basis of a New Fusion Project," Nucl. Tech./Fusion, ___, ...
19. Y-K.M. Peng, "Spherical Torus, Compact Fusion at Low Field," ORNL/FEDC-84/7, Oak Ridge National Laboratory, February 1985.
20. Y-K.M. Peng, "Features of Spherical Torus Plasmas of Ultra-Low Aspect Ratio and Large Elongation," EPS mtg. on Plasma Phys. and Cont. Fusion, Budapest, Hungary, September 2-6, 1985.
21. D.L. Jassby, Comm. Plasma Phys. and Contr. Fusion, 3, 151 (1978).
22. Y-K.M. Peng and R.A. Dory, ORNL/TM-6535, Oak Ridge National Laboratory (1978).
23. N.J. Fisch and C.F.F. Karney, PPPL-2132, Princeton Plasma Physics Laboratory (1984).
24. K.F. Schoenberg et al., J. Appl. Phys. 56, 2519 (1984).
25. P.M. Bellan, Phys. Fluids, 27, 2191 (1984).
26. Y-K.M. Peng et al., "Spherical Torus: An Approach to Compact Fusion at Low-Field - Initial Ignition Assessments," Fusion Tech., 8(1), 338 (1985).
27. R.D. Stambaugh et al., in Plasma Phys. Contr. Nucl. Fusion Res., (IAEA, Vienna 1985) Vol. 1, 217 (1985).
28. D. Palumbo, Nuovo Cimento, 53, Part B, 507 (1968).
29. J.B. Taylor, Phys. Rev. Lett., 33, 1139 (1974).
30. T.H. Batzer et al., "Conceptual Design of a Mirror Reactor for a Fusion Engineering Research Facility (FERF)," UCRL-51617, Lawrence Livermore National Laboratory, 1974.
31. W.D. Nelson, "MFTF- α +T Progress Report," ORNL/FEDC-83-9, Fusion Engineering Design Center, Oak Ridge National Laboratory, 1985.
32. B. Badger, et al., "TASKA, A Tandem Mirror Fusion Engineering Facility," UWFDM-500, KfK-3311, FPA-82-1, University of Wisconsin-Madison, March 1982.
33. B. Badger, et al., "TASKA-M: A Low Cost, Near Term Tandem Mirror Device for Fusion Technology Testing," FPA-83-7, KfK-3680, UWFDM-600, Fusion Power Associates, December 1983.

34. "Fusion Engineering Test Facilities based upon Mirror Plasma Confinement," Nuclear Eng. & Design/Fusion, Special Issue, 2(3), 1985.
35. P. Thullen and K.F. Schoenberg (eds.), "ZT-H Reversed-Field Pinch Experiment Technical Proposal," Los Alamos National Laboratory report LA-UR-84-2601 (1984).
36. R.S. Massey, et al., "Status of the ZT-40M RFP Experimental Program," Fusion Tech., 1(2), 1571 (1985).
37. K.F. Schoenberg, et al., "F- θ Pumping and Field Modulation Experiments on a Reversed Field Pinch Discharge," Phys. Fluids 27 (3), 548 (1984).
38. K.F. Schoenberg, R.F. Gribble and D.A. Baker, "Oscillating Field Current Drive for Reversed Field Pinch Discharges," J. Appl. Phys. 56 (9), 2519 (1984).
39. C.G. Bathke and R.A. Krakowski, "A Comparison Study of Toroidal- Field and Bundle Divertors for a Compact Reversed-Field Pinch Reactor," Fusion Tech., 1(2), 1616, (1985).
40. C. Copenhaver, et al., "Compact Reversed-Field Pinch Reactors (CRFPR): Fusion-Power-Core Integration Study," Los Alamos National Laboratory report LA-10500-MS (August 1985).
41. H.A.B. Bodin and A.A. Newton, "Review Paper: Reversed-Field Pinch Research," Nucl. Fus. 20, 1255 (1980).
42. J.B. Taylor, "Relaxation of Toroidal Plasma and Generation of Reversed Magnetic Field," Phys. Lett. 33, 1139 (1974).
43. R.L. Hagenson, et al., "Compact Reversed-Field Pinch Reactors (CRFPR): Preliminary Engineering Considerations," Los Alamos National Laboratory report LA-10200-MS (August 1984).
44. K.F. Schoenberg, R.F. Gribble and J.A. Phillips, "Zero-Dimensional Simulations of Reversed-Field Pinch Experiments," Nucl. Fus. 22, 1433 (1982).
45. R. Gerwin and R. Keinigs, "Dynamo Theory: Can Amplification of Magnetic Field Profiles Arise from a Cross-Field Alpha Effect," Los Alamos National Laboratory report LA-9290-MS (April 1982).
46. K.F. Schoenberg, R.W. Moses and R.L. Hagenson, "Plasma Resistivity in the Progress of a Reversed-Field Dynamo," Phys. Fluids 27 (7), 1671 (1984).
47. M.K. Bevir and J.W. Gray, "Relaxation, Flux Consumption and Quasi Steady State Pinches," Proc. RFP Theory Workshop, April 28-May 2, 1980, Los Alamos National Laboratory report LA-8944-C, p. 176 (January 1982).
48. H.A.B. Bodin and G. Rogstani, "The RFX Experiment Technical Proposal," Culham Laboratory report RFX-R1 (April 15, 1981).
49. "INTOR - Summary of Cost/Schedule/Manpower," FEDC-M-81-SE-062, 1981.

APPENDIX A

BLANKET DEVELOPMENT PLANNING CONSIDERATIONS

TABLE OF CONTENTS

APPENDIX A BLANKET DEVELOPMENT PLANNING CONSIDERATIONS

	<u>Page</u>
A.1 Introduction.....	A-1
A.2 Decision Framework.....	A-2
A.3 Objectives, Sub-objectives and Attributes.....	A-5
A.4 Issues and Facilities for First Wall/Blanket Development.....	A-7
A.4.1 First Wall/Blanket Development Issues.....	A-8
A.5 Useful Nuclear Technology Facilities.....	A-10
A.6 Consistency with Magnetic Fusion Program Plan (MFPP).....	A-12
A.6.1 General Time Phasing of Development.....	A-12
A.6.2 Periodic Re-evaluation.....	A-13
A.6.3 Frugality and Near Term Planning.....	A-13
A.6.4 Long Term Planning.....	A-14
A.6.5 Summary.....	A-14

LIST OF TABLES

<u>Table</u>	<u>Page</u>
A-1 Summary of First Wall/Blanket Issues.....	A-9
A-2 First Wall/Blanket Issues/Facilities Matrix.....	A-11

APPENDIX A. BLANKET DEVELOPMENT PLANNING CONSIDERATIONS

A.1 Introduction

A key goal of the FINESSE program is to construct development pathways, or dynamic test plans, which can result in attractive options for blankets and other fusion nuclear components (e.g., tritium systems, shielding, plasma interactive components). The approach is to construct a focused set of development objectives for the year 2000 timeframe which can be used to motivate concept improvements and direct the resolution of feasibility and performance issues consistent with the Magnetic Fusion Program Plan and funding constraints. Constructing development pathways requires making several difficult decisions, often based on very little information. Test planning decisions can be made by: the judgement of a strong leader, consensus of an expert group and/or a more formal decision analysis process using numerical scoring. Example test plans, based on expert consensus, are given in Chapter 2.

Although the objectives for the development pathways anticipate a sequence of experiments which lead to an adequate understanding of the technology, it is important to note that success in developing any given component (regardless of funding) is not assured. Consequently, the pathways should provide sufficient breadth and flexibility to allow for redirection in response to failures in development. Conversely, it is expected that novel ideas leading to potentially significant improvements in performance and/or reliability will be proposed and must be accommodated during development.

The sequence of study in FINESSE has been as follows:

- Select representative fusion-electric blanket concepts
- Identify and prioritize their key issues
- Investigate and isolate those features of the fusion environment that must be simulated to resolve the issues

- Define and cost a generic set of experiments and facilities that are capable of resolving the issues
- Construct development pathways consistent with a reasonable set of objectives and constraints.

For the most part, the first four of the above steps were completed during 1984 and 1985. The fifth step has been addressed in the test plans in Chapter 2. These test plans outline only two of many possible development pathways. Further work is required, primarily to evaluate the impact of varying constraints on the test plans. Our work in this area, emphasizing the development of a reasonable approach to this important task, is described in this appendix.

A.2 Decision Framework

The selection of high priority, near-term, blanket technology experiments and the construction of development pathways extending to the ~2000 timeframe is a problem in decision analysis. That is, a stated preference for one development option (e.g., blanket type) or experimental program over another implies that a value judgement regarding the relative importance of the two options can be made. The basis for such a judgement can derive from a more or less rigorous approach towards determining the utility (or value) of alternative experimental programs.

For example, nominal test sequences for solid and liquid breeder blankets were described earlier in this report. In each case, ~100 \$M is expected to be required to provide an adequate resolution of the key issues. It can be argued that a decision between these options, as early as technically justified, could result in an overall expenditure which is more affordable but does not sacrifice ultimate product attractiveness. Alternately, if (say) only 100 \$M were available, spending 50 \$M on each of two principal options might be preferred over spending 100 \$M on a marginally preferred option (if neither is disqualified).

Historically, such decisions have evolved from one of the following types of management approaches:

- The expert judgement and control of a strong leader
- The consensus opinion of a larger group of experts
- A more formal decision analysis process using mathematical techniques (i.e., linear programming) and numerical scoring

Each of these approaches toward reaching decisions has unique advantages and drawbacks. The expert judgement and control of a single leader may, at first, seem to be intrinsically flawed because no such leader can be expected to grasp the entire problem and because the decision would be suspect with respect to fairness. However, if a benevolent and qualified leader does exist, he or she can solicit opinions from the expert community and can be expected to provide a reasonably consistent decision, even lacking the development of extensive documentation regarding the process which was used. Furthermore, such strong individuals, when they exist, have historically been most effective in providing continuity and implementing programs.

The second approach, consensus within a small group of experts, has the advantage that more cross-fertilization of ideas and tolerance of alternatives is likely to result. An expert group is less likely to pursue a radically bold approach (whether advantageous or not), but is more likely to represent the diversity of the community at large. Such diversity can be further encouraged by seeking wide community review. Relative to the single strong leader approach, the consensus approach requires a more detailed documentation of goals and objectives because it is important that inconsistencies in interpretation be avoided.

The third approach, a more formal decision analysis process, can be interpreted as a method by which subjective trade-off (e.g., addressing more blankets in a test program versus addressing fewer in more depth) can be made to be visible and uniformly applied. This type of approach, involving well defined statements of measurable objectives and associated attributes (i.e., quantifiable parameters) with numerical scoring techniques, has been used successfully in the past and has the advantage that a few (possibly one) integrated figures-of-merit can be developed and used to select a preferred solution. This method requires that the value of achieving a certain level of

performance or design predictability can be estimated and that the value of such an achievement can be quantitatively compared against the value of an achievement in an unrelated area (e.g., MHD pressure drop versus tritium release for a liquid metal blanket). The areas which are compared must be unrelated so that the decision problem can be divided into "orthogonal" (or independent) pieces.

Unfortunately, for a decision problem as complex and interactive as that of blanket development, there is a reasonable doubt regarding an ability to develop a quantitative methodology which is capable of discerning the subtle trade-off involved. For example, a zeroth order understanding would indicate that blanket "improvements" allowing an increased neutron wall loading (e.g., to 10 MW/m²) will result in large benefits. However as the loading increases, reliability/availability penalties due to first wall erosion, non-uniform heat fluxes, blanket replacement times, and so on increase in importance. Our current understanding of these and many other trade-offs is very poor, so that a quantitative representation of such relationships will be more difficult to construct and defend than a consensus opinion among a group of experts who are aware of such interactions. In this sense, we are reminded that, for many applications, the human mind remains a much more powerful pattern recognition device (i.e., more "intelligent") than the fastest computer.

Rather than adopt a numerical model for the decision problem in FINESSE, it was decided (after considerable discussion regarding the application of such methods) that the preferred approach will be to structure the logic of the decision process by following the first steps of a formal decision analysis process, while avoiding an integrated numerical tabulation and comparison. More specifically, the following key features will form the FINESSE approach to decision analysis for the construction of blanket development pathways:

- A formal planning objective, a set of planning sub-objectives and a set of quantifiable attributes for each sub-objective will be defined.
- A small group of experts within the FINESSE Program will be required to form a consensus regarding the most useful experiments and facilities.

- Pathway options will be developed and preferred pathways will be selected based upon a comparative evaluation with respect to their ability to satisfy the above sub-objectives (i.e., by comparison with the attributes at a fixed level of funding). An integrated figure of merit for each pathway will not be developed.
- Extensive community review of the proposed pathways will be solicited.

A.3 Objectives, Sub-objectives and Attributes

As a first step in the blanket development planning process, it is appropriate to define an objective, sub-objectives, attributes and nominal goals. The objective should address an assessment of blanket technologies to be provided in the 2000 timeframe consistent with the objectives of the DOE Magnetic Fusion Program Plan. The sub-objectives, in turn, should address lower level measures of success in achieving the overall objectives. These lower level sub-objectives will also be likely to imply different levels of programmatic emphasis in the development program.

In principal, the utility of a given development pathway (i.e., set of experiments) in satisfying a sub-objective can be expressed as a complex function of a complete set of measurable parameters (attributes) which are expected to change as a result of pursuing that pathway. However, the functional relationship may not be known (e.g., the attributes may be functionally related to one another), and the expected outcome may not be realized since it depends upon experimental results of current and precursor experiments in the pathway. However, goal values (minimum, maximum, nominal) and expected values can be established (e.g., 5 MW/m^2 neutron wall load) based upon conventional wisdom. The progress in meeting a sub-objective can then be evaluated by comparing the expected values of a set of attributes against the goal values.

A broad statement of overall objectives for the development of fusion first wall/blanket components follows:

First Wall Blanket Development Planning Objective: Show that it will be possible to develop attractive first wall/blanket technologies for fuel and energy production and recovery. Provide a predictive capability which can be used to assess the performance of first wall/blanket components.

Two sub-objectives which address lower level measures of success in achieving the overall objective for first wall/blanket development follow:

- Attractiveness Sub-Objective: Identify first wall/blanket technologies which can provide attractive performance levels and safety/environmental features to satisfy the requirements of all candidate magnetic fusion confinement concepts and fusion applications.
- Predictability Sub-Objective: Establish a predictive capability to reduce the levels of uncertainty in anticipated performance and reliability such that the risk in extrapolation to reactor application will be minimal.

These can be further broken down to emphasize distinctions between performance/economics and environment/safety as they relate to attractiveness, as well as to emphasize distinctions between our understanding of fusion-unique fundamental phenomena (e.g., MHD flow effects) and other engineering uncertainties as they relate to predictability.

Attributes (and goal values) which can be used to measure progress towards achievement of the attractiveness sub-objective are listed below:

- Neutron wall load (nominal goal = 5 MW/m²)
- Surface heat flux (nominal goal = 1.25 MW/m²)
- Tritium breeding (minimum 3-D TBR = 1.05)
- $M \cdot \eta_t$ product (nominal goal = 0.60)
- B/FW/S and power conversion cost (nominal goal = \$250M or 20% plant cost)
- Lifetime fluence (minimum = 15 MW-yr/m²)
- Inboard BFW/S thickness (nominal goal = 1.0 m)
- Blanket sector MTBF (nominal goal = 250,000 hr)
- Blanket sector MTTR (nominal goal = 730 hr)
- Routine radioactivity release (maximum = 1 mrem/yr = 10Ci/d trit.)

- Response to loss-of-coolant flow (nominal goal = passive safety)
- Short term activation (maximum = 10^8 km³ BHP or 10^4 AFT)
- Vulnerable tritium inventory (nominal goal = 15 g)
in one component
- Long-Term disposal Hazard (nominal goal = on-site burial)

Attributes which can be used to measure progress towards achievement of the predictability sub-objective can also be defined. Specifically, the predictability attributes are the uncertainties in understanding fusion blanket phenomena (fusion-unique and otherwise) that strongly influence the attractiveness attributes which measure the overall attractiveness of the first wall/blanket. As such, the predictability attributes provide a measure of our ability to predict a specified performance level. For example, the uncertainty in achievable neutron wall load will be a function of the uncertainties in various heat transfer coefficients pressure drops and stress levels within the blanket.

A.4 Issues and Facilities for First Wall/Blanket Development

During the past several years, a wide variety of potentially attractive first wall/blanket concepts have been proposed. The principal concepts can be characterized according to the choice of coolant/tritium breeding material/structural material/neutron multiplier. These classes of blankets (and materials options within a particular class) are based upon the following combinations:

- Helium/Lithium Oxide or Lithium Aluminate/Vanadium Alloy or Ferritic Steel/Beryllium
- Helium/Lithium or Lead-Lithium/Vanadium or Ferritic Steel/(Beryllium)
- Helium/Flibe/Vanadium or Ferritic Steel/Beryllium
- Lithium or Lead-Lithium/Vanadium or Ferritic Steel/(Beryllium)
- Water/Lithium Dioxide or Lithium Aluminate/Ferritic Steel/Beryllium
- Water/Lead-Lithium/Ferritic Steel/(Beryllium)

Beryllium in parentheses indicates that a beryllium multiplier is desirable but may not be required. It is important to note that fusion breeder blankets would utilize similar materials combinations but would also introduce fertile materials (^{232}Th , ^{238}U) into the blanket. Similarly, fusion synfuels blankets require high temperature ceramics (SiC).

For fusion systems with neutron wall loads in a range of 3-5 MW/m², there is a high level of confidence that one of the above first wall/blanket technologies can be developed to achieve safe and reliable levels of operation. Nevertheless, each of the above technologies suffers from one or more feasibility issues. Therefore, the establishment of "predictability" will require that feasibility issues be addressed to the extent that an informal selection among the various candidates can be made.

A.4.1 First Wall/Blanket Development Issues

The first wall/blanket issues are summarized in Table A.-1. These issues and associated sub-issues are discussed in Chapters 3 and 4. The symbols used in the table to describe the potential impact on a particular design configuration are shown below:

Feasibility Issues

- F1 - May close design window
- F2 - May result in unacceptable safety risk
- F3 - May result in unacceptable reliability, availability, or lifetime

Attractiveness Issues

- A1 - Reduced system performance
- A2 - Reduced component lifetime
- A3 - Increased system cost
- A4 - Less desirable safety or environmental impact

The order in which the sub-issues appear in Table A-1 does not imply a relative priority. The level of concern reflects the potential impact, design specificity and other issues relating to the importance of a given issue. For example, some critical issues (i.e., liquid metal MHD effects) are not generic but the alternative issues (e.g., solid breeder tritium inventory, tritium control in helium) are equally serious.

Table A-1. Summary of First Wall/Blanket Issues

<u>Issue</u>	<u>Potential Impact</u>	<u>Design Specificity</u>	<u>Level Concern</u>
A) Tritium and/or Fissile Fuel Breeding for all designs	A1, A3	Specific issues	High
B) Solid Breeder Tritium Inventory a) Tritium Inventory and Transport in Solid Breeder and Multiplier b) Solid Breeder Form and Mechanical Interactions	F1, A4	Solid breeder blankets	Critical
C) Tritium Permeation and Recovery a) Tritium Permeation and Recovery in Helium Systems b) Tritium Permeation and Recovery in Liquid Breeder Systems	F3, A3	Specific issues for all designs	Critical
D) Compatability of Coolant/Structure/Breeder a) Helium/Vanadium Compatibility b) Solid Breeder Compatibility and Transfer c) Liquid Breeder Compatibility and Mass Transfer d) Fusion Breeder Pebble Fuel Flow	F3, A1	Specific issues for all designs	Critical
E) Liquid Metal MHD Flow Effects a) MHD Pressure Drop, Heat Transfer, and Fluid Flow b) Electrical Insulators for Flowing Liquid Metal Systems	F1, A1	Specific issues for all designs	High
F) Structural Response and Component Lifetime a) Structural Response and Lifetime for Fusion Blankets b) Development of Ceramics Technologies for Blankets c) Beryllium Form and Lifetime	F3, A1	Specific issues for all designs	High
G) Reliability, Failure Modes, and Accident Consequences a) Failure Modes and Reliability b) Radioactive Release Pathways and Consequences	F2, A4	Specific issues for all designs	High
H) Fusion Breeder Fuel Reprocessing Costs	A1, A3	Fission suppressed Fusion Breeder	High

A.5 Useful Nuclear Technology Facilities

A first attempt at relating facilities to issues for the blanket and first wall is outlined in Table A-2. The issues and facilities are described in further detail in the preceding chapters. The rankings L=low, M=medium, and H=high are intended to distinguish the relative potential level of usefulness of each type of facility for addressing each issue. All the experiments designated L, M, H will provide valuable and/or necessary information. Each facility has been considered individually, without regard for duplication in other facilities. However, if results from previous facilities would be required to obtain or interpret results from the currently considered facility, they are assumed to have been performed.

Bench top experiments are relatively small scale (and cost) experiments that can be (or have been) performed with standard equipment. For example, measurements of the heat capacity of liquid lead-lithium would fall in this category. High heat flux facilities include PMTF at Sandia National Laboratories. Non-liquid metal corrosion/compatibility loop refers to loop experiments for studying materials compatibility. Heat transfer and testing of irradiated samples may be included.

Small-scale liquid metal facilities include loops without magnets and those with small magnets and limited volume. Intermediate scale loops tend to have more interactive conditions, such as both heat flux and magnetic field, as well as being larger.

The partially integrated test facility (PITF) is intended to incorporate as many reactor relevant operating parameters as possible without neutrons. The emphasis here is on testing interactive phenomena. The specifics of a PITF vary greatly depending on the blanket design or designs being tested and the outcome of prior testing, which may result in the emphasis of one area and the de-emphasis of another.

Fission reactor tests are divided into small specimen tests, purged assemblies (capsule or larger) and core-side experiments. Larger volume is available at core-side but fluxes are much lower than those in the core. Under point neutron sources, neutronic measuring facilities are broken out because of their much lower flux requirements and much more stringent source characterization requirements. The other point neutron source facilities are

Table A-2. First Wall/Blanket Issues/Facilities Matrix

FACILITIES ISSUES	NON-NEUTRON FACILITIES						FISSION REACTORS				POINT NEUTRON SOURCES				FUSION DEVICES			
	BENCH TOP EXPERIMENTS	HIGH HEAT FLUX FACILITY	NON-LM COMPATIBILITY LOOP	LIQUID METAL FACILITIES		TRITIUM FUEL PROCESSING FACILITY	SPECIMEN IN-CORE TEST	PURGED IN-CORE ASSEMBLIES	CORE SIDE FACILITY	NEUTRONIC MEASURE FACILITY	SPECIMEN TESTS		SMALL VOLUME INTERACTIVE	CONFIRMATION EXPERIMENT	EXISTING DT EXPERIMENT	NEAR-TERM IGNITION EXPERIMENT	FUSION TEST FACILITY	
				SMALL SCALE	INTERMEDIATE SCALE						LOW FLUENCE	HIGH FLUENCE						
A. TRITIUM AND/OR FISSILE FUEL BREEDING	L					M		M	H	M	M	L		M	M	H		
B. SOLID BREEDER TRITIUM INVENTORY																		
a. INVENTORY AND TRANSPORT	L				L	L	M	H	M			M			M	H		
b. BREEDER FORM AND MECH. INTERACTION	L				M		M	M	M	L	M	H			L	H		
C. TRITIUM PERMEATION AND RECOVERY																		
a. TRITIUM PERMEATION AND RECOVERY IN HELIUM SYSTEMS	L				L	M	L	M	M	L	L	M		L	M	H		
b. TRITIUM PERMEATION AND RECOVERY IN LIQUID BREEDER SYSTEMS	L					H	L	L	M					L	M	H		
D. COMPATIBILITY OF COOLANT/STRUCTURE/ BREEDER																		
a. HELIUM/VANADIUM COMPATIBILITY	L		H		H											H		
b. SOLID BREEDER COMPATIBILITY AND MASS TRANSFER	L		M		L		M	H	M	L	L	M			L	H		
c. LIQUID BREEDER COMPATIBILITY AND MASS TRANSFER	L			M	H	H	L	L	M							H		
d. FUSION BREEDER PEBBLE FUEL FLOW	L		L	L	M	L	L	L								H		
E. LIQUID METAL MHD FLOW EFFECTS																		
a. MHD PRESSURE DROP, HEAT TRANSFER, AND FLUID FLOW	L			M	M	H										H		
b. ELECTRICAL INSULATORS FOR FLOWING LIQUID METAL SYSTEMS	L			M	M	M	L	L			L	L				H		
F. STRUCTURAL RESPONSE AND COMPONENT LIFETIME																		
a. STRUCTURAL RESPONSE AND LIFETIME FOR FUSION BLANKETS	L	H		L	M	H		M	M						M	H		
b. DEVELOPMENT OF CERAMICS TECHNOLOGIES FOR BLANKETS	L	M	M	M	M	M	L	M	L	L	M	M		L	L	H		
c. BERYLLIUM FORM AND LIFETIME	L				L	L	L	M	M	L	M	M		L	L	H		
G. RELIABILITY, FAILURE MODES, AND ACCIDENT CONSEQUENCES																		
a. FAILURE MODES AND RELIABILITY	L	L	L	L	M	L	L	M	M	L	L	M	L	L	L	H		
b. RADIOACTIVE RELEASE PATHWAYS AND CONSEQUENCES	L	L	L	L	L	L	L	M	L	M	L	M	L	L	L	H		
H. FUSION BREEDER FUEL REPROCESSING	L			L	M	H										H		

USEFULNESS OF TEST FACILITY:

L = LOW; VALUABLE OR NECESSARY CONTRIBUTION
M = MEDIUM; SIGNIFICANT, BUT NOT DEFINITIVE
H = HIGH; POTENTIALLY DEFINITIVE FOR THE STATED ISSUE OF ONE OF ITS SUB-ISSUES

primarily for materials testing. Low fluence facilities would include RTNS-II and high fluence would include the proposed FMIT. The small volume interactive facility would require high energy and high fluence over a volume on the order of 10 cm^3 , allowing limited interactive testing.

Fusion confinement experiments include most existing and planned plasma confinement machines. The existing DT experiments refer to TFTR and JET, although they have not yet burned DT. Near-term ignition experiments would burn tritium and produce useful fusion neutron fluxes, although fluence would be negligible. A fusion test facility, (Chapter 9), would include or emphasize fusion nuclear technology testing, with long-burn and moderate neutron wall load and fluence.

A.6 Consistency with Magnetic Fusion Program Plan (MFPP)

The development pathway must be consistent with the objectives and constraints (implicit and explicit) provided in the U.S. MFPP of 1985 and in other DOE guidance. The MFPP is aimed at an assessment of the attractiveness of fusion energy in the 2000 timeframe. Thus, the goal of FINESSE planning is to develop a data base regarding performance and reliability, but not necessarily fully integrated and tested components. In this context, a major fusion engineering research facility for nuclear testing may not be required within the FINESSE planning horizon. Indeed, if overall funding in the nuclear technology area is constrained to $\leq 20\%$ of the magnetic fusion budget during 1990-2000, then the implementation (design, construction, initial operation) of a fusion test facility in addition to a base program in the nuclear technology area may be difficult or impossible to achieve. Without a FERF or similarly expensive facility, the cost of a thorough nuclear technology program is not expected to exceed 10-15% of the overall magnetic fusion budget.

A.6.1 General Time Phasing of Development

Consistent with satisfying both the attractiveness and predictability sub-objectives, it will be necessary to phase the blanket development program in such a way that the expected result will be a narrowing down from several

potential blanket technologies to a few, or possibly one, as the design requirements associated with magnetic confinement options and potential fusion applications become better defined over the next 15-20 years. In this context, it will be prudent to emphasize the resolution of key feasibility and high leverage attractiveness issues in the near term, and concept improvement and predictability issues following the elimination of some blanket design options.

A.6.2 Periodic Re-evaluation

Because the successful development of any blanket design option cannot be assured, the development pathways must provide for programmatic re-evaluations on a 3-5 year timescale, depending upon the particular set of experiments involved. In such re-evaluations, the changing requirements for confinement schemes (e.g., first wall erosion, magnetic field strength), applications (e.g., fusion-electric versus fusion breeder) and reactor systems level performance (e.g., wall load, fluence) must be considered. Also, the desirability of allocating a fraction of the budget to pursue new design innovations must be assessed.

A.6.3 Frugality and Near Term Planning

Frugality, in the context of minimizing the prospect of spending large fractions of the overall development budget on investigating blanket design concepts which have a high probability of failing, is a worthwhile goal of any development program. In a practical sense, frugality requires that, when possible, inexpensive experiments which are directly applicable to decisions regarding the resolution of concept feasibility issues should be implemented on a high priority basis in the near-term.

The highest priority near-term experiments will be those that fall into the following categories:

- Impact feasibility (potential to disqualify one or more design approaches)

- Relatively Inexpensive
- Widely applicable (implies separate rather than multiple effects since they are, in general, applicable to a wide variety of blankets)

These should provide the largest benefit/cost ratio. They would be followed by experiments which fall into only one or two of the above categories, (widely applicable will become less important as concepts are eliminated and better defined) then by experiments which emphasize improvements in performance and/or predictability.

A.6.4 Long Term Planning

In the longer term (beyond the first one or two sets of programmatic evaluations), the general features of large multiple effect and/or integrated testing facilities can already be anticipated, but the final specification of such facilities can not be anticipated prior to the resolution of earlier experiments. Consequently, a detailed specification of such facilities (beyond general anticipated characteristics and costs) is not required. Indeed, unanticipated levels of failure or success in earlier experiments could entirely eliminate the need for the larger facility (i.e., the underlying approach might not be feasible or phenomena might be so well predicted by earlier experiments that the larger facility becomes unnecessary). Recognizing these possibilities, it will be prudent to base large facilities upon nominal anticipated requirements and plan on "intermediate" results.

A.6.5 Summary

Fusion blanket development plans must remain flexible in order to respond to experimental results and changes in schedule and funding. Several considerations have been outlined that will lead to a set of pathway options based on evaluation of the current state of knowledge, expert judgement, and community review. During FY'86, additional specific pathway options will be developed and preferred pathways selected based upon evaluation in light of

the sub-objectives discussed above. Various funding and schedule scenarios will be considered and extensive community review of the proposed pathways will be solicited.